HAL
archives-ouvertes.fr

Phytochemical screening of two Thai tropical rainforest Dipterocarps : Hopea odorata Roxb. and Dipterocarpus costatus Gaertn.f.

Malaï Satiraphan

▶ **To cite this version:**

Malaï Satiraphan. Phytochemical screening of two Thai tropical rainforest Dipterocarps : Hopea odorata Roxb. and Dipterocarpus costatus Gaertn.f.. Other. Université René Descartes - Paris V, 2012. English. <NNT : 2012PA05P623>. <tel-01124074>

HAL Id: tel-01124074

https://tel.archives-ouvertes.fr/tel-01124074

Submitted on 6 Mar 2015

HAL is a multi-disciplinary open access archive for the deposit and dissemination of scientific research documents, whether they are published or not. The documents may come from teaching and research institutions in France or abroad, or from public or private research centers.

L'archive ouverte pluridisciplinaire **HAL**, est destinée au dépôt et à la diffusion de documents scientifiques de niveau recherche, publiés ou non, émanant des établissements d'enseignement et de recherche français ou étrangers, des laboratoires publics ou privés.

UNIVERSITE PARIS DESCARTES
SILPAKORN UNIVERSITY

Année : 2012 **Série : Pharmacie**

THÈSE DE DOCTORAT EN COTUTELLE

DE L'UNIVERSITÉ PARIS DESCARTES
ET DE L'UNIVERSITÉ SILPAKORN

SPÉCIALITÉ : PHARMACOGNOSIE

Par : Malaï SATIRAPHAN

Etude phytochimique de deux Dipterocarpaceae de la forêt thaïlandaise : *Hopea odorata* Roxb. et *Dipterocarpus costatus* Gaertn.f.

Soutenue le 27 septembre 2012

Composition du jury:

M. Marc LITAUDON, Dr	**Rapporteur**
Mme Busaban SIRITHUNYALUG, Dr	**Rapporteur**
Mme Sylvie MICHEL, Pr	**Examinateur**
Mme Christiane GARBAY, Pr	**Examinateur**
M. Chavalit SITTISOMBUT, Dr	**Examinateur**
M. Uthai SOTANAPHUN, Dr	**Examinateur**
M. Xavier CACHET, Dr	
Mme Françoise RAYNAUD, Dr	

Ce travail est dédié à la mémoire du Professeur François TILLEQUIN (1950-2011)

REMERCIEMENTS

Aux membres du jury, pour avoir accepté de participer au jury de ma thèse,
Mr Marc LITAUDON, Ingénieur de recherche CNRS-HDR, ICSN Gif SurYvette,
Mme Busaban SIRITHUNYALUG, Professeur associé à la Faculté de Pharmacie, Université de Chiang Mai,
Mme Christiane GARBAY, Professeur de l'Université Paris Descartes,
Mme Sylvie MICHEL, Professeur de l'Université Paris Descartes,
M. Chavalit SITTISOMBUT, Professeur assistant à la Faculté de Pharmacie, Université de Silpakorn,
M. Uthai SOTANAPHUN, Professeur associé à la Faculté de Pharmacie, Université de Silpakorn,
M. Xavier CACHET, Maître de conférences à la Faculté de Pharmacie, Université Paris Descartes.
A toutes les personnes qui m'ont soutenues en France et en Thaïlande au cours de ma thèse,
le professeur Marie-Jose FOGLIETTI, les professeurs associés Sindchai KEOKITICHAI et Jurairat NUNTHANID,
les membres titulaires du laboratoire de Pharmacognosie de l'Université Paris Descartes : les professeur Michel KOCH, Brigitte DEGUIN et Marie-Christine LALLEMAND, les docteurs Hanh DUFAT, Sabrina BOUTEFNOUCHET, Marina KRITSANIDA, Raphaël GROUGNET, François-Hugues POREE, Thomas GASLONDE, les membres de l'équipe technique : Chouaha BOUZIDI, Maryse ROUXEL, Oumar KANTE, Olivier HERMET, les étudiants (en particulier Linh HOANG pour son aide au cours de l'évaluation biologique des composés et M.Quoc Dang THAI pour son travail sur les cycloartanes),
Elise PROST (IGE), Meryam TAGHI (ASI), Anne REGAZZETTI (IGE),
les docteurs Perayot PAMONSINLAPATHAM et docteurs Chalermphong RATTANABORDIN pour avoir réalisé les tests de cytotoxicité,
ma famille, tous mes amis de Faculté de Pharmacie de l'Université Silpakorn-Bangkok,
Enfin je tiens à remercier tout particulièrement pour leur soutien financier : la Faculté de Pharmacie de l'Université de Silpakorn, ainsi que le Ministère des Affaires Etrangères et Européennes (Programme Hubert Curien (PHC) Thaïlande, 2009-2010).

This work is dedicated to the memorial of Professor François TILLEQUIN (1950-2011)

ACKNOWLEDGEMENTS

It is a great pleasure to acknowledge the guidance and support of Prof. Sylvie MICHEL and Dr.Xavier CACHET throughout this work. I am deeply indebted to them for their enthusiasm patience, and friendship.

I am extremely grateful to Assoc. Prof. Sindhchai KEOKITICHAI and Prof. Marie-Jose FOGLIETTI for their great assistance at the beginning of this collaboration, Prof. Christiane GARBAY for her cytotoxicity laboratory support as well as Assoc. Prof. Jurairat NUNTHANID for her continuing support from Silpakorn University.

I am grateful to Assist. Prof. Chavalit SITTISOMBUT for his supply of the plant material, solvents for extraction and cytotoxic assays in preliminary study, Assoc. Prof. Uthai SOTANAPHUN for his guidance of the study plan and Prof.Marc LITAUDON together with

Assoc. Prof. Busaban SIRITHUNYALUG for their commentation.

I would like to thank all the people who have contributed information and supplies for my work: Dr.Perayot PAMONSINLAPATHAM, Dr.Chalermphong RATTANABORDIN, and Ms Linh HOANG for their bioactivity experiments, along with Mr.Quoc Dang THAI for his absolute configuration determination; Mme Elise PROST for the suggestion of NMR experiments; Meryam TAGHI and Anne REGAZZETTI for MS measurements.

I would like to acknowledge the love and support of professors and everyone in Pharmacognosy laboratory at University of Paris Descartes.

- Prof.Michel KOCH
- Prof.Brigitte DEGUIN, Prof.Marie-Christine LALLEMAND, Dr.Hanh DUFAT, Dr.Sabrina BOUTEFNOUCHET, Dr.Marina KRITSANIDA
- Dr.Raphael GROUGNET, Dr.François-Hugues POREE, Dr.Thomas GASLONDE
- Chouaha BOUZIDI, Maryse ROUXEL, Oumar KANTE, Olivier HERMET

Financial support came from Pharmacy Faculty, Silpakorn University, along with French and Thai Commission on Higher Education and universities through Programme Hubert Curien Thaïlande (PHC) Year 2009-2010. I am really grateful.

Finally, I would like to thank all my family, for their continued encouragement with powerful impulsion and being source of strength. Also all of my friends in Pharmacy Faculty at Silpakorn University have shown continuing concern for me and interest in my work, and for these things I am grateful.

ABSTRACT

Preliminary study of the extracts from *Hopea odorata* leaves and *Dipterocarpus costatus* wood showed that the hexane extracts of both plants exhibited cytotoxicity against breast cancer (MCF-7) and small cell lung cancer (NCI-H187), in conjuction with potent anti-malarial (against *Plasmodium falciparum* K1 strain) activity of *D.costatus* wood hexane extract.

Phytochemical studies of *H. odorata* leaves hexane extract led to the isolation of 16 terpenoids in the series lupane (n = 8), 3,4-*seco*-cycloartane (n = 4), friedelane (n = 2) and oleanane (n = 2). Among lupanes, 3,30-dioxolup-20(29)-en-28-oic acid was isolated for the first time from a natural source. Cytotoxicity of lupanes triterpenes against four human cancer cell lines (PC3, MDA-MB-231, HT-29 and HCT116) was evaluated and showed the structure- activity relationship related to the oxidation degree at position 3, 28 and 30. Among cycloartanes two new 3,4-*seco*-cycloartanes were identified. They are saturated fatty acid esters of (24*S*,25*S*,26)-trihydroxy-3,4-*seco*-cycloart-4(29)-en-3-oic acid.

Isolation of *D. costatus* wood hexane extract discovered 30 terpenoids of which 12 triterpenes are new, including 5 norlupanes, 3 dammaranes, 2 nordammaranes and 2 *seco*-dammaranes. The biological activities of all isolated compounds were evaluated through cytotoxicity against human cancer cell lines mentioned above and rat myoblast-derived cells L-6, as well as antimalarial activity against *Plasmodium falciparum* FcB1 strain. Interestingly, the norlupane **36**, possessing an endoperoxide group, showed a strong antiplasmodial activity associated with low cytotoxicity.

Keywords : Dipterocarpaceae, *Hopea odorata*, *Dipterocarpus costatus*, terpenoids, cytotoxicity, 3,4-*seco*-cycloartanes, lupane, norlupane, dammarane, nordammarane, 2,3-*seco*-dammarane

LIST OF TABLES

Table		page
1	Some reported bioactive terpenoids and phenolic compounds in low polarity fraction of the family Dipterocarpaceae extracts.	12
2	Discovery of lupane-type triterpenes in some plants.	15
3	Cytotoxicity of betulonic acid against various cell lines	21
4	Cytotoxicity of other lupane-type triterpenes	22
5	Anti-inflammatory activity of some lupanes (effect on NO and PGE2 production)	23
6	Anti HIV-1 activity of some lupanes	24
7	Discovery of dammarane-type triterpenes in some plants.	25
8	*In vitro* antiviral activity of dammaranes.	30
9	*In vitro* bioactivity assays of *H.odorata* leaves extract	42
10	Fractionation and isolated compounds from a small portion of *H.odorata* leaves hexane extract.	45
11	Fractionation of *H.odorata* leaves hexane extract isolation by MPLC.	47
12	Fractionation of Fraction B23 isolated by MPLC.	51
13	Cytotoxic activity against HCT116, HT29, MDA-MB231 and PC3 cell lines.	58
14	The ^{1}H NMR data for (*S*)-MTPA and (*R*)-MTPA ester of compound **18a**.	63
15	The ^{1}H-NMR (400 MHz) and ^{13}C-NMR (75 MHz) data of **1** and **4** (in $CDCl_3$)	74
16	The ^{1}H-NMR (400 MHz) and ^{13}C-NMR (75 MHz) data of **2** and **6** (in $CDCl_3$)	76
17	The ^{1}H-NMR (400 MHz) and ^{13}C-NMR (75 MHz) data of **3**, **7** and **8** (in $CDCl_3$)	78
18	The ^{1}H-NMR (400 MHz) data of **5**, **10**, **11**, **12** and **13** (in $CDCl_3$)	82
19	The ^{1}H-NMR (400 MHz) data of **14**, **16** and **17** (in $CDCl_3$)	83
20	The ^{13}C-NMR (75 MHz) data of **5**, **10**, **11**, **12**, **13**, **14**, **16** and **17** (in $CDCl_3$)	84
21	The ^{1}H-NMR (400 MHz) and ^{13}C-NMR (75 MHz) data of **9** (in $CDCl_3$)	87
22	The ^{1}H-NMR (400MHz) and ^{13}C-NMR (75 MHz) data of **15** (in $CDCl_3$	88
23	The ^{1}H-NMR (300 MHz) of **18**, **18a**, **18b** and **19** (in $CDCl_3$).	92
24	The ^{13}C-NMR (75 MHz) of **18**, **18a**, **18b** and **19** (in $CDCl_3$).	93
25	The ^{1}H-NMR (300 MHz) and ^{13}C-NMR spectrum (75 MHz) of **20** and **20a** (in $CDCl_3$).	94
26	*In vitro* bioactivity assays of *D.costatus* wood extract	108
27	Fractionation of *D.costatus* wood hexane extract isolation by MPLC.	110
28	% Cell proliferation inhibition of the isolated compounds	117
Table		Page
29	Screening test for in vitro antiplasmodial activity and cytotoxicity of the isolated triterpenes	119
30	Antiplasmodial potency of compound **36**	120
31	The ^{1}H-NMR (400 MHz) and ^{13}C-NMR spectrum (75 MHz) data of **21** (in $CDCl_3$)	143
32	The ^{1}H-NMR (300 MHz) and ^{13}C-NMR (75 MHz) of **22** and **31** (in $CDCl_3$)	146

33	The ^{1}H-NMR (300 MHz) of **23**, **33** (in $CDCl_3$) and **48** (in acetone)	149
34	The ^{1}H-NMR (300 MHz) of **40**, **44** and **46** (in $CDCl_3$)	150
35	The ^{13}C-NMR (75 MHz) of **23**, **33**, **40**, **44** and **46** (in $CDCl_3$) and **48** (in acetone)	151
36	The ^{1}H-NMR (300 MHz) and ^{13}C-NMR (75 MHz) of **45** (in acetone)	152
37	The ^{1}H-NMR (300 MHz) and ^{13}C-NMR (75 MHz) of **29**, **32** and **38** (in $CDCl_3$)	154
38	The ^{1}H-NMR (300 MHz) of **30**, **34**, **37** and **47** (in $CDCl_3$)	156
39	The ^{13}C-NMR (300 MHz) of **30**, **34**, **37** and **47** (in $CDCl_3$)	157
40	The ^{1}H-NMR (300 MHz) and ^{13}C-NMR (75 MHz) of **27**, **28** and **35** (in $CDCl_3$)	159
41	The ^{1}H-NMR (300 MHz) and ^{13}C-NMR (75 MHz) of **26**, **39** and **49** (in $CDCl_3$)	161
42	The ^{1}H-NMR (300 MHz) of **24**, **25**, **36**, **41** and **42** (in $CDCl_3$)	164
43	The ^{13}C-NMR (75 MHz) of **24**, **25**, **36**, **41** and **42** (in $CDCl_3$)	165
44	Compounds isolated from *Hopea odorata* leaves hexane extract and *Dipterocarpus costatus* wood hexane extract	174

LIST OF FIGURES

Figure		page
1	Structure of some reported bioactive terpenoids and phenolic compounds in the family Dipterocarpaceae.	9
2	Some reported lupane-type triterpenes structures.	18
3	Some reported dammarane-type triterpenes structures.	27
4	Two Mosher conformers showing the (*S*)-MTPA and (*R*)-MTPA derivatives proposed by Mosher.	31
5	The (*S*)-MTPA ester presenting the $H_{A,B,C,X,Y,Z}$ instead of group R^1 and R^2.	31
6	Some tetrazolium salts for cell proliferation and cell viability measurement.	32
7	Reduction of WST-1by NADH.	32
8	The principle of REMA method.	33
9	Characteristics of *H.odorata* Roxb.	37
10	Distribution of *H.odorata* in Thailand.	38
11	Structure of lupane triterpenes from *H.odorata* leaves hexane extract.	69
12	Structures of compounds **1** and **4**	73
13	Structures of compounds **2** and **6**	75
14	Structures of compounds **3**, **7** and **8**	77
15	Structures of the isolated lupanes	79
16	Selected HMBC correlations of **5, 10, 11, 12, 13, 14, 16, and 17**	80
17	Selected NOE correlations of compound **16**	86
18	Structure of caryophyllene oxide (**9**)	87
19	Structure and Selected HMBC correlations of compound **15**	88
20	Structures of compounds **18**, **18a** and **18b** and selected HMBC correlations of **18**	89
21	Proposed configuration of **18**	91
22	Structures of compounds **19** and **19a** and Selected HMBC correlations of **19a**	94
23	Structures and selected HMBC correlations of compound **20** and **20a**.	95
24	Characteristics of *D.costatus* Gaertn.f.	102
25	Distribution of *D.costatus* in Thailand	103
26	Proposed structure of isolated secondary metabolites from *D.costatus* wood hexane extract.	121
27	The possible degradation products of the 20,24,25-triol dammarane.	140
28	Selected HMBC correlations of **21**	143
29	Selected HMBC correlations of **22** and **31**	144
30	Fragmentation of dammarenediol II	145
31	Selected HMBC correlations of compounds **23**, **33**, **40**, **44**, **46** and **48**	147
Figure		page
32	Selected HMBC correlations of compound **45**	151
33	Selected HMBC correlations of compounds **29**, **32** and **38**	153
34	Seleted HMBC correlations of compounds **30**, **34**, **37** and **47**	155
35	Seleted HMBC correlations of compounds **27**, **28** and **35**	158
36	Seleted HMBC correlations of compounds **26**, **39** and **49**	160
37	Seleted HMBC correlations of compounds **24**, **25**, **36**, **41** and **42**	163
38	Selected NOE and stereoscopic view of compound **41**	163
39	Comparison of 3D model of 19α- and 19β-orientation of compound **24**	166
40	Selected NOE and stereoscopic view of compound **42**	167
41	The ^{1}H (300 MHz) and ^{13}C NMR (75 MHz) spectrum of **2 and 6** (in	200

	$CDCl_3$)	
42	The ^1H (300 MHz) and ^{13}C NMR (75 MHz) spectrum of **3**, **7 and 8** (in $CDCl_3$).	201
43	The ^1H (300 MHz) and ^{13}C NMR (75 MHz) spectrum of **14** (in $CDCl_3$).	202
44	The HMBC correlation of **14** (in $CDCl_3$).	203
45	IR spectrum of **14**. (dry film)	204
46	The ^1H (300 MHz) and ^{13}C NMR (75 MHz) spectrum of **16** (in $CDCl_3$).	205
47	Expanded HSQCedited spectrum of **16** in the range of δ_H 0.7-5.1 ppm and δ_C 10-110 ppm.	206
48	The HMBC correlation of **16** (in $CDCl_3$).	206
49	The expanded NOESY spectrum of **16** (in $CDCl_3$) in the range of δ_H 0.8-4.0 ppm.	207
50	The ^1H (300 MHz) and ^{13}C NMR (75 MHz) spectrum of **17** (in $CDCl_3$).	208
51	Expanded HSQCedited spectrum of **17** (in $CDCl_3$) in the range of δ_H 0.7-5.2 ppm and δ_C 0-160 ppm.	209
52	The HMBC correlation of **17** (in $CDCl_3$).	209
53	The ^1H and ^{13}C NMR spectrum (300 MHz) of **18** (in $CDCl_3$).	210
54	Expanded HSQCedited spectrum of **18** (in $CDCl_3$) in the range of δ_H 0.4-2.8 ppm and δ_C 10-55 ppm.	211
55	Expanded HSQCedited spectrum of **18** (in $CDCl_3$) in the range of δ_H 3.2-5.0 ppm and δ_C 60-120 ppm.	211
56	HMBC correlation of **18** (in $CDCl_3$).	212
57	Expanded HMBC correlation of **18** (in $CDCl_3$) in the range of a) δ_H 0.3-2.8 ppm and δ_C 10-80 ppm. b) δ_H 1.5-4.5 ppm and δ_C 10-80 ppm. c) δ_H 3.2-5.0 ppm and δ_C 10-80 ppm.	213
58	The ^1H NMR spectrum (300 MHz) of **18**,**18a** and **18b** (in $CDCl_3$).	214
59	The ^{13}C NMR spectrum (75 MHz) of **18**,**18a** and **18b** (in $CDCl_3$).	215
60	The ^1H NMR spectrum (300 MHz) of **18a** and **19a** (in $CDCl_3$).	216
Figure		page
61	The ^{13}C NMR spectrum (75 MHz) of **18a** and **19a** (in $CDCl_3$).	217
62	The HSQCedited spectrum of **19a** (in $CDCl_3$).	218
63	The HMBC spectrum of **19a** (in $CDCl_3$).	218
64	The ^1H NMR spectrum (300 MHz) of **20** (in $CDCl_3$) and expanded spectrum in the range of 0.3-2.7 ppm.	219
65	The ^{13}C NMR spectrum (75 MHz) of **20** (in $CDCl_3$) and expanded spectrum in the range of 10.0-54.0 ppm.	220
66	The HSQCedited correlation of **20** (in $CDCl_3$) and expanded spectrum in the range of δ_H 0.2-2.8 ppm and δ_C 10-58 ppm.	221
67	The HMBC correlation of **20** (in $CDCl_3$) and expanded spectrum in the range of δ_H 0.3-7.0 ppm and δ_C 10-56 ppm.	222
68	The ^1H NMR spectrum (300 MHz) of **20** and **20a** (in $CDCl_3$)	223
69	The ^{13}C NMR spectrum (75 MHz) of **20** and **20a** (in $CDCl_3$).	224
70	The HSQCedited correlation of **20a** (in $CDCl_3$) and expanded spectrum in the range of δ_H 0.3-2.6 ppm and δ_C 0-56 ppm.	225
71	The HMBC correlation of **20a** (in $CDCl_3$) and expanded spectrum in the range of δ_H 0.4-2.6 ppm and δ_C 12-59 ppm.	226
72	The ^1H NMR spectrum (300 MHz) of **22** and **31** (in $CDCl_3$).	227
73	The ^{13}C NMR spectrum (75 MHz) of **22** and **31** (in $CDCl_3$).	228
74	The HMBC correlation of **22** and **31** (in $CDCl_3$).	229

75	The expanded HMBC correlation of **22** and **31** (in $CDCl_3$) and expanded spectrum in the range of δ_H 0.7-1.8 ppm and δ_C 15-58 ppm.	230
76	The ^1H NMR spectrum (300 MHz) of **24** (in $CDCl_3$) and expanded spectrum in the range of 0.7-2.1 ppm.	231
77	The ^{13}C NMR spectrum (300 MHz) of **24** (in $CDCl_3$) and expanded spectrum in the range of 13-56 ppm. (with trace of dipterocarpol)	232
78	The HSQCedoted correlation of **24** (in $CDCl_3$) and expanded spectrum in the range of δ_H 0.7-3.8 ppm and δ_C 13-72 ppm.	233
79	The HMBC correlation of **24** (in $CDCl_3$) and expanded spectrum in the range of δ_H 2.9-3.8 ppm, δ_C 10-50 ppm and δ_H 1.2-1.8 ppm, δ_C 81-84ppm.	234
80	The ^1H NMR spectrum (300 MHz) of **25** (in $CDCl_3$) and expanded spectrum in the range of 0.95-1.10 ppm.	235
81	The ^{13}C NMR spectrum (75 MHz) of **25** (in $CDCl_3$) and expanded spectrum in the range of 16-60 ppm.	236
82	The expanded HSQCedited correlation of **25** (in $CDCl_3$) in the range of δ_H 0.8-4.9 ppm and δ_C 16-110 ppm.	237
83	The HMBC correlation of **25** (in $CDCl_3$) and expanded spectrum in the range of δ_H 4.7-4.9 ppm, δ_C 20-55 ppm and δ_H 0.9-2.0 ppm, δ_C 18-57ppm.	238
Figure		page
84	The expand ^1H NMR spectrum (300 MHz) of **26** (in $CDCl_3$).	239
85	The ^{13}C NMR spectrum (75 MHz) of **26** (in $CDCl_3$) and expanded spectrum in the range of 13-58 ppm.	240
86	The expanded HSQCedited correlation of **26** (in $CDCl_3$) in the range of δ_H 0.8-2.7 ppm and δ_C 13-58 ppm.	241
87	The expanded HMBC correlation of **26** (in $CDCl_3$) in the range of δ_H 0.7-2.7 ppm, δ_C 13-59 ppm and δ_H 1.0-2.7 ppm, δ_C 211-219 ppm.	242
88	The expand ^1H NMR spectrum (300 MHz) of **27** and **28** (in $CDCl_3$) δ_H 0.7-2.7 ppm.	243
89	The ^{13}C NMR spectrum (75 MHz) of **27** and **28** (in $CDCl_3$).	244
90	The expanded ^{13}C NMR spectrum (75 MHz) of **27** and **28** (in $CDCl_3$) in the range of δ_H 10-60 ppm.	245
91	The expanded HSQCedited correlation of **27** (in $CDCl_3$) in the range of δ_H 0.8-2.8 ppm and δ_C 13-58 ppm.	246
92	The HMBC correlation of **27** (in $CDCl_3$) and expanded spectrum in the range of δ_H 0.9-2.8 ppm, δ_C 15-57 ppm.	247
93	The ^1H NMR spectrum (300 MHz) of **29** (in $CDCl_3$) and expanded spectrum in the range of 0.85-1.20 ppm.	248
94	The ^{13}C NMR spectrum (75 MHz) of **29** (in $CDCl_3$).	249
95	The HSQCedited correlation of **29** (in $CDCl_3$) in the range of δ_H 4.31-4.36 ppm, δ_C 89.00-90.50 ppm and δ_H 5.00-5.11 ppm, δ_C 113.00-115.50 ppm.	250
96	The HMBC correlation of **29** (in $CDCl_3$)and expanded spectrum in the range of δ_H 1.78-1.82 ppm, δ_C 86.00-150.00 ppm and δ_H 1.17-1.22 ppm, δ_C 32.00-80.00 ppm	251
97	The ^1H NMR spectrum (300 MHz) of **32** (in $CDCl_3$) and expanded spectrum in the range of 0.7-2.2 ppm.	252
98	The ^{13}C NMR spectrum (75 MHz) of **32** (in $CDCl_3$).	253
99	The HSQCedited correlation of **32** (in $CDCl_3$).	254
100	The HMBC correlation of **32** (in $CDCl_3$).	255
101	The ^1H NMR spectrum (300 MHz) of **36** (in $CDCl_3$) and expanded	256

spectrum in the range of 0.8-2.6 ppm.
102 The ^{13}C NMR spectrum (300 MHz) of **36** (in $CDCl_3$) and expanded spectrum in the range of 11-58 ppm. 257
103 The HSQCedited correlation of **36** (in $CDCl_3$) and expanded spectrum in the range of δ_H 0.9-2.6 ppm and δ_C 10-56 ppm. 258

Figure		page
104	The HMBC correlation of **36** (in $CDCl_3$) and expanded spectrum in the range of δ_H 0.9-2.1 ppm, δ_C 13-58 ppm and δ_H 3.5-4.3 ppm, δ_C 19.5-22.0 ppm.	259
105	The ^1H NMR spectrum (300 MHz) of **39** (in $CDCl_3$) and expanded spectrum in the range of 0.7-2.7 ppm.	260
106	The ^{13}C NMR spectrum (75 MHz) of **39** (in $CDCl_3$) and expanded spectrum in the range of 10-58 ppm.	261
107	The HSQCedited correlation of **39** (in $CDCl_3$) and expanded spectrum in the range of δ_H 0.9-2.9 ppm and δ_C 12-58 ppm.	262
108	The HMBC correlation of **39** (in $CDCl_3$) and expanded spectrum in the range of δ_H 0.6-2.7 ppm and δ_C 10-80 ppm.	263
109	IR spectrum of **39**. (dry film).	264
110	The ^1H NMR spectrum (300 MHz) of **41** (in $CDCl_3$).	265
111	The ^{13}C NMR spectrum (300 MHz) of **41** (in $CDCl_3$) and expanded spectrum in the range of 10-59 ppm.	266
112	The expanded HSQCedited correlation of **41** (in $CDCl_3$) in the range of δ_H 0.8-3.0 ppm and δ_C 11-57 ppm.	267
113	The HMBC correlation of **41** (in $CDCl_3$) and expanded spectrum in the range of δ_H 0.7-2.6 ppm and δ_C 10-59 ppm.	268
114	The NOE correlation of **41** (in $CDCl_3$).	269
115	The ^1H NMR spectrum (300 MHz) of **42** (in $CDCl_3$) and expanded spectrum in the range of 0.8-2.6 ppm.	270
116	The ^{13}C NMR spectrum (75 MHz) of **42** (in $CDCl_3$) and expanded spectrum in the range of 12-84 ppm.	271
117	The expanded HSQCedited correlation of **42** (in $CDCl_3$) in the range of δ_H 0.8-3.6 ppm and δ_C 11-80 ppm.	272
118	The HMBC correlation of **42** (in $CDCl_3$) and expanded spectrum in the range of δ_H 0.7-3.7 ppm and δ_C 13-90 ppm.	273
119	The NOE correlation of **42** (in $CDCl_3$) and expanded spectrum in the range of δ_H 0.7-2.7 ppm.	274
120	The ^1H NMR spectrum (300 MHz) of **45** (in acetone) and expanded spectrum in the range of 0.8-2.6 ppm.	275
121	The ^{13}C NMR spectrum (75 MHz) of **45** (in acetone) and expanded spectrum in the range of 10-58 ppm.	276
122	The HSQCedited correlation of **45** (in acetone) and expanded spectrum in the range of δ_H 0.8-2.6 ppm and δ_C 10-58 ppm.	277

Figure		page
123	The HMBC correlation of **45** (in acetone) and expanded spectrum in the range of δ_H 0.6-4.2 ppm and δ_C 10-85 ppm.	278
124	The ^{1}H NMR spectrum (300 MHz) of **46** (in $CDCl_3$) and expanded spectrum in the range of 0.7-2.7 ppm.	279
125	The ^{13}C NMR spectrum (75 MHz) of **46** (in $CDCl_3$) and expanded spectrum in the range of 10-58 ppm.	280
126	The HSQCedited correlation of **46** (in $CDCl_3$) and expanded spectrum in the range of δ_H 0.8-2.6 ppm and δ_C 10-58 ppm.	281
127	The HMBC correlation of **46** (in $CDCl_3$) and expanded spectrum in the range of δ_H 0.6-4.2 ppm and δ_C 10-85 ppm.	282
128	The ^{1}H NMR spectrum (300 MHz) of **47** (in $CDCl_3$) and expanded spectrum in the range of 0.6-2.8 ppm.	283
129	The ^{13}C NMR spectrum (75 MHz) of **47** (in $CDCl_3$) and expanded spectrum in the range of 10-52 ppm.	284
130	The HSQCedited correlation of **47** (in $CDCl_3$) and expanded spectrum in the range of δ_H 0.8-2.6 ppm and δ_C 10-58 ppm.	285
131	The HMBC correlation of **47** (in $CDCl_3$) and expanded spectrum in the range of δ_H 0.7-2.8 ppm and δ_C 10-90 ppm.	286
132	The ^{1}H NMR spectrum (300 MHz) of **48** (in acetone) and expanded spectrum in the range of 0.8-2.8 ppm.	287
133	The ^{13}C NMR spectrum (75 MHz) of **48** (in acetone) and expanded spectrum in the range of 10-55 ppm.	288
134	The HSQCedited correlation of **48** (in acetone) and expanded spectrum in the range of δ_H 0.9-2.7 ppm and δ_C 13-52 ppm.	289
135	The HMBC correlation of **48** (in acetone) and expanded spectrum in the range of δ_H 0.8-2.7ppm and δ_C 15-53 ppm.	290
136	The ^{1}H NMR spectrum (300 MHz) of **49** (in $CDCl_3$).	291
137	The ^{13}C NMR spectrum (75 MHz) of **49** (in $CDCl_3$) and expanded spectrum in the range of 10-60 ppm.	292
138	The expanded HSQCedited correlation of **49** (in $CDCl_3$) in the range of δ_H 0.9-2.8 ppm and δ_C 12-58 ppm.	293
139	The expanded HMBC correlation of **49** (in $CDCl_3$) in the range of δ_H 0.9-2.7ppm, δ_C 15-53 ppm and δ_H 1.1-2.8ppm, δ_C 170-220 ppm.	294

LIST OF SCHEMES

Scheme		page
1	Taxonomic classification of genus *Hopea* and *Dipterocarpus*.	5
2	Biosynthesis pathway of dammarane and lupanes triterpene.	13
3	Extraction and bioactivity assay of preliminary study of *H.odorata* leaves.	43
4	Extraction of *H.odorata* leaves for phytochemical study.	44
5	Isolation of main compounds from *H.odorata* leaves hexane extract.	46
6	Isolation of *H.odorata* leaves extract by MPLC (SiO_2).	49
7	Further purification of fraction B23.	50
8	Further purification of Fraction C39.	55
9	Purification of fraction C41.	55
10	Mosher's esterification of compound **18a**.	56
11	Purification of fraction C42.	57
12	Hydrolysis of **20a** from fraction C41 and C42.	57
13	Reaction mechanism of methylation of carboxylic acid	70
14	Reaction mechanism of transesterification at C-24 and hydrolysis at C-3 of 18a.	70
15	Reaction mechanism of saponification of 20a.	71
16	Reaction mechanism of **18a** in modified Mosher's method	71
17	Proposed biosynthesis of **20** from mangiferonic acid	72
18	Extraction and bioactivity assay of preliminary study of *D. costatus* wood	107
19	Extraction of *D. costatus* wood for phytochemical study.	109
20	Purification of *D. costatus* wood hexane extract.	115
21	Semisynthesis of octanordammarane-3,17-dione (**26**) from (20*S*,24*R*)-20,24-epoxydammarane-3α,17α,25-triol.	136
22	Semisynthesis of cabralealactone (**28**), 3-epicabraleahydroxylactone (**35**) and 3*β*-acetoxy-17-oxo-octanordammarane from dipterocarpol (**22**).	137
23	Proposed mechanism of ocotillol formation from dammarenediol derivative (in plant).	138
24	Oxidation reaction of cabraleone (**30**) to cabralealactone (**28**).	139
25	The possible biosynthesis of dammarane found in *D.costatus*. (based on derivatization on the side chain).	172

ABBREVIATIONS

δ	chemical shift
λmax	wavelength at maximum absorptivity
ν_{max}	wavenumber at maximum absorption
$[\alpha]_D$	optical rotation
μg	Microgram
^{13}C-NMR	carbon-13 nuclear magnetic resonance
1D	one dimension
^{1}H-NMR	proton nuclear magnetic resonance
1-methoxy PMS	1-Methoxy-5-methylphenazinium methylsulfate
2D	two dimension
4-DMAP	4-dimethylaminopyridine
br	broad (for NMR spectra)
cc	column chromatography
CCl_4	carbon tetrachloride
$CDCl_3$	Deuterochloroform
CH_2Cl_2	Dichloromethane
CH_3I	methyl iodide
$CHCl_3$	Chloroform
cHex	Cyclohexane
cm	Centrimeter
COSY	correlation spectroscopy
d	doublet (for NMR spectra)
db	double bond
dbh	diameter at breast height. Breast height is defined as 4.5 feet (1.37m) above the forest floor on the uphill side of the tree.
dd	doublet of doublet (for NMR spectra)
DEPT	distortionless enhancement by polarization transfer
DMSO	Dimethylsulfoxide
dt	doublet of triplet (for NMR spectra)
EI	electron impact
ESI	electrospray ionization
Et_3N	Triethylamine
EtOAc	ethyl acetate
EtOH	Ethanol
fam	Family
fr	Fraction
g	Gram
GC	gas chromatography
h	Hour
H_2O	Water
HMBC	heteronuclear multiple bond correlation
HRESI	high resolution electrospray ionization
HSQCedited	edited heteronuclear single quantum correlation
IC_{50}	The 50% inhibitory concentration
IR	Infrared
J	coupling constant
KBr	potassium bromide
LiOH	lithium hydroxide
m	multiplet (for NMR spectra)

m/z	mass to charge ratio
MeOH	Methanol
mg	Milligram
MHz	mega hertz
MIC	minimum inhibitory concentration

TABLE OF CONTENTS

page

REMERCIEMENT i
ACKNOWLEDGEMENT ii
ABSTRACT iii
LIST OF TABLES iv
LIST OF FIGURES vi
LIST OF SCHEMES xii
ABBREVIATIONS xiii
TABLE OF CONTENTS xv
INTRODUCTION 1
LITERATURE REVIEWS 3
- Dipterocarpaceae 3
- Thai Dipterocarpaceae 4
- Bioactive components in Dipterocarpaceous plants. 6
- Biosynthesis of lupane and dammarane-type triterpenes in plants 13
- Lupane triterpenoids 14
- Dammarane triterpenoids 25
- Determination of the absolute configuration by modified Mosher's method. 31
- Cytotoxic evaluation by WST-1 method. 32
- Cytotoxic evaluation by REMA method. 33

PART I : Phytohemical study of *Hopea odorata.* 34
I. Botanical study 35
- Genus *Hopea*. 35
- *Hopea odorata* Roxb. 35

II. Previous chemical work on genus *Hopea* 36
III. Experimental part 39
3.1 Plant material 40
3.2 Method and apparatus 41
3.3 Preliminary study 41
3.3.1 Preliminary extraction by soxhlet extraction 42
3.3.2 *In vitro* bioactivity assays 42
3.4 Extraction and isolation of *H. odorata* leaves hexane extract 43
3.4.1 Extraction by maceration 43
3.4.2 Isolation of major compounds with a small portion of hexane extract. 44
3.4.2.1 Isolation by silica gel column chromatography 44

page

45
3.4.2.2 Isolation by sephadex column chromatography 46
3.4.3 Isolation of a large portion of hexane extract 49
3.4.4 Purification of HML10 58
3.5 Cytotoxic evaluation of 8 isolated lupanes 59
3.6 Physical characteristics and spectrum of isolated compounds

IV. Personnel work 65
4.1 Plant material 66
4.2 Preliminary study 66
4.3 Extraction and Isolation of *H. odorata* leaves hexane extract 66
4.4 Identification and structural study of isolated compounds 73
4.4.1 Friedelin (**1**) and *Epi*friedelanol (**4**) 73
4.4.2 *β*-Amyrin (**2**) and Saturated Fatty Acid Ester of *β*-Amyrin (**6**) 75
4.4.3 *β*-Sitosterol (**3**), *β*-Sitosterol Palmitate (**7**) and Mixture of Saturated and Unsaturated Fatty Acid Ester of *β*-Sitosterol (**8**) 77
4.4.4 Betulonic Acid (**5**), *Epi*betulinic Acid (**10**), Betulone (**11**), 30-Hydroxy-3-oxolup-20(29)-ene (**12**), Betulinic Acid (**13**), 3,30-Dioxolup-20,29-en-28-oic Acid (**14**)*, 28,30-Dihydroxylup-20(29)-en-3-one (**16**)** and Messagenic Acid G (**17**)** 79
4.4.5 Caryophyllene oxide (**9**) 87
4.4.6 Mangiferonic acid (**15**) 88
4.4.7 26-Fatty acid ester of (24*S*,25*S*)-24,25,26-trihydroxy-3,4-*seco*-cycloart-4(29)-en-3-oic acid (**18**)***, its 3-methyl ester (**18a**) and its triterpene moiety (transesterification product, **18b**) 89
4.4.8 C-24 Fatty acid ester of (24*S*,25*S*)-24,25,26-trihydroxy-3,4-*seco*-cycloart-4(29)-en-3-oic acid (**19**)*** and its 3-methyl ester (**19a**) 95
4.4.9 3,4-*Seco*-cycloart-4(29), 24-diene-3,26-dioic acid (**20**)*** and its 3,26-dimethyl ester (**20a**) 95
4.5 Cytotoxic evaluation of 8 isolated lupanes 97
4.6 Conclusion 98
PART II : Phytochemical study of *Dipterocarpus costatus* 99
I. Botanical study 100
page
- Genus *Dipterocarpus*. 100
- *Dipterocarpus costatus* Gaertn.f. 101

II. Previous chemical work on genus *Dipterocarpus* 104
III. Experimental part 106
3.1 Plant material 107
3.2 Method and apparatus 107
3.3 Preliminary study 107
3.3.1 Preliminary extraction by soxhlet extraction 107
3.3.2 *In vitro* bioactivity assays 108
3.4 Extraction and isolation of *D.costatus* wood hexane extract 109
3.4.1 Extraction by maceration 109
3.4.2 Isolation 109
116

3.5 Cytotoxic evaluation of isolated triterpenes 118
3.6 *In vitro* antiplasmodial activity of isolated triterpenes 121
3.7 Physical characteristics and spectrum of isolated compounds
IV. Personnel work 133
4.1 Plant material 134
4.2 Preliminary study 134
4.3 Extraction and isolation of *D.costatus* wood hexane extract 134
4.4 Identification and structural study of isolated compounds 143
4.4.1 *β*-Sitosterol (**3**), Caryophyllene oxide (**9**) and clovane-2,9-diol (**43**) 143
4.4.2 *β*-Elemene (**21**) 144
4.4.3 Dipterocarpol (**22**) and Dammarenediol II (**31**) 147
4.4.4 Isofouquierone peroxide (**23**), isofouquierol peroxide (**33**), isofouquierone (**40**), isofouquierol (**44**), (20*S*,23*E*)-20,25,26-trihydroxydammar-23-en-3-one (**46**)*** and (20*S*,23*E*)-25-hydroperoxy-20-hydroxy-2,3-*seco*-dammar-23-en-2,3-dioic acid (**48**)*** 151
4.4.5 (20*S*,22*E*)-20,24,25-Trihydroxydammar-22-en-3-one (**45**)*** 152
4.4.6 20(*S*)-Hydroxy-24-perhydroxy-dammar-25-en-3-one (**29**)***, cereotagaloperoxide (**32**)** and (20*S*,24*S*)-20,24-dihydroxydammar-25-en-3-one (**38**) 155
4.4.7 Cabraleone (20*S*,24*S*) (**30**), ocotillone (20*S*,24*R*) (**34**), ocotillol II (**37**) and (20*S*,24*R*)-20,24-epoxy-25-hydroxy-2,3-*seco*-dammarane-2,3-dioic acid (**47**)*** page 158
160
4.4.8 Isocabralealactone (20*R*) (**27**)**, cabralealactone (20*S*) (**28**) and 3-*epi*cabraleahydroxylactone (**35**)
4.4.9 Octanordammarane-3,17-dione (**26**)*, (20*S*,23*E*)-20-hydroxy-27-nordammar-23-ene-3,25-dione (**39**)*** and (20*S*)-20-hydroxy-3-oxo-24,25,26,27-tetranordammar-23-oic acid (**49**)*** 162
4.4.10 (20*R*)-17*α*,29-Epoxy-28-norlupan-3-one (**24**)***, 17*α*-hydroxy-28-norlupan-20(29)-en-3-one (**25**)***, (20*S*)-29-Hydroxy-17*α*,20-peroxy-28-norlupan-3-one (**36**)***, 17*α*-Hydroxy-28,29-dinorlupan-3,20-dione (**41**)*** and (20*R*)-20-Hydroxy-17*α*,29-epoxy-28-norlupan-3-one (**42**) *** 168 169 170
4.5 Cytotoxic evaluation of isolated triterpenes
4.6 *In vitro* antiplasmodial activity of isolated triterpenes
4.7 Conclusion
GENERAL CONCLUSION 173
BIBLIOGRAPHY 183

APPENDIX 198
- Spectroscopic spectrum of new compounds 199

INTRODUCTION

It has been long known that plants are a rich source of bioactive compounds that mankind has learned to use throughout history. Natural products have been used by man since antiquity for a number of applications, such as drugs, pigments and flavours. However, mankind was not aware of the specific importance and distinct chemical nature of such compounds until the end of the 19th century, and it has only been during the last century that natural products have experienced a great surge in phytochemistry. Many factors have led to this change, including the development of new and more powerful spectroscopic and chromatographic techniques and the change in the perception of society about chemicals. During the 20th century, phytochemical studies and, subsequently, natural products studies led to the discovery of an enormous number of compounds with a variety of chemical structures (many of them are bioactive), all of which are presented in the chemical composition of living organisms (from unicellular to higher organisms) [1]. Plants provide a broad spectrum of potential drug substances. Several researches reported about phytochemistry of various plants to investigate their bioactivity. The active molecules isolated from traditional medicinal plants might not only provide valuable drugs but are also valuable as "lead molecule" which might be modified chemically, or serve as a template for the design of synthetic molecules incorporating the pharmacophore responsible for the activity [2]

The situation of cancer in the world is seriously concerned. WHO [3] indicated that cancer was a leading cause of death worldwide and the total number of cases globally was increasing. The number of global cancer deaths is projected to increase 45% from 2007 to 2030 (from 7.9 million to 11.5 million deaths), influenced in part by an increasing and aging global population. New cases of cancer in the same period are estimated to jump from 11.3 million in 2007 to 15.5 million in 2030. In most developed countries, cancer is the second largest cause of death after cardiovascular disease, and epidemiological evidence points to this trend emerging in the less developed world. This is particularly true in countries in "transition" or middle-income countries, such as in South America and Asia. Already more than half of all cancer cases occur in developing countries. On the other hand, Malaria is one of the diseases that cause morbidity and mortality in the world for many decades. Although world malaria report 2011 of WHO showed continued progress for the malaria control and the incidence of disease was reduced more than 50% between 2000 to 2010 in 43 of the 99 countries, the resistance to artemisinins – a vital component of drugs used in the treatment of *Plasmodium falciparum* malaria – has been reported in a growing number of countries in South-East Asia [4]. This will cause the problem in malaria control in the future. Hence, many researchers worked on prevention and control of these diseases. Scientists are interested to find bioactive agents from natural sources, especially from traditional herbal medicine.

During recent decades, the biodiversity awareness in Thailand is growing to improve and sustain management of natural resources and to support the knowledge of traditional herbal medicine. Diptercarpaceae, constituted dominant and economically

important trees of lowland forest of the country, was known as a family which was enrich of resveratrol oligomer. A number of researches have reported about resveratrol oligomers in this family [5-20]. Since resveratrol oligomers possess polyphenol in the structure, they are in more polar extract. Yet, the nonpolar hexane extracts of *Hopea odorata* Roxb. leaves and *Dipterocarpus costatus* Gaertn.f. wood were also interesting because of their cytotoxic activities against several cancer cell lines [21].

H. odorata is a folk medicine which its wood has been used for treatment of yaws, blood disorder, fever, and as expectorant. Its dried stem latex was ground and used for wound healing [22]. As well as, the previous study of dammar resin from *D. costatus* found many dammaranes that possessed anti-HIV activity [23]. All of these made the inspiration for the investigation in this project.

In this thesis, we describe the isolation and structure elucidation of isolated compounds from the hexane extract of *H.odorata* leaves and *D. costatus* wood. A number of new compounds in different triterpenoid types, as well as several known triterpenoids, were discovered. Some isolated compounds were then evaluated for cytotoxic activity.

LITERATURE REVIEW

- Dipterocarpaceae
- Thai Dipterocarpaceae
- Bioactive components in Dipterocarpaceous plants.
- Biosynthesis of lupane and dammarane-type triterpenes in plants
- Lupane triterpenoids
- Dammarane triterpenoids
- Determination of the absolute configuration by modified Mosher's method.
- Cytotoxic evaluation by WST-1 method.
- Cytotoxic evaluation by REMA method.

Dipterocarpaceae [20, 24-29]

The Dipterocarpaceae is a medium-sized family with about 680 species and represents typically by resinous buttressed tropical rain forest trees. The largest genera are *Shorea* (196 species), *Hopea* (104 species), *Dipterocarpus* (70 species), and *Vatica* (65 species). The family is characterized by winged fruits in which the wings are developed from persistent sepals, fleshy bilobed unequal cotyledons, simple stipulate leaves, and dimorphic shoot systems. This predominantly Asian family is divided into three subfamilies; Dipterocarpoideae, Monotoideae, and Pakaraimoideae. Dipterocarpoideae, the largest subfamily with 13 genera and about 470 species, is restricted to tropical Asia, while the subfamily Monotoideae, 3 genera and more than 30 species, occurs in mainland Africa and Madagascar, and the subfamily Pakaraimoideae, one genus and one species, is indigenous to northern South America (Scheme 1).

The subfamily Dipterocarpoideae plants have conspicuously large stipules and basifixed anthers, 2-3 celled ovary and 2 ovules in each cell. The petals are longer than the sepals. The wood rays are multiserate. The wood, leaves and ovaries have resin or secretory ducts. The fruits of dipterocarps offer a good generic character, only a few exceptions, if one gives an attention. *Shorea* have three lobes of the fruiting calyx larger than the other two, and *Hopea* have two lobes larger than the other three. *Dipterocarpus* have two large lobes and three auricles. Only a few species of these genera have wingless fruits. Several plants in this subfamily such as plants in genus *Shorea, Dipterocarpus, Hopea* and *Neobalanocarpus* are considered as important economically timber used for construction and furniture. They are also known as oleoresin-producing trees in tropical Asia. For example the oleoresin from genus *Dipterocarpus*, especially *D. alatus*, is used for illumination, waterproofing baskets and boats, and for making paint, varnish and lacquer. Therefore, *D.alatus* is considered as a highly important economic plant in Southeast Asia. Furthermore, *Dryobalanops aromatic* is a source of camphor mainly used in China. This subfamily is divided into two groups;

- *Valvate-Dipterocarpi* group (tribe *Dipterocarpeae*) consists of genus *Vateria, Vateriopsis, Stemonoporus, Vatica, Cotylelobium, Upuna, Anisoptera,*

Dipterocarpus (the characteristics: valvate sepals in fruit, solitary vessels, scattered resin canals, and basic chromosome number x =11).

- *Imbracate-Shoreae* group (tribe *Shoreae*) consists of genus *Shorea, Parashorea, Hopea, Neobalanocarpus, Dryobalanops* (the characteristics: imbricate sepals in fruit, grouped vessels, resin canals in tangential bands, and basic chromosome number x= 7).

The plants in subfamily Monotoideae have basi-versatile anthers, 4-5 celled ovary, 2-4 ovules in each cell and small and caducous stipules. The petals are longer than the sepals, and the wood rays are uniseriate. The wood, flowers, and leaves of these trees do not produce a resin or have secretory ducts. The plants in genus *Monotes* have secretory cavities instead of resin canals as found in the Dipterocarpoideae plants.

The morphological characteristics of Pakaraimoideae plants, the third subfamily, in term of the anthers (basi-versatile), stipules (small and caduceus), and the lack of resin ducts are similar to those of the Monotoideae. The petals are shorter than the sepals, and the wood rays are dominantly biserate. The subfamily Pakaraimoideae seems to be closer to the monotoideae than the Dipterocarpoideae. The lack of resin canals in wood of both the Monotoideae and the Pakaraimoideae constitutes a major distinction from the Dipterocarpoideae.

Diversity of opinions still exists for generic divisions, especially with the genus *Shorea* and the group of genera *Vatica* and *Cotylelobium*. However, certain well defined genera exist, such as *Dryobalanops, Dipterocarpus, Anisoptera* and *Upuna*.

Thai Dipterocarpaceae [25, 30, 31]

Dipterocarpaceae in Thailand was first described in "Florae Siamensis Enumeratio" by Craib (1925), followed by Smitinand (1954) who published his "Identification Keys to Genera and Species of the Dipterocarpaceae of Thailand" and continued the work with his co-worker, Satisuk and Plengklai, by publishing "The Manual of Dipterocarpaceae of Mainland South-East Asia". In year 2001, Pooma reviewed "Checklist of Dipterocarpaceae in Thailand" and included this paper in his thesis report "Dipterocarpaceae in Thailand: Taxonomic and Biogeographical Analysis" in 2003.

Thai Dipterocarpaceous plants, deciduous or semi-evergreen trees, consists only in the subfamily Dipterocarpoideae which is represented by about 65 species in 8 genera; *Valvate-Dipterocarpi* group (*Anisoptera, Cotylelobium, Dipterocarpus, Vatica)* and *Imbricate-Shoreae* group (*Hopea, Neobalanocarpus, Shorea* and *Parashorea*).

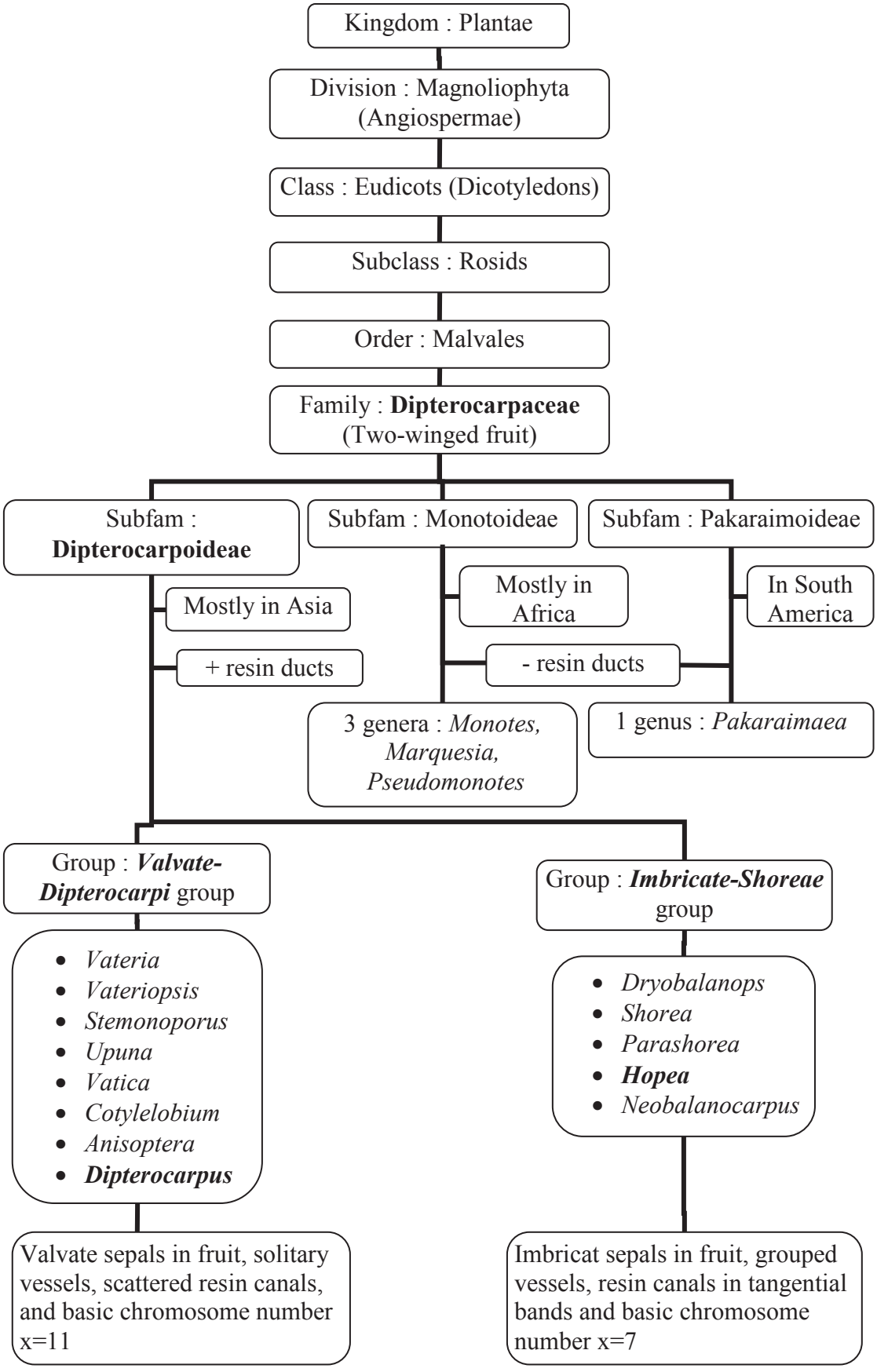

Scheme 1. Taxonomic classification of genus *Hopea* and *Dipterocarpus* [20, 25, 28, 32]

Bioactive components in Dipterocarpaceous plants

The review of Seo and Kinghorn [20] stated that, in addition to oligostilbenoids, the bioactive constituents in Dipterocarpaceous plants, especially in Dipterocarpoideae subfamily, were terpenoids, coumarins, ellagic acid derivatives, flavonoids, phenolics and quinones. The study of several Dipterocarpaceaous plants is in the following table. The researchers were interested in oligostilbenoids rather than other groups of compounds. Thus, most studies worked on high polarity extract, not in hexane extract as in this research.

The plants belonging to the family Dipterocarpaceae have been known to produce oligostilbenoids (or resveratrol oligomers), which are limited in only a number of families, namely, the Cyperaceae, Dipterocarpaceae, Gnetaceae, Leguminosae, and Vitaceae. They occur in subfamily *Dipterocarpoideae* as di-, tri-, tetra-, hexa-, hepta-, and octastilbenoids, containing various molecular frameworks as a result of different condensation of the resveratrol monomer. Some of these polyphenol compounds show interesting biological activities, such as antioxidant [6], anti-inflammatory [33], antibacterial [34], antiviral [35], and cytotoxic effects [8, 36], as well as acetylcholinesterase inhibitor activity [7]. Hopeaphenol, the first resveratrol oligomer to be structurally characterized from the subfamily Dipterocarpapoideae, was isolated initially from the heartwood of *Hopea odorata* and *Balanocarpus heimii* and its structure was determined in 1966. Hopeaphenol strongly inhibited murine leukemia P-388 cells [37].

A number of resins from some genera in the subfamily Dipterocarpoideae were investigated and found to contain several sesquiterpenes and triterpenes.

- The resin from five species of the genus *Doona* (*Shoreae* group) were examined (1966) [38] and reported to contain sesquiterpene such as humulene, *β*-elemene, caryophyllene, and copaene, and triterpenes such as *β*-amyrin (largely predominated among all triterpenes), ψ-taraxasterol, dammarenediol-I, hydroxydammarenone-I, and ursolic acid. Moreover, asiatic acid, dipterocarpol and dihydroxyolean-12-en-28-oic acid were also isolated from the *D.congestiflora* resin of the work of Bandaranayake et al (1975) [39].
- Chemical analysis of the neutral fraction of the resin from the genus *Dipterocarpus* was revealed by Bisset et al and Bandaranayake et al [39, 40]. Several sesquiterpenes and triterpenes were identified: sesquiterpene - humulene, caryophyllene, copaene, α-gurjunene, calerene, γ-gurjunene, alloaromadendrene, cyperene, caryophyllene oxide, farnesane, dehydrofarnesane; triterpene – diptercarpol, dammarenediol-II, dammaradienone, and ocotillone, together with asiatic acid and 2,3-dihydroxyurs-12-en-28-oic acid. The triterpenes showed little variation with the most abundant – dipterocarpol (ca 48% of the neutral fraction) while the sesquiterpene were much more variable. The mixture of caryophyllene, humulene and alloaromadendrene (ca 24%) was the next

most abundant and the compounds were present in the ratio 7:10:3, respectively.

- The following polyterpenes from the resin of thirty-five species of the genus *Shorea* were characterized [41]: the sesquiterpene hydrocarbon - *β*-elemene, caryophyllene, α-gurjunene and cyperene; the sesquiterpene alcohol - spathulenol; the triterpenes - *β*-Amyrin, ursolic aldehyde, dipterocarpol, dammarenediol II (20S), dammaradienone and hydroxyhopanone, including acid constituents as shoreic acid and dammarenolic acid. In genus *Shorea*, the sesquiterpene hydrocarbon showed only little variation; the variable occurrence of the sesquiterpene alcohol and the triterpenes enabled the sub-genus *Anthoshorea* to be distinguished from the sub-genera *Shorea*, *Richetia* and *Rubroshorea*. The copaene, *β*-elemene, and caryophyllene association was a feature peculiar to the genus and the occurrence of shoreic acid and oxygenated sesquiterpenes appeared to be specific to the genus *Shorea*. Further study of *Shorea robusta* resin [42, 43] led to finding of more ursene and oleanene triterpenes eg. asiatic acid (the largest amount), α-amyrin, ursolic acid and uvaol, together with mangiferonic acid.
- Triterpenes from *Dryobalanops aromatica* (*Shoreae* group) resin were investigated by Cheung and Wong [44]. Asiatic acid was found as one of the most abundant components, accompanying oleanolic acid, hedragonic acid, dryobalanonolic acid, dryobalanolide,

Burger et al (2009) established taxonomic characterization of dammar resin by GC-MS [45]. Dammar resin displayed a similar characteristic profile containing ursane and oleanane derivatives; 2,3-dihydroxyolean-12-en-28-oic acid, 2,3-dihydroxyurs-12-en-28-oic acid, 2,3-dihydroxyoleanadien-28-oic acid and 2,3-dihydroxyursadien-28-oic acid (in large quantity). Betulonal was reported as a biomarker characteristic of genus *Dipterocarpus* but not found in the *Shorea* one.

The triterpenes isolated from 8 species of bark and timber of *Stemonoporus* (*Dipterocarpi* group) belong only to the ursene or oleanene series [46]. All the species examined had the pentacyclic triterpenes *δ*-amyrenone, *α*-amyrin and ursolic acid, sitosterol and sitosteryl-*o*-methoxybenzoate. The most outstanding feature of the chemistry of the genus was the absence of the tetracyclic dammarane skeleton which was otherwise widespread in the family. *δ*-Amyrenone, *α*-amyrin along with ursolic acid presented in all the species of *Stemonoporus* studied and could be considered to be the triterpenoid marker for this genus [46]. Moreover, bergenin (isocoumarin), was found in large quantity of bark extracts from 5 studied species, whereas timber extractives contained two other aromatic compounds, 4-hydroxybenzaldehyde and methyl 2,4-dihydroxybenzoate. The chemical constituent study of *Dipterocarpus hispidus* bark found betulinic acid, dipterocarpol and dammarenediol II whilst the timber contained dipterocarpol and asiatic acid [39]. A study of Geevanada et al [47] illustrated phenolic compounds and triterpenes from bark and timber of 11 species belonging to the genera

Cotylelobium, *Hopea*, *Shorea*, *Vateria* and *Vatica*. The result yielded fatty acid ester of sitosteryl, *β*-amyrin acetate, *β*-amyrin, dipterocarpol, ursolic acetate, lupeol, sitosterol, ursolic acid, betulinic acid, hexamethyl-coruleoellagic acid, tetramethylellagic acid, chrysophanol (anthraquinone), and scopoletin (coumarin).

Isolation of ethyl acetate extract of *Vatica diospyros* stem and chloroform extract of *Vatica cinerea* leaves and twigs (*Dipterocarpi* group) [48, 49] yielded mangiferonic acid, betulin, betulinic acid as the major triterpenoids which exhibited mild anti-HIV activity.

Most of the isolated terpenoids have been reported to be biologically active as indicated in Table 1, although such work has occurred on these compounds isolated from plants of other family [20, 50-52]. For example, the common triterpenoids, betulonic acid and betulinic acid, were reported having cytotoxicity against several cell lines (see lupane triterpene). The characteristic triterpenes in family Dipterocarpaceae could be summarized in pentacyclic (lupanes, ursanes and oleananes) and tetracyclic (dammaranes and cycloartanes) triterpenes.

Furthermore, a lot of flanovoids are already known as antioxidants. A flavonoid aglycone survey [53, 54] was carried out on the leaves of 7 genera of the family Dipterocarpaceae: *Cotylelobium*, *Dipterocarpus*, *Hopea*, *Shorea*, *Stemonoporus*, *Vateria* and *Vatica*. After acid hydrolysis of the leaves material, the main flavonoid aglycones found were the flavonols quercetin and kaempferol, and the flavones apigenin. The flavones luteolin was defined as a chemotaxonomic significance in the genus *Shorea* because it was present only in this genus and absent in the rest of the species of the family. The genus *Shorea* and *Dipterocarpus* were considered as the most primitive with respect to the presence of myricetin and proanthocyanidins (cyanidin and delphinidin) and the other five genera have more advanced patterns, recognizing *Stemonoporus* as the most advanced with an increase of apigenin.

Resveratrol oligomers (=oligostilbenoids)

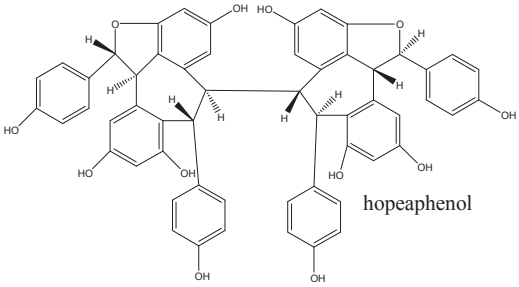

hopeaphenol

Steroid

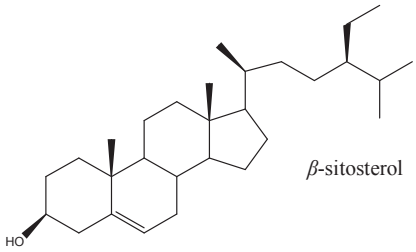

β-sitosterol

Sesquiterpene

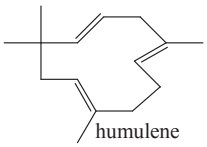

humulene

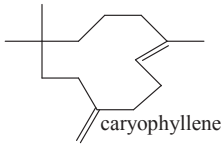

caryophyllene

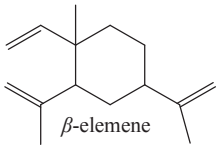

β-elemene

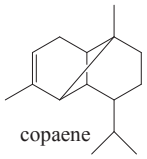

copaene

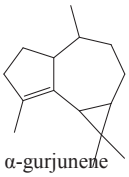

α-gurjunene

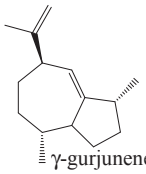

γ-gurjunene

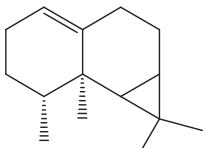

β-gurjunene (calarene)

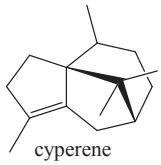

cyperene

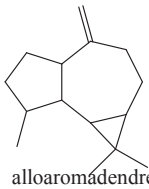

alloaromadendrene

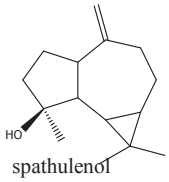

spathulenol

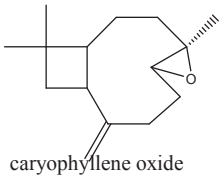

caryophyllene oxide

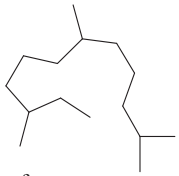

farnesane

Triterpene

Oleanane

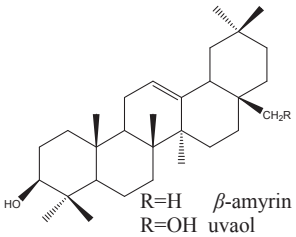

R=H *β*-amyrin
R=OH uvaol

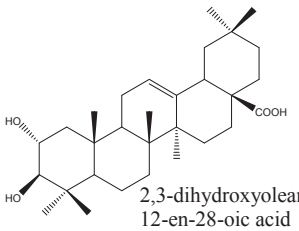

2,3-dihydroxyolean-12-en-28-oic acid

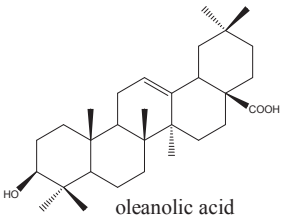

oleanolic acid

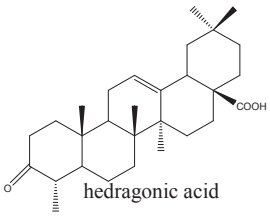

hedragonic acid

Ursane

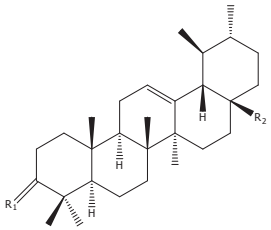

R_1=COOH
R_2=H, *β*-OH ursolic acid
R_2=O ursonic acid
R_1=CHO
R_2=H, *β*-OH ursolic aldehyde

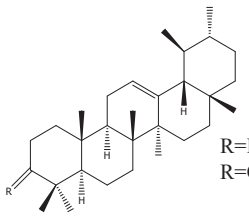

R=H, *β*-OH *α*-amyrin
R=O *α*-amyrenone

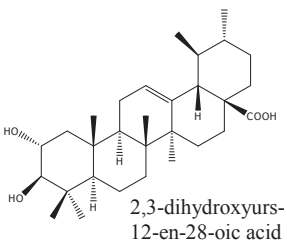

2,3-dihydroxyurs-12-en-28-oic acid

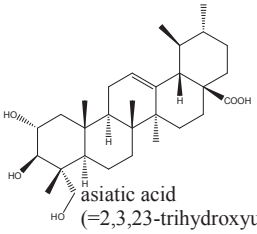

asiatic acid (=2,3,23-trihydroxyurs-12-en-28-oic acid)

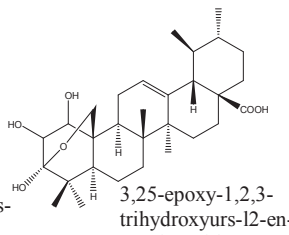

3,25-epoxy-1,2,3-trihydroxyurs-l2-en-28-oic acid

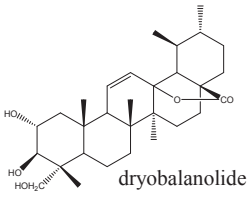

dryobalanolide

Figure 1. Structure of some reported bioactive terpenoids and phenolic compounds in the family Dipterocarpaceae.

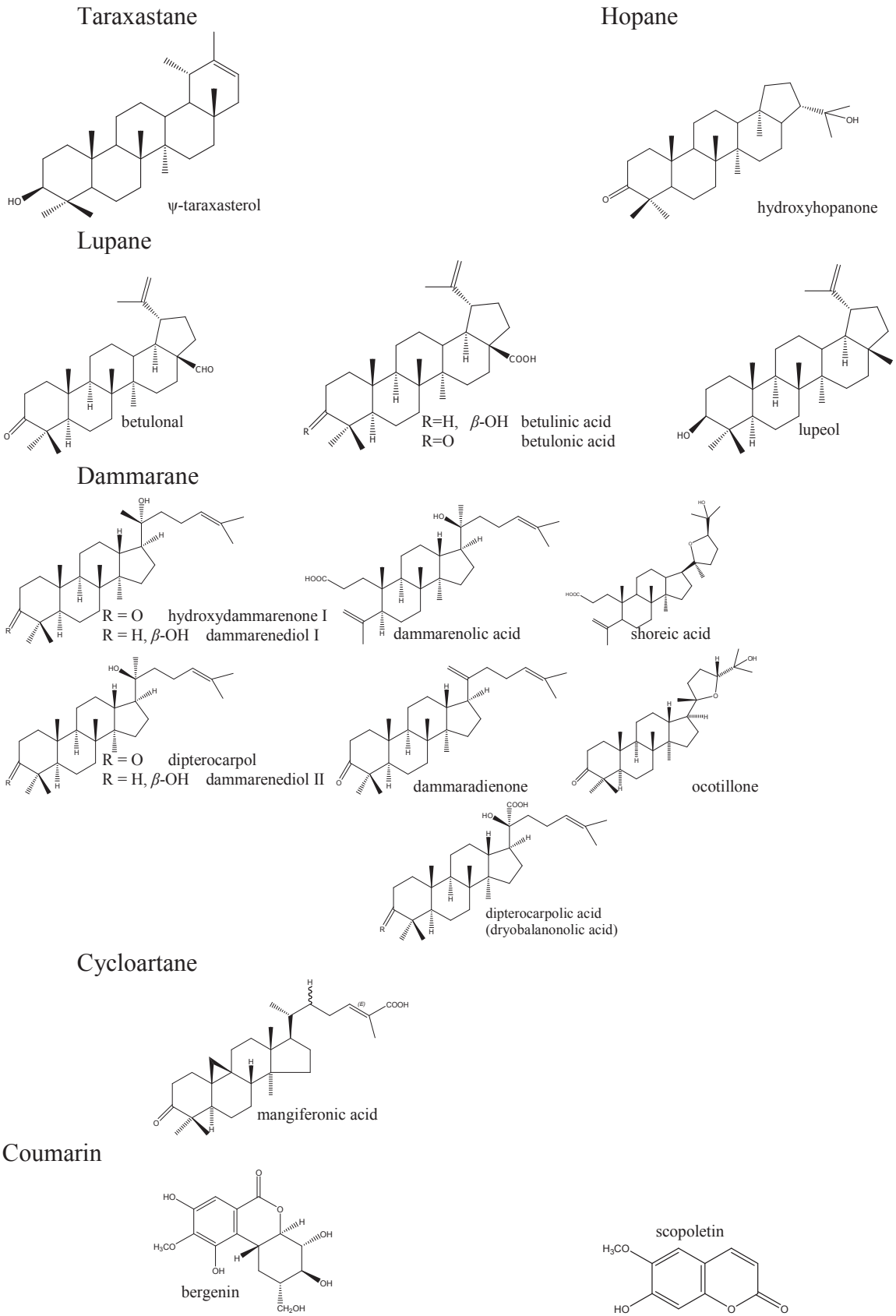

Figure 1. Structure of some reported bioactive terpenoids and phenolic compounds in the family Dipterocarpaceae (continued).

Flavanoids

Flavonol

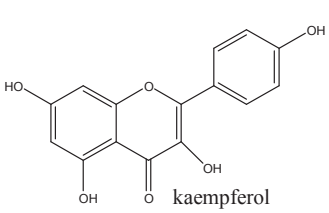

kaempferol

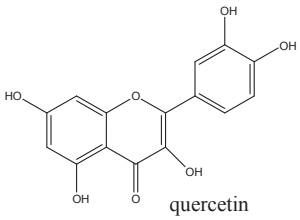

quercetin

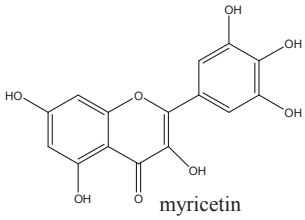

myricetin

Flavone

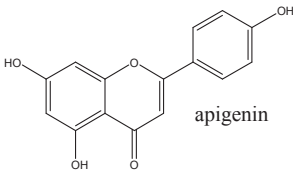

apigenin

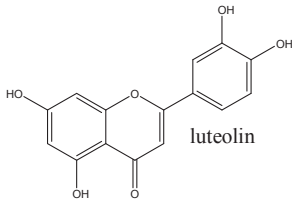

luteolin

Proanthocyanidin

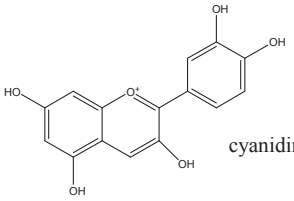

cyanidin

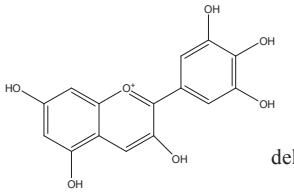

delphinidin

Miscellenous

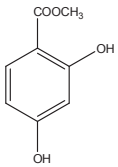

methyl-2,4-dihydroxy-benzoate

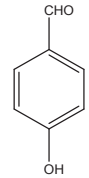

4-hydroxybenzaldehyde

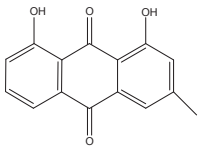

chrysophanol

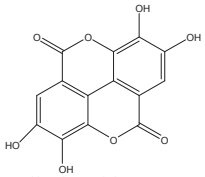

ellagic acid

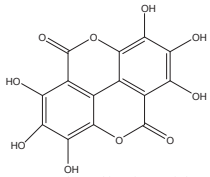

coruleoellagic acid

Figure 1. Structure of some reported bioactive terpenoids and phenolic compounds in the family Dipterocarpaceae (continued).

Table 1. Some reported bioactive terpenoids and phenolic compounds in low polarity fraction of the family Dipterocarpaceae extracts.

Terpenoids	Bioactivity [reference]	Plant source (part)[reference]
Sesquiterpenes		
β-Elemene	Antitumor [50]	*Doona* sp. (re) [38], *Shorea* sp. (re) [41]
Caryophyllene	Anti-inflammatory, antibiotic, antioxidant, anticarcinogenic and local anaesthetic activities [55]	*Doona* sp. (re) [38], *Shorea* sp. (re) [41]
Copaene	Male medfly attractant [56]	*Doona* sp. (re) [38], *Shorea* sp. (re) [41]
Humulene	Anticancer [55]	*Doona* sp. (re) [38]
Caryophyllene oxide	Anti-microbial [57], antimalarial [58]	*Dipterocarpus* sp. (re) [40],
Spathulenol	Immunomodulator [59], Anti-microbial[57],Antifungus [60]	*Shorea* sp. (re) [41]
Triterpenes		
β-Amyrin, *α*-amyrin	Antinociception [61], hepato-protectant [62]	*Doona* sp. (re) [38], *Stemonoporus* sp. (b,t) [46]
Ursolic acid	Antiangiogenesis [63]	*Stemonoporus* sp. (b,t) [46], *Doona macrophylla* (re) [39]
Ursonic acid	Antitumor [64], Anti-HSV [23]	*Stemonoporus affinis*, *S.lancifolius* (b,t) [46]
Dryobalanolide	Antimicrobial [65]	*Dryobalanops aromatic* (re) [44]
Asiatic acid	Anti-inflammatory [66], cytotoxic [51]	*Dipterocarpus pilosus (re)*[67], *D.hispidus* (re, t), *D.zeylaicus* (re), *Doona macrophylla* and *D.congestiflora* (re) [39], *Dryobalanops aromatic* (re) [44]
ψ-Taraxasterol	Antioedema [68]	*Doona* sp. (re) [38]
β-Sitosterol	Analgesic [69]	*Stemonoporus* sp. (b,t) [46]
hydroxyhopanone	Anti-HSV [23]	*Shorea* sp. (re) [41], Dammar resin [70]
Hydroxydammarenone I	Anti-HSV [23]	Dammar resin [23], *Doona* sp. (re) [38]
Betulinic acid	Cytotoxic [52], anti-HIV [49]	*Dipterocarpus hispidus* (t, b) [39], genera *Cotylelobium*, *Hopea*, *Shorea*, *Vateria* and *Vatica* (t,b) [47, 49]
Betulonic acid	Cytotoxic [52], anti-HIV [49]	*Vatica cinerea* (l) [49]
Hydroxydammarenone II (=dipterocarpol)	Anti-HSV [23]	*Shorea* sp. (re) [41], Dammar resin [23, 70],*Dipterocarpus glandiflorus* (w)[71]
Dammarenediol II	Anti-HSV [23]	*Shorea* sp. (re) [41], Dammar resin [23, 70]
Dammarenolic acid	Anti-HSV [23], Anti-HIV [72]	*Shorea* sp. (re) [41], Dammar resin[23]
Shoreic acid	Anti-HSV [23]	*Shorea* sp. (re) [41], Dammar resin[23]
Ocotillone	Cytotoxic [73]	*Dipterocarpus* sp. (re) [40]
Coumnarins		
Bergenin	Antibacteria and Antioxidant [74]	*Stemonoporus* sp. (b) [46]
Scopoletin	Acetylcholenesterase inhibitor [75]	Genus *Cotylelobium*, *Hopea*, *Shorea*, *Vateria* and *Vatica* (t,b) [47], *Dipterocarpus hasseltii* (b) [37]
Anthraquinones		
Chrysophanol	Antimicrobial [76]	Genus *Cotylelobium*, *Hopea*, *Shorea*, *Vateria* and *Vatica* (t,b) [47]
Ellagic acid derivatives		
Ellagic acid	Antimalaria [77]	Genus *Cotylelobium*, *Hopea*, *Shorea*, *Vateria* and *Vatica* (t,b) [47]
Coruleoellagic acid	Antimalaria [77]	

re=resin, b=bark, t=timber, w= wood, l=leaves

Biosynthesis of lupane and dammarane-type triterpenes in plants

The terpenoids constitute the largest family of natural products derived from C_{30} precursors; over 22,000 individual compounds of this class have been described since 1991 [78]. Because various triterpenes are an increasing promising group of plant metabolites, the utilization of different plants as their sources is of interest [79]. Nearly 200 different triterpene skeletons are known from natural sources or enzymatic reactions that are structurally consistent with being cyclization products of squalene, oxidosqualene, or bis-oxidosqualene [80].

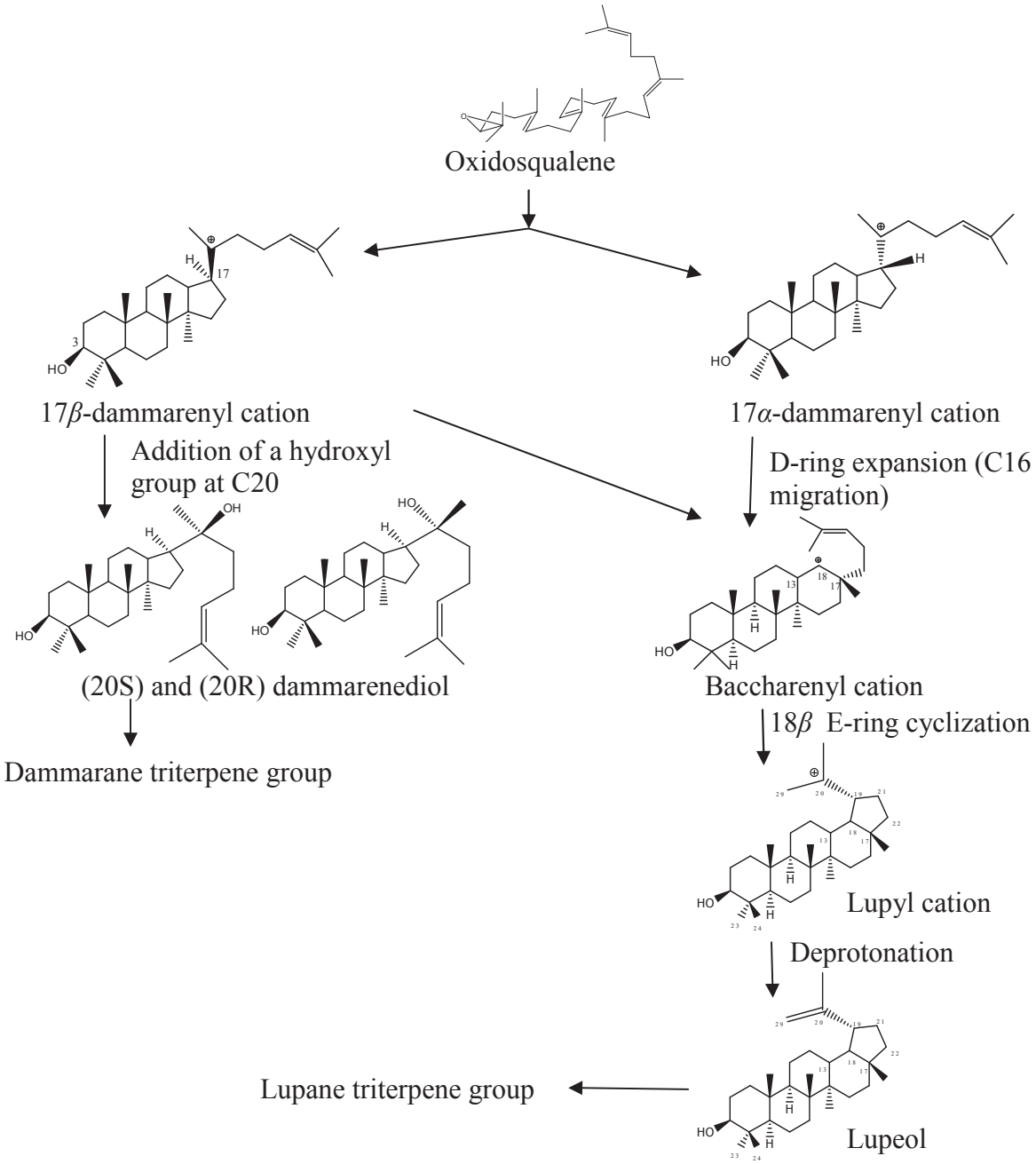

Scheme 2. Biosynthesis pathway of dammarane and lupanes triterpene [80]

Biosynthesis of most 3β-OH-triterpenes is proposed to be arisen from oxidosqualene, although squalene cyclization followed by oxidation at C-3 is also

plausible [80]. A large variety of triterpene alcohols arise from one of two epimeric dammarenyl cations, 17*β*-dammarenyl cation or 17*α*-dammarenyl cation, which are 6-6-6-5 tetracycles with all-chair configurations. Initial cyclization might form a 6-6-5 tricyclic ring, and follow by ring expansion and D-ring annulations. Addition of a hydroxyl group at C-20 to 17*β*-dammarenyl cation without rearrangement generated dammarenediol, which was a precursor for dammarane triterpene.

Then, most of the widespread pentacyclic triterpene alcohols in plants such as lupeol and *β*-amyrin could be synthesized from the dammarenyl cation after D-ring expansion via C-16 migration followed by 18*β* E-ring cyclization and sometimes, further E-ring expansion. The lupyl cation, with *trans*-D,E ring junction, is generated from either 17*β*- or 17*α*-dammarenyl cation by D-ring expansion (C-16 migration) to form baccharenyl cation followed by E-ring closure to the β-face of C-18. Direct deprotonation without rearrangement provides lupeol, a precursor of a variety of lupane derivatives. Lupyl cation could also undergo E-ring expansion and finally produce ursane, oleanane and taraxastane- type triterpenes.

Lupane-type triterpenes

Pentacyclic triterpenes are one group of promising secondary plant metabolites for cancer treatment with multifaceted effects and targets. The pentacyclic triterpenes such as lupeol, betulin, betulinic acid, oleanolic and ursolic acid are proposed to be multitarget agents. They fit to the concept of modern cancer therapy, by treating cancer from different sides, including the tumour environment and the immune system [79]. Lupane triterpenoids are pentacyclic compounds with 30 carbon atoms, biosynthetically derived from the cyclization of squalene, and a vast class of natural products whose structural diversity includes a wide array of functional groups. Lupane-containing plants are systematically widespread within the angiosperms and are found predominantly among trees and bushes. They were found wide spread distribution in several family; Betulaceae, Celastraceae, Apocyaceae, Euphorbiaceae, Anacardiaceae and Leguminoseae etc. Not many norlupanes were also found in family Myrtaceae and Betulaceae. Only one study obtained 2,3-*seco*-lupane, a rare structure, from *Microtropis jokienensis* (Cealastraceae) and very few obtained 3,4-*seco*-lupane.(Table 2.)

In addition to cytotoxicity, compounds of this class are reported to be bioactive with antitumor-promoting, antiviral, and anti-inflammatory activities [81].

Table 2. Discovery of lupane-type triterpenes in some plants

Family	Plant	Lupanes found	Reference
Anacardiaceae	*Ozoroa insignis* (root)	betulonic acid; betulinic acid	[82]
	Rhus chinensis (stem)	betulin; betulonic acid	[83]
Apocyaceae	*Nerium oleander* (leaves)	Oleanderol (=lupa-12,20(29)-dien-3*β*,27,28-triol); betulin; betulinic acid	[84]
Betulaceae	*Betula alleghaniensis* (outer bark)	lup-20(29)-ene-28-ol-3-one-30-al; 29-norlupan-3,20-dione; 29-norlupan-28-ol-3,20-dione; lupan-20,28-diol-3-one; 29-norlupan-3 *β*-ol-20-one; lupeol; lupenone; betulone; betulin; betulonic acid; lupenyl formate; lup-20(29)-ene-30-ol-3-one; lup-20(29)-ene-3*β*,30-diol; lup-20(29)-ene-28-ol-30-al; lupan-20-ol-3-one; lupan-3*β*,20-diol; lupan-3 *β* -ol-29-oic acid.	[85]
	B. platyphylla var.*japonica* (floral spike)	Betulonic acid	[86]
	B. pubescens (bark)	betulin; lupenone; betulonic acid; lupeol; betulinic acid	[87]
	B. verrucosa (bark)	betulinol; lupeol; betulinic acid; lupan-3*β*-,20-diol; lupan-3*β*,20,28 -triol	[88]
Celastraceae	*Cassine papillosa* (stem bark)	3-oxolup-20-en-30-ol; lup-20-en-3β,30-diol	[89]
	Hippocratea celastroides (aerial part)	3-oxolup-20-en-30-ol; lup-20-en-3β,30-diol	[90]
	Maytenus Canariensis (aerial part)	3*β*,28,30-lupan-20(29)-ene-triol; 28,30-dihydroxy-lup-20(29)-en-3-one; Lup-20(29)-ene-3*β*,30-diol	[91]
	M.imbricate (stem)	3-oxo-lup-20(29)-en-23-al; 30-OH-lupan-20(29)-en-3-one; 11α-OH-lup-20(29)-en-3-one; lup-20(29)-en-3β,29-diol;	[92]
	M.chiapensis (leaves)	3*β*,6*β*-dihydroxylup-20(29)-ene; 6*β*,28-dihydroxy-3-oxolup-20(29)-ene; 6*β*-hydroxy-3-oxolup-20(29)-en-28-oic acid; glochidone; lupeol; betulin; lupenone; betulone; betulonealdehyde; 3-*epi*-glochidiol; glochidonol; Messagenin; 28,30-dihydroxy-3-oxolup-20(29)-ene; betulin-3*β*-caffeate	[93]
	M. cuzcoina (root bark)	nepeticin; rigidenol; glochidone;, lupeol; betulin; betulinic aldehyde; 3-*epi*betulin; 3-*epi*betulinic aldehyde; 3-*epi*betulinic acid; lupenone; betulone; betulone aldehyde; betulonic acid; glochidiol; 3-*epi*-glochidiol; glochidonol; 11α-hydroxyglochidone.	[93]

Family	*Plant*	Lupanes found	Reference
	M.nemerosa (wood and stem)	3-oxo-20(29)-lupen-30-al; 30-hydroxy-20(29)-lupen-3-one; lup-20(29)-ene-3β,30-diol,	[94]
	Microtropis jokienensis (stem)	7*β*-hydroxy-methyl betulinate; 7*β*-senecioyl betulinic acid; 30-hydroxy-2,3-*seco*-lup-20(29)-ene-2,3-dioic acid; 3-*epi*-thurberogenin	[95]
	Perrottetia arisanensis (stem)	3-*epi*-thurberogenin; 3-*epi*-thurberogenin-22*β*-dodecanoate; 3-*epi*-thurberogenin-22*β*-tetra-decanoate; 3-*epi*-thurberogenin-22*β*-hexadecanoate;	[95]
	Microtropis jokienensis (stem) + *Perrottetia arisanensis* (stem)	28-hydroxy-3-oxo-lup-20(29)-en-30-al; betulinic acid; 3-*epi*betulinic acid; 3-*epi*betulin; 30-hydroxylupeol; 30-hydroxybetulin; 30-hydroxylup-20(29)-en-3-one; 28,30-dihydroxy-3-oxolup-20(29)-ene; 3-methoxy-betulinic acid; lupeol; 3-*epi*betulinaldehyde; thurberonenin; thurberogenone	[95]
	Rzedowskia tolantonguensis (aerial part)	3-oxo-lup-20-en-30-ol; lup-20-en-3β,30-diol, betulin	[96]
	Solacia chinensis (leaves)	30-OH-lup-20(29)-en-3-one; 3*β*-OH-20-oxo-30-norlupane; betulin; betulinic acid	[97]
	S. cordata (stem bark)	28-OH-lup-20(29)-en-3-one; 30-OH-lup-20(29)-en-3-one; 15,28-DiOHlup-20(29)-en-3-one; betulin	[98]
Cornaceae	*Cornus capitata* (leaves)	Lupeol; betulin; *epi*betulin; betulinic acid; *epi*betulinic acid (not so much lupanes)	[99]
Euphorbiaceae	*Bischofia javanica* (bark)	Betulinic acid; betulonic acid	[100]
Hamamelidaceae	*Liquidamber styraciflua* (cone)	6*β*-OH-3-oxolup-20(29)-en-28-oicacid; 6*β,30*-DiOH-3-oxolup-20(29)-en-28-oic acid;	
Leguminoseae	*Acacia mellifera* (stem bark)	28-hydroxy-3-oxo-lup-20(29)-en-30-al; 3-oxo-lup-20(29)-en-30-al; 3-hydroxy-lup-20(29)-en-30-al; 28-hydroxy-lup-20(29)-en-3-one; (20*R*)-3-oxolupan-30-al; (20*S*)-3-oxolupan-30-al; (20*R*)-28-hydroxylupan-30-al-3-one; (20*S*)-3β-hydroxylupan-30-al; 30-hydroxylup-20(29)-en-3-one; 30-hydroxylup-20(29)-en-3β-ol; lupenone; lupeol; betulin; betulinic acid; betulonic acid; 3-(*E*)-trans-coumaroylbetulin, 3-(*Z*)-cis-coumaroylbetulin	[101-103]
	Melilotus messanensis (aerial part)	messagenin (=30-norlupane-3*β*,28-diol-20-one); betulinic acid; lupeol; betulinaldehyde; betulin; 3-oxoplatanic acid; messagenic acid D, F, G, H, I	[104]

Family	*Plant*	Lupanes found	Reference
	Platypodium elegans (leaves)	lupeol; lupeone; betulone; 28-OH-lup-20(29)-ene-3-one, canaric acid (3,4-*seco*-lupane); dihydrocanaric acid	[105]
Moraceae	*Ficus microcarpa* (aerial root)	acetylbetulinic acid; betulonic acid (only small quantity of lupanes)	[106]
Myrtaceae	*Melaleuca ericifolia* (leaves)	28-norlup-20(29)-en-3*β*-hydroxy-17 *β* –hydroperoxide; 28-norlup-20(29)-en-3*β*-hydroxy-17*α*-hydroperoxide; 20*S*-17*β*,29-epoxy-28-norlupan-3 *β*-ol*; betulinic acid, betulin, betulinaldehyde	[107]
	M.leucadendron (leaves)	28-norlup-20(29)-ene-3*β*,17*β*-diol; betulinic acid; betulonic acid	[108]
	Syzygium formosanum (leaves)	betulin; betulinic acid; lupeol (not so much lupanes)	[109]
Rhamnaceae	*Alphitonia zizyphoides* (dried bark)	betulinic acid	[110]
	Zizyphus jujube (dried fruit)	Betulinic acid	[111]
Rhizophoraceae	*Cassipourea madagascariensis*	3-oxolup-20-en-30-ol; lup-20-en-3β,30-diol	[112]
Simaroubaceae	*Picramma pentundra* (bark)	*epi*betulinic acid (major)	[113]
Verbenaceae	*Junellia tridens* (aerial part)	*epi*betulinic acid (not so much)	[114]
Zygophyllaceae	*Peganum nigellastrum* (aerial part)	3α,27-dihydroxy lup-20(29)-en-28-oic acid methyl ester; 3α-acetoxy-27-hydroxylup-20(29)-en-28-oic acid methyl ester; betulinic acid; 3-acetoxy-betulinic aicd; *epi*betulinic acid; 3-acetoxy-*epi*betulinic acid	[115]
Dipterocarpaceae	*Vatica cinerea* (leaves and stem)	betulinic acid; betulin; betuonic acid	[49]
	Vatica diospyros (stem)	betulin, betulinic acid	[48]

The underlined compounds demonstrated the major lupane in the extract.

* There was argument that it was impossible to have the configuration at C-17 and C-19 as described in this paper [116].

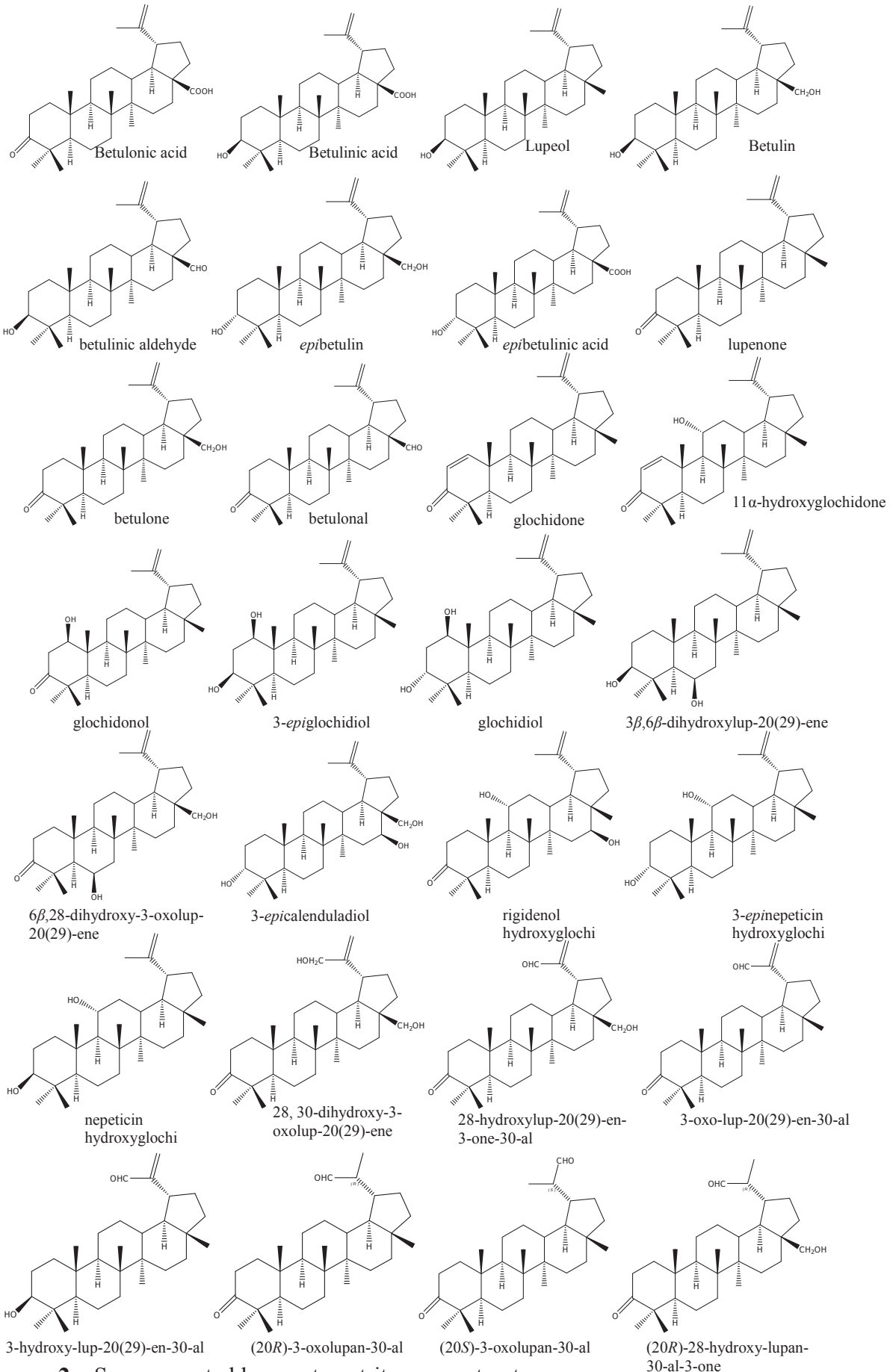

Figure 2. Some reported lupane-type triterpenes structures.

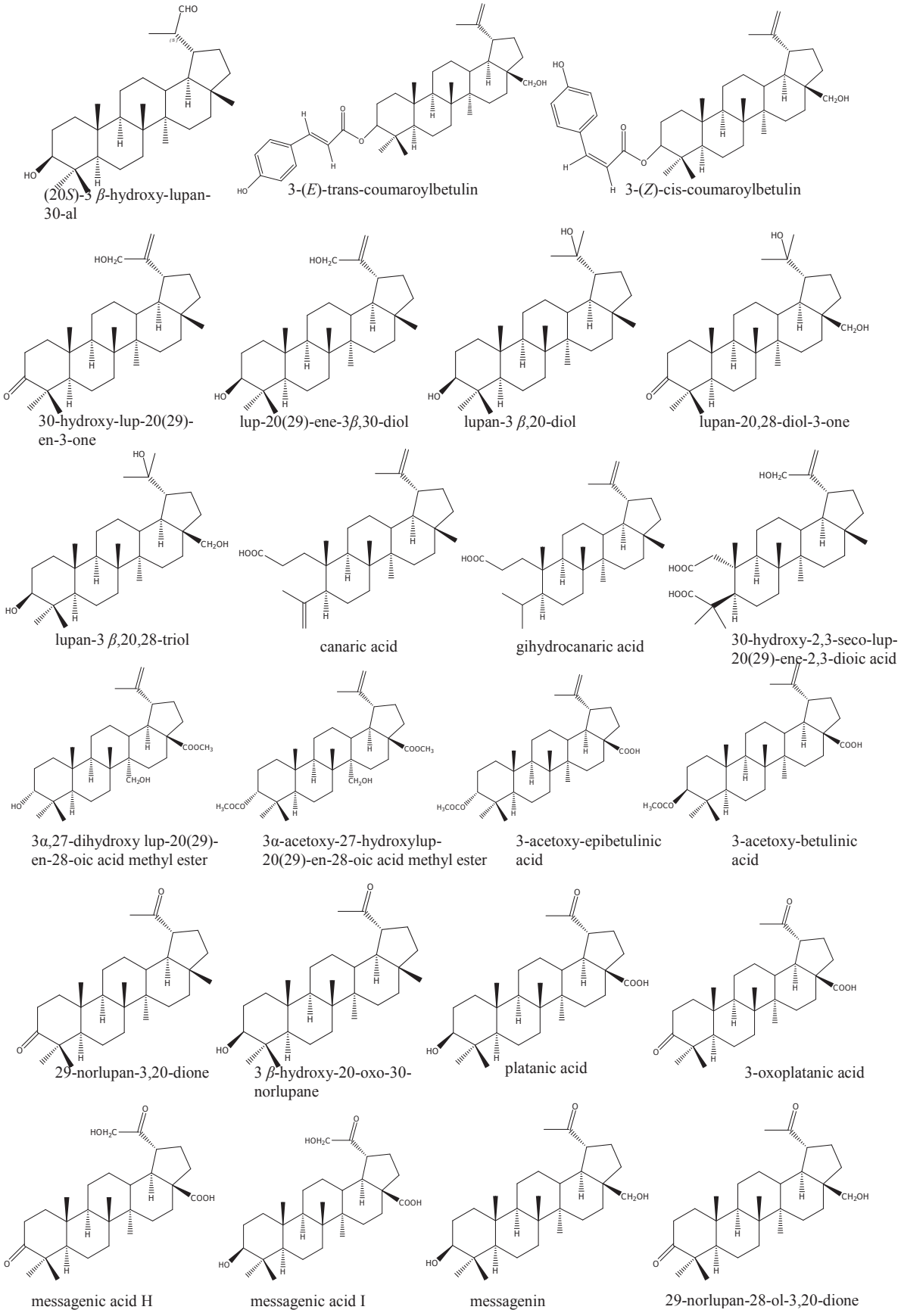

Figure 2. Some reported lupane-type triterpenes structures (continued)

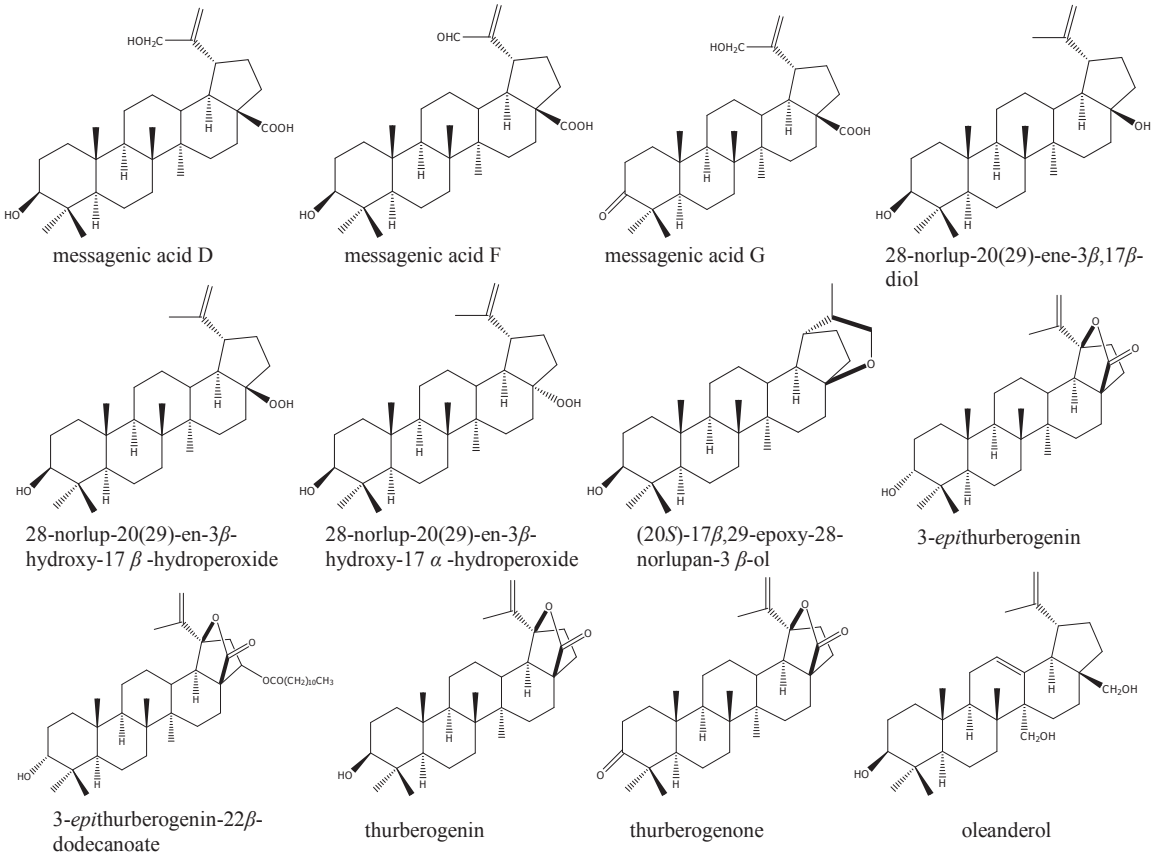

Figure 2. Some reported lupane-type triterpenes structures (continued)

Cytotoxicity

Betulinic acid and betulonic acid had been known as potent antiproliferative agents (Table 3) [52, 86, 106, 117-120]. DNA Topoisomerases II (Topo II) are target enzymes for anticancer chemotherapeutic drug development. Wada et al suggested that betulinic acid and its derivatives were catalytic inhibitors of Topo II activities [100]. Zhang et al [121] reported that the antitumor action of betulonic acid might be inducing apoptosis through inhibiting the PI3K, AKT pathways and promoting caspase-3,9 activities. The modification of betulonic acid and betulinic acid at C-3, C-28 and isopropenyl group could produce a number of potential antimelanoma activity [52] and anti-HIV activity [122, 123]. In a study on relationships between structure and activity of lupane triterpenes, a carboxylic group at C-28 was an important part for cytotoxicity [106]. Hata works [124, 125] showed that the keto group at C-3 and carbonyl group at C-17 were necessary for antiproliferative effect against some cancer cells. The structural similarities of the lupane groups from Mutai work [101] indicated that the presence of at least one hydroxyl group is important for cytotoxic activity. Furthermore, the position of the hydroxyl on C-3 is more important than on C-28, the presence of the conjugated carbonyl influences the activity very slightly and finally the presence of two hydroxyls (on C-3 and C-28) results in a reduction of activity. A number of amino acid conjugates of betulinic acid at C-28 carboxylic acid position showed improved water solubility as well as selective cytotoxicity [126].

Since the finding that betulinic acid was a highly promising anticancer drug after inducing apoptosis in melanoma cell lines in 1995, various experimental works focused on the apoptosis inducing mechanisms of betulinic acid and other triterpenes (Table 4). The antitumor effects were subsequently confirmed in a series of cancer cell lines from other origins, for example breast, colon, lung and neuroblastoma. Many studies have shown further effects that justify the expectation that lupane triterpenes are useful to treat cancer by several modes of action [79]. Lupane-type triterpenes, such as betulin, betulinic acid and lupeol, displayed anti-inflammatory activity which often accompanied by immune modulation. Although up to now no clinical trial has been published using these triterpenes in cancer therapy, the pharmacological potential of the lupane seems high.

Table 3. Cytotoxicity of betulinic acid and betulonic acid against various cell lines

Cell	Cell type	IC_{50} (μM)		references
		Betulonic acid	Betulinic acid	
A549	Alveolar basal epithelial cells	15	146 2.8 μg/mL	[117] [95]
HT29	Human colon adenocarcinoma grade II cell line	17 >10	89	[117] [106]
DU145	Human prostate carcinoma epithelial-like cell line	36	196	[117]
PC-3	Human prostate cancer cell line	15	91	[117]
MEL-1	Human melanoma cell	16.0 μg/mL	3.3 μg/mL	[118]
MEL-2	Human melanoma cell	0.9 μg/mL 0.1 μg/mL	1.2 μg/mL 1.0 μg/mL	[52] [118]
SK-Mel2	Human melanoma cell	26	21	[117]
K562	Human erythroleukenia cell line	6 16.1	56	[117] [86]
MCF-7	Human breast adenocarcinoma cell line	29 49	143 4.0 μg/mL	[117] [86] [95]
MDA-MB231	Human breast cancer		3.5 μg/mL	[95]
CEM	Human T-Lymphoblastoid CEM cell line	17	27	[117]
K562 tax	Leukemia cell	17	112	[117]
HL60	Human leukemia cell		2.0 μg/mL	[95]
COLO205	Colon carcinoma	36.8		[86]
KB	Epidermoid carcinoma	3.8 8.2 2.5 μg/mL	 >20 μg/mL	[86] [106] [52]
KB-C2	Colchicine-resistant KB	2.3		[86]
HONE-1	Nasopharyngeal carcinoma	4.9		[106]
SGC7901	Human gastric cancer cell	68.14		[120]
HepG-2	Human liver cancer cell	110.77	 3.1 μg/mL	[120] [95]
Hep3B	Hepatoma cell		1.7 μg/mL	[95]
FS-5	Human foreskin fibroblast		20.7 μg/mL	[119]
OVCAR-3	Human ovarian adenocarcinoma		0.9 μg/mL	[119]
HeLa	Cervical carcinoma		0.8 μg/mL	[119]

Table 4. Cytotoxicity of other lupane-type triterpene

compound	Tested cell lines (IC_{50})	Reference
*Epi*betulinic acid	HeLa (2.1 μg/mL), Hep-2 (3.1 μg/mL)	[93]
	HL60 (2.3 μg/mL)	[95]
	A549 (9.7 μg/mL)	
	MCF-7 (9.7 μg/mL)	
	MDA-MB231 (9.2 μg/mL)	
	Hep3B (8.1 μg/mL)	
	HepG2 (9.3 μg/mL)	
28,30-Dihydroxy-3-oxolup-20(29)-ene	HeLa (4.0 μg/mL), Hep-2 (7.1 μg/mL)	[93]
28-Hydroxy-3-oxo-lup-20(29)-en-30-al	NSCLC-N6 (15 μg/mL)	[101]
	HL60 (1.6 μg/mL)	[95]
	Ca9-22 (1.4 μg/mL)	
	MCF-7 (2.9 μg/mL)	
	MDA-MB231 (7.9 μg/mL)	
	Hep3B (4.7 μg/mL)	
Betulin	HL60 (1.7 μg/mL)	[95]
	MCF-7 (16.0 μg/mL)	
	A549 (15.7 μg/mL)	
	Hep3B (9.3 μg/mL)	
	HepG2 (6.7 μg/mL)	
(20*R*)-28-Hydroxylupan-30-al-3-one	NSCLC-N6 (39.5 μM)	[102]
3-Oxo-lup-20(29)-en-30-al	KB (cytotoxic at conc 10 μg/mL)	[94]
3-Hydroxy-lup-20(29)-en-30-al	NSCLC-N6 (11 μg/mL)	[101]
Betulone	NSCLC-N6 (30 μg/mL)	[101]
Lupeol	NSCLC-N6 (>30 μg/mL)	[101]
28-Norlup-20(29)-en-3*β*-hydroxy-17*β*-hydroperoxide	Malignant +SA (15.5 *μ*M)	[107]
28-Norlup-20(29)-en-3*β*-hydroxy-17*α*-hydroperoxide	Malignant +SA (20.6 *μ*M)	[107]
(20*S*)-17*β*,29-Epoxy-28-norlupan-3*β*-ol	Malignant +SA (18.1 *μ*M)	[107]
28-Norlup-20(29)-ene-3*β*,17*β*-diol	Malignant +SA (18.7 *μ*M)	[107]

HeLa = human carcinoma of cervix
Hep-2 = human carcinoma of larynx
HL60 = human leukemia cell
Ca9-22 = gingival cancer
MDA-MB231, MCF7 = breast cancer
HepG2, Hep3B = hepatoma cancer
A549 = lung cancer
Malignant +SA = Malignant +SA mouse mammary epithelial cell
NSCLC-N6 = human non-small-cell bronchopulmonary carcinoma.

Anti-inflammatory activity

A number of lupane triterpenes from *Maytenus* sp were evaluated for potential anti-inflammatory activity [127], and several compounds exhibited *in vitro* potent inhibitory effects on NO and prostaglandin E2 production in mouse macrophages (RAW264.7) stimulated with bacterial endotoxin. Compounds able to reduce the excessive production

of these mediators had a potential for the prevention and treatment of different inflammatory pathologies. The structure–activity relationship was discussed. The substitution of a C-28 methyl by a hydroxyl methyl group (betulin, betulone) increased the potency mainly on NO, whereas the presence of a C-28 carboxyl group (betulonic acid, *epi*betulinic acid) increased both the potency on NO and PGE2 production and the cytotoxicity. In contrast, the introduction of C-28 carbonyl aldehyde (betulinic aldehyde) or C-20 carbonyl ketone group (28-hydroxy-3,20-dioxo-29-norlupane) was detrimental. On the other hand, the presence of the *α*-hydroxyl group at C-11 (11-*α*-hydroxy-glochidone) resulted in a higher inhibitory activity, especially for NO. The acetylation of betulin at C-28 increased the potency and reduced the cytotoxicity of this compound, although the double acetylation at C-28 and C-3 strongly reduced the activity. Also, the acetylation at C-11 or the chlorination at C-30 of rigidenol increased the potency of the compound.

Table 5. Anti-inflammatory activity of some lupanes (effect on NO and PGE2 production) [93]

Compound	%Viability[a] (10μM)	NO		PGE_2	
		% inhibition[b]	IC_{50}[c](μM)	% inhibition[b]	IC_{50}[c](μM)
Betulonic acid	72.1±2.9	69.2±5.1	0.3	58.4±3.9	2.7
*Epi*betulinic acid	67.1±4.1	89.1±4.4	0.7	68.7±5.7	0.6
28-Hydroxy-3,20-dioxo-29-norlupane	94.9±3.3	19.4±2.8	N.D.	0.0±0.0	N.D.
Betulinic aldehyde	100.0±0.0	19.5±4.0	N.D.	0.0±0.0	N.D.
11-*α*-Hydroxy-glochidone	88.4±1.9	53.1±4.2	8.2	53.6±5.9	5.4
Glochidone	100.0±0	00.0±0.0	N.D.	33.2±0.6	N.D.
Betulin	69.9±1.2	50.1±3.0	5.0	47.7±4.3	12.9
*Epi*betulin	91.0±5.3	44.9±5.7	12.8	49.3±2.7	9.6
Betulone	100.0±0.0	27.3±2.3	N.D.	34.5±12.7	N.D.
Rigidenol	100.0±0.0	42.7±1.7	12.9	44.6±4.7	20.7

[a] Compounds were assayed at 10 μM.
[b] Percentages of inhibition for NO and PGE2 production were obtained at 5 μM.
[c] Values represent the concentration required to produce 50% inhibition of the response, along with the 95% confidence limits.

In accordance with 30% in EPP-induced rat ear oedema inhibition of 0.5 mg/ear betulinic acid [128], Danstan et al reported 52% inhibition of prostaglandin biosynthesis by betulinic acid [110].

Antiviral activity

Some lupanes expressed antiviral activity with low selectivity to virus. Betulin, betulinic acid and betulonic acied were reported as anti-HIV agent, however, selectivity indexes, concentration ratio of 50% cytotoxic response of media cell (CC_{50}) to 50% inhibition of HIV-1 replication (IC_{50}) were low [49]. Sun et al suggest that the modification at C-3 and C-28 of betulin and betulinic acid (by addition of 3',3'-dimethylglutaryl group) could enhance the activity with the higher TI value [122]. It was suggested that the carboxylic group at C-28 of betulinic acid analogous was essential for anti-HIV-1 while a hydroxyl or ketone group at C-3 has little effect on the anti-HIV-1 activity [83].

Table 6. Anti HIV-1 activity of some lupanes

	CC_{50}	IC_{50}	TI	reference
Betulin	19.5 μM	13.8 μM	1.4	[49][a]
	2.14 μg/mL	No suppression	-	[129][c]
Betulinic acid	36.0 μM	32.5 μM	1.1	[49][a]
Betulonic acid	105.1 μM	21.4 μM	4.9	[49][a]
	30.66 μM	5.81 μM	5.27	[83][b]
	1.8 μg/mL	0.22 μg/mL	8	[129][c]

CC_{50} = Concentration mediating a 50% cytotoxic response
IC_{50} = Concentration mediating a 50% inhibition of HIV-1 replication
TI = CC_{50}/ IC_{50}
HIV-1 = human immunodeficiency virus type 1
[a] media = human osteosarcoma cell (HOS)
[b] media = T cell leukemia lymphocyte (C-8166)
[c] media = T lymphoid cell line (H-9)

Betulin, betulonic acid and betulinic acid were also active against herpes simplex and ECHO 6 virus with low TI too [130].

Miscelleneous activity

Antimalarial activity - Santos's work [131] studied the antimalarial activity of betulinic acid and its derivative compounds, betulonic acid, betulinic acid acetate, betulinic acid methyl ester, and betulinic acid methyl ester acetate was evaluated. These substances showed potent antiplasmodial activity against chloroquine-resistant *Plasmodium falciparum* parasites *in vitro*, with IC_{50} values of 9.89, 10.01, 5.99, 51.58, and 45.79 μM, respectively.

Antimicrobial activity – Mutai's work [103] discovered antimicrobial activity of 2 lupanes against different test organism. They reported that 3-(*Z*)-cis coumaroylbetulin exhibited a very strong activity against *Pseudomonas aeruginosa* and a strong activity against *Staphylococcus aureus* at a concentration of 0.1 mg/disc while 30-hydroxylup-20(29)-en-3*β*-ol also showed pronounced effects against *Pseudomonas aeruginosa*s, *Staphylococcus aureus*, *Microsporum gypseum*, and *Trichophyton mentagrophytes*. The latter compound presented higher antifungal activity against *Microsporum gypseu* at a concentration of 0.1mg/disc. The hydroxyl substituent at C-3 of 30-hydroxylup-20(29)-en-3*β*-ol was important for the ability to inhibit microorganism growth by comparison to inactive 30-hydroxylup-20(29)-en-3-one. The result also confirmed the important of conformation of molecule because 3-*E*-trans coumaroylbetulin showed lower activity.

Antituberculosis – *Epi*betulinic acid showed antituberculosis activity with MIC 50 *μ*g/mL. This agreed with the finding that low polarity pentacyclic triterpenes with a hydroxyl or keto group in the A or B rings and an acid group in the E ring possess moderate antitubercular activity. In addition, the lipophilicity of these triterpenes is likely to allow them to rapidly penetrate the lipid-rich mycobacterial cell wall [114].

Allelopathic activity - The allelopathic activity of lupane derivatives (lupeol, betulinic acid, betuladehyde, betulin and messagenin) has been reported in Macias' work [104]. These triterpenes possessed potential allelopathic activity in particular over dicotyledon species.

Protective effect against the cytotoxicity of Cadmium - Betulone exhibited protective effect against Cd cytotoxicity at a high concentration (20μM) without any cell damage [101].

Dammarane-type triterpene

Dammarane triterpene is a characteristic triterpene in Dipterocarpaceae family. However, it also appears as the main triterpene in Betulaceae, Compositae, Meliaceae and Oleaceae families [60, 86, 132-145]. Dammarenyl cation was a cyclization product of oxidosqualene and was proposed to be the precursor of most triterpene alcohols in lupane, ursane and oleanane skeletons [80]. Many publications have reported bioactivity of dammarane triterpenes especially antiviral activity [23].

Table 7. Discovery of dammarane-type triterpenes in some plants

Family	Plant	dammaranes found	Reference
Anacardiaceae	*Rhus javanica* (stem bark)	semialactone, semialatic acid, isofouquierone peroxide, fouquierone	[146]
Apocyanaceae	*Nerium oleander* (leaves)	ocotillol II, 24-*epi*-ocotillol	[147]
Betulaceae	*Alnus javanica* (flower)	Me (24*E*)-3,4-*seco*-dammara-4(28),20,24-trien-26-oic acid-3-oate, (24*E*)-3,4-*seco*-dammara-4(28),20,24-trien-3,26-dioic acid, (20*S*,24*S*)-20,24-dihydroxy-3,4-*seco*-dammara-4(28),25-dien-3-oic acid, (23*E*)(20*S*)-20,25-dihydroxy-3,4-*seco*-dammara-4(28),23-dien-3-oic acid, (23*E*)(20*S*)-20,25,26-trihydroxy-3,4-*seco*-dammara-4(28),23-dien-3-oic acid, (23*E*)(12*R*,20*S*)-12,20,25-trihydroxy-3,4-*seco*-dammara-4(28),23-dien-3-oic acid.	[134]
	Betula platyphylla var.*japonica* (floral spikes)	3-*epi*ocotillol II (and its acetate, 3-*O*-methylmalonyl, 3-*O*-malonyl), ocotillone, cabraleone (only a little), 12*β*-acetoxy-20(*S*),24(*R*)-epoxy-3*α*,25-diOH-dammarane (and its 3*α*-acetoxy ester), papyriferic acid and its methyl ester, methyl shoreate, betulafolientriol oxide, cabraleahydroxylactone, 20(*S*),24(*R*)-diOHdammara-26-en-3-one, dipterocarpol	[86, 135]
	Betula manschurica (leaves)	20(*S*),24(*S*)-dihydroxydammara-25-en-3-one, dipterocarpol, ocotillone	[136]
Burseraceae	*Commiphora dalzielii* (stem bark)	cabraleone, cabraleadiol (and its acetate), isofouquierone	[148]
	Boswellia carterii (gum resin)	isofouquierol (only a few)	[149]
Capparaceae	*Cleome brachycarpa*	cabralealactone	[150]
Celastraceae	*Celastrus rosthormianus*	3*β*,20(*S*),24(*S*)-trihydroxydammar-25-ene-3-caffeate, 3*β*,20(*S*),24(*R*)-trihydroxydammar-25-ene-3-caffeate (fouquierol-3-caffeate), 3*β*,20(*S*),24(*S*)-trihydroxydammar-23(Z)-ene-3-caffeate	[151]
Dipterocarpaceae	*Dryobalanops aromatica* (resin)	dipterocarpol, dammarenediol II, dryobalanone, ocotillol II,	[152]
	Dipterocarpus pilosus (oleoresin)	dipterocarpol, dammardienone, hallongdinone, ocotillone, dammarenediol II, ocotillol II, dipterocarpolic acid	[67]
Euphorbiaceae	*Phylanthus flexuosus* (stem bark)	ocotillol II	[153]

Family	Plant	dammaranes found	Reference
Fouquieriaceae	*Fouquieria splendens* (stem bark)	ocotillol II, isofouquierol, fouquierol	[154, 155]
Meliaceae	*Aglaia elaeagnoides* (bark)	cabraleone	[137]
	Aglaia forbesii (seed)	isoeichlerialactone, isoeichlerianic acid, isocabralealacone, aglinin A, spathulenol	[60]
	Aglaia foveolata (bark)	3-*epi*ocotillol, shoreic acid, eichlerianic acid, foveolin A, foveolin B	[138]
	Aglaia lawii (leaves)	aglinin A, cabraleone, eichlerianicacid, shoreicacid,	[139]
	Aglaia rubiginosa (leaves)	(20*S*,24*S*)-dihydroxydammar-25-en-3-one (fouquierone), (20S,25)-dihydroxy-dammar-23-en-3-one (=isofouquierone)	[140]
	Aglaia silvertris (root bark)	isoeichlerianic acid, methyl isoeichlerianate	[141]
	Aglaia tomentosa (leaves)	cabraliadiol-3-acetate, cabraleone, 3-*epi*ocotillol	[139]
	Amoora yunnanensis (bark)	cabraliadiol, cabraleahydroxylactone, ocotillone, cabraleone, shoreic acid, aglinin A, 20(*S*),24-epoxy-24,25-dihydroxydammar-3-one	[142]
	Cabralea eichleriana (wood)	eichlerianic acid, shoreic acid, cabraleone, cabraleadiol, ocotillone, cabralealactone, cabraleahydroxylactone, dammarenolic acid, eichlerialactone	[143]
	Cabralea polytricha (fruits)	cabraleadiol, cabraleone, cabralealactone, cabraleahydroxylactone, eichlerianic acid, shoreic acid, dammarenolic acid, eichlerialactone	[133]
	Dysoxylum malabaricum (leaves)	ocotillone, shoreic acid, dymalol	[144]
	Dysoxylum richii (fruit)	ocotillone, cabraleone, shoreic acid, eichlerianic acid, richenone, richenol, richenoic acid, methyl richenoate	[145]
Moraceae	*Ficus pumila* (fruit)	3*β*-acetoxy-22,23,24,25,26,27-hexanordammarane-20-one, 3*β*-acetoxy-20,21,22,23,24,25,26,27-octanordammarane-17*β*-ol, 3*β*-acetoxy-(20*R*,22*E*,24*RS*)-20,24-dimethoxydammaran-22-en-25-ol, 3*β*-acetoxy-(20*S*,22*E*,24*RS*)-20,24-dimethoxydammaran-22-en-25-ol	[156]
Oleaceae	*Olea madagascariensis* (fruit lipid)	dammaradienol, dipterocarpol	[132]
Palmae	*Copernicia cerifera* (canuaba wax from leaves)	24(*R*)-methyldammara-21,25-diene-3-ol, 24(*R*)-24-methyldammara-25-ene-3-one, (*E*)-25-hydroperoxydammar-23-ene-3,20-diol, carnaubadiol (=24*R*-methyldammar-25-ene-3,20-diol)	[157]
Rhizophoraceae	*Ceriops tagal* (fruit)	dammarenediol II, cereotagaloperoxide, ocotillol II, fouquierol, isofuoquierol,cereotagalol A, cereotagalol B	[158]
Rosaceae	*Cawania mexicana* (twig and leaves)	damarenediol II	[23]
	Gierocarpus intricarpus (leaves and flower)	isofouquierol	[23]
Velloziaceae	*Barbacenia bicolor* (root, stem)	3*β*,20(*R*)-dihydroxydammar-24-ene, 20(*R*)-dihydroxydammar-24-ene-3-one	[159]
Theaceae	*Camelia japonica* (seed oil)	3-*epi*carbraleahydroxylactone, 3-*epi*cabraleadiol, ocotillol II, ocotillol I, dammarenediol II	[160]

The underlined compounds demonstrated the major dammarane in the extract.

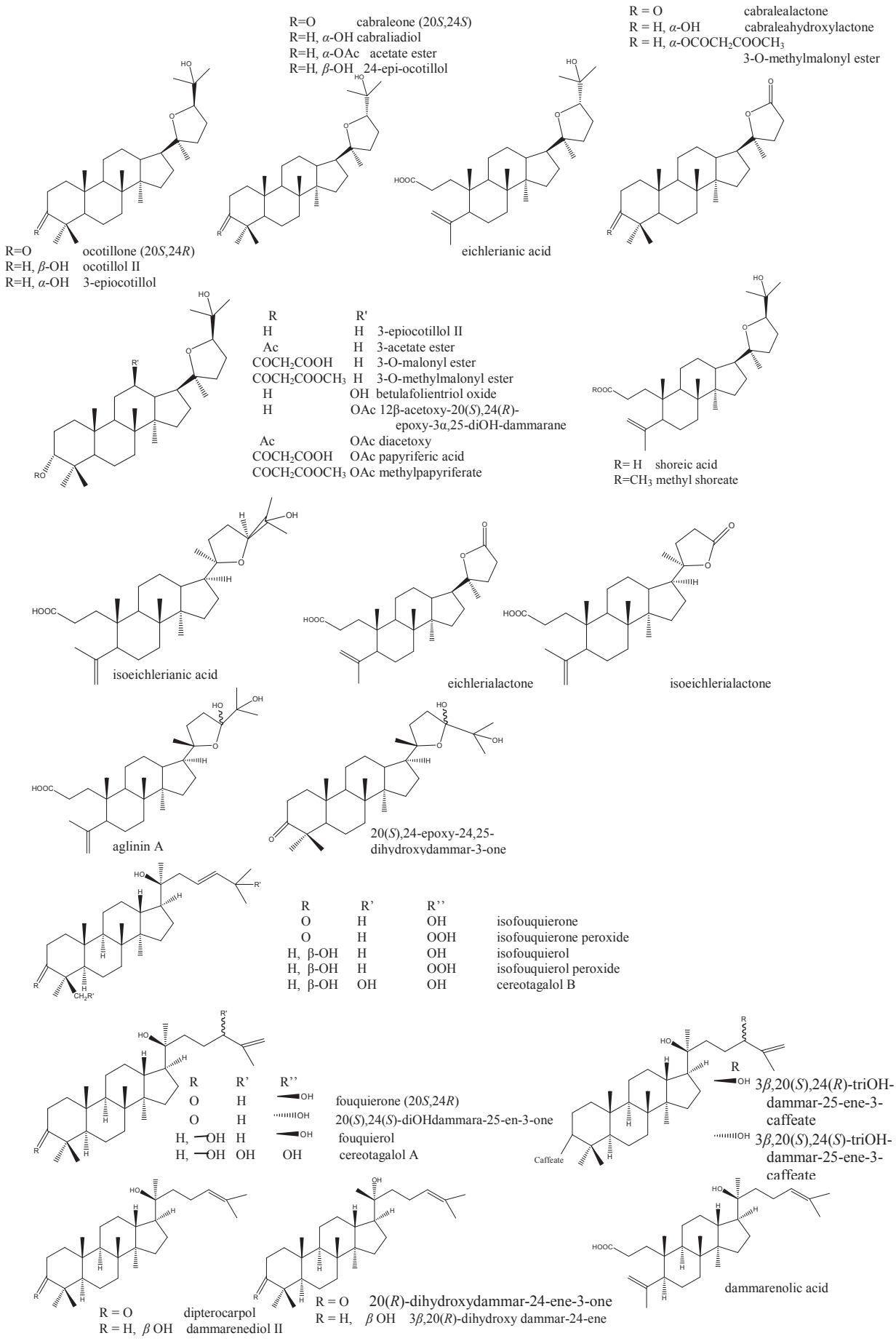

Figure 3. Some reported dammarane-type triterpenes structures.

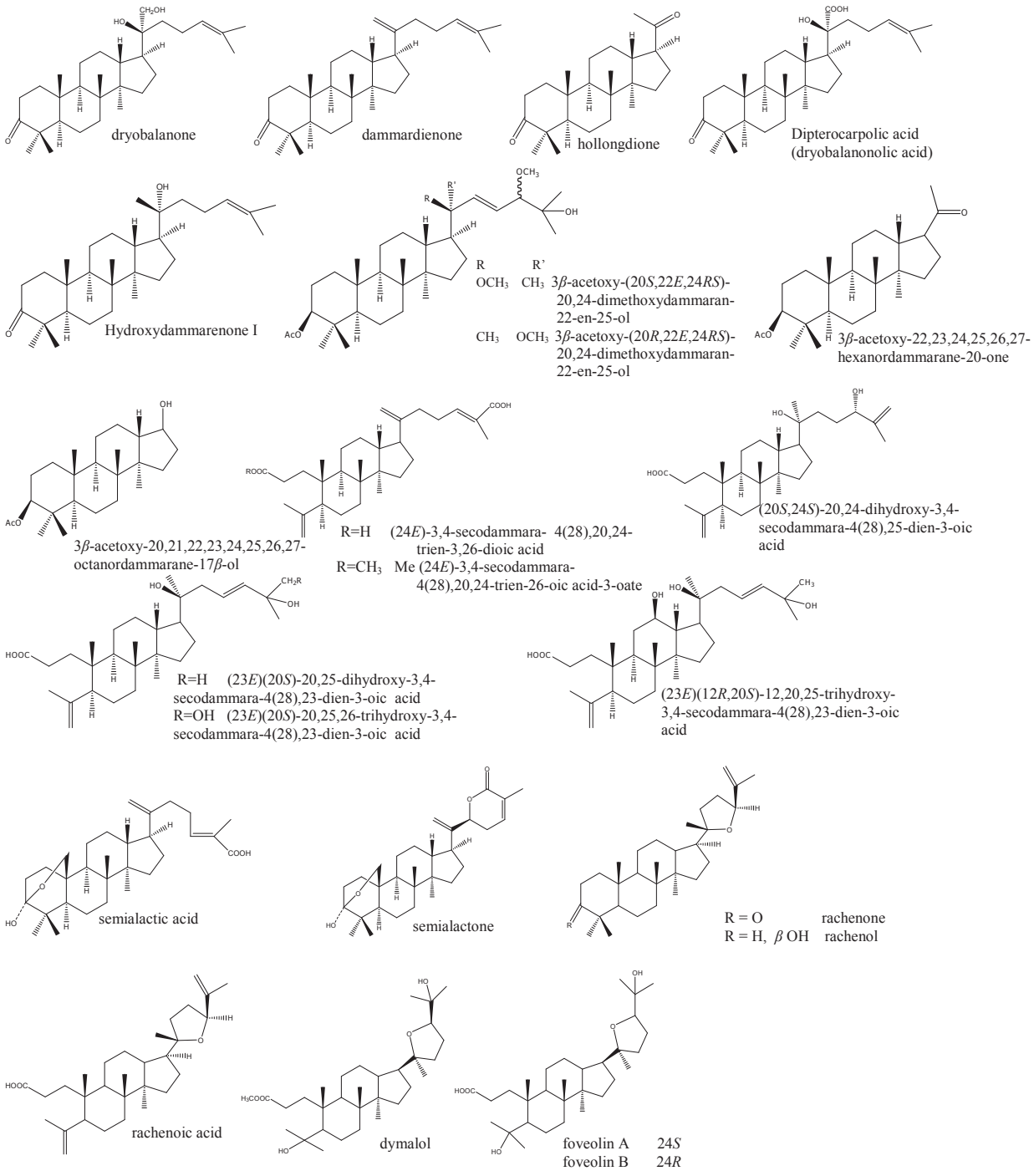

Figure 3. Some reported dammarane-type triterpenes structures.(continued)

Cytotoxicity

Cabralealactone exhibited cytotoxic activity against P388 leukemia cells with IC_{50} 3.8 µg/mL [161]. However the relationship between structure and cytotoxic activity could not be deduced. Nevertheless, it also presented multidrug resistance-reversing effect [86]. It presented moderate cytotoxic activity against KB-C2 cells (multidrug resistant human epidermoid carcinoma of the nasopharynx cells), with IC_{50} =28.5 µM in the presence of 2.5 µM colchicine although cabralealactone itself was not cytotoxic (IC_{50} >100 µM). The report also showed the recovery of cytotoxicity of 2.5 µM colchicine against KB-C2 in the presence of cabralealactone 2.5 and 5 µg/mL with IC_{50} 5.7 and 3.0 µM, respectively, compared to 18.2 µM when cabralealactone was absent [86].

According to MTT cytotoxic assay, 20(*S*),24(*S*)-dihydroxydammar-25-en-3-one showed weak cytotoxic activity and showed enhanced cytotoxicity against KB-C2 in the presence of 2.5µM (non toxic concentration) colchicine as compared with those in the absence of colchicine [86].

With the inhibitory effect against EBV-EA (Epstein-Barr virus-early antigen) activation, dammarenediol II (IC_{50} = 300 mol ratio/32 pmol TPA compare to 397 mol ratio/32 pmol TPA of *β*-carotene as reference compound) was suggested to be a valuable antitumor promoter (potential cancer chemopreventive agent). The intensively study showed that epoxidation at C-20 – C-24 of the side chain leads to a decrease in the activity as observed for 3-*epi*cabraleahydroxylactone, 3-*epi*cabraleadiol, ocotillol II and ocotillol I, with IC_{50} = 587, 553, 571 and 525 mol ratio/32 pmol TPA, respectively [160].

Cell growth inhibitory activity of ocotillol II was examined. It showed strong cytotoxicity to WI-38 (normal human lung cell) with IC_{50} 1.3 µM but moderate to weak cell growth inhibitory activities to VA-13 (malignant lung tumor) and HepG2 cells (human liver cancer) with IC_{50} 15 and 136 µM [147], then it is not suitable for anticancer.

Ocotillone showed moderate cytotoxicity against leukemia cells (L-1210, IC_{50} 20µg/mL) [73]

Wang et al [151] performed the experiments to show that the caffeoyl derivative of 3*β*,20(*S*),24(*S*)-trihydroxydammar-25-ene, fouquierol and 3*β*,20(*S*),25-trihydroxydammar-23(Z)-ene could increase the cytotoxicity of these compounds against human cervical squamous carcinoma (Hela) cell line (with IC_{50} 6.4, 5.3 and 6.5 µg/mL, respectively.) The hydrolysates of three compounds gave IC_{50} 26.4, 35.3 and 5.6 µg/mL, respectively.

Anti-inflamatory Activity

Dammarenediol-II showed anti-inflammatory activity, with a 50% inhibitory dose (ID_{50}) of 0.3 mg/ear, which was more inhibitive than quercetin (ID_{50}=1.6 mg/ear), a known inhibitor of TPA-induced inflammation in mice [162].

Inhibitory Effects on Production of NO in LPS (lipopolysaccharide)-Activated Macrophages

The inorganic free radical NO has been implicated in physiologic and pathologic processes, such as vasodilation, nonspecific host defense, ischemia-reperfusion injury, and chronic or acute inflammation. NO is produced by the oxidation of L-arginine by NO synthase (NOS). In the family of NOS, inducible NOS (iNOS) is specifically involved in pathologic aspects with the overproduction of NO and can be expressed in response to proinflammatory agents such as interleukin-1β, tumor necrosis factor-α, and LPS in various cell types including macrophages, endothelial cells, and smooth muscle cells. Isofouquierol (100μM) showed 86.6% inhibitory effect on NO production induced by LPS in mouse peritoneal macrophages[149].

Antiviral activity

In vitro antiviral activity of some dammarane was initially investigated by Poehland et al [23]. The result showed potent antiviral activity against HSV-1 and HSV-2 (table 8).

Table 8. *In vitro* anti-herpes activity of dammar resin [23]

Compound	IC_{50} (μg/mL)	
	HSV-1	HSV-2
Dammaradienol	2.5	3.0
Hydroxydammarenone I	2.0	5.0
Damarenediol II	7.0	7.0
Dammarenolic acid	3.0	2.0
Shoreic acid	7.0	8.0
Eichlerianic acid	7.0	8.0

HSV-1=McIntyre stain (ATCC VR-539), HSV-2=MS stain (ATCC VR-540)

Isofouquierol from twigh, leaves and flower of *Gierocarpus intricarpus* (Rosaceae) was also reported as a major anti-herpes active [23].

Antifungal activity

Terpenoid constituents and their antifungal activity of *Aglaia forbesii* seed were studied. The 3,4-*seco*-dammarane triterpenes, isoeichlerialactone, isoeichlerianic acid and aglinin A, showed a broader antifungal spectrum against *Phytophthora botryosa*, *P.palmivora*, and *Rigidoporus microporus* whereas the dammaran-3-one derivative, isochlerialactone, and spathulenol were only active against *R.microporus* [60]. It was proposed that the 3,4-*seco*-3-acid skeleton could account for antifungal property.

Insect antifeedant

Ocotillone exhibited insect antifeedant and growth-regulating activities against *Spodoptera litura* [163].

Determination of the absolute configuration by modified Mosher's method.

The high-field FT NMR application of modified Mosher's method has been reliably utilized for determining the absolute configuration of secondary alcohols and primary amines [149, 164-169]. This method involoves derivatization of the secondary alcohol with both (*R*)-MTPA-Cl and (*S*)-MTPA-Cl affording two diastereoisomeric ester [(*S*)- and (*R*)-ester, respectively]. The ester derivatives of α-methoxy-α-trifluoromethylphenylacetic acid (MTPA) have proved especially useful in this regard. Mosher proposed that, in solution, the carbinyl proton, ester carbonyl and trifluoromethyl groups of the MTPA moiety were in the same plane (Figure 4). The ^{1}H NMR signal of R^1 of the (*R*)-MTPA ester will appear upfield relative to that of the (*S*)-MTPA ester due to the diamagnetic effect of the benzene ring [It is important to be noted that (*R*)-MTPA-Cl yields (*S*)-MTPA ester]. The chemical shif differences of the ester proton at R^1 and R^2 were then calculated ($\Delta\delta=\delta_S-\delta_R$) ($R^1$:$\Delta\delta>0$ and R^2:$\Delta\delta<0$) [168]. Ohtani and his co-worker [169] extended this method to longer chain secondary alcohols (Figure 5). The values of $\Delta\delta$ ($=\delta_S-\delta_R$) could be measured for protons residing within group R^1 and R^2 (as many proton signals as possible with respect to each of the (*S*)-MTPA and (*R*)-MTPA ester). The $H_{A,B,C...}$ NMR signals of the (*R*)-MTPA ester were relatively more shielded and should appear upfield relative to those of the (*S*)-MTPA ester. The reverse should be true for the $H_{X,Y,Z...}$. Therefore, the values of $\Delta\delta$ ($=\delta_S-\delta_R$) of the $H_{A,B,C...}$ would be positive value ($\Delta\delta>0$) while those of the $H_{X,Y,Z...}$ would be negative values ($\Delta\delta<0$). This method was applied to determine the absolute configuration at position 24 of compound **18a**.

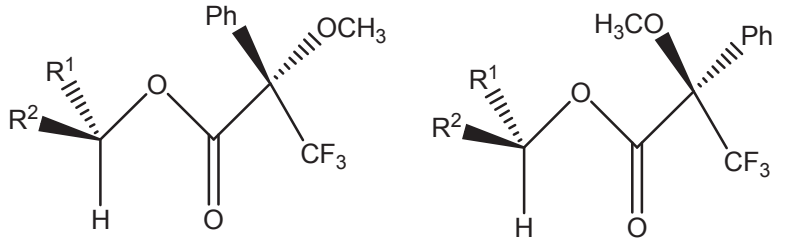

(*S*)-MTPA ester (*R*)-MTPA ester

Figure 4. Two Mosher conformers showing the (*S*)-MTPA and (*R*)-MTPA derivatives proposed by Mosher.

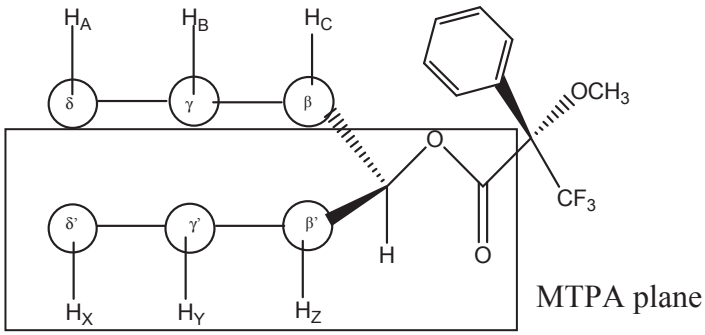

Figure 5. The (*S*)-MTPA ester presenting the $H_{A,B,C,X,Y,Z}$ instead of group R^1 and R^2

Cytotoxic evaluation by WST-1 method.

Sodium salt of 4-[3-(4-iodophenyl)-2-(4-nitrophenyl)-2*H*-5-tetrazolio]-1,3-benzene disulfonate (WST-1) is one of tetrazolium salts which are available to measure cell proliferation or cell viability [170-172].

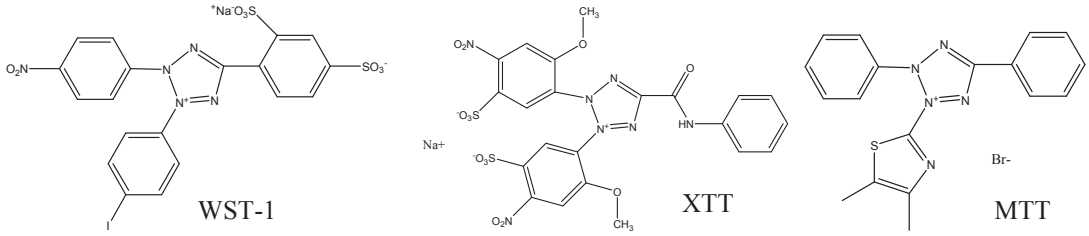

Figure 6. Some tetrazolium salts for cell proliferation and cell viability measurement

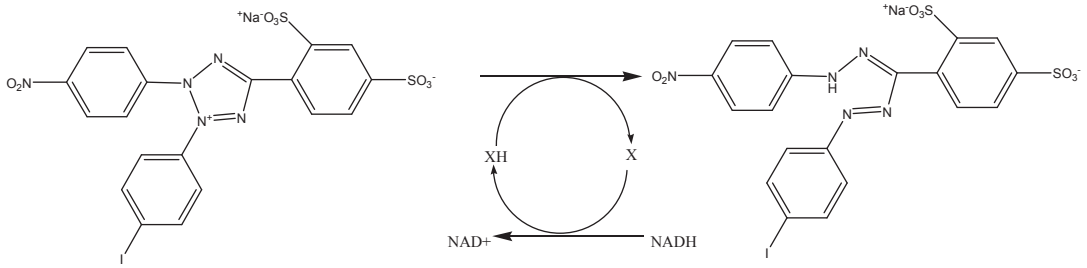

Figure 7. Reduction of WST-1by NADH; X=electron coupling reagent, NADH = reduced nicotinamide adenine dinucleotide. (1-Methoxy PMS, used as Electron coupling reagent, is easily dissolved by water and alcohol.)

The use of tetrazolium salts, such as MTT (3-(4,5-dimethylthiazole-2-yl)-2,5-diphenyltetrazolium bromide) and WST-1, is based on the fact that live cells reduce tetrazolium salts into highly colored formazan compounds whose absorbance is in direct proportion to the number of viability cells. The biochemical procedure is based on the activity of the succinate-tetrazolium reductase, a mitochondrial enzyme, which is inactivated shortly after cell death. So, this method was found to be very efficient in assessing the viability of cells. An increase in number of living cells results in an increase in the overall activity of mitochondrial dehydrogenases in the sample. This increase directly correlates to the amount of formazan formed, as monitored by the absorbance. However, due to neutrality of the solution, the use of MTT produces a water-insoluble formazan compound which is disadvantage when spectrophotometric measurement of formazan products is required. It needs an extra step to solubilize this insoluble product. The compound producing highly water-soluble formozan was developed. WST-1, containing two sulfonate groups to improve water-solubility, was proved to be more sensitive than MTT and less cytotoxic than XTT (a former water-soluble tetrazolium salt, 2,3-bis(2-methoxy-4-nitro-5-sulfophenyl)-5-[(phenylamono)carbonyl]-2H-tetrazolium hydroxide), in the proliferation assay using P388 cell lines. Therefore, WST-1 is of value as a viability indicator in cell proliferation assay.

Cytotoxic evaluation by REMA (resazurin microplate assay) method [173-175]

Resazurin (7-Hydroxy-3*H*-phenoxazin-3-one-10-oxide) is an oxidation–reduction indicator used for the evaluation of cell growth, particularly in various cytotoxicity assays. It has also been used for decades to demonstrate bacterial and yeast contamination of milk and provided a convenient index of cell proliferation following irradiation. Resazurin is a blue non-fluorescent and non-toxic dye that becomes pink and fluorescent when reduced to resorufin that could be further reduced to hydroresorufin (colorless and non-fluorescent). This conversion is intracellular, facilitated by mitochondrial, microsomal and cytosolic oxidoreductases, then, the reduced product could be excreted into the medium. Resorufin, the result of resazurin bioreduction, is measured colorimetrically or fluorometrically. Reduction of the fluorescent resorufin into a further reduced non-fluorescent product may lead to aberrant results in which living cells produced a weak signal and dying cells, which could not sustain further reduction, yielded a high fluorescent signal.

Resazurin is non-toxic to cells and stable in culture medium, allowing continuous measurement of cell proliferation *in vitro* as either a kinetic or endpoint assay. Toxic insult that impairs cell viability and proliferation also affects the capacity of cultures to reduce resazurin, and the rate of dye reduction is directly proportional to the number of viable cells present.

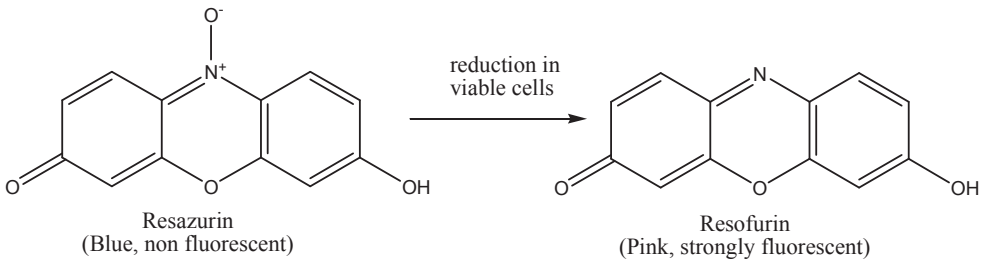

Figure 8. The principle of REMA method

The certain precaution should be taken in REMA method. First, it is worth checking the cross-reactivity of resazurin with any compound to be tested, without any cells in the medium. Second, the reduction rate by cells in culture should also be checked so that conditions for resazurin concentration and incubation time are optimized in order to avoid over-reduction of resazurin into the colourless and non-fluorescent hydroresorufin. Third, resazurin is more valuable as an endpoint measurement for cytotoxicity rather than as a kinetic measure for monitoring cell growth. All these initial steps may be seen as cumbersome and lengthening a process which is supposed to be quick and simple. However, once established for routine screening, high throughput screening is probably the most obvious application for this test, since this reagent is not as expensive as the reagents of other method.

PART I

Phytochemical Study of *Hopea odorata* Roxb leaves.

I. BOTANICAL STUDY

Genus *Hopea* [25, 26, 31]

The genus *Hopea* is distributed from Sri Lanka, to Bangladesh, India, Myanmar, South China, Hainan, Indochina and Malaysia. There are 14-15 species in Thailand.

Genus description : Big or vast trees resinous, with transparent resin. Stipule oblong to linear-lanceolate, small, caducous. Leaves not plicate, symmetrical or asymmetrical at base, chartaceous or coriaceous; secondary nerves pinnate or dryobalanoid, arched near to margin; intermediate nerves present in dryobalanoid type; tertiary nerves scalariform or reticulate. Domatia frequently present. Flowers rather small in panicled unilateral racemes. Sepal 2 external, 3 internal, imbricate. Petal silky or tomentose on the part exposed in bud only, contort, narrow, yellow, red or white. Stamen usually 15, rarely 10. Anther ovate with 4 pollen sac. Ovary 3 celled, 2-ovuled each. Fruit surrounded by 5 enlarged sepal, free to base, 2 outer wings long linear, 3 inner ones not longer than fruit, connate in a cup at base, closely appressed to the small nut. Cotyledon fleshy, bilobed, unequal. Bark usually smooth, paper flaky, or distantly fissured. Timber light red and rather soft.

Hopea odorata **Roxb.** [25, 27, 176, 177]

Common name : Iron wood.

Vernacular name : Takhian thong (ตะเคียนทอง), Takhian (ตะเคียน) are preferred name. Khaen (แคน) - used in the northeast. Koki (โกกิ) – for Karen hill tribe in Chiengmai.

Diagnostic characters : Very large buttressed tree to 1.8 m dbh and up to 45 m tall with dense, dark green crown and large spreading branches with slender, droopling twigs. In evergreen forest. Bark dark brown flaky bark, becoming scaly with age, inner bark dull yellow, with conspicuous white droplets of resin (dammar). Leaves 8-16 * 3-7.5 cm ovate to ovate-oblong to lanceolate, slightly asymmetrical, falcate, apex long acuminate and blunt or rounded base, secondary nerves 8-12 pairs. Young leaves densely covered with grey star-shaped hairs. Mature leaves dark green, almost smooth except for tiny tufts of blackish hairs (domatia) in or below the vein axils. Stalk 1-1.8 cm, slender with tiny, triangular stipule. Domatia pore-like. Glabrous. Connectives ± as long as anthers. Flowers 0.8-1 cm, yellow, slightly fragrant, in flattened, branching sprays of up to 50 flowers at end of twigs and upper leaf axils, 5-7 cm long. Calyx minute, petals 3-5 mm. Spreading with narrow, finely fringed tips, twisted and fused together at base, falling as a rosette with stamens attached. 15 stamens with long pointed tips on top of anthers, style slender, ovary as long as style. Fruit 2 long wings with 9-11 main veins, 4-6 * 1 cm, slightly narrowed towards the base. 3 much shorter wings < 0.5 cm overlapping but not completely covering the nut.

Note tree dbh (= diameter at breast height) is outside bark diameter at breast height. Breast height is defined as 4.5 feet (1.37m) above the forest floor on the uphill side of the tree.

Distribution : A wide spread species distributed from the Western Ghats, Bangladesh (type locality), Andaman and Nicobar Islands, lower Myanmar, throughout Indochina including North Vietnam and Peninsular Malaysia (Perak and Trengganu northwards). In Thailand, it is widespread throughout the country in lowland evergreen dipterocarp to dry evergreen forests up to 900 m altitude, occasionally found by streams, open forest near beaches and peat swamp forest. However, large trees are rare in the forest except in well-protected or inaccessible places.

Phenology: Flowering: January-December
Fruiting: January-August

A

B

Figure 9. Characteristics of *H.odorata* Roxb. A. from reference [176] B. from reference [27]

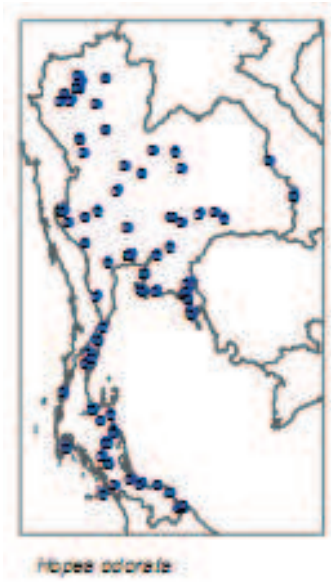

Figure 10. Distribution of *H.odorata* in Thailand [25]

II. PREVIOUS CHEMICAL WORK ON GENUS *HOPEA*

Aqueous and ethanolic crude extracts of *Hopea utilis* screened for antibacterial and cytotoxic activities were studied. Antibacterial activity of ethanolic extracts of *H. utilis* were more successful with the pathogens *Salmonella typhi* and *Streptococcus aureus* (MIC = 25 mg/mL and 36 mg/L, respectively). The results of both extracts (aqueous and ethanolic) of *H. utilis* showed the brine shrimp lethality assay LD_{50} values at 1.64 µg/mL and 1.34 µg/mL, respectively [34].

Oligostilbenoids from *Hopea hainanansis*, hopeahainol A, a dimer, and neohopeaphenol A, a tetramer, were found to be acetylcholinesterase inhibitors with an IC_{50} value of 4.33 µM, and 7.66 µM, respectively [7, 11].

Hopeanolin, an unusual resveratrol trimer with an *ortho*-quinone nucleus, was isolated and characterized from the stem bark of *Hopea exalata*. Also obtained were six known stibenoids, shoreaphenol, vaticanol G, α-viniferin, pauciflorol A, vaticanol A, and *trans*-3,5,4'-trihydroxystilbene-2-*C*-glucoside. Hopeanolin demonstrated antifungal activity in the MIC value range 0.1−22.5 µg/mL [178].

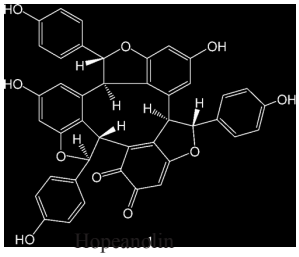

Hopeanolin

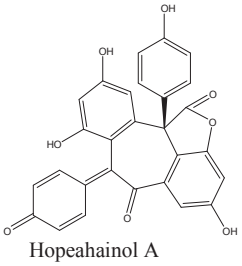

Hopeahainol A

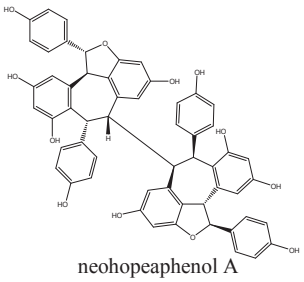

neohopeaphenol A

Timber/bark of *Hopea cordifolia* and *H. jucunda* [47] contained sitosterol, lupeol, ursolic acid, β–amyrin, betulinic acid, dipterocarpol (in the order of quantity from high to low). On the other hand, it showed that there was more lupane triterpene in genus *Hopea* than dammarane triterpene.

The isolation of the extract from the stem bark of *Hopea odorata*, *H. mengarawan* and *H. nigra*, found seven known resveratrol derivatives, named balanocarpol, heimiol A, vaticanol G, vaticanol B, hopeaphenol, ampelopsin H, and hemlesyanol C. Hopeaphenol was more active in antioxidant than ascorbic acid whereas vaticanol B and ampelopsin H were very active against HeLa-S3 (human epithelial carcinoma cell line) and Raji cell (human Burkitt's lymphoma cell line) [6]. Nguyen et al [179] also isolated two oligostilbene, hopeaphenol and malibatol A, from the methanolic extract of the stem bark of *Hopea odorata* Roxb. Malibatol A had been reported to have significant effect against cancer cell line CEM-SS (human T lymphoblastoid cell line) with the IC_{50} = 21 µg/mL.

Quercetin, kaempferol, apigenin and quercetin-3-glucoside were isolated in the study of flavanoid pattern of *H. odorata* leaves [54].

III. EXPERIMENTAL PART

3.1 Plant material

3.2 Method and apparatus

3.3 Preliminary study
- 3.3.1 Preliminary extraction by soxhlet extraction
- 3.3.2 *In vitro* bioactivity assays

3.4 Extraction and isolation of *H. odorata* leaves hexane extract
- 3.4.1 Extraction by maceration
- 3.4.2 Isolation of major compounds with a small portion of hexane extract.
  - 3.4.2.1 Isolation by silica gel column chromatography
  - 3.4.2.2 Isolation by sephadex column chromatography
- 3.4.3 Isolation of a large portion of hexane extract
- 3.4.4 Purification of HML10

3.5 Cytotoxic evaluation of 8 isolated lupanes

3.6 Physical characteristics and spectrum of isolated product

3.1 PLANT MATERIAL

Sample of the leaves of *H. odorata* was collected from Chiang Mai (Maerim district), a northern province of Thailand in September, 2004, and identified by Dr.Chavalit Sittisombut. A voucher specimen was deposited at the herbarium of the Department of Pharmacognosy, Faculty of Pharmacy, Silpakorn University, Nakhon Pathom, Thailand.

3.2 METHOD AND APPARATUS

- 1D AND 2D NMR spectra were recorded on Bruker AC300 (300 MHz) and Avance 400 (400 MHz).
  - Chemical shifts were given in parts per million (ppm, δ) relative to solvent peaks as internal standards (δ: $CDCl_3$: 7.27 ppm (^1H), 77.0 ppm (^{13}C)).
  - Coupling constants (J) were expressed in hertz (Hz).
  - Multiplicity of ^1H-NMR spectrum: s = singlet, d = doublet, t = triplet, q = quartet, dd = doublet of doublet, dt = doublet of triplet, m = multiplet.
- MS
  - Low resolution MS was run on Thermo Finnergan LCQ Advantage (ESI-ion trap)
  - High resolution MS was run on LCT Premier Waters® (ESI-TOF)
  - GC/MS analyses for sesquiterpenes and fatty acid analysis were carried out in a Hewlett Packard 6890 GC coupled to a 5975 quadrupole MS.
- IR spectrum was recorded using Nicolet 510 FT-IR spectrophotometer as film on NaCl pellets. The positions were presented in wave number (ν, cm^{-1}).
- Specific rotations ($[\alpha]_D^{20}$) were measured on a Perkin-Elmer Model 341 polarimeter with the D-ray of Na (always at 589 nm) at 20°C. The concentration was expressed in g/100mL.
- MPLC (medium pressure liquid chromatography) BUCHI684 Fraction collector was used for rough fractionation.
- Silica gel 60A C.C.20-45μm chromagel sds from CARLOERBA was used in column chromatography
- Lipophilic Sephadex® LH20100-100G (10 g for 100 mg extract)
- TLC was carried on a Merck® aluminium sheet 20x20 cm silica gel 60 F_{254}. Spots were detected under UV (254 and 366 nm) before spraying with vanillin-sulfuric acid solution followed by heating the plate at 110°C for 5 minute.

3.3 PRELIMINARY STUDY

3.3.1 Preliminary extraction by soxhlet extraction

The 50.4128 g dried and powdered leaves was first extracted by soxhlet apparatus. The extraction gave the 1.7908 g (3.55%) and 10.6608 g (21.15%) of the hexane and ethanol extracts, respectively. Then, both extracts were examined for bioactivity (Scheme 3).

3.3.2 *In vitro* bioactivity assays

The *in vitro* cytotoxic and antifungal activities of both extracts were performed by the Resazurin Microplate assay (REMA)[173], while antituberculosis and antimalarial activity were measured by green fluorescent protein microplate assay (GFPMA) and microculture Radioisotope Technique, respectively. All samples were tested by BIOTEC, Thailand. The results were shown in the following table.

Table 9. *In vitro* bioactivity assays of *H.odorata* leaves extract

	IC_{50} (µg /mL)				
	Anti MCF-7	Anti NCI-H187	Antifungus	Antimalaria	Anti-TB
H.odorata leaves hexane extract	36.67	9.5	Inact.	Inact.	Inact.
H.odorata leaves ethanol extract	Inact.	Inact.	Not tested	Not tested	Not tested

Inact. = inactive at the level of 50 µg/mL.

The method for each assay was as follows:

Cytotoxicity against MCF-7 (breast cancer)

Method Resazurin Microplate assay (REMA)

Negative control 0.5% DMSO

IC_{50} of positive control Ellipticine=-µg/mL, Doxorubicine = 0.817 µg/mL

Maximum final concentration of tested sample 50 µg/mL

Cytotoxicity against NCI-H187 (small cell lung cancer)

Method Resazurin Microplate assay (REMA)

Negative control 0.5% DMSO

IC_{50} of positive control Ellipticine=0.441 µg/mL, Doxorubicine = 0.065 µg/mL

Maximum final concentration of tested sample 50 µg/mL

Antifungal activity against *Candida albicans*

Method Resazurin Microplate assay (REMA)

Negative control 0.5% DMSO

IC_{50} of positive control Amphotericin B = 0.034 µg/mL

Maximum final concentration of tested sample 50 µg/mL

Antituberculosis (anti-TB) against *Mycobacterium tuberculosis* H37Ra strain

Method Green fluorescent protein microplate assay (GFPMA)

Negative control 0.5% DMSO

MIC of positive control Rifampicin = 0.003-0.012 µg/mL, Streptomycin= 0.156-0.313 µg/mL, Isoniazid = 0.023-0.046 µg/mL, Ofloxacin = 0.391-0.781 µg/mL

Maximum final concentration of tested sample 50 µg/mL

Antimalaria against *Plasmodium falciparum* K1 strain

Method Microculture Radioisotope Technique

Negative control 0.1% DMSO

IC50 of positive control Dihydroartemisinine 4.5 nM

Maximum final concentration of tested sample 10 μg/mL

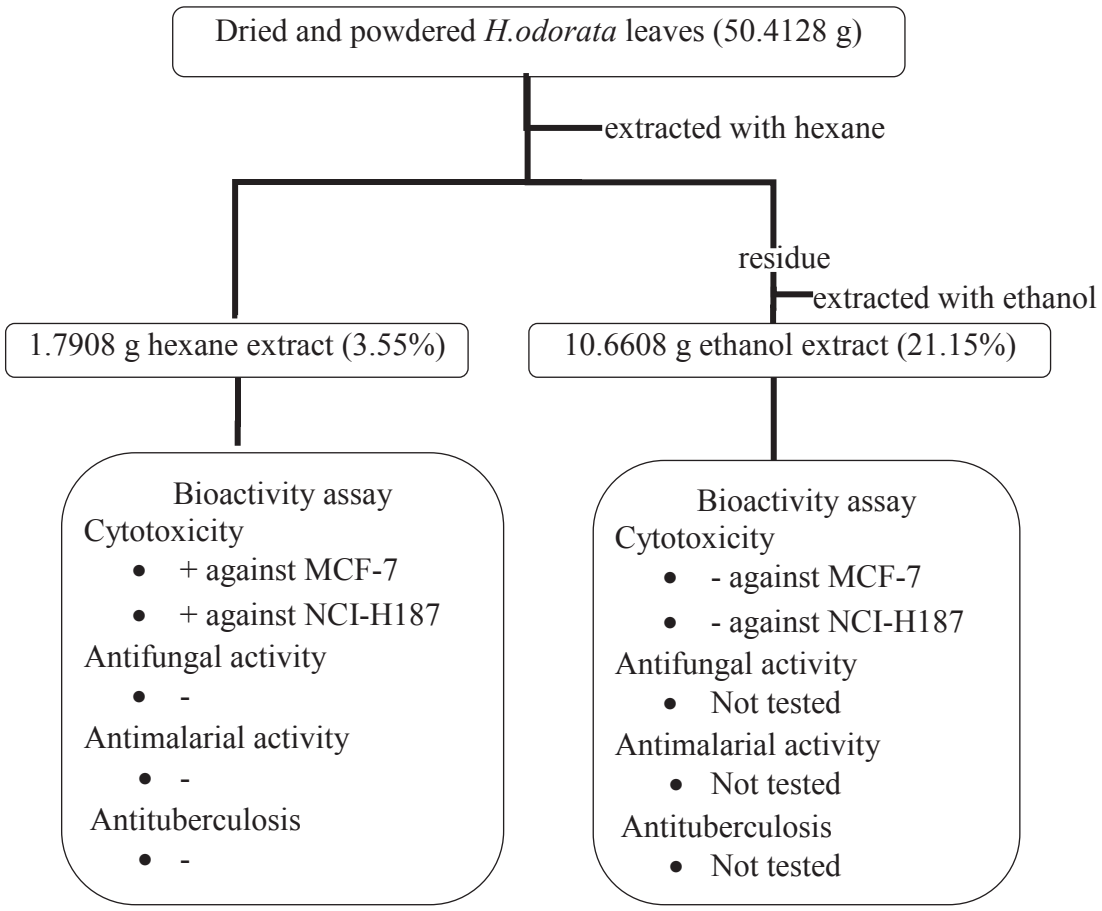

Scheme 3. Extraction and bioactivity assay of preliminary study of *H. odorata* leaves.

3.4 EXTRACTION AND ISOLATION OF *H. odorata* LEAVES HEXANE EXTRACT.

3.4.1 Extraction by maceration

The dried and powdered leaves (1,077.30 g) of *H.odorata* was sequentially extracted by maceration with hexane and ethanol (3L*48h*3, each). Each extract was concentrated in reduced pressure to dark green residues of both hexane extract (19.52 g, 1.81%) and ethanol extract (216.63 g, 20.10%) (Scheme 4).

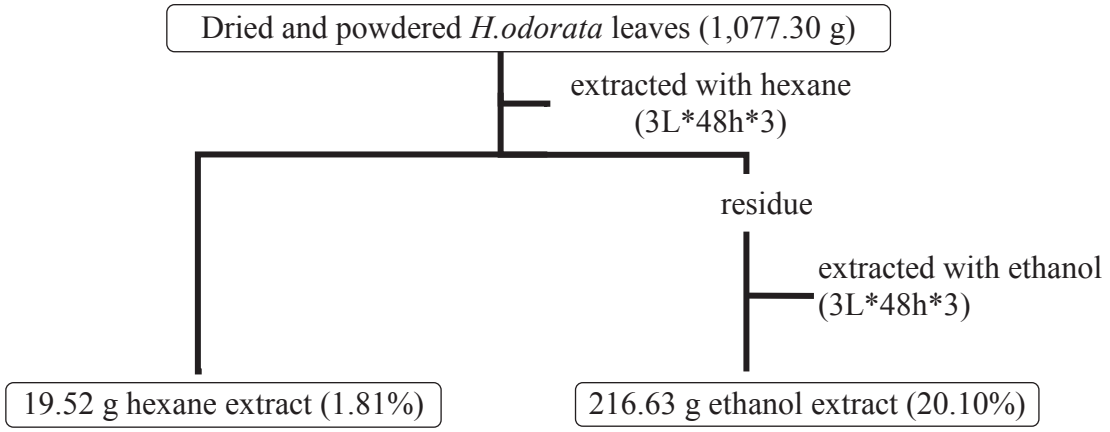

Scheme 4. Extraction of *H.odorata* leaves for phytochemical study.

3.4.2. Isolation of major compounds with a small portion of hexane extract.

3.4.2.1 Isolation with silica gel column chromatography

A small portion (2.03 g) of the hexane extract was fractionated by column chromatography (column ID 5 cm) on silica gel (35-70 μm, 98.83 g) and was eluted with hexane, hexane-CH_2Cl_2 mixture (9:1, 7:3, 6:4, 5:5, 3:7, 1:9, 5:95), CH_2Cl_2 and methanol. Fractionation was achieved by comparison of each fraction on TLC (hexane-CH_2Cl_2 1:9). Then, 19 fractions were collected (A01-A19). The fractions of interest were isolated by SiO_2 cc with various solvent systems (Scheme 5, Table 10). The isolated compounds had been determined based on spectroscopic data and comparison to the previous data.

Study of fraction A07

The existing stain on the wall of fraction A07 was not dissolve in hexane but had to be dissolved with CH_2Cl_2. After drying, it provided a small white needle crystal that was characterized by spectroscopic data as friedelin (**1**, 8 mg).

Study of fraction A10

Fraction A10 was subjected through silica gel (20-45 μm) cc and eluted with cHex-EtOAc 6:1. A small white crystal of *β*-amyrin (**2**, 20 mg) was found.

Study of fraction A11

Fraction A11 was purified in silica gel (20-45 μm) cc with silica gel cc using cHex-EtOAc (5:1) as eluent. A white powder of *β*-sitosterol (**3**, 35 mg) was obtained.

Study of fraction A17

Fraction A17 (15.1 mg) was purified with a small silica gel (20-45 μm) cc and eluted with cHex – EtOAc 10 : 1 system. Friedelin (**1**, 3 mg) and *epi*friedelanol (**4**, 3 mg) were isolated.

Table 10. Fractionation and isolated compounds from a small portion of *H. odorata* leaves hexane extract.

Fraction	Moble phase (cHex-CH_2Cl_2, %)	Characteristic	Weight (mg)	Isolated compound
A01	100:0	White gel	164.6	
A02	100:0	White oily semisolid	42.3	
A03	100:0 90:10	White crystalline solid	12.7	
A04	70:30	Pale yellow gel	351.1	
A05	70:30	Yellow solid	36.1	
A06	70:30	White + orange solid	24.9	
A07	70:30	Yellow gel	50.6	
		White powder on the surface of tube	10.8	Friedelin (**1**, 8 mg)
A08	60:40	Yellow solid	19.4	
A09	60:40	Yellow solid	53.8	
A10	60:40 50:50	Yellow + orange solid	108.7	*β*-amyrin (**2**, 20 mg)
A11	30:70	Yellow solid + yellow oil	184.4	*β*-sitosterol (**3**, 35 mg)
A12	30:70	Pale green solid	51.8	
A13	30:70	Pale green solid	29.6	
A14	30:70	Green oily solid	48.3	
A15	10:90	Dark green oily solid	77.7	
A16	5:95 0:100	Dark green solid	54.8	
A17	MeOH 100% wash	Dark green + white solid	15.1	Friedelin (**1**, 3 mg) and *epi*friedelanol (**4**, 3 mg)
		White solid on the surface of tube	2.8	
A18	MeOH 100% wash	Dark green oily solid + yellow oil	1.44 gm	
A19	MeOH 100% wash	Pale green solid	13.8	

3.4.2.2. Isolation with sephadex column chromatography

A portion of hexane extract (100 mg) was subjected to sephadex (10 gm sephadex swelled in dichloromethane) cc and eluted with CH_2Cl_2 (Scheme 5). Each fraction was examined on TLC (cH-EtOAc = 5:1). Chlorophyll (green band) and carotene (yellow band) were removed from the column quickly. Continuing collection obtained 12 mg of betulonic acid (**5**) which was further purified by a silica gel cc (cHex-EtOAc = 5:1 as eluent).

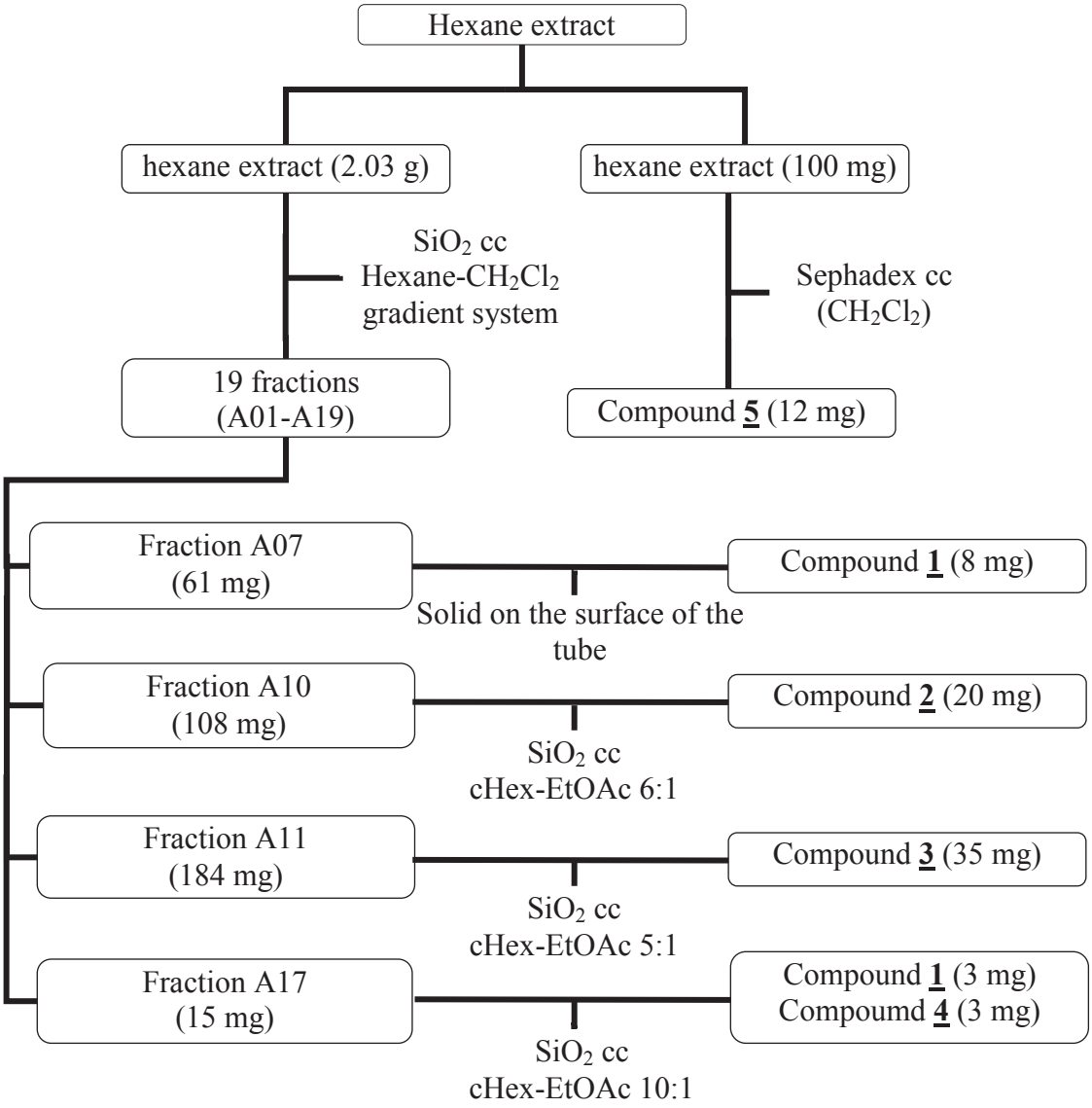

Scheme 5. Isolation of main compounds from *H. odorata* leaves hexane extract.

3.4.3 Isolation of a large portion by MPLC.

The hexane extract of *H. odorata* leaves (10.35 g) was deposited on 10 g dry silica gel and then subjected to medium pressure column chromatography (MPLC) (sample compartment column: ID 3 cm length 25 cm, isolation column: ID 7.5 cm and length 45 cm) over silica gel; eluted with cHex, cHex-CH_2Cl_2 gradient mixture (with 5% increasing in each 500 mL portion), CH_2Cl_2 and methanol. The eluated liquid was collected in 250-ml tubes. The tubes were then combined according to their TLC patterns (system cHex-CH_2Cl_2 20:1 and 10:1) (Scheme 6, Table 11). Then, 24 fractions (B01-B24) were collected. Fraction B11-

B12, B14, B15-B16 and B21 were rechromatographed on silica gel, while B23 was subjected to MPLC (SiO_2) again for more purification (Scheme 7).

Table 11. Fractionation of *H.odorata* leaves hexane extract isolation by MPLC.

Fraction	Mobile phase (cHex-CH_2Cl_2,%)	Weight (mg)	description	Isolated compounds
B01	100-90 : 0-10	92.5	Colorless semisolid	
B02	90 : 10	4.2	Colorless semisolid	
B03	85 : 15	5.3	Colorless semisolid	
B04	80 : 20	6.1	Colorless semisolid	
B05	75 : 25	32.6	Colorless semisolid	
B06	75 : 25	16.9	Orange-brown solid	
B07	75 : 25	10.7	Yellow solid (pink spot on TLC)	
B08	70 : 30	7.7	Yellow solid (pink spot on TLC)	
B09	65 : 35	8.6	Yellow solid	
B10	60 : 40	2.9	Yellow solid	
B11	55 : 45	19.5	Yellow solid	Saturated fatty acid ester of *β*-amyrin (**6**, 25 mg)
B12	55 : 45	30.5	Yellow solid	
B13	50 : 50	7.2	White solid	
B14	50 : 50	217.7	Pale yellow and white solid	Palmitic acid ester of *β*-sitosterol (**7**, 45 mg)
B15	45-40 : 55-60	404.9	Pale green semisolid	Mixture of satd. and unsatd. fatty acid ester of *β*-sitosterol (**8**, 133 mg)
B16	35-30 : 65-70	137.4	Yellow semisolid	Mixture of satd. and unsatd. fatty acid ester of *β*-sitosterol (**8**, 25 mg)
B17	30-25 : 70-75	32	Yellow-white solid	
B18	25-20 : 75-80	70.7	Orange solid	
B19	20-15 : 80-85	94.7	Orange solid	
B20	10-5 : 90-95	152.6	Orange solid	
B21	100% CH_2Cl_2	110.2	Orange white solid	Friedelin (**1**, 10 mg)
B22	100% CH_2Cl_2	318.1	Orange white solid	
B23	100% MeOH	7.43 g	Dark green solid	rechromatograph with MPLC
B24	100% MeOH	0.81 g	Dark green solid	

Study of fraction B11 and B12

Fraction B11 and B12 were pooled (50 mg) and chromatographed over silica gel column and eluted with mixture of cHex- CH_2Cl_2 (10:1). It yielded a white amorphous solid (25 mg) which showed the characteristic of saturated fatty acid ester of *β*-amyrin (**6**, 25 mg) by spectroscopic consideration.

Study of fraction B14

Fraction B14 (217 mg) was submitted through silica gel cc using cHex-EtOAc 80:1 as mobile phase. The elution yielded 155 mg of white solid which was sequentially purified with sephadex column (System: $CHCl_3$-MeOH = 1.5:0.5). A white wax of fatty acid ester of *β*-sitosterol (76 mg) was obtained and then transesterification of the ester was perfomed

Transesterification of fatty acid ester [180]

An aliquot of the ester (45 mg) was refluxed in dry MeOH (20 mL) with sodium methoxide (20 mg) overnight. The reaction product was extracted with H_2O and CH_2Cl_2. The organic phase was separated, dried over Na_2SO_4 and evaporated. Dried CH_2Cl_2 phase was then subjected to silica gel cc using cHex-EtOAc 5:1 as eluent. The eluted compounds were analyzed by GCMS. Methyl ester of saturated fatty acid; palmitic acid (main) with a little of stearic acid, together with *β*-sitosterol were obtained. Then, the main ester was determined as *β*-sitosterol palmitate (**7**).

Study of fraction B15

Fraction B15 (404 mg) was submitted to cc on SiO_2 eluted with cHex/EtOAc (80:1). The fractions were grouped. The fraction of interest was sequentially submitted to purification through sephadex column using $CHCl_3$-MeOH = 1.5:0.5 as moblile phase and gave fatty acid ester compound **8** (133 mg). Transesterification (as same as fraction B14) followed by identification with GC-MS of compound **8** gave *β*-sitosterol (**7**) and the mixture of saturated fatty acid (palmitic acid) and unsaturated fatty acid (linoleic and oleic acid). The result was in agreement with NMR determination.

Study of fraction B16

Fraction B16 (137 mg) was further purified by SiO_2 cc using cHex/EtOAc (70:1) system as mobile phase. After fractionation, the first isolated fraction (25 mg) gave the same pattern of ^1H NMR and HSQCedit spectrum as compound **8** from fraction B15.

Study of fraction B21

Fraction B21 (110 mg) was submitted through column chromatography on silica gel using cychlohexane-CH_2Cl_2 1:2 as mobile phase. The elution yielded 10 mg small white needle crystal of friedelin (**1**).

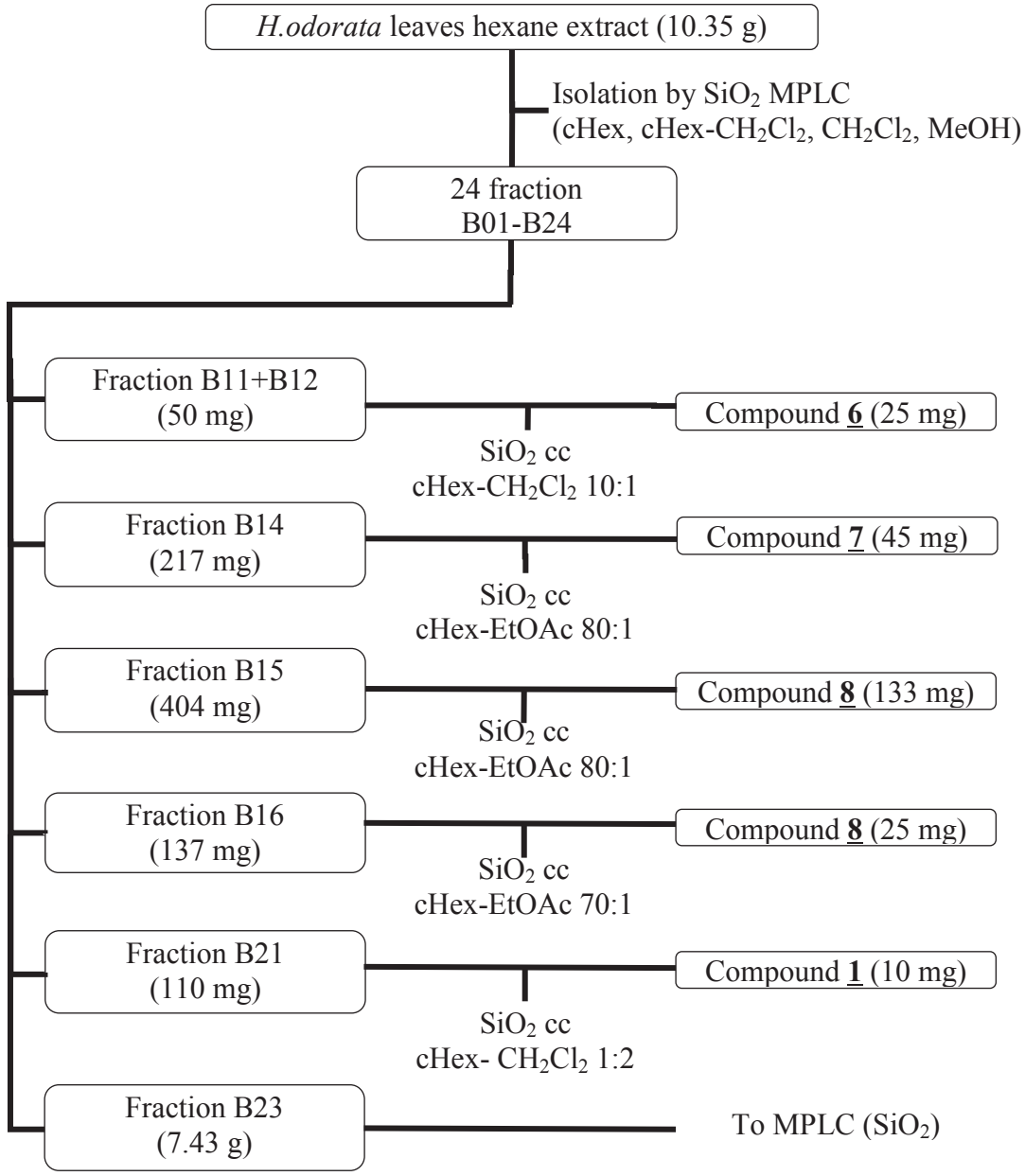

Scheme 6. Isolation of *H.odorata* leaves extract by MPLC (SiO_2).

3.4.4 Purification of fraction B23

Fraction B23 (7.28 g) was deposited on 7 g dry silica gel and was isolated over silica gel medium pressure liquid chromatography (MPLC) (column for sample compartment 3 cm ID, 10 cm length and isolation column 7.5 cm ID and 45 cm length), which was

successively eluted with dichloromethane, dichloromethane-ethyl acetate gradient mixtures, ethyl acetate and methanol (Scheme 7, Table 12). The flow rate of applied eluent was set at 50 mL/min. Then, 48 fractions were collected based on TLC patterns using system hexane-dichloromethane (1:10) and hexane-ethyl acetate (5:2). The results of the chromatography were shown in Table 12. Crystals of *β*-Sitosterol (**3**, 324 mg) and betulonic acid (**5**, 424 mg) were obtained from fraction C12 and C22-C25, respectively.

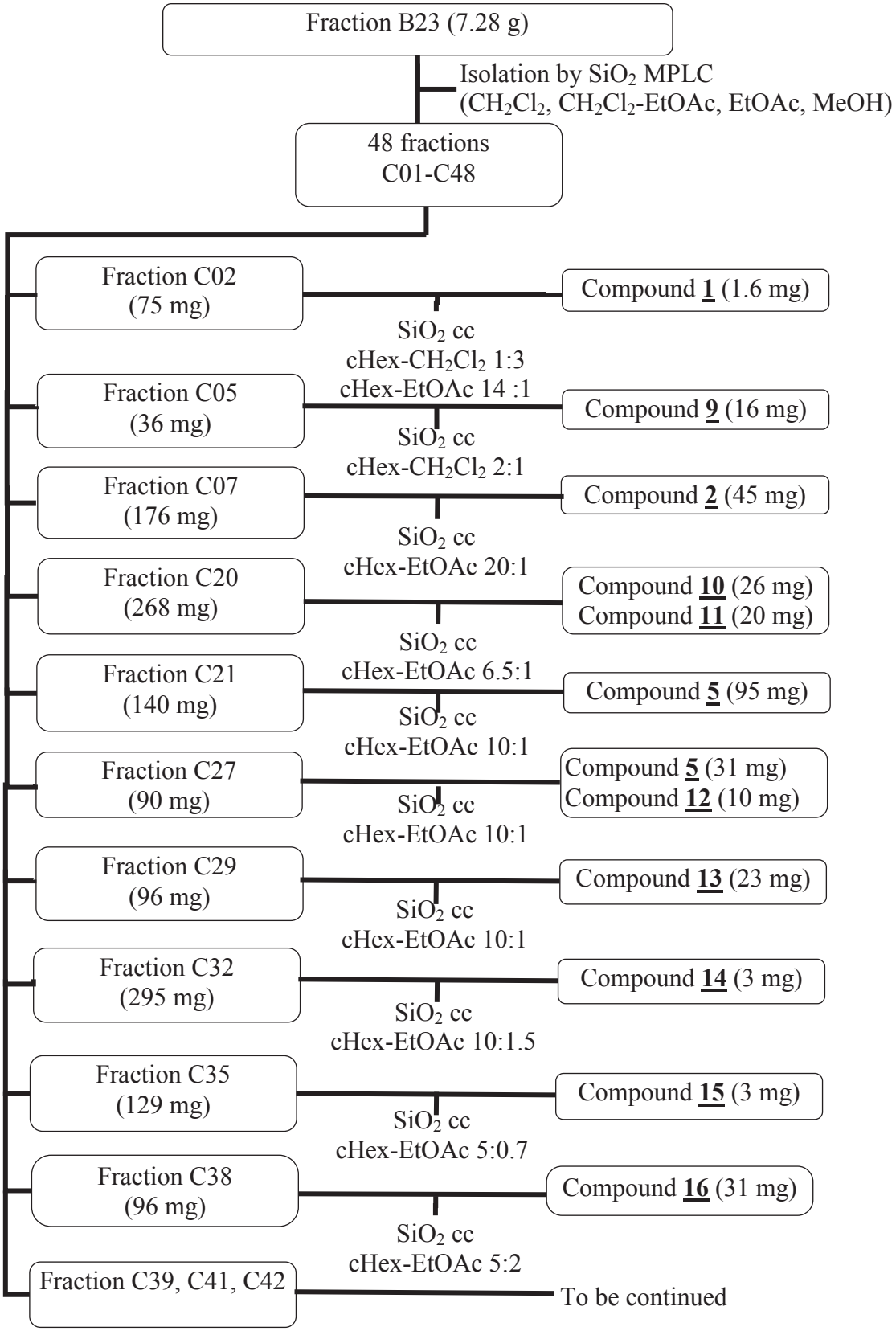

Scheme 7. Further purification of fraction B23

Table 12. Fractionation of Fraction B23 isolated by MPLC

Fraction	Eluent (CH_2Cl_2-EtOAc,%)	Weight (mg)	Isolated compounds
C01	100 : 0	39.7	
C02	100 : 0	75.8	Friedelin (**1**, 1.6 mg)
C03	100 : 0	56.4	
C04	100 : 0	37.7	
C05	100 : 0	36.8	(-)-caryophyllene oxide (**9**, 16 mg)
C06	100 : 0	52.9	
C07	100 : 0	176.9	β-amyrin (**2**, 45 mg)
C08	100 : 0	38.4	
C09	100 : 0	31.9	
C10	100 : 0	125.6	
C11	100 : 0	23.7	
C12	100 : 0	324.5	β-sitosterol (**3**, 324 mg)
C13	100 : 0	14.1	
C14	100 : 0	25.1	
C15	100 : 0	97	
C16	98 : 2	65	
C17	98 : 2	87.9	
C18	98 : 2	128.2	
C19	98 : 2	198.4	
C20	98 : 2	268.1	*Epi*betulinic acid (**10**, 26 mg) Betulone (**11**, 20 mg)
C21	98 : 2	140.0	Betulonic acid (**5**, 95 mg)
C22	98 : 2	327.3	Betulonic acid (**5**, 424 mg)
C23	98 : 2	11.3	
C24	96 : 4	44.2	
C25	96 : 4	41.5	
C26	96-94 :4-6	43.4	
C27	94 : 6	96.2	Betulonic acid (**5**, 31 mg) 30-hydroxy-3-oxolup-20(29)-ene (**12**, 18 mg)
C28	92-90 : 8-10	167.7	
C29	90 : 10	96.6	Betulinic acid (**13**, 20 mg)
C30	90 : 10	67.7	
C31	90-88 : 10-12	61.3	
C32	90-86 : 10-14	295	3,30-dioxo-lup-20(29)-en-28-oic acid (**14**, 3 mg)*
C33	86-84 : 14-16	174.4	
C34	84 : 16	99.3	
C35	84-82 : 16-18	129.2	Mangiferonic acid (**15**, 3.7 mg)
C36	80 : 20	77.6	
C37	80-75 : 20-25	96.8	
C38	75-70 : 25-30	96.9	28,30-dihydroxy-3-oxolu-20(29)-ene (**16**, 31 mg)**

Table 12. Fractionation of Fraction B23 isolated by MPLC (continued)

Fraction	Eluent (CH_2Cl_2-EtOAc)	Weight (mg)	Isolated compounds
C39	70-65 : 30-35	218.2	C-26 fatty acid ester of 24,25,26-trihydroxy-3,4-*seco*-cycloart-4(29)-en-3-oic acid (**18**, 3 mg)*** Messagenic acid G (**17**, 12 mg)**
C40	65 : 35	123.1	
C41	60-55 : 40-45	228.7	**18** (10 mg) **18**+**19** (C-24 fatty acid ester of 24,25,26-trihydroxy-3,4-*seco*-cycloart-4(29)-en-3-oic acid) (32 mg) **18**+**20** (3,4-*seco*-cycloart-4(29), 24-diene-3,26-dioic acid) (64 mg)
C42	55-25 : 45-75	324.3	**18** (3.8 mg) **19** (only a little) *** **20** (only a little) **19**+**20** (26 mg)
C43	25-20 : 75-80	52.6	
C44	20-0 : 80-100	229.5	
C45	100-97 : 0-3 EtOAc : MeOH (from this fraction)	134.0	
C46	97-95 : 33-5	178.1	
C47	95-93 : 5-7	220.3	
C48	90-60 : 10-40	443.3	

* the compound found for the first time in the nature.
** the compounds whose complete NMR data were first reported.
*** New compounds.

Study of fraction C02

Fraction C02 (75 mg) was further rechromatographed over SiO_2 cc with cHex-CH_2Cl_2 (1:3) and further purified using SiO_2 cc. Elution with cHex-EtOAc (14:1) yielded friedelin (**1**, 1.6 mg)

Study of fraction C05

Fraction C05 (36 mg) was subjected to SiO_2 cc using cHex-CH_2Cl_2 (2:1) system as eluent. After elution, caryophyllene oxide (**9**, 16 mg) was obtained.

Study of fraction C07

Fraction C07 (176 mg) was resubmitted through column chromatography on silica gel (cHex-EtOAc 20:1). The elution yielded 45 mg *β*-amyrin (**2**).

Study of fraction C20

Fraction C20 (268 mg) was chromatographed over silica gel (cHex-EtOAc 6.5:1) and yielded *epi*betulinic acid (**10**, 26 mg) and betulone (**11**, 20 mg).

Study of fraction C21

Fraction C21 (140 mg) was further purified by SiO_2 cc using the mixture of cHex-EtOAc 10:1 as eluent to obtain betulonic acid (**5**, 95 mg).

Study of fraction C27

Fraction C27 (90 mg) was chromatographed over SiO_2 cc and eluted with the mixture of cHex-EtOAc 10:1 to yield betulonic acid (**5**, 31 mg) and 30-hydroxy-3-oxolup-20(29)-ene (**12**, 18 mg).

Study of fraction C29

Further separation of fraction C29 (96 mg) by SiO_2 cc (cHex-EtOAc 10:1) provided betulinic acid (**13**, 20 mg).

Study of fraction C32

Compound **14** (3,30-dioxo-lup-20(29)-en-28-oic acid, 3 mg) was crystallized after successive chromatography of fraction C32 (295 mg) over SiO_2 cc with system cHex-EtOAc 10:1.5.

Partial systhesis of 14 Selective SeO_2 allylic oxidation of **5**, as previously described by F.A. Macias et al [181, 182], afforded compounds **14** and **17** in 22 and 29% yield, respectively. Briefly, **5** (28 mg) was stirred in 20 ml $CHCl_3$, (3 mM), with 1.6 mg of SeO_2, and 0.05 ml of *tert*-butyl hydroperoxide (*t*-ButOOH) during 24 hr at room temperature. The crude reaction was filtered and washed through silica gel using $CHCl_3$, and EtOAc. Polar EtOAc fraction was then purified using silica gel cc. The elution was begun with the system cHex-EtOAc 10:1 and followed by 5:2.

Study of fraction C35

Fraction C35 (129 mg) afforded compound **15** (mangiferonic acid, 3 mg) by further purification with silica gel cc eluting with system cHex-EtOAc 5:0.7.

Study of fraction C38

From fraction C38 (96 mg), repeating purification on SiO_2 cc with cHex-EtOAc 5:2 obtained green oil of 28,30-dihydroxy-3-oxolup-20(29)-ene (**16**, 31 mg).

Study of fraction C39

Fraction C39 (218 mg) was applied to a silica gel cc and eluted with cHex-EtOAc gradient system to give 30 subfractions (C39-01 to C39-30) in increasing polarity (Scheme 8). Subfraction C39-24 and C39-25 were combined and further purified by SiO_2 cc with cHex-EtOAc 2:1 system to obtained messagenic acid (**17**, 12 mg). Subfraction C39-18 and C39-19 were pooled and subjected to SiO_2 cc with cHex-EtOAc 5:1 to yield 26-fatty acid ester of (24*S*,25*S*)-24,25,26-trihydroxy-3,4-*seco*-cycloart-4(29)-en-3-oic acid (**18**, 3 mg).

Study of fraction C41

Fraction C41 (228 mg) was rechromatographed over a silica gel cc and eluted with cHex-EtOAc gradient system to obtain 10 mg of **18**, **19** (very few amount), 32.8 mg of the mixture of **18** and **19** (24-fatty acid ester of (24*S*,25*S*)-24,25,26-trihydroxy-3,4-*seco*-

cycloart-4(29)-en-3-oic acid), and 64.5 mg of the mixture of **18** and **20** ((24*E*)-3,4-*seco*-cycloart-4(29),24-diene-3,26-dioic acid) (Scheme 9).

Methylation of the mixture of 18+19 This mixture was dissolved in 3.5 mL anhydrous DMF under argon in a 10-mL flask. Sodium bicarbonate (2 eq, 0.2 mmol, 16.8 mg) was added. Methyl iodide (3 eq, 28.4 mg, 12.5 µL) was added dropwise at room temperature and magnetic stirring was maintained 24 h. The reaction could be monitored by TLC (cHex-EtOAc 2:1). After this period, 10 mL EtOAc and 5 mL of distilled water were added. The organic phase was separated. The residual aqueous phase was extracted with 10 mL EtOAc (2 times). The organic phases were combined and washed with distilled water (2 x 5mL), then dried over $MgSO_4$, filtered and evaporated under reduced pressured [183]. The residue was chromatographed on silica gel cc (cHex-EtOAc 5:1) to isolate 3-methyl ester of compound **18** (=**18a**) and 3-methyl ester of **19** (=**19a**). The NMR experiments of both compounds were performed.

Hydrolysis of 18a In a 10 mL flask, compound **18a** (10.4 mg) was dissolved in 3 mL of anhydrous dichloromethane. A small catalytic amount of sodium methoxide (2 mL) was added to the solution. The reaction mixture was stirred and refluxed for 4 h at 50°C. The reaction was monitored by TLC (cHex-EtOAc 2:1). The solvent was evaporated under vacuum. The residue was dissolved in CH_3COOH-H_2O 3:1. The reaction products were extracted with CH_2Cl_2 to obtain a mixture of two acids. The solvent was again evaporated under vacuum. To isolate 2 compounds, the mixture was extracted with MeOH-H_2O (3:1) and cHex. Methyl arachidate and (24*S*,25*S*)-24,25,26-trihydroxy-3,4-*seco*-cycloart-4(29)-en-3-oic acid (=**18b**) were obtained.

Methylation of the mixture of 18+20 Methylation was performed as aboved procedure. The reaction products were isolated by silica gel cc (cHex-EtOAc 5:1) to obtain 3-methyl ester of **18** (**18a**, 19 mg) and 3,26-dimethyl ester of **20** (**20a**, 6 mg). Compound **18a** was reacted with MTPA to determine the absolute configuration (Scheme 10) whereas compound **20a** was pooled with **20a** from fraction C42 and saponified for structural elucidation (Scheme 12)

Preparation of (*R*)- and (*S*)-MTPA ester of 18a. Compound **18a** was dissolved in 0.5 mL anh CH_2Cl_2. Then, 1.36 mg triethyl amine (Et_3N, 2µL), 4.6 mg 4-dimethylaminopyridine (4-DMAP) and 5.36 mg (+)-*S*-MTPA-Cl (4 µL) were subsequently added. The reaction mixture was stirred at room temperature under nitrogen for 24 h (Scheme 10). The reaction was monitored by TLC (cHex-EtOAc 5:1). The solvent was evaporated under vacuum system and the residue was chromatographed on a SiO_2 cc (cHex-EtOAc 9:1) to isolate (*R*)-MTPA ester of **18a**. Reaction of **18a** with 5.36 mg (-)-*R*-MTPA-Cl (4 µL) according to the same procedure yielded the (*S*)-MTPAester of **18a** [168, 184]. The absolute stereostructure of **18a** was determined by the application of modified Mosher's method. The proton chemical shift differences of both esters ($\Delta\delta=\delta_S-\delta_R$) at adjacent positions to C-24 were measured (Table 14).

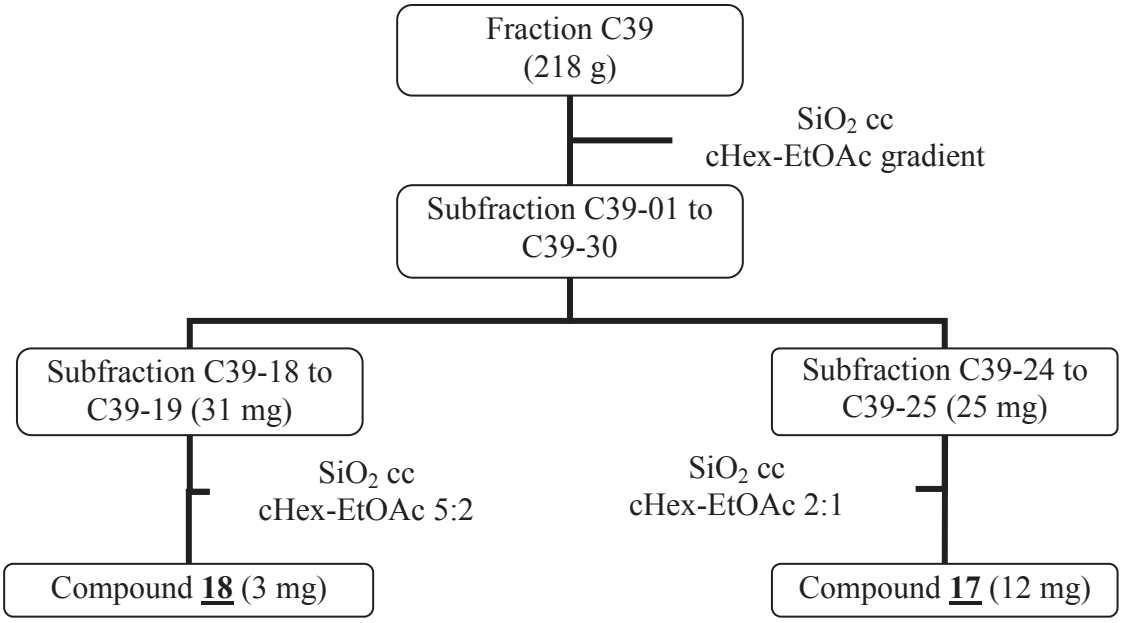

Scheme 8. Further purification of Fraction C39

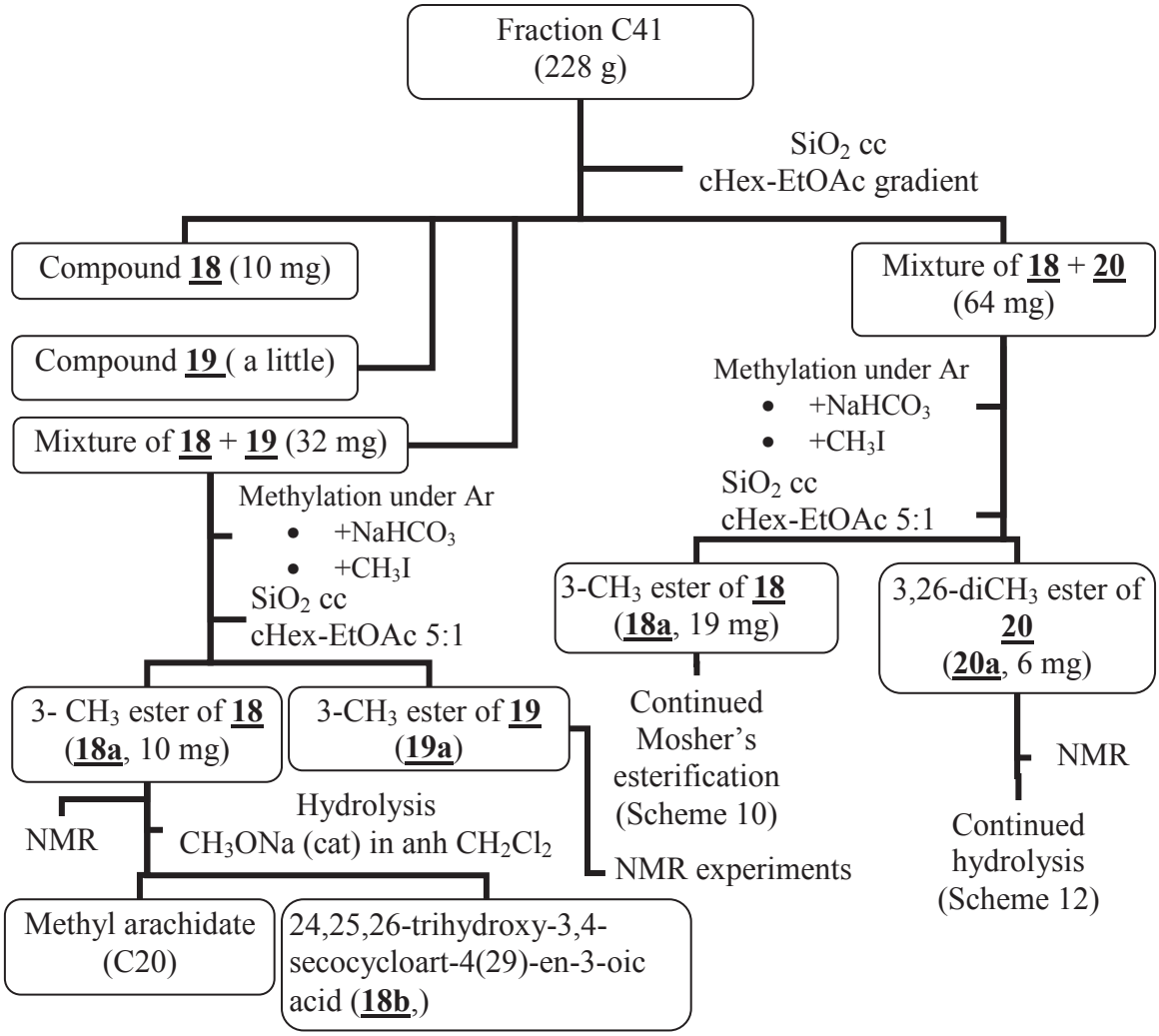

Scheme 9. Purification of fraction C41

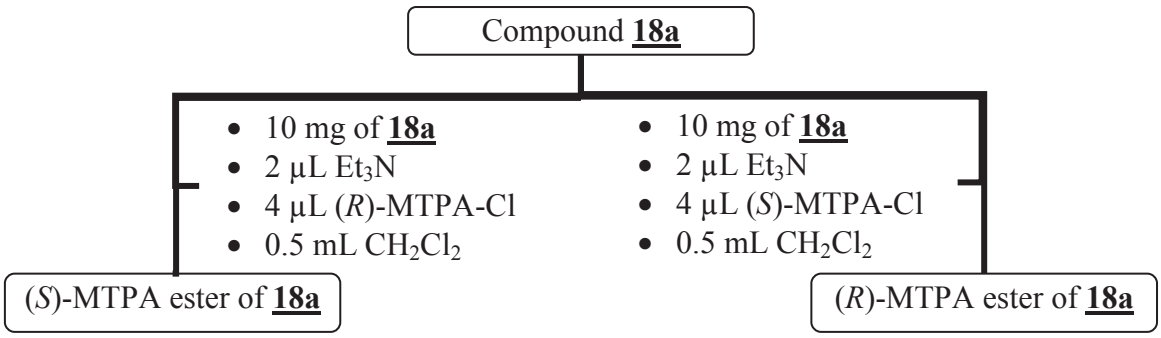

Scheme 10. Mosher's esterification of compound **18a**

Study of fraction C42

Fraction C42 (280 mg) was subjected over a silica gel cc (Scheme 11). After elution with cHex-EtOAc gradient system, 3.8 mg of **18**, **19** (very few amount), **20** (a few amount) and 26.7 mg of the mixture of **19** and **20** were obtained.

Methylation of the mixture of 19 + 20 The same reaction as of the mixture of **18** + **19** was performed. The reaction products were isolated over a silica gel cc with cHex-

EtOAc 5:1 to give 3-methyl ester of **19** (**19a**, 7.5 mg) and 3,26-dimethyl ester of **20** (**20a**, 4.4 mg).

Hydrolysis of 20a. Within a 10-mL flask, 3,26-dimethyl ester of **20** (=**20a**) from fraction C41 and C42 were pooled and dissolved in 3 mL of THF-H_2O (1:2) with a small amount of $LiOH.H_2O$ (3 mg) as a catalyst (Scheme 12). The reaction was stirred for 24 h at room temperature under N_2. The reaction was monitored via TLC (cHex-EtOAc 2 :1). The products were neutralized by 3%HCl to pH6, then extracted with EtOAc. The solvent was evaporated by reduced pressure to give **20** (8 mg).

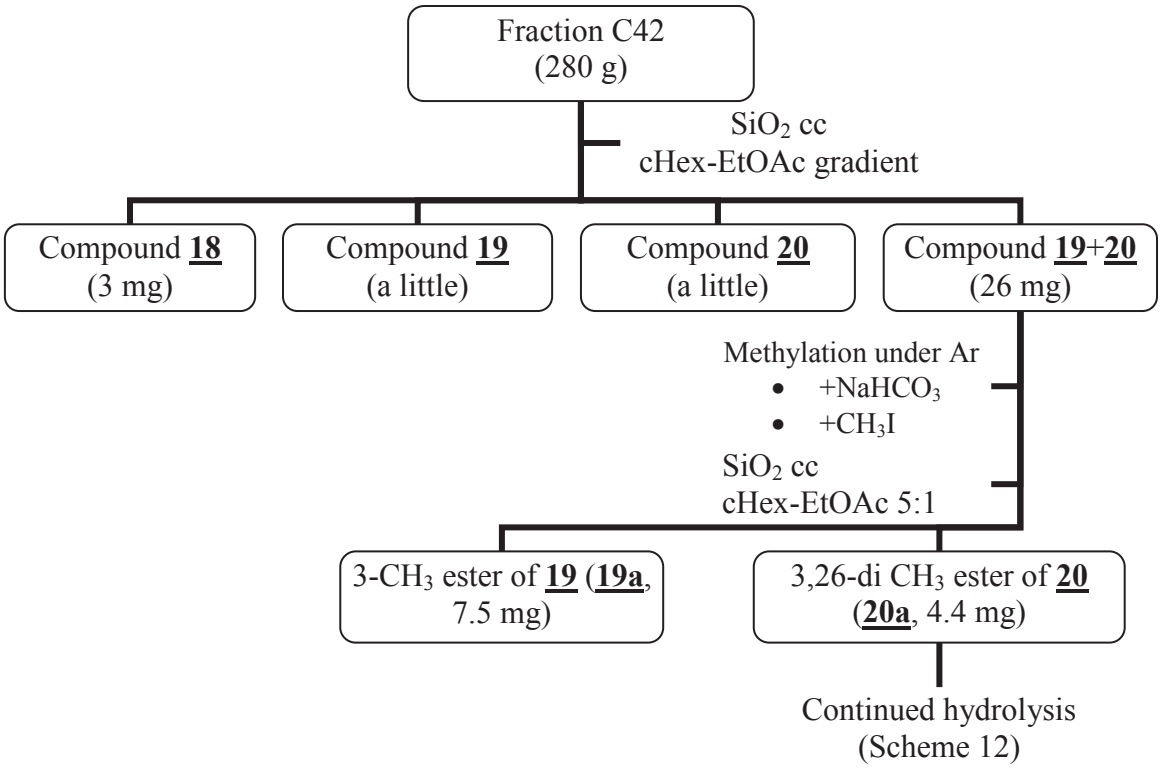

Scheme 11. Purification of fraction C42

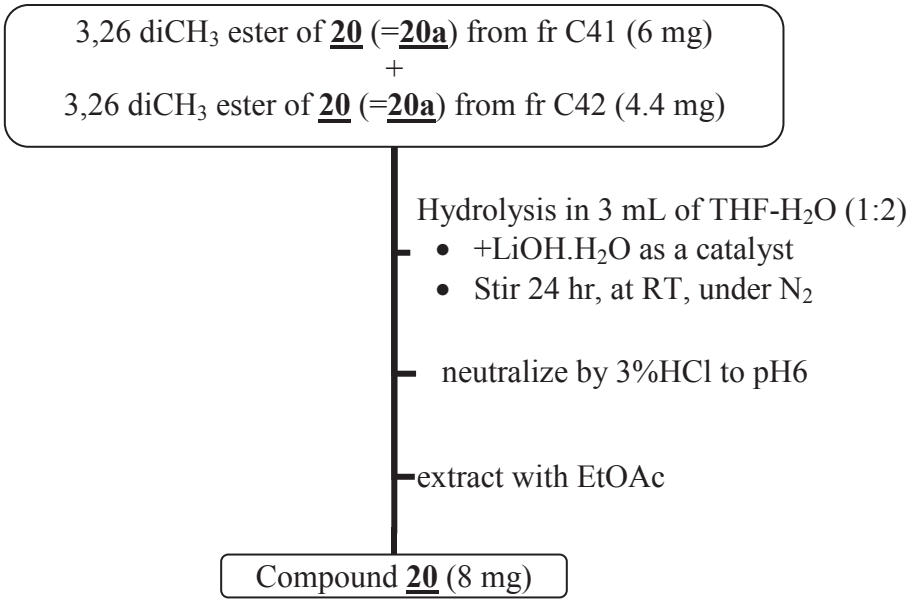

Scheme 12. Hydrolysis of **20a** from fraction C41 and C42

3.5 CYTOTOXIC EVALUATION OF 8 ISOLATED LUPANES.

The effect of the isolated lupanes on various cell lines was evaluated using WST-1 method (Table 13). The assay principle is based upon the reduction of the tetrazolium salt WST-1 to formazan by cellular mitochondrial succinate tetrazolium reductase. Difference cell lines; prostate cancer cell line (PC3), human breast adenocarcinoma cell line (MDA-MB-231), colorectal adenocarcinoma cell line (HT-29) and colorectal carcinoma cell line (HCT 116), were selected and seeded onto 96-well plates at a cell density of 5,000 cells/well in 5% CO_2 incubator at 37°C. After 24 h incubation, cells were exposed to various concentrations of compound **5**, **10**, **11**, **12**, **13**, **14**, **16** and **17** (3 wells for each dilution) for 24 h. Then, the tetrazolium salt WST-1 solution was added and cultured for further 4 h. To determine the cell survival, Optical Density (OD) was measured with a Bio-Rad Coda microplate analyzer at a wavelength of 450 nm (reference wavelength: 600 nm). Cisplatin was used as a positive control. Results in Table 13 were expressed as IC_{50}, the concentration required for 50% inhibition cell growth of treated cells compared to untreated controls.

Statistical analysis: IC_{50} are shown as mean ± standard deviation (SD) of triplicates from each independent experiment. Cell proliferation form WST-1 activities were analyzed using the student's t-test. P-values less than 0.05 were considered statistically significant.

Table 13. Cytotoxic activity against HCT116, HT29, MDA-MB231 and PC3 cell lines

Cpd	IC_{50} (µM)[a]			
	HCT 116[b]	HT-29[c]	PC3[d]	MDA-MB-231[e]
5	85.60±37.61*	/[f]	139.00±3.64*	/[f]
13	/[f]	/[f]	>500	/[f]
10	/[f]	/[f]	/[f]	/[f]
11	/[f]	/[f]	>300	/[f]
12	/[f]	/[f]	/[f]	/[f]
14	/[f]	/[f]	282±17.78*	/[f]
16	/[f]	/[f]	/[f]	/[f]
17	43.50±16.26*	/[f]	>500	/[f]
cisplatin	4.74±2.01	17.50±17.87	19.93±10.30	21.20±23.36

[a] Concentration required for 50% cell growth inhibition. Determined according to WST-1 method, [b]colorectal carcinoma cell line, [c] colorectal adenocarcinoma cell line, [d]human prostate cancer cell line, [e]human breast adenocarcinoma cell line, [f]Inactive compounds: less than 50% inhibition at the threshold concentration of 200 µg/mL. * P-values less than 0.05 compared between tested compound and cisplatin.

3.6 PHYSICAL CHARACTERISTICS AND SPECTRUM OF ISOLATED COMPOUNDS

Friedelin (1) [185, 186]

Molecular formula	$C_{30}H_{50}O$	**MW**	426.72
Description	small needle white crystal		
Retention factor	R_f =0.65 (cHex-EtOAc =5:1)		
Specific rotation	$[\alpha]_D^{23}$ -21 ($CHCl_3$, *c* 0.3) (lit.[186] -21.5 ($CHCl_3$, *c*=1, 22 ^oC))		
IR spectrum	ν_{max} (film) 2926, 2862, 1715, 1389 cm^{-1}		
Mass spectrum	GC-EI-MS	*m/z*: 426 $[M]^+$, 273, 205, 125, 123, 109	
	ESI-MS (ES+)	*m/z*: 449 $[M+Na]^+$, 413, 236	
NMR spectrum	^1H– and ^{13}C NMR– see Table 14		

β-amyrin (2) [187]

Molecular formula	$C_{30}H_{50}O$	**MW**	426.72
Description	a small white crystal		
Retention factor	R_f =0.41 (cHex-EtOAc 5:1)		
Specific rotation	$[\alpha]_D^{20}$ +47.87 ($CHCl_3$, *c* 0.175)		
IR spectrum	ν_{max} (film) 3353, 2917, 2844, 1463, 1385, 1035, 759 cm^{-1}		
Mass spectrum	GC-EI-MS	*m/z* : 426 $[M]^+$, 218 (100%), 203	
NMR spectrum	^1H– and ^{13}C NMR– see Table 15		

β-sitosterol (3) [188]

Molecular formula	$C_{29}H_{50}O$	**MW**	414.72
Description	white powder		
Retention factor	R_f = 0.20 (cHex-EtOAc =5:1)		
Specific rotation	$[\alpha]_D^{20}$ -14.44 ($CHCl_3$, *c* 0.18)		
IR spectrum	ν_{max} (film) 3390, 2934, 2864, 1464, 1378, 1061, 757 cm^{-1}		
Mass spectrum	ESI-MS	*m/z* (ES+): 437 $[M+Na]^+$	
	GC-EI-MS *m/z*: 414$[M]^+$, 396, 381, 329, 303, 273, 255, 213		
NMR spectrum	^1H– and ^{13}C NMR– see Table 16		

*Epi*friedelanol (4) [189, 190]

Molecular formula	$C_{30}H_{52}O$	**MW**	428.73
Description	white needle crystal		
Retention factor	R_f =0.21 (cHex-EtOAc =5:1)		
Specific rotation	$[\alpha]_D^{20}$ +4 ($CHCl_3$, *c* 0.025)		
IR spectrum	ν_{max} (film) 2921, 2844 cm^{-1}		
Mass spectrum	GC-EI-MS *m/z*: 428 $[M]^+$, 413, 275, 165, 125, 109, 96, 95		
NMR spectrum	^1H– and ^{13}C NMR– see Table 14		

Betulonic acid (5) [129]

Molecular formula	$C_{30}H_{46}O_3$ **MW** 454.68
Description	white crystal
Retention factor	R_f=0.22 (cHex-EtOAc =5:1) R_f=0.61 (cHex-EtOAc =5:2)
Specific rotation	$[\alpha]_D^{20}$ +12.22 ($CHCl_3$, *c* 0.09) (lit.[129] +40.1 ($CHCl_3$, *c* 0.86))
IR spectrum	ν_{max} (film) 3120, 3066, 2917, 2849, 2863, 1703, 1694 cm^{-1}
Mass spectrum	ESI-MS *m/z* (ES-) : 453 $[M-H]^-$, 255
NMR spectrum	^1H NMR - see Table 17, ^{13}C NMR – see Table 19

Saturated fatty acid ester of β-amyrin (6)

Description	white amorphous solid
NMR spectrum	^{13}C NMR– see Table 15

β-Sitosterol palmitate (7)

Description	white wax		
Mass spectrum	GC-EI-MS	palmitic acid, methyl ester	*m/z* 270 $[M]^+$
		β-sitosterol	*m/z* 414 $[M]^+$
NMR spectrum	^{13}C NMR– see Table 16		

Saturated and unsaturated fatty acid ester of β-sitosterol palmitate (8)

Description	white wax	
Mass spectrum	GC-EI-MS of methyl acid ester after transesterification	
	Palmitic acid, methyl ester	*m/z* 270 $[M]^+$
	Linoleic acid (18:2), methyl ester	*m/z* 294 $[M]^+$
	Oleic acid (18:1), metyl ester	*m/z* 296 $[M]^+$
NMR spectrum	^{13}C NMR– see Table 16	

Caryophyllene oxide (9) [58, 191, 192]

Molecular formula	$C_{15}H_{24}O$ **MW** 220.35
Description	yellow oil
Retention factor	R_f=0.42 (cHex-EtOAc =10:1) R_f=0.15 (cHex-CH_2CL_2 =1:1)
Specific rotation	$[\alpha]_D^{20}$ -34.83 ($CHCl_3$, *c* 0.29) (lit.[58] -46.40 ($CHCl_3$, *c* 5.60, 29°C))
IR spectrum	ν_{max} (film) 3066 (=CH_2), 2960, 2856, 1732, 1456, 1289, 1123(C-O), 1073 (C-O), 743 cm^{-1}
Mass spectrum	GC-EI-MS *m/z*: 220 $[M]^+$, 109, 93, 79 (100%)
NMR spectrum	^1H– and ^{13}C NMR– see Table 21

***Epi*betulinic acid (<u>10</u>)** [81, 84, 113, 127, 185, 193] and **betulinic acid (<u>13</u>)** [39, 47, 84, 111]

	*Epi*betulinic acid (10)	Betulinic acid (13)
Molecular formula (MW)	$C_{30}H_{48}O_3$ (456.71)	$C_{30}H_{48}O_3$ (456.71)
Description	White solid	White crystal
Retention factor	R_f=0.50 (cHex-EtOAc =5:2)	R_f=0.40 (cHex-EtOAc =5:2)
Specific rotation	$[\alpha]_D^{20}$ -3.33 ($CHCl_3$,*c* 0.09) (lit.[113] -11 (*c* 0.2, 26°C))	$[\alpha]_D^{20}$ +2.67 ($CHCl_3$, *c* 0.075) (lit.[39] +13 ($CHCl_3$, 26°C))
IR spectrum	ν_{max} (film) 3700-2500 (br), 3428, 3069, 2914, 2844, 1700, 1459, 1295, 762 cm^{-1}	ν_{max} (film) 3600-2500 (br), 3466, 3069, 2926, 2851, 1687, 1455 cm^{-1}
Mass spectrum	ESI- *m/z* (ES-) : 455 $[M-H]^-$	ESI- *m/z* (ES-) : 455 $[M-H]^-$
NMR spectrum	^1H NMR - see Table 17, ^{13}C NMR – see Table 19	

Betulone (<u>11</u>) [125, 194, 195]

Synonym 3-oxobetulin
Molecular formula $C_{30}H_{48}O_2$ **MW** 440.71
Description white wax
Retention factor R_f=0.47 (cHex-EtOAc =5:2)
Specific rotation $[\alpha]_D^{20}$ +21.67 ($CHCl_3$, *c* 0.12) (lit.[125] +52.7 ($CHCl_3$, *c* 0.3, 25°C))
IR spectrum ν_{max} (film) 3435, 3065, 2917, 2847, 1705, 1463, 1376, 1025 cm^{-1}
Mass spectrum ESI-MS *m/z* (ES+) : 463 $[M+Na]^+$
NMR spectrum ^1H NMR - see Table 17, ^{13}C NMR – see Table 19

30-Hydroxy-3-oxolup-20(29)-ene (<u>12</u>) [92, 98]

Molecular formula $C_{30}H_{48}O_2$ **MW** 440.71
Description white wax
Retention factor R_f=0.42 (cHex-EtOAc =5:2)
Specific rotation $[\alpha]_D^{20}$ +14.44 ($CHCl_3$, *c* 0.18) (lit.[98] +20 ($CHCl_3$, *c* 0.26))
IR spectrum ν_{max} (film) 3448, 3085, 2937, 2851, 1705 cm^{-1}
Mass spectrum ESI-MS *m/z* (ES+) : 463 $[M+Na]^+$
NMR spectrum ^1H NMR - see Table 17, ^{13}C NMR – see Table 19

3,30-Dioxolup-20,29-en-28-oic acid (<u>14</u>)* [181]

Molecular formula $C_{30}H_{44}O_4$ **MW** 468.68
Description colorless crystal
Retention factor R_f=0.42 (cHex-EtOAc =5:2)
Specific rotation $[\alpha]_D^{20}$ +30.63 ($CHCl_3$, *c* 0.18) (lit.[181] +16 ($CHCl_3$, *c* 0.08))

IR spectrum	ν_{max} (film) 3700-2500 (br), 3069, 2924, 2845, 1731, 1685, 1463, 1276 cm^{-1}
Mass spectrum	ESI-MS *m/z* (ES-) : 467 $[M-H]^-$
	HRESI-MS m/z (ES-) : 467.3146 ($C_{30}H_{43}O_4$ calc. 467.3161)
NMR spectrum	^1H NMR - see Table 18, ^{13}C NMR – see Table 19

Mangiferonic acid (<u>15</u>) [49, 196, 197]

Molecular formula	$C_{30}H_{46}O_3$ **MW** 454
Description	white wax
Retention factor	R_f =0.48 (cHex-EtOAc =2:1)
Specific rotation	$[\alpha]_D^{20}$ +8.89 ($CHCl_3$, *c* 0.225)
IR spectrum	ν_{max} (film) 3700-2500 (br), 2925, 2854, 1708, 1464, 1281 cm^{-1}
Mass spectrum	ESI-MS *m/z* (ES-) : 453 $[M-H]^-$
NMR spectrum	^1H and ^{13}C NMR – see Table 22

28,30-Dihydroxylup-20(29)-en-3-one (<u>16</u>)** [91]

Molecular formula	$C_{30}H_{48}O_3$ **MW** 456.71
Description	green oil
Retention factor	R_f =0.29 (cHex-EtOAc =1:1)
Specific rotation	$[\alpha]_D^{20}$ +3.03 ($CHCl_3$, *c* 0.33) (lit.[95]+7.6 (MeOH, *c* 0.19))
IR spectrum	ν_{max} (film) 3434, 2937, 1698, 1456 cm^{-1}
Mass spectrum	ESI-MS *m/z* (ES+) : 479 $[M+Na]^+$
NMR spectrum	^1H NMR - see Table 18, ^{13}C NMR – see Table 19

Messagenic acid G (<u>17</u>)** [181]

Synonym	30-hydroxy-3-oxolup-20(29)-en-28-oic acid
Molecular formula	$C_{30}H_{46}O_4$ **MW** 470.70
Description	amorphous solid
Retention factor	R_f =0.40 (cHex-EtOAc =1:1)
Specific rotation	$[\alpha]_D^{20}$ +14.29 ($CHCl_3$, *c* 0.14) (lit.[181] +22 ($CHCl_3$, *c* 0.50))
IR spectrum	ν_{max} (film) 3700-2500 (br), 3074, 2938, 2864, 1695 cm^{-1}
Mass spectrum	ESI-MS *m/z* (ES-) : 469 $[M-H]^-$
NMR spectrum	^1H NMR - see Table 18, ^{13}C NMR – see Table 19

26-Arachidic acid ester of (24*S*,25*S*)-24,25,26-trihydroxy-3,4-*seco*-cycloart-4(29)-en-3-oic acid (<u>18</u>)***

Molecular formula	$C_{50}H_{88}O_6$ **MW** 785.23
Description	White semisolid
Retention factor	R_f =0.68 (cHex-EtOAc =1:1)
Specific rotation	$[\alpha]_D^{20}$ +26.32 ($CHCl_3$, *c* 0.19)

IR spectrum ν_{max} (film) 3700-2500 (br), 2924, 2854, 1713, 1456, 1376 cm^{-1}

Mass spectrum HRESI-MS *m/z* (ES+) : 807.6495 ($C_{50}H_{88}O_6$+Na calc 807.6479)
HRESI-MS *m/z* (ES+) triterpene after transesterification **18b** :
513.3572 ($C_{30}H_{50}O_5$+Na calc 513.3556)

NMR spectrum ^{1}H NMR - see Table 23, ^{13}C NMR – see Table 24

3-Methyl ester of 18 (=18a)

Specific rotation $[\alpha]_D^{20}$ +74 ($CHCl_3$, 0.10)

IR spectrum ν_{max} (film) 3700-2500 (br), 2924, 2861, 1740, 1457 cm^{-1}

NMR spectrum ^{1}H NMR - see Table 23, ^{13}C NMR – see Table 24

Table 14. The ^{1}H NMR data for (*S*)-MTPA and (*R*)-MTPA ester of compound **18a**

Position	(*S*)-MTPA ester	(*R*)-MTPA ester	$\Delta\delta=\delta_S-\delta_R$ (ppm)
H-20	1.4012	1.3976	+0.0036
H-21	0.8400	0.8392	+0.0008
H-22a	1.4800	1.3741	+0.1059
H-22b	1.0000	1.0000	0.0000
H-26a	3.9782	4.3252	-0.3470
H-26b	3.8741	4.1466	-0.2725
H-27	1.1620	1.2041	-0.0421

3-Methyl ester of 24-Stearic acid ester of (24*S*,25*S*)-24,25,26-trihydroxy-3,4-*seco*-cycloart-4(29)-en-3-oic acid (19a)***

Specific rotation $[\alpha]_D^{20}$ +31.3 ($CHCl_3$, *c* 0.15)

IR spectrum ν_{max} (film) 2924, 1739, 1456 cm^{-1}

Mass spectrum HRESI-MS *m/z* (ES+) : 793.6293 ($C_{49}H_{86}O_6$+Na calc 793.6322)

NMR spectrum ^{1}H NMR - see Table 23, ^{13}C NMR – see Table 24

(24*E*)-3,4-*Seco*-cycloart-4(29), 24-diene-3,26-dioic acid (20) [217]

Molecular formula $C_{30}H_{46}O_4$ **MW** 470.70

Description White solid

Retention factor R_f = 0.5 (cHex-EtOAc =1:1)

Specific rotation $[\alpha]_D^{20}$ +31 ($CHCl_3$, *c* 0.07) (lit.[217] +23 (MeOH, *c* 0.36))

IR spectrum ν_{max} (film) 2927, 1695, 1262, 1021, 801 cm^{-1}

Mass spectrum EI-MS *m/z* 469 $[M-H]^-$; HRESI-MS : found m/z 469.33333 ;
calculated for $C_{30}H_{45}O_4$ ($[M-H]^-$) :469.3318.

NMR spectrum ^{1}H and ^{13}C NMR NMR - see Table 25

3,26-dimethyl ester of 20 (20a)

Molecular formula	$C_{32}H_{50}O_4$	**MW**	498.75
Description	colorless liquid		
Specific rotation	$[\alpha]_D^{20}$ +43 ($CHCl_3$, *c* 0.07)		
Mass spectrum	ESI-MS *m/z* 499 $[M+H]^+$		
NMR spectrum	^1H and ^{13}C NMR NMR - see Table 25		

IV. PERSONAL WORK

4.1 Plant material

4.2 Preliminary study

4.3 Extraction and isolation of *H. odorata* leaves hexane extract

4.4 Identification and structural study of isolated compounds

4.5 Cytotoxic evaluation of 8 isolated lupanes

4.6 Conclusion

4.1 PLANT MATERIAL

H.odorata leaves were collected in Chiangmai, a province with biodiversity in plants. Chiangmai is in the northern part of Thailand. It is located among the highest mountains in the country including the deciduous forest association of lowlands and the evergreen forest of the upland. Plant sample was prepared for the study by drying and chopping.

4.2 PRELIMINARY STUDY

From preliminary study, *H. odorata* leaves were extracted by soxhlet apparatus. Plant sample was first extracted with hexane, then, extraction was continued with ethanol. After drying using reduced-pressure evaporator, the *in vitro* cytotoxic and antifungal activities of both extracts were performed by the Resazurin Microplate assay (REMA), while antituberculosis and antimalarial activity were measured by green fluorescent protein microplate assay (GFPMA) and microculture radioisotope technique, respectively. The hexane extract showed stronger cytotoxic activity against both cell lines, especially against NCI-H187. Hence, it was chosen to be separated by repeated column chromatography.

4.3 EXTRACTION AND ISOLATION OF *H. odorata* LEAVES HEXANE EXTRACT.

After repeated column chromatography of *H.odorata* leaves hexane extract, two new fatty acid esters of 3,4-*seco*-cycloartanes (**18** and **19**) were obtained together with one lupane (**14**) which was found for the first time in the nature. Phytochemical study of this extract also led to the isolation of other seventeen known compounds. The structures of isolated compounds were established conclusively based on UV, IR, MS and extensive ^{1}H- and ^{13}C- NMR spectra analysis. The spectra of known compounds were compared to literature data. One sesquiterpene and five types of triterpenes were identified. Isolated terpenoids are as follows:

Sesquiterpene : caryophyllene oxide (**9**)

Triterpenes :

- Friedelane type : friedelin (**1**) and *epi*friedelanol (**4**)
- Oleanane type : *β*-amyrin (**2**) and its saturated fatty acid ester (**6**)
- Steroidal type : *β*-sitosterol (**3**) and its saturated and unsaturated fatty acid esters (**7**, **8**)
- Lupane type : betulonic acid (**5**), *epi*betulinic acid (**10**), betulone (**11**), 30-hydroxylup-20(29)-en-3-one (**12**), betulinic acid (**13**), 3,30-dioxolup-20(29)-en-28-oic acid (**14**), 28,30-dihydroxy-3-oxolup-20(29)-ene (**16**), messagenic acid G (**17**)
- Cycloartane and *seco*-cycloartane type : mangiferonic acid (**15**), 26-arachidic acid ester of (24*S*,25*S*)-24,25,26-trihydroxy-3,4-*seco*-

cycloart-4(29)-en-3-oic acid (**18**), 24-stearic acid ester of (24*S*,25*S*)-24,25,26-trihydroxy-3,4-*seco*-cycloart-4(29)-en-3-oic acid (**19**), (24*E*)-3,4-*seco*-cycloartane-4(29),24-diene-3,26-dioic acid (**20**)

Friedelane-, oleanane- and steroidal-types triterpenes in this study are wide-spread triterpenes found in plants. However, it should be noted that fatty acid esters of *β*-sitosterol and *β*-amyrin were also obtained.

When the polarity of mobile phase was increased, the elution of isolated compound was in the order of fatty acid ester of *β*-amyrin (**6**) and fatty acid esters of *β*-sitosterol (**7**, **8**), friedelin (**1**), caryophyllene oxide, *β*-amyrin (**2**), *β*-sitosterol (**3**), lupane triterpenes with less polarity (**5**, **10**, **11**, **12**, **13**, **14**, **16**), mangiferonic acid, more polar lupane (messagenic acid G, **17**), fatty acid ester of 3,4-*seco*-cycloartane-3-oic acid (**18**, **19**), and finally, 3,4-*seco*-cycloartane dioic acid (**20**). From the previous literatures [20, 47, 49], the common terpenenoids such as *β*-amyrin, *β*-sitosterol, friedelin and caryophyllene oxide, as well as betulinic acid, betulonic acid and mangiferonic acid have been reported in Dipterocarpaceous plants. The major compounds in this extract were betulonic acid, *β*-sitosterol and *β*-amyrin.

It has been reported that *β*-amyrin and its palmitate ester exhibited antidepressant and antinociceptive properties [61, 198, 199] as well as anti-inflammatory activity [200].

β-Sitosterol is one of the most prevalent phytosterols which is ubiquitous throughout the plant kingdom. It is structurally related to cholesterol. *β*-Sitosterol has an amazing array of scientifically acknowledged benefits for key areas of health in immune dysfunction, inflammatory disorder and rheumatoid arthritis, hypercholesterolemia, breast cancer, colon cancer and, especially, benign prostatic hypertrophy [201]. Caryophyllene oxide showed a variety of bioactivity such as a potent antimalarial, mild cytotoxic [58] and anti-inflammatory activity [202].

All lupanes gave blue-violet spot with vanillin-sulfuric TLC reagent. The TLC trace and the amount of each fraction showed that betulonic acid (**5**) was the most abundant compound in this extracts. Among the family containing lupanes as major triterpenoids, this *H. odorata* leaves hexane extract gave much more betulonic acid, an oxidation product at C-3, than betulinic acid. Accompanied by oxidation at C-28 and C-30, it showed higher degree of oxidation in the metabolism system. Moreover, the higher oxidized derivatives at C-30 normally exhibited a narrower distribution and this is the first report of compound **10**, **11**, **12**, **14**, **16 and 17** in the family Dipterocarpaceae. In addition to cytotoxic activity, they also possessed anti HIV [83], antimalarial [131], anti-inflammatory [127] activities.

*Epi*betulinic acid (**10**) was not found as much as **5** and **13** and not normally distributed in the same family as **13**. It has been isolated from Simaroubaceae [113], Verbenaceae [114], Zygophyllaceae [115] and Cornaceae [99]. It is interesting to note the co-occurrence of betulinic and *epi*betulinic acid in *H. odorata*. This incident was found

only in *Cornus capitata* leaves (Cornaceae) [99] and the aerial part of *Peganum nigellastrum* (Zygophyllaceae) [115]. The cytotoxic and anti-inflammatory activity of this compound were reported [93, 127] together with moderate anti-tuberculosis activity [114].

Betulone (**11**) has been achieved from the plants of Betulaceae [85], Celastraceae [97, 127] and Leguminoseae [101, 105]. It exhibited only mild cytotoxicity in Mutai's work, however, it possessed protective effect against Cd cytotoxicity at a high concentration (20μM) without any cell damage. [194]

Compound **12** (30-hydroxy-3-oxo-lup-20(29)-ene) was one of the major compounds of plants in family Celastraceae [92, 97, 98] and appeared here just as a minor component. It has never been reported in family Dipterocarpaceae. It exhibited weak cytotoxic activity against A2780 (Human ovarian cancer cell line) with the IC_{50} value of 16.4 μg/mL [112] as well as antimalarial activity against *P.falciparum* [203]. Mambu's work suggested that in comparison to the C-30 aldehyde and the C-3 ketone, a C-30 hydroxyl group possed lower antimalarial activity and with hydroxyl at both C-3 and C-30 the activity diminished considerably.

This was the first finding of 3,30-dioxolup-20(29)-en-28-oic acid (**14**) as a natural product in plant. It was a co-product in the synthesis of messagenic acid G from betulinic acid [181]. Since this compound was obtained only in small amount, in order to confirm the proposed structure, a partial synthesis was performed using betulonic acid, which was isolated in large amounts from *H. odorata*, as starting material. Selective SeO_2 allylic oxidation of betulonic acid, as described by Macias *et al*.[181, 182], gave 3,30-dioxolup-20(29)-en-28-oic acid, **14**, (22%) and messagenic acid G, **17**, (29%). The NMR data of synthesized product were in good agreement with the proposed structure. The incomplete ^{1}H NMR data was reported in the study of Macias et al [181], however no ^{13}C-NMR data has been provided. The complete NMR data were provided in this research.

Compound **16** (28,30-dihydroxylup-20(29)-en-3-one) is one of rare lupanes in the nature. Until now, there are only 3 papers about this compound from plants in family Celastraceae) [91, 93, 95] and never been reported in Dipterocarpaceous plant. However, the structure elucidation in previous study was based mainly on the comparison to the ^{1}H-NMR spectrum of 3β,28,30-lup-20(29)-ene triol and the data obtained from chemical reaction. Only incomplete NMR spectra has been reported [91]. The complete 1D and 2D NMR data of 28,30-dihydroxy-3-oxolup-20(29)-ene were reported for the first time in this study. Nunez et al [93] reported its moderate cytoxicity against HeLa (human carcinoma of cervix, IC_{50} 4.0 μg/mL=8.75 μM) and Hep-2 (human carcinoma of larynx, IC_{50} 7.1 μg/mL=15.55 μM).

Compound **17** (messagenic acid G) has been reported only in *Melilotus messanensis* (Leguminosae) [181] and *Liquidamber styraciflua* (Hamamelidaceae) [204]. It could be synthesized from oxidization of betulinic acid in which compound **14** was a co-product. It showed the effect on the germination and growth of dicotyledons [181].

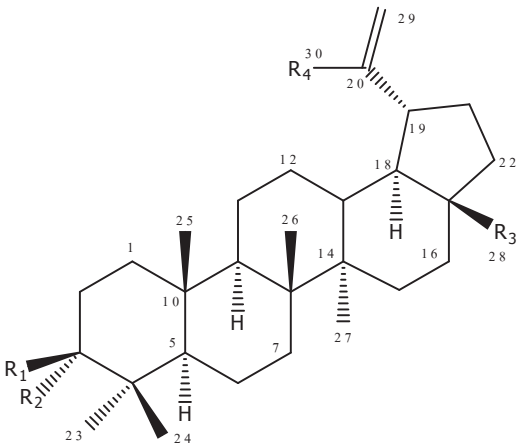

R_1,R_2=O, R_3=COOH, R_4=CH_3	Betulonic acid, **5**
R_1=OH, R_2=H, R_3=COOH, R_4=CH_3	Betulinic acid, **13**
R_1=H, R_2=OH, R_3=COOH, R_4=CH_3	*Epi*betulinic acid, **10**
R_1,R_2=O, R_3=CH_2OH, R_4=CH_3	Betulone, **11**
R_1,R_2=O, R_3= CH_3, R_4= CH_2OH	30-Hydroxylup-20(29)-en-3-one, **12**
R_1,R_2=O, R_3=COOH, R_4=CHO	3,30-Dioxolup-20(29)-en-28-oic acid, **14**
R_1,R_2=O, R_3=CH_2OH, R_4=CH_2OH	28,30-Dihydroxylup-20(29)-en-3-one, **16**
R_1,R_2=O, R_3= COOH, R_4= CH_2OH	Messagenic acid G, **17**

Figure 11. Structure of lupane triterpenes from *H.odorata* leaves hexane extract

Compound **15** (mangiferonic acid) is one of common cycloartane triterpenes in Dipterocarpaceae [43, 49, 205, 206]. It has been reported in *Tillandsia* sp. (Bromeliaceae) [207] and *Mangifera* sp (Anacardiaceae) [197, 208].

In fraction C41 and C42, the use of silica gel as stationary phase did not allows satisfactory separation. The compounds were eluted in mixtures such as the mixtures of **18** + **19**, **18** + **20** and the mixture of **19** + **20**. Only a little amount of each compound was obtained as pure and it was not possible to get NMR spectrum of sufficient quality. (However, it should be noted that the revelation of TLC by the vanillin-sulfuric reagent is very sensitive, much more than the sensitivity of NMR analysis.) To facilitate the purification, the mixtures with carboxylic acid group in the structure were subjected to methylation with sodium bicarbonate and methyl iodide in anhydrous DMF (Scheme 13). Then, after reaction, methyl ester of each compound (**18a**, **19a**, **20a**) was succesfully isolated through silica gel column chromatography. Compound **18a** was performed transesterification at C-26 with small quantity of CH_3ONa (as a catalyst) and hydrolysis of the carboxymethylate at C-3 was suddenly taken place after redissolved in CH_3COOH-H_2O 3:1, an aqueous acidic condition (Scheme 14). The reaction with *(S)*-and *(R)*-MTPA-Cl by means of modified Mosher's method was carried out to detect the absolute

configuration at C-24 of **18a** (Scheme 16). After reaction, the *(R)*-MTPA and *(S)*-MTPA ester were produced, respectively.

Pure methyl ester product of **20** (**20a**) was saponified to its original molecule by LiOH. The mechanism diagrams were shown in Scheme 15.

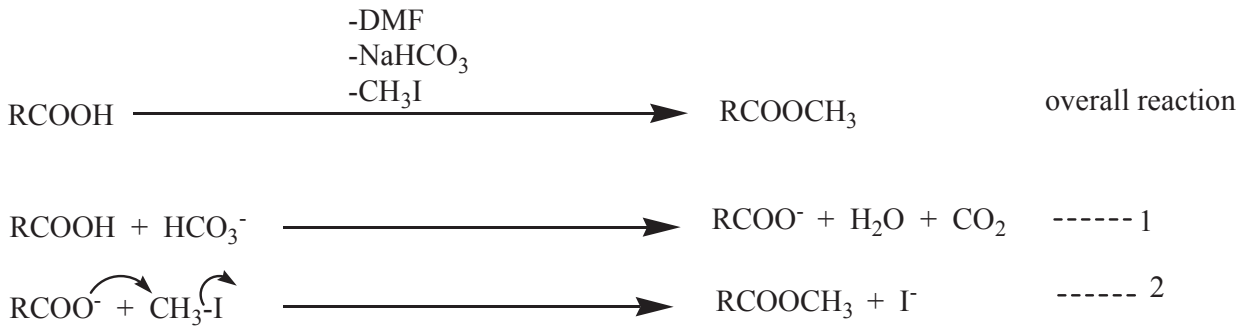

Scheme 13. Reaction mechanism of methylation of carboxylic acid

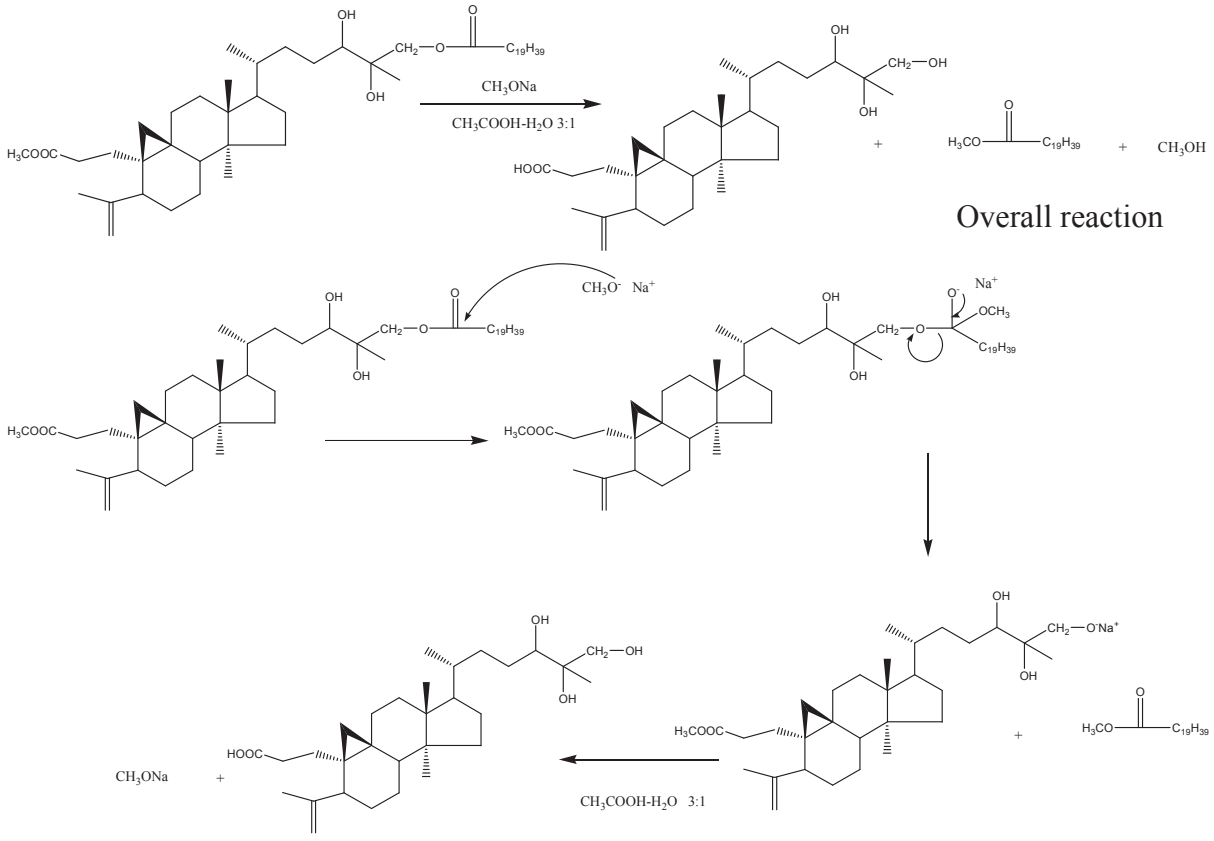

Scheme 14. Reaction mechanism of transesterification at C-26 and hydrolysis at C-3 of 18a.

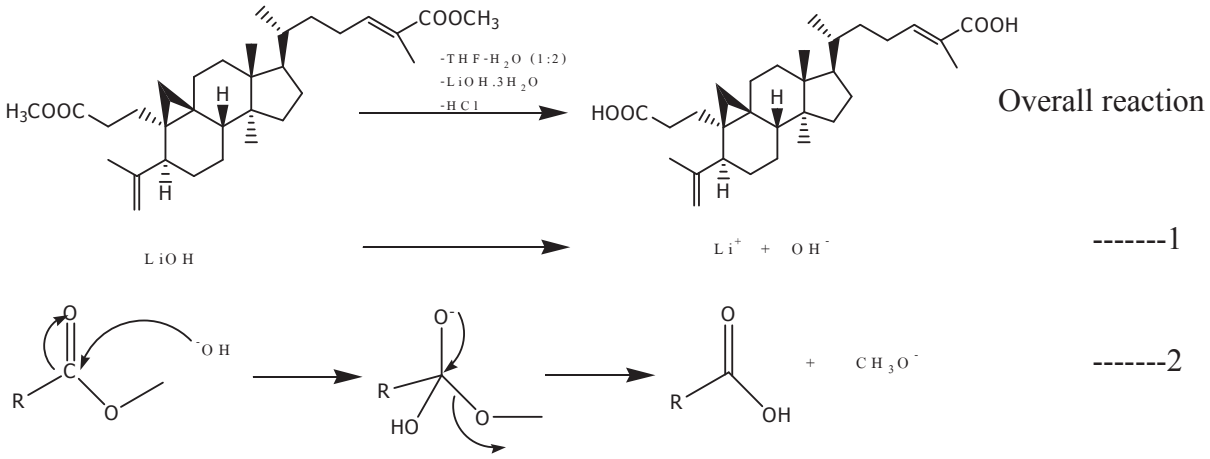

Scheme 15. Reaction mechanism of hydrolysis of 20a

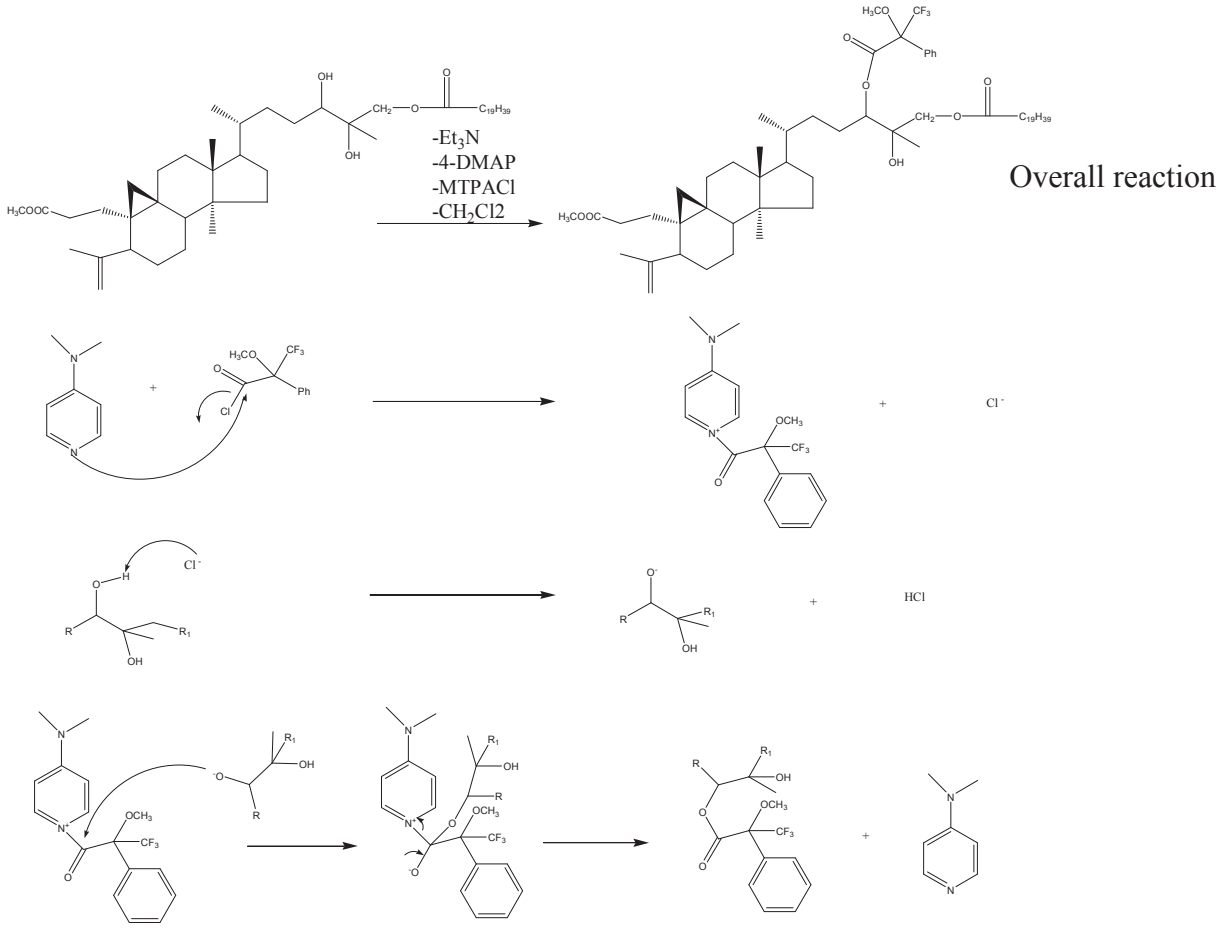

Scheme 16. Reaction mechanism of **18a** in modified Mosher's method

The 3,4-*seco*-cycloartanes are comparatively rare in the nature, although several closely related compounds such as cycloartanes were known. It has been found mostly in family Rubiaceae (genus *Gardenia* [209-211] and genus *Antirhea* [212, 213]), along with family Schisandraceae (genus *Kadsura, Schisandra* [214, 215]), family Bromeliaceae (genus *Tillandsia* [216]) and family Magnoliaceae (genus *Illicium* [196]). Compound **18** and **19** are fatty acid esters of the same triterpene moiety but different in the position of ester. They are considered to be new products. Although the absolute configuration on C-

24 of **18a** from modified Mosher's reaction seemed to be *R*-form with some ambiguity in the raw data, finally, the actual configuration was clearly determined as 24*S*,25*S*. The detail was discussed under the topic of compound **18**, **18a**, and **18b** in section 4.4 "Identification and structural study of isolated compounds". The breakage of C-3 and C-4 bond of 3,4-*seco*-cycloartane-3-oic acid (**18**, **19** and **20**) was explained through the oxidation process. Compound **20** could be proposed as the oxidation product of mangiferonic acid (**15**), a known cycloartane presented in this extract, as same as oxidation of schizandronic acid in *Schisandra micrantha* (Schisandraceae) [214]. During the course of this work, compound **20** has been isolated from the aerial parts of *Abies georgei* (Pinaceae) [217] and named abiestrine J, while its dimethyl ester (**20a**) had been isolated from *Tillandsia usneoides* (Bromeliaceae) [216]. Up to now, compound **18** and **19** have never been discovered from any other sources. The amount of 3,4-*seco*-cycloartane triterpenes was not sufficient for cytotoxic assay.

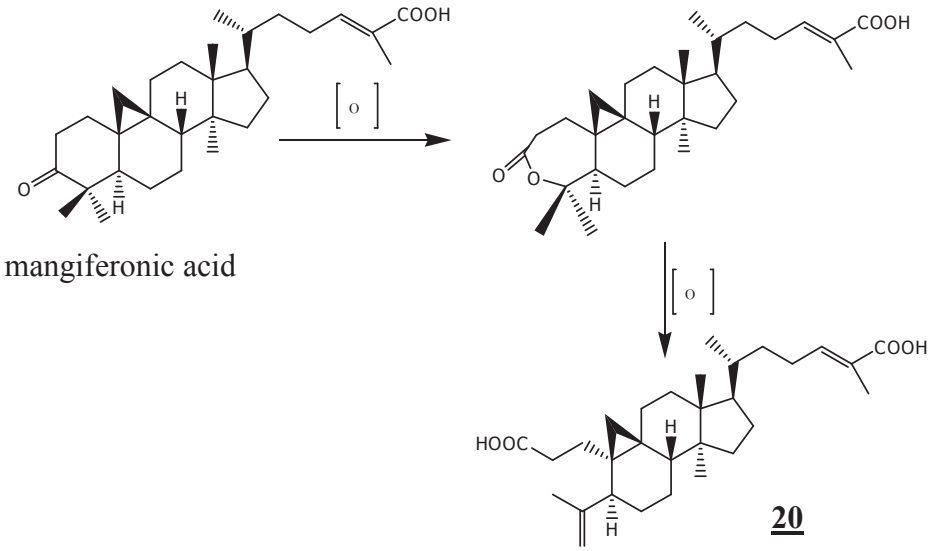

Scheme 17. Proposed biosynthesis of **20** from mangiferonic acid

4.4 IDENTIFICATION AND STRUCTURAL STUDY OF ISOLATED COMPOUNDS.

4.4.1 Friedelin (1) and *Epi*friedelanol (4)

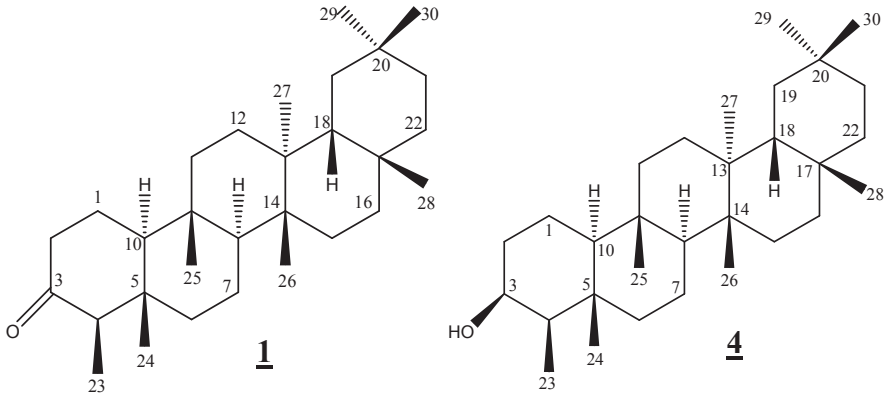

Figure 12 Structures of compounds **1** and **4**

The ^{13}C-NMR, DEPT and HSQCedited spectrum of compound **1** showed 30 carbon signals, representing 8 methyl, 11 methylene, 4 methine and 7 quaternary carbons. The shifted upfield δ_C of 23-methyl group to 6.84 ppm, together with the δ_C 31-35 ppm of 3 methyl groups at C-28 to C-30, was in harmony with the characteristic of 3-oxo-friedelane triterpene. The quaternary carbon signal at δ_C 213.3 ppm was assigned to C-3. No hydroxyl and double bond signals were found in the ^{1}H and ^{13}C-NMR spectra. The δ_C data were compared to friedelin from previous report [185, 186]. The compound **1** was then defined as friedelin with the confirmation data from MS.

The starting point for the assignments of compound **4** was the hydrogen (δ_H 3.78) attached to the oxygenated C-3 (δ_C 72.8). From COSY spectrum, this hydrogen (H-3) showed a correlation with two hydrogen atoms of H-2 (δ_H 1.67 and 1.93) and H-4 (δ_H 1.30). The proton signal at H-23 (δ_H 0.98, d) also showed a correlation with the signal at H-4. The δ_C of C-23 (δ_C 11.6) was shifted upfield than other methyl groups but downfield compared to friedelane with α-OH configuration on C-3 (δ_C 10.0) [190] and 3-oxo friedelane. The remaining δ_C and δ_H were compared to the literature data [189, 190] and the structure was identified as *epi*friedelanol (synonym: 3β-friedelinol). The EI-MS spectrum confirmed this conclusion.

The ^{1}H and ^{13}C-NMR data of both compounds were compared in Table 15.

Table 15 The ^{1}H-NMR (400 MHz) and ^{13}C-NMR (75 MHz) data of **1** and **4** (in $CDCl_3$); δ in ppm; J in Hz

position	**1**		**4**	
	δ_H	δ_C	δ_H	δ_C
1	2.02 (m) 1.74 (dd, *J*=13.0, 5.3)	22.3	1.58 (m) 1.49 (d, *J*=7.3)	15.8
2	2.44 (m) 2.36 (m)	41.5	1.67 (m) 1.93 (m)	35.3
3		213.3	3.78 (br.s)	72.8
4	2.32 (m)	58.2	1.30 (m)	49.2
5		42.2		37.8
6	1.80 (m) 1.32 (m)	41.3	1.78 (dd, *J*=13.1, 2.8) 1.03 (d, *J*=10.3)	41.7
7	1.53 (m) 1.44 (m)	18.2	1.44 (d, *J*=2.5) 1.41 (d, *J*= 2.5)	17.5
8	1.44 (m)	53.1	1.33 (dd, *J*=10.4, 3.5)	53.2
9		37.4		37.1
10	1.60 (m)	59.5	0.95 (dd, *J*=2.3, 11.3)	61.3
11	1.52 (m)	35.6	1.59 (m, 1H) 1.26 (m, 1H)	35.5
12	1.39 (m)	30.5	1.39 (m, 1H) 1.35 (m, 1H)	30.6
13		39.7		39.7
14		38.3		38.4
15	1.32 (m)	32.4	1.56 (dd, *J*=10.1,4.2) 1.33 (dd, *J*=10.4,3.5)	32.3
16	1.40 (m)	36.0	1.50 (m) 1.17 (m)	36.1
17		30.0		30.0
18	1.62 (dd, *J*=1.8, 6.0)	42.8	1.59 (m)	42.8
19	1.27 (m)	35.3	1.39 (m) 1.24 (m)	35.2
20		28.2		28.2
21	1.54 (m)	32.8	1.51 (d, 10.9) 1.29 (dt, *J*=6.6,3.2)	32.8
22	1.56 (d, *J*=4.3) 1.00 (m)	39.3	1.54 (m) 0.97 (m)	39.3
23	0.94 (s)	6.8	0.99 (d, *J*= 6.4)	11.6
24	0.77 (s)	14.7	1.01 (s)	16.4
25	0.92 (s)	18.0	0.91 (s)	18.2
26	1.06 (s)	20.3	1.04 (s)	20.1
27	1.10 (s)	18.7	1.06 (s)	18.7
28	1.23 (s)	32.1	1.22(s)	32.1
29	1.01 (s)	35.0	1.00 (s)	35.0
30	1.06 (s)	31.8	1.05 (s)	31.8

4.4.2 *β*-Amyrin (2) and Saturated Fatty Acid Ester of *β*-Amyrin (6)

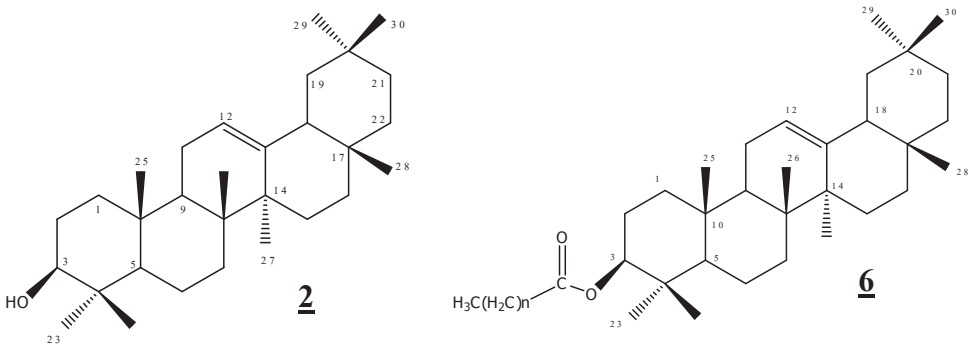

2 6

Figure 13 Structures of compounds **2** and **6**

The carbon multiplicities of compound **2** were determined by the ^{13}C NMR spectrum and the HSQCedited correlation. The presence of 8 methyl, 10 methylene, 5 methine, and 7 quaternary carbons was thus established. The signals in the ^{13}C NMR spectrum for oxymethine ($\delta_{C\text{-}3}$ 79.0), double bond with methine and quaternary carbons ($\delta_{C\text{-}12}$ 121.7 and $\delta_{C\text{-}13}$ 145.2) in conjunction with the signals in the ^{1}H NMR spectrum at $\delta_{H\text{-}3}$ 3.25 and $\delta_{H\text{-}12}$ 5.19 were in good agreement with the presence of *β*-amyrin. The rest of assignment was compared to the literature data [187]. This structure was then characterized as *β*-amyrin. It was confirmed by the EI-MS spectrum that was compatible with the reference spectrum.

The identification of the triterpene moiety of **6** as being *β*-amyrin was possible by direct comparison of the NMR data of **6** with the spectra of compound **2** (Table 16). The ^{1}H NMR spectrum was very close to that of *β*-amyrin (Figure 41). The ^{13}C NMR spectrum of **6** corresponded to that of *β*-amyrin with methine and quarternary carbon signals ($\delta_{C\text{-}12}$ 121.7 and $\delta_{C\text{-}13}$ 145.2), a characteristic of oleanene triterpenes. Detail analysis of the extra δ_C in this spectrum indicated that this triterpene was esterified with fatty acid. This observation was supported by the presence of an additional methyl (δ_C 14.2), many methylenes (δ_C 29-30) and acyl group (δ_C 173.7). In addition, the oxymethine carbon (C-3) appeared at higher chemical shift (δ_C 80.6) than that observed for *β*-amyrin (δ_C 79.0). This phenomenon also appeared in $\delta_{C\text{-}3}$ of 3-fatty acid ester of *β*-sitosterol (**7** and **8**) (Table 17, Figure 42) and implied esterification at C-3. Moreover, there was no additional signal of carbon with double bond then this fatty acid should be saturated fatty acid. However, its amount was not enough for transesterification to establish the complete structure.

Table 16 The ^{1}H-NMR (400 MHz) and ^{13}C-NMR (75 MHz) data of **2** and **6** (in $CDCl_3$); δ in ppm; J in Hz

position	**2**		**6**
	δ_H	δ_C	δ_C
1	1.73 (m) 1.03 (m)	38.6	39.8
2	1.67 (dd, J=14.0, 6.6) 1.61 (m)	27.2	26.9
3	3.27 (ddd, J=11.1, 4.3)	79.0	80.6
4		38.8	38.2
5	0.80 (dd, J=14.2, 4.2)	55.2	55.2
6	1.59 (m) 1.44 (m)	18.4	18.3
7	1.58 (ddd, J=18.3, 12.2, 4.8,) 1.38 (m)	32.6	32.5
8		39.8	39.8
9	1.59 (m)	47.6	47.5
10		36.9	36.8
11	1.95 (m) 1.91 (m)	23.5	23.7
12	5.19 (m)	121.7	121.6
13		145.2	145.2
14		41.8	41.7
15	1.81 (m) 1.01 (m)	26.1	26.1
16	2.05 (m) 0.86 (m)	26.9	26.9
17		32.5	32.5
18	1.99 (m)	47.2	47.2
19	1.71 (m) 1.06 (m)	46.8	46. 8
20		31.1	31.1
21	1.42 (d, J=12.2) 1.15 (d, J=13.1)	34.7	34.7
22	1.46 (m) 1.27 (m)	37.1	37.1
23	1.05 (s)	28.1	28.1
24	0.84 (s)	15.5	16.8
25	0.99 (s)	15.6	15.6
26	1.02 (s)	16.8	16.8
27	1.18 (s)	26.0	26.0
28	0.88 (s)	28.4	28.4
29	0.92 (s)	33.3	33.4
30	0.92 (s)	23.7	23.7
CH_3-$(CH_2)_n$-(CO)O-			173.7
CH_3-$(CH_2)_n$-(CO)O-			25.2, 29-30
CH_3-$(CH_2)_n$-(CO)O-			14.2

4.4.3 *β*-Sitosterol (3), *β*-Sitosterol Palmitate (7) and Mixture of Saturated and Unsaturated Fatty Acid Ester of *β*-Sitosterol (8)

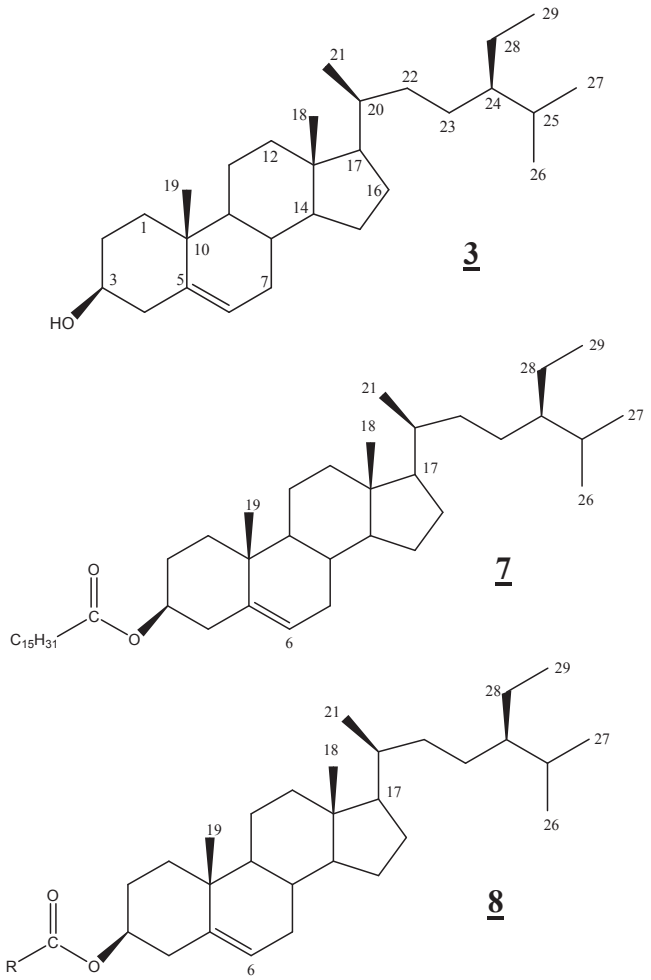

Figure 14 Structures of compounds **3**, **7** and **8**

The ^{13}C NMR spectrum of **3** showed the presence of 29 carbon signals that were contributed to 6 methyl, 11 methylene, 9 methine, and 3 quaternary carbons. From the HSQCedited spectrum, one methine carbon signal at 71.8 ppm correlated to $\delta_{H\text{-}3}$ 3.58 and an olefin carbon at $\delta_{C\text{-}6}$ 121.7 ppm correlated to $\delta_{H\text{-}6}$ 5.40. The ^{13}C-NMR data of **3** was then compared to the previous literature [188] and then it was identified as *β*-sitosterol. This was supported by the ESI-MS spectrum ($[M+Na]^+$ *m/z* at 437) and GC-EI-MS spectrum (comparison to the reference spectrum).

The ^{1}H-NMR of **7** showed protons of H-3 and H-6 at δ_H 4.10 and δ_H 5.41, respectively. The position of H-3 was shifted down field compare to that of *β*-sitosterol (Figure 42). The ^{13}C NMR spectrum also showed characteristics of *β*-sitosterol (C-3 oxymethine at δ_C 73.66 and quaternary and methine carbon signals at δ_C 139.7 and 122.6), with additional carbon signals of fatty acid ester (methylenes at δ_C 29-30 and acyl group at δ_C 174.0). Transesterification of **7** yielded *β*-sitosterol and methyl palmitate (*m/z* 270) which were characterized by GC-MS analysis. Although small amount of methyl stearate was also found in MS spectrum, the main ester was determined as *β*-sitosterol palmitate (**7**).

The ^{1}H-NMR and ^{13}C-NMR spectra of compound **8** were consistent with those of **7**, except more δ_C signals of double bond (127.9, 128.0 and 130.2 ppm) (Figure 42). After transesterification, methyl palmitate, methyl linoleate and methyl oleate were obtained by means of GC-MS determination. However, the amount of palmitate ester was still more than the other 2 unsaturated fatty acid esters.

Table 17 The ^{1}H-NMR (400 MHz) and ^{13}C-NMR (75 MHz) data of **3**, **7** and **8** (in $CDCl_3$); δ in ppm; J in Hz

position	**3**		**7**	**8**
	δ_H	δ_C	δ_C	δ_C
1	1.90 (dd, *J*=9.6,3.6) 1.13 (dd, *J*=6.4,3.5)	37.3	37.0	37.0
2	2.02 (m) 1.58 (m)	31.7	31.9	31.5
3	3.58 (m)	71.8	73.7	73.7
4	2.31 (m)	42.3	42.3	42.3
5		140.8	139.7	139.7
6	5.40 (d, *J*=4.8)	121.7	122.6	122.6
7	1.59 (m)	31.9	31.9	31.9
8	1.49 (d, *J*=4.6)	31.9	31.9	31.9
9	0.95 (s)	50.1	50.0	50.0
10		36.5	36.5	36.6
11	1.54 (d, *J*=1.6)	21.1	21.0	21.0
12	2.07 (m) 1.20 (d, *J*=4.2)	39.8	39.7	39.7
13		42.3	42.3	42.3
14	1.03 (s)	56.8	56.7	56.7
15	1.64 (m) 1.33 (s)	24.3	24.3	24.3
16	1.92 (m) 1.30(s)	28.3	28.3	28.2
17	1.16 (s)	56.0	56.0	56.0
18	0.73 (s)	11.9	11.9	11.9
19	1.06 (s)	19.4	19.3	19.3
20	1.39 (m)	36.2	36.2	36.2
21	0.97 (d, *J*=6.5)	18.8	18.8	18.8
22	1.36 (m) 0.93 (s)	33.9	33.9	33.9
23	1.21 (m)	26.0	26.1	26.0
24	0.95 (s)	45.8	45.8	45.8
25	1.71 (m)	29.1	29.1	28.7
26	0.88 (d, *J*=1.8)	19.8	19.8	19.8
27	0.86 (s)	19.0	19.0	19.0
28	1.27 (s)	23.1	23.1	23.1
29	0.89 (s)	12.0	12.0	12.0
-O<u>C</u>(=O)$(CH_2)_{14}CH_3$			174.0	
-OC(=O)<u>(CH_2)</u>$_{14}CH_3$			29.2-29.6	
-OC(=O)$(CH_2)_{14}$<u>CH_3</u>			14.1	
-O<u>C</u>(=O)R				173.3
CH_2 of fatty acid				22.7, 29.1-29.7, 31.9
double bond of fatty acid				127.9, 128.0, 130.2
terminal methyl of fatty acid				14.1

4.4.4 Betulonic Acid (5), *Epi*betulinic Acid (10), Betulone (11), 30-Hydroxy-3-oxolup-20(29)-ene (12), Betulinic Acid (13), 3,30-Dioxolup-20,29-en-28-oic Acid (14), 28,30-Dihydroxylup-20(29)-en-3-one (16) and Messagenic Acid G (17)

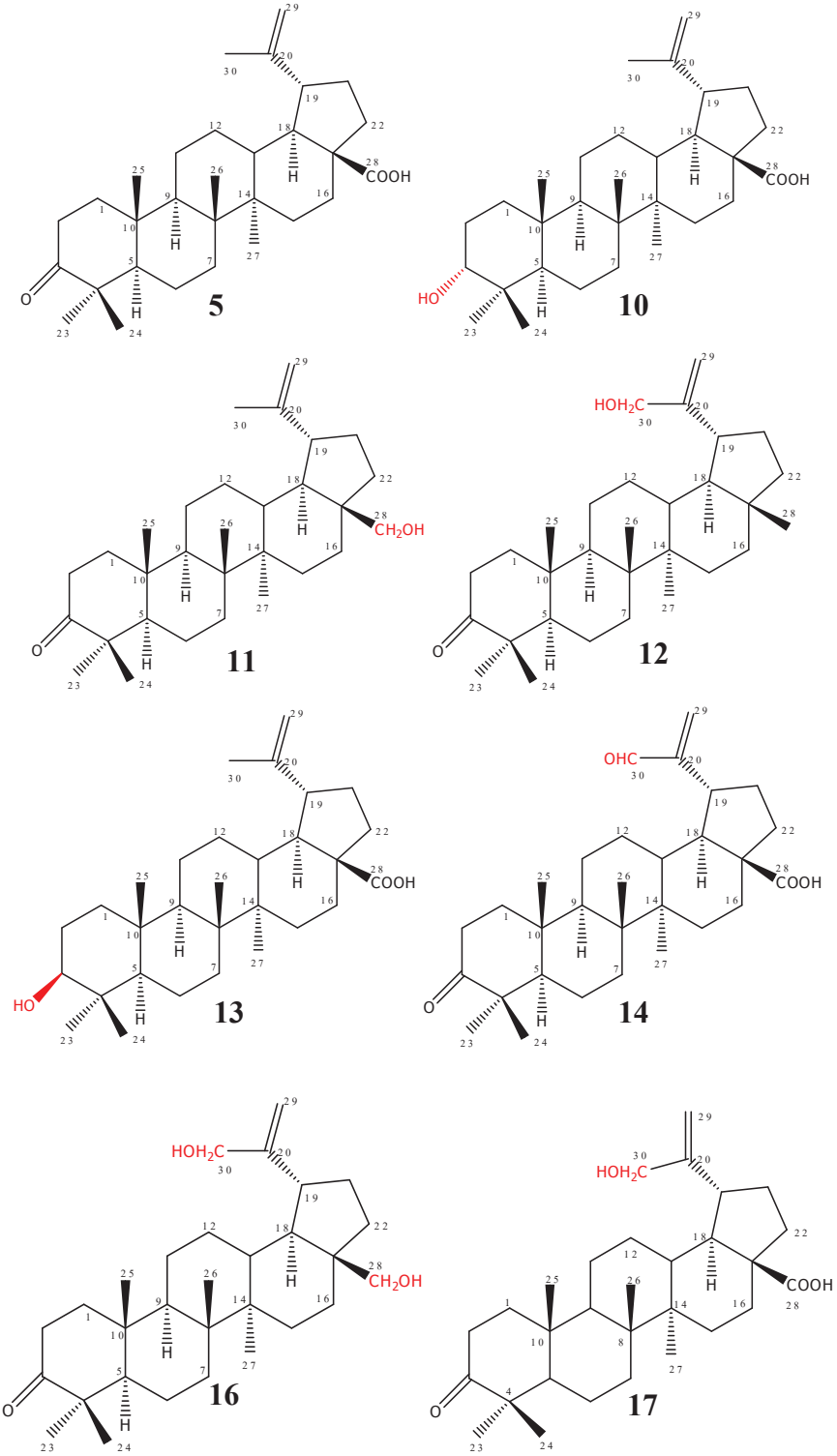

Figure 15 Structures of the isolated lupanes

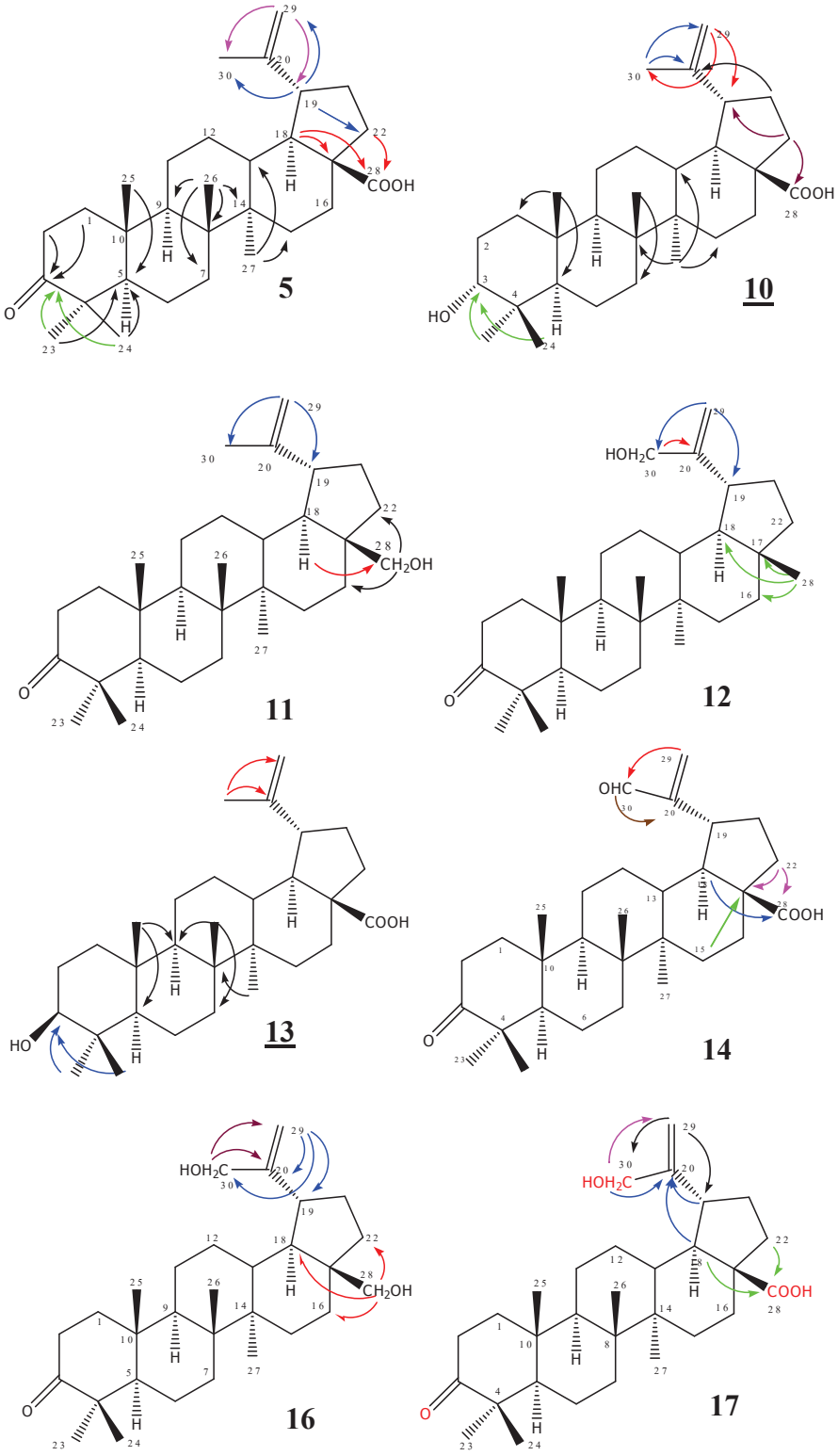

Figure 16. Selected HMBC correlations of **5**, **10**, **11**, **12**, **13**, **14**, **16**, and **17**

The isolated compounds in this group were lupane triterpenes. All lupanes gave blue-violet spot with vanillin-sulfuric TLC reagent.

IR spectrum of compound **5** obviously showed the presence of carboxylic (3500-2500 cm^{-1}, broad band) and carbonyl (about 1705 cm^{-1}, sharp) groups. The ^{13}C-NMR and

HSQCedited spectra of compound **5** showed 30 carbon siganls representing 6 methyl, 11 methylene, 5 methine and 8 quaternary carbons. The δ_C value displayed one ketone (δ_C 218.2), one carboxylic group (δ_C 180.8) and one double bond (δ_C150.3 (Civ) and 109.8 (CH_2))

The HSQCedited correlation of compound **5** indicated 2 terminal olefenic protons at 4.75 and 4.62 ppm attached on the same δ_C 109.8 ppm that confirmed the terminal methylene structure. The HMBC spectrum showed the correlation between these 2 olefinic protons and a methyl carbon at 19.36 ppm (C-30) as well as a quaternary carbon at 46.9 ppm (C-19) (Figure 12). Lupane group normally had 7 methyl groups. However, one methyl group was oxidized to carboxylic group that shown at 180.8 ppm of ^{13}C-NMR spectrum. The oxidation at C-28 made δ_C of C-16 and C-22 upfield shift. There were also the correlations between ketone carbon (δ_C 218.2) and the protons of 2 methyl groups (δ_H 1.08, 1.03) that indicated carbonyl group on ring A at position 3.

After searching for chemical constituents of Dipterocarpaceaous plant and comparison to previous NMR data [129], compound **5** was identified as betulonic acid. It was supported by the MS (ES- : *m/z* 453 of $[M-H]^-$). The TLC trace and the amount of each fraction showed that betulonic acid (**5**) was the most abundant compound in this extracts.

Both compound **10** and **13** exhibited the equal mass $[M-H]^-$ *m/z* at 455 amu representing molecular formula of $C_{30}H_{48}O_3$. Their IR spectrum obviously showed the presence of carboxylic (3500-2500 cm^{-1}, broad band) and hydroxyl (about 3400 cm^{-1}) groups. The NMR spectra of both compounds were very close to betulonic acid (**5**) and indicated that a hydroxyl group was substituted at C-3 instead of a keto group. Selected HMBC correlations of both compounds were shown in Figure 16. The difference between **10** and **13** was only the stereochemistry of this position. H-3 of **13** resonated at δ_H 3.21. Its splitting pattern (dd, *J*= 11.2, 4.8 Hz) indicated it was arranged in axial orientation [39, 47, 84, 111]. On the other hand, H-3 of **10** resonated at δ_H 3.40 and its equatorial orientation was suggested based on the splitting pattern (t, *J*=2.7 Hz) [81, 84, 113, 127, 185, 193]. Furthermore, δ_C of CH_3-24 which was the axial methyl group at the C-4 was strongly influenced by the stereochemistry of the hydroxyl group at C-3. Indeed, $\delta_{C\text{-}24}$ of **13** showed upperfield shift (Δ+7 ppm) compared to that of **10**. Moreover, δ_C of C-1 and C-5

of **13** shifted to lower field as compared to those of **10** on account of γ-effect. The δ_C of C-

2, C-3 and C-4 of **13** also shifted lower field, compared to those of **10**, but with lesser degree. From all of these data, compounds **10** and **13** were elucidated as *epi*betulinic and betulinic acid, respectively.

Table 18. The ^{1}H-NMR (400 MHz) data of **5**, **10**, **11**, **12** and **13** (in $CDCl_3$); δ in ppm; *J* in Hz

position	**5**	**10**	**11**	**12**	**13**
1	1.38 (m) 1.91 (m)	1.28 (m) 1.46 (m)	1.42 (d, *J*=2.4) 1.94 (t, *J*=5.1)	1.38 (m) 1.90 (m)	0.98 (m) 1.73 (m)
2	2.42 (m) 2.50 (m)	1.56 (m)	2.45 (m) 2.55 (m)	2.43 (m) 2.50 (m)	1.66 (m)
3		3.40 (t, *J*=2.7)			3.21(dd, *J*=11.2,4.8)
5	1.35 (m)	1.27 (m)	1.38 (m)	1.32 (m)	0.70 (d, *J*=9.3)
6	1.52 (m)	1.41 (m)	1.38 (m) 1.52 (d, *J*=2.8)	1.47 (m)	1.42 (m) 1.67 (m)
7	1.44 (m)	1.45 (m)	1.50 (m)	1.45 (m)	1.42 (m)
9	1.38 (m)	1.45 (m)	1.45 (m)	1.38 (m)	1.33 (m)
11	1.34 (m) 1.44 (m)	1.52 (m)	1.47 (m)	1.28 (m) 1.42 (m)	1.49 (m)
12	1.06 (m) 1.73 (m)	2.00 (m)	1.69 (m)	1.13 (m) 1.36 (m)	1.78 (m)
13	2.23 (m)	2.23 (dt, *J*= 12.4, 3.4)	1.70 (m)	1.68 (m)	2.23(m)
15	1.42 (m) 1.99 (m)	1.46 (m) 2.05 (m)	1.77 (m)	1.06 (m) 1.71 (m)	1.46 (m) 2.06 (m)
16	1.44 (m) 2.28 (m)	1.47 (m)	1.47 (m) 2.00 (m)	1.40 (m) 1.52 (m)	1.47 (m)
18	1.64 (m)	1.66 (m)	1.65 (m)	1.47 (m)	1.66 (m)
19	3.02 (td, *J*=10.7,4.8)	3.02 (dt, *J*=10.5,4.9)	2.47 (dd, *J*=7.4, 4.7)	2.34 (td, *J*=10.8,5.3)	3.04 (dt, *J*=10.7,4.8)
21	1.22 (m) 1.54 (m)	1.25 (m) 1.58 (m)	1.98 (m)	1.33 (m) 2.08 (m)	1.58 (m)
22	1.47 (m) 1.99 (m)	1.55 (m) 2.04 (m)	1.92 (m)	1.28 (m) 1.40 (m)	1.55 (m) 2.04 (m)
23	1.08 (s)	0.94 (s)	1.08 (s)	1.08 (s)	0.96 (s)
24	1.03 (s)	0.82 (s)	1.03 (s)	1.03 (s)	0.78 (s)
25	0.94 (s)	0.84 (s)	0.93 (s)	0.93 (s)	0.82 (s)
26	0.99 (s)	0.94 (s)	1.07 (s)	1.07 (s)	0.92 (s)
27	1.00 (s)	1.00 (s)	1.00 (s)	0.96 (s)	0.98 (s)
28			3.36 (d, *J*=10.8) 3.81 (d, *J*=11.0)	0.80 (s)	
29	4.62 (s) 4.75 (s)	4.62 (s) 4.75 (s)	4.59 (s) 4.69 (s)	4.91 (s) 4.95 (s)	4.62 (s) 4.75 (s)
30	1.70 (s)	1.70 (s)	1.70 (s)	4.17 (s, br)	1.71 (s)

Table 19. The ^{1}H-NMR (400 MHz) data of **14**, **16** and **17** (in $CDCl_3$); δ in ppm; J in Hz

position	**14**	**16**	**17**
1	1.37 (m) 1.89 (m)	1.38 (m) 1.88 (m)	1.39 (m) 1.90 (m)
2	2.41 (m) 2.47 (m)	2.42 (m) 2.49 (m)	2.43 (m) 2.50 (m)
5	1.31 (m)	1.33 (m)	1.33 (m)
6	1.46 (m)	1.47 (m)	1.47 (m)
7	1.43 (m)	1.45 (m)	1.43 (m)
9	1.35 (m)	1.38 (m)	1.38 (m)
11	1.31 (m) 1.38 (m)	1.27 (m) 1.43 (m)	1.32 (m) 1.45 (m)
12	0.91 (m) 1.34 (m)	1.02 (m) 1.41 (m)	1.48 (m)
13	2.22 (m)	1.67 (m)	2.21 (m)
15	1.23 (m) 1.55 (m)	1.12 (m) 1.73 (m)	1.23 (m) 1.54 (m)
16	1.51 (m) 2.32 (m)	1.13 (m) 1.90 (m)	1.46 (m) 2.31 (m)
18	2.02 (m)	1.72 (m)	1.77 (t, J =11.5)
19	3.35 (td, J=11.2,4.6)	2.31 (m)	2.90 (td, J=11.0,4.5)
21	1.42 (m) 2.16 (m)	1.31 (m) 1.96 (m)	1.42 (m) 2.11 (m)
22	1.75 (m) 2.00 (m)	1.43 (m) 2.12 (m)	1.57 (m) 1.98 (m)
23	1.07 (s)	1.07 (s)	1.08 (s)
24	1.01 (s)	1.02 (s)	1.02 (s)
25	0.91 (s)	0.92 (s)	0.92 (s)
26	0.96 (s)	1.06 (s)	0.97 (s)
27	0.96 (s)	0.99 (s)	1.02 (s)
28		3.33 (d, J= 10.8) 3.80 (d, J=10.8)	
29	5.93 (s) 6.31 (s)	4.91 (s) 4.96 (s)	4.94 (s) 4.99 (s)
30	9.53 (s)	4.12 (m)	4.14 (s)

Table 20. The ^{13}C-NMR (75 MHz) data of **5**, **10**, **11**, **12**, **13**, **14**, **16** and **17** (in $CDCl_3$); δ in ppm

position	**5**	**10**	**11**	**12**	**13**	**14**	**16**	**17**
1	39.6	33.2	39.6	39.6	38.7	39.6	39.6	39.6
2	34.1	25.4	34.1	34.2	27.4	34.1	34.1	34.1
3	218.2	76.3	218.3	218.3	79.0	218.2	218.2	218.1
4	47.3	37.5	47.4	47.3	38.9	47.3	47.3	47.3
5	54.9	49.0	54.9	54.9	55.3	54.9	54.9	54.9
6	19.6	18.2	19.7	19.7	18.3	19.6	19.6	19.6
7	33.6	34.2	33.5	33.6	34.3	33.6	33.5	33.6
8	40.6	40.9	40.9	40.8	40.7	40.6	40.9	40.6
9	49.9	50.3	49.7	49.7	50.5	49.7	49.7	49.8
10	36.9	37.3	36.9	36.9	37.2	36.9	36.8	36.9
11	21.4	20.7	21.4	21.5	20.8	21.3	21.4	21.5
12	25.4	25.5	25.2	26.7	25.5	27.2	26.8	26.8
13	38.5	38.4	37.4	38.1	38.4	38.4	37.3	38.4
14	42.5	42.5	42.8	42.8	42.4	42.4	42.7	42.4
15	30.5	30.6	27.0	27.4	30.5	29.6	27.0	29.7
16	32.1	32.2	29.3	35.4	32.1	31.8	33.8	32.0
17	56.3	56.4	47.8	43.0	56.3	56.4	47.8	56.3
18	49.2	49.2	48.7	48.8	49.2	50.5	49.3	49.9
19	46.9	47.0	47.8	43.8	46.9	38.4	43.5	42.5
20	150.3	150.5	150.4	154.7	150.4	156.2	154.4	154.6
21	29.7	29.6	29.6	31.8	29.7	31.8	31.7	32.3
22	37.0	37.1	34.0	39.8	37.1	36.9	29.1	36.8
23	26.6	28.3	26.6	26.7	28.0	26.6	26.7	26.7
24	21.0	22.1	21.1	21.1	15.4	21.3	21.0	21.0
25	16.0	15.9	15.8	16.0	16.1	15.9	16.0	16.0
26	15.8	16.0	16.0	15.8	16.1	15.8	15.8	15.8
27	14.6	14.8	14.7	14.5	14.7	14.5	14.7	14.6
28	180.8	181.2	60.5	17.7	180.5	181.7	60.2	180.7
29	109.8	109.7	109.8	106.9	109.7	134.2	107.2	107.0
30	19.4	19.4	19.1	64.9	19.4	195.0	65.0	65.3

The molecular formula of $C_{30}H_{48}O_2$ of compound **11** was suggested by the MS *m/z* at 463 amu $[M+Na]^+$. The NMR data of compound **11** were similar to betulonic acid (**5**). The ^{13}C-NMR and HSQCedited spectrum displayed 6 methyl, 12 methylene, 5 methine, 7 quaternary carbons with the presence of 1 hydroxy methylene (δ_C 60.5; δ_H 3.36 and 3.81), 1 pair of terminal olefin carbons (δ_C 150.4 and 109.8) and 1 carbonyl carbon (δ_C 218.3). The ^{1}H-NMR showed signals of H-23, -24, -25, -26, -27, -30 of methyl groups at δ 1.08, 1.03, 0.93, 1.07, 1.00 and 1.70 ppm, respectively. A hydroxyl methylene, in stead of carboxylic group, at position 28 was suggested based on two downfield δ_H 3.36 (d) and 3.81 (d) which attached on a downfield δ_C at 60.51. It also showed δ_H of terminal methylene group C-29 at 4.69 and 4.59. The HMBC correlations: H-29 (δ_H 4.59, 4.69) and C-19 (δ_C 47.8), C-30 (δ_C 19.1) confirmed the presence of terminal olefin group, whereas those from H-28 (δ_H 3.36, 3.81) to C-16 (δ_C 29.6) and C-22 (δ_C 34.0) as well as from H-18 (δ_H 1.65) to C-28 (δ_C 60.5) confirmed the presence of a hydroxyl group at C-28 (Figure 16). The physical properties and spectroscopic data were compared to previous literature [125, 194, 195]. Then, it was identified as betulone.

The MS of compound **12** showed the same mass as compound **11**. The ^{13}C-NMR spectrum exhibited the presence of 30 carbon signals which were assigned by the 2D HSQCedited experiment as 6 methyl, 10 methylene, 5 methine, 5 quatenary carbons, two olefinic carbons, 1 hydroxy methylene and 1 carbonyl carbons. Its NMR data were close to compound **11**. In the ^{1}H-NMR spectrum, the signals at δ_H 4.17 showed the hydroxyl group, as well as two olefinic protons at δ_H 4.91 and 4.95. The HMBC correlations between $\delta_{H\text{-}29}$ 4.91/4.95 and $\delta_{C\text{-}30}$ 64.9 and -$\delta_{C\text{-}19}$ 43.8 together with between $\delta_{H\text{-}30}$ 4.17 and $\delta_{C\text{-}20}$ 154.7 (Figure 16) allowed to the assignment of the OH group at C-30. With the comparison to other lupanes in this study (**5**, **10**, **11**, **13**), C-28 of this compound was a methyl carbon. This methyl group significantly affected C-17 (upfield) and C-16 as well as C-22 (comparable downfield shift). The C-28 methyl group also was suggested by the HMBC correlations of $\delta_{H\text{-}28}$ at 0.80 ppm with δ_C at 35.4, 43.3 and 48.8 ppm of C-16, C-17 and C-18, respectively. With all of this spectroscopic data and comparison to the literature [92, 98], compound **12** was identified as 30-hydroxy-3-oxolup-20(29)-ene.

The molecular formula $C_{30}H_{44}O_4$ of compound **14** was suggested on the basis of the $[M-H]^-$ ion at *m/z* 467.3146 (calcd $C_{30}H_{43}O_4$ at *m/z* 467.3161). The ^{13}C-NMR data showed the presence of 30 signals which were attributed (by HSQCedited correlation) to 5 methyl, 11 methylene, 6 methine and 8 quaternary carbons. The NMR spectrum of **14** was very close to those of betulonic acid (**5**), except an aldehyde signals at δ_H 9.53 and δ_C 195.0 instead of the methyl signal of C-30. The presence of aldehyde functional group was confirmed by IR band at 1731 cm^{-1}. The HMBC correlations from the aldehyde proton (δ_H 9.53) to C-20 (δ_C δ_C 156.2) and from deshield H-29 (δ_H 5.93 and 6.31 ppm) to the aldehyde carbon (194.9 ppm) (Figure 16) suggested the position of this functional group at C-30. The presence of dienone system (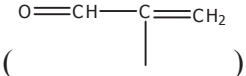) caused this compound detected under UV

at 254 nm on TLC. Then, compound **16** was defined as 3,30-dioxolup-20,29-en-28-oic acid.

The ESI-MS spectrum of **16** showed a $[M+Na]^+$ at *m/z* 479 corresponding to the molecular formula $C_{30}H_{48}O_3$. The difference between the NMR data of **16** and betulonic acid (**5**) was obviously seen through the chemical shift at position 30 and 28. The signal at δ_H 4.12 ppm (s, 2H) represented the protons at C-30 while the germinal coupling protons at δ_H 3.33 and 3.80 ppm were the protons at C-28. The HMBC spectrum presented the correlations between 2 olefinic protons (δ_H 4.96 and 4.91 ppm) and hydroxy C-30 (δ_C 65.0) as well as C-20 and C-19 (Figure 16). These olefinic H-29 signals were presented at lower field because of the effect of hydroxyl group at C-30. From HSQCedited spectrum, the 2 hydroxyl protons ($\delta_{H\text{-}28}$ at 3.33 and 3.80) attached on the same carbon at δ_C 60.2 ppm and, from HMBC, correlated with C-22 (δ_C 31.7), C-16 (δ_C 33.8) and C-18 (δ_C 49.3) (Figure 16). From NOESY spectrum, the stereochemistry of C-28 was comfirmed from the correlation between H_{28a} and H-13, H-15 and H-26 as well as the correlation of H_{28b} with H-19, H_{21b} and H_{22b}. The remaining signals were in agreement with those of betulonic acid (**5**). It was finally deduced that this compound was 28,30-dihydroxylup-20(29)-en-3-one [91].

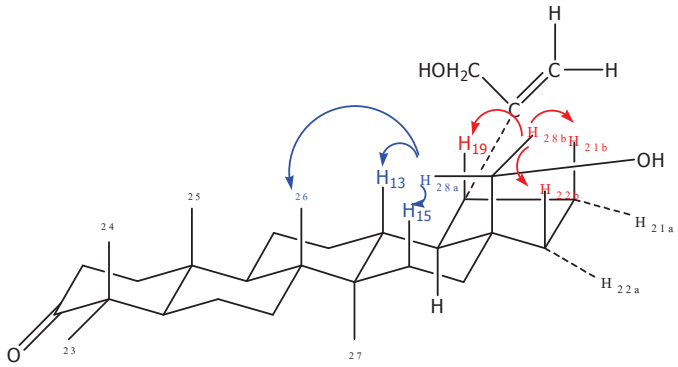

Figure 17. Selected NOEs of compound **16**

The ESI (-) MS of **17** showed $[M-H]^-$ at 469 representing the molecular formula of $C_{30}H_{46}O_4$. The spectrums of HSQCedited and ^{13}C NMR showed 30 carbons: 5 methyl, 12 methylene, 5 methine and 8 quaternary carbons. The NMR data of **17** were close to **16** except the chemical shift at position 28. The downfield shift of $\delta_{C\text{-}17}$ to 56.3 indicated the position of the acidic group at C-28. The C-28 (δ_C 180.7) of carboxylic group exhibited the HMBC correlations with H-18 (δ_H 1.77) and H-22 (δ_H 1.98) (Figure 16). The other assignment of carbon and proton positions was consistent to those of **16**. Finally, it was identified as 29-hydroxy-3-oxolup-20(30)-en-28-oic acid or messagenic acid G.

4.4.5 Caryophyllene oxide (9)

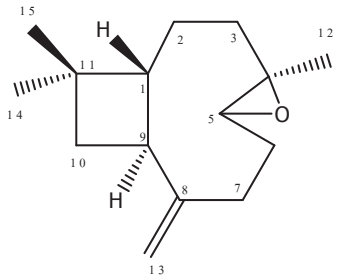

Figure 18 Structure of caryophyllene oxide (**9**)

Caryophyllene oxide was identified by using GC-EI-MS ($[M]^+$ ion at *m/z* 220 and high matching quality with caryophyllene oxide spectrum). The ^{13}C-NMR and HSQCedited spectrum showed 15 carbon signals representing 3 methyl, 6 methylene, 3 methine and 3 quaternary carbons. The δ_C values suggested 1 oxy-quaternary carbon (δ_C 59.9), 1 oxy-methine carbon (δ_C 63.8) and two terminal olefinic carbons (δ_C 151.8 and 112.8). Based on HSQCedited spectrum, The ^{1}H and ^{13}C-NMR spectrum agreed with caryophyllene oxide in previous literature [58, 191, 192].

Table 21 The ^{1}H-NMR (400 MHz) and ^{13}C-NMR (75 MHz) data of **9** (in $CDCl_3$); δ in ppm; *J* in Hz

position	δ_H	δ_C
1	1.80 (dd, *J*=19.8, 10.3)	50.8
2	1.72 (m), 1.48 (m)	27.2
3	2.13 (dd, *J*=7.9, 4.7), 1.05 (s)	39.1
4		59.9
5	2.93 (dd, *J*=10.5, 4.2)	63.8
6	2.30 (td, *J*=16.3, 8.1, 4.1), 1.36 (m)	30.2
7	2.40 (td, *J*=12.5, 8.1, 4.5), 2.17 (m)	29.8
8		151.8
9	2.67 (dd, *J*=18.8, 9.4)	48.7
10	1.73 (d, *J*=8.3), 1.68 (d, *J*=10.5)	39.8
11		34.0
12	1.25 (s)	17.0
13	5.03 (s), 4.91 (s)	112.8
14	1.04 (s)	29.9
15	1.06 (s)	21.6

4.4.6 Mangiferonic acid (15)

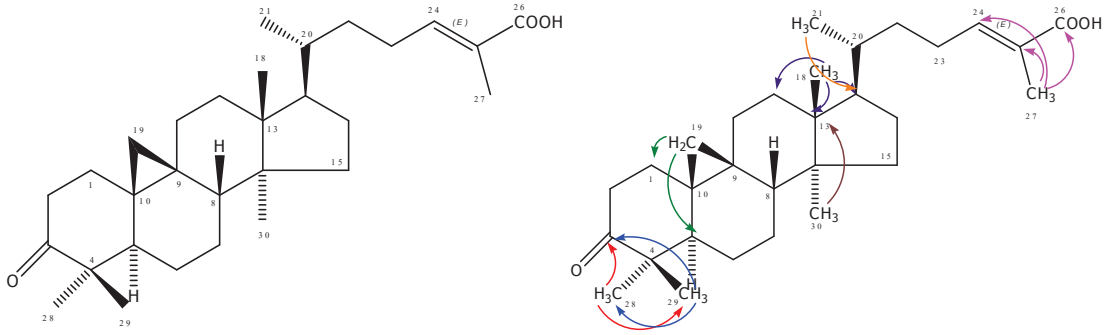

Figure 19 Structure and Selected HMBC correlations of compound **15**

The ^{1}H-NMR spectrum of compound **15** indicated the presence of a cycloartane skeleton. The typical doublets at δ_H 0.63 and 0.84 (J=4.1 Hz) were the characteristic of a cyclopropane methylene (H_2-19). A keto group at C-3 was suggested based on δ_C at 216.8 which showed HMBC correlations with H_3-28 and H_3-29 (Figure 19). Its $[M-H]^-$ ion at m/z 453 corresponded to the molecular formula $C_{30}H_{46}O_3$.

Table 22 The ^{1}H-NMR (400MHz) and ^{13}C-NMR (75 MHz) data of **15** (in $CDCl_3$); δ in ppm; J in Hz

position	δ_H	δ_C	position	δ_H	δ_C
1	1.60 (m) 1.95 (m)	33.4	16	1.35 (m)	28.2
2	2.34 (m) 2.77 (m)	37.5	17	1.86 (d, J=8.1)	52.2
3		216.8	18	1.05 (s)	18.1
4		50.3	19	0.63 (d, J=4.1) 0.84 (d, J=4.1)	29.5
5	1.76 (d, J=4.4)	48.4	20	1.48 (s)	36.0
6	1.60 (m)	21.5	21	0.98 (s)	18.1
7	1.42 (m)	25.9	22	1.20 (m)	26.0
8	1.62 (d, J=3.8)	47.9	23	2.40 (m)	34.7
9		21.1	24	6.95 (t, J=7.0)	145.9
10		26.0	25		126.5
11	1.24 (m)	26.7	26		172.7
12	1.71 (m)	32.8	27	1.90 (s)	12.0
13		45.4	28	1.10 (s)	22.2
14		48.7	29	1.15 (s)	20.8
15	1.36 (m)	35.5	30	0.96 (s)	19.3

A trisubstituted olefin group was indicated based on an olfinic proton ($\delta_{H\text{-}24}$ 6.95) and two olefinic carbons ($\delta_{C\text{-}24}$ 145.9 and $\delta_{C\text{-}25}$ 126.5). A carboxylic and a methyl were suggested for substitution on C-25 since there were HMBC correlations between the methyl protons ($\delta_{H\text{-}27}$ 1.90) and the olefinic carbons together with the carboxylic carbons ($\delta_{C\text{-}26}$ 172.7) (Figure 19). The conjugated double bond was established to be in the E-conformation due to the downfield shifted of the double bond proton caused by the close proximity of the carbonyl carbon (δ_H 6.09 for Z-form of schizandronic acid) [196]. It was clearly supported

by the chemical shift of the CH_3-27 (δ_C 12.00), since it was shielded by steric interaction with the C-23 methylene (δ_C 20.6 for *Z*-form) [196].

The data of compound **15** were in agreement with the reported data [196] of mangiferonic acid which was one of common cycloartane triterpenes in Dipterocarpaceae [43, 49, 205, 206].

4.4.7 26-Fatty acid ester of (24*S*,25*S*)-24,25,26-trihydroxy-3,4-*seco*-cycloart-4(29)-en-3-oic acid (18), its 3-methyl ester (18a) and its triterpene moiety (transesterification product, 18b)

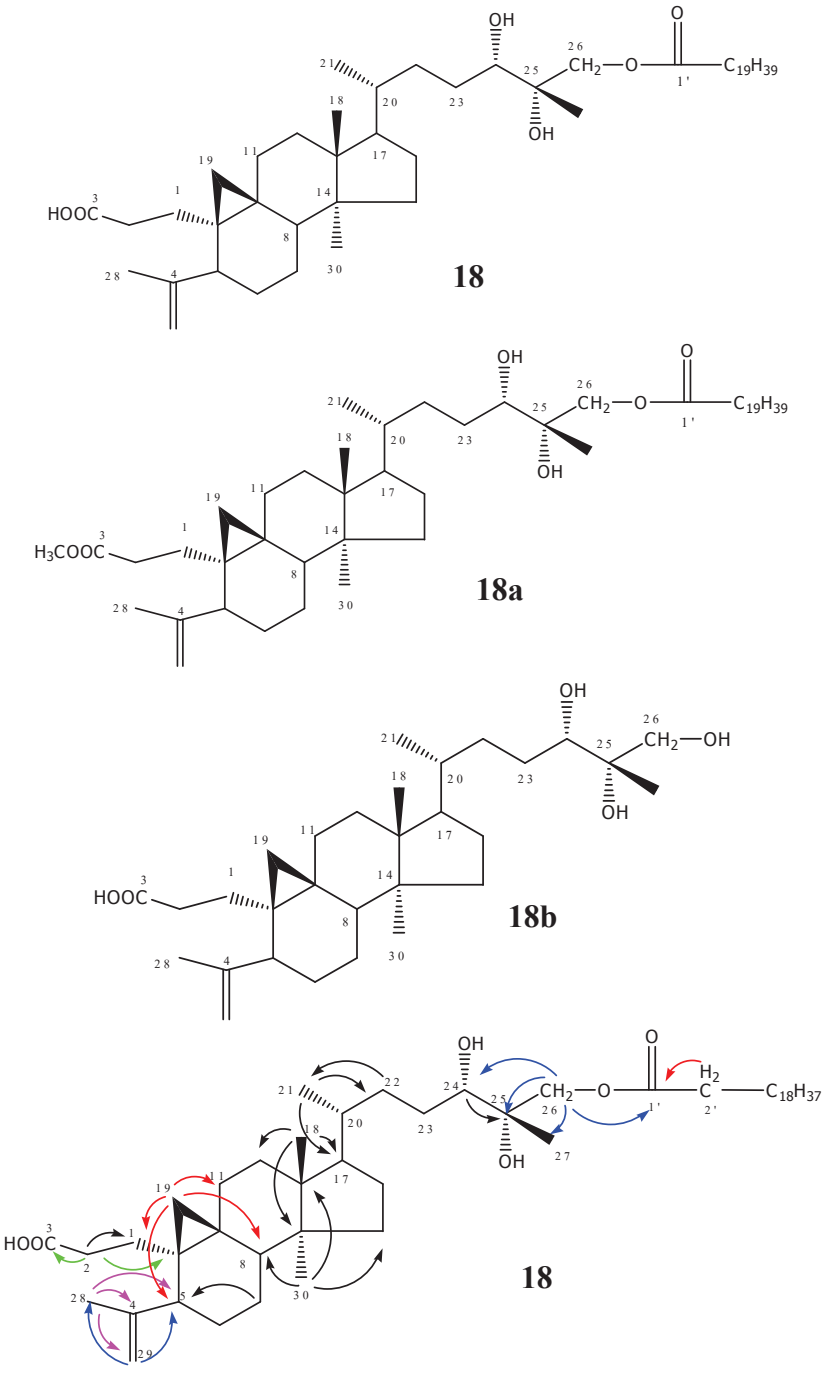

Figure 20 Structures of compounds **18**, **18a** and **18b** and selected HMBC correlations of **18**

Compound **18**, obtained as a white semisolid, was shown to possess a molecular formula $C_{50}H_{88}O_6$ by HRESI-MS. Its IR spectrum showed a broad absorption band at 1712 cm^{-1} indicating overlap of two carbonyl groups.

Compound **18** exhibited a characteristic pair of doublets at δ_H 0.42 (J=4 Hz) and 0.73 (J=4 Hz), corresponding to the methylene protons of the cyclopropane ring of a cycloartane triterpene. Position of these two protons at C-19 was concluded from their HMBC correlations to C-1, C-5, C-8 and C-11 (δ_C 28.8, 45.9, 47.7 and 26.9, respectively) (Figure 22). One carboxylic group (C-3) at δ_C 178.20 ppm showed long range correlation to H-2 (δ_H 2.57) which subsequently correlated to C-1(δ_C 28.8). The HMBC correlations were also observed among protons and carbons at position 4, 5, 28 and 29, but no long range correlations from these protons and carbons to those at positions 1, 2 and 3 (Figure 22). This suggested the clevaging of ring A at positions 3-4. Then, a 3,4-*seco*-cycloartane skeleton was suggesteded for this compound. However, this compound possessed more 20 carbons than normal cycloartane. Based on NMR data, a C20 fatty acid side chain was suggested.

The chemical shifts δ_C at 34.3, 31.9, 29.1-29.7, 22.7 and 14.2 ppm revealed the methylene and methyl groups of fatty acid. No additional data of double bond in fatty acid chain was observed. The oxy-methylene protons (δ_H 4.29/4.03) at position 26 of 3,4-*seco*-cycloartane displayed HMBC correlation to the carbonyl carbon of this fatty acid (δ_C 174.3) (Figure 20). These evidences suggested saturated fatty acid ester at C-26.

Examining the NMR spectrum of **18a** gave the correlation of methyl proton (δ_H 3.65) with C-3 (δ_C 178.2). Finally, after transesterification, the HRESI-MS indicated the molecular formula of triterpene as $C_{30}H_{50}O_5$ (**18b**) and of fatty acid as $C_{20}H_{40}O_2$. Analysis of the data enabled compound **18** to be proposed as 26-arachidic acid ester of 24,25,26-trihydroxy-3,4-*seco*-cycloart-4(29)-en-3-oic acid, a new natural product.

According to Ohtani et al.[169], the stereochemistry of the substituents adjacent to the secondary hydroxyl group was determined by difference in their ^{1}H NMR resonances in the (*S*) and (*R*)-MTPA esters ($\Delta\delta=\delta_S-\delta_R$). The absolute configuration of **18a** at position 24 created using modified Mosher's method was supposed to be *R*-form due to positive values of $\Delta\delta$ obtained for H-20, H-21, and H-22b, as well as opposite results for H-26a, H-26b, and H-27. However, there were some difficulties in the rate of reaction, quantity of reaction product and some unclear ^{1}H-NMR data. First, esterification reactions with both *S*- and *R*-MTPA-Cl were not clean and/or conversion rates were low. Only 2 mg of ester was isolated from the reaction with *S*-MTPA-Cl and most of starting molecules were still unchanged. The low yields of esterification might be resulted from the hindered reaction due to long chain fatty acid at position 26. In case of reaction with *R*-MTPA-Cl, the reaction took very long time and the conversion was very low too. Furthermore, ^{1}H-NMR spectrum of product fraction showed a mixture of two compounds (in a 1:2.45 ratio). This suggested epimerization of the product and calculation was made on the major compound. Secondly, very low difference values, $\Delta\delta$ = +0.0008 and +0.0036, were calculated for H-

21 and H-20, respectively. Other signals on the left of side chain, H-22b and H-23, were difficult to be assigned because of low amount of the ester product. It is consistent with the results from Banskota et al's work [218]. They found that the advanced Mosher's method could not be applied to determine the configuration of a cycloartane which hydroxylated at C-24 and C-25. The presence of C-25 hydroxylated group made unusual conformation and caused dehydration into olefin (double bond between C-25 and C-27). Then, in our work, the presence of ester group at both C-24 and C-26 may promote epimerization at C-25. A better way to determine the actual configuration has recently been reported through an asymmetric synthesis of four isomers of ganodermanotriol [219] (a lanostane-type triterpene bearing a triol side chain similar to compound **18b**). By comparison to the ^{13}C-NMR data of those four synthetic isomer (recorded in $CDCl_3$), the absolute configuration was clearly determined as 24*S*,25*S*.

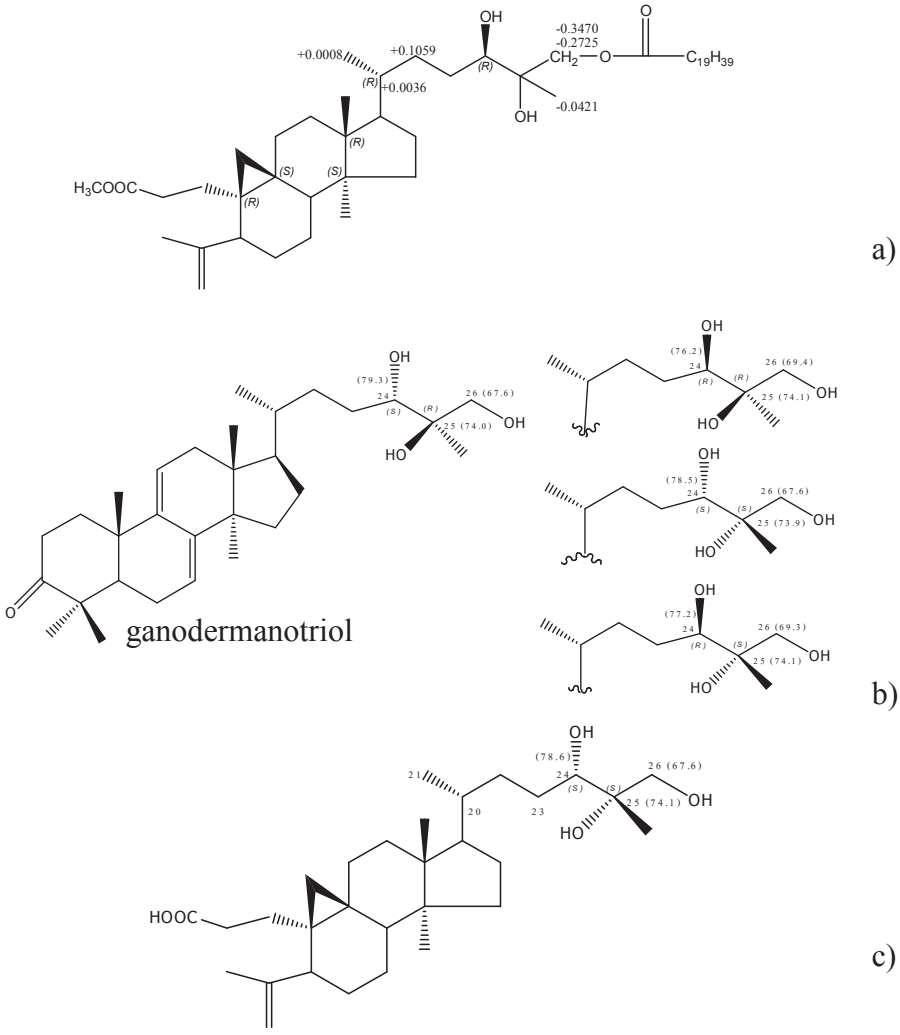

Figure 21. Proposed configuration of **18**

a) The proton chemical shift differences (δ_S-δ_R) of protons around C-24 of **18a**-MTPA ester

b) $\delta_{C\text{-}24}$ to $\delta_{C\text{-}26}$ (in parenthesis) of ganodermanotriol (24*S*,25*R*) and its stereoisomers (reference [219])

c) proposed configuration of **18b** according to four isomers in b) and related δ_C.

Table 23. The ^{1}H-NMR (400MHz) of **18**, **18a**, **18b** and **19a** (in $CDCl_3$) ; δ in ppm ; J in Hz.

position	δ_H			
	18	**18a**	**18b**	**19a**
1 CH_2	2.07 (m) 1.39 (m)	2.05 (m) 1.38 (m)	2.12 (m) 1.35 (m)	2.05 (m) 1.38 (m)
2 CH_2	2.57 (m)) 2.37 (m)	2.51 (m) 2.27 (m)	2.57 (m) 2.35 (m)	2.51 (m)
3 -C(=O)-O-				
4 Civ db				
5 CH	2.43 (m)	2.43 (m)	2.46 (m)	2.43 (m)
6 CH_2	1.50 (m) 1.08 (m)	1.53 (m) 1.50 (m)	1.61 (m)	1.53 (m) 1.09 (m)
7 CH_2	1.31 (m) 1.10 (m)	1 .31 (m) 1.10 (m)	1.10 (m)	1 .33 (m) 1.11 (m)
8 CH	1.57 (m)	1.57 (m)	1.60 (m)	1.57 (m)
9 Civ				
10 Civ				
11 CH_2	2.11 (m) 1.23 (m)	2.11 (m) 1.23 (m)	2.11 (m) 1.11 (m)	2.10 (m) 1.25 (m)
12 CH_2	1.66 (m)	1.66 (m)	1.51 (m)	1.66 (m)
13 Civ				
14 Civ				
15 CH_2	1.30 (m)	1.30 (m)	1.27 (m)	1.29 (m)
16 CH_2	1.93 (m) 1.29 (m)	1.90 (m) 1.29 (m)	1.32 (m)	1.89 (m) 1.29 (m)
17 CH	1.60 (m)	1.59 (m)	1.63 (m)	1.58 (m)
18 CH_3	0.97 (s)	0.97 (s)	0.99 (s)	0.97 (s)
19 CH_2	0.73 (d, J=4) 0.42 (d, J=4)	0.73 (d, J=4.1) 0.41 (d, J=4.1)	0.76 (d, J=4.3) 0.43 (d, J=4.3)	0.73 (d, J =4.3) 0.41 (d, J= 4.3)
20 CH	1.43 (m)	1.41 (m)	1.41 (m)	1.42 (m)
21 CH_3	0.90 (d, J=3.3)	0.93 (d, J=4.2)	0.90 (d, J=6.2)	0.88 (d, J=4.6)
22 CH_2	1.49 (m) 1.30 (m)	1.48 (m) 1.31 (m)	1.29 (m)	1.74 (m) 1.40 (m)
23 CH_2	1.47 (m) 1.41 (m)	1.46 (m) 1.41 (m)	1.33 (m)	1.80 (m) 1.68 (m)
24 CH-O-	3.43 (d, J=9.2)	3.42 (d, J=8.8)	3.55 (m)	4.73 (overlap with H_{29b})
25 Civ –O-				
26 CH_2-O-	4.29 (d, J=11.5) 4.03 (d, J= 11.5)	4.28 (d, J=11.4) 4.04 (d, J=11.4)	3.87 (d, J=11.6) 3.50 (d, J=11.6)	3.38 (d, J=12) 3.23 (d, J=12)
27 CH_3	1.21 (s)	1.20 (s)	1.13 (s)	1.06 (s)
28 CH_3	1.75 (s)	1.69 (s)	1.70 (s)	1.69 (s)
29 CH_2 db	4.83 (s) 4.75 (s)	4.81 (s) 4.74 (s)	4.87 (s) 4.79 (s)	4.81 H29a (s) 4.73 (overlap with H-24)
30 CH_3	0.94 (s)	0.94 (s)	0.96 (s)	0.93 (s)
3-O$\underline{CH_3}$		3.65 (s)		3.65 (s)
1'-($\underline{CH_2}$)$_n$-CH_3		2.37 (t, J=7.5) 1.30 (m)		2.38 (t, J=7.5) 1.26 (m)
1'-$(CH_2)_n$-$\underline{CH_3}$		0.93 (s)		0.87 (s)

Table 24. The ^{13}C-NMR (75 MHz) of **18**, **18a**, **18b** and **19a** (in $CDCl_3$); δ in ppm; J in Hz.

position	δ_C			
	18	**18a**	**18b**	**19a**
1 CH_2	28.8	29.0	28.8	29.0
2 CH_2	31.1	31.4	31.3	31.4
3 -C(=O)-O-	178.2	174.5	179.0	174.4
4 Civ db	149.4	149.5	149.5	149.5
5 CH	45.9	45.8	45.8	45.8
6 CH_2	27.7	27.8	27.8	27.7
7 CH_2	25.0	25.0	25.0	25.1
8 CH	47.7	47.7	47.8	47.7
9 Civ	21.3	21.3	21.3	21.3
10 Civ	26.9	27.0	26.9	27.0
11 CH_2	26.9	26.9	26.9	26.9
12 CH_2	33.0	33.0	33.1	33.0
13 Civ	45.1	45.1	45.1	45.1
14 Civ	49.0	49.0	49.0	49.0
15 CH_2	35.6	35.6	35.6	35.6
16 CH_2	28.2	28.2	28.2	28.1
17 CH	52.3	52.3	52.4	52.2
18 CH_3	18.1	18.1	18.2	18.0
19 CH_2	29.7	30.0	30.1	29.9
20 CH	35.9	35.8	36.0	35.6
21 CH_3	18.2	18.2	18.2	18.1
22 CH_2	33.3	33.2	33.3	32.7
23 CH_2	27.6	27.6	27.8	24.6
24 CH-O-	76.4	76.4	78.6	75.5
25 Civ –O-	73.9	73.9	74.1	73.2
26 CH_2-O-	68.4	68.4	67.6	66.9
27 CH_3	20.7	20.7	21.3	17.6
28 CH_3	19.7	19.8	19.8	19.8
29 CH_2 db	111.6	111.5	111.6	111.5
30 CH_3	19.3	19.3	19.3	19.3
3-O$\underline{CH_3}$		51.4		51.5
1’	174.3	174.3		175.7
1’-($\underline{CH_2}$)$_n$-CH_3	34.3, 29.2-29.8, 22.7	34.3, 29.2-29.8, 22.7		34.5, 29.2-29.8, 24.6
1’-(CH_2)$_n$-$\underline{CH_3}$	14.2	14.2		14.2

4.4.8 C-24 Fatty acid ester of (24*S*,25*S*)-24,25,26-trihydroxy-3,4-*seco*-cycloart-4(29)-en-3-oic acid (19) and its 3-methyl ester (19a)

Compound **19** was always obtained in the mixture with **18** or **20**. Methylation was performed to enable them to separate from each other by SiO_2 cc. Pure compound **19** from fraction C41 and C42 was so few that we cannot run with enough quality of NMR spectrum. However, it was possible to establish the spectrum of methylation product of **19** (=**19a**).

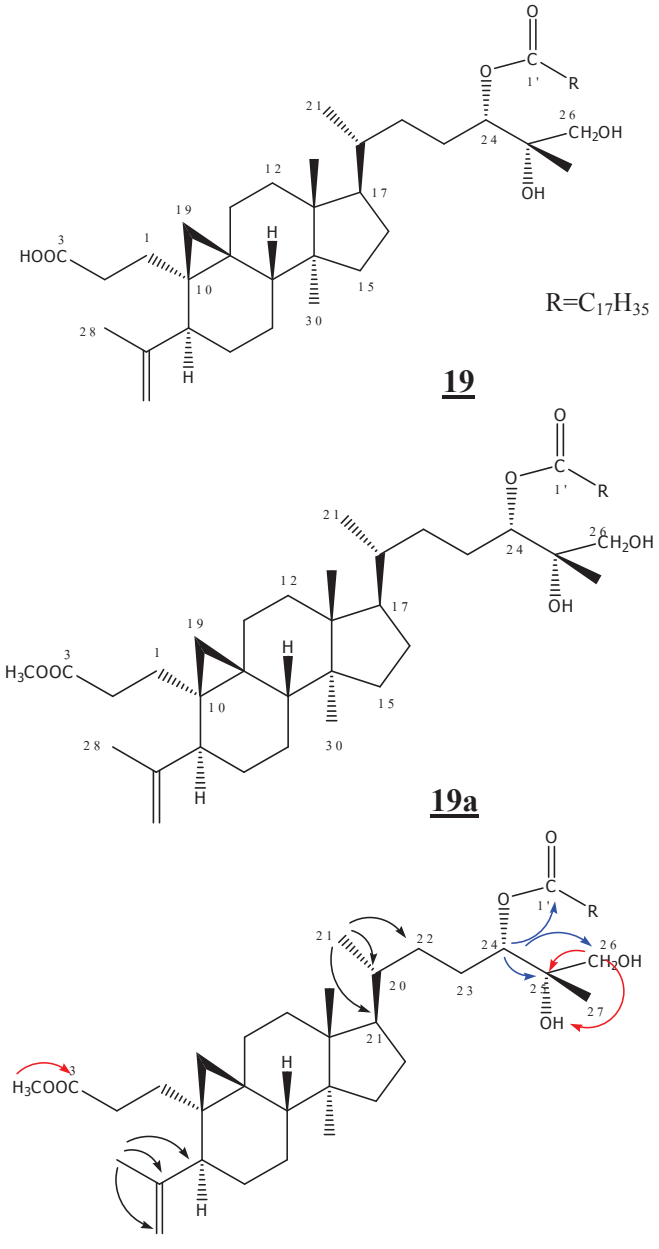

Figure 22. Structures of compounds **19** and **19a** and Selected HMBC correlations of **19a**

NMR assignments of compound **19a** were compared to those of **18a**, with significant differences noted only for resonances associated with position 22 to 27. As same as compound **18** and **18a**, there were the HMBC correlations of H-21 (δ_H 0.88) with C-17 (δ_C 52.3), C20 (δ_C 35.6) and C-22 (δ_C 32.7), indicating side chain at C-17 (Figure 22). The

HMBC spectrum also showed the correlatations of H-24 (δ_H 4.73) to C-25 (δ_C 73.2) and C-27 (δ_C 17.6), and the correlations of H-27 to C-25 and C-26. However, the resonances of H-22, H-23 and H-24 were downfield shift whereas those of H-26 and H-27 were undergone upfield. Another interesting difference from **18** and **18a** was that the HMBC correlations of carbonyl carbon of fatty acid (δ_C 175.7) with methine proton H-24 (δ_H 4.73) instead of methylene protons H-26 (δ_H 3.38 and 3.23). These data indicated that esterification was on hydroxy group of C-24 instead of C-26. The difference between the HRESI-MS of **19a** and **18b** suggested stearic acid as the fatty acid of compound **19**. Hence, the proposed structure of **19** was proposed as 24-stearic acid ester of (24*S*,25*S*)-24,25,26-trihydroxy-3,4-*seco*-cycloart-4(29)-en-3-oic acid. Nevertheless, the amount of **19a** was too low to investigate more reaction.

4.4.9 3,4-*Seco*-cycloart-4(29), 24-diene-3,26-dioic acid (20) and its 3,26-dimethyl ester (20a)

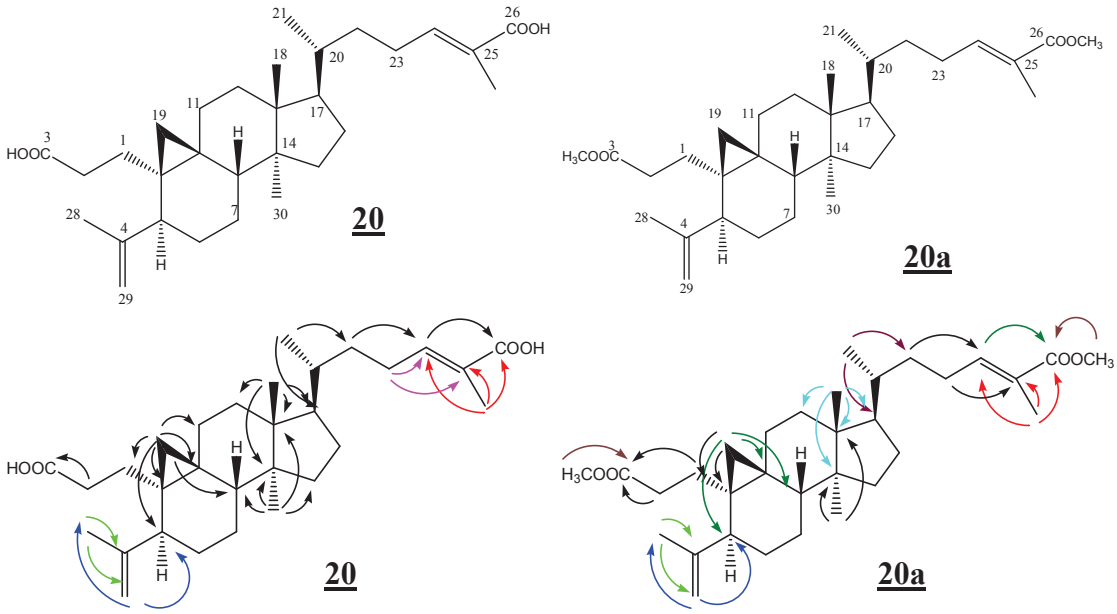

Figure 23. Structures and selected HMBC correlations of compound **20** and **20a**.

Inspection of the 1D-NMR spectrum of compound **20** demonstrated a carboxylic group (δ_C 180.2), a terminal alkene (δ_C 149.4, 111.6; δ_H 4.82, 4.74), and the methylene protons of a cyclopropane ring (δ_H 0.75, 0.42; d, J=4 Hz). These various functional groups were incorporated into the 3,4-*seco*-cycloartane skeleton with one carboxylic acid group.

Compound **20** was obtained from the mixtures of **18**+**20** and **19**+**20** which were methylated to be able to separate each compound and then pure methyl ester product of **20** (**20a**) was hydrolyzed to its original molecule by LiOH. However, the amount of pure separated compound **20** was too low for extensive NMR study.

Table 25. The ^{1}H-NMR (400 MHz) and ^{13}C-NMR (75 MHz) data of **20** and **20a** (in $CDCl_3$); δ in ppm; J in Hz

position	δ_H		δ_C	
	20	**20a**	**20**	**20a**
1 CH_2	2.08 (m) 1.37 (m)	2.05 (m) 1.38 (m)	28.8	29.0
2 CH_2	2.55 (m) 2.30 (m)	2.52 (m) 2.27 (m)	31.4	31.4
3 C(=O)-O			180.2	174.4
4 Civ db			149.4	149.5
5 CH	2.44 (dd, *J*=10.9, 5.3)	2.43 (dd, *J*=11.0, 4.8)	45.8	45.8
6 CH_2	1.52 (m) 1.08 (m)	1.52 (m) ; 1.09 (m)	27.7	27.7
7 CH_2	1.31 (m) 1.10 (m)	1.31 (m) 1.12 (m)	25.0	25.0
8 CH	1.56 (m)	1.58 (m)	47.7	47.7
9 Civ			21.3	21.3
10 Civ			26.9	27.0
11 CH_2	2.10 (m) 1.26 (m)	2.10 (m) 1.26 (m)	26.9	26.9
12 CH_2	1.66 (m)	1.66 (m)	33.0	33.0
13 Civ			45.2	45.2
14 Civ			49.0	49.0
15 CH_2	1.30 (m)	1.30 (m)	35.6	35.6
16 CH_2	1.90 (m) 1.29 (m)	1.91 (m) 1.29 (m)	28.1	28.1
17 CH	1.60 (m)	1.60 (m)	52.2	52.1
18 CH_3	0 .97 (s)	0.96 (s)	18.1	18.0
19 CH_2	0.75 (d, *J*=4) 0.42 (d, *J*=4)	0.73 (d, *J*=4) 0.41 (d, *J*=4)	30.0	29.9
20 CH	1.42 (m)	1.43 (m)	36.0	36.0
21 CH_3	0.92 (d, *J*=6.4)	0.91 (d, *J*=6.4)	18.1	18.1
22 CH_2	1.57 (m) 1.18 (m)	1.58 (m) 1.17 (m)	34.7	34.9
23 CH_2	2.26 (m) 2.13 (m)	2.24 (m) 2.10 (m)	26.0	25.7
24 CH db	6.91 (t, *J*=6.9)	6.77 (t, *J*=7.0)	146.0	143.2
25 Civ db			126.6	127.1
26 C(=O)-O			173.6	168.8
27 CH_3	1.84 (s)	1.84 (s)	12.0	12.4
28 CH_3	1.69 (s)	1.69 (s)	19.7	19.7
29 CH_2 db	4.82(s) 4.74(s)	4.81(s) 4.73 (s)	111.6	111.5
30 CH_3	0.94 (s)	0.93 (s)	19.3	19.3
3-OCH_3		3.64 (s)		51.5
26-OCH_3		3.73 (s)		51.7

Compound **20** established the molecular formula of $C_{30}H_{46}O_4$ by ESI-MS at *m/z* 469 $[M-H]^-$. Twenty eight amu increasing mass of methylation product (**20a**) indicated two carboxylic groups were presented in the structure. This information was campatible with two additional methoxyl proton signals at δ_H 3.64 and 3.73. More information of the side chain was obtained from the HMBC experiment which gave a good agreement with the side chain of mangiferonic acid (**15**) as shown in Figure 23. The stereochemistry of olefin

at C-24 and C-25 was assigned as *E*-form according to the downfield shift of H-24 of **20** (δ_H 6.9 instead of 6.0). Dimethyl esters of **20a** at position 3 and 26 were supported by the HMBC correlation of δ_H 3.64 to δ_C 174.4 (C-3) and δ_H 3.73 to δ_C 168.8 (C-26). On the basis of the above spectroscopic studies the structure of **20** was identified as (24*E*)-3,4-*seco*-cycloartane-4(29),24-diene-3,26-dioic acid [217].

4.5 CYTOTOXIC EVALUATION OF 8 ISOLATED LUPANES.

In the present study, cytotoxic evaluation of 8 lupane triterpenes using WST-1 antiproliferative method revealed that all compounds were inactive against HT29 and MDA-MB231cell lines. Betulonic acid (**5**) exhibited cytotoxicity against both HT116 and PC3 cell lines, with IC_{50} values of 85.60±37.61 and 139.00±3.64 μM, respectively. Compounds **14** displayed weak cytotoxicity against PC3 cells (IC_{50} 282±17.78 μM). Compounds **13**, **11**, **17** were shown slightly cytotoxic effects against PC3 cell line. Interestingly, messagenic acid G (**17**, IC_{50} 43.5±16.26 μM), which differs from betulonic acid (**5**) by the presence of an additional hydroxyl group at the C-30 position, was about 2 fold more potent in inhibiting the growth of HCT116 cells than **5**. In contrast, C-30 aldehyde diminished this activity. These results showed that 3-keto and 17-COOH groups were necessary for cytotoxicity against PC-3 cell line whereas the hydroxyl group at C-30 could enhance this activity.

4.6 CONCLUSION

Phytochemical study of *H.odorata* leaves hexane extract presented the major triterpenes as betulonic acid, *β*-sitosterol and *β*-amyrin, in the order from high to low quantity. Compound **18** and **19** are new, while compound **14** is isolated for the first time in the nature. Within this investigation, *H.odorata* provides various different triterpene compositions. Lupane triterpenes are the main triterpenes in this plant with the minor of cycloartanes and 3,4-*seco*-cycloartanes.

The chemotaxonomic marker in this extract should be lupane- and *seco*-cycloartane-type triterpenes. This work is the first research that studied deeply about triterpenes in *H. odorata* leaves. Besides compound **5** and **13**, other lupanes are characterized for the first time in family Dipterocarpaceae. Most of lupanes in this study have been found to be major components in plants from family Celastraceae [92, 127], Leguminosae [101] and Betulaceae [220]. On the other hand, this study shows an interesting relationship among these families. Purified lupanes exhibit closed structural similarities and differed from each other in the degree of oxidation, particularly at the positions C-3, C-28 and C-30. These findings underlined the chemotaxonomic significance of lupane triterpenes in *H. odorata* Roxb. This results are not in accordance with the conclusion of Geevananda et al [47] indicating lupeol as a marker for the genus *Hopea*, but it is betulonic acid.

The proposed of biosynthesis of **18**, **19** and **20** was based on the oxidation between C-3 and C-4 bond. The relationship between compound **20** and mangiferonic acid (**15**), found in this extract as well, was observed through the similarity of the side chain. Since compound **18**, **19** and **20** were isolated from higher polarity fraction than the others, more free triterpenes of **18**, **19** and **20** might be obtained from the ethanol extract because of their higher polarity (compared to other isolated compounds).

In this research, we evaluated the cytotoxic activity of betulonic acid and its derivatives against four cell lines: PC3, MDA-MB-231, HT-29 and HCT 116. Cytotoxicity of this hexane extract might be from betulonic acid that obtained about 5% of dried extract. The result supports a specific activity against prostate cancer cells PC3, as previously described for betulonic acid [221]. The structure-activity realationship of lupanes is in agreement with the previous literature. The potency of activity was mainly based on the degree of oxidation at positon 3, 28 and 30. Moreover, messagenic acid G, **17**, was found to display a significant cytotoxic activity against HCT116 cells. More extensive investigations are therefore needed for a better understanding of the structure-activity relationships of cytotoxic lupanes and to elucidate their mechanism of action. Because of higher oxidation degree at C-3 of *seco*-cycloartanes, in case it is possible to obtain more quantity, it is interesting to assess bioactivity of cycloartane and *seco*-cycloartane groups too.

PART II

Phytochemical Study of *Dipterocarpus costatus* wood.

I. BOTANICAL STUDY

Genus *Dipterocarpus* [25-27, 177]

The genus *Dipterocarpus* is widely distributed from Sri Lanka, India, South China to Indochina and Malaysia but not east of Wallace's Line. The resin takes the form of wood-oil and is obtained by cutting a large hole in the tree-trunk and burning it within. In Thailand, fourteen species have been recorded.

Genus description: Small to large evergreen or deciduous trees, usually buttressed in evergreen species. Bark scaly in evergreen species, roughly cracked or V-shape fissured in deciduous species. Stipule enlarged into protecting bud, lanceolate, caducous, with distinct ring-like stipular scar on twigs. Leaves coriaceous, symmetrical at base, distinctly plicate. usually large, sometimes sinuate-crenate; Straight, parallel side veins, bending just before margin. Domatia not present. Flowers white or pink, very fragrant. 5 Petals, twisted together into an open-mouthed funnel, fused at base & falling as one piece. Calyx-tube free. Stamens numerous with long pointed projections on top of anthers. Anther narrowly-lanceolate, with 4 subequal pollen sacs. Filament compressed in upper half, broad at lower half. Ovary 3-celled, 2 ovules in each. Inflorescences usually raceme (unbranched panicle), axillary or terminal, with 3-4 large flowers, zig-zag arrangement. Flower buds almost sessile or with short pedicels. Fruit large with 2 long and 3 much shorter wings (calyx lobes), fused together at base and completely covering the nut. Nut usually with apically conical stylopodium. Cotyledon thin, convolute.

Dipterocarpus costatus Gaertn.f. [25-27, 177]

Synonyms: *Dipterocarpus angustifolius*, *Dipterocarpus insularis*, *Dipterocarpus artocarpifolius*, *Dipterocarpus parvifolius*

Vernacular name: Yang pai (ยางปาย) and Yang phrai (ยางพราย) are both preferred names. Yang kaen (ยางแกน) and Yang hi (ยางฮี) are also locally used in the north. Yang bai iat (ยางใบเอียด) and Yang hua waen (ยางหัวแหวน) are recognized in the peninsula.

Diagnostic characters: Deciduous tree to 40 m with very tall, straight trunk and rather open spherical crown. Bark pale brown peeling in thin rounded flakes leaving a distinctive swirling pattern, reminiscent of temple motifs. Indumentum dark brown tufted hairs on young twigs, buds, petioles and racemes. Leaves 8-14 * 4-8 cm, usually elliptic to ovate with slightly pointed tip and blunt or slightly heart-shaped base, more or less hairy on both surface, secondary nerves 10-18 pairs. Young leaves densely covered with star-shaped hairs, mature leaves with scattered short hairs on veins and lower surface. Stalks 1.5-2.7 cm, stout, usually with long shaggy hairs and fairly persistent narrow stipules, 5 mm. Flowers 2 cm, pale orange, in short unbranched clusters of 3-6 flowers at axils of young leaves. Calyx narrowly ridged, coarsely hairy, 8-12 stamens. Fruits 2 long wings, 8-12 cm, 3-5 main veins, 3 short wings <1cm, rounded and deeply folded. Body of fruit 1.2-1.5 cm globose with 5 narrow ridges, <2 mm wide, roughly hairy. Young fruits bright red, standing out clearly against the dark green leaves, often produced in great profusion

Distribution: A widespread species, distributed from the Andaman Islands, Bangladesh to lower Myanmar, Indochina except North Vietnam, and Peninsular Malaysia (from Negri Sembilan northwards). Found throughout Thailand, occasionally by streams, 50-1,300 m altitude. It also occurs in association with *Pinus merkusii* in disturbed lowland semi-evergreen forest and in typical deciduous dipterocarp forest at Khong Chiam, Ubon Ratchathani. (Figure 24)

Phenology Flowering: January-December
Fruiting: January-December

Putative hybrids : *Dipterocarpus costatus* x *D. obtusifolius* has been reported several times, especially at high elevation in deciduous dipterocarp forest, Doi Suthep, and also in Myanmar, but can also be found in lowland areas, under 100 m altitude, in the same area as the hybrid *D.alatus* x *D. costatus*. The leaves resemble those of *D.obtusifolius*, the bark and fruits are closer to *D. costatus* in size and shape.

a)

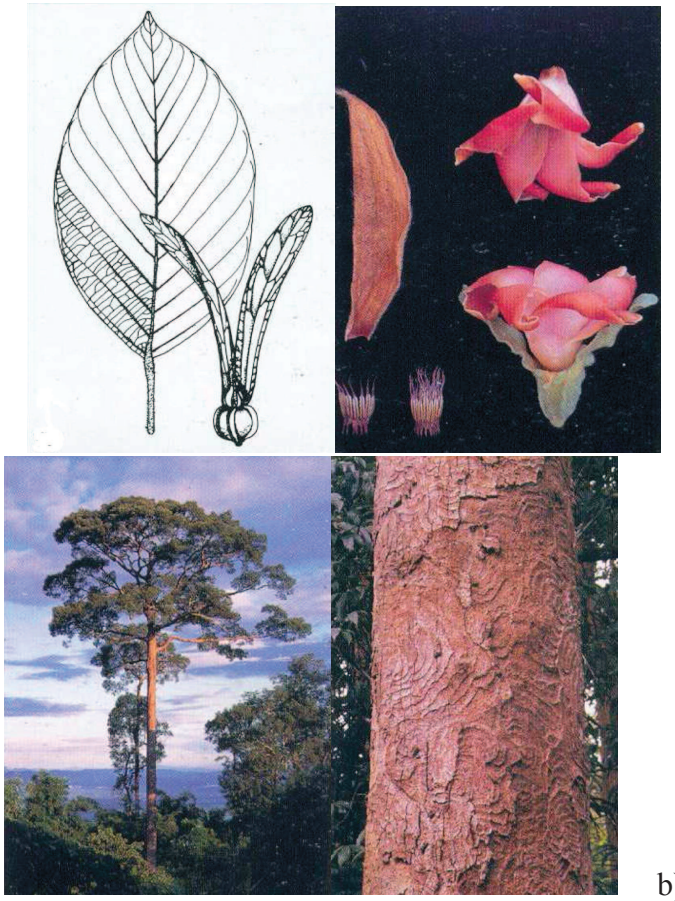

b)

Figure 24. Characteristics of *D. costatus* Gaertn.f. a)-sketch : A. Seeding with enlarged bud. B. Flowering branch. C. Flowing bud. D. Fruit [25, 29]

b) Characteristics of *D. costatus* Gaertn.f. [27]

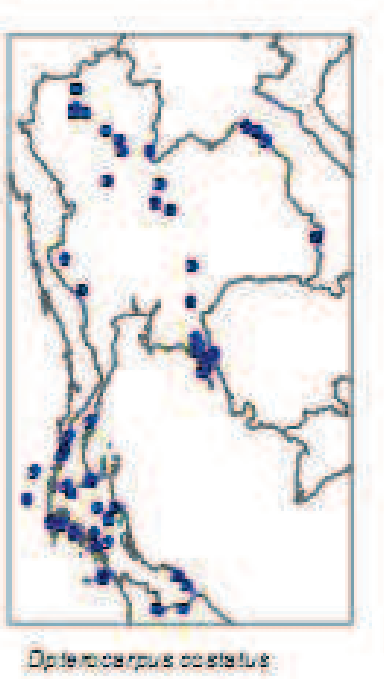

Figure 24. Distribution of *D. costatus* in Thailand [25]

II. PREVIOUS CHEMICAL WORK ON GENUS *DIPTEROCARPUS*

Though some studies have been conducted on the bark and timber, the phytochemical study of genus *Dipterocarpus* have been mostly based on the resin which plays an important economical role in South Eastast Asian countries. The major constituents are in terpenoids especially, dammarane and ursane [39, 40, 67, 71, 222]. The most abundant terpene of the extracts from the genus *Dipterocarpus* is dipterocarpol.

The main neutral triterpenes of dammar resin from the early study were dammadienone, dammadienol, two isomeric hydroxydammarenones and their related diols, and a third ketol, hydroxyhopanone. Based on acid triterpenes, in addition to dammarolic acid, three acids were isolated ursolic acid, dammarenolic acid and dammarenonic acid, the latter obtained only in small yield as its methyl ester (1955) [222]. The work of McLean and Watts (1960) demonstrated dipterocarpol from light petrolatum extract of *D.verrucosis* and *D.glandiflorus* wood [71].

The following chemical analysis of the resin from 42 different species of the genus *Dipterocarpus* by Bisset et al. (1966) [40] revealed the presence of the following sesqui- and triterpenoids: humulene, caryophyllene, copaene, α-gurjunene, calarene, γ-gurjenene, alloaromadendrene, cyperene, caryophyllene oxide, farnesane, dehydrofarnesane, dipterocarpol (hydroxydammarenone-II), dammarenediol-II, dammaradienone, and ocotillone. The triterpene of the various species showed little variation. The sesquiterpenes were much more variable, and caused defining of six groups in the genus, on the basis of the composition of the sesquiterpene fraction of their resins.

Gupta and Dev (1971) [67] worked on the triterpene fraction of oleoresin from *Dipterocarpus pilosus* and found dipterocarpol with several dammaranes (dammara-20,24-dien-3-one, dammara-24-ene-3,20-diol, ocotillone-II, hollongdione, and dipterocarpolic acid), accompanying two ursane derivatives - asiatic acid (with two of its acetyl derivatives), and 2*α*-hydroxyursolic acid.

Bandaranayake et al (1975) [39] isolated terpenoids from resin and bark of 2 *Dipterocarpus* species (*D.hispidus* and *D.zeylanicus*). Dipterocapol was found in large quantities accompanied by asiatic acid, ocotillone, dammarenediol 20S, betulinic acid, humulene and alloaromadendrene. It has been shown that dipterocarpol, the major component of the neutral fraction of *D. costatus* resin, was present to the extent of ca 48%. The mixture of sesquiterpenoids, caryophyllene, humulene and alloaromadendrene was the next most abundant (ca 24%) and the compounds were present in the ratio 7:10:3, respectively. Ocotillone 20R and ocotillone 20S were isolated in yields of *ca* 0.05%, and *ca* 0.04% respectively. The petrol insoluble fraction of the resin was shown to contain 2 component ; 2*α*,3*β*-dihydroxyurs-12-en-28-oic acid (minor, 0.13%) and asiatic acid (major, ca 15%, 2α,3β,23α-trihydroxyurs-12-en-28-oic acid).

A resveratrol tetramer, named diptoindonesin E, was isolated from the acetone extract of the tree bark of *Dipterocarpus hasseltii*, together with (−)-ε-viniferin, laevifonol,

(−)-α-viniferin, vaticanol B, (−)-hopeaphenol, and a coumarin, scopoletin. Hopeaphenol strongly inhibited murine leukemia P-388 cells [37].

A study of flavonoid pattern of *D. costatus* leaves found the same aglycone as *H.odorata* (quercetin, kaempferol and apigenin) but different flavonoid glycoside (quercetin 3-rutinoside) [54].

III. EXPERIMENTAL PART

3.1 Plant material

3.2 Method and apparatus

3.3 Preliminary extraction

3.3.1 Preliminary extraction by soxhlet extraction

3.3.2 *In vitro* bioactivity assays

3.4 Extraction and isolation of *D. costatus* wood hexane extract

3.4.1 Extraction by maceration

3.4.2 Isolation

3.5 Cytotoxic evaluation of isolated triterpenes

3.6 *In vitro* antiplasmodial activity of isolated triterpenes

3.7 Physical characteristics and spectrum of isolated compounds

3.1 PLANT MATERIAL

Dipterocarpus costatus wood was collected from Chiang Mai (Maerim district), a northern province of Thailand in September, 2004, and identified by Dr.Chavalit Sittisombut. A voucher specimen was deposited at the herbarium of the Department of Pharmacognosy, Faculty of Pharmacy, Silpakorn University, Nakhon Pathom, Thailand.

3.2 METHOD AND APPARATUS

As same as those for *H. odorata*.

3.3 PRELIMINARY EXTRACTION

3.3.1 Preliminary extraction by soxhlet extraction

Dried wood of *D. costatus* (50.4210 g) was cut in pieces and was soxhlet extracted with hexane and ethanol. Both solutions were separately concentrated in vacuo to give 1.0367 g (2.56%) hexane and 1.3755 g (2.73%) ethanol extracts.

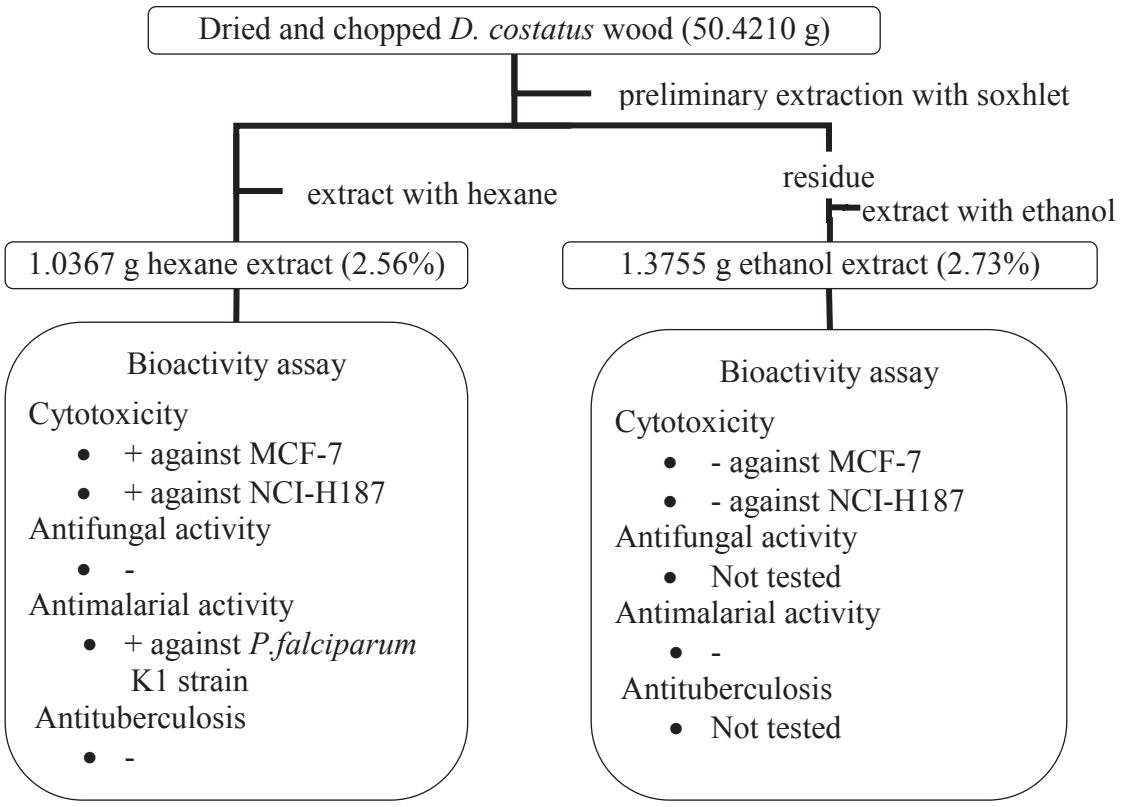

Scheme 18. Extraction and bioactivity assay of preliminary study of *D. costatus* wood

3.3.2 *In vitro* bioactivity assays

The hexane and the ethanol extracts were assayed for biological activity with the same method as applied for *H.odorata* extract. The result was shown in Table 26.

Table 26. *In vitro* bioactivity assays of *D. costatus* wood extract

	IC_{50} (µg /mL)				
	Anti MCF-7	Anti NCI-H187	Antifungus	Antimalaria	Anti-TB
D. costatus wood/ hexane	25.55	9.06	Inact.	3.20	Inact.
D. costatus wood/ ethanol	Inact	Inact	Not tested	Inact	Not tested

Inact. = inactive at the level of 50 µg/mL.
MCF-7 = breast cancer, NCI-H187 = small cell lung cancer, antifungal = anti – *Candida albicans*, antimalaria = anti – *Plasmodium falciparum*, anti – TB = anti – *Mycobacterium tuberculosis*.

The method for each assay was as follows:

Cytotoxicity against MCF-7 (breast cancer)

Method Resazurin Microplate assay (REMA)

Negative control 0.5% DMSO

IC_{50} of positive control Ellipticine=-µg/mL, Doxorubicine = 1.09 µg/mL

Maximum final concentration of tested sample 50 µg /mL

Cytotoxicity against NCI-H187 (small cell lung cancer)

Method Resazurin Microplate assay (REMA)

Negative control 0.5% DMSO

IC_{50} of positive control Ellipticine=0.390 µg/mL, Doxorubicine = 0.040 µg/mL

Maximum final concentration of tested sample 50 µg/mL

Antimalarial activity against *Plasmodium falciparum* K1 strain

Method Microculture Radioisotope Technique

Negative control 0.1% DMSO

IC50 of positive control Dihydroartemisinine 4.1 nM

Maximum final concentration of tested sample 10 µg/mL

Antifungal activity against *Candida albicans*

Method Resazurin Microplate assay (REMA)

Negative control 0.5% DMSO

IC_{50} of positive control Amphotericin B = 0.034 µg/mL

Maximum final concentration of tested sample 50 µg/mL

Antituberculosis (anti-TB) against *Mycobacterium tuberculosis* H37Ra strain

Method Green fluorescent protein microplate assay (GFPMA)

Negative control 0.5% DMSO

MIC of positive control Rifampicin = 0.003-0.012 µg/mL, Streptomycin= 0.156-0.313 µg/mL, Isoniazid = 0.023-0.046 µg/mL, Ofloxacin = 0.391-0.781 µg/mL

Maximum final concentration of tested sample 50 µg/mL

3.4 EXTRACTION AND ISOLATION OF *D. costatus* WOOD HEXANE EXTRACT

3.4.1 Extraction by maceration

The dried and chopped heartwood (2,645 gm.) of *D. costatus* was macerated with hexane (3L*48h*3), then maceration continued with dichloromethane, ethyl acetate and ethanol (3L*48h*3, each), one by one, at room temperature. All extracts were separately filtered and concentrated under vacuum. (Scheme 19)

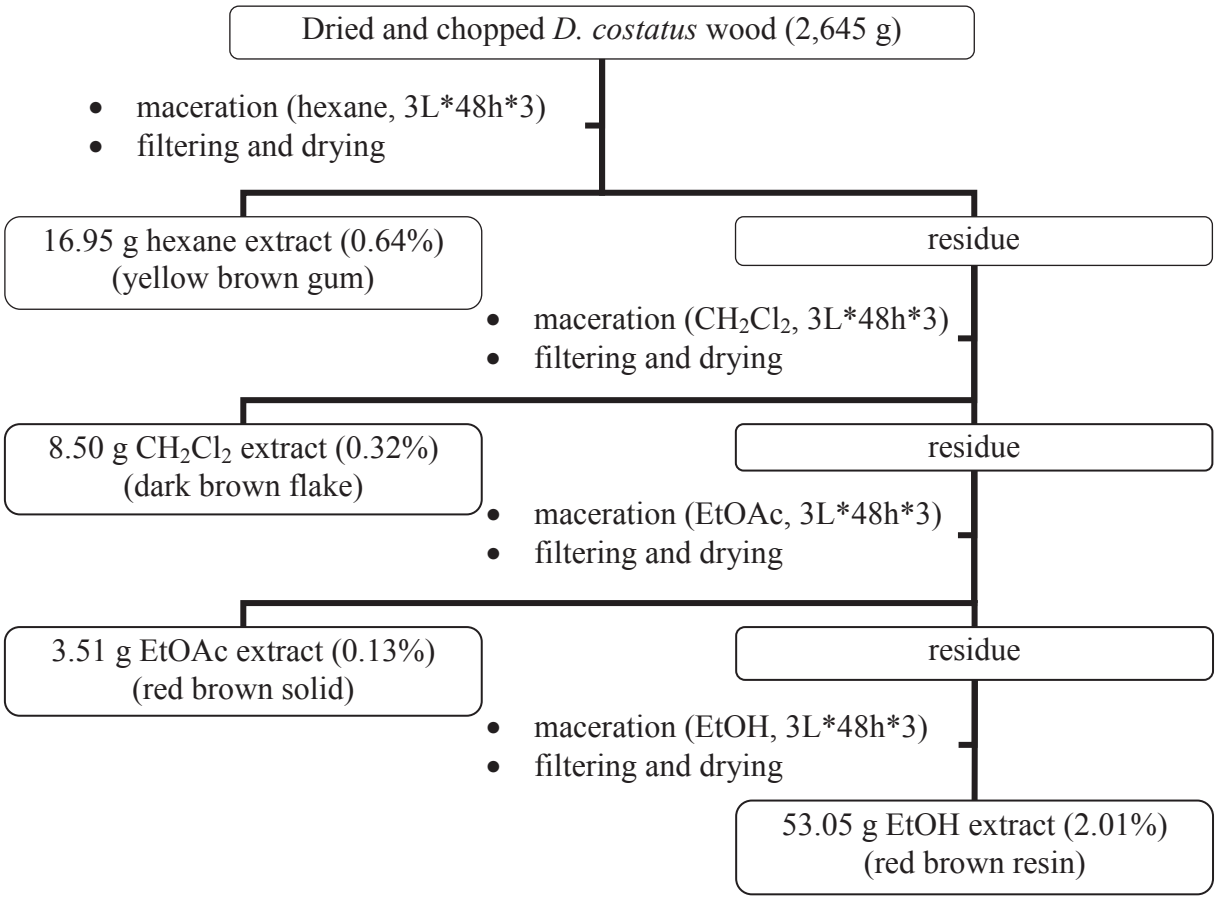

Scheme 19. Extraction of *D. costatus* wood for phytochemical study

3.4.2 Isolation.

The hexane extract (12 g) was adsorbed on silica gel (12 g), then, fractionated by silica gel medium pressure liquid chromatography (MPLC), and successively eluted with gradually increasing polarity of eluents; cyclohexane, gradient mixtures of cyclohexane-dichloromethane, dichloromethane, gradient mixtures of dichloromethane-ethyl acetate, ethyl acetate, gradient mixtures of ethyl acetate-methanol, and methanol. The elution afforded 70 fractions (D01-D70, as described in table 19) on the basis of their TLC. Fraction D02 (colorless semisolid) and fraction D50 (yellow gum) showed only one spot on TLC (cHex-EtOAc 100:1 and 1:1, respectively, sprayed with H_2SO_4/vanillin reagent). After spectroscopic analysis, they were identified as *β*-elemene (**21**, 10.6 mg) for fraction

D02 and isofouquierone (**40**, 119 mg) for fraction D50. When fraction D16 was dried, its characteristic was a white flake which showed a broad single spot on TLC (cHex-EtOAc 2:1, sprayed with H_2SO_4/vanillin reagent) with some pale spots of impurity. The spectroscopic data indicated the structure of *β*-sitosterol (**3**, 200 mg). Other fractions were purified by rechromatography over SiO_2 column chromatography.

Table 27. Fractionation of *D. costatus* wood hexane extract isolation by MPLC.

Fraction	Eluent (cHex-CH_2Cl_2-EtOAc-MeOH, %)	Weight (mg)	Isolated compounds
D01	cHex-CH_2Cl_2 100-90:0-10	91.1	
D02	cHex-CH_2Cl_2 85:15	10.6	*β*-elemene (**21**, 10.6 mg)
D03	cHex-CH_2Cl_2 80-70:20-30	11.9	
D04	cHex-CH_2Cl_2 65-55:35-45	15.2	
D05	cHex-CH_2Cl_2 50-45:40-55	118.9	
D06	cHex-CH_2Cl_2 40-35:60-65	24.6	
D07	cHex-CH_2Cl_2 30-25:70-75	21.2	
D08	cHex-CH_2Cl_2 20-10:80-90	18.1	
D09	cHex-CH_2Cl_2 5-0:95-100	143.6	
D10	cHex-CH_2Cl_2 0:100	58.6	
D11	cHex-CH_2Cl_2 0:100	375.5	caryophyllene oxide (**9**, 150 mg)
D12	cHex-CH_2Cl_2 0:100	164.6	
D13	cHex-CH_2Cl_2 0:100	117.8	
D14	cHex-CH_2Cl_2 0:100	35.1	
D15	cHex-CH_2Cl_2 0:100	57.5	
D16	cHex-CH_2Cl_2 0:100	200	*β*-sitosterol (**3**, 200 mg)
D17	CH_2Cl_2-EtOAc 100-96:0-4	62.1	
D18	CH_2Cl_2-EtOAc 94:6	227.5	
D19	CH_2Cl_2-EtOAc 94:6	102.6	
D20	CH_2Cl_2-EtOAc 94:6	38.4	
D21	CH_2Cl_2-EtOAc 94:6	242.0	
D22	CH_2Cl_2-EtOAc 92:8	502.5	dipterocarpol (**22**, 400 mg) isofouquierone peroxide (**23**, 20 mg)
D23	CH_2Cl_2-EtOAc 92:8	962.8	
D24	CH_2Cl_2-EtOAc 92:8	539.7	(20*R*)-17 *α*,29-epoxy-28-norlupan-3-one (**24**, 20 mg) *** dipterocarpol (**22**, 70 mg) 17*α*-hydroxy-28-norlupan-20(29)-en-3-one (**25**, 72 mg) *** octanordammarane-3,17-dione (**26**, 16 mg) * isocabralealactone (20*R*) (**27**, 42 mg) ** cabralelactone (**28**, 131 mg) isofouquierone peroxide (**23**, 11 mg) (20*S*)-20-hydroxy-24-perhydroxy-dammar-25-en-3-one (**29**, 6 mg) ***
D25	CH_2Cl_2-EtOAc 90:10	179.4	
D26	CH_2Cl_2-EtOAc 90:10	270.7	

Table 27. Fractionation of *D. costatus* wood hexane extract isolation by MPLC. (continued)

Fraction	Eluent (cHex-CH_2Cl_2-EtOAc-MeOH, %)	Weight (mg)	Isolated compounds
D27	CH_2Cl_2-EtOAc 88:12	617.6	cabraleone (**30**, 350 mg) dammarenediol II (**31**, 233 mg) cereotagaloperoxide= (20*S*)-3 *β*,20-dihydroxy-24-perhydroxydammar-25-ene (**32**, 3 mg) ** isofouquierol peroxide (**33**, 11 mg)
D28	CH_2Cl_2-EtOAc 88:12	656.7	cabraleone (**30**, 28 mg) ocotillone (**34**, 456 mg) cabralealactone (**28**, 14 mg) 3-*epi*cabraleahydroxylactone (**35**, 20 mg) isofouquierol peroxide (**33**, 8 mg)
D29	CH_2Cl_2-EtOAc 86:14	432.2	
D30	CH_2Cl_2-EtOAc 86-84:14-16	252.8	
D31	CH_2Cl_2-EtOAc 84:16	136.9	
D32	CH_2Cl_2-EtOAc 82:18	143.0	(20*S*)-29-hydroxy-17 *α*,20-peroxy-28-norlupan-3-one (**36**, 4 mg) ***
D33	CH_2Cl_2-EtOAc 82:18	129.0	
D34	CH_2Cl_2-EtOAc 82:18	60.2	
D35	CH_2Cl_2-EtOAc 80:20	265.2	ocotillol II (**37**, 40 mg) (20*S*,24*S*)-20,24-dihydroxydammar-25-en-3-one (**38**, 5 mg)
D36	CH_2Cl_2-EtOAc 80:20	50.6	
D37	CH_2Cl_2-EtOAc 80:20	473.7	isofouquierone peroxide (**23**, 80 mg) (20*S*,23*E*)-20-hydroxy-27-nordammar-23-ene-3,25-dione (**39**, 8 mg) *** isofouquierone (**40**, 37 mg)
D38	CH_2Cl_2-EtOAc 80-78:20-22	191.0	ocotillol II (**37**, 5 mg) isofouquierone peroxide (**23**, 6 mg) 17*α*-hydroxy-28,29-dinorlupan-3,20-dione (**41**, 6 mg) *** (20*S*,23*E*)-20-hydroxy-27-nordammar-23-ene-3,25-dione (**39**, 40 mg) ***
D39	CH_2Cl_2-EtOAc 78:22	136.8	
D40	CH_2Cl_2-EtOAc 78-76:22-24	109.2	
D41	CH_2Cl_2-EtOAc 76:24	143.7	
D42	CH_2Cl_2-EtOAc 74-72:26-28	267.3	(20*R*)-20-hydroxy-17 *α*,29-epoxy-28-norlupan-3-one (**42**, 17 mg) *** (20*S*,24*S*)-20,24-dihydroxydammar-25-en-3-one (**38**, 73 mg)
D43	CH_2Cl_2-EtOAc 72:28	93.8	
D44	CH_2Cl_2-EtOAc 72:28	112.9	(20*S*,24*S*)-20,24-dihydroxydammar-25-en-3-one (**38**, 15 mg)
D45	CH_2Cl_2-EtOAc 70:30	92.0	
D46	CH_2Cl_2-EtOAc 70-68:30-32	58	
D47	CH_2Cl_2-EtOAc 68:32	116.4	
D48	CH_2Cl_2-EtOAc 66:34	90.2	
D49	CH_2Cl_2-EtOAc 66-62:34-38	549.2	
D50	CH_2Cl_2-EtOAc 62:38	119.3	isofouquierone (**40**,119 mg)
D51	CH_2Cl_2-EtOAc 60:40	97.5	
D52	CH_2Cl_2-EtOAc 60-58:40-42	69.9	
D53	CH_2Cl_2-EtOAc 58-56:42-44	98.2	clavone-2,9-diol (**43**)

Table 27. Fractionation of *D. costatus* wood hexane extract isolation by MPLC. (continued)

Fraction	Eluent (cHex-CH_2Cl_2-EtOAc-MeOH, %)	Weight (mg)	Isolated compounds
D54	CH_2Cl_2-EtOAc 56:44	62.6	
D55	CH_2Cl_2-EtOAc 54-50:46-50	163.2	isofouquierol (**44**, 54 mg)
D56	CH_2Cl_2-EtOAc 50-48:50-52	41.4	
D57	CH_2Cl_2-EtOAc 48-44:52-56	36.2	
D58	CH_2Cl_2-EtOAc 44-40:56-60	59.6	(20*S*,22*E*,24*R*)-20,24,25-trihydroxydammar-22-en-3-one (**45**, 6 mg) ***
D59	CH_2Cl_2-EtOAc 40-35:60-65	48	(20*S*,22*E*,24*R*)-20,24,25-trihydroxydammar-22-en-3-one (**45**, 5 mg) ***
D60	CH_2Cl_2-EtOAc 35-30:65-70	26.4	
D61	CH_2Cl_2-EtOAc 25:75	33.5	
D62	CH_2Cl_2-EtOAc 25-20:75-80	37.7	
D63	CH_2Cl_2-EtOAc 15:85	17.5	
D64	CH_2Cl_2-EtOAc 15-0:85-100	80.0	(20*S*,23*E*)- 20,25,26-trihydroxydammar-23-en-3-one (**46**, 8 mg) ***
D65	EtOAc-MeOH 100-95:0-5	58.0	(20*S*,23*E*)- 20,25,26-trihydroxydammar-23-en-3-one (**46**, 4 mg) ***
D66	EtOAc-MeOH 90:10	286.3	(20*S*,24*R*)-20,24-epoxy-25-hydroxy-2,3-*seco*-dammarane-2,3-dioic acid (**47**, 16 mg) *** (20*S*, 23*E*)- 25-hydroperoxy-20-hydroxy-2,3-*seco*-dammar-23-en-2,3-dioic acid (**48**, 5 mg) ***
D67	EtOAc-MeOH 85:15	106.9	
D68	EtOAc-MeOH 80:20	138.7	(20*S*)-20-hydroxy-3-oxo-24,25,26,27-tetranordammar-23-oic acid (**49**, 5 mg) *** (20*S*,24*R*)-20,24-epoxy-25-hydroxy-2,3-*seco*-dammarane-2,3-dioic acid (**47**, 8 mg) ***
D69	EtOAc-MeOH 75-65:25-35	161.2	
D70	EtOAc-MeOH 50-0:50-100	164.0	

* the compound found for the first time in the nature.
** the rare compound in the nature.
*** New compounds.

Study of fraction D11

Fraction D11 (375 mg) was further chromatographed over SiO_2, using cHex-EtOAc 30:1 as mobile phase, to yield caryophyllene oxide (**9**, 150 mg)

Study of fraction D22

Fraction D22 (502 mg) was subjected to SiO_2 cc using cHex-EtOAc (8:1) system as eluent. After elution, dipterocarpol (**22**, 400 mg) and isofouquierone peroxide (**23**, 20 mg) were obtained.

Study of fraction D24

Fraction D24 (539 mg) was purified by SiO_2 cc with cHex-EtOAc 8:1 and 4:1 to afford 8 compounds; (20*S*)-17α,29-epoxy-28-norlupan-3-one (**24**, 20 mg), dipterocarpol (**22**, 70 mg), 17α-hydroxy-28-norlupan-20(29)-en-3-one (**25**, 72 mg), octanordammarane-3,17-dione (**26**, 16 mg), isocabralealactone (20R) (**27**, 42 mg), cabralelactone (**28**, 131 mg), isofouquierone peroxide (**23**, 11 mg) and (20*S*)-20-hydroxy-24-perhydroxydammar-25-en-3-one (**29**, 6 mg).

Study of fraction D27

Fraction D27 (617 mg) was subjected to SiO_2 cc using cHex:EtOAc = 8:1, followed by 5:1 and 3:1, as mobile phase. The elution gave 4 compounds: cabraleone (**30**, 350 mg), dammarenediol II (**31**, 233 mg), cereotagaloperoxide (**32**, 3 mg) and isofouquierol peroxide (**33**, 11 mg).

Study of fraction D28

Fraction D28 (656 mg) was subjected to SiO_2 cc with cHex-EtOAc 6:1 and 3:1 as eluent to give 5 compounds: cabraleone (**30**, 28 mg), ocotillone (**34**, >250 mg), cabralealactone (**28**, 14 mg), 3-*epi*cabraleahydroxylactone (**35**, 20 mg) and isofouquierol peroxide (**33**, 8 mg).

Study of fraction D32

Fraction D32 (142 mg) was purified by SiO_2 cc with cHex-EtOAc (4:1) system. A star crystal of (20*S*)-29-hydroxy-17α,20-peroxy-28-norlupan-3-one (**36**, 4 mg) was obtained and washed with cold EtOAc.

Study of fraction D35

Fraction D35 (265 mg) was separated chromatographically over SiO_2 cc with cHex-EtOAc (3.5:1) system. The elution provided ocotillol II (**37**, 40 mg) and (20*S*,24*S*)-20,24-dihydroxydammar-25-en-3-one (**38**, 5 mg).

Study of fraction D37

Fraction D37 (473 mg) was further chromatographed over SiO_2 cc using cHex-EtOAc (4:1) to yield isofouquierone peroxide (**23**, 80 mg), (20*S*,23*E*)-20-hydroxy-27-nordammar-23-ene-3,25-dione (**39**, 8 mg) and isofouquierone (**40**, 37 mg).

Study of fraction D38

Fraction D38 (191 mg) was purified by SiO_2 cc using cHex-EtOAc (4:1) to afford 4 compounds: ocotillol II (**37**, 5 mg), isofouquierone peroxide (**23**, 6 mg), 17α-hydroxy-28,29-dinorlupan-3,20-dione (**41**, 6 mg) and (20*S*,23*E*)-20-hydroxy-27-nordammar-23-ene-3,25-dione (**39**, 40 mg).

Study of fraction D42 and D43

Fraction D42 and D43 were combined (360 mg) and chromatographed over SiO_2 cc, eluting with cHex:EtOAc (3:1) to give (20*R*)-20-hydroxy-17*α*,29-epoxy-28-norlupan-3-one (**42**, 17 mg) and (20*S*,24*S*)-20,24-dihydroxydammar-25-en-3-one (**38**, 73 mg).

Study of fraction D44

Compound **38** (15 mg) was crystallized in fraction D44 and was characterized as (20*S*,24*S*)-20,24-dihydroxydammar-25-en-3-one (**38**).

Study of fraction D53

Fraction D53 (98 mg) was chromatographed by SiO_2 cc with cHex-EtOAc (1:1) and further purified using GC-MS to give an unidentified sesquiterpene and clovane-2,9-diol (**43**)

Study of fraction D55

Fraction D55 (163 mg) was chromatographed over SiO_2 cc, eluting with cHex-EtOAc (1.5:1) to give isofouquierol (**44**, 54 mg).

Study of fraction D58 and D59

Fraction D58 (59 mg) and D59 (48 mg), upon further chromatography over SiO_2 cc using cHex-EtOAc (1:1), furnished (20*S*,22*E*,24*R*)-20,24,25-trihydroxydammar-22-en-3-one (**45**, 6 and 5mg, respectively).

Study of fraction D64 and D65

Chromatography of fraction D64 (80 mg) and D65 (58 mg) over SiO_2 cc with cHex-

EtOAc (1:8) afforded (20*S*,23*E*)-20,25,26-trihydroxydammar-23-en-3-one (**46**, 8 and 4

mg, respectively).

Study of fraction D66

Fraction D66 (286 mg) was subjected to silica gel column chromatography with CH_2Cl_2:MeOH (30:1) and addition of a little of acetic acid gave (20*S*,24*R*)-20,24-epoxy-25-hydroxy-2,3-*seco*-dammarane-2,3-dioic acid (**47**, 16 mg) and (20*S*,23*E*)-25-hydroperoxy-20-hydroxy-2,3-*seco*-dammar-23-en-2,3-dioic acid (**48**, 5 mg).

Study of fraction D68

Fraction DML68 (138 mg) was rechromatographed over silica gel (cHex-Acetone-MeOH = 20:4:1) to give (20*S*)-20-hydroxy-3-oxo-24,25,26,27-tetranordammar-23-oic acid (**49**, 5

mg) and (20*S*,24*R*)-20,24-epoxy-25-hydroxy-2,3-*seco*-dammarane-2,3-dioic acid (**47**, 8 mg).

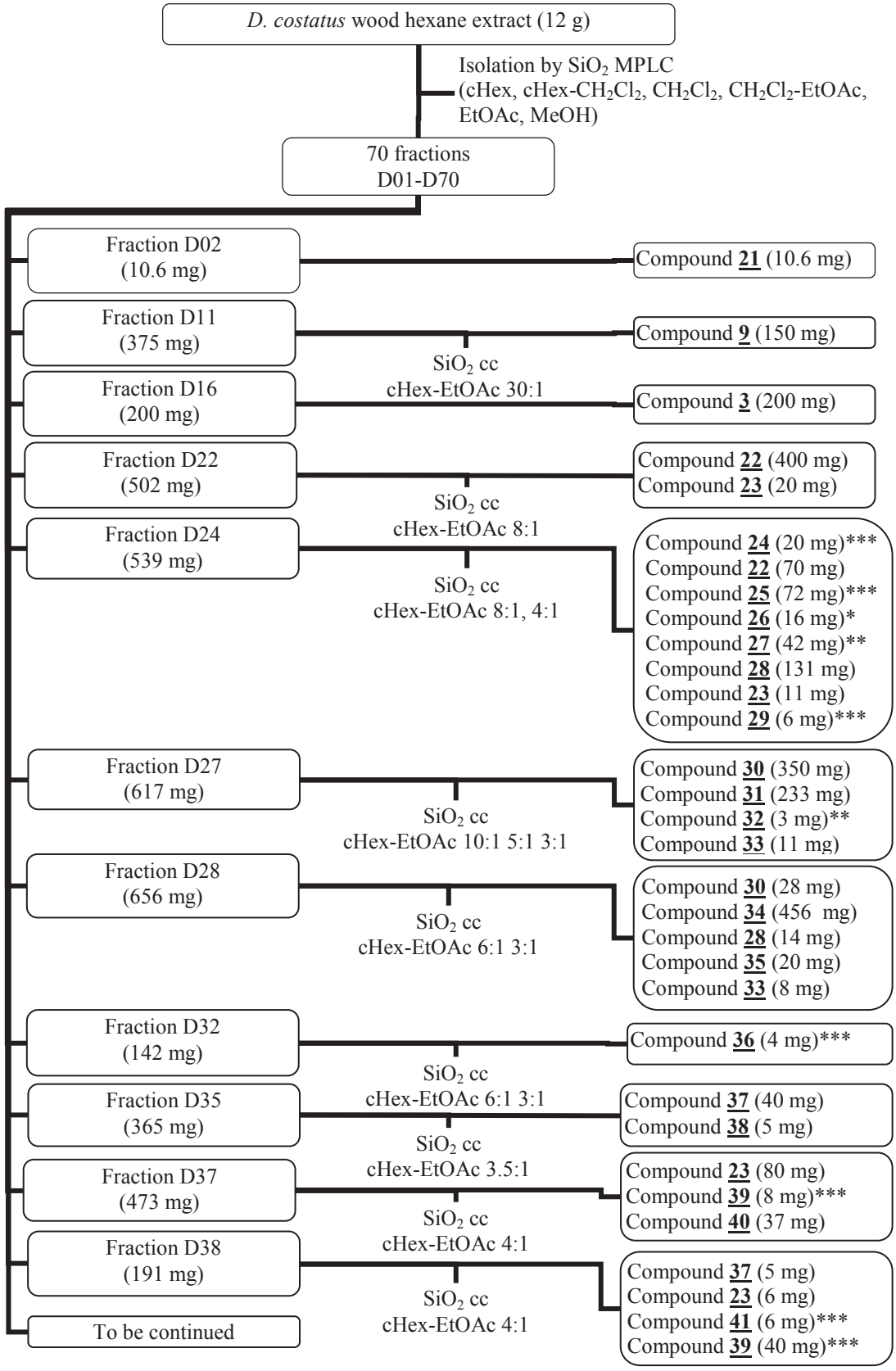

Scheme 20. Purification of *D. costatus* wood hexane extract.

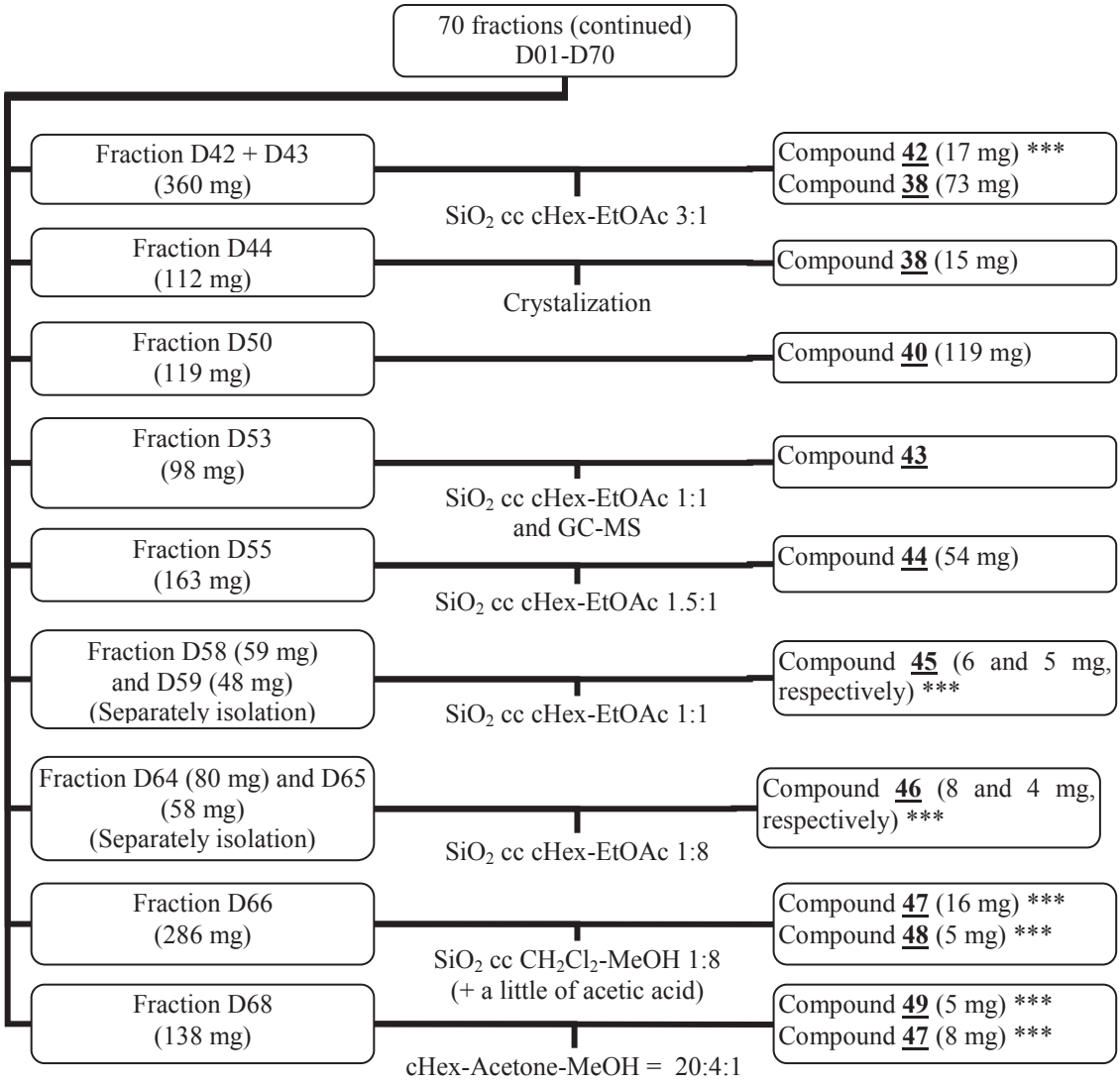

* the compound found for the first time in the nature.
** the rare compound in the nature.
*** New compounds.

Scheme 20. Purification of *D. costatus* wood hexane extract (continued).

3.5 CYTOTOXIC EVALUATION OF ISOLATED TRITERPENES

The cytotoxic effect of the isolated triterpenes against various cell lines was evaluated using WST-1 method as same as that of lupane triterpenes. The result was shown in Table 20. The cytotoxic activity against prostate cancer cell line (PC3), human breast adenocarcinoma cell line (MDA-MB-231), colorectal adenocarcinoma cell line (HT-29) and colorectal carcinoma cell line (HCT 116) were determined. Briefly, cells were seeded in 96-well plates and incubated at 37°C for 24 h. Cells were then treated with the isolated compounds (about 7-10 μM). After 72 h incubation in 5%CO_2 and 37^{o}C, WST-1 reagent was added to the test wells and further incubated at 37^{o}C for 1 h. The absorbance of each culture was read at 455 nm. The results were compared to negative control (no compound

added) and expressed as % inhibition of cell proliferation. Cisplatin (1 and 18 μM) was used as positive control.

Table 28. % Cell proliferation inhibition of the isolated triterpenes

No.	Group of compound	Concentration (μM)	% cell proliferation inhibition			
			PC3	MDA-MB231	HT-29	HCT 116
24	Norlupane group		NT	NT	NT	NT
25	Norlupane group	8.67	NT	NT	11.64	61.88
36	Norlupane group	8.07	NT	NT	0.00	0.00
41	Norlupane group	8.63	NT	NT	0.00	8.16
42	Norlupane group	8.36	NT	NT	0.00	12.23
26	Nordammarane group	10.00	19.84	6.29	3.26	12.20
39	Nordammarane group	10.00	8.22	1.97	0.00	11.96
49	Nordammarane monoacid		NT	NT	NT	NT
22	Dipterocarpol group	10.00	20.12	2.47	15.92	29.19
31	Dipterocarpol group	8.32	NT	NT	3.69	15.35
27	Lactone group	10.00	10.76	10.07	15.30	23.99
28	Lactone group	10.00	6.94	0.65	12.94	25.02
35	Lactone group	10.00	3.43	9.25	1.93	18.49
29	Fouquierone group		NT	NT	NT	NT
32	Fouquierone group	7.76	NT	NT	0.00	17.49
38	Fouquierone group	10.00	0.00	5.33	6.59	10.66
45	Fouquierone group (tri-OH)	10.00	9.75	13.71	0.00	8.28
40	Isofouquierone group	10.00	10.00	17.11	11.63	21.18
44	Isofouquierone group	10.00	9.35	0.00	0.00	1.18
46	Isofouquierone group (tri-OH)	10.00	12.62	17.93	9.66	24.30
23	Isofouquierone OOH group	10.00	7.81	5.37	1.19	15.78
33	Isofouquierone OOH group	7.76	NT	NT	9.12	0.00
48	Isofouquierone OOH (dioic acid)	7.08	NT	NT	25.09	1.05
30	Ocotillone group	10.00	15.66	3.07	2.81	11.60
34	Ocotillone group	10.00	11.99	0.17	0.00	14.35
37	Ocotillone group	10.00	5.91	5.01	2.65	18.31
47	Ocotillone group (dioic acid)	7.30	NT	NT	4.27	0.00
	Cisplatin (+control)	1.00	51.91	40.29	0.77	40.14
	Cisplatin (+control)	18.00	NT	NT	54.65	44.40

NT = not tested

3.6 *IN VITRO* ANTIPLASMODIAL ACTIVITY OF ISOLATED TRITERPENES

3.6.1 *In vitro* antiplasmodial activity

Theory - The antiplasmodial activity of various triterpenes was determined according to Desjardins et al 1979 [223-225]. To evaluate the *in vitro* growth of *Plasmodium falciparum* FcB1 strain, [^{3}H]hypoxanthine was added to parasite microcultures. Inhibition of uptake of a radiolabeled nucleic acid precursor ([^{3}H]hypoxanthine) by the parasite served as the indicator of antimalarial activity. [^{3}H]hypoxanthine incorporation was directly proportional to the number of parasitized erythrocytes in culture. The isolated triterpenes were dissolved in dimethylsulfoxide (DMSO) and tested at a concentration of 10 μM for screening assay. The compounds showing significant inhibition rates were submitted to serial dilution with culture medium before being added to parasite cultures (1% parasite and 2% hematocrite) in 96-well microplates. The growth inhibition for each concentration was determined by comparing the radioisotope incorporated in the treated cultured with that in the control culture maintained on the same plate. The concentrations causing 50% and 90% inhibition of parasite growth (IC_{50}, IC_{90}) were calculated from the drug concentration-response curves. All assays were done in triplicate. The experiments were prepared using strict aseptic techniques inside a laminar flow hood in the following procedure.

Screening test - A 96-well plate, with 8 rows and 12 columns, were used to prepared 300 μL of the mixture of 20 μM tested triterpenes and culture medium in DMSO. Take 100 μL of each mixture to the second and third plates (The experiments were triplicate in 3 plates). Then, add 100 μL of parasite culture to make total 200 μL each well. The plates were placed in the incubator at 37^{o}C for 24 h in the atmosphere without oxygen. After the 24-h incubator period, the plates were removed and 25 μL of [^{3}H]hypoxanthine was added to each well. The plates were then returned to the incubutor with the same temperature for an additional 24 h in the atmosphere with oxygen. The experiment was stopped by freezing at -25^{o}C. Incorporation of [^{3}H]hypoxanthine into DNA of parasites was measured using 1450 Microbeta trilux (Wallac) liquid scientillation and luminescence counter. An untreated parasite control was included. The result was shown in Table 29.

Determination of IC_{50} and IC_{90} – The obviously potent triterpenes were prepared in serial dilution from 100 to 0.195 μM with the parasite culture as above. After incubation of 48 h at 37^{o}C under anaerobic atmosphere, [^{3}H]hypoxanthine was added to all wells and the plates were again incubated for 24 h at 37^{o}C under aerobic condition. The reaction was stopped by freezing the plate at -25^{o}C. The result was expressed as the IC_{50} and IC_{90} values of the selected triterpene (Table 30). Chloroquine was used as a positive control.

3.6.2 Cytotoxicity test on mammalian cells

Rat myoblast-derived cells L-6 was seeded into 96-well microplates and treated with 10 and 1μM of isolated triterpenes from antiplasmodial screening test for 24 h, at 37^{o}C under a 5% CO_2 atmosphere. Cytotoxicity was determined using the colorimetric MTT assay. After incubation sterile MTT solution was added to each well and incubated for another 2 h. The absorbance reduction percentages at 540 nm for the treated cultures and the untreated control culture were obtained and compared. The % growth inhibition of L-6 cell was then calculated. All assays were done in triplicate. The result was shown in Table 29.

Table 29. Screening test for *in vitro* antiplasmodial activity and cytotoxicity of the isolated triterpenes

	Antiplasmodial activity	Cytotoxicity against L-6 cells	
Compound	% growth inhibition at 10 μM	% cell proliferation inhibition at 10 μM	% cell proliferation inhibition at 1 μM
22	14.21±11.36	0.00±0.00	0.65±7.75
23	17.98±2.28	5.53±2.83	3.58±15.81
24	0.00±0.00	8.67±10.84	0.14±8.92
25	7.76±8.78	4.23±5.62	2.55±5.43
26	26.67±0.93	9.61±2.69	11.69±6.00
27	7.49±3.40	33.85±6.83	1.59±11.32
28	13.90±0.89	10.72±10.29	6.20±6.97
30	19.44±16.59	2.89±12.13	0.00±0.00
31	11.35±10.18	0.33±13.26	6.33±4.39
32	27.80±5.26	0.00±0.00	6.10±5.71
33	4.15±10.92	0.83±8.73	24.13±5.06
34	17.85±12.01	0.00±0.00	3.16±5.81
35	0.00±0.00	3.81±3.23	0.00±0.00
36	90.94±1.48	15.57±2.90	13.94±5.38
37	0.00±0.00	0.75±0.34	0.00±0.00
38	22.95±18.43	0.00±0.00	0.00±0.00
39	27.81±4.87	0.00±0.00	0.00±0.00
40	17.52±6.06	0.00±0.00	7.28±5.78
41	0.00±0.00	2.88±10.47	12.18±4.67
42	14.83±2.26	0.80±2.65	12.91±5.90
44	1.26±3.78	8.01±2.43	0.92±3.05
45	23.71±9.72	4.33±2.30	4.59±0.61
46	14.38±9.36	13.53±6.15	12.03±4.22
47	7.62±4.25	5.24±0.69	9.84±1.84
48	3.65±1.48	0.34±6.52	8.67±5.03

Table 30. Antiplasmodial potency of compound **36**

Antimalarial activities against *P. falciparum* (FcB1 strain)	
IC_{50} (μM)	IC_{90} (μM)
3.74±0.76	10.31±0.62

IC_{50} for chloroquine was 72.6±7.4 nM

3.7 PHYSICAL CHARACTERISTICS AND SPECTRUM OF ISOLATED PRODUCTS

Common steroid

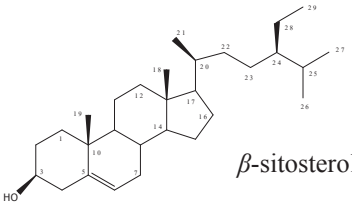

β-sitosterol (**3**)

Sesquiterpenes

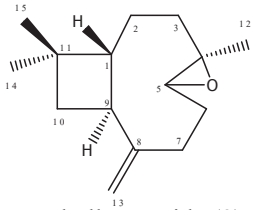

caryophyllene oxide (**9**)

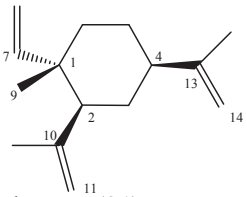

β-elemene (**21**)

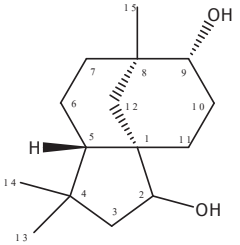

clovane-2,9-diol (**43**)

Norlupane triterpenes

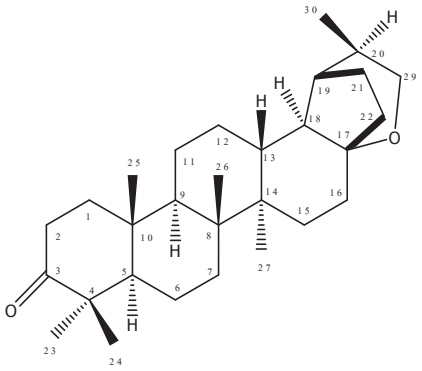

(20*S*)-17*α*,29-epoxy-28-norlupan-3-one (**24**)***

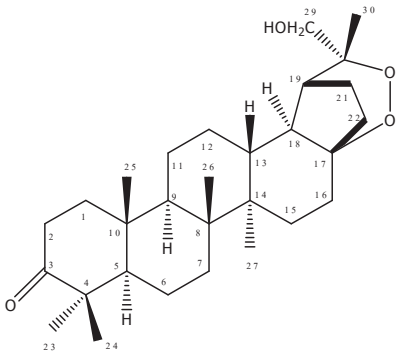

29-OH-17*α*,20-peroxy-28-norlupan-3-one (**36**)***

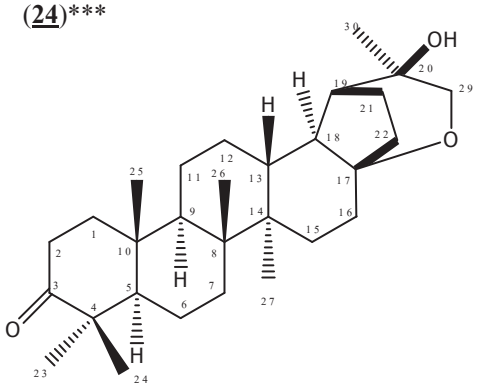

20-OH-17*α*,29-epoxy-28-norlupan-3-one (**42**)***

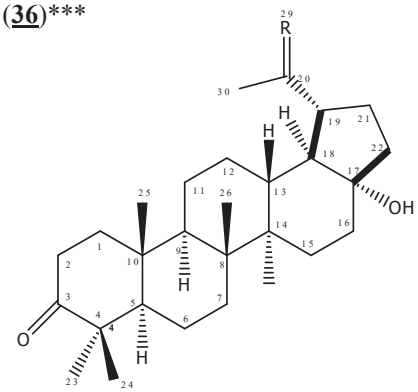

R= CH_2 17*α*-OH-28-norlupan-20(29)-en-3-one (**25**)***
R= O 17*α*-OH-28,29-dinorlupan-3,20-dione (**41**)***

Figure 26. Proposed structure of isolated compounds from *D. costatus* wood hexane extract

Nordammarane triterpane

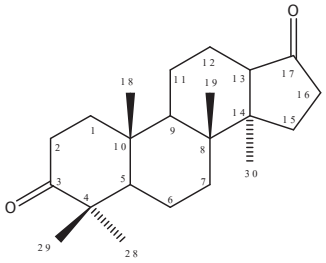

octanordammarane-3,17-dione (**26**)*

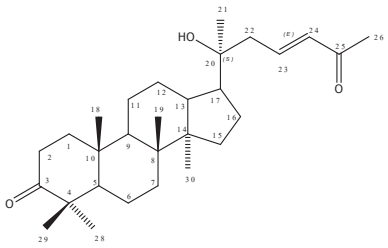

(20*S*)-20-OH-27-nordammar-23(*E*)-ene-3,25-dione (**39**)***

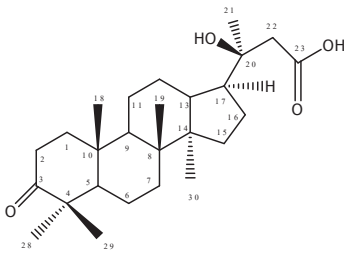

(20*S*)-20-OH-3-oxo-24,25,26,27-tetranordammar-23-oic acid (**49**)***

Dammarane triterpenes (Dipteocarpol group)

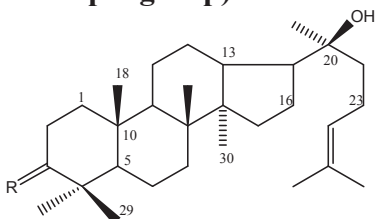

R=O dipterocarpol (**22**)
R=*β*-OH, H dammarenediol II (**31**)

Dammarane triterpenes (isofouquierone group)

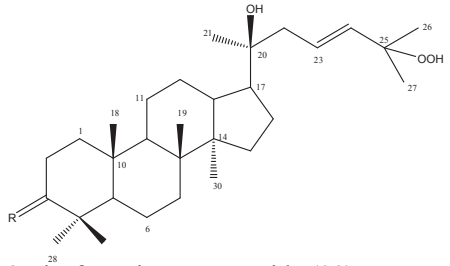

R=O isofouquierone peroxide (**23**)
R=*β*-OH, H isofouquierol peroxide (**33**)

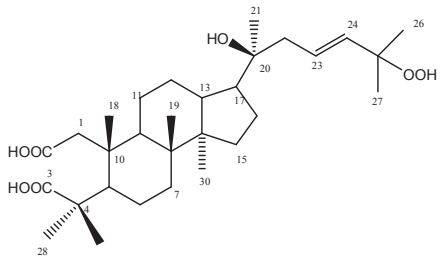

(20*S*, 23*E*)- 25-hydroperoxy-20-hydroxy-2,3-secodammar-23-en-2,3-dioic acid (**48**)***

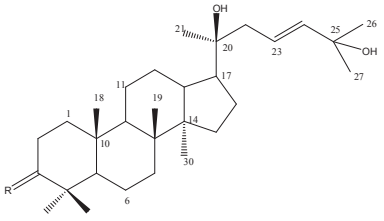

R=O isofouquierone (**40**)
R=*β*-OH, H isofouquierol (**44**)

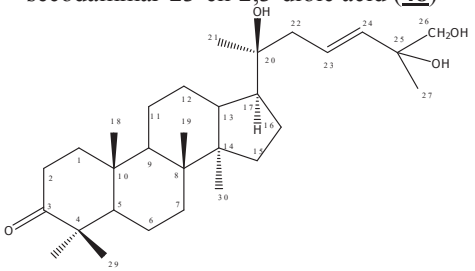

(20*S*,23*E*)- 20,25,26-trihydroxydammar-23-en-3-one (**46**)***

Figure 25. Proposed structures of isolated compounds from *D. costatus* wood hexane extract. (continued)

Dammarane triterpenes (fouquierone group)

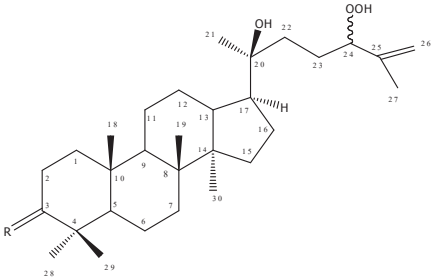

R=O (20*S*)-20-hydroxy-24-perhydroxy-dammar-25-en-3-one (**29**)***
R=*β*-OH, H cereotagaloperoxide (**32**)**

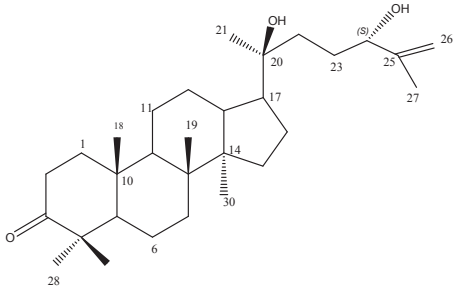

(20*S*,24*S*)-20,24-dihydroxydammar-25-en-3-one (**38**)

Dammarane triterpenes (ocotillone group)

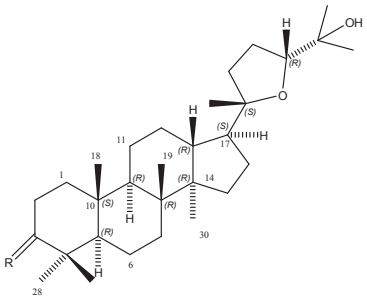

R=O ocotillone (**34**)
R=*β*-OH, H ocotillol II (**37**)

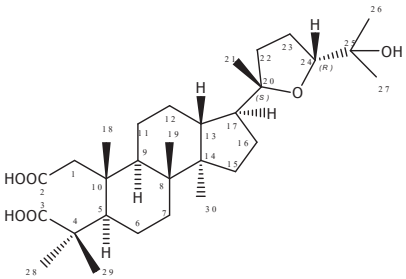

(20*S*,24*R*)-20,24-epoxy-25-hydroxy-2,3-secodammarane-2,3-dioic acid (**47**)***

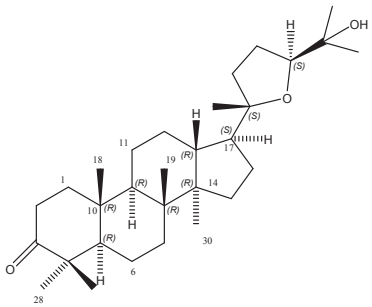

Cabraleone (**30**)

Dammarane triterpene (lactone group)

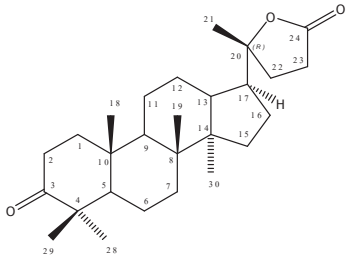

isocabralealactone (20*R*) (**27**)**

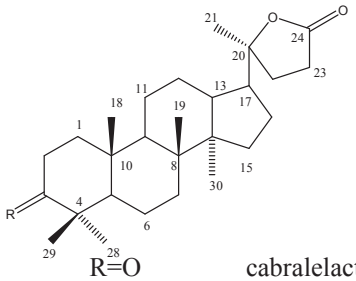

R=O cabralelactone (**28**)
R=*β*-OH, H 3-epicabraleahydroxylactone (**35**)

Dammarane triterpene (miscellaneous)

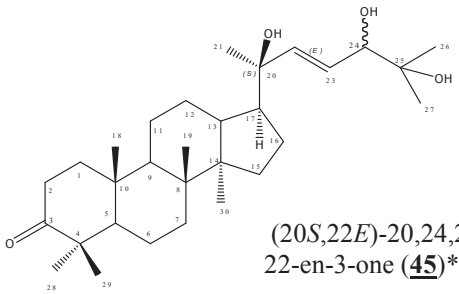

(20*S*,22*E*)-20,24,25-trihydroxydammar-22-en-3-one (**45**)***

Figure 25. Proposed structure of isolated compounds from *D. costatus* wood hexane extract. (continued)

* the compound found for the first time in the nature.
** the rare compound in the nature.
*** New compounds.

β-Sitosterol (3) and caryophyllene oxide (9)

The obtained data were the same as those obtained from *H.odorata* leaves hexane extract.

β-Elemene (21) [226]

Molecular formula	$C_{15}H_{24}$ **MW** 204
Description	colorless resin
Retention factor	R_f=0.73 (cHex-EtOAc =100:1)
Specific rotation	$[\alpha]_D^{20}$ +3.2 ($CHCl_3$, *c* 0.125) (lit.[226] +15.4 ($CHCl_3$, *c* 0.59, 23°C))
IR spectrum	ν_{max}(film) 3082(=C-H stretching), 2926, 2851, 1644,1455,1378 cm^{-1}
Mass spectrum	GC-EI-MS *m/z*: 204 $[M]^+$, 189, 175, 147, 107, 93 (100%), 81, 67
NMR spectrum	^1H and ^{13}C-NMR - see Table 31

Dipterocarpol (22) [39, 67, 71, 227-229]

Molecular formula	$C_{30}H_{50}O_2$ **MW** 442.72
Description	white shiny flakes
Retention factor	R_f=0.50 (cHex-EtOAc =3:1)
Specific rotation	$[\alpha]_D^{20}$ +74.1 ($CHCl_3$, *c* 0.135) (lit.[71] +67 ($CHCl_3$, *c* 1.09, 26°C))
IR spectrum	ν_{max} (film) 3505, 2949, 2864, 1704, 1457, 1377, 1109 cm^{-1}
Mass spectrum	ESI-MS *m/z* (ES+): 907 $[2M+Na]^+$, 465 $[M+Na]^+$
NMR spectrum	^1H and ^{13}C-NMR - see Table 32

Isofouquierone peroxide (23) [146]

Molecular formula	$C_{30}H_{50}O_4$ **MW** 474.72
Description	white powder
Retention factor	R_f=0.17 (cHex-EtOAc =3:1), =0.57 (cHex-EtOAc =1:1)
Specific rotation	$[\alpha]_D^{20}$ +41.0 (MeOH, *c* 0.105) (lit.[146] +67 ($CHCl_3$, *c* 0.29))
IR spectrum	ν_{max} (film) 3412, 2960, 2862, 1695, 1455, 1384 cm^{-1}
Mass spectrum	ESI-MS *m/z* (ES+) : 971$[2M+Na]^+$, 497 $[M+Na]^+$
NMR spectrum	^1H-NMR –see Table 33, ^{13}C-NMR - see Table 35

(20*R*)-17*α*,29-Epoxy-28-norlupan-3-one (24) ***

Molecular formula	$C_{29}H_{46}O_2$ **MW** 426.67
Description	white needle crystal
Retention factor	R_f=0.60 (cHex-EtOAc =3:1)
Specific rotation	$[\alpha]_D^{20}$ +11.3 ($CHCl_3$, *c* 0.115)
IR spectrum	ν_{max} (film) 2926, 2864, 1707, 1456, 1380 cm^{-1}
Mass spectrum	ESI-MS *m/z* (ES+) : 875$[2M+Na]^+$, 449 $[M+Na]^+$ HRMS (ESI-TOF) *m/z* (ES+) : 449.3399 $[M+Na]^+$ (calcd for $C_{29}H_{46}O_2Na$, 449.3396)
NMR spectrum	^1H-NMR –see Table 42, ^{13}C-NMR - see Table 43

17α-Hydroxy-28-norlupan-20(29)-en-3-one (<u>25</u>) ***

Molecular formula	$C_{29}H_{46}O_2$ **MW** 426.67
Description	colorless resin
Retention factor	R_f =0.42 (cHex-EtOAc =3:1)
Specific rotation	$[\alpha]_D^{20}$ +41.3 ($CHCl_3$, *c* 0.155)
IR spectrum	ν_{max} (film) 3441 (OH), 2948, 2868, 1704 (C=O), 1642, 1454, 1384, 756 cm^{-1}
Mass spectrum	ESI-MS *m/z* (ES+) : 875$[2M+Na]^+$, 449 $[M+Na]^+$ HRMS (ESI-TOF) *m/z* (ES+) : 449.3400 $[M+Na]^+$ (calcd for $C_{29}H_{46}O_2Na$, 449.3396)
NMR spectrum	^{1}H-NMR –see Table 42, ^{13}C-NMR - see Table 43

Octanordammarane-3,17-dione (<u>26</u>) *[230]

Molecular formula	$C_{22}H_{34}O_2$ **MW** 330.50
Description	colorless resin
Retention factor	R_f =0.33 (cHex-EtOAc =3:1)
Specific rotation	$[\alpha]_D^{20}$ +94.0 ($CHCl_3$, *c* 0.065)
IR spectrum	ν_{max} (film) 2947, 2869, 1738 (C-17 ketone), 1705 (C-3 ketone), 1455, 1384, 755 cm^{-1}
Mass spectrum	ESI-MS *m/z* (ES+) : 683 $[2M+Na]^+$, 353 $[M+Na]^+$ HRMS (ESI-TOF) *m/z* (ES+) : 353.2466 $[M+Na]^+$, (calcd for $C_{22}H_{34}O_2Na$, 353.2457) and 331.2645 $[M+H]^+$ (calcd for $C_{22}H_{35}O_2$, 331.2637)
NMR spectrum	^{1}H and ^{13}C-NMR - see Table 41

Isocabralealactone (20*R*) (<u>27</u>)** [60, 67, 161, 229, 231]

Synonym	25,26,27-trinordammaran-3-one-20(*R*),24-olide
Molecular formula	$C_{27}H_{42}O_3$ **MW** 414.31
Description	white amorphous powder
Retention factor	R_f =0.23 (cHex-EtOAc =3:1)
Specific rotation	$[\alpha]_D^{20}$ +71.0 ($CHCl_3$, *c* 0.100)
IR spectrum	ν_{max} (film) 2949, 2862, 1767 (lactone), 1704 (ketone), 1460, 1383, 1245, 1193, 754 cm^{-1}
Mass spectrum	ESI-MS *m/z* (ES+) : 851 $[2M+Na]^+$, 437 $[M+Na]^+$, 415 $[M+H]^+$ HRMS (ESI-TOF) *m/z* (ES+) : 437.3023 $[M+Na]^+$ (calcd for $C_{27}H_{42}O_3Na$, 437.3032)
NMR spectrum	^{1}H and ^{13}C-NMR - see Table 40

Cabralealactone (20*S*) (28) [67, 133, 161, 229, 231]

Synonym	25,26,27-trinordammaran-3-one-20(*S*),24-olide
Molecular formula	$C_{27}H_{42}O_3$ **MW** 414.31
Description	white amorphous powder
Retention factor	R_f=0.21 (cHex-EtOAc =3:1)
Specific rotation	$[\alpha]_D^{20}$ +50.0 ($CHCl_3$, *c* 0.115)
IR spectrum	ν_{max} (film) 2954, 2867, 1770 (lactone), 1704 (ketone), 1237, 1193, 755 cm^{-1}
Mass spectrum	ESI-MS *m/z* (ES+) : 851 $[2M+Na]^+$, 437 $[M+Na]^+$, 415 $[M+H]^+$
NMR spectrum	^1H and ^{13}C-NMR - see Table 40

(20*S*)-20-Hydroxy-24-perhydroxy-dammar-25-en-3-one (29)

***[146, 158]

Molecular formula	$C_{30}H_{50}O_4$ **MW** 474.72
Description	colorless resin
Retention factor	R_f=0.11 (cHex-EtOAc =3:1)
Mass spectrum	ESI-MS *m/z* (ES+) : 497 $[M+Na]^+$
NMR spectrum	^1H and ^{13}C-NMR - see Table 37

Cabraleone (20*S*,24*S*) (30) [39, 67, 138, 141, 148]

Molecular formula	$C_{30}H_{50}O_3$ **MW** 458.72
Description	colorless resin
Retention factor	R_f=0.50 (cHex-EtOAc =3:1)
Specific rotation	$[\alpha]_D^{20}$ +60.0 ($CHCl_3$, *c* 0.075) (lit.[133] +54 (*c* 1.0))
IR spectrum	ν_{max} (film) 3473, 2693, 2872, 1705, 1456, 1384, 1059, 756 cm^{-1}
Mass spectrum	EI-MS *m/z* (ES+) : 939 $[2M+Na]^+$, 481 $[M+Na]^+$
NMR spectrum	^1H-NMR –see Table 38, ^{13}C-NMR - see Table 39

Dammarenediol II (31) [23, 39, 67, 132, 159, 227]

Molecular formula	$C_{30}H_{52}O_2$ **MW** 444.73
Description	colorless oil
Retention factor	R_f=0.38 (cHex-EtOAc =5:2)
Specific rotation	$[\alpha]_D^{20}$ +12.9 ($CHCl_3$, *c* 0.155) (lit.[23] +32.8 (*c* 1.05))
IR spectrum	ν_{max} (film) 3444, 2944, 2870,1699,1455,1378, 1216, 1044, 757 cm^{-1}
Mass spectrum	EI-MS *m/z* : 317 $[M\text{-side chain}]^+$, 299 (100%), 207, 189, 109, 95, 69
NMR spectrum	^1H and ^{13}C-NMR - see Table 32

Cereotagaloperoxide (32) [146, 158]

Synonym	20(S)-3β,20-dihydroxy-24-perhydroxydammar-25-ene
Molecular formula	$C_{30}H_{52}O_4$ **MW** 476.73
Description	white solid
Retention factor	R_f=0.15 (cHex-EtOAc =5:2)
Specific rotation	$[\alpha]_D^{20}$ +20.0 ($CHCl_3$, *c* 0.070) (lit.[158] +54.1 (MeOH, *c* 0.04))
IR spectrum	ν_{max} (film) 3405, 2943, 2861, 1453, 1377, 756 cm^{-1}
Mass spectrum	ESI-MS *m/z* (ES+) : 975 $[2M+Na]^+$, 499 $[M+Na]^+$
NMR spectrum	^1H and ^{13}C-NMR - see Table 37

Isofouquierol peroxide (33) [157]

Molecular formula	$C_{30}H_{52}O_4$ **MW** 476.73
Description	white solid
Retention factor	R_f=0.15 (cHex-EtOAc =3:1)
Specific rotation	$[\alpha]_D^{20}$ +21.0 ($CHCl_3$, *c* 0.105) (lit.[157] -0.08 ($CHCl_3$, *c* 0.05))
IR spectrum	ν_{max} (film) 3404, 2943, 2867, 1453, 1377, 1028, 757 cm^{-1}
Mass spectrum	ESI-MS *m/z* (ES+) : 975 $[2M+Na]^+$, 499 $[M+Na]^+$, 477 $[M+H]^+$
NMR spectrum	^1H-NMR –see Table 33, ^{13}C-NMR - see Table 35

Ocotillone (20*S*,24*R*) (34) [39, 67, 138, 141, 148]

Molecular formula	$C_{30}H_{50}O_3$ **MW** 458.72
Description	white needle crystal
Retention factor	R_f=0.44 (cHex-EtOAc =3:1)
Specific rotation	$[\alpha]_D^{20}$ +58.6 ($CHCl_3$, *c* 0.145) (lit.[39] +59 ($CHCl_3$, 26^{o}C))
IR spectrum	ν_{max} (film) 3473, 2965, 2871, 1705, 1456, 1384, 1080, 756 cm^{-1}
Mass spectrum	EI-MS *m/z* (ES+) : 939 $[2M+Na]^+$, 481 $[M+Na]^+$
NMR spectrum	^1H-NMR –see Table 38, ^{13}C-NMR - see Table 39

3-*Epi*cabraleahydroxylactone (20*S*) (35) [160]

Synonym	(20*S*)-3β-hydroxy-25,26,27-trinordammaran-20,24-olide
Molecular formula	$C_{27}H_{44}O_3$ **MW** 416.33
Description	colorless resin
Retention factor	R_f=0.13 (cHex-EtOAc =3:1)
Specific rotation	$[\alpha]_D^{20}$ +34.8^o ($CHCl_3$, *c* 0.115) (lit.[160] +6.7 ($CHCl_3$, *c* 0.21))
IR spectrum	ν_{max} (film) 3473, 2946, 2871, 1761, 1455, 1379, 1191, 1075 cm^{-1}
Mass spectrum	ESI-MS *m/z* (ES+) : 855 $[2M+Na]^+$, 439 $[M+Na]^+$
NMR spectrum	^1H and ^{13}C-NMR - see Table 40

(20*S*)-29-Hydroxy-17α,20-peroxy-28-norlupan-3-one (<u>36</u>) ***

Molecular formula	$C_{29}H_{46}O_4$ **MW** 458.67
Description	white star crystal
Retention factor	R_f =0.41 (cHex-EtOAc =2:1)
Specific rotation	$[\alpha]_D^{20}$ +23.5 ($CHCl_3$, *c* 0.085)
IR spectrum	ν_{max} (film) 3474 (OH), 2948, 2864, 1703 (C=O), 1455, 1384, 1047 (C-O), 755 cm^{-1}
Mass spectrum	ESI-MS *m/z* (ES+) : 939 $[2M+Na]^+$, 481 $[M+Na]^+$, HRMS (ESI-TOF) *m/z* (ES+) : 481.3274 $[M+Na]^+$ (calcd for $C_{29}H_{46}O_4Na$, 481.3294)
NMR spectrum	^{1}H-NMR –see Table 34, ^{13}C-NMR - see Table 35

Ocotillol II (20*S*,24*R*) (<u>37</u>) [67, 135, 147, 153, 154]

Molecular formula	$C_{30}H_{52}O_3$ **MW** 460.73
Description	white needle crystal
Retention factor	R_f =0.52 (cHex-EtOAc =1:1)
Specific rotation	$[\alpha]_D^{20}$ +24.6 ($CHCl_3$, *c* 0.065) (lit.[135] +39.63 ($CHCl_3$, *c* 1.04, 22^{o}C))
IR spectrum	ν_{max} (film) 3439, 2946, 2862, 1462, 1376, 1082, 1043, 754 cm^{-1}
Mass spectrum	EI-MS *m/z* (ES+) : 943 $[2M+Na]^+$, 483 $[M+Na]^+$
NMR spectrum	^{1}H-NMR –see Table 38, ^{13}C-NMR - see Table 39

(20*S*,24*S*)-20,24-dihydroxydammar-25-en-3-one (<u>38</u>) [136, 151, 158]

Molecular formula	$C_{30}H_{50}O_3$ **MW** 458.72
Description	white amorphous powder
Retention factor	R_f =0.33 (cHex-EtOAc =1:1)
Specific rotation	$[\alpha]_D^{20}$ +43.6 ($CHCl_3$, *c* 0.110)
IR spectrum	ν_{max} (film) 3307, 2952, 2867, 1704, 1454, 1368 cm^{-1}
Mass spectrum	ESI-MS *m/z* (ES+) : 939 $[2M+Na]^+$, 481 $[M+Na]^+$
NMR spectrum	^{1}H and ^{13}C-NMR - see Table 37

(20*S*,23*E*)-20-Hydroxy-27-nordammar-23-en-3,25-dione (39) ***

Molecular formula	$C_{29}H_{46}O_3$	**MW**	442.67
Description	White powder		
Retention factor	R_f=0.38 (cHex-EtOAc =1:1)		
Specific rotation	$[\alpha]_D^{20}$ +30.0 ($CHCl_3$, *c* 0.100)		
IR spectrum	ν_{max} (film) 3472(hydroxy group), 2949, 2866, 1702 (carbonyl C-3), 1663 (α,β unsaturated carbonyl C-25), 1622 (C=C st), 1459, 1377, 1256 cm^{-1}		
UV	absorption at 254 nm		
Mass spectrum	ESI-MS *m/z* (ES+) : 907 $[2M+Na]^+$, 465 $[M+Na]^+$, HRMS (ESI-TOF) *m/z* (ES+) : 465.3359 $[M+Na]^+$ (calcd for $C_{29}H_{46}O_3Na$, 465.3345)		
NMR spectrum	^1H and ^{13}C-NMR - see Table 41		

Isofouquierone (40) [148]

Molecular formula	$C_{30}H_{50}O_3$	**MW**	458.72
Description	yellow gum		
Retention factor	R_f=0.30 (cHex-EtOAc =1:1)		
Specific rotation	$[\alpha]_D^{20}$ +29.8 ($CHCl_3$, *c* 0.865) (lit.[148] ($CHCl_3$, *c* 0.1))		
IR spectrum	ν_{max} (film) 3439, 2949, 2867, 1703, 1459 cm^{-1}		
Mass spectrum	ESI-MS *m/z* (ES+) : 939 $[2M+Na]^+$, 481$[M+Na]^+$,		
NMR spectrum	^1H-NMR –see Table 34, ^{13}C-NMR - see Table 35		

17*α*-Hydroxy-28,29-dinorlupan-3,20-dione (41) ***

Molecular formula	$C_{28}H_{44}O_3$	**MW**	428.65
Description	colorless resin		
Retention factor	R_f=0.42 (cHex-EtOAc =1:1)		
Specific rotation	$[\alpha]_D^{20}$ +24.7 ($CHCl_3$, *c* 0.170)		
IR spectrum	ν_{max} (film) 3439 (OH), 2948, 2864, 1704 (C=O), 1455, 1383, 755 cm^{-1}		
Mass spectrum	ESI-MS *m/z* (ES+) : 879 $[2M+Na]^+$, 451 $[M+Na]^+$ HRMS (ESI-TOF) *m/z* (ES+) : 451.3191 $[M+Na]^+$, (calcd for $C_{28}H_{44}O_3Na$, 451.3188)		
NMR spectrum	^1H-NMR –see Table 42, the ^{13}C-NMR - see Table 43		

(20*R*)-20-Hydroxy-17*α*,29-epoxy-28-norlupan-3-one (42) ***

Molecular formula	$C_{29}H_{46}O_3$	**MW**	442.67
Description	colorless resin		
Retention factor	R_f =0.34 (cHex-EtOAc =1:1)		
Specific rotation	$[\alpha]_D^{20}$ +85.3 ($CHCl_3$, *c* 0.075)		
IR spectrum	ν_{max} (film) 3440 (OH), 2954, 2869, 1704 (C=O), 1455, 1377, 1140, 1066, 756 cm^{-1}		
Mass spectrum	ESI-MS *m/z* (ES+) : 465 $[M+Na]^+$, 443 $[M+H]^+$ HRMS (ESI-TOF) *m/z* (ES+) : 443.3533 $[M+H]^+$, (calcd for $C_{29}H_{47}O_3$, 443.3525)		
NMR spectrum	^{1}H-NMR –see Table 42, the ^{13}C-NMR - see Table 43		

Clovane-2,9-diol (43)

Molecular formula	$C_{15}H_{26}O_2$	**MW**	238.37
Mass spectrum	GC-EI-MS *m/z* : 238 $[M]^+$, 220, 182, 164 (100%), 150, 135		

The identification was achieved by GC-MS analysis and comparison to the reference spectrum.

Isofouquierol (44) [148, 155, 158]

Molecular formula	$C_{30}H_{52}O_3$	**MW**	460.73
Description	yellow gum		
Retention factor	R_f =0.45 (cHex-EtOAc =1:5)		
Specific rotation	$[\alpha]_D^{20}$ +28.5 (MeOH, *c* 0.365) (lit.[148] +22 ($CHCl_3$, c0.1))		
IR spectrum	ν_{max} (film) 3381, 2943, 2867, 1453, 1376, 1031, 983 cm^{-1}		
Mass spectrum	ESI-MS *m/z* (ES+) : 943 $[2M+Na]^+$, 483$[M+Na]^+$		
NMR spectrum	^{1}H-NMR –see Table 34 and ^{13}C-NMR - see Table 35		

(20*S*,22*E*)-20,24,25-Trihydroxydammar-22-en-3-one (45) ***

Molecular formula	$C_{30}H_{50}O_4$	**MW**	474.72
Description	colorless resin		
Retention factor	R_f =0.26 (cHex-EtOAc =1:4)		
Specific rotation	$[\alpha]_D^{20}$ +45.0 (MeOH, *c* 0.140)		
IR spectrum	ν_{max} (film) 3405, 2936, 2862, 1701, 1457, 1377 cm^{-1}		
Mass spectrum	ESI-MS *m/z* (ES+) : 971 $[2M+Na]^+$, 497 $[M+Na]^+$ HRMS (ESI-TOF) *m/z* (ES+) : 497.3602 $[M+Na]^+$ (calcd for $C_{30}H_{50}O_4Na$, 497.3607)		
NMR spectrum	^{1}H and the ^{13}C-NMR - see Table 36		

(20*S*,23*E*)-20,25,26-Trihydroxydammar-23-en-3-one (46) ***

Molecular formula	$C_{30}H_{50}O_4$ **MW** 474.72
Description	colorless resin
Retention factor	R_f=0.23 (cHex-EtOAc =1:15)
Specific rotation	$[\alpha]_D^{20}$ +32.0 (MeOH, *c* 0.125)
IR spectrum	ν_{max} (film) 3406, 2939, 2862, 1701, 1456, 1380 cm^{-1}
Mass spectrum	ESI-MS *m/z* (ES+) : 513 $[M+K]^+$, 497 $[M+Na]^+$ HRMS (ESI-TOF) *m/z* (ES+) : 497.3592 $[M+Na]^+$ (calcd for $C_{30}H_{50}O_4Na$, 497.3607)
NMR spectrum	^{1}H-NMR –see Table 34 and ^{13}C-NMR - see Table 35

(20*S*,24*R*)-20,24-Epoxy-25-hydroxy-2,3-*seco*-dammarane-2,3-dioic acid (47) ***

Molecular formula	$C_{30}H_{50}O_6$ **MW** 506.71
Description	colorless resin
Retention factor	R_f=0.50 (CH_2Cl_2-MeOH=10:1- a little amount of acetic acid)
Specific rotation	$[\alpha]_D^{20}$ +29.4 ($CHCl_3$, *c* 0.085)
IR spectrum	ν_{max} (film) 3650-2500 (br), 2966, 2871, 1699, 1455, 1377, 1216, 1166, 757 cm^{-1}
Mass spectrum	ESI-MS *m/z* (ES-) : 1011 $[2M-H]^-$, 505 $[M-H]^-$ HRMS (ESI-TOF) *m/z* (ES-) : 505.3533 $[M-H]^-$ (calcd for $C_{30}H_{49}O_6$, 505.3529)
NMR spectrum	^{1}H-NMR –see Table 38, ^{13}C-NMR - see Table 39

(20*S*,23*E*)- 25-Hydroperoxy-20-hydroxy-2,3-*seco*-dammar-23-en-2,3-dioic acid (48) ***

Molecular formula	$C_{30}H_{50}O_7$ **MW** 522.71
Description	colorless resin
Retention factor	R_f=0.33 (CH_2Cl_2-MeOH=10:1)
Specific rotation	$[\alpha]_D^{20}$ +13.3 ($CHCl_3$, *c* 0.075)
IR spectrum	ν_{max} (film) 3650-2500 (br), 2961, 2875, 1699, 1378, 1156, 756 cm^{-1}
Mass spectrum	ESI-MS *m/z* (ES-) : 521$[M-H]^-$ HRMS (ESI-TOF) *m/z* (ES-) : 521.3486 $[M-H]^-$ (calcd for $C_{30}H_{49}O_7$, 521.3478)
NMR spectrum	^{1}H-NMR –see Table 33 and ^{13}C-NMR - see Table 35

(20*S*)-20-Hydroxy-3-oxo-24,25,26,27-tetranordammar-23-oic acid (<u>49</u>) ***

Molecular formula $C_{26}H_{42}O_4$ **MW** 418.61
Description colorless resin
Retention factor R_f =0.05 (cHex:acetone:MeOH =50 :15 :2.5)
Mass spectrum ESI-MS *m/z* (ES-) : 835 $[2M-H]^-$, 417 $[M-H]^-$
NMR spectrum ^1H and the ^{13}C-NMR - see Table 41

IV. PERSONAL WORK

4.1 Plant material

4.2 Preliminary study

4.3 Extraction and isolation of *D. costatus* wood hexane extract

4.4 Identification and structural study of isolated compounds

4.5 Cytotoxic evaluation of some isolated triterpenes

4.6 *In vitro* antiplasmodial activity of isolated triterpene

4.7 Conclusion

4.1 PLANT MATERIAL

D. costatus wood was also collected in Chiangmai and was prepared for the study by drying and chopping.

4.2 PRELIMINARY STUDY

The plant sample was extracted in soxhlet apparatus, with hexane following by ethanol, and yielded 1.0367 g (2.56%) hexane and 1.3755 g (2.73%) ethanol extracts, respectively. Bioactivity of both extracts was evaluated by BIOTEC. The hexane extract showed cytotoxic activity against MCF7 (breast cancer with IC_{50} 25.55 μg/mL) and NCI-H187 (small cell lung cancer with IC_{50} 9.06 μg/mL). Although the potency of *in vitro* cytotoxicity looked lower than that of the *H.odorata* leaves hexane extract, it was interesting that this extract expressed potent anti-malarial activity with IC_{50} 3.20 μg/mL against *Plasmodium falciparum* K1 strain. This result harmonized with Chavalit's work [21] that only the hexane extract of *D. costatus* wood exhibited cytotoxicity against P-388 (murine lymphocytic leukemia), KB (humnan pharyngeal carcinoma), BCA-1 (human breast cancer), Lu-1 (human lung cancer) and Col-2 (human colon cancer) but was not observed from the ethanol extract.

4.3 EXTRACTION AND ISOLATION OF *D. costatus* WOOD HEXANE EXTRACT

Phytochemicalstudy of the hexane extract of *Dipterocarpus costatus* led to the isolation of 31 compounds. These compounds are as follows

Steroid : *β*-sitosterol (**3**)

Sesquiterpene : caryophyllene oxide (**9**), β-elemene (**21**), clovane- 2,9-diol (**43**)

Triterpenes :

Dammarane and *seco*-dammarane type : dipterocarpol (**22**), dammarenediol II (**31**), isofouquierone peroxide (**23**), isofouquierol peroxide (**33**), isofouquierone (**40**), isofouquierol (**44**), (20*S*,23*E*)-20,25,26-trihydroxydammar-23-en-3-one (**46**), (20*S*,23*E*)-25-hydroperoxy-20-hydroxy-2,3-*seco*-dammar-23-en-2,3-dioic acid (**48**), (20*S*,22*E*)-20,24,25-trihydroxydammar-22-en-3-one (**45**), (*20S*,*24S*)-20,24-dihydroxydammar-25-en-3-one (**38**), (*20S*)-20-hydroxy-24-perhydroxy-dammar-25-en-3-one (**29**), cereotagaloperoxide (**32**), cabraleone (**30**), ocotillone (**34**), ocotillol II (**37**), (20*S*,24*R*)-20,24-epoxy-25-hydroxy-2,3-*seco*-dammarane-2,3-dioic acid (**47**)

Nordammarane type : Isocabralealactone (**27**), Cabralealactone (**28**) and 3-*Epi*cabraleahydroxylactone (**35**), Octanordammarane-3,17-

dione (**26**) (20*S*,23*E*)-20-Hydroxy-27-nordammar-23-ene-3,25-dione (**39**), (20*S*)-20-Hydroxy-3-oxo-24,25,26,27-tetranordammar-23-oic acid (**49**)

Norlupane type : 17α-hydroxy-28-norlupan-20(29)-en-3-one (**25**), 17α-hydroxy-28,29-dinorlupan-3,20-dione (**41**), (20*R*)-17α,29-epoxy-28-norlupan-3-one (**24**), (20*S*)-29-hydroxy-17α,20-peroxy-28-norlupan-3-one (**36**), (20*R*)-20-hydroxy-17α,29-epoxy-28-norlupan-3-one (**42**)

The result is in agreement with the previous reported [39, 40]. The most abundant compound in this extract is dipterocarpol (**22**), following by ocotillone (**34**) and isofouquierone (**40**). Based on TLC trace, dipterocarpol (**22**) was found as a major constituent in fraction D21-D23. The total amount was more than 1 g. The TLC and NMR data showed that betulonic acid always contaminated in the subfraction of dipterocarpol. Ocotillone (**34**) presented totally almost 1 g in fraction D28-D29 while isofouquierone (**40**) was obtained totally more than 500 mg in fraction D49-D51. Cabraleone (**30**), 24*R*-epimer of ocotillone, was also isolated from this extract although in less amount. This suggested cyclization and oxidation on the side chain of dipterocarpol, the basic dammarane. Although both C-3 keto and hydroxyl group were found in this extract, 3-oxodammaranes were major derivatives according to their higher amount.

The high amount of dammarane derivatives is interesting from a pharmacological point of view because of their antitumour activities [132]. Dammarenediol II (**31**) was suggested to be a valuable antitumor promoter (potential cancer chemopreventive agent) [160], an anti-inflammatory agent [162] and antiviral agent [23]. Ocotillone (**34**), the second largest amount of triterpenes in this extract, showed moderate cytotoxicity against leukeamia cells (L-1210, IC_{50} 20µg/mL) [73], and insect antifeedant and growth-regulating activities against *Spodoptera litura* [163]. Cabralealactone (**28**) exhibited potent cytotoxicity against P388 leukemia cells [161], as well as multidrug resistance-reversing effect [86]. With in the same report, the potency of colchicine was also increased with the presence of (20*S*,24*S*)-20,24-dihydroxydammar-25-en-3-one (**38**). Isofouquierol (**44**) at the concentration of 100 µM showed 86.6% inhibitory effect on nitric oxide (NO) production induced by LPS in mouse peritoneal macrophages [149] that related to its anti-inflammatory activity. In contrast, ocotillol II (**37**), which exhibited moderate to weak cell growth inhibitory activities to VA-13 (malignant lung tumor) and HepG2 cells (human liver cancer), displayed strong cytotoxicity to WI-38 (normal human lung cell) [147]. Then, it is not suitable to be developed for anticancer.

Dammarenediol-II (**31**) is, in plants, the primary biosynthetic products of the tetracyclization of (*S*)-2,3-oxidosqualene to be dammaranes, lupanes, ursanes and oleananes [80, 147]. The TLC showed the presence of dammarenediol II as a major component in fraction D26-D27, and its amount should be totally about 400 mg. The dammarenediols were first isolated by Mills in 1956 [222] from dammar resin produced by various Dipterocarpus species (in 0.05% yield). Two Dammarenediols have since been

found esterified with fatty acids in the seed oil of *Cacalia atriplicifola* L.(Asteracea)[232] and as components of extracts from *Cowania mexicana* (Rosaceae) [233]. Dammarenediol-II was found in 3-acetate form in edible *Chrysanthemum morifolium* (Compositeae) [162]. Moreover, it appeared in *0lea madagascariensis* (Oleaceae) [132], in seed oil of *Camellia japonica* (Theaceae) [160] and in the fruit of *Ceriops tagal* (Rhizophoraceae) [158].

Dipterocarpol (**22**), an oxidation product at C-3 of dammarenediol II and first isolated from *Dipterocarpus* species [39, 222, 229], is a constituent of dammar resins and Ginseng sapogenins [227] and is abundant in galls of *Pistacia terebinthus* [234]. It is a common composition in genus *Dipterocarpus*. It was found to be the most abundant triterpene in the neutral fraction of oleoresin of various *Dipterocarpus* species [39, 40, 67, 229]. The configuration of ring D was reported as 13*β*, 17*α*-H.[235]

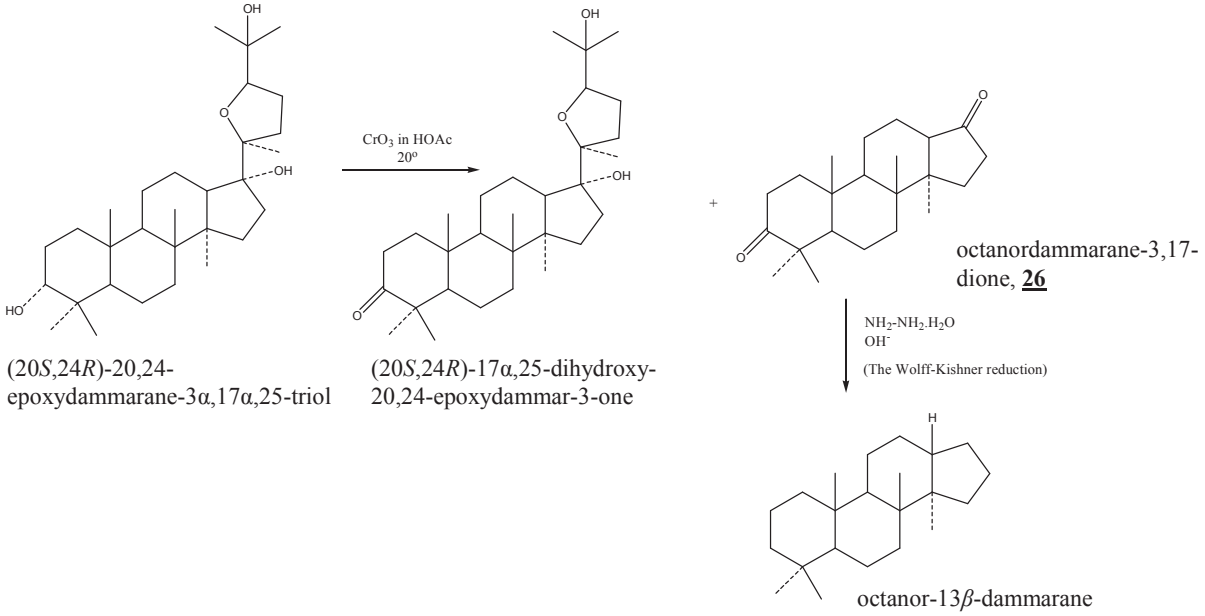

(20*S*,24*R*)-20,24-epoxydammarane-3α,17α,25-triol

(20*S*,24*R*)-17α,25-dihydroxy-20,24-epoxydammar-3-one

octanor-13*β*-dammarane

Scheme 21. Semisynthesis of octanordammarane-3,17-dione (**26**) from (20*S*,24*R*)-20,24-epoxydammarane-3α,17α,25-triol.[230] CrO_3 = chromium trioxide, $NH_2NH_2.H_2O$ = hydrazine hydrate

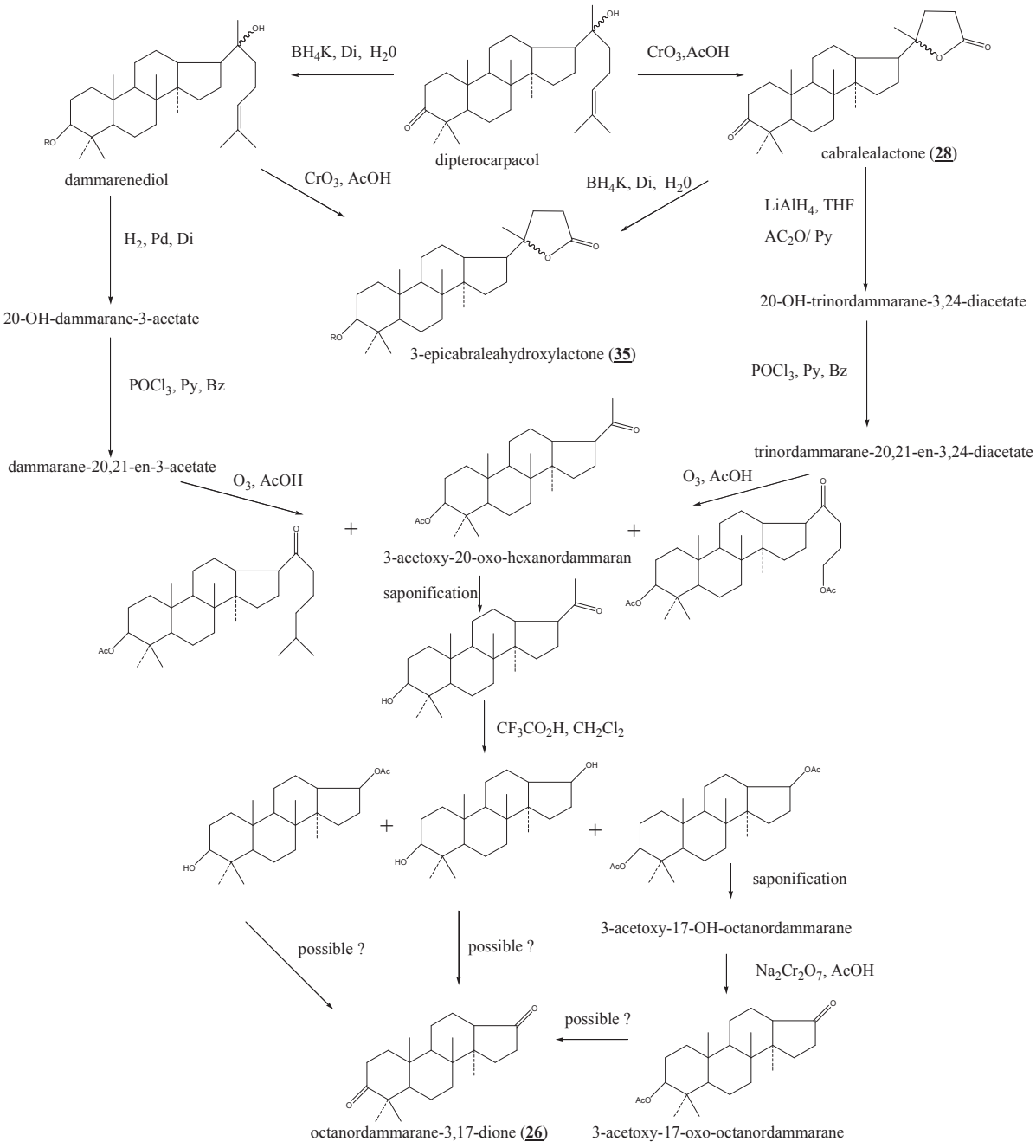

Scheme 22. Semisynthesis of cabralealactone (**28**), 3-*epi*cabraleahydroxylactone (**35**) and 3*β*-acetoxy-17-oxo-octanordammarane from dipterocarpol (**22**) [70, 229, 235]

$POCl_3$ = phosphorous oxychloride, O_3 = ozone, BH_4K = potassium borohydride, CF_3COOH = trifluoroacetic acid, Py = pyridine, CrO_3 = chromium trioxide, Di = dioxane, AcOH = acetic acid, $LiAlH_4$ = lithium aluminium hydride, THF = tetrahydrofuran, Ac_2O = acetic anhydride, $Na_2Cr_2O_7$ = sodium dichromate

Although octanordammarane-3,17-dione (**26**) has previously been semisynthesized from oxidation reaction of 20(*S*),24(*R*)-epoxydammarane-3α,17α,25-triol (scheme 21) [230], to the best of our knowledge, this is the first instance of its isolation from a natural source. Compound **26** could be reduced to be octanor-13*β*-dammarane by the Wolff-Kishner reduction. Furthermore, Biellmann et al [235] reported 3*β*-acetoxy-17-oxo-octanordammarane, which was possible to be converted to **26**, as an oxidation product of 3*β*,17-diacetoxy-octanordammarane, synthesized from dipterocarpol (scheme 22). In this work, octanordammarane-3,17-dione was supposed to be from the second pathway (Biellmann's work) because no 17-hydroxy dammarane was isolated from this extract.

Scheme 22 also showed that cabralealactone (**28**) and 3-*epi*cabraleahydroxylactone (**35**) (lactone group) were the oxidative degradation products from dipterocarpol/dammarenediol. It has been proposed that ocotillone-group dammaranes (ocotillone (**34**), cabraleone (**30**) and ocotillol) were the intermediates in this biosynthesis pathway [133, 154]. Warnhoff et al [154] suggested that ocotillol was probably formed in the plant from a dammarenediol derivative by the formation of 1,2-epoxidation at C_{24}=C_{25} with subsequent oxide opening at C-24 by the C-20 hydroxyl group (scheme 23). The work of Cascon demonstrated oxidation of cabraleone to cabralealactone by Jones reaction and then reduction to 3-*epi*cabraleahydroxylactone with $NaBH_4$ (scheme 24) [133].

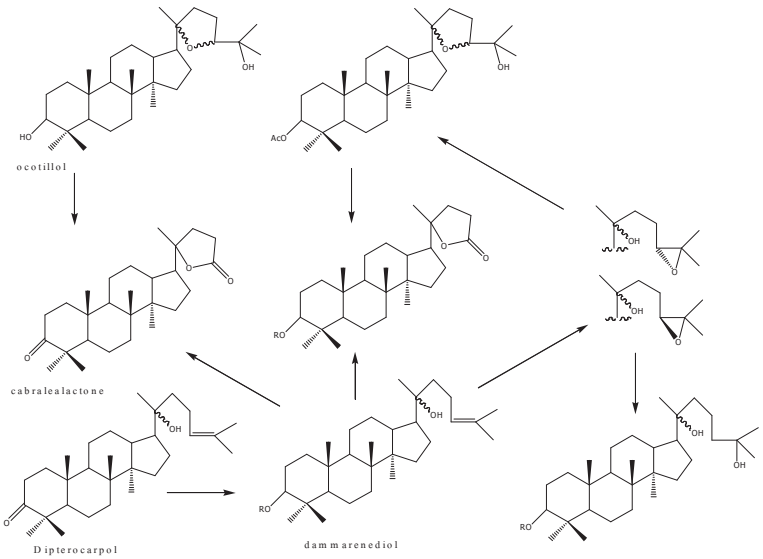

Scheme 23. Proposed mechanism of ocotillol and 3-*epi*cabraleahydroxylactone formation from dammarenediol derivative (in plant)

According to the previous literatures [60, 141], the 20*S* and 20*R* of dammarane triterpenes with a tetrahydrofurryl or lactone sidechain can be easily distinguished by the resonance of C-21, which resonated at about δ_C 23.6-27.2 ppm and at about 21.7-22.0 ppm for the 20*S* isomer and 20*R* isomer, respectively. Consequently, this fact was used to assign either 20*S* or 20*R* configuration of dammarane triterpenes accumulated in this extract. In our study, the stereochemistry at C-20 of all isolated dammaranes except compound **27** was characterized as *S* configured by comparison of the carbon chemical shifts at C-17, C-20, and C-21 with the corresponding reported dammaranes.

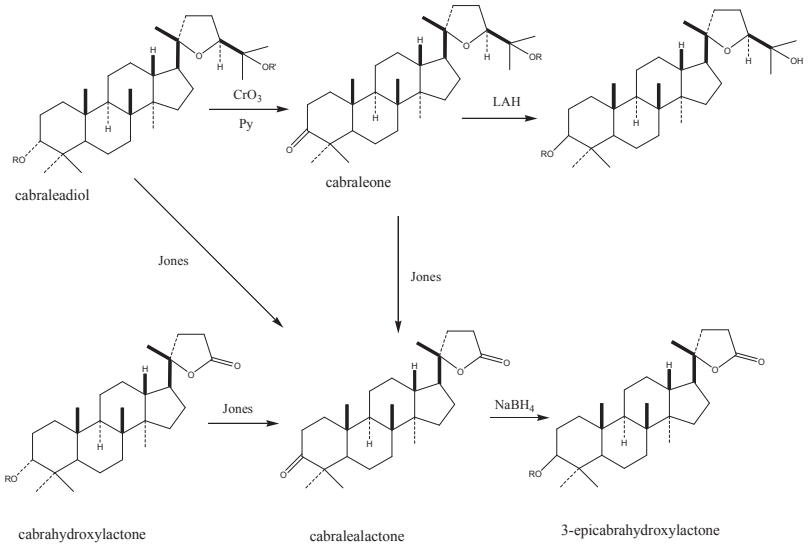

Scheme 24. Oxidation reaction of cabraleone (**30**) to cabralealactone (**28**); R/R' = H/Ac, LAH = lithium aluminium hydride

Isocabralealactone (**27**), 20*R*-epimer of cabralealactone (**28**), has just been reported for the first time in the nature by Joycharat, N. in 2010 [60]. It was a rare compound and only found in *Aglaia forbesii* seed (Meliaceae). Compound **28** was obtained more than **27** so it agreed with the normal configuration (*S*) at C-20 of dammaranes in this extract. Both isomers exhibited the difference in the chemical shift at position 21 and 22, as well as the Specific rotation value. Cabralealactone (**28**) was isolated from family Betulaceae [86], Meliaceae [133, 139, 143] and Capparaceae [150, 161]. 3-*Epi*cabraleahydroxylactone (**35**) was isolated from the seed oil of the camellia (Theaceae) [160].

Ocotillone group was one of the major triterpene intermediates in family Meliaceae [133, 137, 139, 141, 144, 145, 236-239], Betulaceae [86, 135] and Burseraceae [148]. Ocotillone (**34**) has been isolated from family Dipterocarpaceae [40, 67], Meliaceae [133, 141, 145, 236], Betulaceae [86, 135], Julianiaceae [73] and Simaroubaceae [240]. Cabraleone, its 24*S*-epimer, appeared in Meliaceae (especially genus *Cabralea*) [133, 137, 139, 141, 144, 145, 236-239], Fagaceae [241], and Burseraceae [148]. Ocotillol II (**37**), a reduction product of ocotillone (20*S*,24*R*), was found in family Dipterocarpaceae [152], Rhizophoraceae [158], Euphorbeaceae [153], Theaceae [160], and Apocyanaceae [147].

In addition to dipterocarpol, fouquierol and isofouquierol (**44**), acyclic side chain of 3-hydroxydammaranes, have been reported to be biological precursors of 3-hydroxycabralealactone and ocotillol II (**37**), respectively [155]. Fouquierone (**32**, **38**) and isofouquierone groups (**23**, **33**, **40**, **44**) were commonly found in Burseraceae, Betulaceae, Fouquieriaceae, Meliaceae and Anacardiaceae plants[86, 136, 140, 146, 148, 242] but have never been isolated from Dipterocarpaceous plant.

Isofouquierone group is the third most abundant triterpenes in this study. Isofouquierone (**40**), isofouquierone peroxide (**23**), isofouquierol (**44**) and isofouquierol peroxide (**33**) (in the order from high to low quantity in the extract) are known compounds.

Isofouquierone (**40**) and isofouquierol (**44**) were proposed to be alternate pathways besides ocotillone group (cabraleone, cabraleadiol, ocotillone and ocotillol), if the 20,24,25-triol dammarane was viewed as a precursor [148] (figure 27).

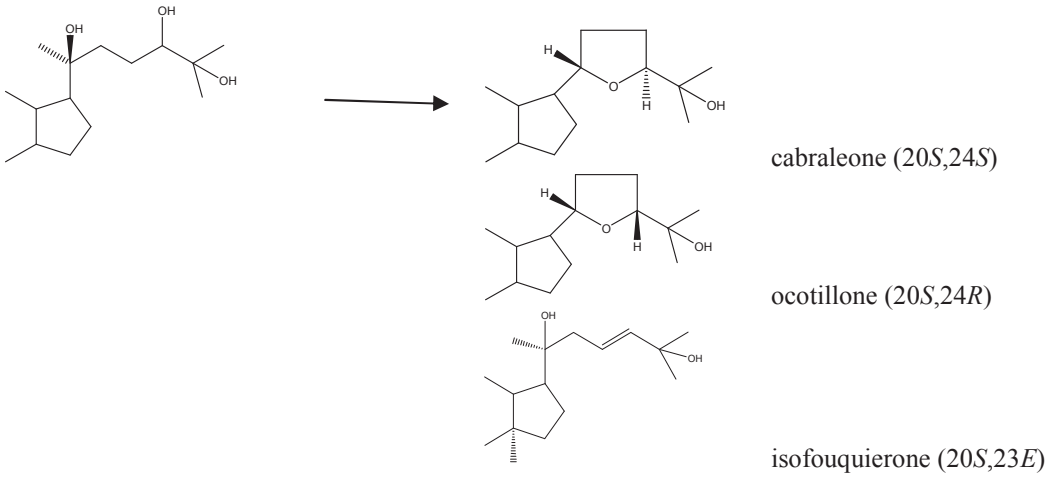

Figure 27. The possible degradation products of the 20,24,25-triol dammarane.

During the NMR experiments (in $CDCl_3$), isofouquierone (**40**) could decomposed by elimination of H_2O from C-25 to C-26 of the side chain 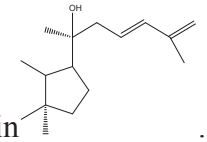 . It has been suggested from the degradation of cycloart-23-ene-3β,25,28-triol in literature [140, 148] that the reaction might have been catalyzed by traces of hydrochloric acid from the $CDCl_3$ solvent. The precise interpretation of these corresponding NMR spectra, with the presence of additional conjugated olefin and disappearance of hydroxyl C-25 group, confirmed this degradation. From this study, isofouquierone was proposed to be the precursor of the compounds in this group. The oxidation of isofouquierone will result in the other 3 compounds (**23**, **46**, **48**). The compounds of this group with the reduction on C-3 carbonyl group (**33**, **44**) were less seen in this extract.

Compound **29**, **32** and **38** were classified as fouquierone group but have not been determined the configuration on C-24 except **38**. They were position isomers of double bond and hydroxyl (or hydroperoxide) group on the side chain of isofouquierone peroxide (**23**) and isofouquierone (**33**). Compound **29** and **38** were 3-oxodammarane while C-3 carbonyl group of **32** was substituted by hydroxyl group. On the other hand, hydroperoxy group were on C-24 of compound **29** and **32** with unidentified configuration, while 24*S*-hydroxyl group appeared in compound **38**. No NMR data have been reported to indicate configuration on hydroperoxy (C-24) carbon of the sidechain of **29** and **32**. Compound **29** should be 20(*S*)-hydroxy-24-perhydroxy-dammar-25-en-3-one with unidentified configuration on C-24 rather than fouquierone as described in literature [146] because of downfield shift of C-24 as well as the MS spectrum at *m/z* 497.05 representing $C_{30}H_{50}O_4Na$ of the $[M+Na]^+$ ion. There was no any reported NMR data for this compound before. Although compound **32** was characterized as cereotagaloperoxide, its proposed structure was closer to fouquierol peroxide because the functional group at C-29 was CH_3

instead of $-CH_2OH$ as in cereotagalol A. Compound **32** has just been found only in *Ceriops tagal* (Rhizophoraceae). In this study, compound **29** and **32** were found only a little quantity and contaminated with isofouquierone peroxide (**23**) and isofouquierol peroxide (**33**), respectively. Each pair of compounds possessed the silimar IR spectrum, exact masses, and R_f value and were difficult to be separated on the column. Compound **38** was found much more than the former 2 compounds as same as its isomer, isofouquierone (**40**), that appeared with much larger amount than the peroxide derivatives. Compound **38** has been isolated from genus *Betula* (family Betulaceae) [86, 136, 140] and was found to exhibit mild cytotoxicity with MDR effect [86].

Compound **45** and **46** were characterized as new acyclic dammarane compounds. The structure of **46** was very close to isofouquierone except C-26 which was oxidized to be hydroxyl methylene group. Adversely, compound **45** looked like fouquierone with the oxidation of C-25 to quaternary hydroxyl carbon and dehydrogenation at C-22 and C-23. The influence of the 2 adjacent hydroxyl group make downfield shift of C-24 and C-25, compared to compound **38** and **40**. Compound **45** was first isolated from fraction D58 but, unfortunately, it degraded in $CDCl_3$ solvent within 24 hours during NMR experiments. The NMR data of degradation product showed an additional double bond with terminal methylene group and the loss of water at position 20 to make double bond. It might be the same reason as compound **40** that traces of hydrochloric acid in $CDCl_3$ solvent caused this degradation. However, it was isolated again in fraction D59. The NMR solvent was changed to deuterated-acetone.

Compound **39** and **49** are new nor-dammarane triperpenes while compound **26** is a nor-dammarane that has been isolated for the first time from plants and has already been discussed on its biosynthesis from the oxidation of dipterocarpol and lactone groups. The side chain of **39** is very close to that of isofouquierone excluding the loss of one C-27 methyl and the substitution of C-25 hydroxyl with a carbonyl carbon. It showed that isofouquierone was possible to be oxidized to compound **39**. Compound **49** was the only tetranordammarane monoacid found in this extract. It was supposed to be produced from the cleavage at C-23 and C-24 of isofouquierone.

In general, ring-A opened triterpenoids have a cleavage between C-3 and C-4, while 2,3-*seco*-triterpenoids, as compound **47** and **48** are rare in the nature. This is the first time that 2,3-*seco*-dammarane derivatives have been isolated from a Dipterocarpaceous plant. They appeared in high polarity fractions. However, 2,3-*seco*-acids have been synthesized by Zorina et al and Wei et al [243, 244] through oxidative scission of A-ring, with the aid of either potassium bichromate in the presence of sulfuric acid or hydrogen peroxide in potassium hydroxide and methanol (H_2O_2/KOH/MeOH). The proposed structure of **47** and **48** revealed that they are 2,3-*seco*-dioic acid derivatives of ocotillone and isofouquierone peroxide, compounds with high quantity in this extract. Compound **48** was then performed NMR experiment in acetone to avoid dehydration.

A group of norlupane derivative was isolated. The plausible pathway for the formation of 17α-hydroxy-28-norlupan-20(29)-en-3-one (**25**) might be from C-28 (β-

orientation) decarboxylation of betulonic acid (found in trace amount with dipterocarpol subfraction) and the attachment of 17α-hydroxyl group to be the new norlupane. The NOE correlations of compound **41** confirmed the C-17 α-hydroxyl configuration, that were consistent with the suggestion of previous assumption [107, 108]. This result was refered to C-17 of compound **25** as well. Compound **25** was assigned to be the precursor of the other isolated norlupanes. Cyclization between C-29 and 17α-hydroxyl group of C-17 produced compound **24**. Compound **36** and **42** were the oxidation products at C-20 of **25** to be hydroxyl group instead of terminal olefin, nevertheless cyclization took place on different position. Cyclization of compound **42** happened between one of methyl group and hydroxyl group of C-17 while one of methyl group after C-20 oxidation of **36** was continually oxidized to be methylene alcohol and cyclization was formed between two hydroxyl groups of C-17 and C-20. Moreover, oxidation of C-29 olefin of **25** to make keto group on C-20 generated compound **41**. The NOE correlations of compound **42** showed that the assumption of 17-hydroxyl configuration from the chemical shifts of C-13 as described in literature [107, 108] could not applied to the ring side chain at C-17. As the result, the α-configuration was assigned on C-17 and C-19 of compound **24**, **36** and **42**.

The 3β-OH derivative of compound **24** showed stronger potency of antiproliferative activity against the malignant SA mouse mammary epithelial cells than that of betulinic acid [107]. Hence, cytotoxicity of this norlupane group is interesting to be investigated.

4.4 IDENTIFICATION AND STRUCTURAL STUDY OF ISOLATED COMPOUNDS.

4.4.1 *β*-Sitosterol (3), Caryophyllene oxide (9) and clovane-2,9-diol (43)

The spectroscopic data of **3** and **9** were campared to the data from phytochemical study of *H.odorata* leaves hexane extract. Caryophyllene oxide was again confirmed by GC-MS analysis. More caryophyllene oxide was found in *D. costatus* than in *H.odorata*. Clovane-2,9-diol (**43**) was found in trace amount and was identified by GC-EI-MS.

4.4.2 *β*-Elemene (21)

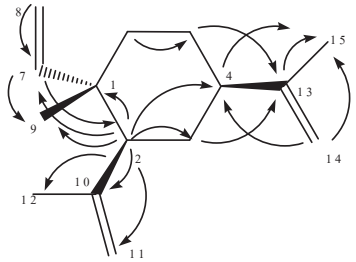

Figure 28. Selected HMBC correlations of **21**

This compound was obtained as a colorless resin which was characterized by GC-MS analysis with comparison to reference data. The identification was supported by the 1D NMR data and the HMBC correlations. The ^{1}H and ^{13}C NMR spectrum showed the presence of methyl, metylene and methine carbon with olefin moiety.

Table 31. The ^{1}H-NMR (400 MHz) and ^{13}C-NMR spectrum (75 MHz) data of **21** (in $CDCl_3$) ; δ in ppm ; J in Hz

position	δ_H	δ_C
1 Civ		32.87
2 CH	2.08 (dd, 1H, *J*=6.7, 15.0 Hz)	52.72
3 CH_2	1.51 (m, 2H)	39.90
4 CH	1.99 (m, 1H)	45.69
5 CH_2	1.48 (m, 1H) 1.57 (m, 1H)	39.82
6 CH_2	1.51 (m, 1H) 1.67 (m, 1H)	26.82
7 CH db	5.88 (dd, 1H, *J*=10.8, 17.6Hz)	150.34
8 CH_2db	4.97 (d, 1H, *J*=5.4Hz) 4.93 (s, 1H)	109.85
9 CH_3	1.06 (s, 3H)	16.60
10 Civ db		147.76
11 CH_2db	4.64 (s, 3H) 4.87 (s, 3H)	112.08
12 CH_3	1.71 (s, 3H)	24.80
13 Civ db		150.45
14 CH_2db	4.76 (s, 1H) 4.77 (s, 1H)	108.24
15 CH_3	1.80 (s, 3H)	21.11

4.4.3 Dipterocarpol (22) and Dammarenediol II (31)

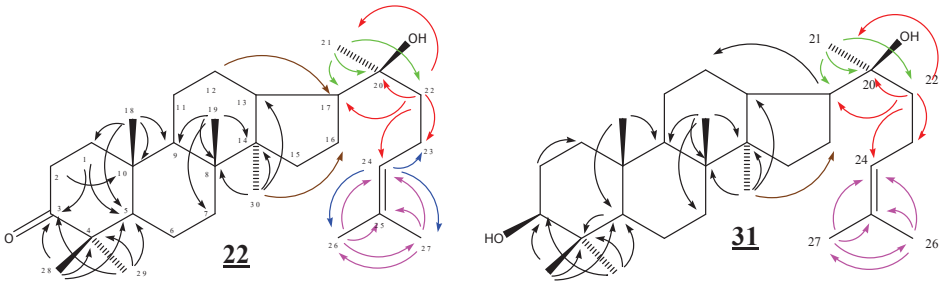

Figure 29. Selected HMBC correlations of **22** and **31**

Compound **22** was obtained as a white shiny flakes with the highest amount among all triterpenes in the extract. Its molecular formula of $C_{30}H_{50}O_2$ was deduced by a combination of ESI-MS (*m/z* 465 of the $[M+Na]^+$ ion) and NMR data. Analysis of the ^1H and ^{13}C NMR data (Tables 32) suggested the 3-oxodammarane skeleton. The side chain consisted of a hydroxyl group as well as one double bond between quaternary carbon and methine carbon. In the HMBC spectrum, the correlations of the methyl proton at δ_H 1.17 (H-21) with δ_C 49.8 (C-17), δ_C 75.4 (hydroxyl quaternary carbon C-20) and δ_C 40.4 (C-22) were dicisive to establish a hydroxyl group and a methyl group attached on C-20. Indeed, the methyl protons ($\delta_{H\text{-}26}$ 1.71 and $\delta_{H\text{-}27}$ 1.64) also showed correlations with quaternary C-25 (δ_C 131.7) and methine C-24 (δ_C 124.7) of double bond. In addition, HMBC correlations of methylene protons at δ_H 1.54 (H-22) with the carbon signals at δ_C 49.8 (C-17), 75.4 (C-20), 22.6 (C-23) and 124.7 (C-24) confirmed the presence of a double bond with 2 terminal methyl groups, together with 2 methylenes between hydroxyl carbon (C-20) and methine carbon of double bond (C-24).

As the result of a detailed spectroscopic analysis and comparison with the published data, the structure of **22** was identified as dipterocarpol, a common triterpene in Dipterocarpaceous plants.

The NMR data of **31** corresponded to those of dipterocarpol except the ^1H and ^{13}C resonance of position 2, 3, 4 and 29. The chemical shift indicated the presence of C-3 methine alcohol in stead of carbonyl group. The HMBC spectrum also exhibited the similar correlations with those of dipterocarpol such as the correlation of H-21 with C-17, C-20 and C-22, including that of H-26 and H-27 with C-25 and C-24 (figure 29).

GC-EI-MS investigation for **31** became available for the present study. It was significant that the [M]+ ions in this compound was not visible in the spectra [39]. MS spectra of **31** showed the tetracyclic dammarane fragments at *m/z* 317, 299, 207 and 189 (Figure 30). Peak at *m/z* 207 indicated the A, B and C rings of the tetracyclic skeleton limiting the choice to the dammarane ring system and excluding euphane or lanostane type skeletons. Peak at *m/z* 317 was due to the wreckage of the bond between C-17 and C-20. A number of peaks at m/z 109, 95 and 69 represented the side chain fragments. The fragment *m/z* 109 corresponded to water loss from the side chain ($C_8H_{15}O$) [39] which lose one more methylene in the fragment at *m/z* 95.

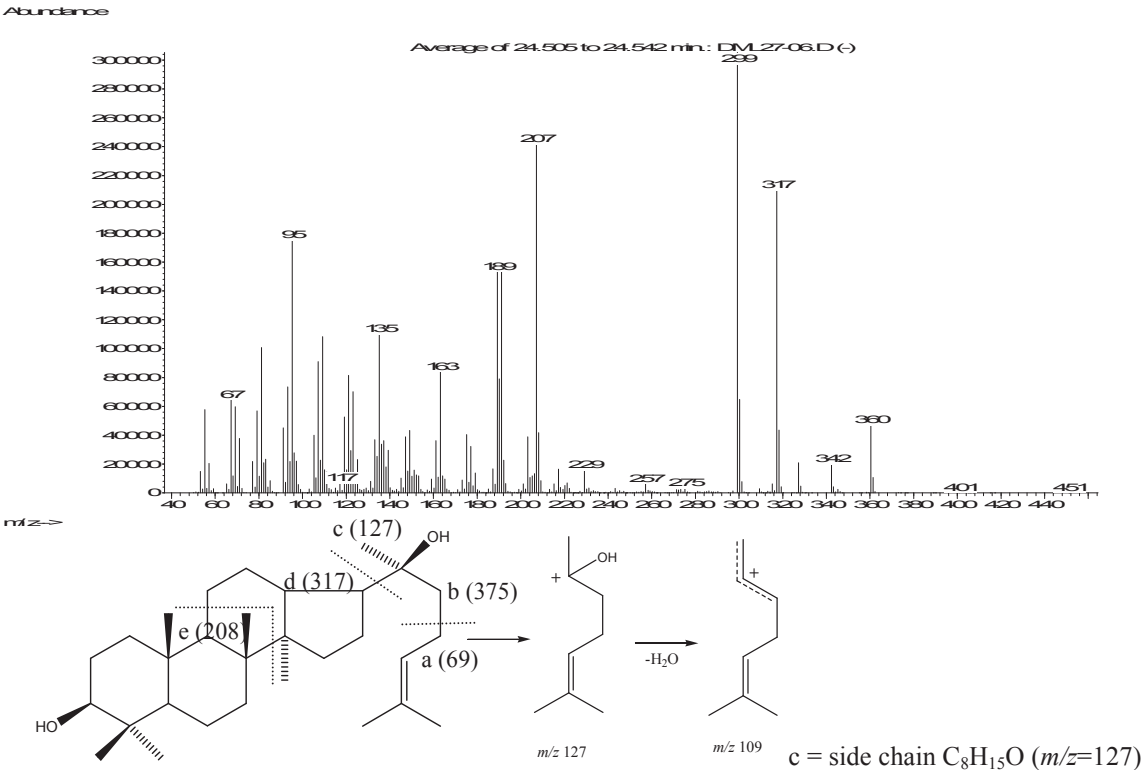

Fragment	*m/z*
a	69
a-2 (2H)	67
b-15 (CH_3)	360
b-15 (CH_3)-18 (H_2O)	342
c-18 (H_2O)	109
c-18 (H_2O) – 14 (CH_2)	95
d	317
d-18 (H_2O)	299
e-1 (H)	207
e-1 (H) – 18 (H_2O)	189

Figure 30 . Fragmentation of dammarenediol II (**31**)

The difference between dammarenediol I and II is *S*-configuration at C-20 in II and *R*-configuration in I derivative. The two C-20 epimers of dammrenediol exhibited similar retention factor, and retention time values on TLC and GC, respectively, and mass spectra [132]. Therefore, the occurrence of only 20*S*-configuration was confirmed by comparison of the ^{13}C NMR spectra of these components with the reference [159, 227, 233]. The chemical shift differences of the carbons around the C-20 epimers such as C-21 and C-22 were used to determine the C-20 configuration [227]. The resonance of the (20*S*)-epimer for C-21 is more deshielded while C-22 is more shielded than that of the (20*R*)-epimer [132] (*R*: δ_C= 23.5, 41.8; *S*: δ_C= 24.9, 40.5 for C-21 and C-22, respectively [159])

From the literature [39, 148, 159] and NMR data, compound **31** was considered to be dammaranediol-II.

Table 32. The ^{1}H-NMR (300 MHz) and ^{13}C-NMR (75 MHz) of **22** and **31** (in $CDCl_3$) ; δ in ppm ; J in Hz (dipterocarpol group – dammarane triterpene)

position	δ_H		δ_C	
	22	**31**	**22**	**31**
1	1.50 (m) 1.97 (m)	1.00 (m) 1.70 (m)	39.9	39.0
2	2.50 (m) 2.57 (m)	1.62 (m)	34.1	27.4
3		3.21 (dd, J=10.9, 5.2)	218.3	79.8
4			47.4	39.0
5	1.42 (d, J=11.2)	0.75 (d, J=11.1)	55.3	55.8
6	1.53 (m) 1.60 (m)	1.46 (m) 1.51 (m)	19.6	18.3
7	1.36 (m) 1.61 (m)	1.30 (m) 1.55 (m)	34.5	35.2
8			40.3	40.4
9	1.48 (m)	1.31 (m)	50.0	50.6
10			36.8	37.1
11	1.32 (m) 1.55 (m)	1.27 (m) 1.51 (m)	22.0	21.5
12	1.55 (m) 1.80 (m)	1.50 (m) 1.75 (m)	24.8	24.8
13	1.71 (m)	1.62 (m)	42.4	42.3
14			50.3	50.3
15	1.13 (m) 1.51 (m)	1.47 (m) 1.07 (m)	31.1	31.2
16	1.33 (m) 1.91 (m)	1.27 (m) 1.82 (m)	27.5	27.5
17	1.80 (m)	1.75 (m)	49.8	49.8
18	0.96 (s)	0.86 (s)	16.0	16.2
19	1.02 (s)	0.97 (s)	15.2	15.5
20			75.4	75.4
21	1.17 (s)	1.15 (s)	25.5	25.4
22	1.54 (m)	1.48 (m)	40.4	40.5
23	2.10 (m)	2.05 (m)	22.6	22.6
24	5.12 (tt, J=7.1, 1.4)	5.13 (t, J=7.1)	124.7	124.7
25			131.7	131.6
26	1.71 (s)	1.70 (s)	25.8	25.7
27	1.64 (s)	1.64 (s)	17.7	17.7
28	1.10 (s)	0.99 (s)	26.7	28.0
29	1.06 (s)	0.79 (s)	21.0	15.4
30	0.91 (s)	0.89 (s)	16.3	16.5

4.4.4 Isofouquierone peroxide (23), isofouquierol peroxide (33), isofouquierone (40), isofouquierol (44), (20*S*,23*E*)-20,25,26-trihydroxydammar-23-en-3-one (46)* and (20*S*,23*E*)-25-hydroperoxy-20-hydroxy-2,3-*seco*-dammar-23-en-2,3-dioic acid (48)*****

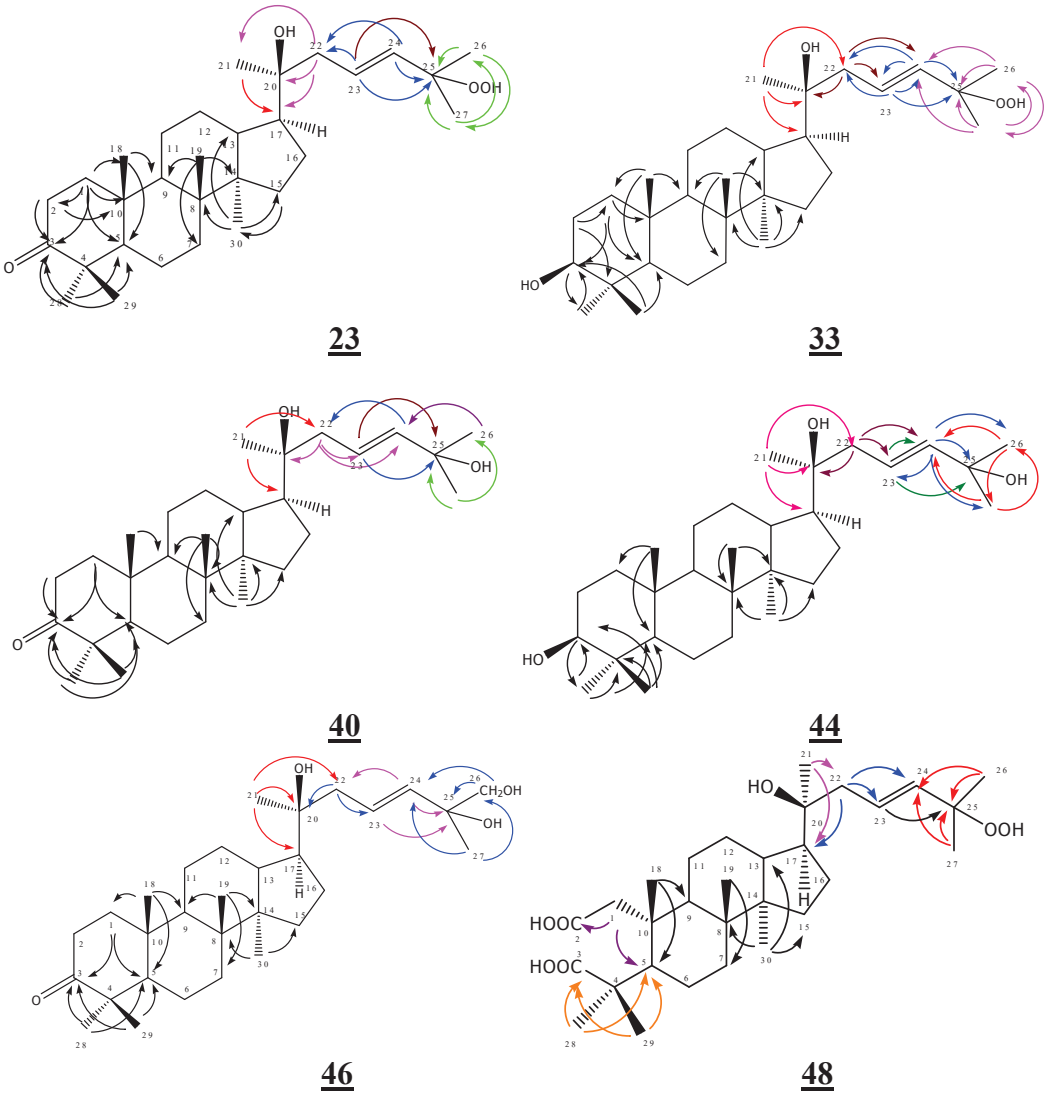

Figure 31. Selected HMBC correlations of compounds **23**, **33**, **40**, **44**, **46** and **48**

The NMR specta of compounds **23**, **33**, **40** and **44** showed the nature of tetracyclic dammarane ring with the same patterns of HSQCedited and HMBC spectra except for the difference in the chemical shifts around C-3 and C-25. The compounds with OH group at C-3 (**33**, **44**) expressed the $\delta_{H\text{-}3}$ about 3.2 and the $\delta_{C\text{-}3}$ 79.0, together with upfield shifts of C-2, C-4 and C-29 compared to those with keto group, whereas compounds **23** and **40** with C-3 keto carbon showed the $\delta_{C\text{-}3}$ at 218.1-218.3. The ^{1}H NMR spectra showed two methyl groups as singlets at δ_H around 1.36-1.37 of H-26 and H-27. The doublet ($J_{23\text{-}24}$ = 15 Hz) and the doublet of triplet ($J_{23\text{-}24}$ = 15, $J_{22\text{-}23}$ = 7 Hz) of compound **23** and **33** due to one proton each at δ_H 5.6 and 5.8 were attributed to olefinic protons at positions 24 and 23, respectively. The coupling constant value indicated *E*-form of double bond. The signals of two methyl groups (C-26 and C-27) bonding to C-25 and olefinic carbons

(C-23 and C-24) were assigned through the HMBC correlations of H-26 and H-27 with C-24 and C-25, of H-23 with C-25, along with the correlations of H-22 with C-23 and C-24 (Figure 31). Another difference among four compounds was the presence of OOH or OH group at C-25. From the HSQCedited and HMBC spectra, the hydroperoxidized quaternary carbon signal of C-25 at δ_C 82 of **23**, **33**, shifted downfield compared to that of **40** and **44** with OH group (δ_C 70.8). Adversely, the δ_C of C-26 and C-27 of **23**, **33** (δ_C 24.1-24.5) were shifted upfield compared to δ_C about 29.9 of **40**, **44**. An addition oxygen atom of hydroperoxide was also supported by the ESI-MS spectra of **23** and **33** that showed 16 amu more mass than those of **40** and **44**, respectively. The HMBC spectrum of all compounds (Figure 31) showed the normal correlations of H-21 with C-17 and C-20. The 20*S* configuration was elucidated by the same downfield shift signal of C-21 as compounds **22** and **31** in previous section.

From above data, the structure of **23** was thus deduced as isofouquierone peroxide that was reported only from the stem bark of *Rhus javanica* (Anacardiaceae) [146]. The ESI-MS of compound **33** showed the $[M+Na]^+$ ion at *m/z* 499, indicating 2 protons more than that of **23**. With the comparison of NMR data to **23** and the previous publication [157], **33** was deduced to isofouquierol peroxide. Finally, the comparison to the literature [148, 155, 158] made the identification of **40** and **44** as isofouquierone and isofouquierol, respectively.

The ^{13}C-NMR spectrum of compound **46** showed 30 carbon signals which resembled to those of isofouquierone (**40**) except for the signals for C-26. The ^{1}H, ^{13}C and HSQCedited data showed that position 26 was hydroxymethylene. The HMBC spectrum (Figure 34) exhibited the correlations between 2 olefinic protons ($\delta_{H\text{-}23}$=5.86, $\delta_{H\text{-}24}$=5.62) and C-25 ($\delta_{C\text{-}25}$=73.3), together with the correlations of C-24 ($\delta_{C\text{-}24}$=137.7) with H-26 ($\delta_{H\text{-}26}$=3.52) and H-27 ($\delta_{H\text{-}27}$=1.32). The downfield shifted of $\delta_{C\text{-}25}$ and upfield shift of $\delta_{C\text{-}24}$ and $\delta_{C\text{-}27}$ were the effect from 26-OH. This compound was thus elucidated as (20*S*,23*E*)-20,25,26-trihydroxydammar-23-en-3-one, a new 3-oxo-dammarane with acyclic side chain and three hydroxyl functional groups.

The molecular formula of compound **48** was established as $C_{30}H_{50}O_7$ from the HRESI (-) MS at *m/z* 521.3486 for $[M-H]^-$, calc $C_{30}H_{49}O_7$ 521.3478. The ^{13}C-NMR data of compound **48** were close to compound **23**. Additional signals of two carbonyl carbons were observed at δ_C 172.3 and 180.4. The six degrees of unsaturation implied from molecular formula together with the presence two carbonyl groups and one pair of double bond suggested three cyclic rings of the structure. A broad band IR absorption spectrum at 3650-2500 cm^{-1} exhibited the presence of carboxylic acid group. In the HMBC spectrum of **48** (Figure 34), the correlations were observed from the proton signals at δ_H 2.46 and 2.66 (H-1) to the carbon signals at δ_C 172.3 (C-2) and 48.1 (C-5) and between the proton signals at δ_H 1.26 (H-28)/1.29 (H-29) and the carbon signals at δ_C 180.4 (C-3)/48.1 (C-5). These indicated the carboxylic groups at C-2 and C-3. Two carboxyl groups and a germinal dimethyl group at C-4 suggested a *seco*-dammarane structure having a cleavage between C-2 and C-3 rather than C-3 and C-4. This ring opening was supported by

downfield shift of $\delta_{H\text{-}5}$ and $\delta_{H\text{-}9}$ (2.57 and 2.53 ppm, respectively) compared to those of **23**. The shift resulted from anisotropic deshielding effect of both carbonyl groups in 3D conformation. The δ_H and δ_C of the rest positions were consistently with compound **23**. On the basis of the above spectroscopic data, the structure of compound **48** was assigned as (20*S*,23*E*)-25-hydroperoxy-20-hydroxy-2,3-*seco*-dammar-23-en-2,3-dioic acid, a new 2,3-*seco*-dioic dammarane derivative. .

Table 33. The ^{1}H-NMR (300 MHz) of **23**, **33** (in $CDCl_3$) and **48** (in acetone) ; δ in ppm ; J in Hz (isofouquierone group – dammarane triterpene)

position	δ_H		
	23	**33**	**48**
1	1.48 (m) 1.97 (m)	1.02 (m) 1.73 (m)	2.46 (d, *J*=17.3) 2.66 (d, *J*=17.3)
2	2.48 (m)	1.61 (m) 1.67 (m)	
3		3.22 (dd, *J*=11.1, 5.2)	
4			
5	1.42 (m)	0.78 (d, *J*=10.7)	2.57 (m)
6	1.48 (m) 1.53 (m)	1.48 (m) 1.55 (m)	1.49 (m) 1.70 (m)
7	1.32 (m) 1.57 (m)	1.32 (m) 1.57 (m)	1.25 (m) 1.63 (m)
8			
9	1.44 (m)	1.36 (m)	2.53 (m)
10			
11	1.32 (m) 1.51 (m)	1.27 (m) 1.55 (m)	1.64 (m)
12	1.54 (m) 1.76 (m)	1.53 (m) 1.77 (m)	1.68 (m)
13	1.73 (m)	1.68 (m)	1.82 (m)
14			
15	1.13 (m) 1.48 (m)	1.13 (m) 1.51 (m)	1.07 (m) 1.48 (m)
16	1.32 (m) 1.93 (m)	1.29 (m) 1.85 (m)	1.20 (m) 1.92 (m)
17	1.77 (m)	1.78 (m)	1.78 (m)
18	0.96 (s)	0.97 (s)	1.00 (s)
19	1.02 (s)	0.86 (s)	1.03 (s)
20			
21	1.16 (s)	1.14 (s)	1.14 (s)
22	2.26 (dd, *J*=7.1, 3.2)	2.25 (dd, *J*=7.0, 3.1)	2.21 (d, *J*=7.2)
23	5.82 (dt, *J*=15.8, 7.1)	5.79 (dt, *J*=15.7, 7.1)	5.76 (dt, *J*=15.9, 7.2)
24	5.64 (d, *J*=15.8)	5.63 (d, *J*=15.8)	5.62 (d, *J*=16.0)
25			
26	1.37 (s)[a]	1.37 (s)[a]	1.29 (s)
27	1.36 (s)[a]	1.36 (s)[a]	1.29 (s)
28	1.10 (s)	0.99 (s)	1.26 (s)
29	1.06 (s)	0.79 (s)	1.29 (s)
30	0.90 (s)	0.89 (s)	0.91 (s)

[a] interchangeable

Table 34. The ^{1}H-NMR (300 MHz) of **40**, **44** and **46** (in $CDCl_3$) ; δ in ppm ; J in Hz (isofouquierone group – dammarane triterpene)

position	δ_H		
	40	**44**	**46**
1	1.49 (m) 1.96 (m)	1.02 (m) 1.73 (m)	1.52 (m) 1.97 (m)
2	2.50 (m)	1.61 (m) 1.67 (m)	2.49 (dd, *J*=14.8, 9.0) 2.57 (dd, *J*=14.8, 9.0)
3		3.25 (dd, *J*=11.1, 4.8)	
4	1.41 (m)	0.78 (d, *J*=11.2)	1.42 (d, *J*=10.7)
5	1.51 (m) 1.59 (m)	1.48 (m) 1.56 (m)	1.52 (m) 1.60 (m)
6	1.35 (m) 1.60 (m)	1.32 (m) 1.57 (m)	1.38 (m) 1.61 (m)
7	1.47 (m)	1.36 (m)	1.47 (t, *J*=11.9)
8	1.32 (m) 1.54 (m)	1.29 (m) 1.55 (m)	1.35 (m) 1.58 (d, *J*=2.5)
9	1.55 (m) 1.77 (m)	1.55 (m) 1.78 (m)	1.58 (m) 1.80 (d, *J*=2.8)
10	1.72 (m)	1.69 (m)	1.72 (m)
11	1.13 (m) 1.50 (m)	1.09 (m) 1.48 (m)	1.17 (m) 1.54 (dd, J=22.6,10.6)
12	1.30 (m) 1.90 (m)	1.29 (m) 1.88 (d, *J*=7.6)	1.31 (dd, *J*=10.3,5.6) 1.90 (m)
13	1.78 (m)	1.78 (m)	1.79 (d, *J*=5.5)
14	0.98 (s)	089 (s)	1.05 (s)
15	1.04 (s)	1.01 (s)	0.99 (s)
16	1.17 (s)	1.18 (s)	1.20 (s)
17	2.24 (broad)	2.25 (s)	2.29 (d, *J*=8.1)
18	5.73 (m)	5.74 (m)	5.86 (m)
19	5.73 (m)	5.74 (m)	5.62 (dd, *J*=15.8, 6.9)
20	1.36 (s)	1.37(s)	3.52 (dd, *J*=24.0, 10.4)
21	1.36 (s)	1.37(s)	1.32 (m)
22	1.12 (s)	1.08 (s)	1.13 (s)
23	1.07 (s)	0.82 (s)	1.09 (s)
24	0.91 (s)	0.92 (s)	0.93 (s)
25	1.49 (m) 1.96 (m)	1.02 (m) 1.73 (m)	1.52 (m) 1.97 (m)
26	2.50 (m)	1.61 (m) 1.67 (m)	2.49 (dd, *J*=14.8, 9.0) 2.57 (dd, *J*=14.8, 9.0)
27		3.25 (dd, *J*=11.1, 4.8)	
28	1.41 (m)	0.78 (d, *J*=11.2)	1.42 (d, *J*=10.7)
29	1.51 (m) 1.59 (m)	1.48 (m) 1.56 (m)	1.52 (m) 1.60 (m)
30	1.35 (m) 1.60 (m)	1.32 (m) 1.57 (m)	1.38 (m) 1.61 (m)
	In acetone		
23	5.74 (m)		
24	5.64 (d, *J*=15.7)		

Table 35. The ^{13}C-NMR (75 MHz) of **23**, **33**, **40**, **44**, **46** (in $CDCl_3$) and **48** (in acetone); δ in ppm; *J* in Hz (isofouquierone group – dammarane triterpene)

position	**23**	**33**	**40**	**44**	**46**	**48**
1	39.9	39.0	39.9	39.0	39.9	42.1
2	34.1	27.4	34.1	27.4	34.1	172.3
3	218.1	79.0	218.3	79.0	218.2	180.4
4	47.4	39.0	47.4	39.0	47.4	46.4
5	55.3	55.8	55.3	55.8	55.3	48.1
6	19.6	18.3	19.6	18.6	19.6	21.2
7	34.5	35.2	34.5	35.2	34.5	34.3
8	40.3	40.4	40.3	40.4	40.3	40.0
9	50.0	50.6	50.0	50.6	50.0	42.2
10	36.8	37.1	36.8	37.1	36.8	41.8
11	22.0	21.5	22.0	21.5	22.0	22.3
12	24.9	24.9	24.8	24.8	24.8	24.5
13	42.6	42.5	42.5	42.4	42.6	42.1
14	50.3	50.3	50.3	50.3	50.3	50.6
15	31.1	31.1	31.1	31.1	31.1	31.0
16	27.5	27.5	27.5	27.5	27.5	27.7
17	50.1	50.2	49.8	49.9	50.0	49.5
18	16.0	16.2	16.0	16.2	15.2	19.5
19	15.2	15.5	15.2	15.5	16.1	14.7
20	75.0	75.2	75.0	75.1	75.0	73.9
21	25.8	25.7	25.7	25.9	25.5	25.7
22	43.4	43.4	43.4	43.4	43.5	44.3
23	127.2	127.2	122.4	122.3	125.9	126.4
24	137.4	137.4	142.1	142.0	137.7	137.2
25	82.1	82.1	70.8	70.8	73.3	80.7
26	24.1[a]	24.1[a]	29.9	29.9	70.0	24.0[a]
27	24.4[a]	24.5[a]	29.9	29.9	24.4	24.1[a]
28	26.7	28.0	26.7	28.0	26.7	26.4
29	21.0	15.4	21.0	15.4	21.0	24.2
30	16.3	16.4	16.3	16.4	16.4	16.0

[a] interchangeable

4.4.5 (20*S*,22*E*)-20,24,25-Trihydroxydammar-22-en-3-one (**45**)***

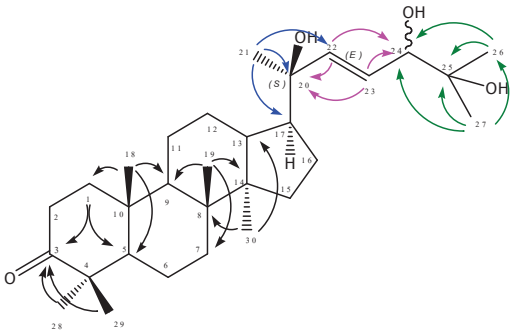

Figure 32. Selected HMBC correlations of compound **45**

The HRESI-MS of **45** at *m/z* 497.3602 $[M+Na]^+$ ion, represented the molecular formula of $C_{30}H_{50}O_4Na$ (calc mass 497.3607). IR absorption showed C=O stretching and O-H stretching at 1701 and 3405 cm^{-1}, respectively. Thirty carbon signals in the ^{13}C-NMR spectrum corresponded to 3-oxodammarane skeleton as dipterocarpol (**22**) [227] but with differences in the signals of the side chain. Three oxygenated carbons, which were one

methine and two quaternary carbons, together with three methyl carbons and two olefinic carbons, were presented for the side chain in the HSQCedited spectrum. The HMBC spectrum showed the correlations of the olefinic protons ($\delta_{H\text{-}22}$ 5.85, $\delta_{H\text{-}23}$ 5.78) with 2 oxygenated carbons ($\delta_{C\text{-}20}$ 74.5 and $\delta_{C\text{-}24}$ 79.2). This suggested the structure of a double bond between 2 oxygenated carbons. This double bond was assigned to be at position 22-23 based on HMBC correlations from methyl protons at position 21 ($\delta_{H\text{-}21}$ 1.24) to a olifinic carbon ($\delta_{C\text{-}22}$ 127.1) and from a olefinic proton ($\delta_{H\text{-}22}$ 5.85) to C-20 ($\delta_{C\text{-}20}$ 74.5) (Figure 32). The configuration of the double bond was *E*-form because of the large coupling constant (*J*=15.8 Hz) between the olefinic protons.

Thus, the structure of compound **45** was determined to be a new dammarene triterpene with a acyclic trihydroxyl side chain, (20*S*,22*E*)-20,24,25-trihydroxydammar-22-en-3-one.

Table 36. The ^{1}H-NMR (300 MHz) and ^{13}C-NMR (75 MHz) of **45** (in acetone); δ in ppm; *J* in Hz

position	δ_H	δ_C	position	δ_H	δ_C
1	1.50 (m) 1.93 (m)	39.6	16	1.31 (m) 2.03 (m)	27.4
2	2.41 (dd, *J*=15.4, 8.1) 2.50 (dd, *J*=15.4, 8.1)	33.6	17	1.79 (m)	50.8
3		215.6	18	0.96 (s)	15.5
4		46.9	19	1.01 (s)	14.8
5	1.47 (m)	55.0	20		74.5
6	1.50 (m) 1.61 (m)	19.4	21	1.24 (s)	28.0
7	1.31 (m) 1.62 (m)	34.5	22	5.85 (d, *J*=15.8)	137.8
8		40.2	23	5.78 (dd, *J*=15.8, 6.1)	127.1
9	1.52 (m)	50.0	24	3.88 (d, *J*=6.1)	79.2
10		36.7	25		71.9
11	1.31 (m) 1.51 (m)	21.8	26	1.15 (s)[a]	25.6[a]
12	1.49 (m) 1.71 (m)	25.1	27	1.13 (s)[a]	24.0[a]
13	1.78 (m)	42.9	28	1.05 (s)	26.1
14		50.0	29	1.01 (s)	20.4
15	1.04 (m) 1.50 (m)	31.0	30	0.92 (s)	15.9

[a] interchangeable

4.4.6 20(*S*)-Hydroxy-24-perhydroxy-dammar-25-en-3-one (29)***, cereotagaloperoxide (32)** and (20*S*,24*S*)-20,24-dihydroxydammar-25-en-3-one (38)

Comparison to the ^{13}C NMR spectrum of **22**, compound **38** showed 30 carbon resonances, which the carbon signals agreed well with 3-oxodammarane skeleton. The difference was on acyclic side chain. The signals of olefinic methine protons and one methyl group were disappeared. Signals of oxymethine (δ_H 4.06, δ_C 76.5), together with terminal methylene (δ_H 4.98, 4.86; δ_C 111.0) were observed for instead. The HMBC correlations from H_3-27 to these oxymethine and methylene carbons (Figure 33) suggested their positions to be at 24 and 26, respectively. The oxymethine at position 24 was also confirmed by the HMBC

correlations from H-24 to C-27, C-25 and C-22. Compound **38** was then elucidated as (20*S*,24*S*)-20,24-dihydroxydammar-25-en-3-one or 24*S*-epimer of fouquierone. Its 24*S*-configuration was determined by comparing its NMR data and specific rotation to the literature [136, 151, 158].

Compound **29** showed very similar NMR data to those of **38** except for the chemical shift around C-24. The δ_C 89.8 was assigned to be the signal of C-24 carbon according to its HMBC correlation to H-27 (δ_H 1.80) (Figure 33). Downfield shift of $\delta_{C\text{-}24}$ at 89.8 ppm suggested the presence a hydroperoxyl substitution rather than a hydroxyl one. This was supported by the ESI-MS of the $[M+Na]^+$ ion at *m/z* 497, representing $C_{30}H_{50}O_4Na$, which showed one more oxygen atom than that of **38**. The stereochemistry of C-24 could not be investigated because very small quantity with impurity of compound **29** was isolated. From the above information, compound **29** was characterized as (20*S*)-20-hydroxy-24-perhydroxy-dammar-25-en-3-one. With the best of our knowledge, this compound was new.

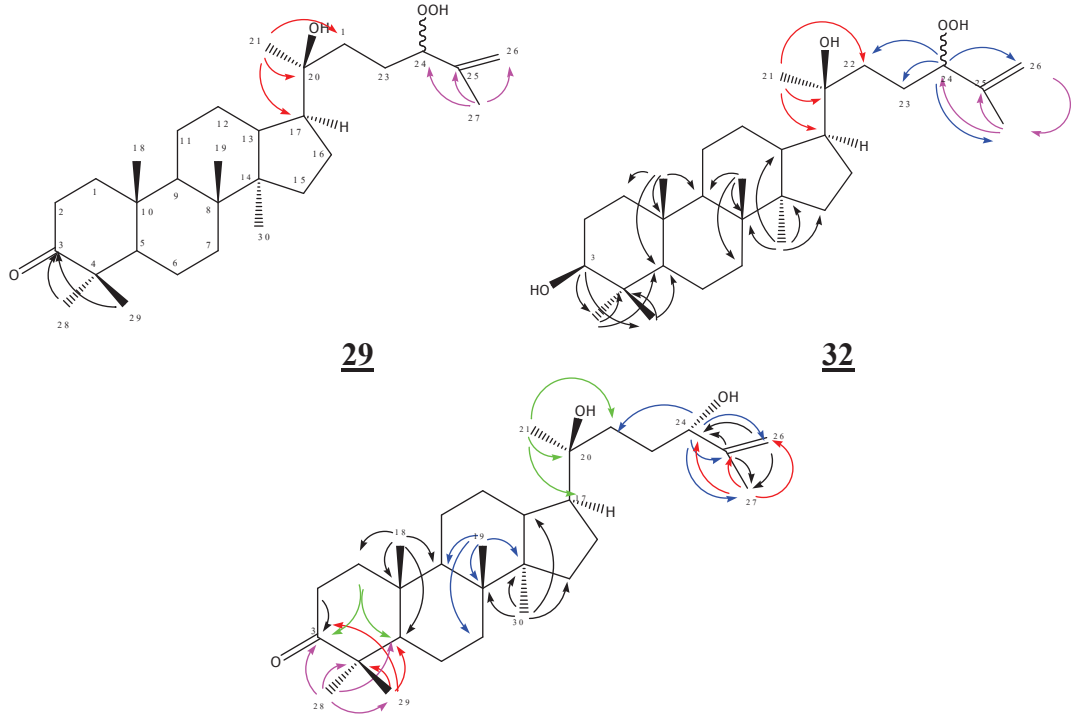

29 **32** **38**

Figure 33. Selected HMBC correlations of compounds **29**, **32** and **38**

The 1D and 2D NMR spectrum of **32** were very close to those of **29** except for the chemical shift around C-3. The ESI-MS revealed a pseudomolecular ion peak at *m/z* 499. $[M+Na]^+$, corresponding to the molecular formula $C_{30}H_{52}O_4$ which was two more hydrogen atoms than **29**. The presence of δ_H 3.22 and δ_C 79.0, as well as the absence of δ_C 218.3 made it more likely to be a hydroxyl rather than a keto group at C-3. It was supported by the chemical shifts of C-2 (δ_C 27.4), C-4 (δ_C 39.0) and C-29 (δ_C 15.4) together with the HMBC correlations of H-28 (δ_H 1.02) and H-29 (δ_H 0.82) to C-3 (δ_C 79.0) (Figure 33). With comparison to the reported data [146, 158], this compound was

determined as (20*S*)-3β,20-dihydroxy-24-perhydroxydammar-25-ene or cereotagaloperoxide that has just been found only from *Ceriops tagal* (Rhizophoraceae) [158].

Table 37. The ^{1}H-NMR (300 MHz) and ^{13}C-NMR (75 MHz) of **29**, **32** and **38** (in $CDCl_3$) ; δ in ppm ; *J* in Hz (fouquierone group – dammarane triterpene)

position	δ_H			δ_C		
	29	**32**	**38**	**29**	**32**	**38**
1	1.46 (m) 1.94 (m)	0.94 (m) 1.71 (m)	1.50 (m) 1.97 (m)	39.9	39.2	39.9
2	2.48 (m)	1.61 (m)	2.50 (m) 2.55 (m)	34.1	27.4	34.1
3		3.22 (dd, *J*=10.9,5.2)		218.3	79.0	218.2
4				47.4	39.0	47.4
5	1.43 (m)	0.75 (d, *J*=10.8)	1.40 (m)	55.3	55.8	55.3
6	1.52 (m) 1.61 (m)	1.47 (m) 1.51 (m)	1.52 (m) 1.60 (m)	19.6	18.3	19.6
7	1.38 (m) 1.63 (m)	1.28 (m) 1.51 (m)	1.38 (m) 1.60 (m)	34.5	35.2	34.5
8				40.3	40.4	40.3
9	1.45 (m)	1.31 (m)	1.48 (m)	50.0	50.6	50.0
10				36.8	37.1	36.8
11	1.34 (m) 1.57 (m)	1.26 (m) 1.50 (m)	1.35 (m) 1.58 (m)	22.0	21.5	22.0
12	1.55 (m) 1.80 (m)	1.49 (m) 1.73 (m)	1.55 (m) 1.80 (m)	24.9	24.8	24.9
13	1.72 (m)	1.63 (m)	1.70 (m)	42.5	42.3	42.5
14				50.3	50.3	50.3
15	1.15 (m) 1.53 (m)	1.06 (m) 1.48 (m)	1.16 (m) 1.53 (m)	31.1	31.2	31.1
16	1.33 (m) 1.90 (m)	1.27 (m) 1.85 (m)	1.33 (m) 1.91 (m)	27.5	27.5	27.5
17	1.80 (m)	1.74 (m)	1.81 (m)	49.9	50.1	50.1
18	0.96 (s)	1.00 (s)	0.96 (s)	16.0	16.2	16.0
19	1.01 (s)	0.89 (s)	1.01 (s)	15.2	15.5	15.2
20				75.1	75.3	75.1
21	1.16 (s)	1.17 (s)	1.17 (s)	25.3	25.2	25.5
22	1.53 (m) 1.63 (m)	1.48 (m) 1.60 (m)	1.55 (m) 1.63 (m)	36.4	36.1	36.6
23	1.76 (m)	1.65 (m)	1.67 (m)	26.9	25.0	29.2
24	4.31 (t, *J*=6.4)	4.33 (t, *J*=6.3)	4.06 (t, *J*=5.8)	89.8	89.8	76.5
25				143.1	143.7	147.6
26	5.05 (br s)	5.04 (br s)	4.86 (s) 4.98 (s)	114.1	114.1	111.0
27	1.80 (s)	1.80 (s)	1.75 (s)	17.6	17.6	17.8
28	1.10 (s)	1.02 (s)	1.10 (s)	26.7	28.0	26.7
29	1.06 (s)	0.82 (s)	1.05 (s)	21.0	15.4	21.0
30	0.90 (s)	0.92 (s)	0.90 (s)	16.3	16.5	16.4

4.4.7 Cabraleone (20*S*,24*S*) (30), ocotillone (20*S*,24*R*) (34), ocotillol II (37) and (20*S*,24*R*)-20,24-epoxy-25-hydroxy-2,3-*seco*-dammarane-2,3-dioic acid (47)***

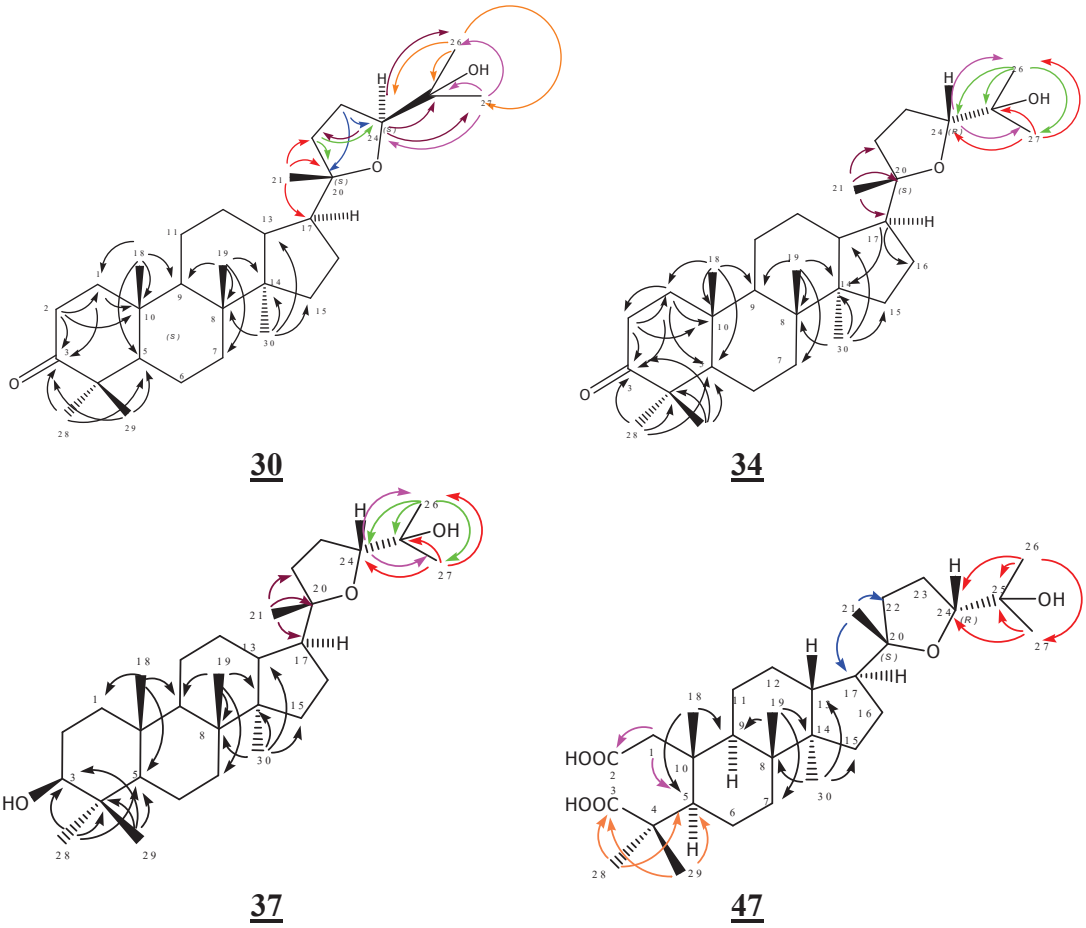

Figure 34 Seleted HMBC correlations of compounds **30**, **34**, **37** and **47**

From the ESI-MS spectra, both compounds **30** and **34** gave pseudo-molecular ions at *m/z* 481 $[M+Na]^+$, representing $C_{30}H_{50}O_3Na$. The IR spectra showed bands at 3473 and 1705 cm^{-1} of hydroxyl and carbonyl groups, respectively. The 1D and 2D NMR spectra revealed the similar structures of both compounds and demonstrated a 3-oxo-dammarane skeleton. The ^1H NMR spectrum showed eight methyl signals while the ^{13}C NMR spectrum showed 30 carbon signals. Two downfield signals of oxygenated carbons at δ_C 86.4 and 83.3 of compound **34**, as well as δ_C 86.5 and 86.4 of compound **30**, suggested the structures of furan ring and were assigned to C-20 and C-24 carbons, respectively, whereas the δ_C 71.5 and 70.2, of **34** and **30** respectively, was assigned to C-25. The 2D NMR spectra of both compounds showed the similar patterns of correlation. The HMBC correlations were found from H-21 to C-17, C-20, and C-22, in addition to the correlations from H-24 to C-26 and C-27 (Figure 34). The NMR data of **30** and **34** were compared to the data from the previous reports [39, 67, 138, 141, 148] and they were identified as cabraleone and ocotillone, respectively. From previous study [141], stereochemistry at C-20 was determined as *S*-configuration. These two compounds were 24-epimers. The signal of 24*S* epimer (**30**) at δ_C 86.4 was more downfield than that of 24*R* epimer (**34**) at δ_C 83.3.

Table 38. The ^{1}H-NMR (300 MHz) of **30**, **34**, **37** and **47** (in $CDCl_3$) ; δ in ppm ; J in Hz (ocotillone group – dammarane triterpene)

position	δ_H			
	30	**34**	**37**	**47**
1	1.46 (m) 1.94 (m)	1.46 (m) 1.94 (m)	0.98 (m) 1.70 (m)	2.51 (d, *J*=19.0) 2.66 (d, *J*=19.0)
2	2.45 (m) 2.53 (m)	2.43 (m) 2.53 (m)	1.63 (m)	
3			3.21 (dd, *J*=10.9,5.2)	
4				
5	1.35 (d, *J*=10.1)	1.35 (d, *J*=9.7)	0.74 (dd, *J*=11.2, 2.0)	2.53 (m)
6	1.49 (m) 1.57 (m)	1.48 (m) 1.57 (m)	1.45 (m) 1.57 (m)	1.60 (m)
7	1.30 (m) 1.58 (m)	1.30 (m) 1.57 (m)	1.29 (m) 1.55 (m)	1.33 (m) 1.67 (m)
8				
9	1.43 (m)	1.46 (m)	1.31 (m)	2.53 (m)
10				
11	1.26 (m) 1.54 (m)	1.28 (m) 1.53 (m)	1.24 (m) 1.56 (m)	1.48 (m)
12	1.32 (m) 1.81 (m)	1.51 (m) 1.81 (m)	1.49 (m) 1.80 (m)	1.50 (m)
13	1.69 (m)	1.64 (m)	1.63 (m)	1.62 (m)
14				
15	1.11 (m) 1.49 (m)	1.09 (m) 1.51 (m)	1.05 (m) 1.52 (m)	1.10 (m) 1.44 (m)
16	1.26 (m) 1.84 (m)	1.28 (m) 1.81 (m)	1.80 (m)	1.33 (m) 1.89 (m)
17	1.91 (m)	1.81 (m)	1.83 (m)	1.83 (m)
18	0.96 (s)	0.94 (s)	0.85 (s)	0.96 (s)
19	1.02 (s)	1.00 (s)	0.97 (s)	0.98 (s)
20				
21	1.16 (s)	1.14 (s)	1.15 (s)	1.14 (s)
22	1.69 (m) 1.91 (m)	1.63 (m) 1.72 (m)	1.63 (m) 1.74 (m)	1.68 (m)
23	1.87 (m)	1.89 (m)	1.91 (m)	1.78 (m)
24	3.65 (dd, *J*=9.7,5.5)	3.74 (t, *J*=7.2)	3.75 (t, *J*=7.2)	3.75 (t, *J*=7.1)
25				
26	1.20 (s)	1.22 (s)	1.23 (s)	1.21 (s)
27	1.12 (s)	1.13 (s)	1.14 (s)	1.13 (s)
28	1.09 (s)	1.09 (s)	0.99 (s)	1.27 (s)
29	1.05 (s)	1.04 (s)	0.79 (s)	1.22 (s)
30	0.90 (s)	0.89 (s)	0.89 (s)	0.90 (s)

Table 39. The ^{13}C-NMR (75 MHz) of **30**, **34**, **37** and **47** (in $CDCl_3$) ; δ in ppm ; J in Hz (ocotillone group – dammarane triterpene)

position	δ_C			
	30	**34**	**37**	**47**
1	39.9	39.9	39.0	41.9
2	34.1	34.1	27.5	177.9
3	218.3	218.2	79.0	186.7
4	47.4	47.4	39.0	46.0
5	55.3	55.3	55.8	48.8
6	19.7	19.6	18.3	19.8
7	34.6	34.6	35.3	34.6
8	40.3	40.2	40.4	40.2
9	50.2	50.1	50.8	42.3
10	36.8	36.8	37.1	40.2
11	22.3	22.6	21.6	22.2
12	25.8	25.7	25.7	25.8
13	43.0	43.1	43.0	43.0
14	50.0	50.0	50.1	50.5
15	31.4	31.4	31.5	31.4
16	27.0	27.4	27.5	26.4
17	49.8	49.4	49.5	49.4
18	16.1	16.1	16.2	20.7
19	15.2	15.1	15.4	15.3
20	86.5	86.4	86.5	86.5
21	27.3	23.6	23.6	23.5
22	34.7	35.6	35.7	35.8
23	26.4	26.1	26.1	26.2
24	86.4	83.3	83.3	83.3
25	70.2	71.5	71.5	71.7
26	27.8	27.5	27.4	27.8
27	24.1	24.3	24.3	24.2
28	26.7	26.7	28.0	28.7
29	21.0	21.0	15.4	22.5
30	16.3	16.4	16.5	16.5

Comparison to the data of **34**, instead of C-3 keto, NMR spectra of compound **37** exhibited an oxymethine (δ_H 3.21, δ_C 79.0) of which C-3 gave the HMBC correlations to H-28 (δ_H 0.99), and H-29 (δ_H 0.79). As described in the identification of **11** and **13**, the 3β-OH configuration was assigned by upfield shift of $\delta_{H\text{-}3}$ at 3.21 and $\delta_{C\text{-}29}$ at 15.4. Splitting pattern of H-3 as doublet of doublet (J=10.9, 5.2 Hz) also confirmed the stereochemistry of 3β-OH. Remaining NMR data was close to that of ocotillone (**34**). From these spectroscopic evidences and comparison to the previous literatures [67, 135, 147, 153, 154] **37** was identified as ocotillol II.

The molecular formula of **47** was deduced to be $C_{30}H_{50}O_6$ on the basis of HRESI-MS (*m/z* 505.3533 $[M\text{-}H]^-$, calcd $C_{30}H_{49}O_6$ 505.3529). The six degrees of unsaturation were implied by the molecular formula. The presence of two carbonyl signals (δ_C 177.9 and 186.7) without any olefin, suggested 4 cyclic rings. The ^{13}C-NMR and HMBC spectra indicated the same side chain structure as ocotillone (**34**). Prominent differences in the ^{1}H and ^{13}C NMR data between **47** and **34** were observed only in those spectroscopic data pertaining to ring A. In the HMBC spectrum of **47**, the correlations were observed from

H-1 at δ_H 2.51 and 2.66 to the carbon signals at δ_C 177.9 (C-2) and 48.8 (C-5) together with the correlations of the proton signals at δ_H 1.27 (H-28) and 1.22 (H-29) to the carbon signals at δ_C 186.7 (C-3) and 48.8 (C-5) (Figure 34). These indicated that the carboxylic groups were at C-2 and C-3. Two carboxyl groups and a germinal dimethyl group at C-4 suggested a 2,3-*seco*-dammarane structure. The structure of **47** was thus concluded to be a new 2,3-*seco*-dammarane derivative with the same side chain as ocotillone (**34**) and was named as (20*S*,24*R*)-20,24-epoxy-25-hydroxy-2,3-*seco*-dammarane-2,3-dioic acid.

4.4.8 Isocabralealactone (20*R*) (27)**, cabralealactone (20*S*) (28) and 3-*epi*cabraleahydroxylactone (35)

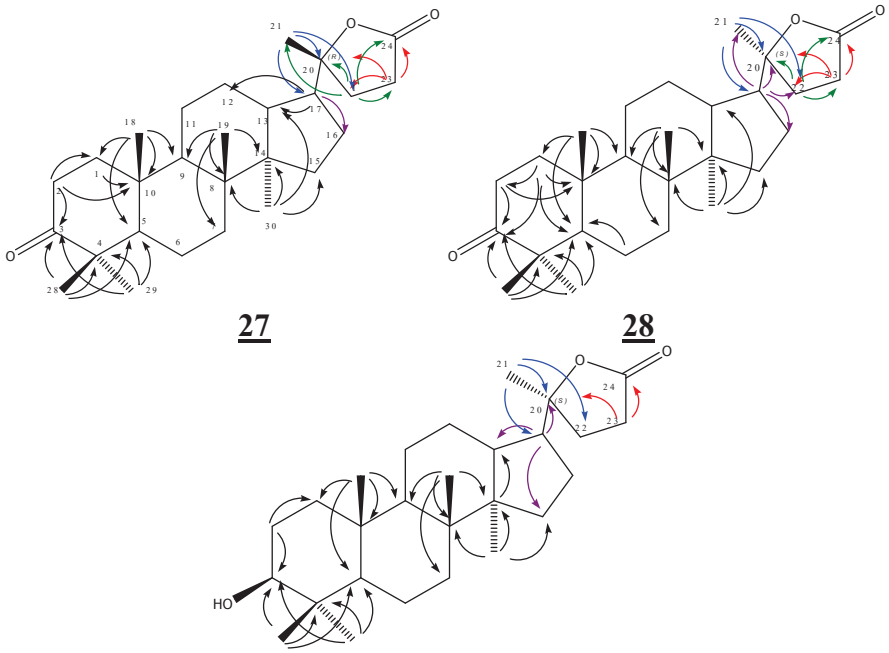

27 **28**

35

Figure 35. Seleted HMBC correlations of compounds **27**, **28** and **35**

The molecular formula of compounds **27** and **28** was assigned as $C_{27}H_{42}O_3$ based on the $[M+Na]^+$ ions at *m/z* 437 from ESI-MS and 437.3023 from HRESI-MS, respectively. Their ^{13}C NMR spectra showed the characteristic of 3-keto tetracyclic dammarane skeleton and were in good agreement with that of ocotillone (**34**) and cabraleone (**30**) except for the downfield signals of the side chain at δ_C 176.8-177.0 (C-24) and disappearance of C-25 to C-27. A lactone ring was indicated based on their strong IR absorption band at 1770 cm^{-1}. The assignment of carbons on the lactone ring was proved through the HMBC correlations (Figure 35). The correlations of H-22 and H-23 to oxygenated C-20 and carbonyl C-24, together with the usual correlations of H-21 to C-17, C-20 and C-22, demonstrated the γ-lactone moiety attached to C-17. Difference between compounds **27** and **28** was only the stereochemistry at C-20. The data from other 20-epimers of this study and the literatures [60, 67, 133, 161, 229, 231] indicated that the chemical shifts of proton and carbon at position 21 of 20*S* epimer were more downfield than those of 20*R* epimer (δ_H 1.34, δ_C 22.08). Chemical shifts of **27** were at δ_H 1.34, δ_C 22.1 whereas those of **28** were at δ_H

1.39, δ_C 25.4. Therefore, the structures of **27** and **28** were assumed to be isocabralealactone and cabralealactone, respectively.

Table 40. The ^{1}H-NMR (300 MHz) and ^{13}C-NMR (75 MHz) of **27**, **28** and **35** (in $CDCl_3$) ; δ in ppm ; J in Hz (lactone group – dammarane triterpene)

position	δ_H			δ_H		
	27	**28**	**35**	**27**	**28**	**35**
1	1.48 (m) 1.96 (m)	1.47 (m) 1.95 (m)	1.00 (m) 1.74 (m)	39.8	39.8	39.0
2	2.50 (m)	2.49 (m)	1.60 (m) 1.67 (m)	34.1	34.1	27.4
3			3.22 (dd, *J*=10.8, 5.3)	218.1	218.0	79.0
4				47.4	47.4	39.0
5	1.42 (m)	1.40 (m)	0.73 (d, *J*=2.1)	55.3	55.2	55.8
6	1.52 (m) 1.60 (m)	1.46 (m) 1.53 (m)	1.55 (m)	19.6	19.6	18.2
7	1.36 (m) 1.62 (m)	1.33 (m) 1.60 (m)	1.29 (m) 1.57 (m)	34.5	34.5	35.2
8				40.3	40.2	40.3
9	1.46 (m)	1.44 (m)	1.31 (m)	50.0	49.8	50.5
10				36.8	36.7	37.1
11	1.31 (m) 1.56 (m)	1.31 (m) 1.54 (m)	1.26 (m) 1.54 (m)	21.8	21.9	21.4
12	1.87 (m)	1.86 (m)	1.87 (m)	25.0	25.0	25.0
13	1.74 (m)	1.64 (m)	1.60 (m)	42.7	43.2	43.2
14				50.1	50.1	50.2
15	1.18 (m) 1.55 (m)	1.15 (m) 1.54 (m)	1.15 (m) 1.53 (m)	31.0	31.0	31.2
16	1.30 (m) 1.97 (m)	1.29 (m) 1.75 (m)	1.25 (m) 1.76 (m)	26.4	26.8	26.8
17	2.00 (m)	2.03 (m)	2.00 (m)	49.4	49.2	49.3
18	0.95 (s)	0.91 (s)	0.96 (m)	16.0	16.0	16.2
19	1.01 (s)	0.97 (s)	0.97 (m)	15.2	15.2	15.5
20				89.9	90.1	90.2
21	1.34 (s)	1.39 (s)	1.38 (m)	22.1	25.4	25.4
22	1.99 (m) 2.09 (m)	1.96 (m) 2.10 (dd, *J*=22.5, 9.7)	1.97 (m) 2.13 (m)	33.2	31.1	31.1
23	2.61 (m)	2.55 (m) 2.66 (dd, *J*=18.1, 9.8)	2.58 (m) 2.66 (dd, *J*=18.7, 8.9)	28.6	29.2	29.2
24				177.0	176.8	176.8
25						
26						
27						
28	1.08 (s)	1.05 (s)	0.99 (s, 3H)	26.7	26.7	28.0
29	1.04 (s)	1.01 (s)	0.79 (s, 3H)	21.0	21.0	15.4
30	0.89 (s)	0.87 (s)	0.90 (s, 3H)	16.1	16.1	16.2

The molecular formula $C_{27}H_{42}O_3$ of compound **35** was deduced from ESI-MS at *m/z* 439 of the $[M+Na]^+$ ion. The appearance of δ_H 3.22 (dd, *J*=10.8, 5.3 Hz) and δ_C 79.0, as well as the HMBC correlations of H-1 (δ_H 1.00, 1.74), H-2 (δ_H 1.60, 1.67), H-28 (δ_H 0.99) and H-29 (δ_H 0.79) with δ_C 79.0 (Figure 35) indicated the 3β-hydroxy structure. The

remaining signals and the HMBC correlation were similar to **28**. With the comparison to the previous publication [160], compound **35** was then determined as 3-*epi*cabraleahydroxylactone.

4.4.9 Octanordammarane-3,17-dione (26)*, (20*S*,23*E*)-20-hydroxy-27-nordammar-23-ene-3,25-dione (39)*** and (20*S*)-20-hydroxy-3-oxo-24,25,26,27-tetranordammar-23-oic acid (49)***

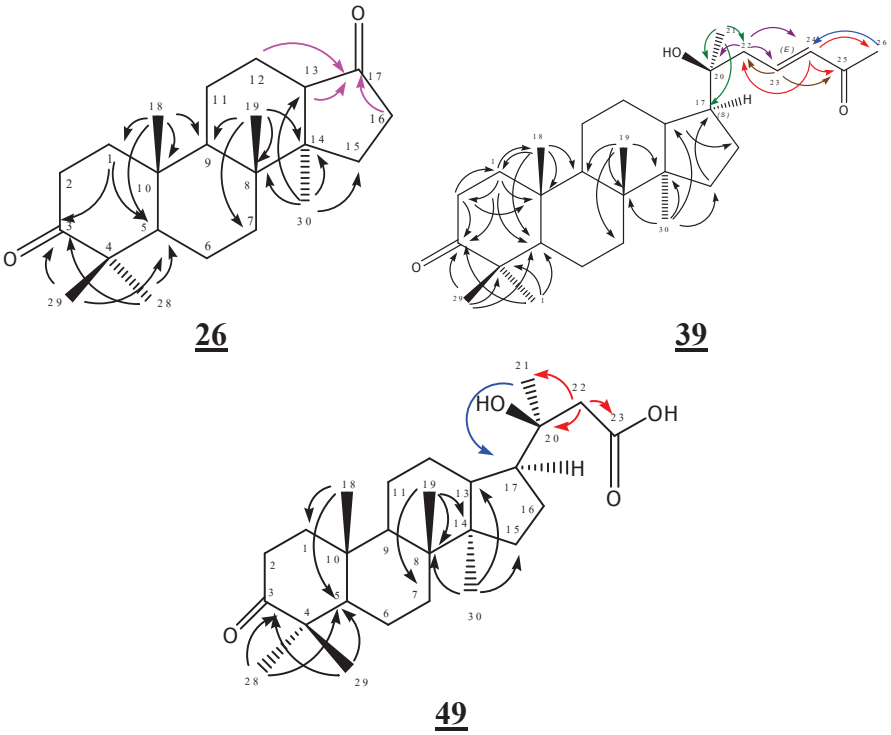

26 **39**

49

Figure 36. Seleted HMBC correlations of compounds **26**, **39** and **49**

The HRESI-MS of compound **26** represented the molecular formula of $C_{22}H_{34}O_2$. The ^{1}H NMR spectrum, showing 5 methyl groups at δ_H 0.92 (CH_3-30), 0.98 (CH_3-18), 1.07 (CH_3-29) and 1.11 (CH_3-19 and CH_3-28), closely resembled to those reported in the literature for octanordammarane-3,17-dione [230]. Its NMR data indicated that the acyclic side chain (C-20 to C-27) at C-17 was disappeared and it was replaced with a keto group. The IR spectrum showed C=O stretching of 2 carbonyl groups at 1738 and 1705 cm^{-1}, which were assigned for C-17 and C-3, respectively. The structure of carbonyl group at C-17 was confirmed by the HMBC correlations of H-12 (δ_H 1.64, 1.94), H-13 (δ_H 2.22) and H-16 (δ_H 2.23) with C-17 (δ_C 218.1) (Figure 36). This carbonyl functional group strongly influenced on the chemical shifts of the surrounding atoms. Compared to dipterocarpol (**22**) and ocotillone (**34**), the ^{13}C resonance of the C-13 showed obviously down field shift (about 8 ppm), as well as that of C-16 with lesser degree, whereas those of C-11, C-12, C-14 and C-15 comparably shifted upfield. The proton signals of H-13 (δ_H 2.22) and H-16 (δ_H 2.23) also downfielded shifted owing to the deshielding effect of the carbonyl group. The specific rotation value was consistent with 17-oxo-3β-acetoxy-octanor-dammarane [235]. Thus, the structure of **26** was identified as octanordammarane-3,17-dione.

Table 41. The ^{1}H-NMR (300 MHz) and ^{13}C-NMR (75 MHz) of **26**, **39** and **49** (in $CDCl_3$) ; δ in ppm ; J in Hz (nordammarane triterpene)

position	δ_H			δ_C		
	26	**39**	**49**	**26**	**39**	**49**
1	1.48 (m) 1.96 (m)	1.50 (m) 1.97 (m)	1.50 (m) 1.95 (m)	40.0	39.9	39.9
2	2.50 (m)	2.54 (m)	2.50 (m)	34.0	34.1	34.1
3				217.8	218.2	218.0
4				47.4	47.4	47.4
5	1.45 (m)	1.42 (m)	1.41 (m)	55.2	55.3	55.3
6	1.48 (m) 1.56 (m)	1.52 (m) 1.60 (m)	1.50 (m) 1.60 (m)	19.6	19.6	19.6
7	1.56 (m)	1.35 (m) 1.60 (m)	1.35 (m) 1.63 (m)	33.7	34.5	34.5
8				40.1	40.3	40.3
9	1.45 (m)	1.47 (m)	1.46 (m)	50.5	49.9	49.9
10				37.0	36.8	36.8
11	1.23 (m)	1.33 (m) 1.57 (m)	1.34 (m) 1.58 (m)	20.6	21.9	21.9
12	1.64 (m) 1.94 (m)	1.53 (m) 1.81 (m)	1.55 (m) 1.78 (m)	20.9	24.9	24.9
13	2.22 (m)	1.74 (d, *J*=11.9)	1.66 (m)	53.9	42.6	42.8
14				46.5	50.3	50.3
15	1.52 (m) 1.97 (m)	1.17 (d, *J*=8.0) 1.53 (m)	1.15 (m) 1.54 (m)	27.8	31.1	31.0
16	2.23 (m)	1.32 (m) 1.90(d, *J*= 6.6)	1.93 (m)	34.9	27.5	27.2
17		1.80 (m)	1.86 (m)	218.1	50.5	50.4
18	0.98 (s)	0.98 (s)	0.96 (s)	16.3	16.0	16.0
19	1.11 (s)	1.04 (s)	1.02 (s)	15.5	15.2	15.2
20					75.3	74.4
21		1.22 (s)	1.30 (s)		26.3	25.7
22		2.41 (d, *J*=8.1) 2.48 (d, *J*=8.1)	2.50 (d, *J*=15.9) 2.65 (d, *J*=15.9)		43.6	43.1
23		6.96 (dt, *J*=15.9, 8.1)			144.6	174.6
24		6.16 (d, *J*=15.9)			133.9	
25					198.5	
26		2.31 (s)			27.0	
27						
28	1.11 (s)	1.12 (s)	1.10 (s)	26.8	26.7	26.7
29	1.07 (s)	1.08 (s)	1.06 (s)	21.0	21.0	21.0
30	0.92 (s)	0.92 (s)	0.91 (s)	16.7	16.3	16.3

The molecular formula of compound **39** was suggested as $C_{29}H_{46}O_3$ with the aid of the HRESI-MS of the $[M+Na]^+$ ion at *m/z* 465.3359. Its ^{13}C-NMR spectrum showed 29 carbon signals with the characteristic of 3-oxodammarane skeleton. Compared to isofouquierone (**40**), the signal of a methyl group at position 27 was missing and an additional carbonyl carbon ($\delta_{C\text{-}25}$ 198.5) on the side chain was observed. This carbonyl group was assigned to be at position 25 with conjugated to double bond at position 23 and 24. UV absorption ability at 254 nm on TLC and IR absorption band at 1663 cm^{-1} confirmed the presence of this α,β unsaturated carbonyl moiety. The HMBC correlations of H-22 (δ_H 2.41 and 2.48) to C-23 (δ_C 144.6), C-24 (δ_C 133.9) and C-20 (δ_C 75.34), of H-23 (δ_H 6.96) and H-24 (δ_H 6.16) to C-25 (δ_C 198.5) and of H-24 (δ_H 6.16) to C-26 (δ_C

27.0) or vice versa concluded the structure of the side chain of compound **39** as shown in Figure 36. Detailed comparison of the ^{13}C-NMR data of **39** showed that the chemical shifts of C-20 to C-26 were very similar to those of rhombenone [245]. The stereochemistry of the double bond was determined as *E*-form based on large coupling constant (J=15.9 Hz) of the olefinic protons. All of these spectroscopic data characterized compound **39** as (20*S*,23*E*)-20-hydroxy-27-nordammar-23-ene-3,25-dione, which was a new nordammarane.

The ESI-MS of compound **49** corresponded to the molecular formula of $C_{26}H_{42}O_4$. Its NMR data were very close to compound **39** with 3 less carbons. Two olefinic carbons and a methyl carbon on the side chain were disappeared. The HMBC spectrum showed correlations of H-21 (δ_H 1.30) with C-17 (δ_C 50.38), C-20 (δ_C 74.39) and C-22 (δ_C 43.06) as same as other dammaranes with 20*S* configuration. Examination of molecular formula and the value of $\delta_{C\text{-}23}$, carbonyl carbon on C-23 should be carboxylic carbon. The HMBC correlations between this carbon and H-22 (δ_H 2.50 and 2.65) confirmed its position at C-23. Identification of the side chain of **49** was supported by the comparision of δ_C to those of the side chain of 3β,20*S*-dihydroxy-23-norchol-5-enoic acid [246] 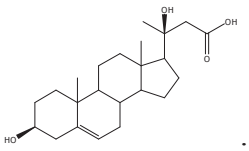 . Therefore, compound **49** was defined as (20*S*)-20-hydroxy-3-oxo-24,25,26,27-tetranordammar-23-oic acid, a new nordammarane.

4.4.10 (20*R*)-17α,29-Epoxy-28-norlupan-3-one (24) ***, 17α-hydroxy-28-norlupan-20(29)-en-3-one (25) ***, (20*S*)-29-Hydroxy-17α,20-peroxy-28-norlupan-3-one (36) ***, 17α-Hydroxy-28,29-dinorlupan-3,20-dione (41) *** and (20*R*)-20-Hydroxy-17α,29-epoxy-28-norlupan-3-one (42) ***

The HRESI-MS at *m/z* 449.3400 of **25** was consistent with a molecular formula of $C_{29}H_{46}O_2$ with seven degree of unsaturation. IR absorptions at 3441 and 1704 cm^{-1} were attributable to a hydroxyl and a carbonyl group, respectively. The ^{13}C and HSQCedited data showed 6 methyl, 10 methylene, 5 methine groups and 8 quaternary carbons. The ^{1}H NMR spectrum showed the 5 methyl groups, appearing as singlets, bonded to quaternary carbons of pentacyclic ring. In addition, an isopropenyl group was evident from a downfield methyl signal (H-30) at δ_H 1.79 and two terminal methylene protons (H-29) at δ_H 4.71 and 4.86. The HMBC data showed the correlations between C-3 (δ_C 218.3) and H-1 (δ_H 1.47, 1.92), H-2 (δ_H 2.47), H-23 (δ_H 1.08) and H-24 (δ_H 1.03) (Figure 37). These data suggested the structure of 3-oxolupane triterpene. An oxygenated quaternary carbon signal at δ_C 81.1 was assigned to C-17 based on the HMBC correlations between this carbon and H-15 (δ_H 1.30), H-16 (δ_H 1.83, 1.90), H-21 (δ_H 1.73, 1.79) and H-22 (δ_H 1.49, 1.89). This information indicated that the structure of this compound was 28-norlupane with 17-OH substitution. The α-orientation of the hydroxyl group was supported by the chemical shift of C-13 (δ_C 44.1) and C-19 (δ_C 52.7). These signals were around 38 and 48 ppm, respectively, for β-configuration [107, 108]. Thus, the structure of **25** was determined as 17α-hydroxy-28-norlupan-20(29)-en-3-one, a new norlupane.

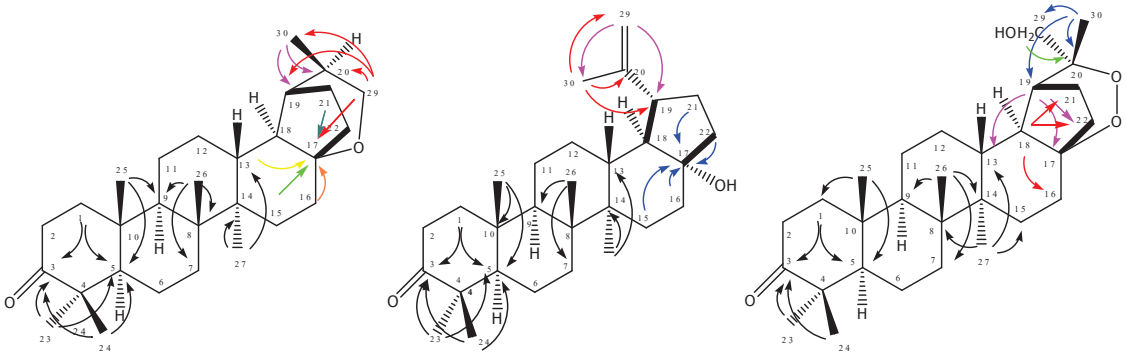

24 **25** **36**

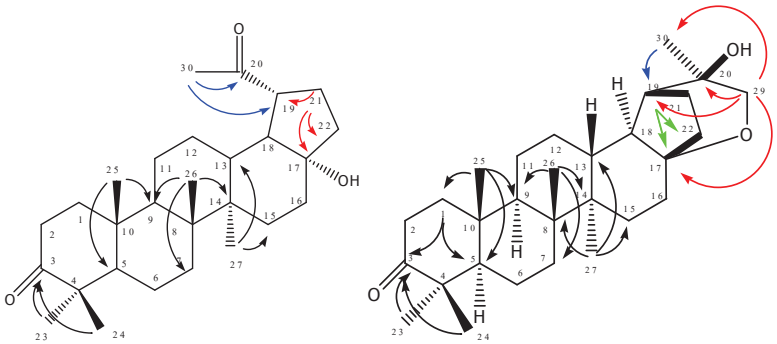

41 **42**

Figure 37. Seleted HMBC correlations of compounds **24**, **25**, **36**, **41** and **42**

The ^{13}C-NMR and 2D NMR data of **41** indicated that this compound was dinorlupane with 28 carbon signals; 6 methyl, 10 methylene, 5 methine and 7 quaternary carbons. The HRESI-MS at *m/z* 521.3486 $[M-H]^-$ of **41** suggested the molecular formula $C_{28}H_{44}O_3$. IR spectrum at 1704 cm^{-1} indicated the presence of carbonyl group. Its NMR data were close to compound **25** except that one carbonyl carbon (δ_C 214.5), instead of an olefinic group, on the side chain was observed. The HMBC correlation of the terminal methyl proton H-30 (δ_H 2.25) to this carbonyl carbon and the methine carbon C-19 (δ_C 55.8) supported a keto group at C-20. The 17α configuration of the hydroxyl group was suggested by the comparison of the chemical shifts of C-13 (δ_C 41.9) and C-19 (δ_C 55.8) to those previously reported [107, 108] ($\delta_{C\text{-}13}$ 38 ppm and $\delta_{C\text{-}19}$ 48 ppm, respectively, in β-configuration). The stereochemistry at C-19 was assigned by the NOESY spectrum that showed the correlations of H-19 with H-12a and H-21a. The structure of compound **41** was then proposed to be 17α-hydroxy-28,29-dinorlupan-3,20-dione.

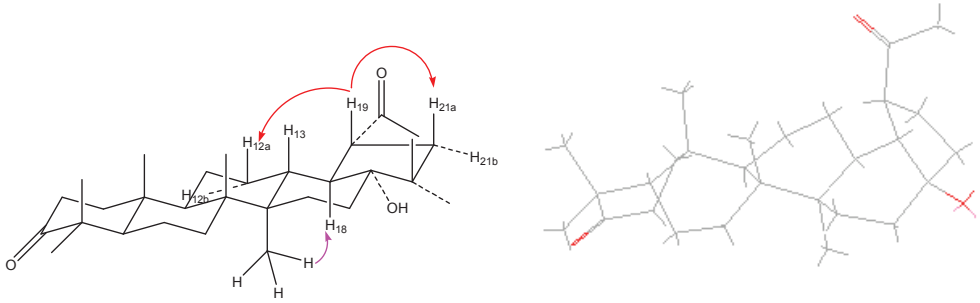

Figure 38. Selected NOE and stereoscopic view of compound **41**.

Table 42. The ^{1}H-NMR (300 MHz) of **24**, **25**, **36**, **41** and **42** (in $CDCl_3$) ; δ in ppm ; J in Hz (norlupane triterpenes)

position	δ_H				
	24	**25**	**36**	**41**	**42**
1	1.46 (m) 1.94 (m)	1.47 (m) 1.92 (m)	1.45 (m) 1.94 (m)	1.47 (m) 1.94 (m)	1.44 (m) 1.93 (m)
2	2.47 (m)	2.47 (m)	2.47 (m)	2.47 (m)	2.46 (m)
3					
4					
5	1.37 (m)	1.40 (m)	1.38 (m)	1.38 (m)	1.36 (m)
6	1.47 (m)	1.49 (m)	1.48 (m)	1.49 (m)	1.48 (m)
7	1.46 (m)	1.44 (m) 1.49 (m)	1.47 (m)	1.41 (m) 1.48 (m)	1.47 (m)
8					
9	1.44 (m)	1.47 (m)	1.42 (d, *J*=2.5)	1.48 (m)	1.43 (m)
10					
11	1.29 (m) 1.52 (m)	1.28 (m) 1.54 (m)	1.29 (m) 1.53 (m)	1.30 (m) 1.56 (m)	1.29 (m) 1.52 (m)
12	1.64 (m) 0.96 (m)	1.71 (m)	1.56 (m) 0.97 (m)	1.64 (m) 1.04 (m)	1.60 (m) 0.94 (m)
13	1.22 (m)	1.17 (m)	1.26 (m)	1.14 (m)	1.23 (m)
14					
15	1.27 (m) 1.51 (m)	1.30 (m)	1.35 (m) 1.59 (m)	1.29 (m) 1.46 (m)	1.30 (m) 1.52 (m)
16	1.63 (m)	1.83 (m) 1.90 (m)	1.56 (m)	1.72-1.84 (m)	1.66 (m)
17					
18	1.39 (d, *J*=11.7)	1.58 (d, *J*=2.4)	1.91 (d, *J*=5.4)	1.71 (m)	1.57 (d, *J*=11.0)
19	2.03 (m)	2.40 (m)	2.02 (m)	2.92 (m)	2.00 (m)
20	1.83 (m)				
21	1.58 (m)	1.73 (m) 1.79 (m)	1.74 (m) 1.99 (m)	1.98 (m)	1.65 (m) 1.91 (m)
22	1.48 (m) 1.91 (m)	1.49 (m) 1.89 (m)	1.94 (m)	1.56 (m) 1.97 (m)	1.55 (m) 1.91 (m)
23	1.09 (s)	1.08 (s)	1.09 (s)	1.09 (s)	1.09 (s)
24	1.03 (s)	1.03 (s)	1.04 (s)	1.04 (s)	1.03 (s)
25	0.94 (s)	0.94 (s)	0.94 (s)	0.94 (s)	0.94 (s)
26	0.99 (s)	0.98 (s)	1.00 (s)	0.98 (s)	0.99 (s)
27	0.99 (s)	0.98 (s)	0.99 (s)	0.97 (s)	0.98 (s)
28					
29	3.25 (t, *J*=11.4,) 3.66 (dd, *J*=11.5, 5.6)	4.70 (s) 4.85 (s)	3.54 (d, *J*=11.4) 4.18 (d, *J*=11.4)		3.42 (d, *J*=11.4) 3.49 (d, *J*=11.4)
30	0.75 (d, *J*=6.7)	1.80 (s)	1.16 (s)	2.23 (s)	1.38 (s)

Table 43. The ^{13}C-NMR (75 MHz) of **24**, **25**, **36**, **41** and **42** (in $CDCl_3$) ; δ in ppm ; J in Hz (norlupane triterpenes)

position	δ_C				
	24	**25**	**36**	**41**	**42**
1	39.8	39.8	39.8	39.8	39.7
2	34.1	34.0	34.0	34.0	34.0
3	218.3	218.3	218.1	218.1	218.2
4	47.3	47.2	47.3	47.3	47.3
5	54.8	54.8	54.8	54.8	54.8
6	19.6	19.6	19.6	19.6	19.6
7	33.2	33.1	33.1	33.1	33.2
8	40.5	40.4	40.6	40.4	40.5
9	50.1	50.5	49.9	50.4	50.0
10	36.9	36.9	36.9	36.9	36.9
11	21.7	21.9	21.4	21.8	21.5
12	25.6	26.8	24.9	27.1	25.2
13	35.9	44.1	35.5	41.9	35.7
14	40.6	40.8	40.6	41.2	40.6
15	28.1	28.3	27.9	28.1	28.0
16	28.4	28.2	24.3	30.5	27.9
17	82.7	81.1	90.2	80.7	83.2
18	54.2	52.2	45.3	52.2	49.2
19	42.5	52.6	42.1	55.8	49.2
20	36.6	150.9	85.3	214.5	70.8
21	21.2	32.2	29.5	25.4	22.2
22	30.0	37.6	23.3	36.8	28.7
23	26.8	26.9	26.8	26.9	26.8
24	21.0	20.9	21.0	20.9	21.0
25	16.3	16.4	16.3	16.4	16.3
26	15.5	15.3	15.5	15.3	15.5
27	13.6	14.5	13.4	14.1	13.5
28					
29	66.9	108.5	64.6		70.4
30	15.2	21.7	20.8	29.7	26.5

The HRESI-MS at *m/z* 449.3399 $[M+Na]^+$ of **24** suggested the molecular formula of $C_{29}H_{46}O_2$. The ^{1}H and ^{13}C NMR data of **24** were consistent with a 3-oxonorlupane skeleton. The chemical shifts of ^{13}C NMR data were close to those of the known

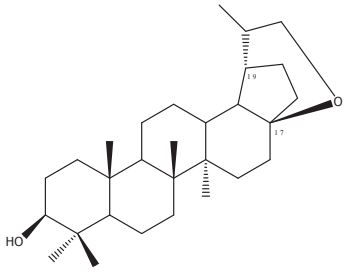

compound, (20*S*)-17β,29-epoxy-28-norlupan-3β-ol [107] except the values of δ_C on rings A and B, especially at C-2, the carbonyl C-3 and C-24. The carbonyl carbon C-3 (δ_C 218.3) was assigned on the basis of its HMBC correlations with the methyl protons (H-23 and H-24) and the methylene protons (H-1 and H-2) (Figure 37). The structure of the isopropyl side chain at C-19 was elucidated based on COSY spectrum which showed the sequential vicinal couplings of H_3-30, H-20 and H_2-29. The HMBC spectrum showed the correlations of the methylene H-29 (δ_H 3.25, 3.66) to the quaternary oxygenated C-17 (δ_C 82.71). This suggested a cyclic structure through an ether

bridge between C-29 and C-17 of the 28-norlupane nucleus. A review of Connelly and Hill [116] noted that it is impossible to have the stereochemistry of the cyclic side chain as the proposed structure of 20*S*-17β,29-epoxy-28-norlupan-3-ol from the work of Abdel-Bar et al [107]. 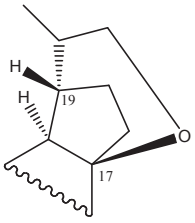

The stereochemistry at C-17 should be in the opposite way, in other words, the bonds between C-19 and C-20, together with C-17 and O, should be in the same plane. That made it conform to the configuration at C-17 and C-19 of compound **25**. The 19α-orientation of isopropyl group was fixed by lupane skeleton and was supported based on the splitting pattern of $\delta_{H\text{-}18}$ (d, *J*=11.7 Hz). From this configuration, the 90^o of the dihedral angle between H-19 and H-18 was possible and it caused H-18 to couple with only H-13. If the 19β-orientation was occurred, this angle would be around 30^o and resulted in doublet of doublet signal of H-18 (Figure 39). The bonds between C-19 and C-20, together with C-17 and oxygen atom, might be in the same plane, therefore, oxygenated substitution at C-17 was also designed as α-orientation. The stereochemistry at C-20 was determined through splitting patterns of H-29. Beside the germinal coupling (*J*=11.4 Hz) between each proton of H-29 the $\delta_{H\text{-}29}$ at 3.25 ppm possessed another axial-axial coupling (*J*=11.4 Hz) with H-20, whereas the other $\delta_{H\text{-}29}$ at 3.66 ppm displayed equatorial-axial coupling (*J*=5.6 Hz) with H-20 (Figure 39). If the structure was 20*S* configuration, the splitting patterns of both protons at position 29 would be changed to doublet of doublet. Thus, the structure of **24** was determined to be (20*R*)-17α,29-epoxy-28-norlupan-3-one.

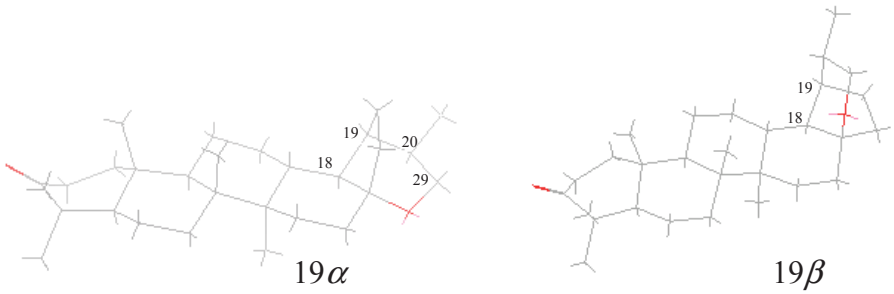

19α 19β

Figure 39. Comparison of 3D model of 19α- and 19β-orientation of compound **24** (by program Chem3D ultra 9.0)

Compound **36** was inferred to have the molecular formula $C_{29}H_{46}O_4$ by the HRESI-MS at *m/z* 481.3294 $[M+Na]^+$. Its ^{13}C-NMR and DEPT data, clearly showed 29 carbon signals; 6 methyl, 11 methylene, 5 methine and 7 quaternary carbons. The ^{13}C NMR data were close to those of **24**, especially, carbon signals of ring A-C. As general 3-oxolupane, there were correlations between C-3 (δ_C 218.1) and H-1(δ_H 1.45, 1.94), H-2 (δ_H 2.47), H-23 (δ_H 1.09) and H-24 (δ_H 1.04). Two oxygenated quaternary carbons and one oxygenated methylene carbon were observed at δ_C 90.2 (C-17), 85.3 (C-20) and 64.6 (C-29) ppm, respectively.

The resonance at unusual low field of both oxygenated quaternary carbons and HMBC correlation suggested the structure of an endoperoxide ring. The assignment of the oxygenated quaternary carbon (δ_C 85.3) at position 20 and an oxygenated methylene carbon (δ_C 64.6) at position 29 were based on the correlations of these carbons to H-30 (δ_H 1.17) and the correlation between H-21(δ_H 1.99) and C-20 (δ_C 85.3) (Figure 37). The position of the other oxy-quaternary carbon at δ_C 90.2 (C-17) was indicated by the correlations with H-19 (δ_H 2.02). As the result, the quaternary carbon should be the head of endoperoxide. The 17α- and 19α-configuration of the substitution on ring E were designed by using the same reason as compound **24**. The 20*S*-configuration was suggested based on downfield shift of $\delta_{H\text{-}18}$ (δ_H 1.91) (compared to those of compound **24** and **42**), resulted from the inductive effect of the oxygen on C-29. Hence, the structure of **36** was then determined as (20*S*)-29-hydroxy-17α,20-peroxy-28-norlupan-3-one.

The HRESI-MS data of **42** at *m/z* 443.3533 $[M+H]^+$ suggested the molecular formula of $C_{29}H_{46}O_2$ with seven degrees of unsaturation. The ^1H and ^{13}C NMR data were consistent with compound **24** and **36** for the linkage between C-17 and C-19. The HSQCedited data showed 6 methyl, 11 methylene, 6 methine and 6 qurternary carbons. The HMBC correlations of H-30 (δ_H 1.42) to C-20 (δ_C 70.8), C-19 (δ_C 49.2) and C-29 (δ_C 70.4) indicated the attachment of an isopropyl group at C-19. Furthermore, the HMBC correlations between H-29 (δ_H 3.49) and the quaternary oxygenated C-17 (δ_C 83.2) indicated a linkage through an ether bridge between C-29 and C-17 of the 28-norlupan nucleus. The α-orientations of both substitutions at C-17 and C-19 were designed by the same reason as compounds **24** and **36**. From NOESY experiment, NOEs of H-30 to H-19 and H-18 indicated the α-configuration of CH_3-30. The structure of **42** was then described as 20-hydroxy-17α,29-epoxy-28-norlupan-3-one.

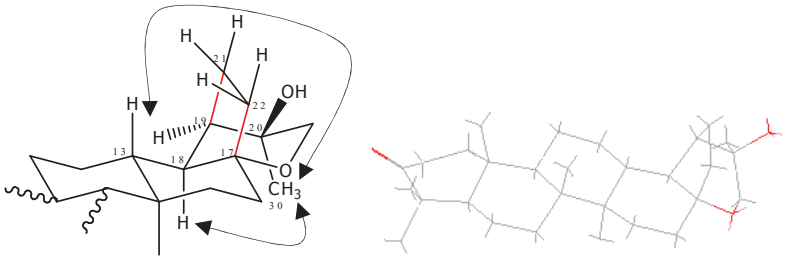

Figure 40 Selected NOE and stereoscopic view of compound **42**

Compound **24**, **25**, **36**, **41** and **42** were classified to 28-norlupane triterpenes. All of them were found herein for the first time.

4.5 CYTOTOXIC EVALUATION OF SOME ISOLATED TRITERPENES

The cytotoxic activities of the isolated compounds were evaluated against a variety of human cancer cell lines, namely, PC3, MDA-MB-231, HT-29 and HCT 116. The results were shown in Table 43. Among these compounds, 17α-hydroxy-28,29-dinorlupan-3,20-dione (**25**) exhibited more than 50% cell proliferation inhibition against HCT 116 at the concentratin of 8.67 μM (3.7 μg/mL). Although antitumor promoter activity of dammarenediol II (**31**) and cytotoxicity against P-388 leukemia cells of ocotillone (**34**) and cabralealactone (**28**) had been reported [73, 160, 161], in this study, they seemed to possess only weak cytotoxicity at the concentration of 10 μM owing that different cell lines were tested.

4.6 *IN VITRO* ANTIPLASMODIAL ACTIVITY OF ISOLATED TERPENOIDS

The antiplasmodial activity of the triterpenes was tested *in vitro* against *Plasmodium falciparum* FcB1 strain, as well as, toxicity against the cell line L-6 of rat (rat skeletal muscle cell line) was evaluated. The growth inhibition of each compound against *P. falciparum* was summarized in Table 29. Antiplasmodial activity of all triterpenes in this study has not previously been reported. Of the 25 compounds tested, the most active specie was compound **36** with 90.94% *P.falciparum* growth inhibition at the concentration of 10µM. The IC_{50} and IC_{90} values of compound **36** against *P.falciparum* were 3.74 and 10.31 µM (1.72 and 4.73 µg/mL), respectively (Table 30). Other 5 triterpenes with the structure in nordammarane (**26**, **39**) and fouquierone (**32**, **38**, **45**) groups showed mild antiplasmodial activity with more than 20% growth inhibition at the concentration of 10 µM. Cytotoxic assay against L-6 cell showed that all compounds exhibited only low activity against normal cell at the concentration of 10 µM.

The presence of endoperoxide group and lupane structure of compound **36** might support our result. Artemisinin is a sesquiterpene lactone with endoperoxide antimalarial drug while antimalarial activity of some lupanes such as betulinic acid has been reported [131].

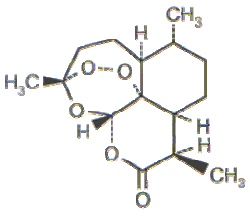

artemisinin

4.7 CONCLUSION

Among 31 isolated compounds, twelve compounds were new. They were (20*R*)-17α,29-epoxy-28-norlupan-3-one (**24**), (20*S*)-20-hydroxy-24-perhydroxy-dammar-25-en-3-one (**29**), (20*S*)-29-hydroxy-17α,20-peroxy-28-norlupan-3-one (**36**), (20*R*)-20-hydroxy-17α,29-epoxy-28-norlupan-3-one (**42**), 17α-hydroxy-28-norlupan-20(29)-en-3-one (**25**), 17α-hydroxy-28,29-dinorlupan-3,20-dione (**41**), (20*S*,23*E*)- 20,25,26-trihydroxydammar-23-en-3-one (**46**), (20*S*,22*E*)-20,24,25-trihydroxydammar-22-en-3-one (**45**), (20*S*,23*E*)-20-hydroxy-27-nordammar-23-ene-3,25-dione (**39**), (20*S*)-20-hydroxy-3-oxo-24,25,26,27-tetranordammar-23-oic acid (**49**), (20*S*,23*E*)-25-hydroperoxy-20-hydroxy-2,3-*seco*-dammar-23-en-2,3-dioic acid (**48**), and (20*S*,24*R*)-20,24-epoxy-25-hydroxy-2,3-*seco*-dammarane-2,3-dioic acid (**47**). Octanordammarane-3,17-dione (**26**) was found for the first time in the nature whereas two dammaranes; cereotagaloperoxide (**32**) and isocabralealactone (**27**), were rare compounds.

Five different side chain groups of dammarane triterpenes were found in this work. Dipterocarpol and ocotillone groups were the common types in this family while isofouquierone, fouquierone and lactone sidechain groups were hitherto never reported in Dipterocarpaceous plants. Dipterocarpol **22**, dammarenediol-II **31**, and ocotillone **34** (no cabraleone) were previously isolated from some species in genus *Dipterocarpus* [40]. It is interesting that the works on genus *Betula* (Betulaceae) also found these 3 dammaranes, as well as lupane triterpene. This finding showed their closely related taxonomy. However, the dammarane derivatives from this extract were close to those found from plants in Meliaceae too.

The presence of 28-norlupane in genus *Dipterocarpus* may be due to the presence of an oxidative enzyme system specific to the conversion of lupanes such as betulonic acid to C-17 oxy-28-norlupane. This is the first report of norlupane in this family.

The isolation of norlupanes, acyclic side chain of fouquierone and isofouquierone-group, 2,3-*seco*-dammaranes together with trihydroxy sidechain dammaranes (**45**, **46**), represented a significant departure from the patterns of triterpene production previously noted [20, 38-40, 43, 44, 46, 47, 205, 206] in the Dipterocarpaceae. Their occurrence is also notable in highlighting the chemotaxonomic significance of plants in the Dipterocarpaceae.

In this investigation, the relationship in the biosynthesis of dammaranes in dipterocarpol, ocotillone and lactone group has been proposed, as well as the biosynthesis of octanordammarane-3,17-dione. It is attractive to make more investigation on synthesis pathway of the compounds with higher oxidation such as compound **45**-**49** (scheme 25). The dammarane derivatives were supposed to be formed by enzymatic oxidation and degradation of the tetracyclic triterpenoid precursor, dipterocarpol. Moreover, the relationship among fouquierone, isofouquierone and dipterocarpol and the stereochemistry at C-24 of compound **29** and **32** should be examined.

In cytotoxic assay, it was interesting that compound **25**, a norlupane triterpene, was active against HCT116 cell line. It showed lower growth inhibition to L-6 cell, a normal mammalian cell, than HCT116 cell, a tumor cell.

The investigation of *in vitro* antiplasmodial activity of new triterpene **36** (an endoperoxide norlupane) demonstrated an important finding for the treatment of malaria with the low cytotoxicity against L-6 of rat, a normal mammalian cell. To ensure the safety of compound **36** usage, its selectivity index (SI) should be carried out. (selectivity index is defined as the ratio of cytotoxicity to antiplasmodial activity, and is determinded by dividing the IC_{50} values for the L-6 cells by the IC_{50} for *P.falciparum*.) In addition, the relationship between structure and activity should be studied intensively.

Moreover, it was found in some study that dammarene triterpenes from dammar resin possesed potent antiviral activity against *Herpes simplex* [23]. Then, it is interesting to investigate this activity of the isolated dammaranes and related compounds from this research too.

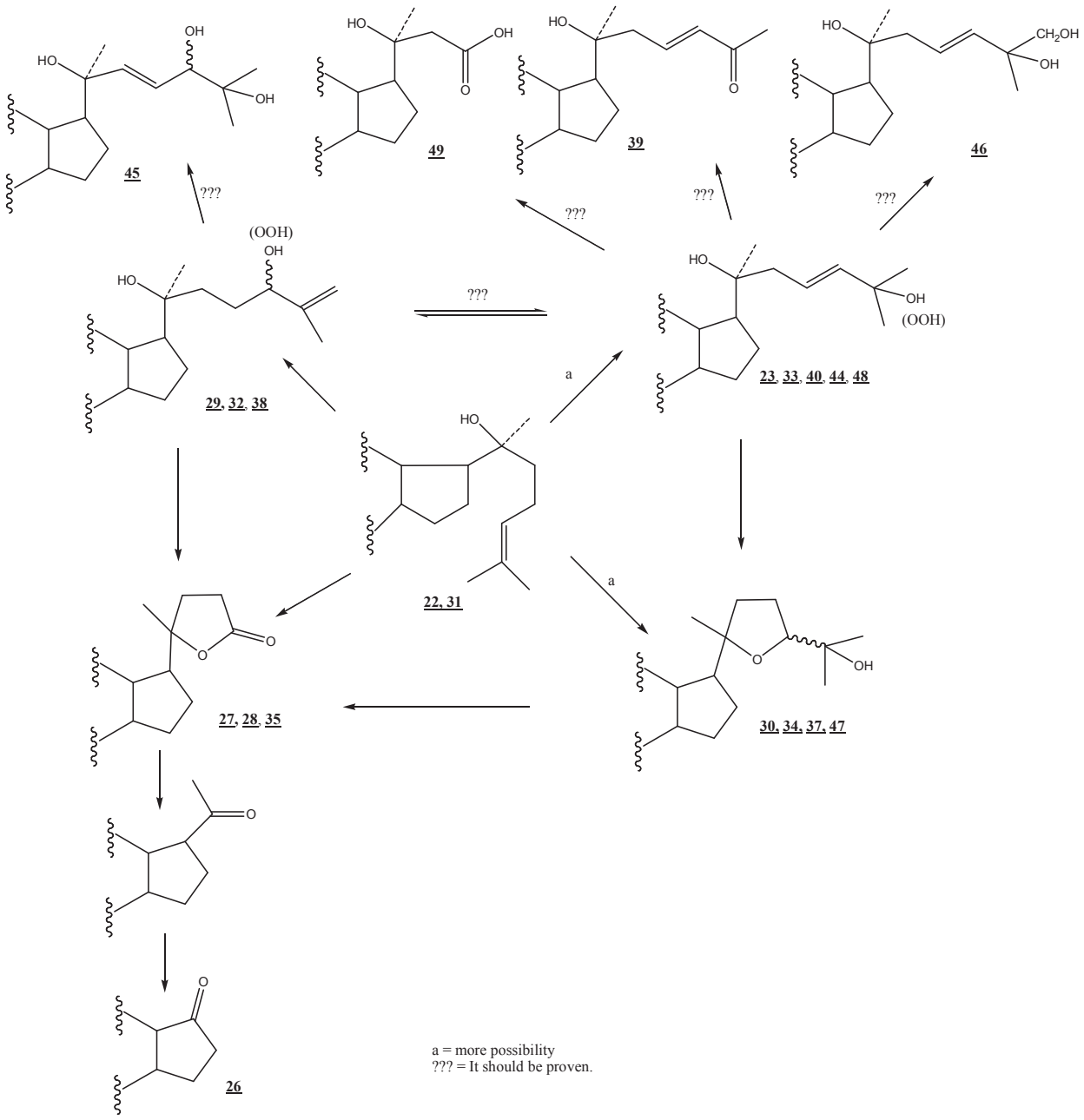

Scheme 25. The possible biosynthesis pathway of dammaranes found in *D. costatus* (based on derivatization on the sidechain).

GENERAL CONCLUSION

Lupane and dammarane are the major triterpenes found in the present study. The result is in agreement with the previous report of chemical constituent in Dipterocarpaceous plants. The relationship in biosynthesis among these triterpenes has been reported [80] and it could explain the triterpenes in this research.

The isolation of *H.odorata* leaves hexane extract yielded 2 new fatty acid esters of 3,4-*seco*-cycloartane triterpenes (**18**-**19**) and 1 lupane first found in the nature (**14**). The chromatography of *D. costatus* wood hexane extract gave the finding of 5 new norlupanes (**24**,**25**,**36**,**41**,**42**), 2 new nordammaranes (**39**,**49**), 3 new dammaranes (**29**,**45**,**46**), 2 new 2,3-*seco*-dammaranes (**47**,**48**), 1 nordammarane first found in the nature (**26**) as well as 3 rare dammaranes (**27**,**29**,**32**).

Dammaranes are the most abundant triterpens in *D. costatus* wood hexane extract whereas *H.odorata* leaves hexane extract is composed of many lupanes. It is interesting that the first tricyclic rings of triterpenes in both extracts are very close to each other. Lupane triterpenes from *H.odorata* extract are pentacyclic ring while *D. costatus* hexane extract contained both norlupane and teracyclic dammarane triterpene with side chain instead of cyclic ring E.

Although both species are in the same family, the major triterpens found are in different groups. However, it should be noted that the close triterpene structure between dammarane and cycloartane are found as well. It means a close metabolism happened in both species. The occurrence of 3,4-*seco*-cycloartane in *H.odorate* extract together with rare 2,3-*seco*-dammarane, trihydroxy sidechain of dammarane, and nordammarane in *D. costatus* extract are of interest and have never been reported from Dipterocarpaceous plants. Furthermore, the finding of a number of dammarane with epoxide and peroxide derivatives make it interesting to further investigation of antimalarial activity in other plants of this family.

Comparison to dammaranes with the same method of assay, lupane triterpenes exhibited higher potency of cytotoxicity. Messagenic acid G showed an attractive potency. The modification at C-3, C-28 and isopropenyl groups could produce the difference potency. Compound **25**, a norlupane triterpene with hydroxyl group at position 17 instead of carboxylic group (compared to betulonic acid), was found potent cytotoxic active against HCT116 cell line. In addition, compound **36**, an endoperoxide norlupane, gave a satisfied antiplasmodial activity. Dammarane triterpenes were less active at the tested concentration. However, it is fascinating to further antiviral activity of all compounds as there are a number of publications reported both activities of these two groups.

Table 44. Compounds isolated from *Hopea odorata* leaves hexane extract and *Dipterocarpus costatus* wood hexane extract

Compound Number	Name (source)	Structure
1	Friedelin (*H. odorata*)	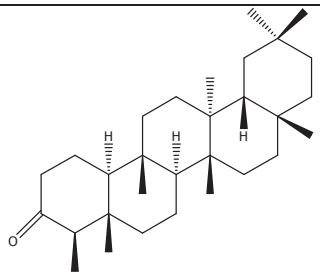
2	*β*-Amyrin (*H. odorata*)	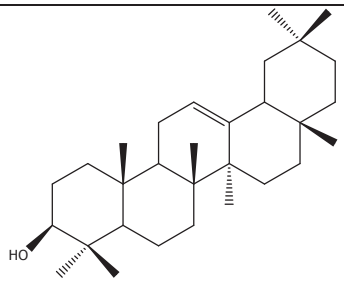
3	*β*-Sitosterol (*H. odorata* and *D. costatus*)	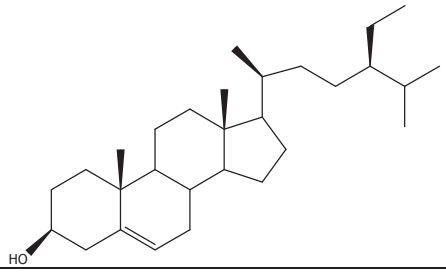
4	*Epi*friedelanol (*H. odorata*)	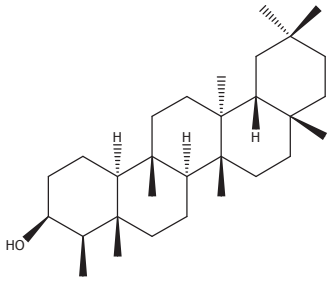
5	Betulonic acid (*H. odorata*)	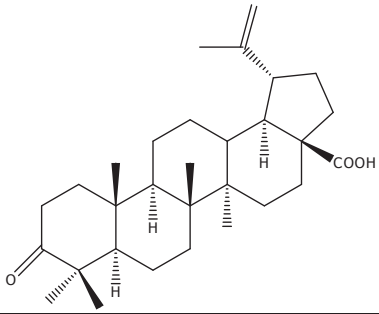

Compound Number	Name (source)	Structure
6	Saturated fatty acid ester of *β*-Amyrin (*H. odorata*)	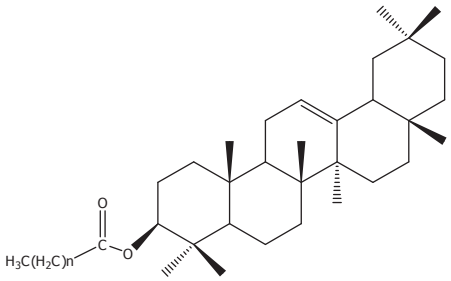
7	*β*-Sitosterol palmitate (*H. odorata*)	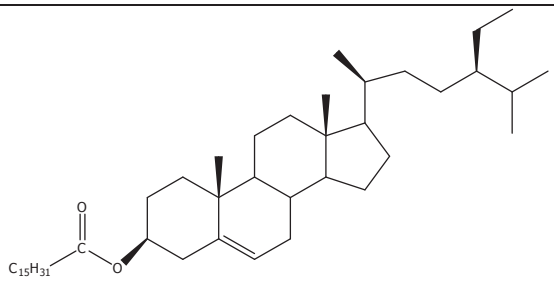
8	Saturated and unsaturated fatty acid ester of *β*-sitosterol (*H. odorata*)	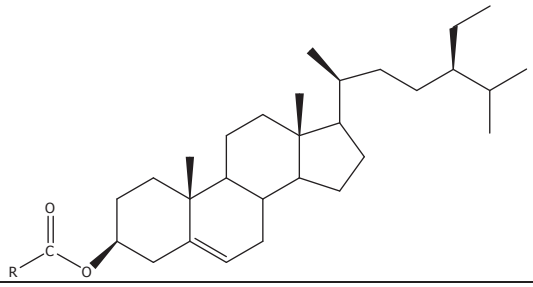
9	Caryophyllene oxide (*H. odorata* and *D. costatus*)	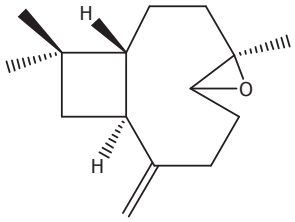
10	*Epi*betulinic acid (*H. odorata*)	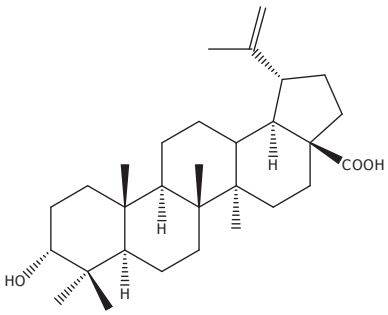

Compound Number	Name (source)	Structure
11	Betulone (*H. odorata*)	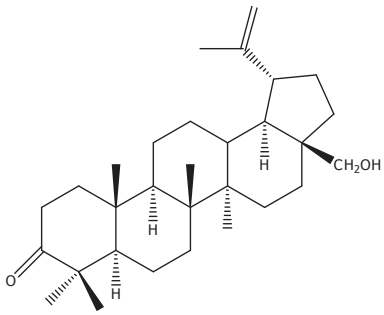
12	30-Hydroxy-3-oxolup-20(29)-ene (*H. odorata*)	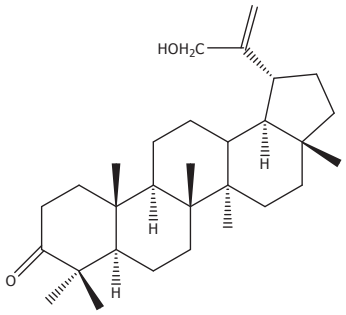
13	Betulinic acid (*H. odorata*)	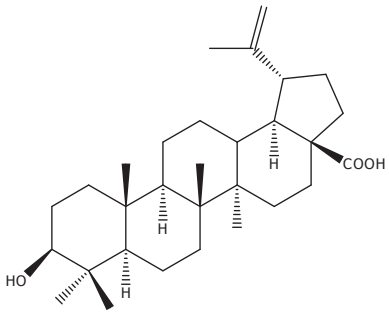
14	3,30-Dioxolup-20(29)-en-28-oic acid (*H. odorata*)	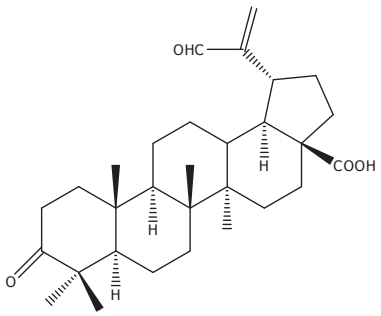
15	Mangiferonic acid (*H. odorata*)	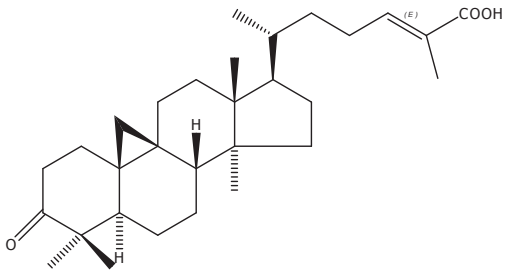

Compound Number	Name (source)	Structure
16	28,30-Dihydroxylup-20(29)-en-3-one (*H. odorata*)	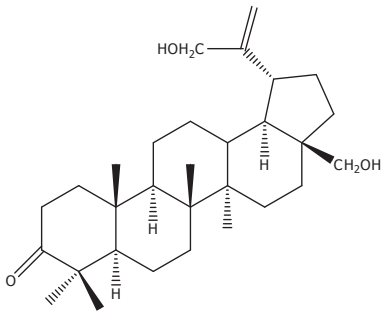
17	Messagenic acid G (*H. odorata*)	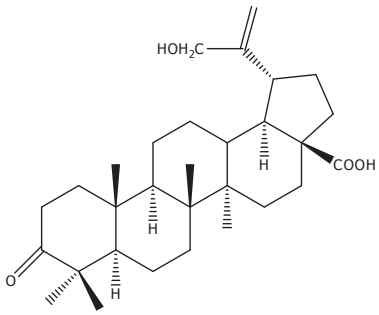
18*	26-Arachidic ester of 24,25,26-trihydroxy-3,4-*seco*-cycloart-4(29)-en-3-oic acid (*H. odorata*)	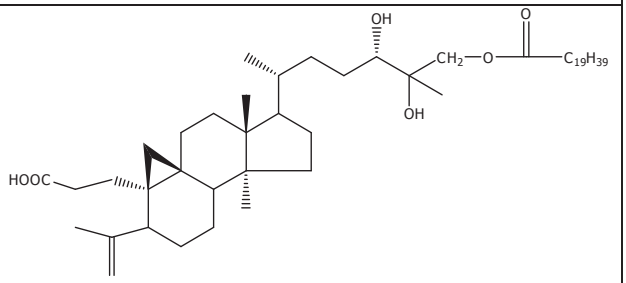
19*	24-Fatty acid ester of 24,25,26-trihydroxy-3,4-*seco*-cycloart-4(29)-en-3-oic acid (*H. odorata*)	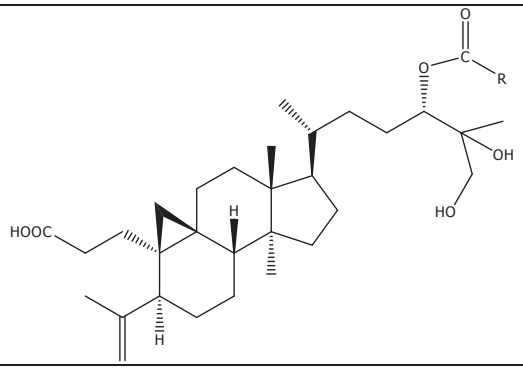
20	(24*E*)-3,4-*Seco*-cycloart-4(29),24-diene-3,26-dioic acid (*H. odorata*)	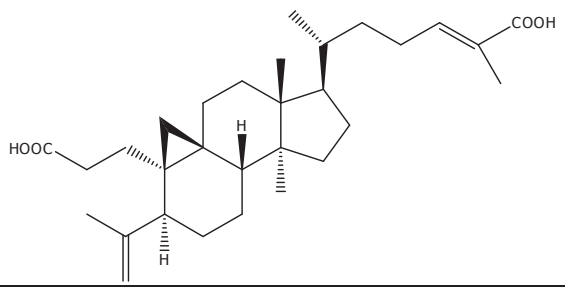

Compound Number	Name (source)	Structure
21	β-Elemene (*D. costatus*)	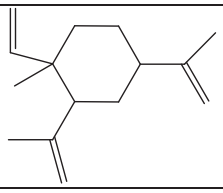
22	Dipterocarpol (*D. costatus*)	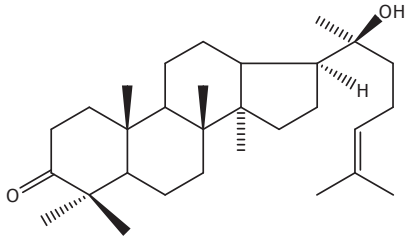
23	Isofouquierone peroxide (*D. costatus*)	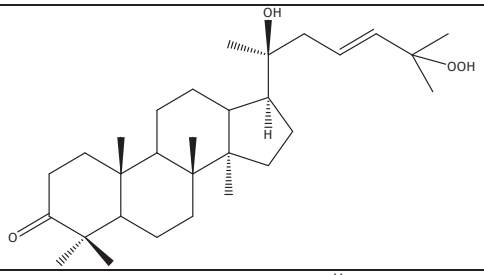
24*	17α,29- Epoxy- 28-norlupane-3-one (*D. costatus*)	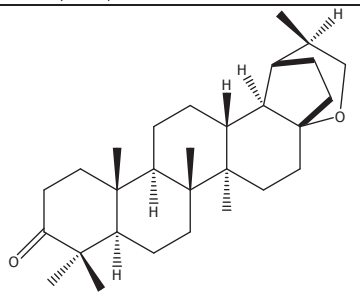
25*	17α-Hydroxy-28-norlupan-20(29)-en-3-one (*D. costatus*)	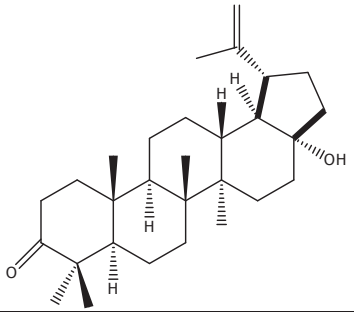
26	Octanordammarane-3,17-dione (*D. costatus*)	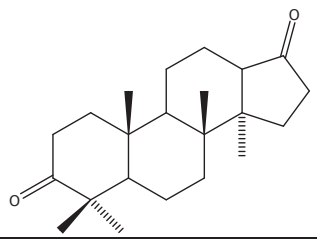

Compound Number	Name (source)	Structure
27	Isocabralealactone (*D. costatus*)	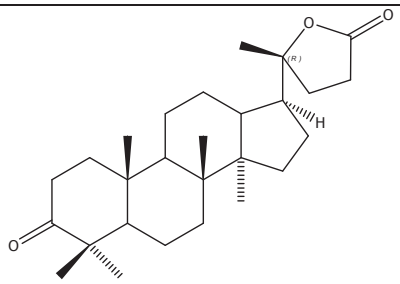
28	Cabralealactone (*D. costatus*)	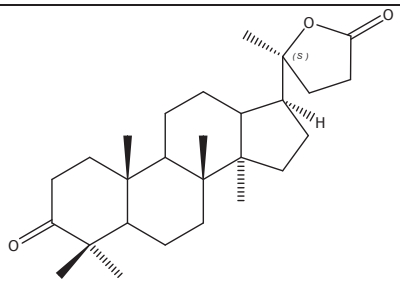
29*	(20*S*)-20-Hydroxy-24-perhydroxydammar-25-en-3-one (*D. costatus*)	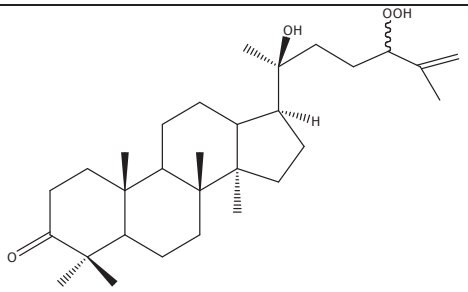
30	Cabraleone (*D. costatus*)	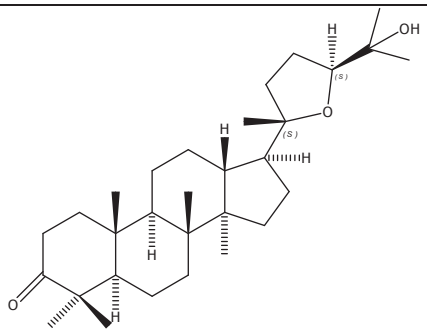
31	Dammarenediol II (*D. costatus*)	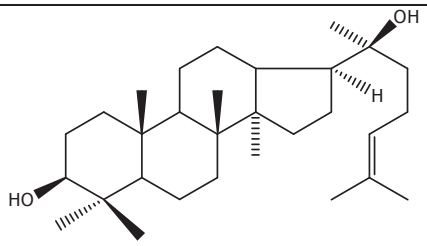
32	Cereotagaloperoxide (*D. costatus*)	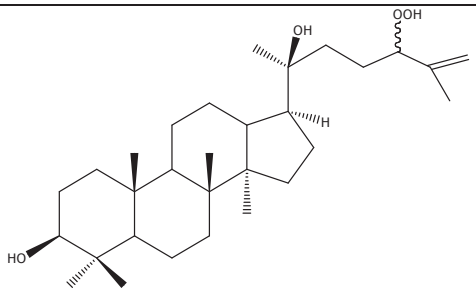

Compound Number	Name (source)	Structure
33	Isofouquierol peroxide (*D. costatus*)	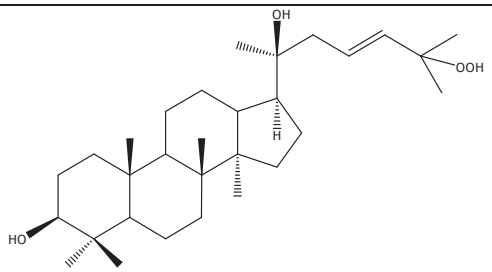
34	Ocotillone (*D. costatus*)	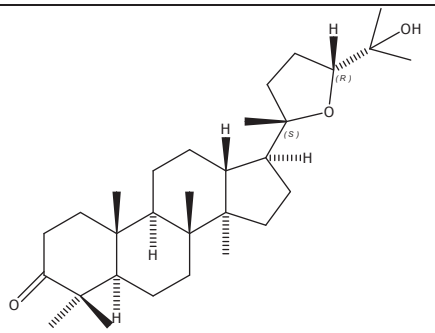
35	3-*Epi*cabraleahydroxy-lactone (*D. costatus*)	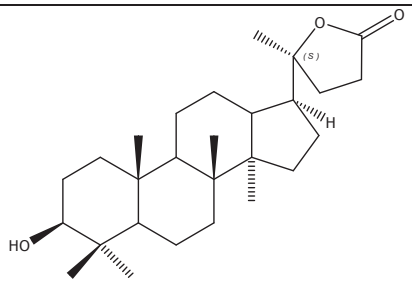
36*	29-Hydroxy-17α,20-peroxy-28-norlupan-3-one (*D. costatus*)	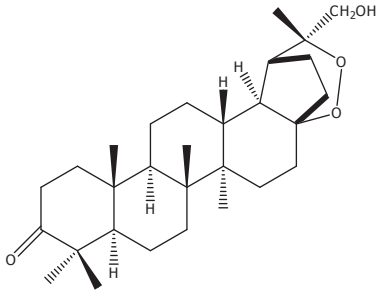
37	Ocotillol II (*D. costatus*)	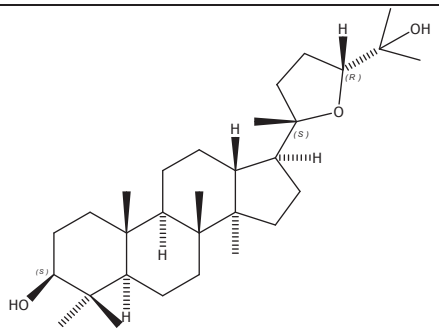

Compound Number	Name (source)	Structure
38	(20*S*,24*S*)-20,24-Dihydroxydammar-25-en-3-one (*D. costatus*)	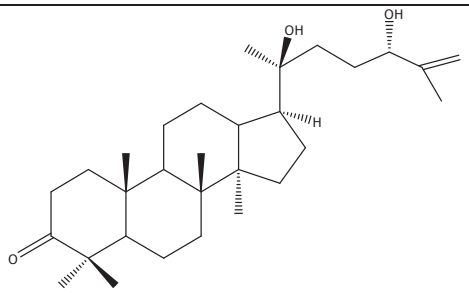
39*	(20*S*,23*E*)-20-Hydroxy-27- nordammar-23-en-3,25-dione (*D. costatus*)	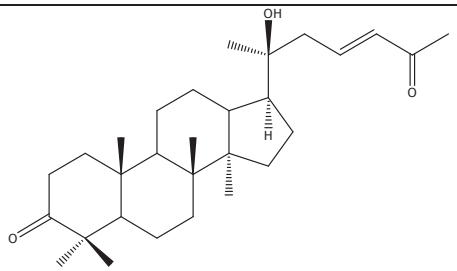
40	Isofouquierone (*D. costatus*)	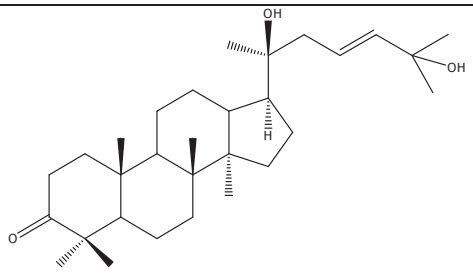
41*	17α,-Hydroxy-28,29-dinorlupan-3,20-dione	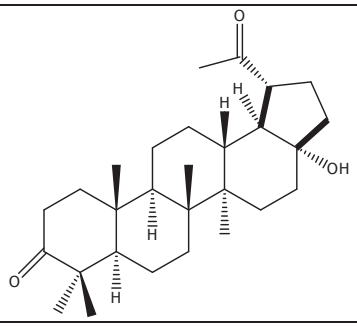
42*	20-Hydroxy-17α,29-epoxy-28-norlupan-3-one (*D. costatus*)	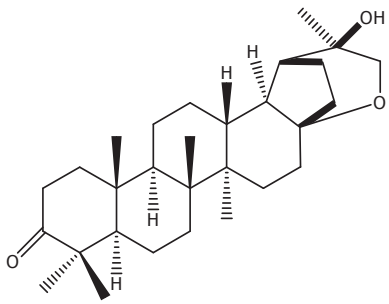
43	Clovane-2,9-diol (*D. costatus*)	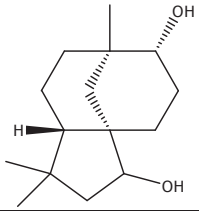

Compound Number	Name (source)	Structure
44	Isofouquierol (*D. costatus*)	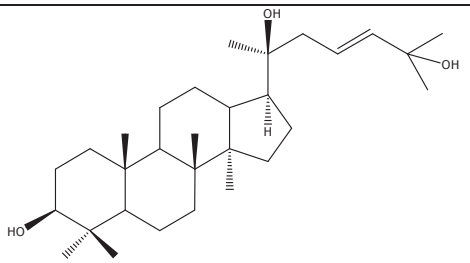
45*	(20*S*,22*E*)-20,24,25-Trihydroxydammar-22-en-3-one (*D. costatus*)	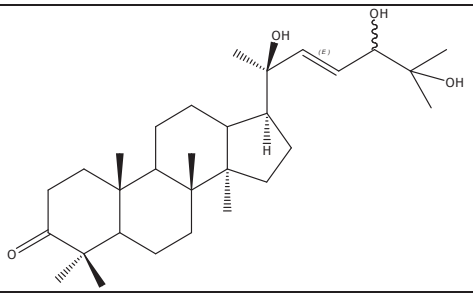
46*	(20*S*,23*E*)-20,25,26-Trihydroxydammar-23-en-3-one (*D. costatus*)	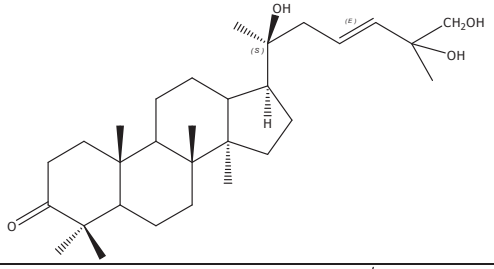
47*	(20*S*,24*R*)-20,24-Epoxy-25-hydroxy-2,3-*seco*-dammarane-2,3-dioic acid (*D. costatus*)	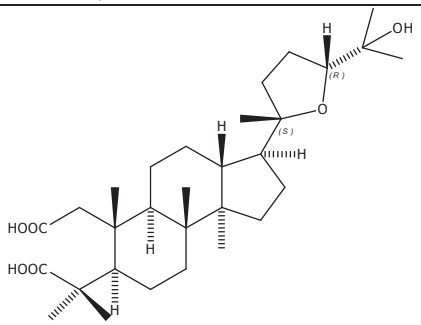
48*	(20*S*,23*E*)-20,24-Epoxy-25-hydroxy-2,3-*seco*-dammarane-2,3-dioic acid (*D. costatus*)	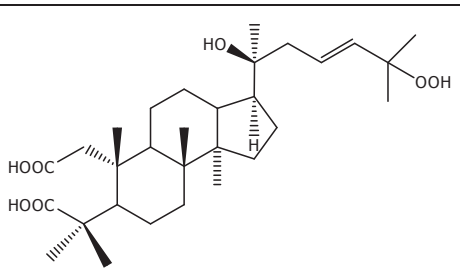
49*	(20*S*)-Hydroxy-3-oxo-24,25,26,27-tetranordammar-23-oic acid (*D. costatus*)	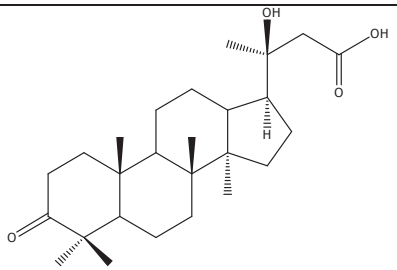

*new compounds

BIBLIOGRAPHY

1. Macias, F.A., J.L.G. Galindo, and J.C.G. Galindo. (2007). "Evolution and current status of ecological phytochemistry." **Phytochemistry** 68: 2917-2936.
2. Antimonova, A.N., et al. (2008). "Synthesis of betulonic acid amides." **Chemistry of Natural Compounds** 44, 3: 327-333.
3. World Health Organization. (2008). **Are the number of cancer cases increasing or decreasing in the world?** Accessed June 17th, 2011. Available from: http://www.who.int/features/qa/15/en/index.html.
4. World Health Organization. (2011). **World malaria report 2011.** Accessed January 4th, 2012. Available from: http://www.who.int/malaria/world_malaria_report_2011/en/.
5. Atun, S., et al. (2006). "Oligostilbenoids from *Hopea Mengarawan* (Dipterocarpaceae)." **Biochemical Systematics and Ecology** 34, 8: 642-644.
6. Atun, S., et al. (2008). "Resveratrol derivatives from stem bark of *Hopea* and their biological activity test." **Journal of Physical Science** 19, 2: 7-21.
7. Ge, H.M., et al. (2008). "Hopeahainol A: an acetylcholinesterase inhibitor from *Hopea hainanensis*." **Chemistry** 14, 1: 376-381.
8. Saroyobudiono, H., et al. (2008). "Oligostilbenoids from *Shorea gibbosa* and their cytotoxic properties against P-388 cells." **Journal of Natural Products** 62: 195-198.
9. Atun, S., et al. (2004). "Oligostilbenoids from *Vatica umbonata* (Dipterocarpaceae)." **Biochemical Systematics and Ecology** 32, 11: 1051-1053.
10. Ito, T., et al. (2005). "Two novel trimeric resveratrol derivatives from Cotylelobium lanceolatum." **Chemistry & Biodiversity** 2, 9: 1200-1216.
11. Liu, J.Y., et al. (2005). "New resveratrol oligomers from the stem bark of *Hopea hainanensis*." **Helvetica Chimica Acta** 88: 2910-2917.
12. Sahidin, et al. (2005). "Cytotoxic properties of oligostilbenoids from the tree barks of *Hopea dryobalanoides*." Z **Naturforsch [C]** 60, 9-10: 723-727.
13. Syah, Y.M., et al. (2003). "Two oligostilbenes, cis- and trans-diptoindonesin B, from *Dryobalanops oblongifolia*." **Phytochemistry** 63, 8: 913-917.
14. Ito, T., et al. (2003). "New resveratrol oligomers in the stem bark of Vatica pauciflora." **Tetrahedron** 59, 28: 5347-5363.
15. Tanaka, T., et al. (2001). "Hopeafuran and a C-glucosyl resveratrol isolated from stem wood of *Hopea utilis*." **Chemical & Pharmaceutical Bulletin (Tokyo)** 49, 6: 785-787.
16. Aminah, N.S., et al. (2002). "Diptoindonesin A, a new C-glucoside of [var epsilon]-viniferin from *Shorea seminis* (Dipterocarpaceae)." **Fitoterapia** 73, 6: 501-507.
17. Ito, T., et al. (2001). "A new resveratrol octamer, vateriaphenol A, in *Vateria indica*." **Tetrahedron Letters** 42, 34: 5909-5912.
18. Tanaka, T., et al. (2000). "Oligostilbenoids in stem bark of *Vatica rassak.*" **Phytochemistry** 54, 1: 63-69.

19. Tanaka, T., et al. (2000). "Stilbenoids in the stem bark of *Hopea parviflora*." **Phytochemistry** 53, 8: 1015-1019.
20. Seo, E.-K. and A.D. Kinghorn. (2000) "Bioactive constituents of the family Dipterocarpaceae." in **Studies in Natural Products Chemistry**, 531-561 edited by Atta-ur-Rahman. Amsterdam: Elsevier.
21. Sittisombut, C., et al. (2006). "Investigation of anti-cancer activity of plants in families of Rutaceae and Dipterocarpaceae in Thailand." Presented at the meeting of Thailand research fund seminar, Phetchaburi, Thailand, October 12th -14th.
22. Chuakul, W., et al. (1997). **Medicinal Plants in Thailand, Volume II.** 1st ed. Bangkok: Amarin Printing and Publishing Public Co., Ltd.
23. Poehland, B.L., et al. (1987). "*In vitro* anitiviral activity of dammar resin triterpenoids." **Journal of Natural Products** 50, 4: 706-713.
24. Ashton, P.S. (2004). "Dipterocarpaceae." in **Tree Flora of Sabah and Sarawak**, **Volume V**, 61-382. Edited by E. Soepadmo, L.G. Saw, and R.C.K. Chung. Kuala Lumpur: Goverment of Malaysia.
25. Pooma, R. (2003). "Dipterocarpaceae in Thailand: Taxonomic and Biogeographical Analysis." Ph.D.dissertation, Department of Botany, Kasetsart University: Bangkok. p.285.
26. Ridley, H.N. (1967). **The Flora of the Malay Peninsula Vol. I.** London: L.Reeve & Co.,LTD.
27. Gardner, S., P. Sidisunthorn, and V. Anusarnsunthorn. (2000). **A Field Guide to Forest Trees of Northern Thailand.** Bangkok: Kobfai Publishing Project. 560.
28. Ashton, P.S. (1982). "Dipterocarpaceae." in **Flora Malesiana**. 237-552. Kuala Lumpur: Goverment of Malaysia.
29. Smitinand, Y., et al.(1980). "The manual of Dipterocarpaceae of mainland South-East Asia." **Thai Forest Bulletin (Botany)** 12: 1-133.
30. Yuwa-Amornpitak, T., T. Vichitsoonthonkul, and M. Tanticharoen. (2006). "Molecular phylogeny of diptercarpaceae in Thailand using trnL-trnF and atpB-rbcL intergenicspacer region in chloroplast DNA." **Pakistan Journal of Biological Sciences** 9, 4: 649-653.
31. Pooma, R. and M. Newman. "Checklist of Dipterocarpaceae in Thailand." **Thai Forest Bulletin (Botany)** 29: 110-187.
32. Wikipedia, The free encyclopedia. (2008). **Dipterocarpaceae.** Accessed September 27th. Available from: http://en.wikipedia.org/wiki/Dipterocarp.
33. Tabata, Y., et al. (2007). "Vaticanol B, a resveratrol tetramer, regulates endoplasmic reticulum stress and inflammation." **American Journal of Physiology Cell Physiology** 293: C411-C418.
34. Maridass, M. (2008). "Antimicrobial and cytotoxic activities of *Hopea utilis* fruits." **Ethnobotanical Leaflets** 12: 570-576.
35. Dai, J.-R., et al. (1998). "HIV-inhibitory and cytotoxic oligostilbenes from the leaves of *Hopea malibato*." **Journal of Natural Products** 61, 3: 351-353.
36. Ito, T., et al. (2003). "Antitumor effect of resveratrol oligomers against human cancer cell lines and the molecular mechanism of apoptosis induced by vaticanol C." **Carcinogenesis** 24, 9: 1489-97.

37. Muhtadi, et al. (2006). "Cytotoxic resveratrol oligomers from the tree bark of *Dipterocarpus hasseltii*." **Fitoterapia** 77: 550-555.
38. Diaz, M.A. and G. Ourisson. (1966). "Etude chimio-taxonomiques dans la famille des Dipterocarpaceaes-I: Introduction generale. Constutuants du genre *Doona* thw." **Phytochemistry** 5: 855-863.
39. Bandaranayake, W.M., et al. (1975). "Tepenes of *Dipterocarpus* and *Doona* species." **Phytochemistry** 14: 2043-2048.
40. Bisset, N.G., et al. (1966). "Etudes chimio-taxonomiques dans la famille des Dipterocarpaceaes-II. Constituants du genre *Dipterocarpus* Gaertn.F. Essai de classification chimio-taxonomique." **Phytochemistry** 5: 865-880.
41. Bisset, N.G., et al. (1971). "Constituants Sesquiterpeniques et Triterpeniques des Resines du Genre *Shorea.*" **Phytochemistry** 10: 2451-2463.
42. Hota, R.K. and M. Bapuji. (1993). "Triterpenoids from the resin of *Shorea robusta.*" **Phytochemistry** 32. 2: 466-468.
43. Misra, L.N. and A. Ahmad. (1997). "Triterpenoids from *Shorea robusta* resin." Phytochemistry 45, 3: 575-578.
44. Cheung, H.T. and C.S. Wong. (1972). "Structures of triterpenes from *Dryobalanops aromatica.*" **Phytochemistry** 11: 1771-1780.
45. Burger, P., et al., 2009. "Archaeological resinous samples from Asian wrecks: taxonomic characterization by GC-MS." **Analytica Chimica Acta** 648: 85–97.
46. Bandaranayake, W.M., et al. (1977). "Triterpenoid taxonomic markers for *Stemonoporus* and other genera of the Dipterocarpaceae." **Phytochemistry** 16: 699-701.
47. Geevananda, Y.A., et al. (1980). "Distribution of some triterpenes and phenolic compounds in the extractives of endemic Dipterocarpaceae species of Sri Lanka." **Phytochemistry** 19, 6: 1099-1102.
48. Seo, E.K., et al. (1999). "Resveratrol tetramers from *Vatica diospyroides.*" **Journal of Organic Chemistry** 64: 6976-6983.
49. Zhang, H.J., et al. (2003). "Natural Anti-HIV Agents. Part IV: Anti-HIV Constituents from *Vatica cinerea*." **Journal of Natural Products** 66, 2: 263-268.
50. Adio, A.M. (2009). "(-)-trans-*β*-Elemene and related compounds: occurrence, synthesis, and anticancer activity." **Tetrahedron** 65: 5145-5159.
51. Cho, C.W., et al. (2006). "Glioblastoma cell death induced by asiatic acid." **Cell Biology and Toxicology** 22: 393-408.
52. Kim, D.S.H.L., J.M. Pezzuto, and E. Pisha. (1998). "Synthesis of betulinic acid derivatives with activity against human melanoma." **Bioorganic & Medicinal Chemistry Letters** 8: 1707-1712.
53. Joshi, K., G.I. Seneviratne, and S.P. Senanayake. (2004). "Leaf flavonoid aglycone patterns in the species of Dipterocarpaceae in Sri Lanka." **Biochemical Systematics and Ecology** 32, 3: 329-336.
54. Joshi, K., (2003). "Leaf flavonoid patterns in *Dipterocarpus* and *Hopea* (Dipterocarpaceae)." **Botanical Journal of the Linnean Society** 143,1: 43-46.

55. Legault, J. and A. Pichette. (2007). "Potentiatine Effect of β-Caryophyllene on anticancer activity of α-humulene, isocaryophyllene and paclitaxel." **Journal of Pharmacy and Pharmacology** 59,12: 1643-1647.
56. Flath, R.A., et al. (1994). "Male Lures for Mediterranean Fruitfly (*Ceratitis capitata* wied.): Structural Analogs of *α*-Copaene" **Journal of Chemical Ecology** 20, 10: 2595-2609.
57. Ulubelen, A., et al. (1994). "Terpenoids from *Salvia sclarea*." **Phytochemistry** 36, 4: 971-974.
58. Kanokmedhakul, S., K. Kanokmedhakul, and R. Lekphrom. (2007). *"Bioactive constituents of the roots of Polyalthia cerasoides.*" **Journal of Natural Products** 70: 1536-1538.
59. Ziaei, A., et al. (2011). "Identification of Spathulenol in *Salvia mirzayanii* and the Immunomodulatory Effects." **Phytotherapy Research** 25, 4: 557-562.
60. Joycharat, N., et al. (2010). "Terpenoid constituents and antifungal activity of *Aglaia forbesii* seed against phytopathogens." **Canadian Journal of Chemistry** 88: 937-944.
61. Otuki, M.F., et al. (2005). "Antinociceptive properties of mixture of *α*-amyrin and *β*-amyrin triterpenes: evidence for participation of protein kinase C and protein kinase A pathways" **Journal of Pharmacology And Experimental Therapeutics Fast Forward** 313: 310-318.
62. Oliveiraa, F.A., et al. (2005). "Protective effect of *α*- and *β*-amyrin, a triterpene mixture from *Protium heptaphyllum* (Aubl.) March. trunk wood resin, against acetaminophen-induced liver injury in mice." **Journal of Ethnopharmacology** 98, 1-2: 103-108.
63. Kanjoormana, M. and G. Kuttan. (2010). "Antiangiogenic activity of ursolic acid." **Integrative Cancer Therapies** 9, 2: 224-235.
64. Kim, S.-H., (1997). "Antitumor Activity and Inhibitory of Topoisomerase-I by ursonic acid." **Korean Journal of Oriental Medical Pathology** 11, 2: 12-15.
65. Tsiri, D., et al. (2008). "Triterpenoids from *Eucalyptus camaldulensis* Dehnh. tissue cultures." **Helvetica Chimica Acta** 91, 11: 2110-2114.
66. Yun, K.-J., et al. (2008). "Inhibition of LPS-induced NO and PGE2 production by asiatic acid via NF-κB inactivation in RAW 264.7 macrophages: Possible involvement of the IKK and MAPK pathways international" **Immunopharmacology** 8, 3: 431-441.
67. Gupta, A.S. and S. Dev. (1971). "Higher Isoprenoids—I, : Triterpenoids from the Oleoresin of *Dipterocarpus pilosus*: Hollongdione and dipterocarpolic acid" **Tetrahedron** 27, 4: 823-834.
68. Zitterl-Eglseer, K., et al. (1997). "Anti-oedematous activities of the main triterpendiol esters of marigold (*Calendula officinalis* L.)" **Journal of Ethnopharmacology** 57, 2: 139-144.
69. Villaseñor, I.M., et al. (2002). "Bioactivity studies on *β*-sitosterol and its glucoside." **Phytotherapy Research** 16, 5: 417-421.

70. Mills, J.S. (1956). "The constitution of the neutral, tetracyclic triterpenes of dammar resin." **Journal of Chemical Society**: 2196-2202.
71. McLean, J. and W.E. Watts. (1960). "Extractives from the Dipterocarpaceae." **Journal of Organic Chemistry** 25, 7: 1263.
72. Esimone, C.O., et al. (2010). "Dammarenolic acid, a *seco*-dammarane triterpenoid from *Aglaia* sp. shows potent anti-retroviral activity *in vitro*." **Phytomedicine** 17, 7: 540-547.
73. Makino, M., T. Motegi, and Y. Fujimoto. (2004). "Tirucallane-type triterpenes from *Juliana adstringens.*" **Phytochemistry**, 65: 891-896.
74. Bizimenyera, E. (2007). "The potential role of antibacterial, antioxidant and antiparasitic activity of *Peltophorum africanum* Sond. (Fabaceae) extracts in ethnoveterinary medicine" Ph.D. dissertation, Paraclinical Sciences, University of Pretoria: Pretoria.
75. Rollinger, J.M., et al. (2004). "Acetylcholinesterase Inhibitory Activity of Scopolin and Scopoletin Discovered by Virtual Screening of Natural Products." **Journal of Medicinal Chemistry** 47, 25: 6248-6254.
76. García-Sosa, K., et al. (2006). "Chrysophanol, an antimicrobial anthraquinone from the root extract of *Colubrina greggii.*" **Journal of the Mexican Chemical Society** 50, 2: 76-78.
77. Sturm, N., et al. (2009). "Compounds structurally related to ellagic acid show improved antiplasmodial activity." **Antimicrobial Agents and Chemotherapy** 53, 2: 622-630.
78. McGarvey, D.J. and R. Croteau. (1995). "Terpenoid metabolism." **The Plant Cell** 7: 1015-1026.
79. Laszczyk, M.N. (2009). "pentacyclic triterpenes of the lupane, oleanane and ursane group as tools in cancer therapy." **Planta Medica** 75: 1549-1560.
80. Xu, R., G.C. Fazio, and S.P.T. Matsuda. (2004). "On the origins of triterpenoid skeletal diversity." **Phytochemistry** 65: 261-291.
81. Monaco, P. and L. Previtera. (1984). "Isoprenoids from the leaves of *Quercus suber.*" **Journal of Natural Products** 47, 4: 673-676.
82. Ng'ang'a, M.M., et al. (2009). "Chemical constituents from the root bark of *Ozoroa insignis*." **Biochemical Systematics and Ecology** 37: 116-119.
83. Gu, Q., et al. (2007). "A new benzofuranone and anti-HIV constituents from the stems of *Rhus Chinensis.*" **Planta Medica** 73: 279-282.
84. Siddiqui, S., et al. (1988). "Oleanderol, a new pentacyclic triterpene from the leaves of *Nerium oleander.*" **Journal of Natural Products** 51, 2: 229-233.
85. Cole, B.J.W., et al. (1991.) "Triterpenoid constituents in the outer bark of *Betula alleghaniensis* (yellow birch)." **Journal of Wood Chemistry and Technology** 11, 2: 209-223.
86. Kashiwada, Y., et al. (2007). "Triterpenoids from the floral spikes of *Betula platyphylla* var. *japonica* and their reversing activity against multidrug-resistant cancer cells." **Journal of Natural Products** 70: 623-627.

87. Abyshev, A.Z., E.M. Agaev, and A.B. Guseinov. (2007). "Studies of the chemical composition of birch bark extracts (cortex betula) from the Betulaceae family." **Pharmaceutical Chemistry Journal** 41: 22-26.
88. Lindgren, B.O. and C.M. Svahn. (1966). "Lupan-3 β-,20-diol and lupan-3 β,20,28-triol in Bark from Birch, *Betula verrucosa* Erh." **Acta Chemica Scandinavica** 20, 6: 1720-1721.
89. Drewes, S.E. and M.J. Mashimbye. (1993). "Flavanoids and triterpenoids from *Cassine papillosa* and the absolute configuration of 11,11-dimethyl-1,3,8,10-tetrahydroxy-9-methoxypeltogynan." **Phytochemistry** 32, 4: 1041-1044.
90. Gonzalez, A.G., et al. (1989). "Triterpenes of *Hippocratea celastroides* (Celastraceae)." **Revista Latinoamericana de Quimica** 20, 1: 17.
91. Gonzalez, A.G., I.A. Jimenez, and A.G. Ravelo. (1992). "Triterpene from *Maytenus canariensis* and synthesis of a derivative from Betulin." **Phytochemistry** 31, 6: 2069-2072.
92. Ribeiro, S., et al. (2005). "Lupane pentacyclic tricyclic triterpenes isolated from stems and branches of *Maytenus imbricata* (Celastraceae)." **Helvetica Chimica Acta** 88: 1102-1109.
93. Nunez, M.J., et al. (2005). "Lupane triterpenoids from *Maytenus Species*." **Journal of Natural Products** 68: 1018-1021.
94. Fang, S.-D., et al. (1984). "The chemistry of toxic principles from *Maytenus nemerosa*." **Phytochemistry** 23, 3: 631-633.
95. Chen, I.-H., et al. (2008). "Lupane-type triterpenoids from *Microtropis fokienensis* and *Perrottetia arisanensis* and the apoptotic effect of 28-hydroxy-3-oxo-lup-20(29)-en-30-al." **Journal of Natural Products** 71, 8: 1352-1357.
96. Gonzalez, A.G., et al. (1987). "Triterpenes and triterpenoquinones of *Rzedowskia tolantoguensis* (Celastraceae)." **Revista Latinoamericana de Quimica** 18, 2: 83-87.
97. Zhang, Y., et al. (2008). "The absolute stereostructures of three rare d:b-friedobaccharane skeleton triterpenes from the leaves of *Salacia chinensis*." **Tetrahedron** 64: 7347-7352.
98. Tinto, W.F., L.C. Blair, and A. Alli. (1992). "Lupane triterpenoids of *Salacia cordata*." **Journal of Natural Products** 55, 3: 395-398.
99. Bhakuni, R.S., Y.N. Shukla, and R.S. Thaku. (1986). "Constituents of *Cornus capitata.*" **Journal of Natural Products** 49, 4: 714-714.
100. Wada, S.I. and R. Tanaka. (2005). "Betulinic acid and its derivatives, potent DNA topoisomerase II inhibitors, from the bark of *Bischofia javanica.*" **Chemistry & Biodiversity** 2: 689-694.
101. Mutai, C., et al. (2004). "Cytotoxic lupane-type triterpenoids from *Acacia mellifera.*" **Phytochemistry** 65: 1159-1164.
102. Mutai, C., et al. (2007). "Lupane triterpenoids from *Acacia mellifera* with cytotoxic activity." **Molecules** 12: 1035-1044.
103. Mutai, C., et al. (2009). "Antimicrobial activity of *Acacia mellifera* extracts and lupane triterpenes." **Journal of Ethnopharmacology** 123: 143-148.

104. Macias, F.A., A.M. Simonetj, and M.D. Esteban. (1994). "Potential allelopathic lupane triterpenes from bioactive fractions of *Melilotus messanensis.*" **Phytochemistry** 36, 6: 1369-1379.
105. Amaral, L.F.G., et al. (2001). "3,4-*Seco*-lupanes and other constituents from *Platypodium elegans.*" **Fitoterapia** 72: 441-443.
106. Chiang, Y.-M., et al. (2005). "Cytotoxic triterpenes from the aerial roots of *Ficus microcarpa.*" **Phytochemistry** 66: 495-501.
107. Abdel-Bar, F.M., et al. (2008). "Antiproliferative triterpenes from *Melaleuca ericifolia.*" **Journal of Natural Products** 71: 1787-1790.
108. Lee, C.-K. (1998). "A new norlupene from the leaves of *Melaleuca leucadendron.*" **Journal of Natural Products** 61: 376-376.
109. Chang, C.-W., et al. (1999). "Terpenoids of *Syzygium formosanum.*" **Journal of Natural Products** 62: 327-328.
110. Dunstan, C.A., et al. (1998). "Alphitol, a phenolic substance from *Alphitonia zizyphoides* which inhibits prostaglandin biosynthesis *in vitro.*" **Phytochemistry** 48, 3: 495-497.
111. Yagi, A., et al. (1978). "Studies on the constituents of *Zizyphi Fructus*. I. Structure of three new *p*-coumaroylates of alphitoic acid." **Chemical & Pharmaceutical Bulletin** 26, 6: 1798-1802.
112. Chaturvedula, V.S.P., et al., (2006). "Cytotoxic diterpenes from *Cassipourea madagascariensis* from the Madagascar rainforest." **Journal of Natural Products** 69: 287-289.
113. Herz, W., P.S. Santhanam, and I. Ahlberg. (1972). "3-*Epi*betulinic acid, a new triterpenoid from *Picramma pentadra.*" **Phytochemistry** 11: 3061-3063.
114. Caldwell, C.G., et al. (2000). "Oleanane triterpenes from *Junellia tridens.*" **Journal of Natural Products** 63: 1611-1614.
115. Ma, Z.-Z., et al. (2000.) "Three new triterpenoids from *Peganum nigellastrum.*" **Journal of Natural Products** 63: 390-392.
116. Connolly, J.D. and R.A. Hill. (2010). "Triterpenoids." **Natural Product Reports** 27: 79-132.
117. Urban, M., et al. (2004). "Synthesis of a-*seco* derivatives of betulinic acid with cytotoxic activity." **Journal of Natural Products** 67, 7: 1100-1105.
118. Kouzi, S.A., et al. (2000). "Microbial transformations of the antimelanoma agent betulinic acid." **Journal of Natural Products** 63: 1653-1657.
119. Lee, S.-S., et al. (1998). "Preparation and cytotoxic effect of ceanothic acid derivatives." **Journal of Natural Products** 61: 1343-1347.
120. Ling, L.-l. (2008). "Preliminary experiental study of intro antitumor activity of betulonic acid." **Heilongjiang Yiyao** 21, 1: 20-21.
121. Zhang, X.J., et al. (2008). "Study of betulonic acid on anti-tumor by inhibiting PI3K/AKT pathways." **Ziran Kexueban** 24, 3: 261-264.
122. Sun, I.-C., et al. (1998). "Anti-AIDS agents.32. Synthesis and anti-HIV activity of betulin derivatives." **Bioorganic & medicinal chemistry Letters** 8: 1267-1272.

123. Sun, I.-C., et al. (1998). "Anti-AIDS agents. 34: Synthesis and structure-activity relationships of betulin derivatives as anti-HIV agents." **Journal of Medicinal Chemistry** 41: 4648-4657.
124. Hata, K., et al. (2003). "Anti-leukemia activities of lup-28-al-20(29)-en-3-one, a lupane tripterpene." **Toxicology Letters** 143: 1-7.
125. Hata, K., K. Hori, and S. Takahashi. (2002). "Differentiation- and apoptosis-inducing activities by pentacyclic triterpenes on a mouse melanoma cell line." **Journal of Natural Products** 65: 645-648.
126. Jeong, H.-J., et al. (1999). "Preparation of amino acid conjugates of betulinic acid with activity against human melanoma." **Bioorganic & medicinal chemistry Letters** 9: 1201-1204.
127. Reyes, C.P., et al. (2006). "Activity of lupane triterpenoids from *Maytenus* species as inhibitors of nitric oxide and prostaglandin E2." **Bioorganic & Medicinal Chemistry** 14, 5: 1573-1579.
128. Recio, M.C., et al. (1995). "Investigations on the steroidal anti-inflammatory activity of triterpenoids from *Diospyros leucomelas*." **Planta Medica** 65: 9-12.
129. Ito, J., et al. (2001). "Anti-AIDS agents. 48: Anti-HIV activity of moronic acid derivatives and the new melliferone-related triterpenoid isolated from Brazilian propolis." **Journal of Natural Products** 64, 10: 1278-1281.
130. Pavlova, N.I., et al. (2003). "Antiviral activity of betulin, betulinic and betulonic acids against some enveloped and non-enveloped viruses." **Fitoterapia** 74, 5: 489-492.
131. Santos, S.M., et al. (2009). "Antimalarial activity of betulinic acid and derivatives *in vitro* against *Plasmodium falciparum* and in vivo in *P. berghei*-infected mice." **Parasitology research** 105, 1: 275-279.
132. Bianchini, J.-P., et al. (1988). "Dammarane derivatives in the fruit lipids of *Olea madagascariensis*." **Phytochemistry** 27, 7: 2301-2304.
133. Cascon, S.C. and K.S.J. Brown. (1972). "*B*iogenetically significant triterpenes in a species of Meliaceae *: Cabralea polytricha A.Juss.*" **Tetrahedron** 28, 2: 315-323.
134. Aoki, T., S. Ohta, and T. Suga. (1988). "Six novel *seco*-dammarane-type triterpenes from male flowers of *Alnus japonica*" **Phytochemistry** 27,9: 2915-2920.
135. Ohmoto, T., T. Nakaido, and M. Ikuse. (1978). "Constituents of pollen. V: Constituents of *Betula platyphylla* var.*japonica.*" **Chemical & Pharmaceutical Bulletin** 26, 5: 1437-1442.
136. Malinovskaya, G.V., et al. (1980). "A new triterpene from the leaves of *Betula mondschurica.*" **Chemistry of Natural Compounds** 16, 3: 257-261.
137. Fuzzati, N., et al. (1996). "Triterpenoids, lignans and a benzofuran derivative from the bark of *Aglaia elaeagnoidea.*" **Phytochemistry** 42, 5: 1395-1398.
138. Roux, D., et al. (1998). "Foeolins A and B, dammarane tritepenes from *Aglaia foveolata.*" **Phytochemistry** 49, 6: 1745-1748.
139. Mohamad, K., et al. (1999). "Dammarane triterpenes and pregnane steroids from *Aglaia lawii* and *A.tomentosa.*" **Phytochemistry** 51: 1031-1037.

140. Weber, S., et al. (2000). "Phytochemical investigation of *Aglaia rubiginosa.*" **Journal of Natural Products** 63: 636-642.
141. Seger, C., et al. (2008). "Isoeichlerianic acid from *Aglaia silverstris* and revision of the stereochemistry of Foveolin B." **Tetrahedron Letters** 49: 4313-4315.
142. Luo, X.-D., et al. (2000). "Dammarane triterpenoids from *Amoora yunnanensis*." **Heterocycles** 53, 12: 2795-2802.
143. Rao, M.M., et al. (1975). "*Cabralea eichleriana* DC.(Meliaceae)-I : Structure and stereochemistry of wood extractives." **Tetrahedron** 31: 333-339.
144. Govindachari, T.R., G. Suresh, and G.N.K. Kumari. (1994). "Triterpenoids from *Dysoxylum malabaricum.*" **Phytochemistry** 37, 4: 1127-1129.
145. Aalbersberg, W. and Y. Singh. (1991). "Dammarane triterpenoids from *Dysoxylum richii.*" **Phytochemistry** 30, 3: 921-926.
146. Lee, I.M., et al. (2001). "Semialactone, isofouquierone peroxide and fouquierone, three new dammarane triterpenes from *Rhus javanica.*" **Chemical & Pharmaceutical Bulletin** 49, 8: 1024-1026.
147. Fu, L.W., et al. (2005). "Three new triterpenes from *Nerium oleander* and biological activity of the isolated compounds." **Journal of Natural Products** 68: 198-206.
148. Waterman, P.G. and S. Ampofo. (1985). "Dammarane triterpenes from the stem bark of *Commiphora dalzielii.*" **Phytochemistry** 24, 12: 2925-2928.
149. Yoshikawa, M., et al. (2009). "Absolute stereostructures of olibanumols A, B, C, H, I, and J from olibanum, gum-resin of boswellia carterii, and inhibitors of nitric oxide production in lipopolysaccharide-activated mouse peritoneal macrophages." **Chemical & Pharmaceutical Bulletin** 57, 9: 957-964.
150. Ahmad, V.U. and K.A. Alvi. (1987). "Deacetoxybrachycarpone, A trinortriterpenoid from *Cleome brachycarpa.*" **Phytochemistry** 26, 1: 315-316.
151. Wang, K.-W., et al. (2006). "Novel bioactive dammarane caffeoyl esters from *Celastrus rosthornianus.*" **Planta Medica** 72: 370-372.
152. Carrick, J., K.C. Chan, and H.T. Cheung. (1968). "A new phytochemical survey of Malaya-chemical screening." **Chemical & Pharmaceutical Bulletin** 16, 12: 2436-2441.
153. Tanaka, R., K. Masuda, and S. Matsunaga. (1993). "Lup-20(29)-en-3β,15α-diol and ocotillol-II from the stem bark of *Phyllanthus flexuosus*" **Phytochemistry** 32, 2: 472-474.
154. Warnhoff, E.W. and M.M. Halls. (1965). "Desert plant constituents II ocotillol: An intermediate in the oxidation of hydroxy isooctenyl side chains." **Canadian Journal of Chemistry** 43: 3311-3323.
155. Butruille, D. and X.A. Dominguez. (1974). "Fouquierol et Isofouquierol: Deux nouveaux triterpenes de la serie du dammarane." **Tetrahedron Letters** 15, 8: 639-642.
156. Kitagima, J., K. kimizuka, and Y. Tanaka. (1999). "New dammarane-type acetylated triterpenoids and their related compouds of *Ficus pumila* fruit." **Chemical & Pharmaceutical Bulletin** 47, 8: 1138-1140.

157. Cysne, J.B., et al. (2006). "^{1}H and ^{13}C NMR spectral assignments of four dammarane triterpenoids from carnauba wax." **Magnetic Resonance in Chemistry** 44, 641-643.
158. Pakhathirathien, C., et al. (2005). "Dammarane triterpenes from the hypocotyls and fruits of *Ceriops tagal*." **Journal of Natural Products** 68: 1787-1789.
159. Baker, P.M., E.J.L. Barreiro, and B. Gilbert. (1976). "Tetracyclic triterpenes of *Barbacenia bicolor*." **Phytochemistry** 15: 785-787.
160. Akihisa, T., et al. (2004). "3-*Epi*cabraleahydroxylactone and other triterpenoids from camellia oil and their inhibitory effects on Epstein–Barr virus activation." **Chemical & Pharmaceutical Bulletin** 52, 1: 153-156.
161. Nagaya, H., et al. (1997). "Cytotoxic triterpenes from *Cleome africana*." **Phytochemistry** 44, 6: 1115-1119.
162. Ukiya, M., et al. (2001). "Constituents of Compositae plants. 2: Triterpene diols, triols, and their 3-o-fatty acid esters from edible Chrysanthemum flower extract and their anti-inflammatory effects." **Journal of Agricultural and Food Chemistry** 49: 3187-3197.
163. Govindachari, T.R., et al. (1995). "Structure-related insect antifeedant and growth regulating activities of some limonoids." **Journal of Chemical Ecology** 21, 10: 1585-1600.
164. Galman, J.L. and H.C. Hailes. (2009). "Application of a modified Mosher's method for the determination of enantiometric ratio and absolute configuration at C-3 of chiral 1,3-dihydroxy ketones." **Tetrahedron: Asymmetry** 20: 1828-1831.
165. Xiao, L., et al. (1997). "Study for the determination of the absolute configuration of fluoromethylated secondary alcohols by the modified Mosher method." **Journal of Fluorine Chemistry** 84: 19-23.
166. Chen, H., et al. (2009). "A route to enantiomerically pure 5-(2'-hydroxyethyl)cyclopent-2-en-1-ol and its absolute configuration by Mosher esters". **Tetrahedron: Asymmetry** 20: 449-456.
167. Kouda, K., T. Ooi, and T. Kusumi. (1999). "Application of the modified Mosher's method to linear 1,3-diols." **Tetrahedron Letters** 40: 3005-3008.
168. Dale, J.A. and H.S. Mosher. (1973). "Nuclear magnetic resonance enantiomer reagents.: Configurational correlations via nuclear magnetic resonance chemical shifts of diastereomeric mandelate, 0-methylmandelate, and α-methoxy-α-trifluoromethylphenylacetate (MTPA) esters." **Journal of the American Chemical Society** 95, 2: 512-519.
169. Ohtani, I., et al. (1991). "High-field FT NMR application of Mosher's method.: The absolute configurations of marine terpenoids." **Journal of the American Chemical Society** 113: 4092-4096.
170. Ishiyama, M., et al. (1993). "A new sulfonated tetrazolium salt that produces a highly water-soluble formazan dye." **Chemiacal & Pharmaceutical Bulletin** 41, 6: 1118-1122.
171. Ishiyama, M., et al. (1995). "Novel disulfonated tetrazolium salt that can be reduced to a water-soluble formazan and its application to the assay of lactate dehydrogenase." **Analyst** 120: 113-116.

172. Vistica, D., et al. (1991). "Tetrazolium-based assays for cellular viability: A critical examination of selected parameters affecting formazan production." **Cancer Research** 51: 2515-2520.
173. Brien, J., et al. (2000). "Investigation of the alamar blue (resazurin) fluorescent dye for the assessment of mammalian cell cytotoxicity." **European Journal of Biochemistry** 267: 5421-5426.
174. Sarker, S.D., L. Nahar, and Y. Kumarasamy. (2007). "Microtitre plate-based antibacterial assay incorporating resazurin as an indicator of cell growth, and its application in the *in vitro* antibacterial screening of phytochemicals." **Methods** 42, 4: 321-324.
175. Anopkumar-Dukie, S., et al. (2005). "Resazurin assay of radiation response in cultured cells." **The British Journal of Radiology** 78: 945-947.
176. Bunyavejchewin, S., et al. (2009). **Forest trees of Huai Kha Khaeng wildlife sanctuary, Thailand: Data from the 50-hectare forest dynamics plot.** Bangkok: National Parks, Wildlife and Plant Conservation Department, Thailand.
177. Suvatti, C. (1978) "Dipterocarpaceae" in **Flora of Thailand**. 870-872. Bangkok: Kurusapha.
178. Ge, H.M., et al. (2006). "Bioactive oligostilbenoids from the stem bark of *Hopea exalata*." **Journal of Natural Products** 69, 12: 1800-1802.
179. Nguyen, Q.H., et al. (2007). "Oligostilbenes from stem bark of *Hopea odorata* Roxb." **Tap Chi Duoc Hoc** 47, 4: 37-39.
180. Berreirosa, M.L., et al. (2002). "Fatty acid esters of triterpenes from *Erythroxylum passerinum.*" **Journal of the Brazilian Chemical Society** 13, 5: 669-673.
181. Macias, F.A., et al. (1998). "Bioactive polar triterpenoids from *Melilotus messanenis*." **Phytochemistry** 49, 3: 709-717.
182. Macias, F.A., J.C.G. Galindo, and G.M. Massanet. (1992). "Potential allelopathic activity of several sesquiterpene lactone models." **Phytochemistry** 31, 6: 1969-1977.
183. Karanewsky, D.S., M.F. Malley, and J.Z. Gougoutas. (1991). "Practical synthesis of an enantiomerically pure synthon for the preparation of mevinic acid analogs." **Journal of Organic Chemistry** 56, 11: 3744-3747.
184. Lamshöft, M., H. Schmickler, and F.-J. Marner. (2003). "Determination of the absolute configuration of hydroxyiridals by chiroptical and NMR spectroscopic methods." **European Journal of Organic Chemistry** 2003, 4: 727-733.
185. Mahato, S.B. and A.P. Kundua. (1994). "^{13}C NMR spectra of pentacyclic triterpenoids—a compilation and some salient features." **Phytochemistry** 37, 6: 1517-1575.
186. Addae-Mensah, I. and H. Achenbach. (1985). "Terpenoids and flavonoids of *Bridelia ferruginea.*" **Phytochemistry** 24, 8: 1817-1819.
187. Bandeira, P.N., et al. (2007). "Obtention of derivatives from the α- and β-amyrin triterpenoid mixture: ^{13}C NMR data." **Revista Brasileira de Farmacognosia** 17, 2: 204-208.

188. Schuhr, C.A., et al. (2003). "Quantitative assesment of crosstalk between the two isoprenoid biosynthesis pathways in plants by NMR spectroscopy." **Phytochemistry Reviews** 2: 3-16.
189. Maldonado, E., et al. (1998). "Acyclic diterpenes from *Perymenium hintonii*." **phytochemistry** 49, 4: 115-118.
190. Salazar, G.C.M., et al. (2000). "Two epimeric friedelane triterpenes isolated from *Maytenus truncata* Reiss: ^{1}H and ^{13}C Chemical shift assignments." **Magnetic Resonance in Chemistry** 38: 977-980.
191. Morten, C.J. and B.A. Sparling. (2007). " **Application of NMR techniques to the structure determination of caryophyllene oxide (unknown #92)**." Accessed November 4th, 2009. Available from: http://ocw.mit.edu/NR/rdonlyres/Chemistry/5-46Spring-2007/0E512A9E-1BAC-4A9C-9FEE-2E3842C90001/0/546_project1.pdf.
192. Skold, M., et al. (2006). "The fragrance chemical b-caryophyllene—air oxidation and skin sensitization." **Food and Chemical Toxicology** 44,: 538-545.
193. Kitajima, J., M. Shindo, and Y. Tanaka. (1990). "Two new triterpenoid sulfates from the leaves of *Schefflera octaphylla*." **Chemical & Pharmaceutical Bulletin** 38, 3: 714-716.
194. Hiroya, K., et al. (2002). "Synthesis of betulin derivatives and their protective effects against the cytotoxicity of cadmium." **Bioorganic & medicinal chemistry** 10: 3229-3236.
195. Komissarova, N.G., et al. (2002). "Selective Oxidation of Betulin by Cr(VI) Reagents." **Chemistry of Natural Compounds** 38, 1: 58-61.
196. Sy, L.-K., R.M.K. Saunders, and G.D. Brown. (1997). "Phytochemistry of *Illicium dunnianum* and the systematic position of the Illiaciaceae." **Phytochemistry** 44, 6: 1099-1108.
197. Anjaneyulu, V., et al. (1985). "Triterpenoids from *Mangifera indica*." **Phytochemistry** 24, 10: 2359-2367.
198. Subarnas, A., et al. (1993). "Pharmacological properties of β-amyrin palmitate, a novel centrally acting compound, isolated from *Lobelia inflata* leaves." **Journal of Pharmacy and Pharmacology** 45, 6: 545-550.
199. Subarnas, A., et al. (1993). "A possible mechanism of antidepressant activity of β-amyrin palmitate isolated from *Lobelia inflata* leaves in the forced swimming test." **Life Sciences** 52, 3: 289-296.
200. Holanda Pinto, S.A., et al. (2008). "Anti-inflammatory effect of α, β-amyrin, a pentacyclic triterpene from *Protium heptaphyllum* in rat model of acute periodontitis." **Inflammopharmacology** 16, 1: 48-52.
201. Murthy, K. and S. Mishra. (2009). "Quantification of β-sitosterol from *Mucuna pruriens* by TL C" **Chromatographia** 69, 1-2: 183-186.
202. Chavana, M.J., P.S. Wakteb, and D.B. Shinde. (2010). "Analgesic and anti-inflammatory activity of caryophyllene oxide from *Annona squamosa* L. bark" **Phytomedicine** 17,2: 149-151.

203. Mambu, L., et al. (2006). "Clerodane and labdane diterpenoids from *Nuxia sphaerocephala*." **Phytochemistry** 67: 444-451.
204. Fukuda, Y., et al. (2006). "Lupane and oleanane triterpenoids from the cones of *Liquidamber styraciflua*." **Journal of Natural Products** 69: 142-144.
205. Cheung, H.T. (1972). "Constituents of Dipterocarpaceae resins IV: Triterpenes of *Shorea acuminata* and *S. resina-nigra*." **Australian Journal of Chemistry** 25: 2003-2012.
206. Bisset, N.G., et al. (1971). "Constituants sesquiterpeniques et triterpeniques des resines du genere *Shorea*." **Phytochemistry** 10: 2451-2463.
207. Cabriela, G.M., M. Gallo, and A.M. Seldes. (1996). "Cycloartane derivatives from *Tillandsia usneoides.*" **Journal of Natural Products** 59: 343-347.
208. Anjaneyulu, V., et al. (1999). "Triterpenoids from *Mangifera indica.*" **Phytochemistry** 50: 1229-1236.
209. Silva, G.L., et al. (1997). "Novel cytotoxic ring-a *seco*-cycloartane triterpenes from *Gardenia coronaria* and *G.sootepensis*." **Tetrahedron** 53, 2: 529-538.
210. Nuanyai, T., et al. (2010). "Cytotoxic 3,4-*seco*-cycloartane triterpenes from the exudate of *Gardenia tubifera.*" **Journal of Natural Products** 73, 1: 51-54.
211. Nuanyai, T., et al. (2009.) "Cytotoxic 3,4-*seco*-cycloartane triterpenes from *Gardenia sootepensis.*" **Journal of Natural Products** 72, 6: 1161-1164.
212. Lee, D., et al. (2001). "Novel 29-nor-3,4-*seco*-cycloartane triterpene methyl esters from the aerial parts of *Antirhea acutata*." **Tetrahedron** 57, 33: 7107-7112.
213. Lee, D., et al. (2001). "Cyclooxygenase-inhibitory and antioxidant constituents of the aerial parts of *Antirhea acutata.*" **Bioorganic & medicinal chemistry Letters** 11: 1565-1568.
214. Li, R.-Y., et al. (2003). "Micranoic acids A and B: two new octanortriterpenoids from *Schisandra micrantha.*" **Chem. Pharm. Bull**. 51, 10: 1174-1176.
215. Sy, L.-K. and G.D. Brown. (1999). "New *seco*-cycloartanes from *Kadsura coccinea* and the assisted autoxidation of a tri-substituted alkene." **Tetrahedron** 55: 119-132.
216. Cabriela, G.M., M. Gallo, and A.M. Seldes. (1995). "A 3,4-*seco*-cycloartane derivative from *Tillandsia usneoides.*" **Phytochemistry** 39, 3: 665-666.
217. Yang, X.-W., et al. (2010). "Abiesatrines A–J: anti-inflammatory and antitumor triterpenoids from *Abies georgei Orr.*" **Organic & Biomolecular Chemistry** 8: 2609-2616.
218. Kennedy, E.M., et al. (2011)., "Semisynthesis and biological evaluation of ganodermanontriol and its stereoisomeric triols." **Journal of Natural Products** 74: 2332-2337.
219. Banskota, A.H., et al. (2000). "Thirteen novel cycloartane-type triterpenes from *Combretum quadrangulare*." **Journal of Natural Products** 63, 1: 57-64.
220. Galgon, T., D. Hoke, and B. Drager. (1999). "Identification and quantification of betulinic acid." **Phytochemical analysis** 10: 187-190.
221. Saxena, B.B., et al. (2006). "Boc-lysinated-betulonic acid: a potent, anti-prostate cancer agent." **Bioorganic & Medicinal Chemistry** 14, 18: 6349-6358.

222. Mills, J.S. and A.E.A. Werner. (1955). "The chemistry of damar resin." **Journal of Chemical Society**: 3132-3140.
223. Mesquita, M.L., et al. (2007). "*In vitro* antiplasmodial activity of *Brazilian cerrado* plants used as traditional remedies." **Journal of Ethnopharmacology** 110: 165-170.
224. Desjardins, R.E., et al. (1979). "Quantitative assessment of antimalarial activity *in vitro* by a semiautomated microdilution technique." **Antimicrobial Agents and Chemotherapy** 16, 6: 710-718.
225. Chulay, J.D., J.D. Haynes, and C.L. Diggs. (1983). "*Plasmodium falciparum*: Assessment of *in vitro* growth by [3h] hypoxanthine incorporation." **Experimental Parasitology** 55: 138-146.
226. Corey, E.J., B.E. Roberts, and B.R. Dixon. (1995). "Enantioselective total synthesis of β-elemene and fuscol based on enantiocontrolled ireland-claisen rearrangement." **Journal of the American Chemical Society** 117: 193-196.
227. Asakawa, J., et al. (1977). "^{13}C NMR study of Ginseng sapogenins and their related dammarane type triterpenes." **Tetrahedron** 33: 1935-1939.
228. Quispel, A., et al. (1989). "Identification of Dipterocarpol as isolation factor for the induction of primary isolation of frankia from root nodules of *Alnus glutinosa* (L.) Gaertner." **Molecular Plant-Microbe Interactions** 2, 3: 107-112.
229. Crabbe, P., G. Ourisson, and T. Takahashi. (1958). "Le Dipterocarpol-I: Preparation de la 8,14-dimethyl 18 -nor-testosterone." **Tetrahedron** 3: 279-302.
230. Malinovskaya, G.V., et al., (1982). "Partial synthesis of octanor-13β-dammarane." **Chemistry of Natural Compounds** 18, 5: 560-564.
231. Yamashita, H., et al. (1998). "Dammarane triterpenoids from rhizomes of *Pyrrosia lingua*." **Phytochemistry** 49, 8: 2461-2466.
232. Spencer, G.F. (1981). "Dammarenediol II esters from *Cacalia atriplicifolia* L. seed oil." **Journal of Natural Products** 44, 2: 166-168.
233. Johnson, W.S., et al. (1999). "The fluorine atom as a cation-stabilizing auxiliary in biomimetic polyene cyclizations: Total synthesis of dl-dammarenediol." **Journal of Organic Chemistry** 64: 9587-9595.
234. Monaco, P., et al. (1973). "Neutral triterpenes from the galls of *Pistacia terebinthus*." **Phytochemistry** 12: 939-942.
235. Biellmann, J.-F., P. Crabbe, and G. Ourisson. (1958). "Le Dipterocarpol-II: Stereochimie en C-13 et en C-17." **Tetrahedron** 3: 303-309.
236. Lao, X.-D., et al. (2000). "Dammarane triterpenoids from *Amoora yunnanensis*." **Heterocycles** 53, 12: 2795-2802.
237. Rivero-Cruz, J.F., et al. (2004). "Cytotoxic constituents of the twigs and leaves of *Aglaia rubiginosa.*" **Journal of Natural Products** 67: 343-347.
238. Hwang, B.Y., et al. (2004). "Silvestrol and *epi*silvestrol, potential anticancer rocaglate derivatives from *Aglaia silvestris.*" **Journal of Organic Chemistry** 69: 3350-3358.
239. Rao, M.M., et al. (1975). "Structure and stereochemistry of limonoids of *Cabralea eichleriana.*" **Phytochemistry** 14: 1071-1075.

240. Arriaga, A.M.C., et al. (2002). "Chemical constituents of *Simarouba versicolor.*" **Annals of the Brazilian Academy of Sciences** 74, 3: 415-424.
241. Thoison, O., et al. (2004). "Insect antifeedant compound from *Nothofagus dombeyi* and *N.pumilio.*" **Phytochemistry** 65: 2173-2176.
242. Pokhilo, N.D., et al. (1985). "Triterpenoids from the leaves of the Siberian species of Birch *Betula nana* and *B.exilis.*" **Chemistry of Natural Compounds** 21, 3: 328-332.
243. Zorina, A.D., et al. (1997). "Synthesis of *seco*-acids of the dammarane series." **Pharmaceutical Chemistry Journal** 31, 6: 330-332.
244. Wei, Y., C.-M. Ma, and M. Hattori. (2009). "Synthesis of dammarane-type triterpene derivatives and their ability to inhibit HIV, and HCV protease." **Bioorganic & Medicinal Chemistry** 17: 3003-3010.
245. Kim, K.-S., et al. (1997). "A novel triterpene f*rom Hedera rhombea.*" **Archives of Pharmacal Research** 20, 2: 191-193.
246. Seldes, A.M., M.S. Maier, and E. Gros. (1986). "^{13}C NMR studies of epimeric 20(*R,S*)-hydroxy-23-norcholanoic acid derivatives." **Magnetic Resonance in Chemistry** 24: 239-242.

APPENDIX

Spectroscopic spectrum of new compounds

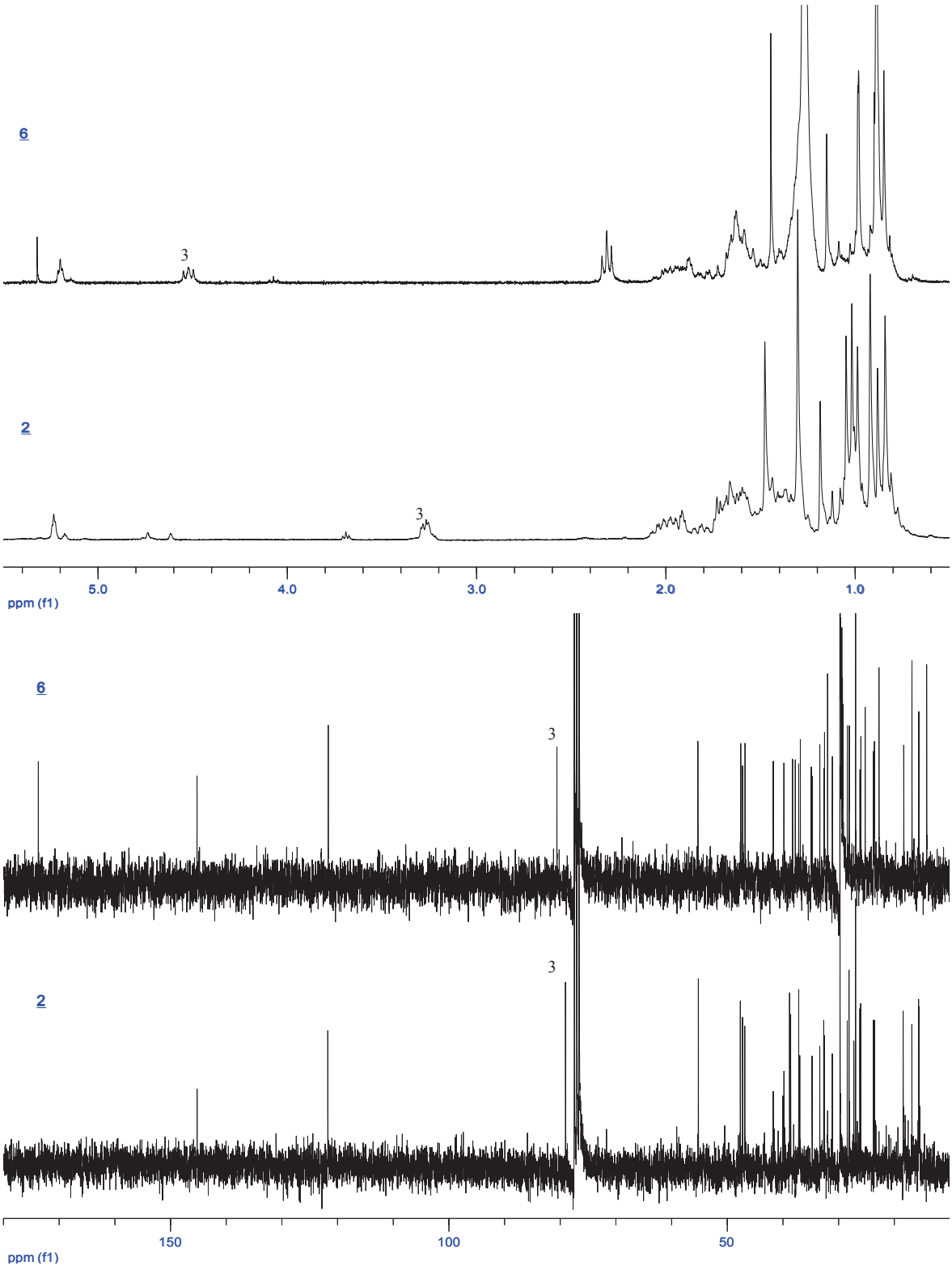

Figure 41. The ^{1}H (300 MHz) and ^{13}C NMR (75 MHz) spectrum of **2 and 6** (in $CDCl_3$)

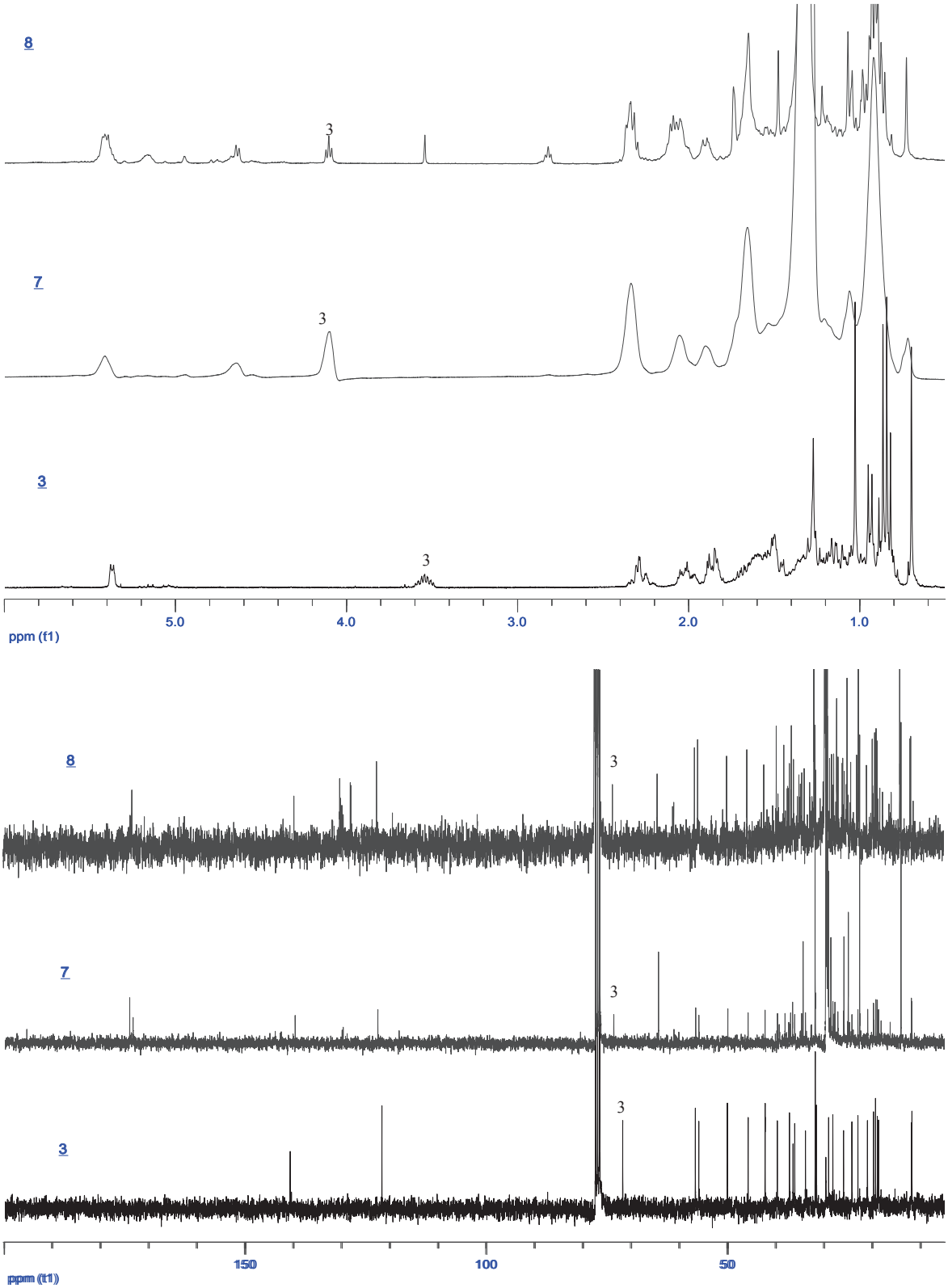

Figure 42. The ^{1}H (300 MHz) and ^{13}C NMR (75 MHz) spectrum of **3**, **7** **and** **8** (in $CDCl_3$).

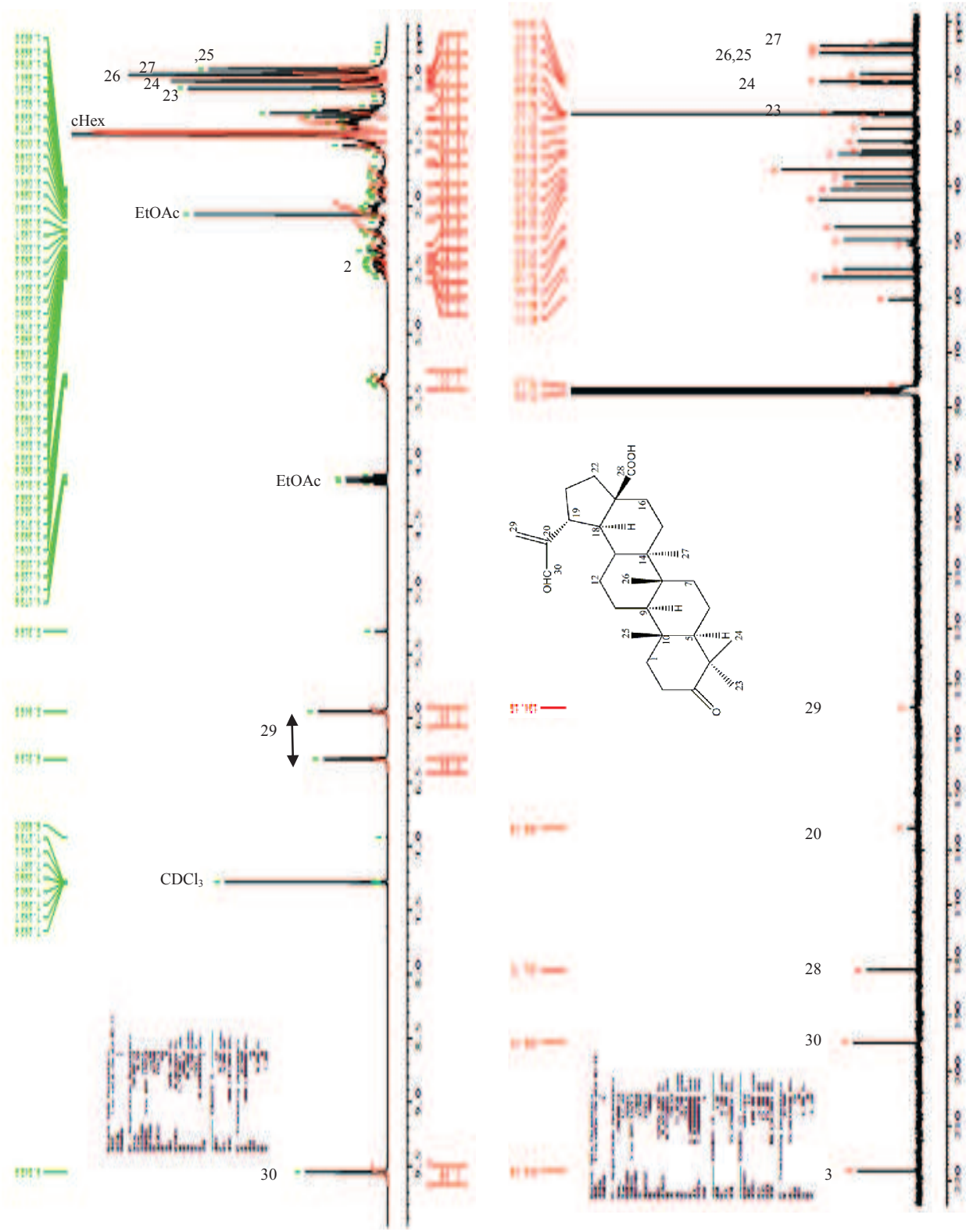

Figure 43. The ^{1}H (300 MHz) and ^{13}C NMR (75 MHz) spectrum of **14** (in $CDCl_3$).

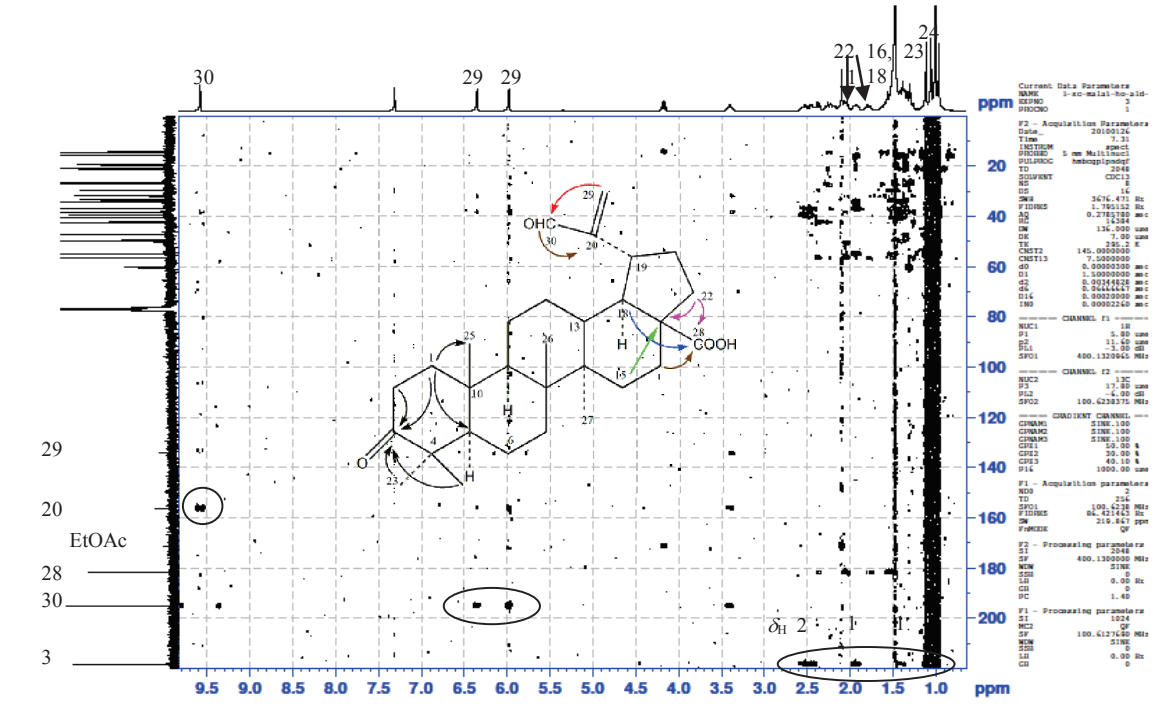

a

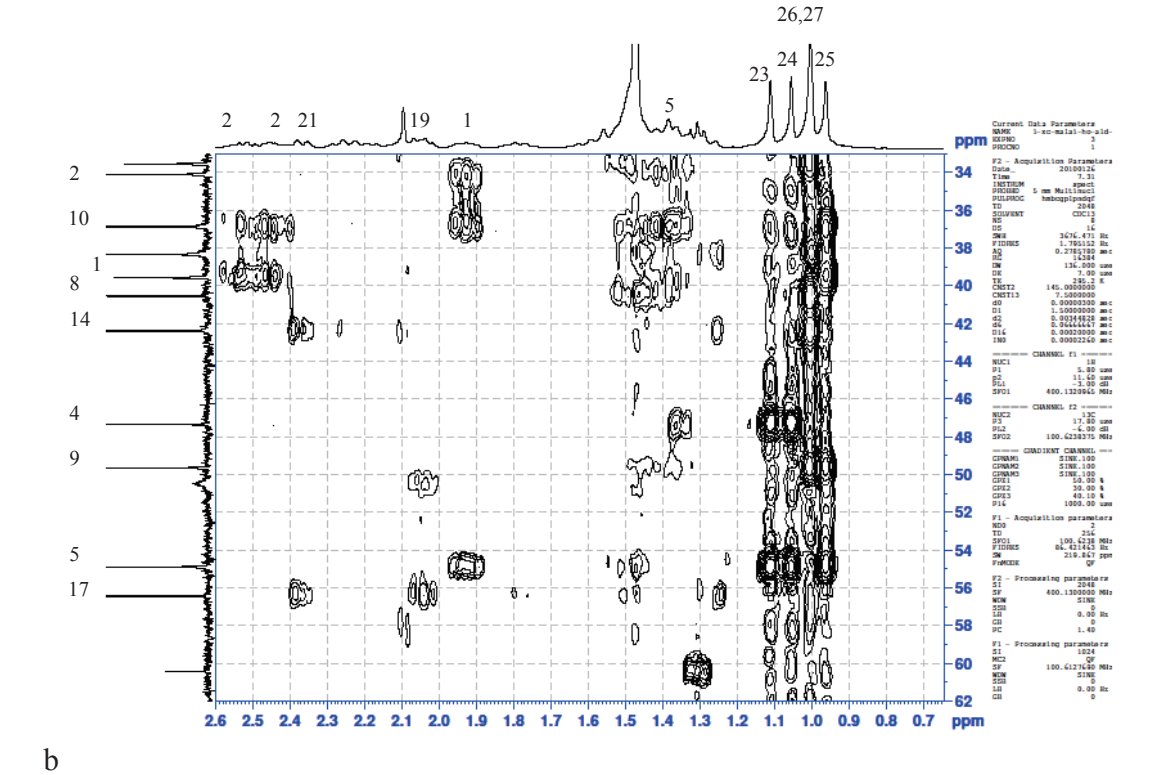

b

Figure 44. The HMBC correlation of **14** (in $CDCl_3$). a) whole spectrum b.) expanded HMBC spectrum in the range of δ_H 0.7-2.6 ppm and δ_C 33-62 ppm.

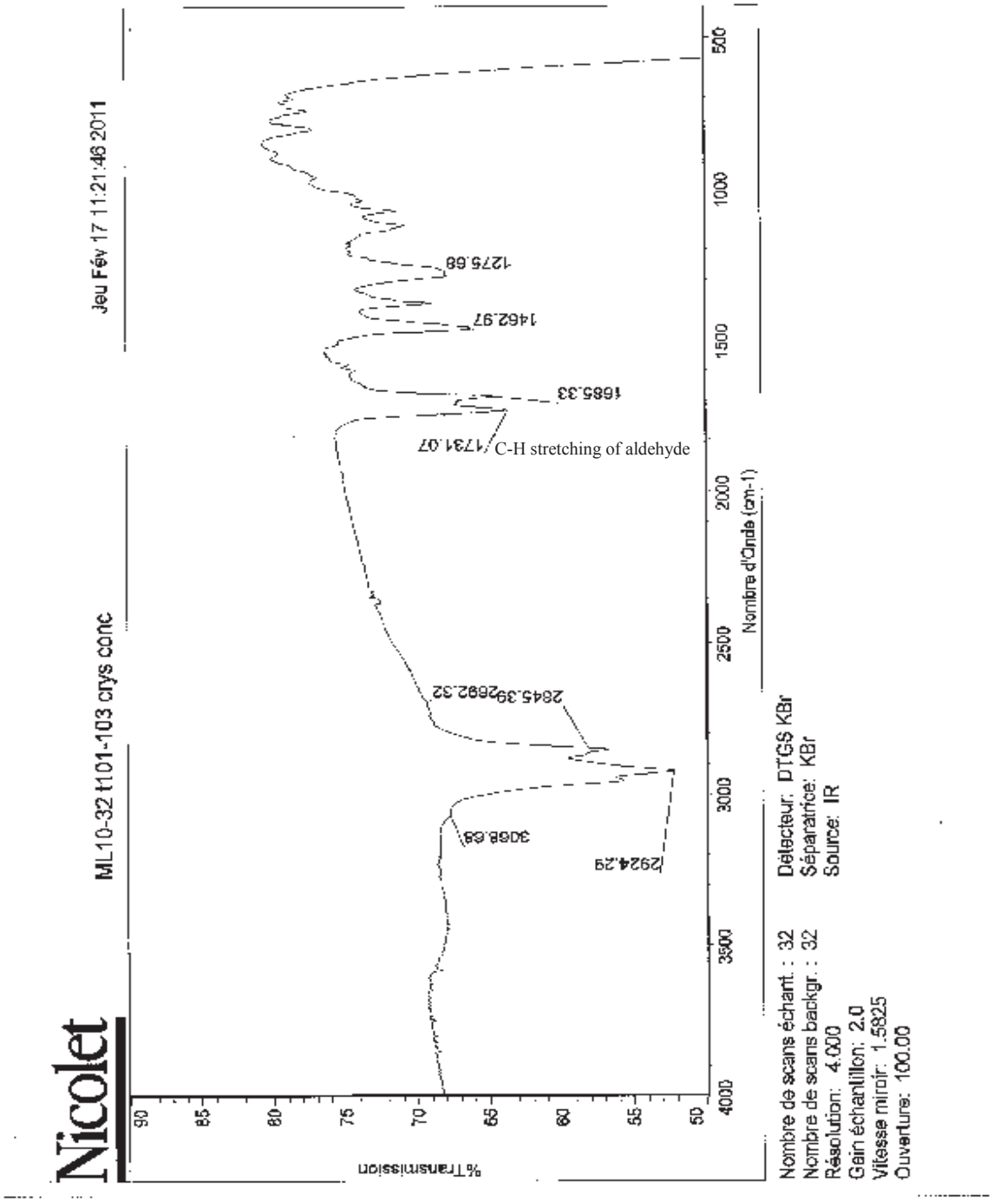

Figure 45. IR spectrum of **14**. (dry film)

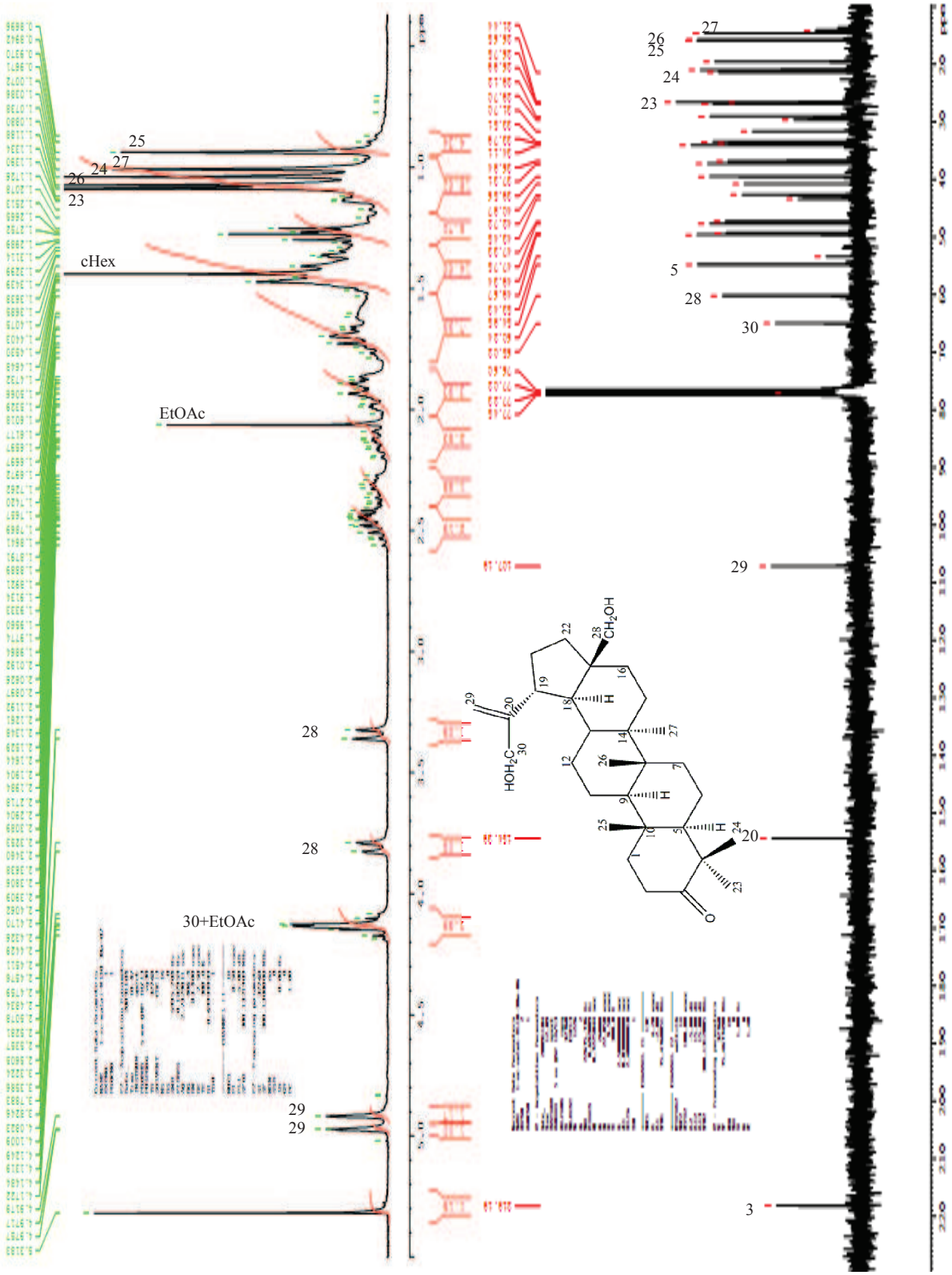

Figure 46. The ^{1}H (300 MHz) and ^{13}C NMR (75 MHz) spectrum of **16** (in $CDCl_3$).

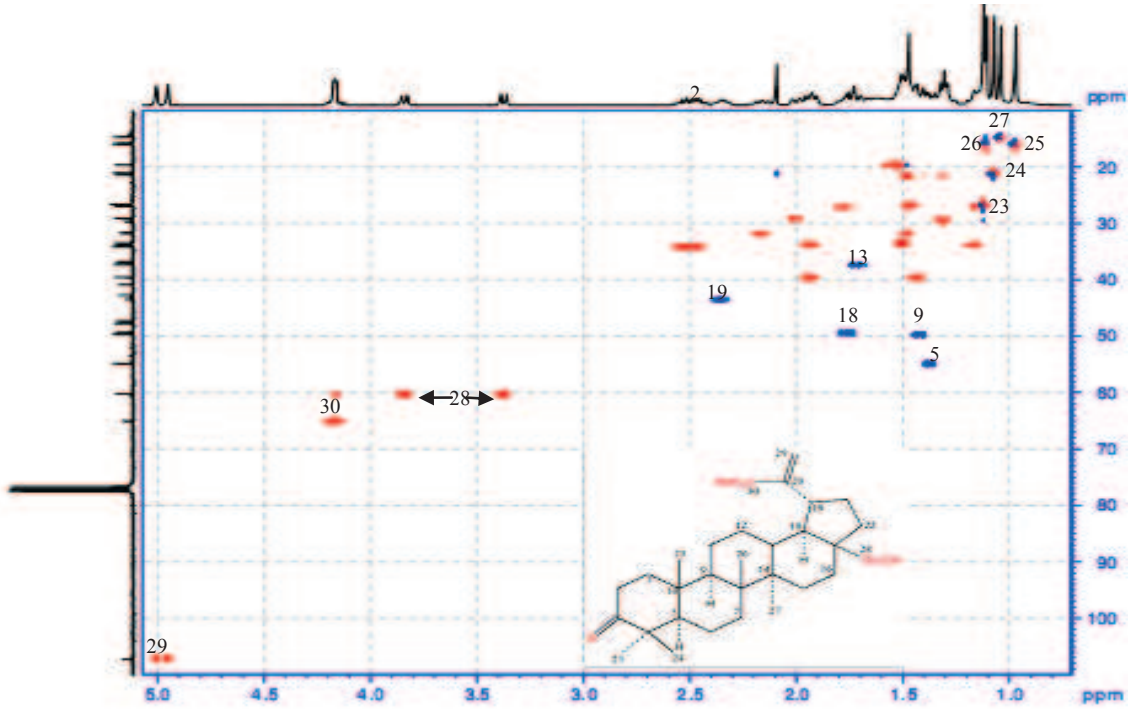

Figure 47. Expanded HSQCedited spectrum of **16** (in $CDCl_3$) in the range of δ_H 0.7-5.1 ppm and δ_C 10-110 ppm.

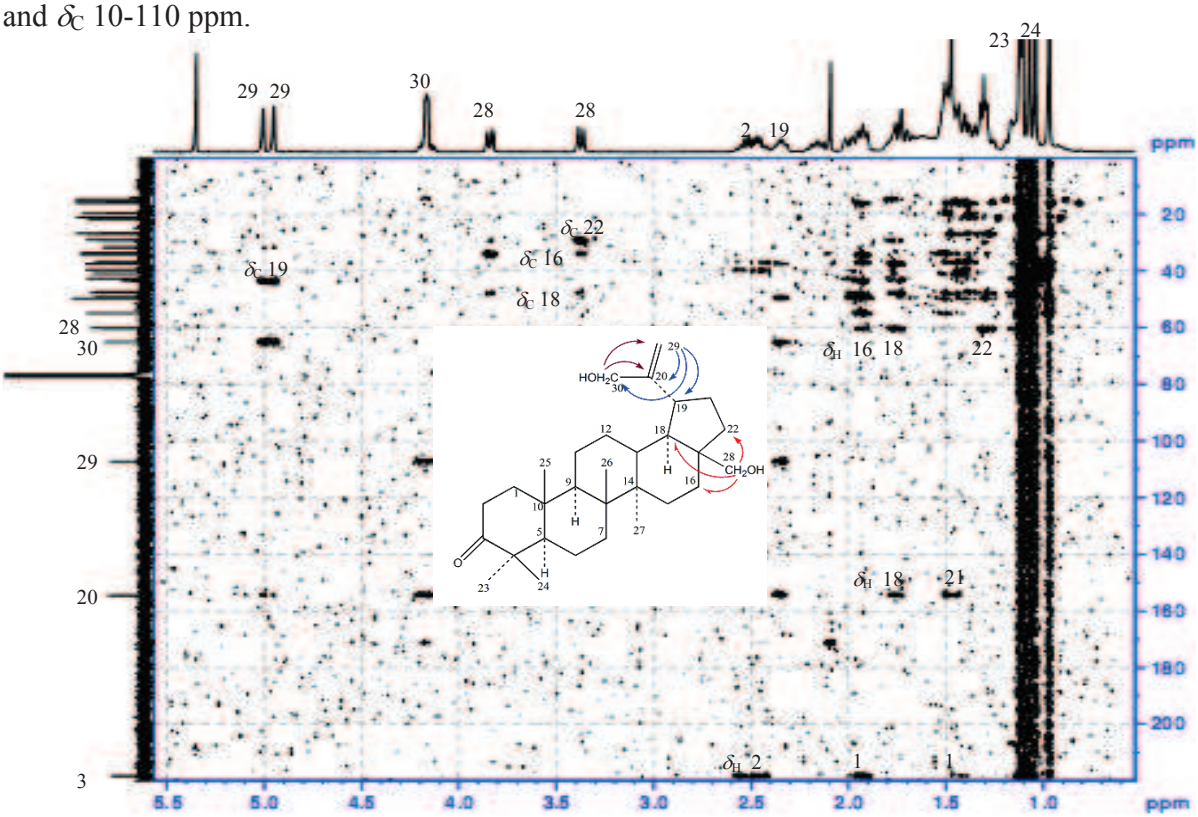

Figure 48. The HMBC correlation of **16** (in $CDCl_3$).

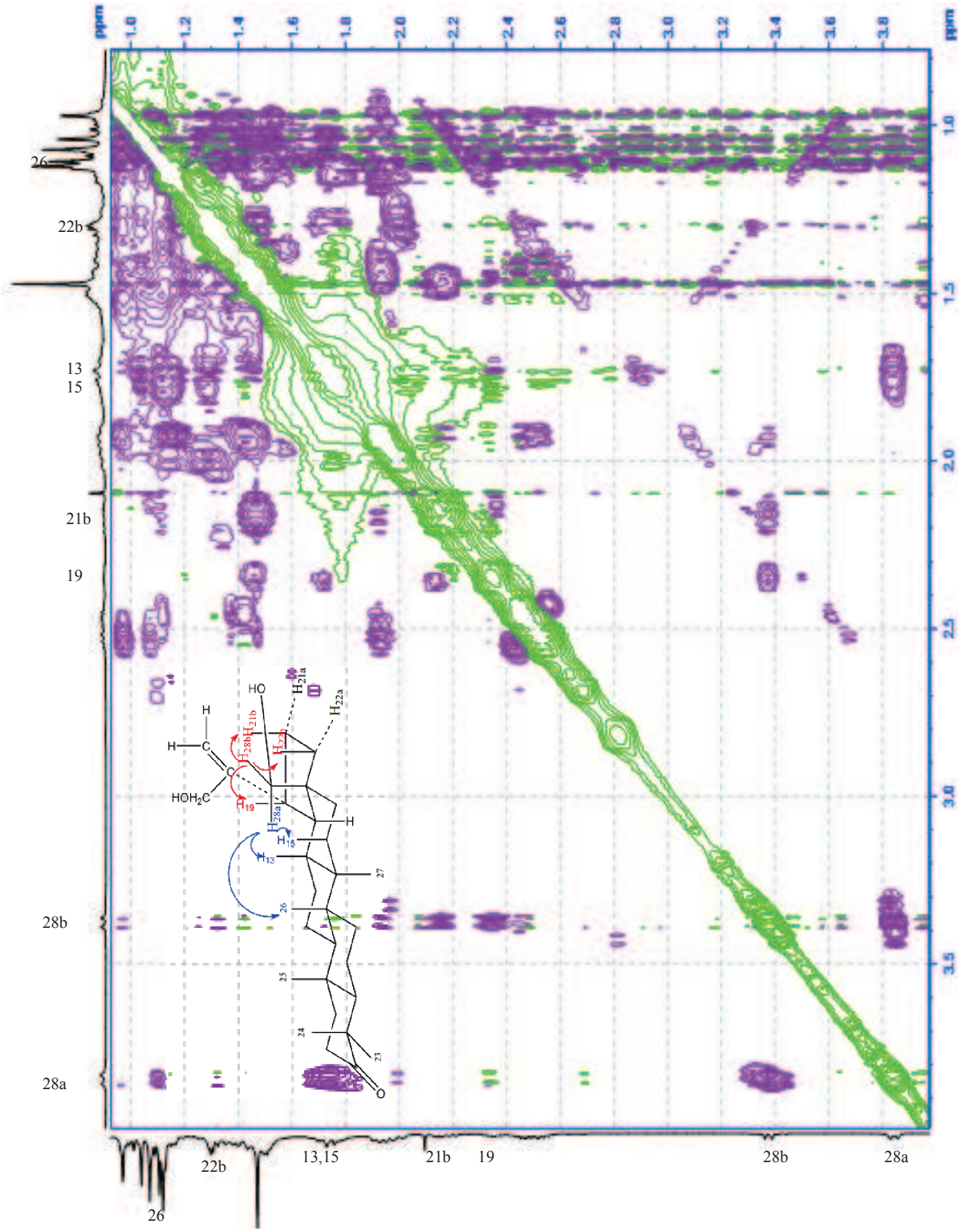

Figure 49. The expanded NOESY spectrum of **16** (in $CDCl_3$) in the range of δ_H 0.8-4.0 ppm.

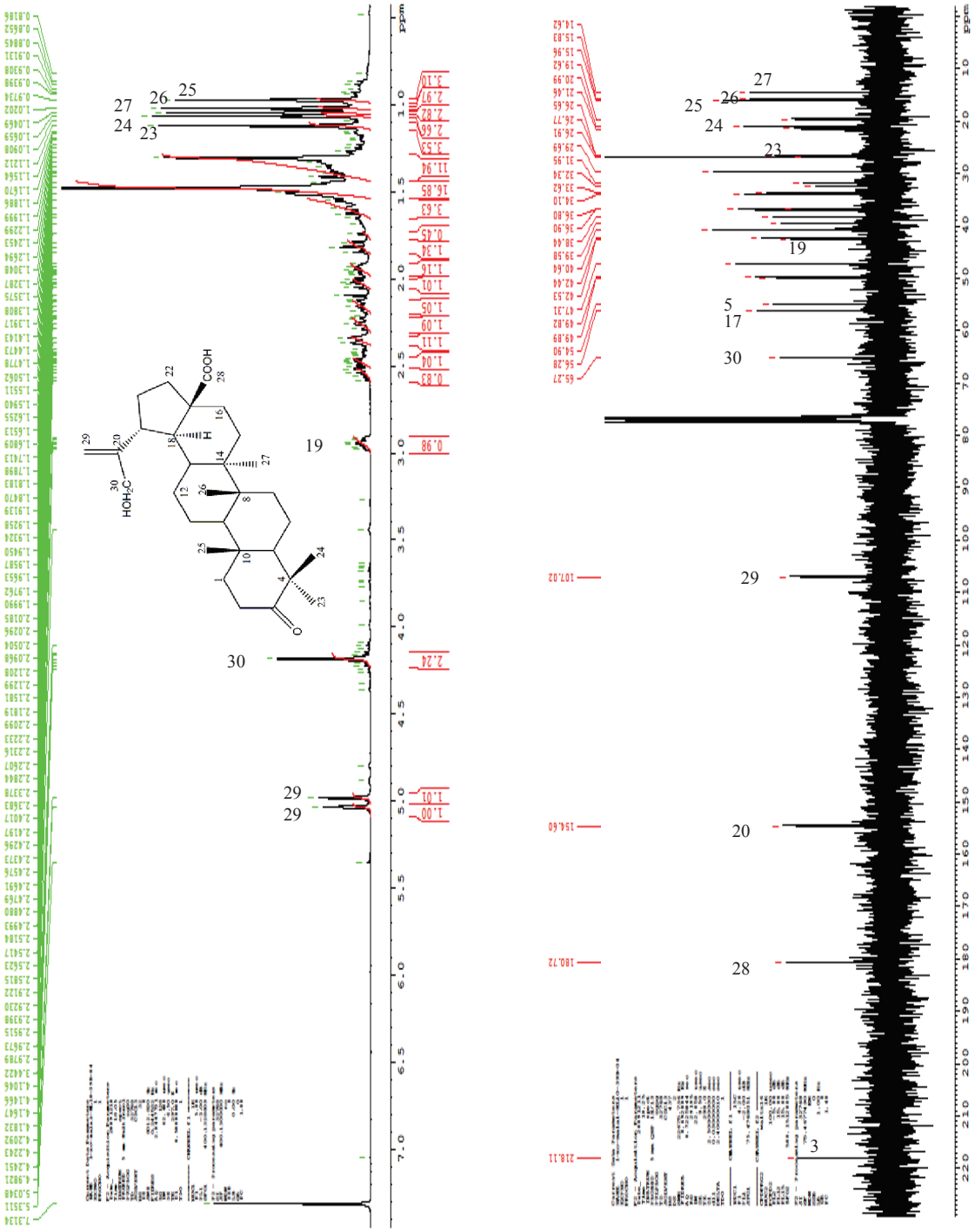

Figure 50. The ^{1}H (300 MHz) and ^{13}C NMR (75 MHz) spectrum of **17** (in $CDCl_3$).

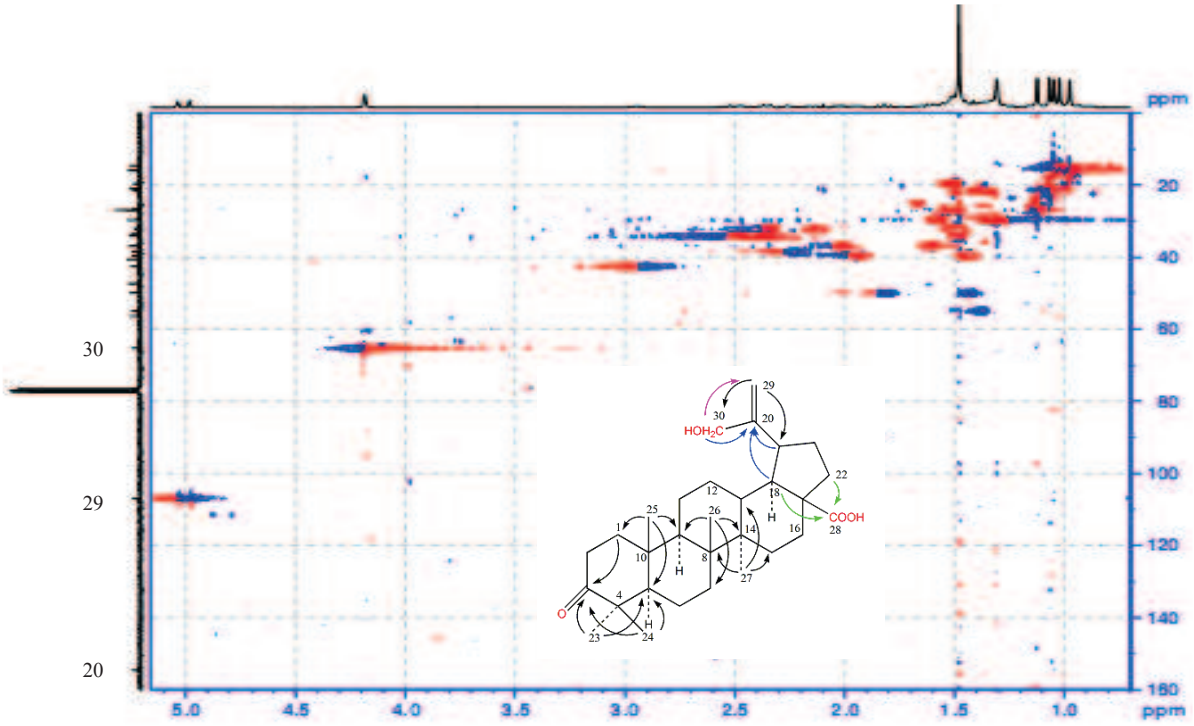

Figure 51. Expanded HSQCedited spectrum of **17** (in $CDCl_3$) in the range of δ_H 0.7-5.2 ppm and δ_C 0-160 ppm.

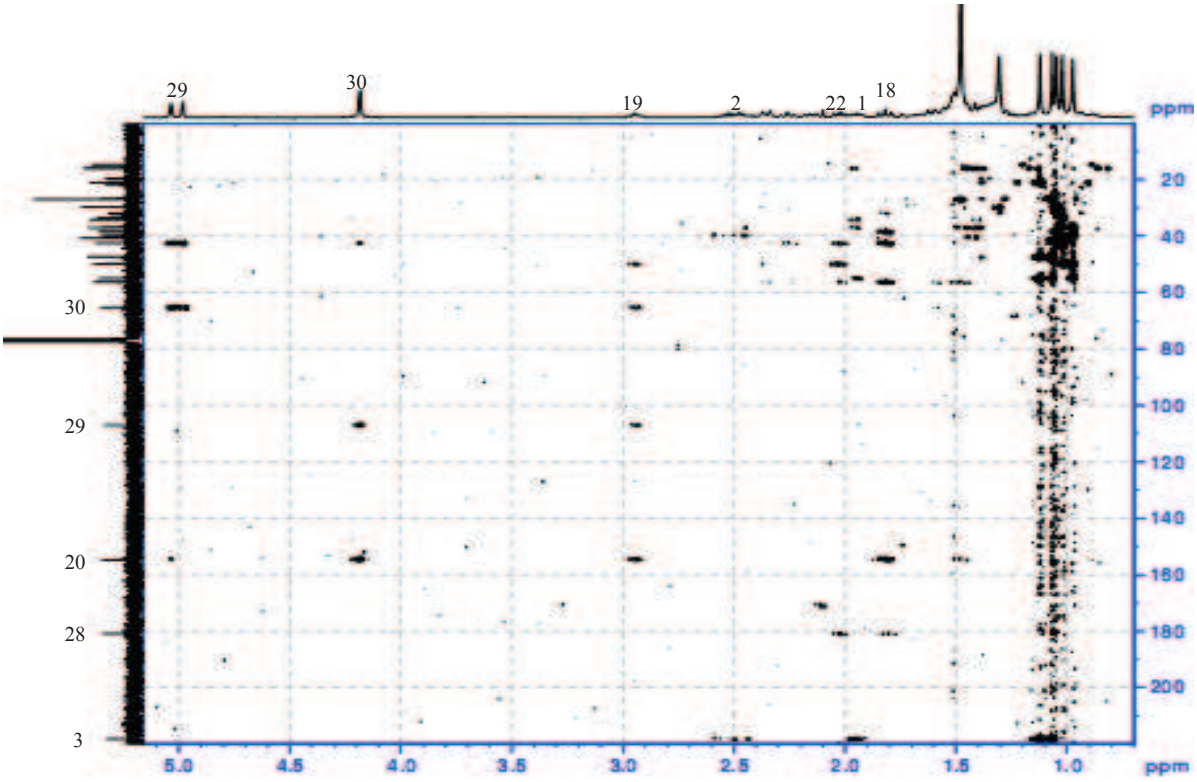

Figure 52. The HMBC correlation of **17** (in $CDCl_3$).

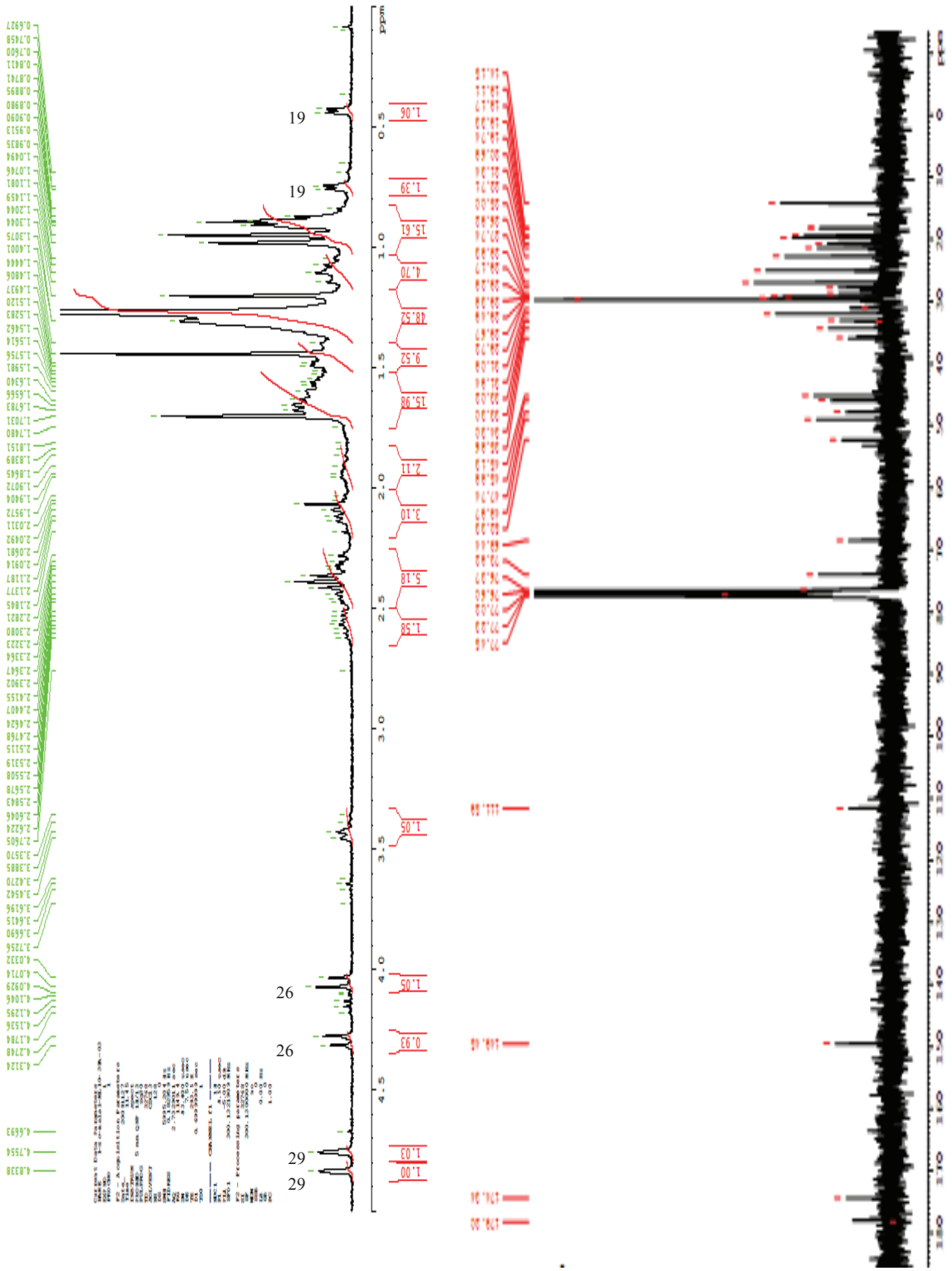

Figure 53. The ^{1}H (300 MHz) and ^{13}C NMR (75 MHz) spectrum of **18** (in $CDCl_3$).

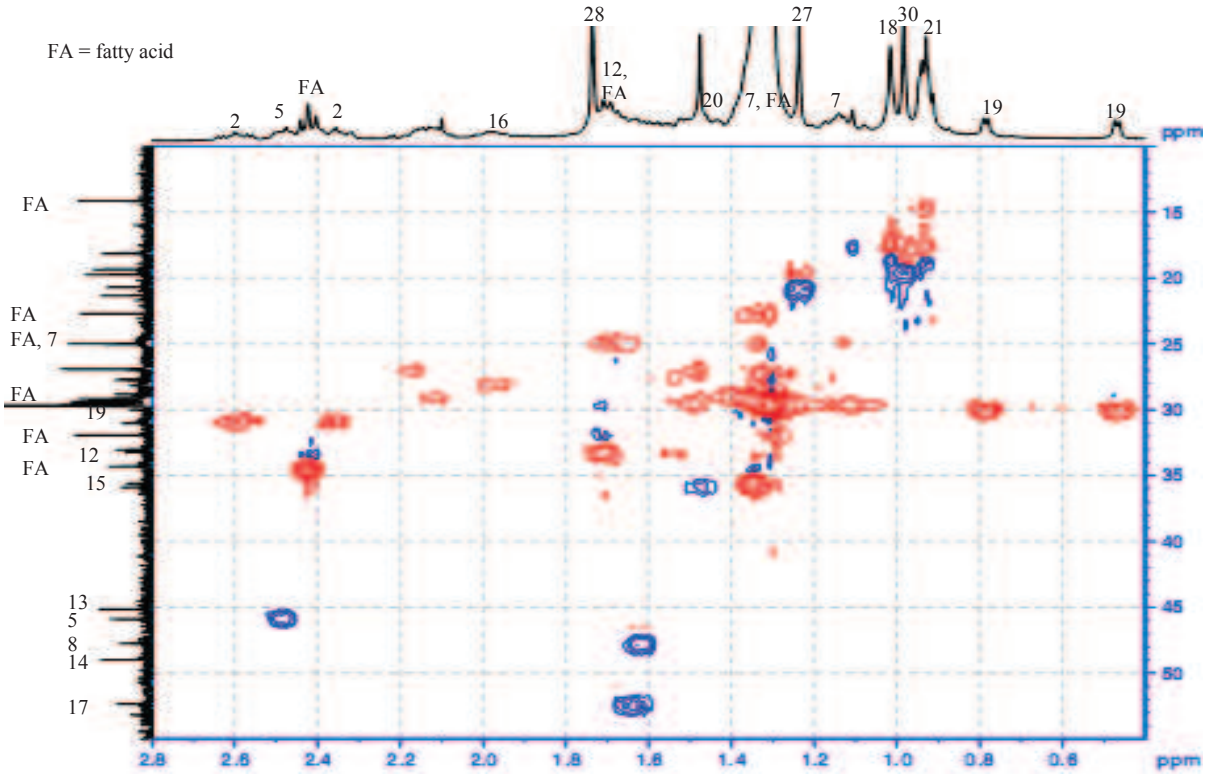

Figure 54. Expanded HSQCedited spectrum of **18** (in $CDCl_3$) in the range of δ_H 0.4-2.8 ppm and δ_C 10-55 ppm.

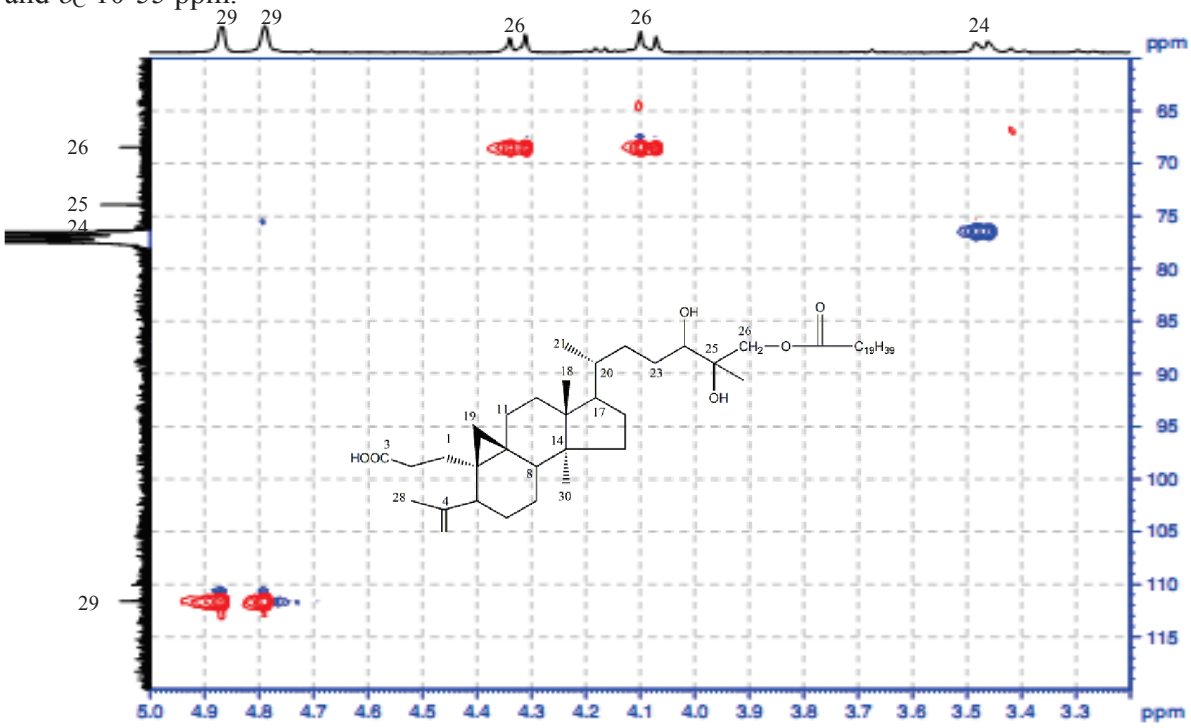

Figure 55. Expanded HSQCedited spectrum of **18** (in $CDCl_3$) in the range of δ_H 3.2-5.0 ppm and δ_C 60-120 ppm.

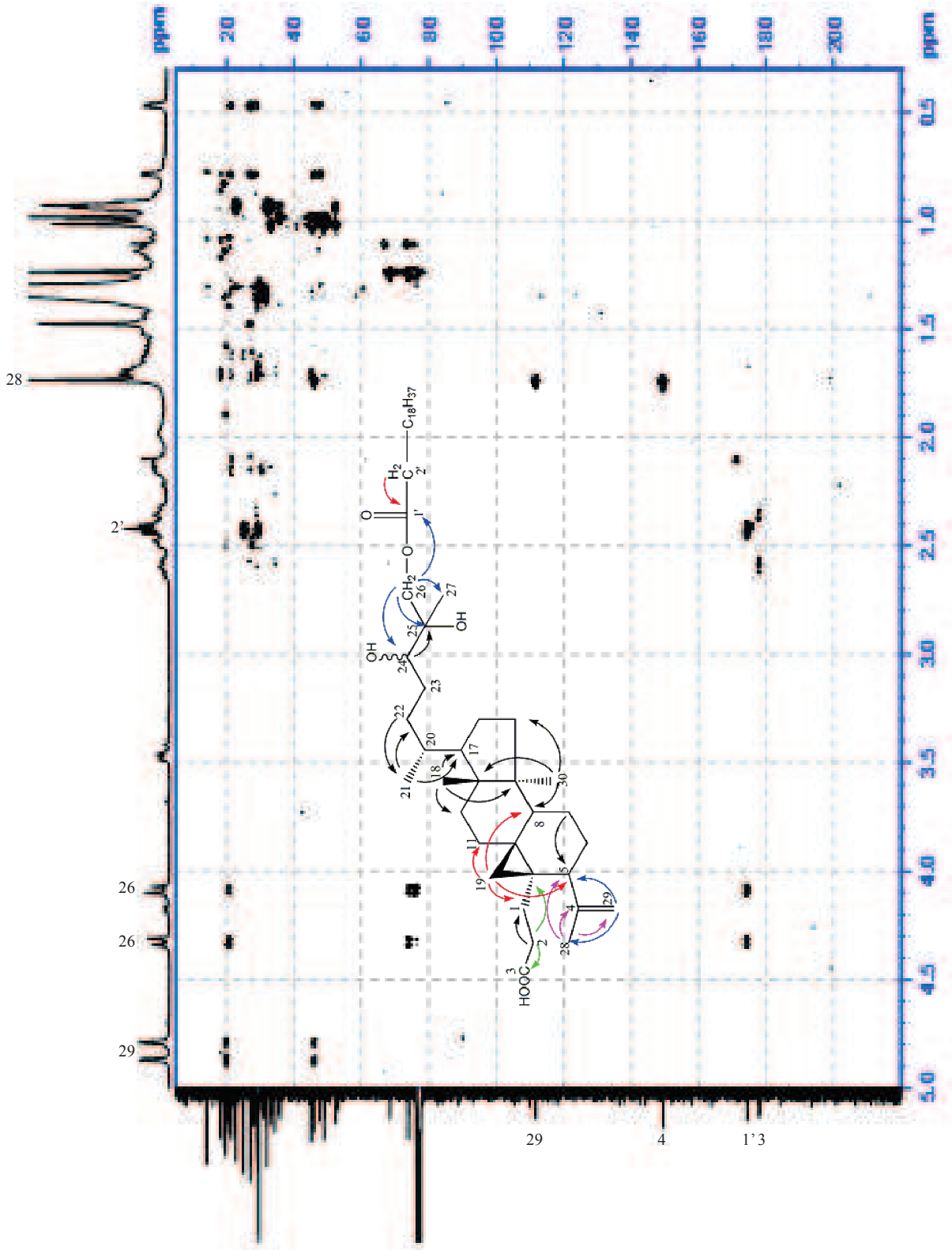

Figure 56. The HMBC correlation of **<u>18</u>** (in $CDCl_3$).

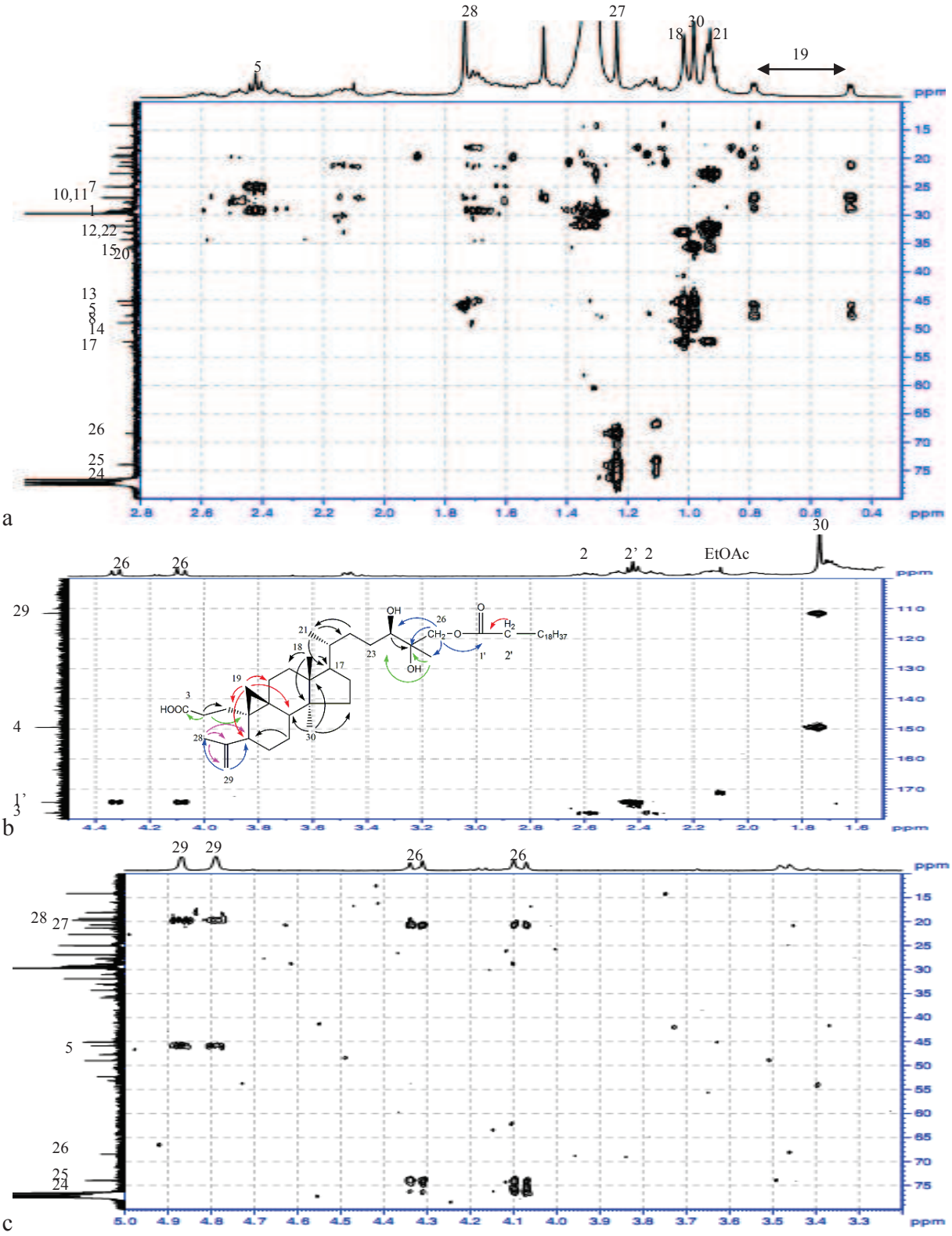

Figure 57. Expanded HMBC correlation of **18** (in $CDCl_3$) in the range of a) δ_H 0.3-2.8 ppm and δ_C 10-80 ppm. b) δ_H 1.5-4.5 ppm and δ_C 10-80 ppm. c) δ_H 3.2-5.0 ppm and δ_C 10-80 ppm.

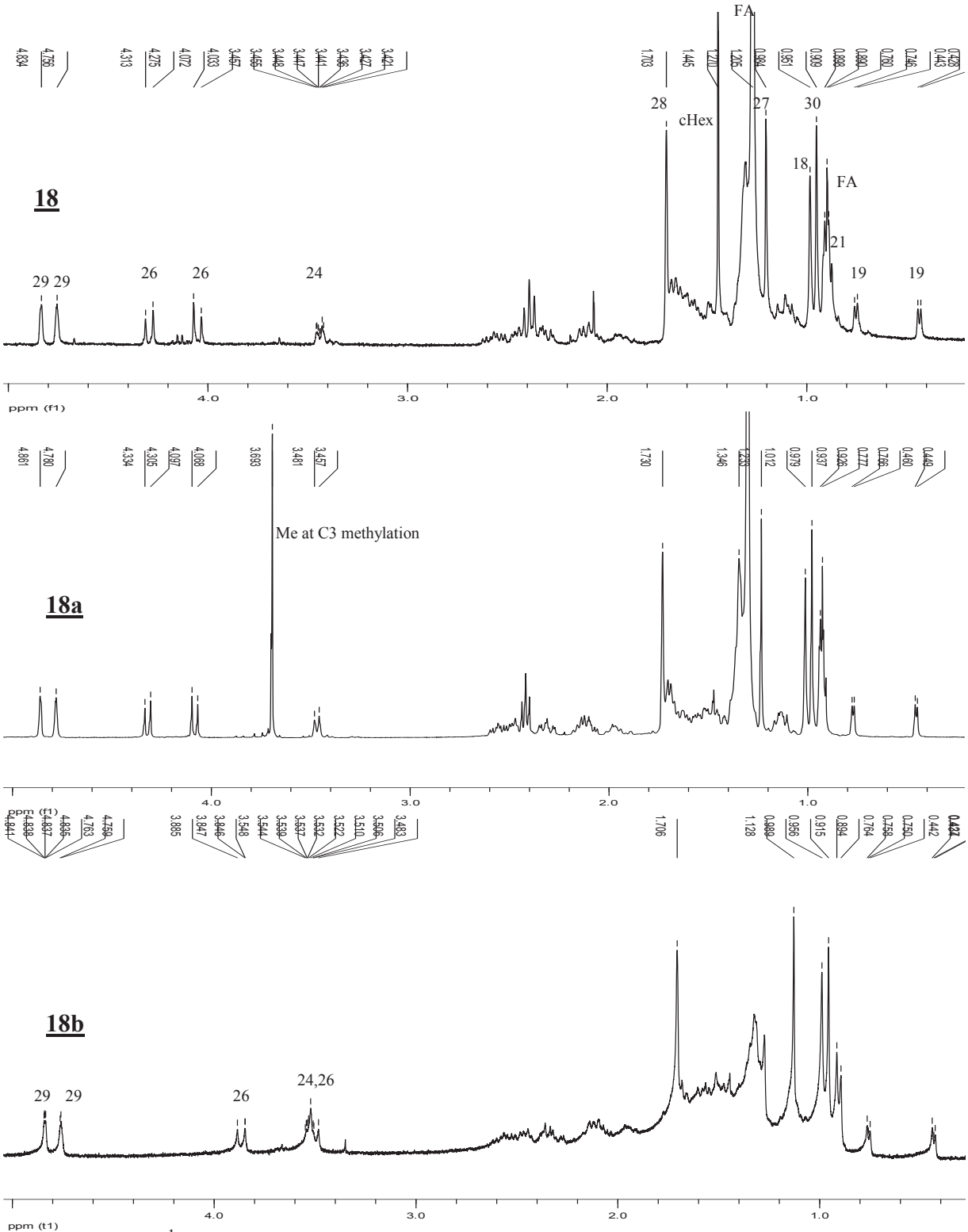

Figure 58. The ^{1}H NMR spectrum (300 MHz) of **18**,**18a** and **18b** (in $CDCl_3$).

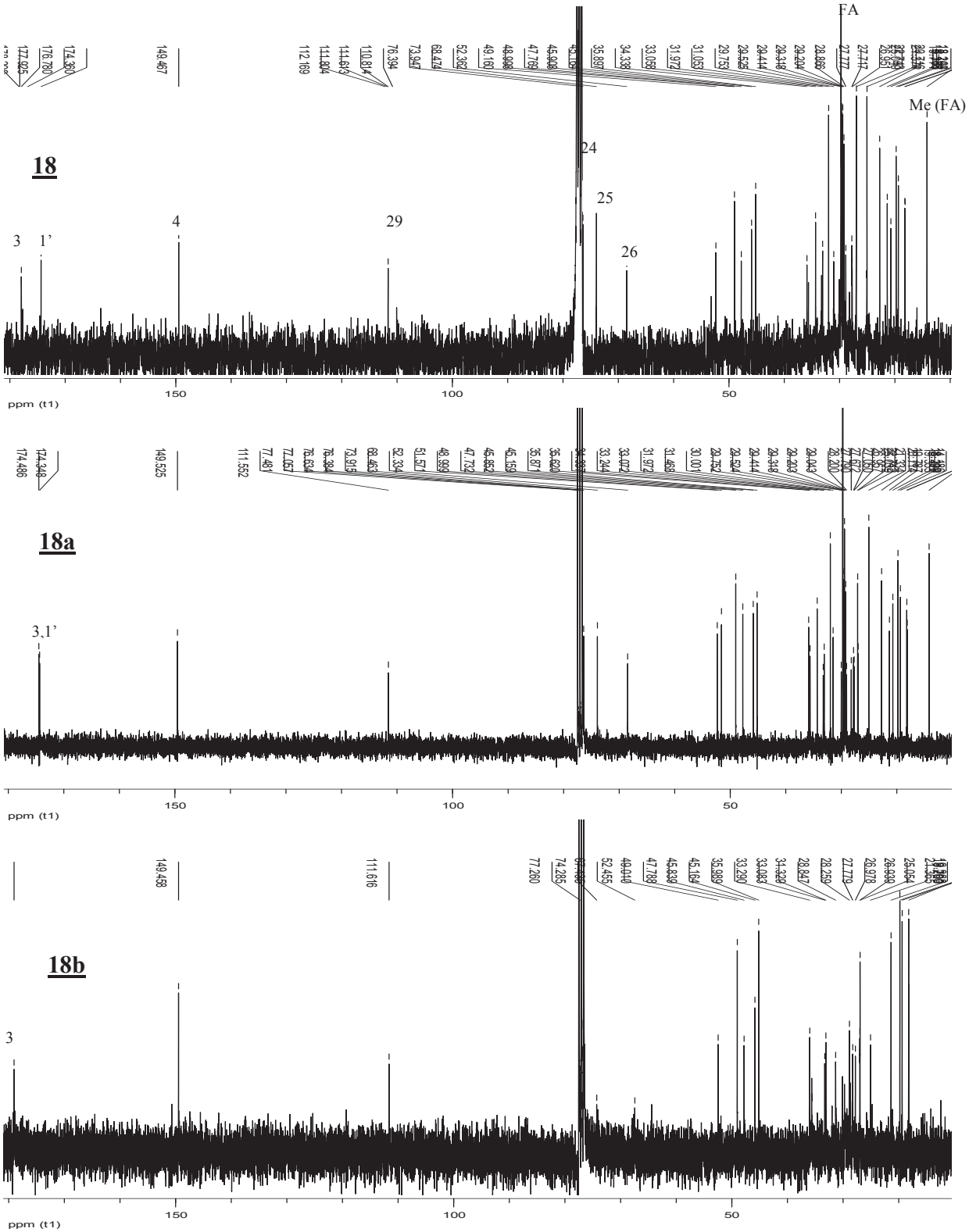

Figure 59. The ^{13}C NMR spectrum (75 MHz) of **18**,**18a** and **18b** (in $CDCl_3$).

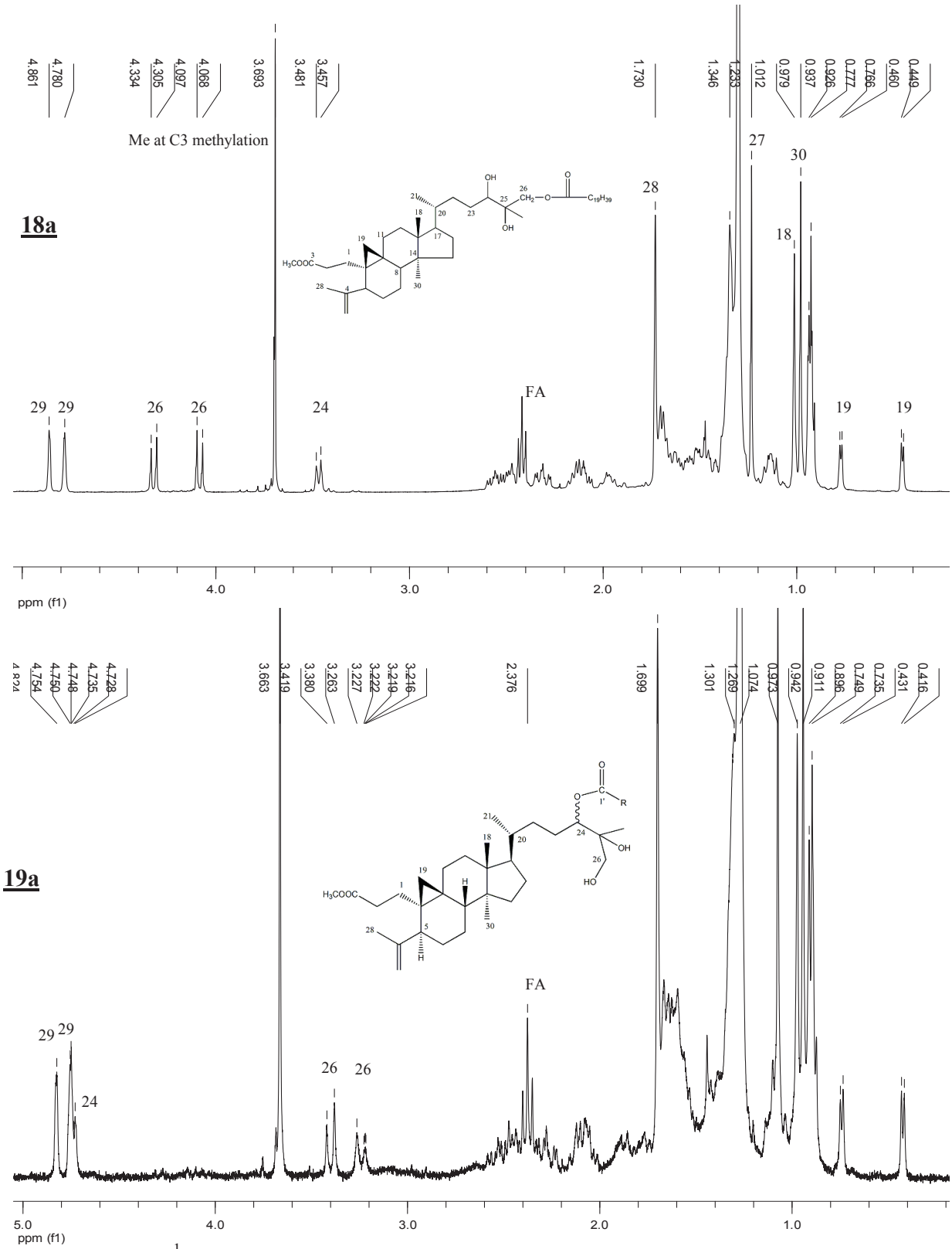

Figure 60. The ^{1}H NMR spectrum (300 MHz) of **18a** and **19a** (in $CDCl_3$).

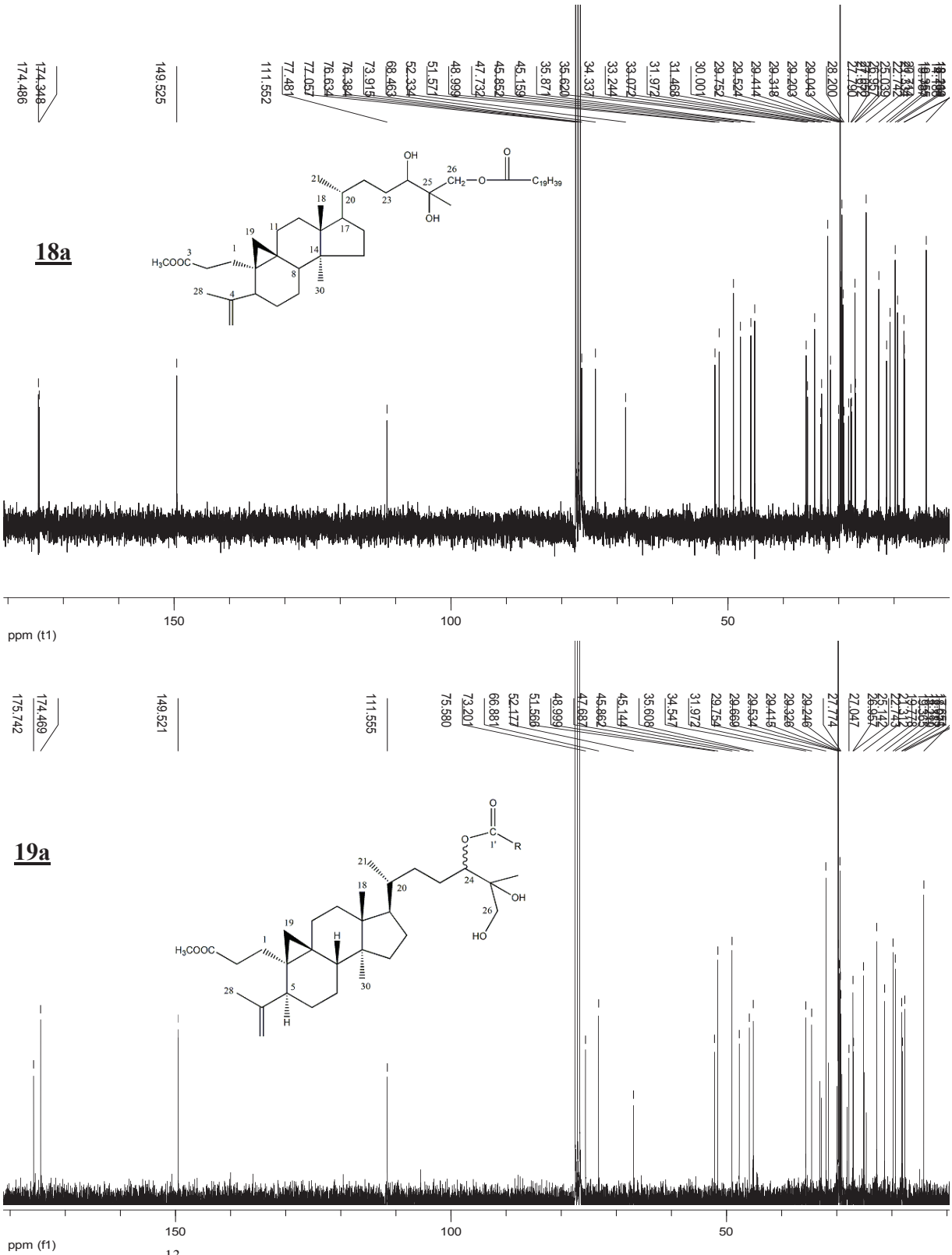

Figure 61. The ^{13}C NMR spectrum (75 MHz) of **18a** and **19a** (in $CDCl_3$).

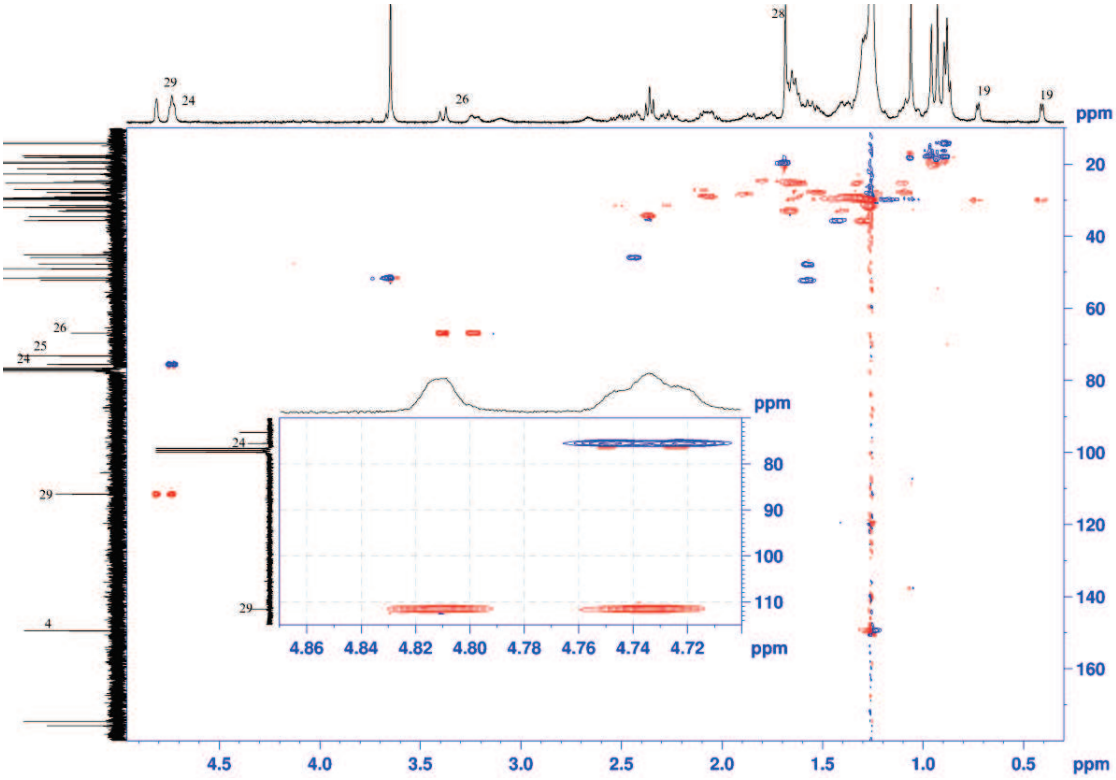

Figure 62. The HSQCedited spectrum of **19a** (in $CDCl_3$).

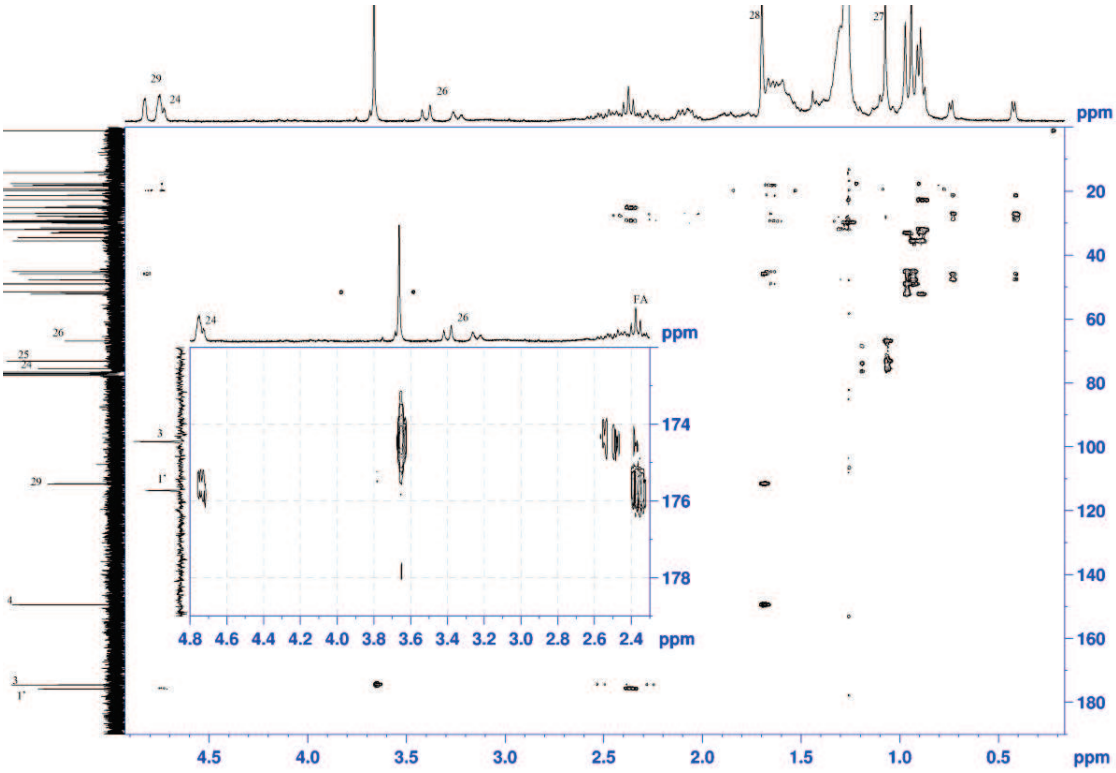

Figure 63. The HMBC spectrum of **19a** (in $CDCl_3$).

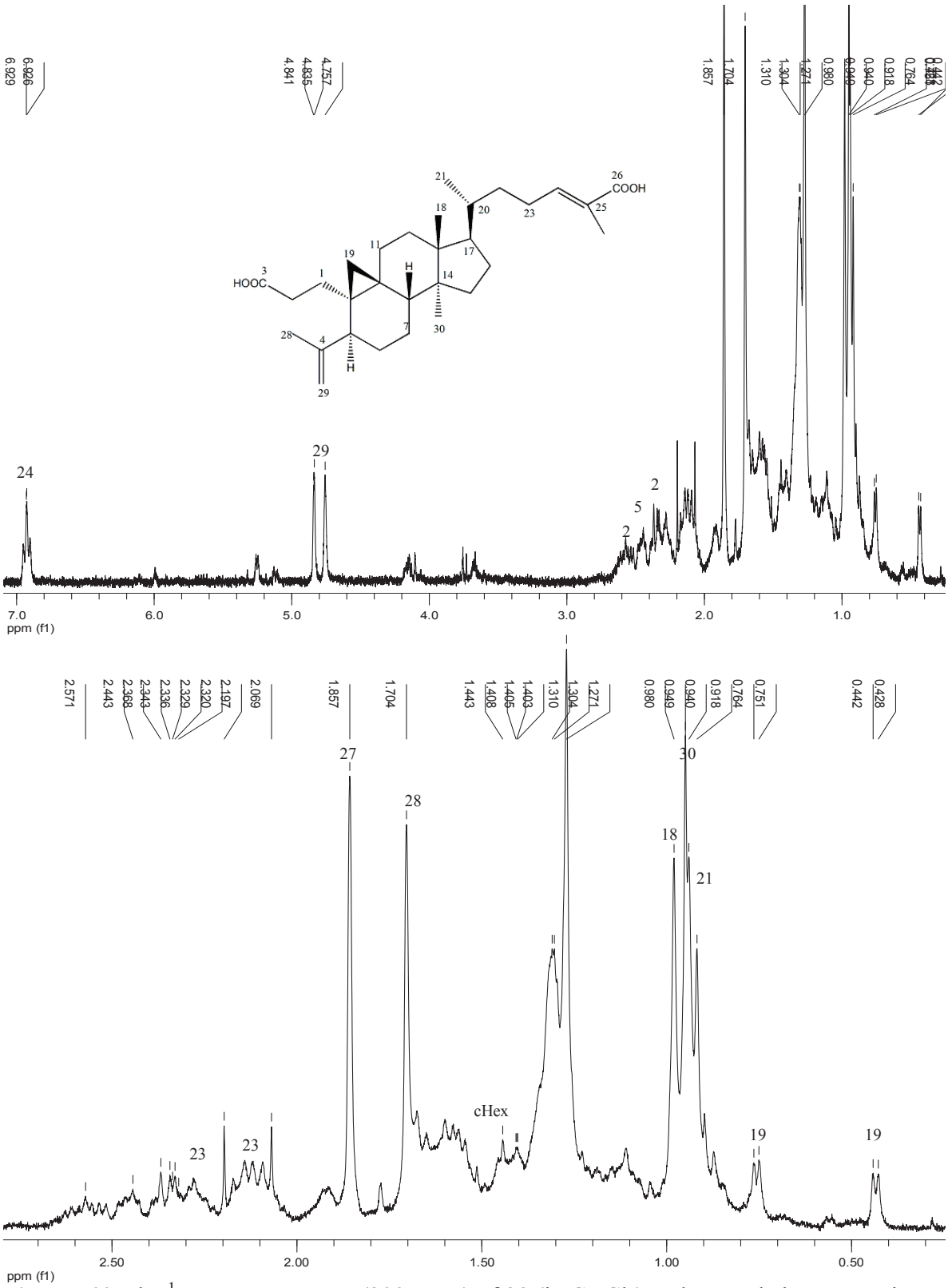

Figure 64. The ^{1}H NMR spectrum (300 MHz) of **<u>20</u>** (in $CDCl_3$) and expanded spectrum in the range of 0.3-2.7 ppm.

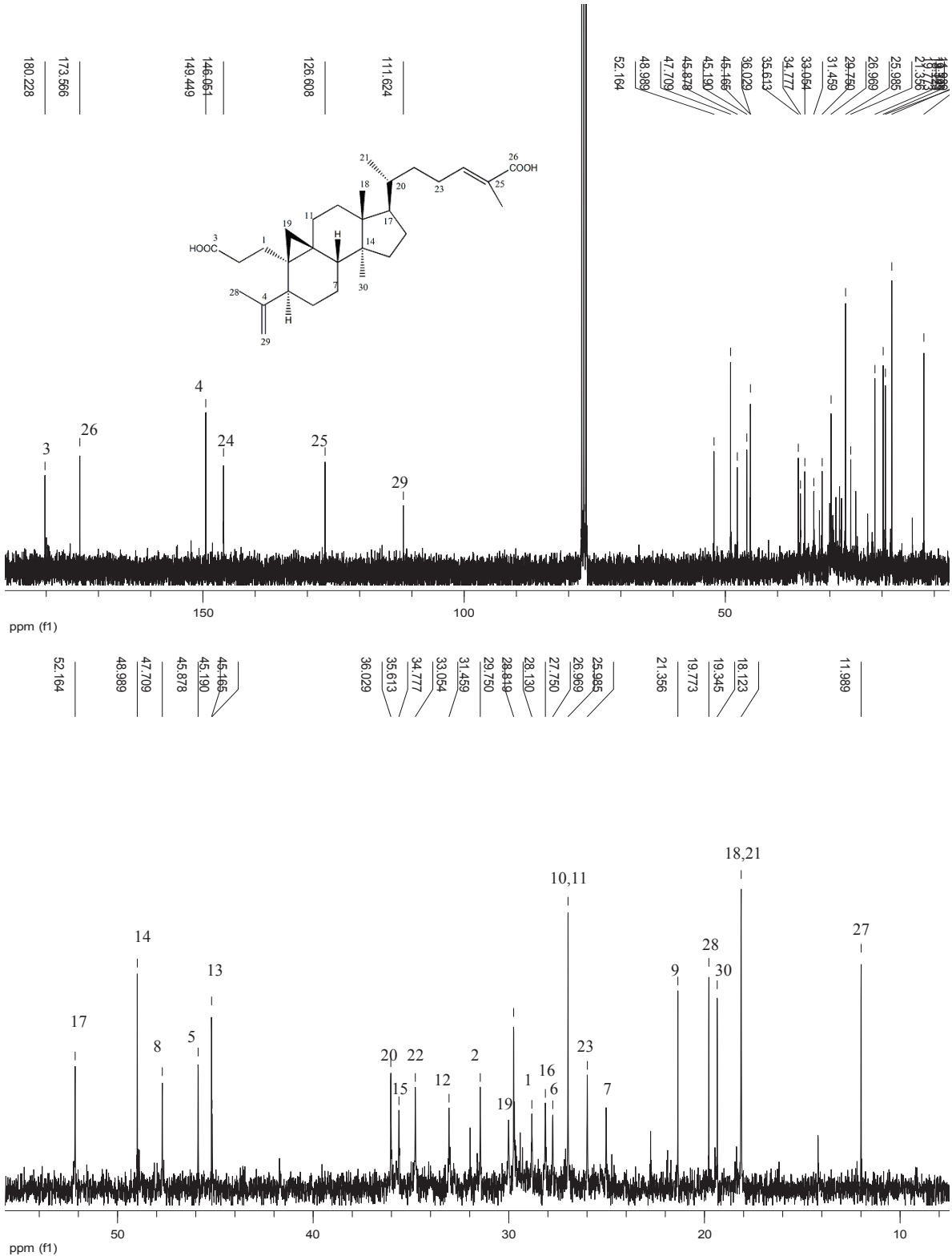

Figure 65. The ^{13}C NMR spectrum (75 MHz) of **20** (in $CDCl_3$) and expanded spectrum in the range of 10.0-54.0 ppm.

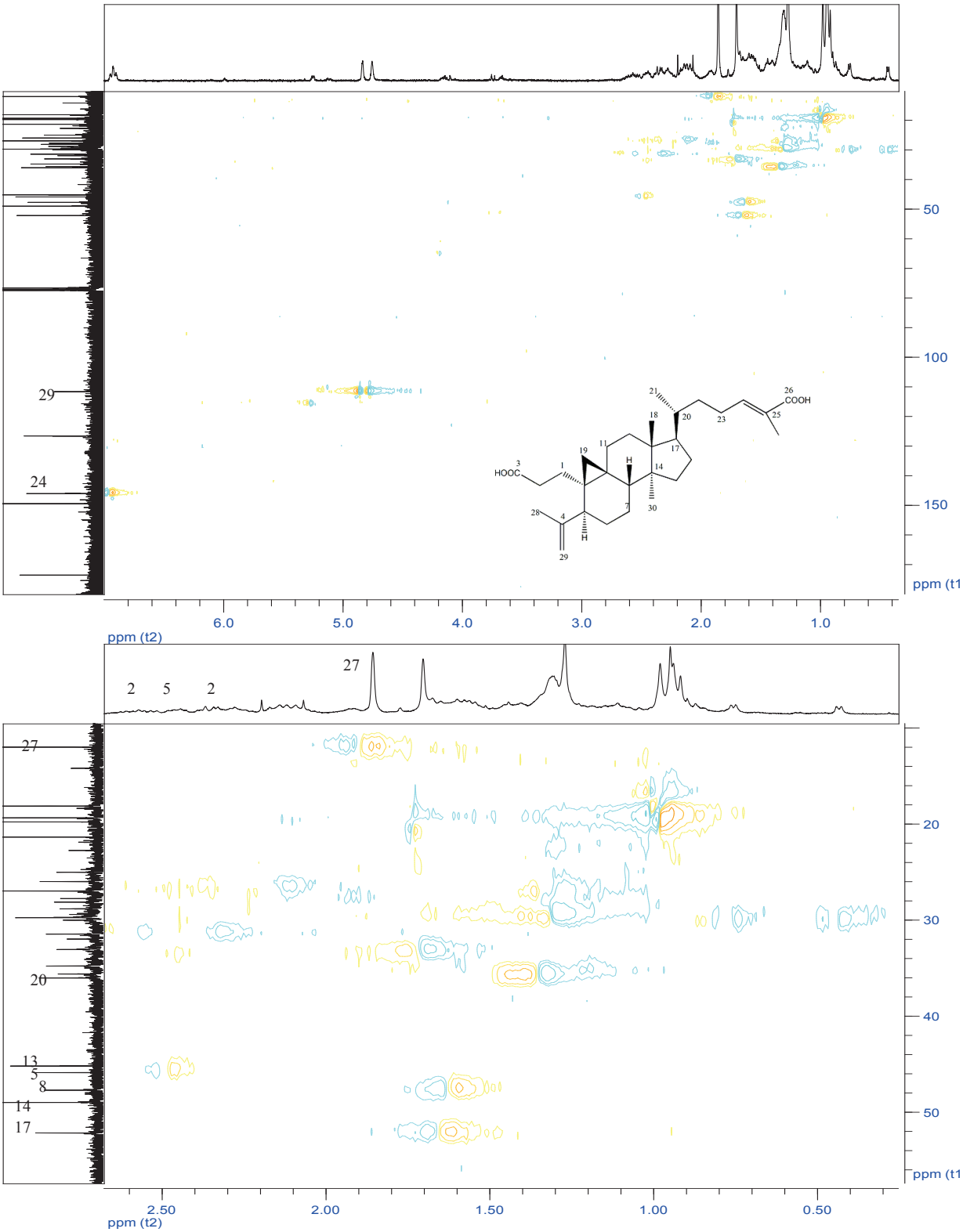

Figure 66. The HSQCedited correlation of **<u>20</u>** (in $CDCl_3$) and expanded spectrum in the range of δ_H 0.2-2.8 ppm and δ_C 10-58 ppm.

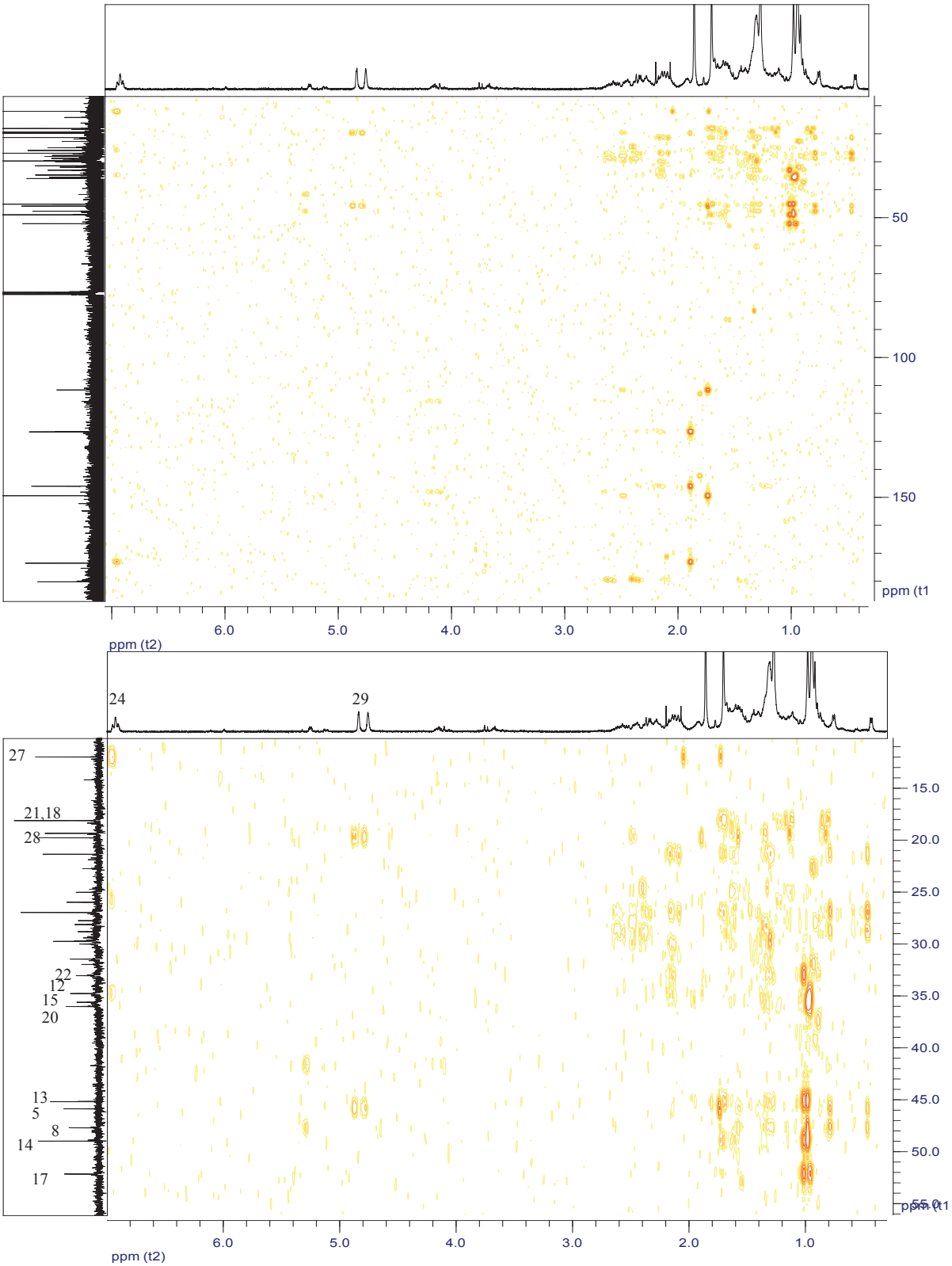

Figure 67. The HMBC correlation of **<u>20</u>** (in $CDCl_3$) and expanded spectrum in the range of δ_H 0.3-7.0 ppm and δ_C 10-56 ppm.

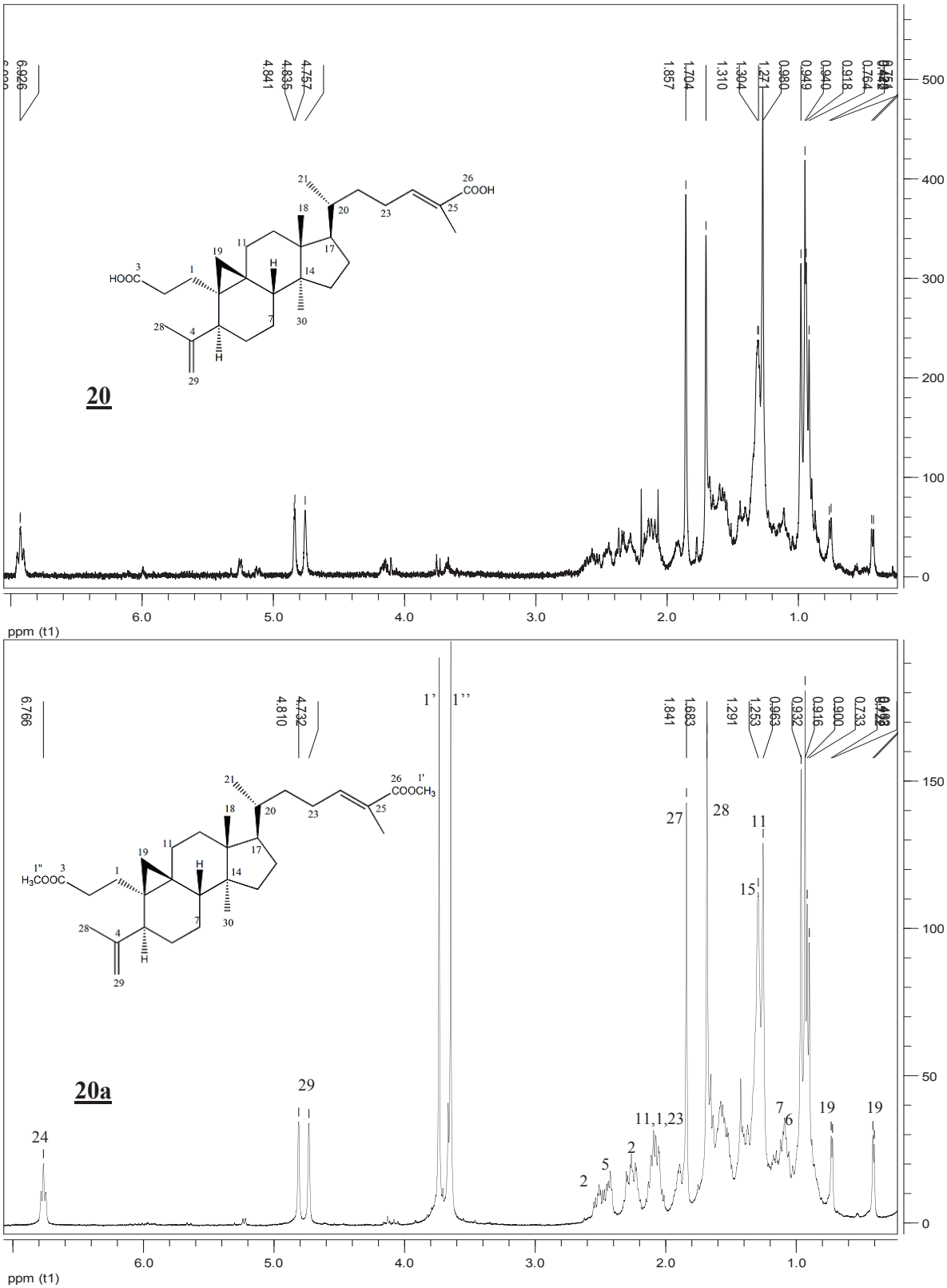

Figure 68. The ^{1}H NMR spectrum (300 MHz) of **20** and **20a** (in $CDCl_3$)

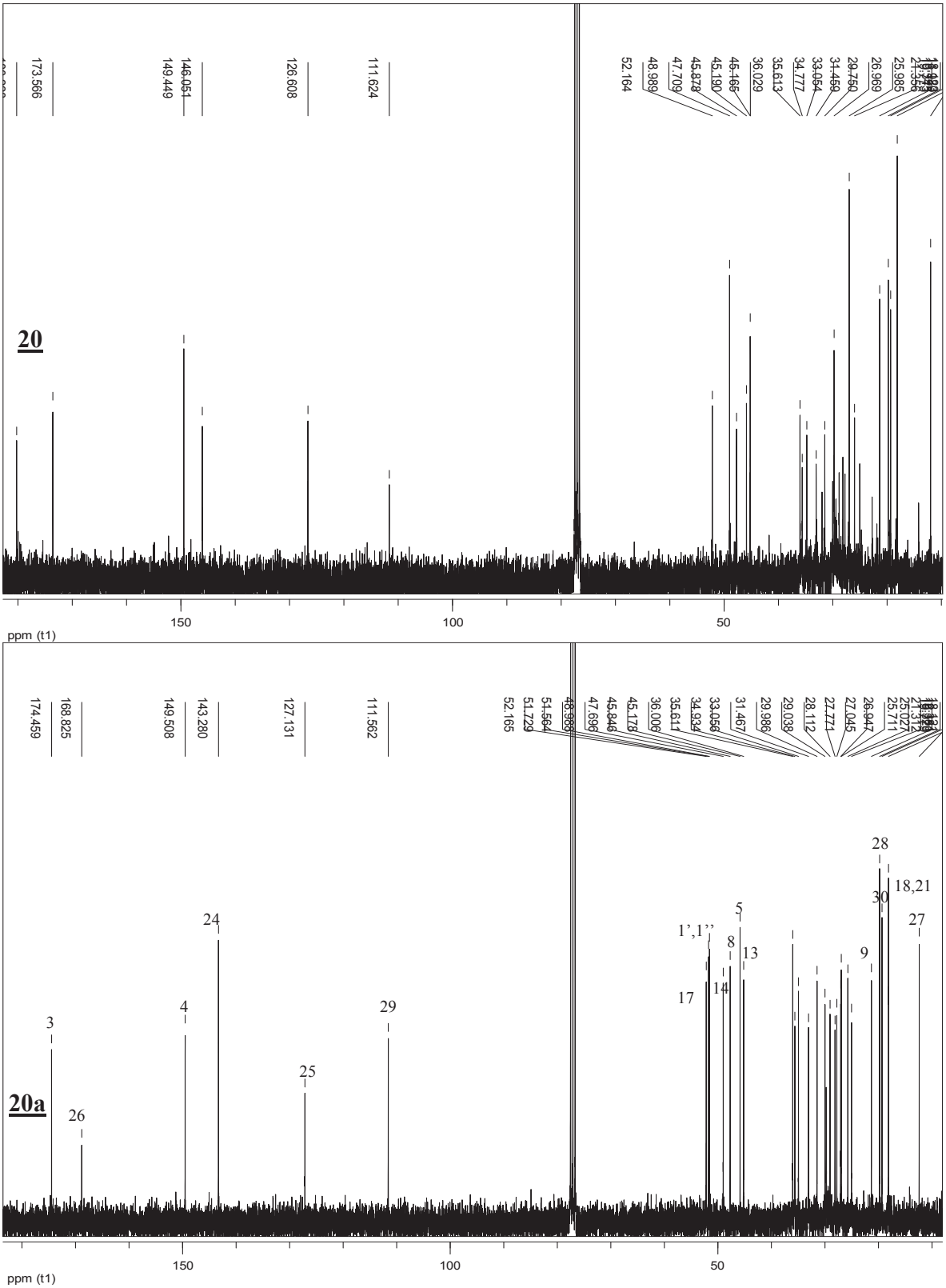

Figure 69. The ^{13}C NMR spectrum (75 MHz) of **20** and **20a** (in $CDCl_3$).

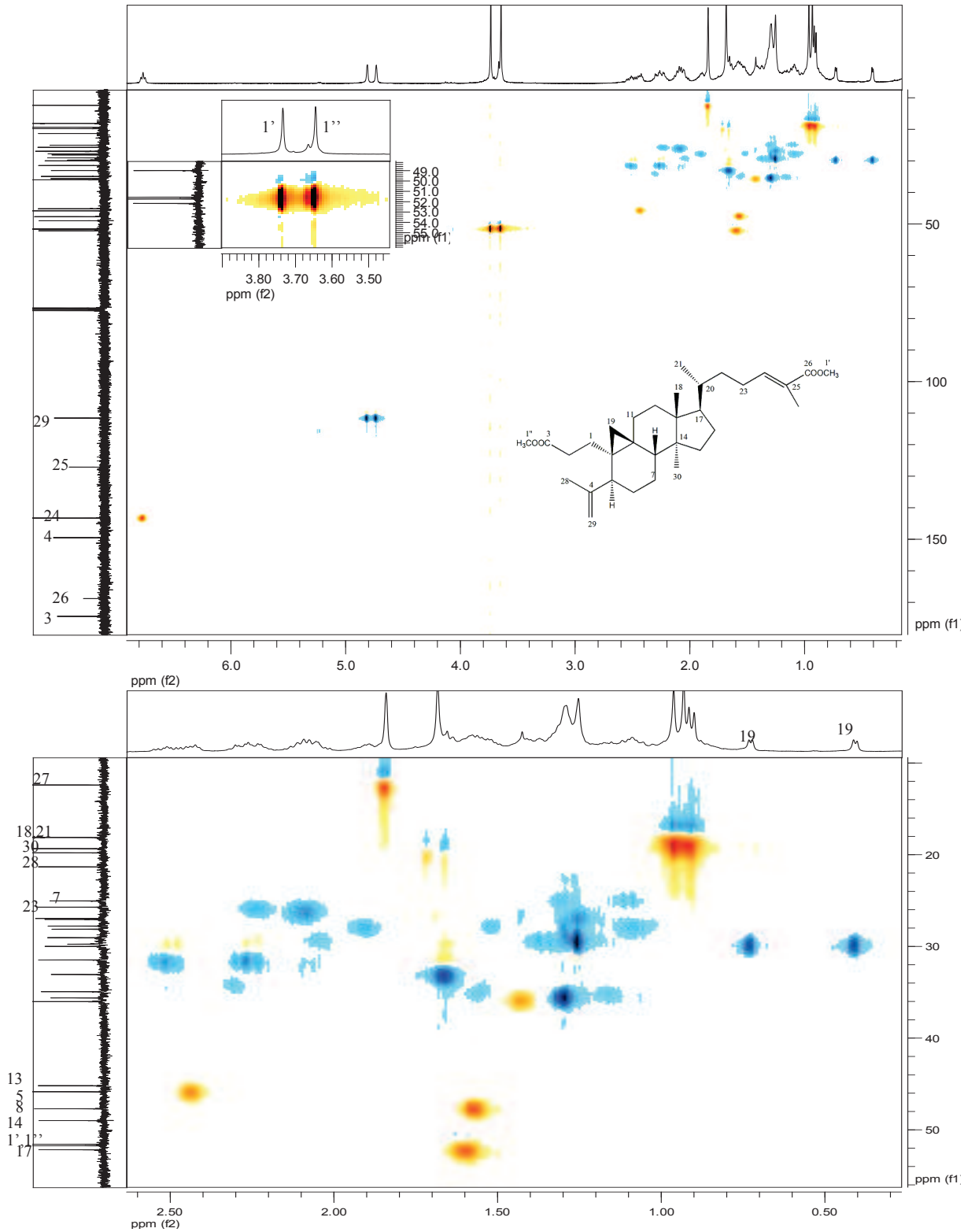

Figure 70. The HSQCedited correlation of **<u>20a</u>** (in $CDCl_3$) and expanded spectrum in the range of δ_H 0.3-2.6 ppm and δ_C 0-56 ppm.

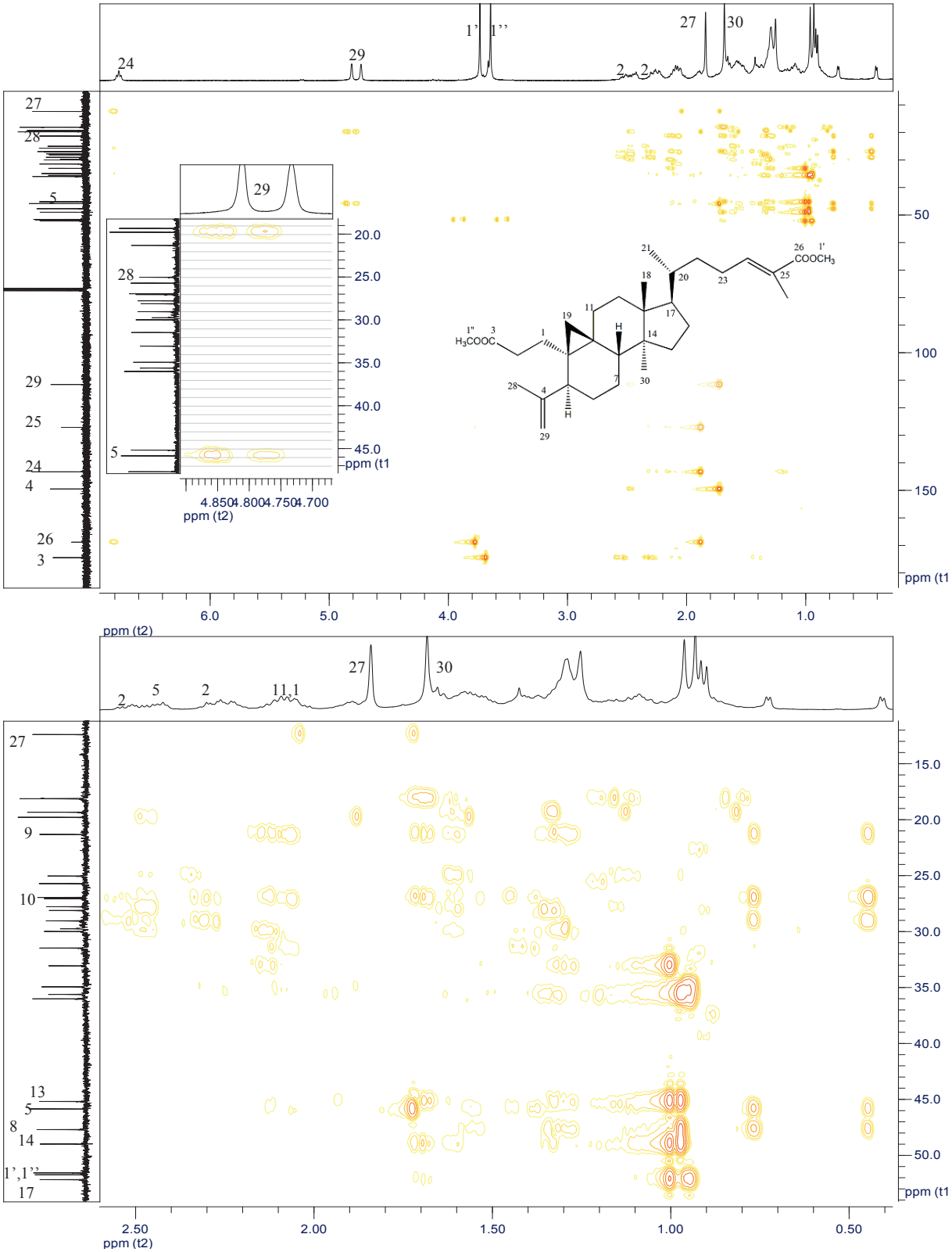

Figure 71. The HMBC correlation of **<u>20a</u>** (in $CDCl_3$) and expanded spectrum in the range of δ_H 0.4-2.6 ppm and δ_C 12-59 ppm.

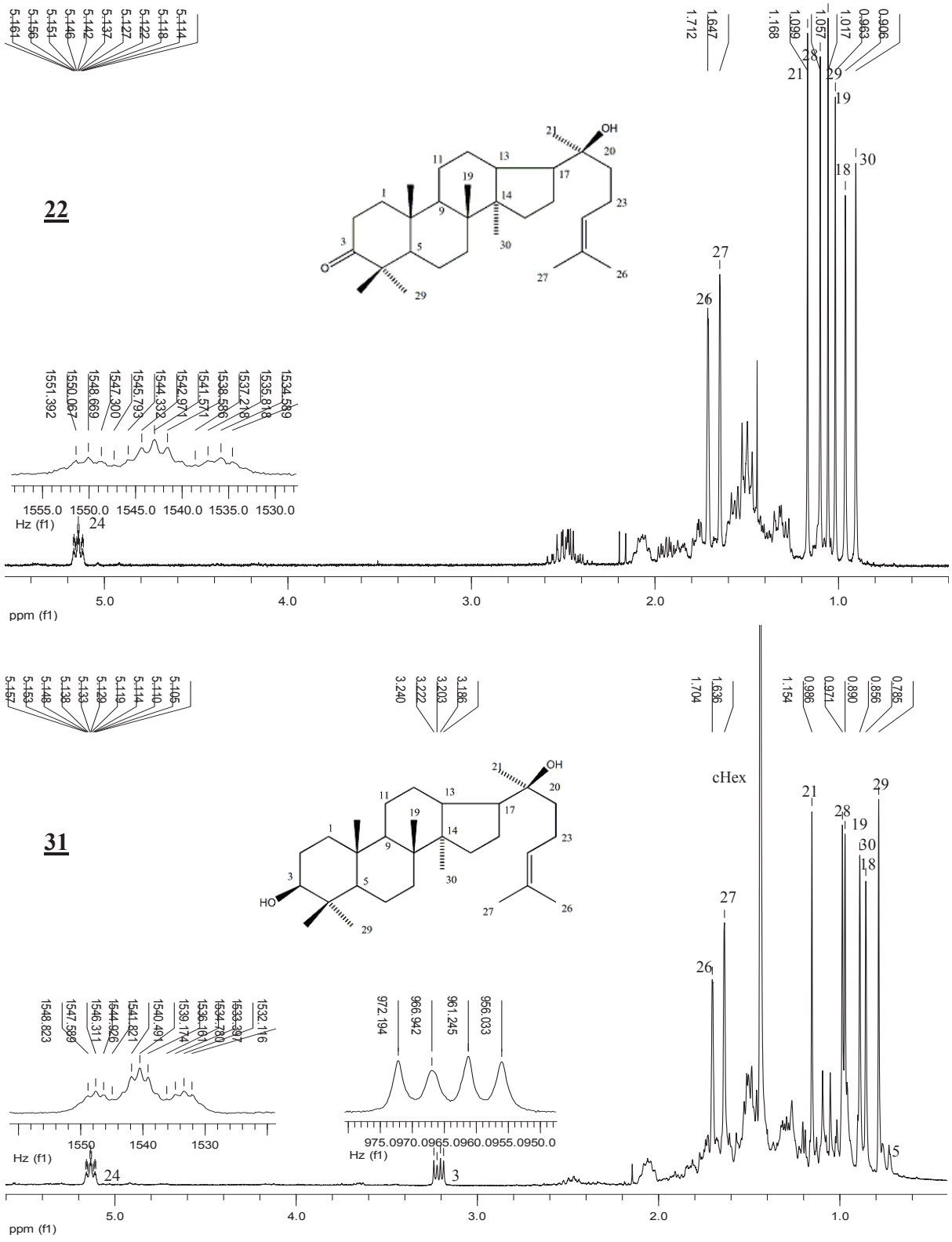

Figure 72. The ^{1}H NMR spectrum (300 MHz) of **22** and **31** (in $CDCl_3$).

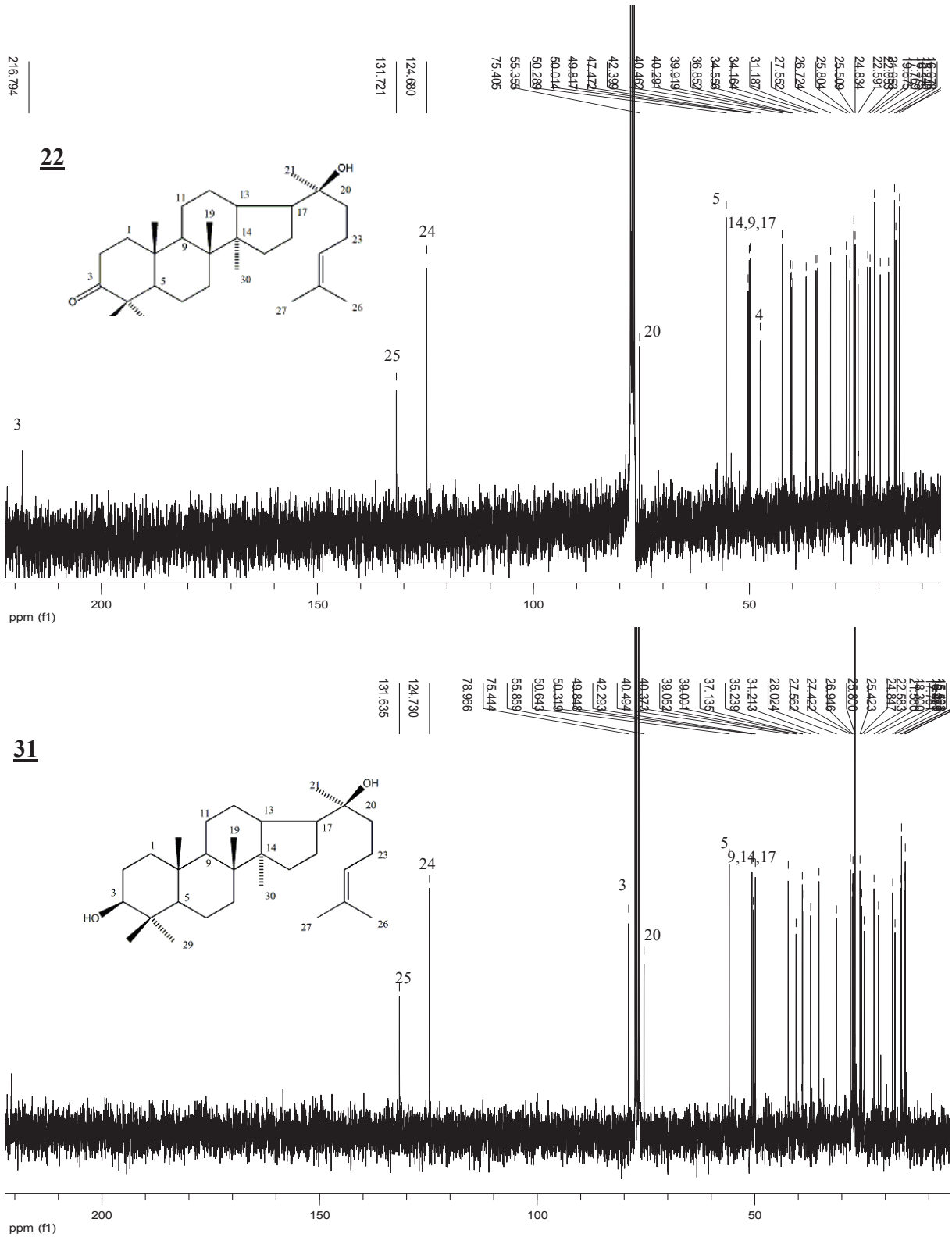

Figure 73. The ^{13}C NMR spectrum (75 MHz) of **22** and **31** (in $CDCl_3$).

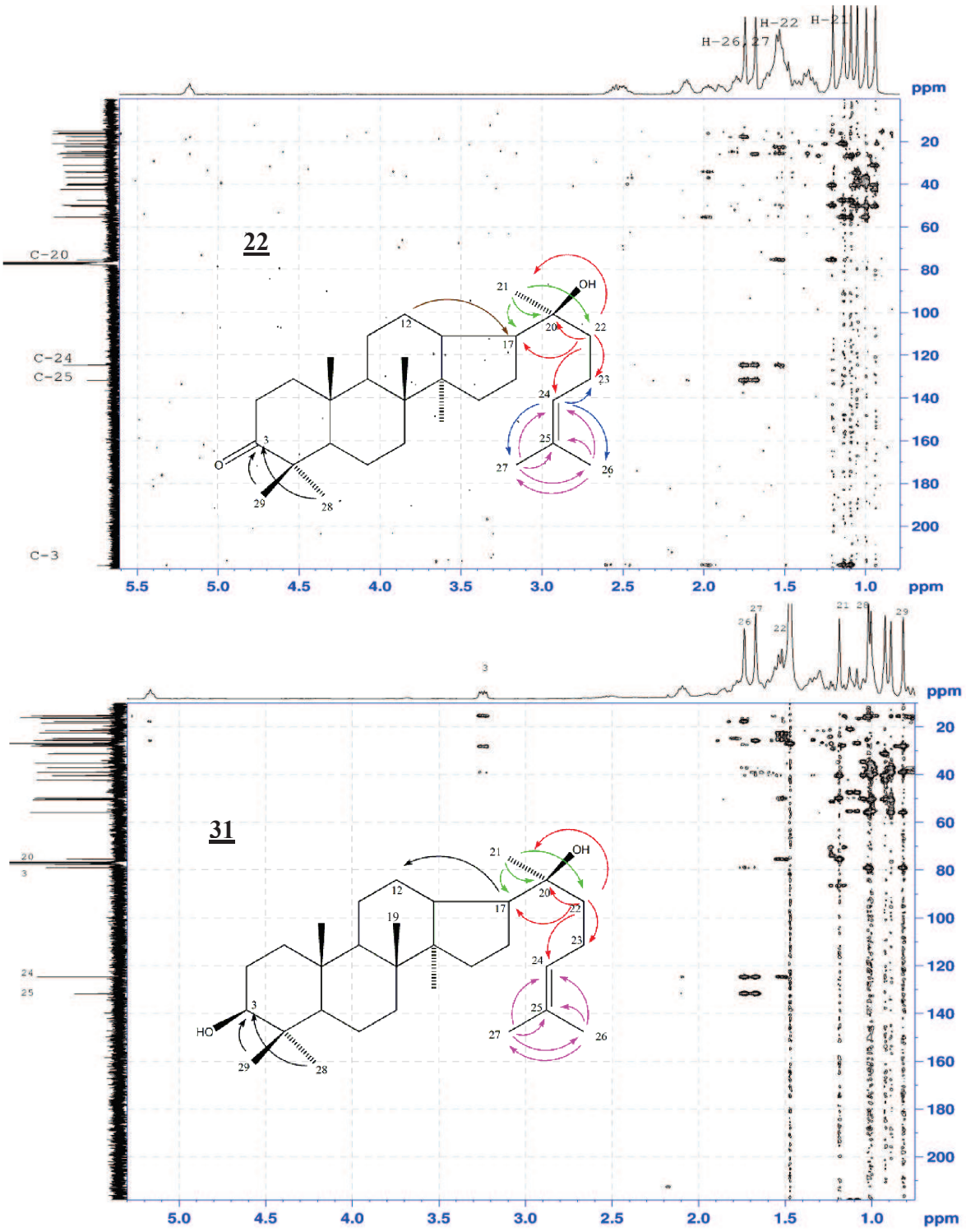

Figure 74. The HMBC correlation of **22** and **31** (in $CDCl_3$).

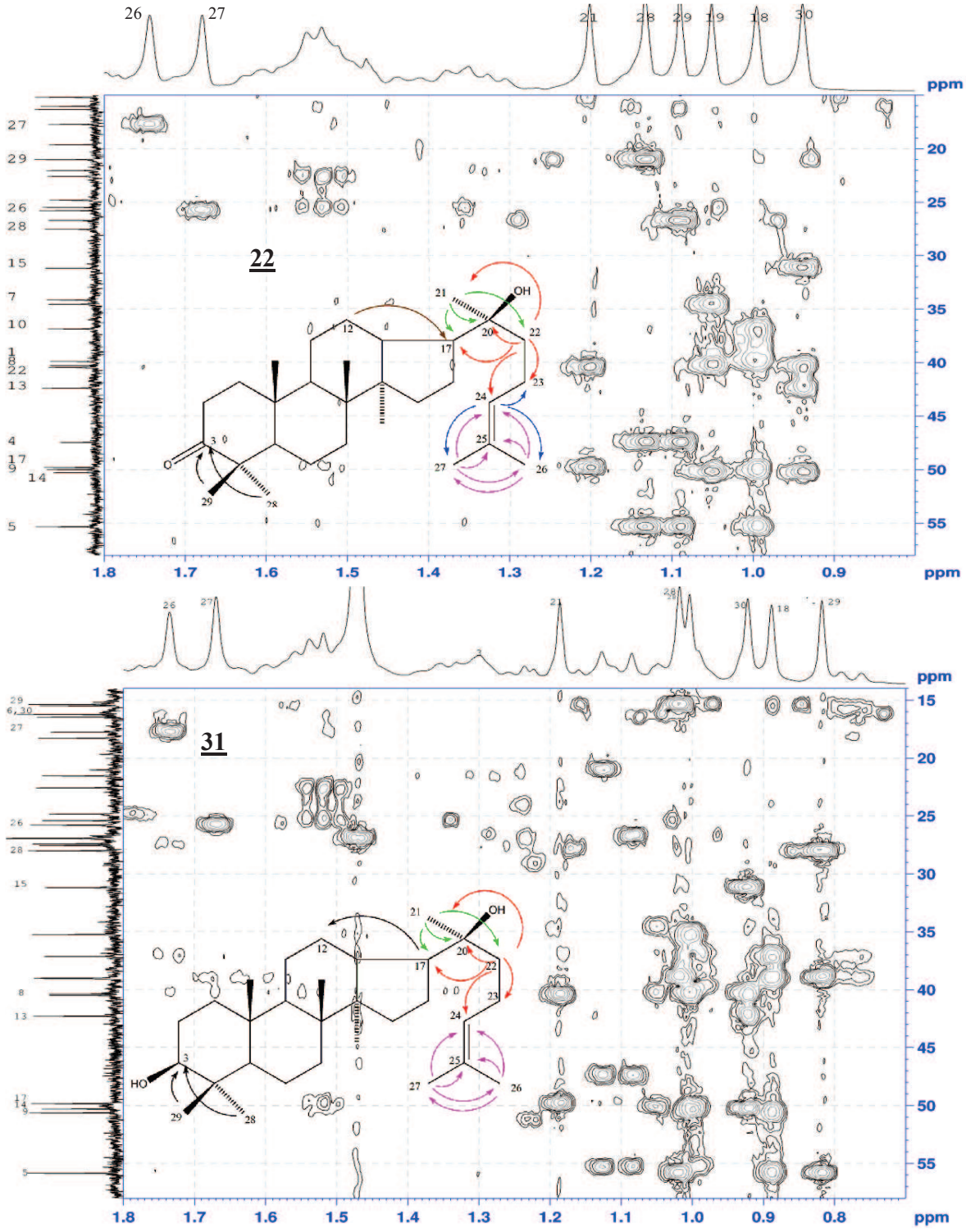

Figure 75. The expanded HMBC correlation of **22** and **31** (in $CDCl_3$) and expanded spectrum in the range of δ_H 0.7-1.8 ppm and δ_C 15-58 ppm.

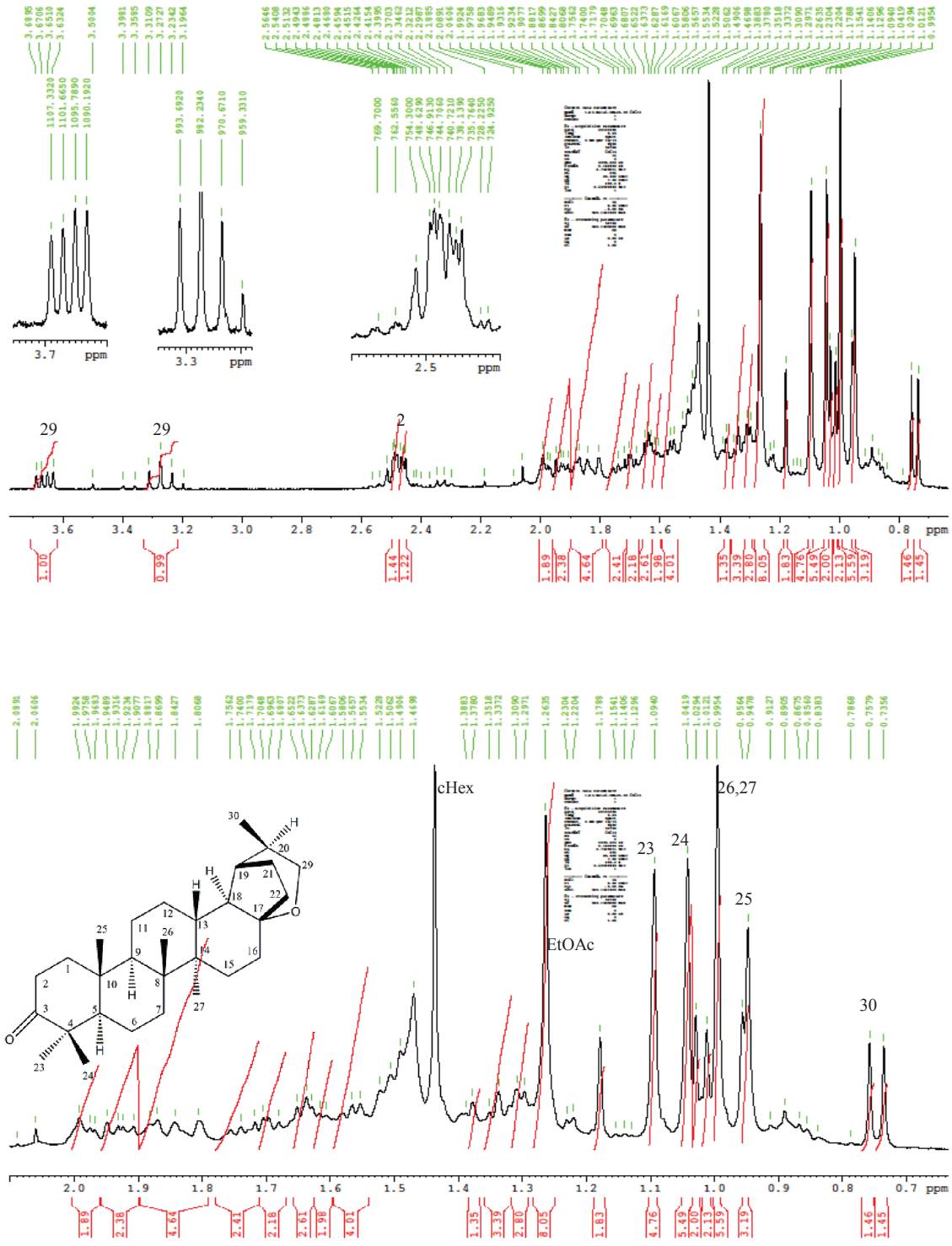

Figure 76. The ^{1}H NMR spectrum (300 MHz) of **24** (in $CDCl_3$) and expanded spectrum in the range of 0.7-2.1 ppm. (with trace of impurity)

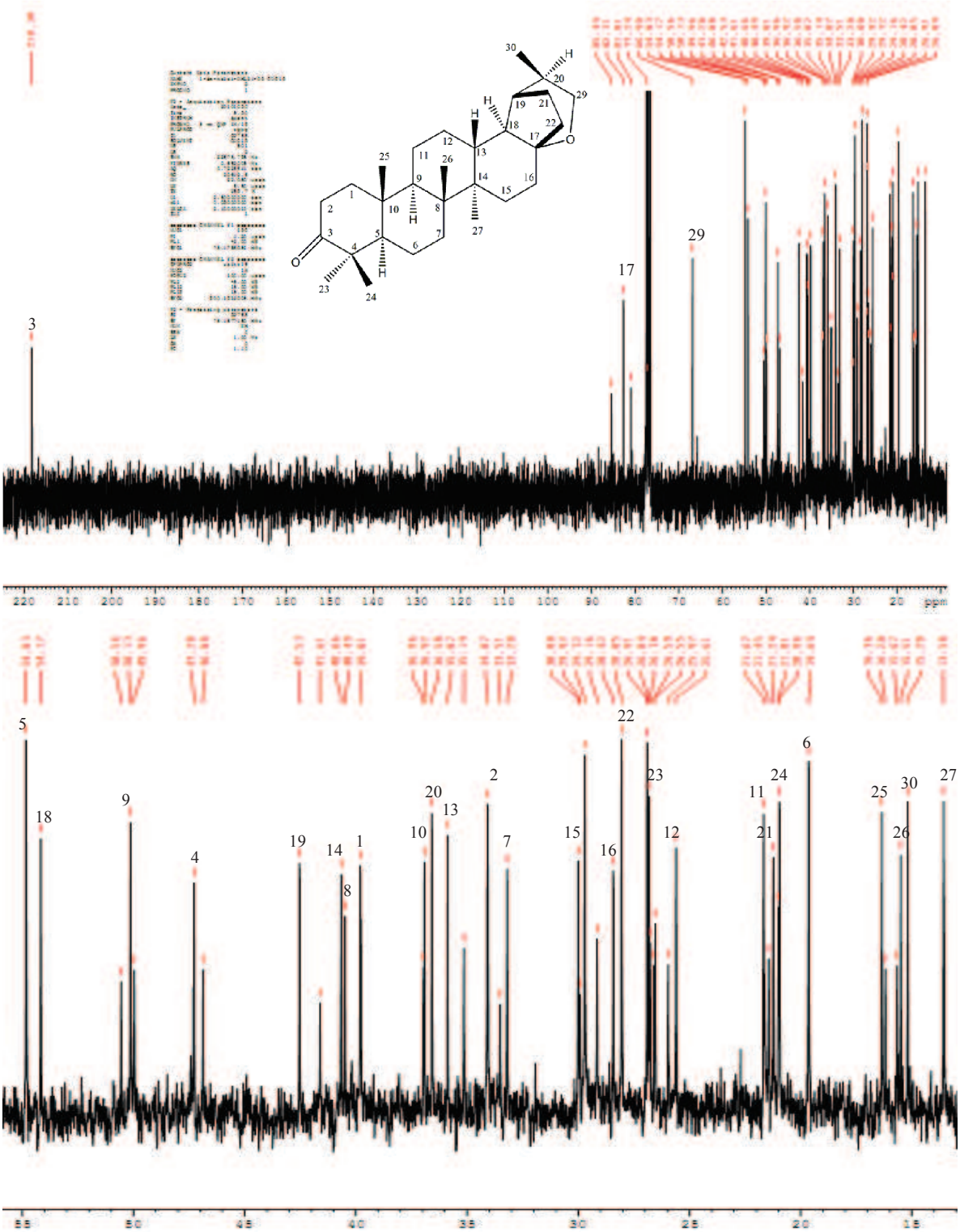

Figure 77. The ^{13}C NMR spectrum (75 MHz) of **<u>24</u>** (in $CDCl_3$) and expanded spectrum in the range of 13-56 ppm. (with trace of dipterocarpol)

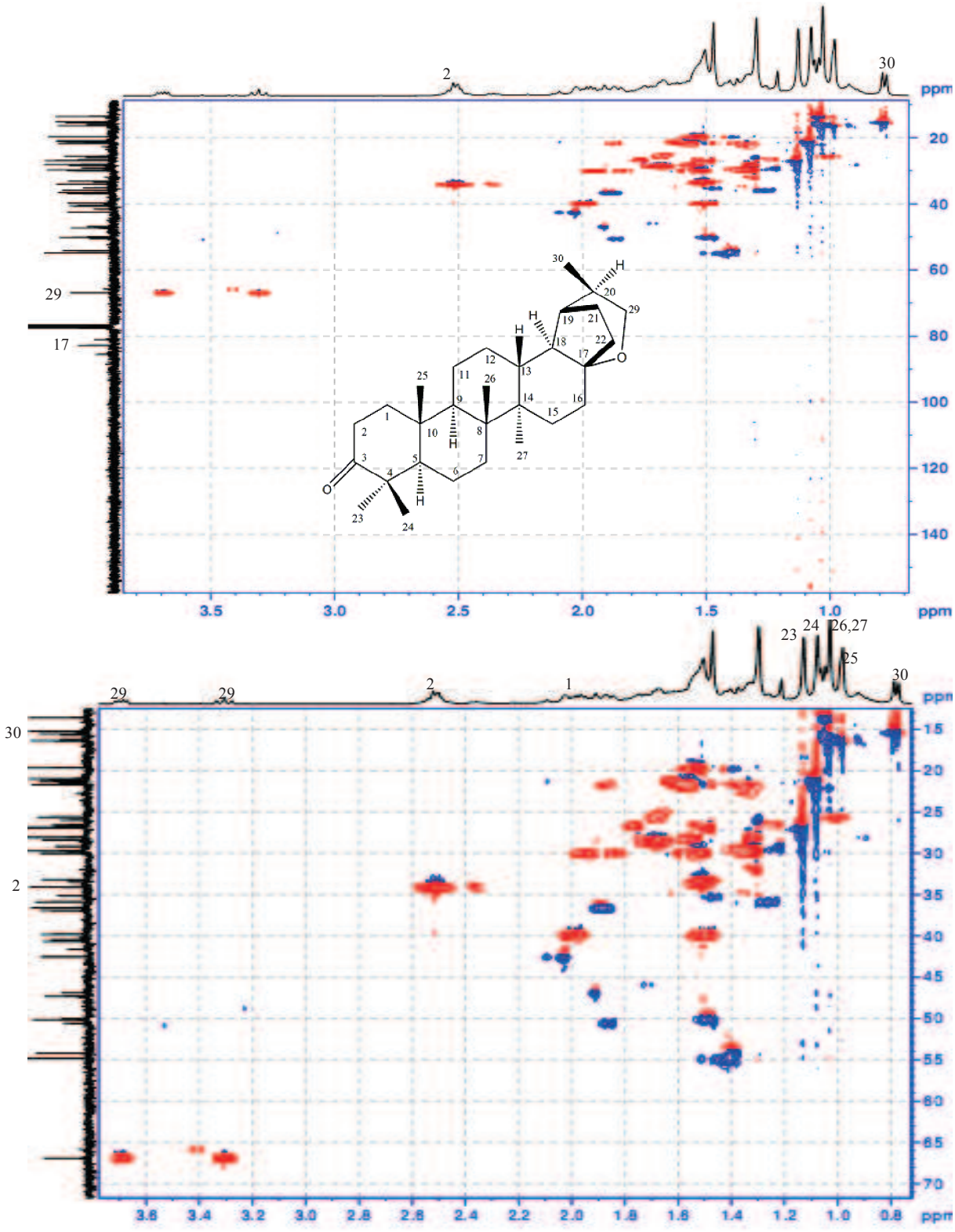

Figure 78. The HSQCedited correlation of **24** (in $CDCl_3$) and expanded spectrum in the range of δ_H 0.7-3.8 ppm and δ_C 13-72 ppm.

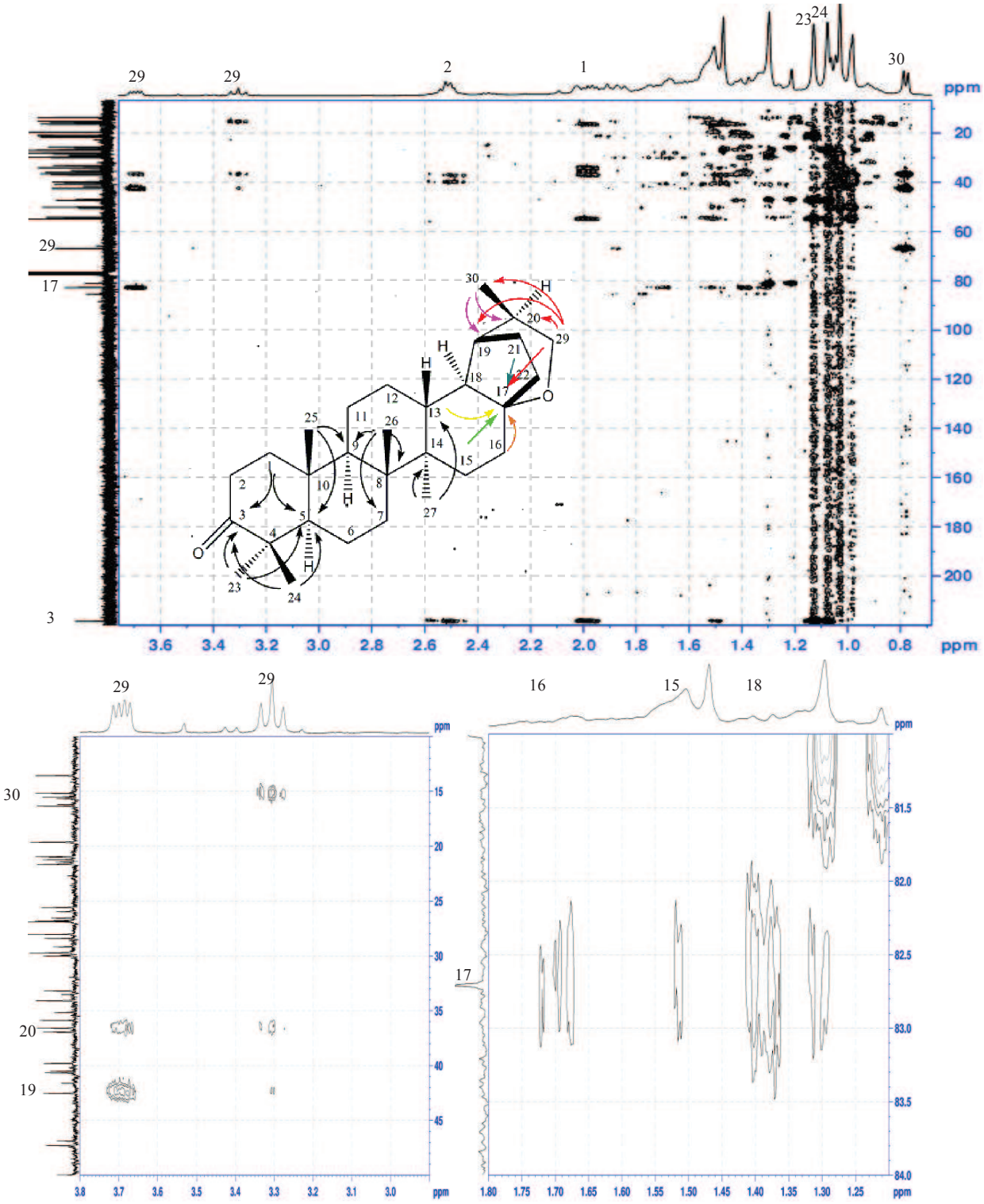

Figure 79. The HMBC correlation of **24** (in $CDCl_3$) and expanded spectrum in the range of δ_H 2.9-3.8 ppm, δ_C 10-50 ppm and δ_H 1.2-1.8 ppm, δ_C 81-84 ppm.

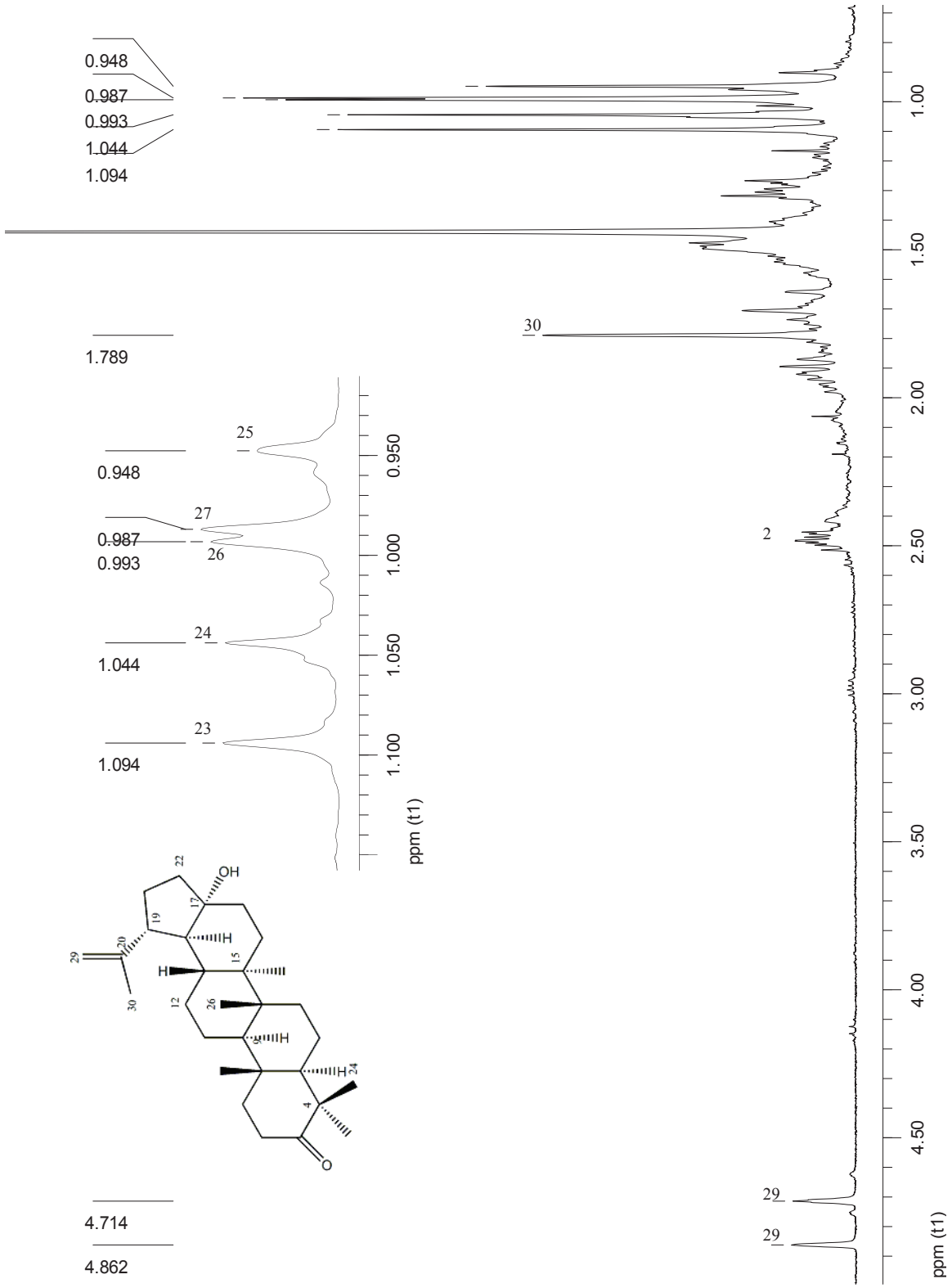

Figure 80. The ^{1}H NMR spectrum (300 MHz) of **25** (in $CDCl_3$) and expanded spectrum in the range of 0.95-1.10 ppm.

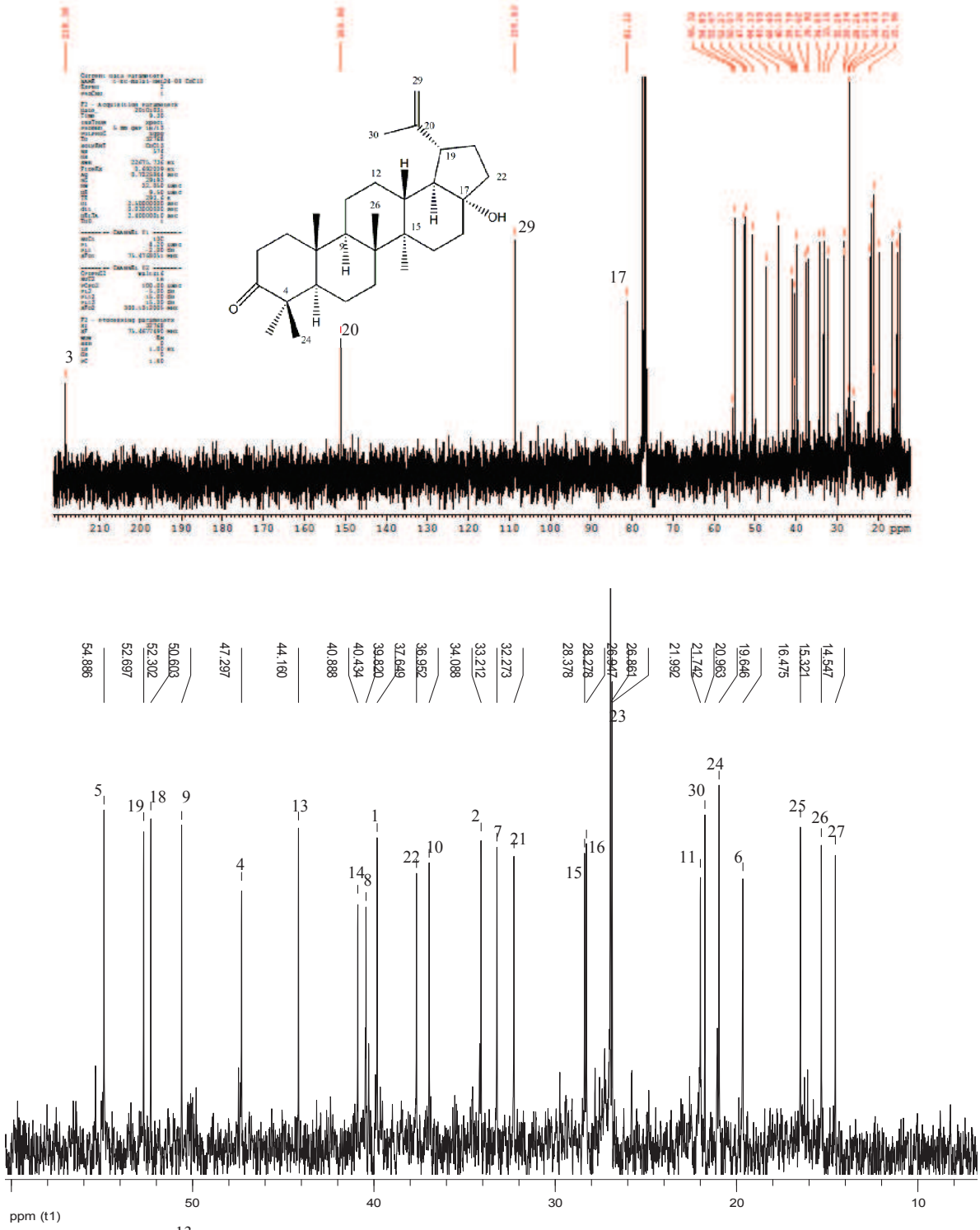

Figure 81. The ^{13}C NMR spectrum (75 MHz) of **25** (in $CDCl_3$) and expanded spectrum in the range of 16-60 ppm.

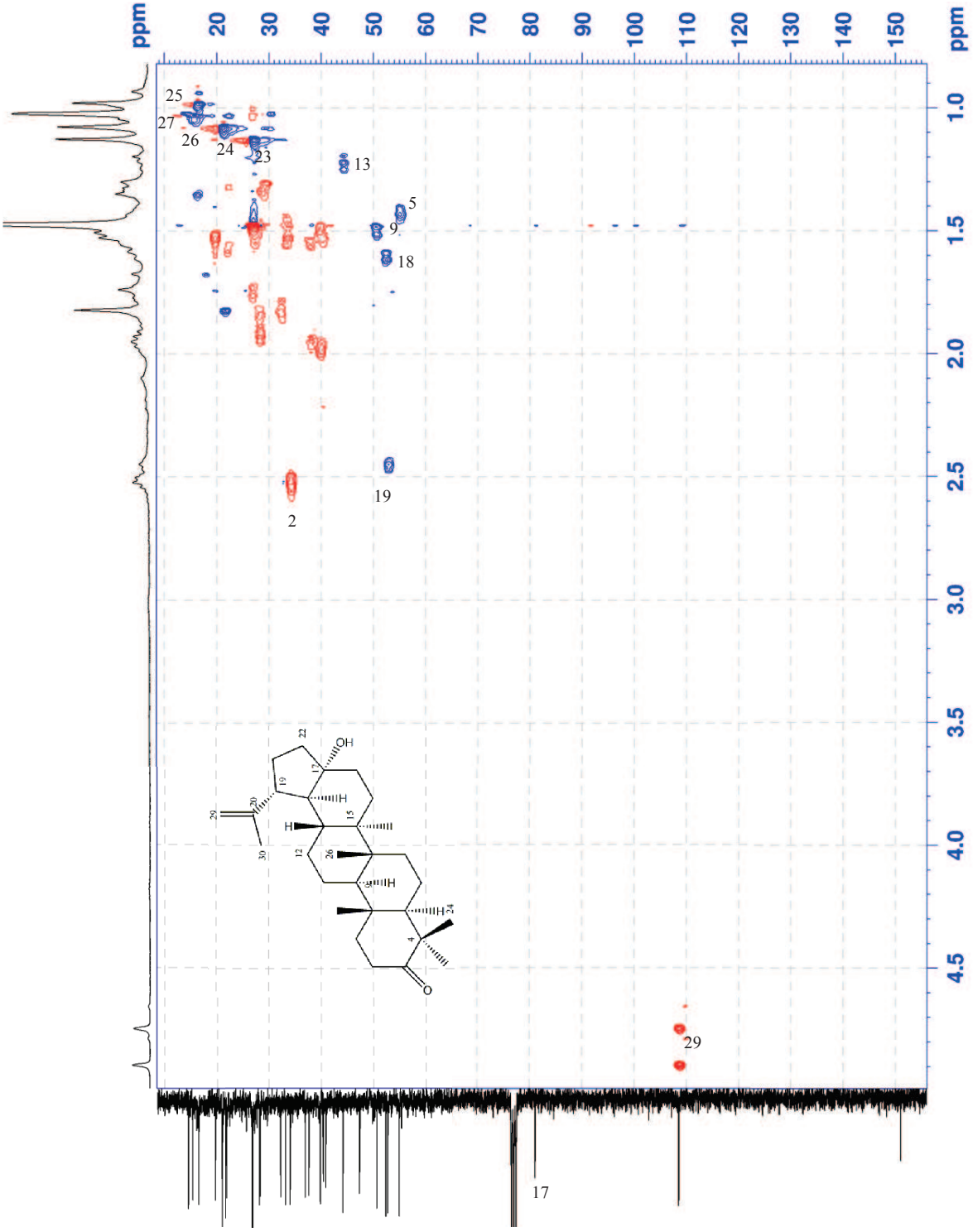

Figure 82. The expanded HSQCedited correlation of **25** (in $CDCl_3$) in the range of δ_H 0.8-4.9 ppm and δ_C 16-110 ppm.

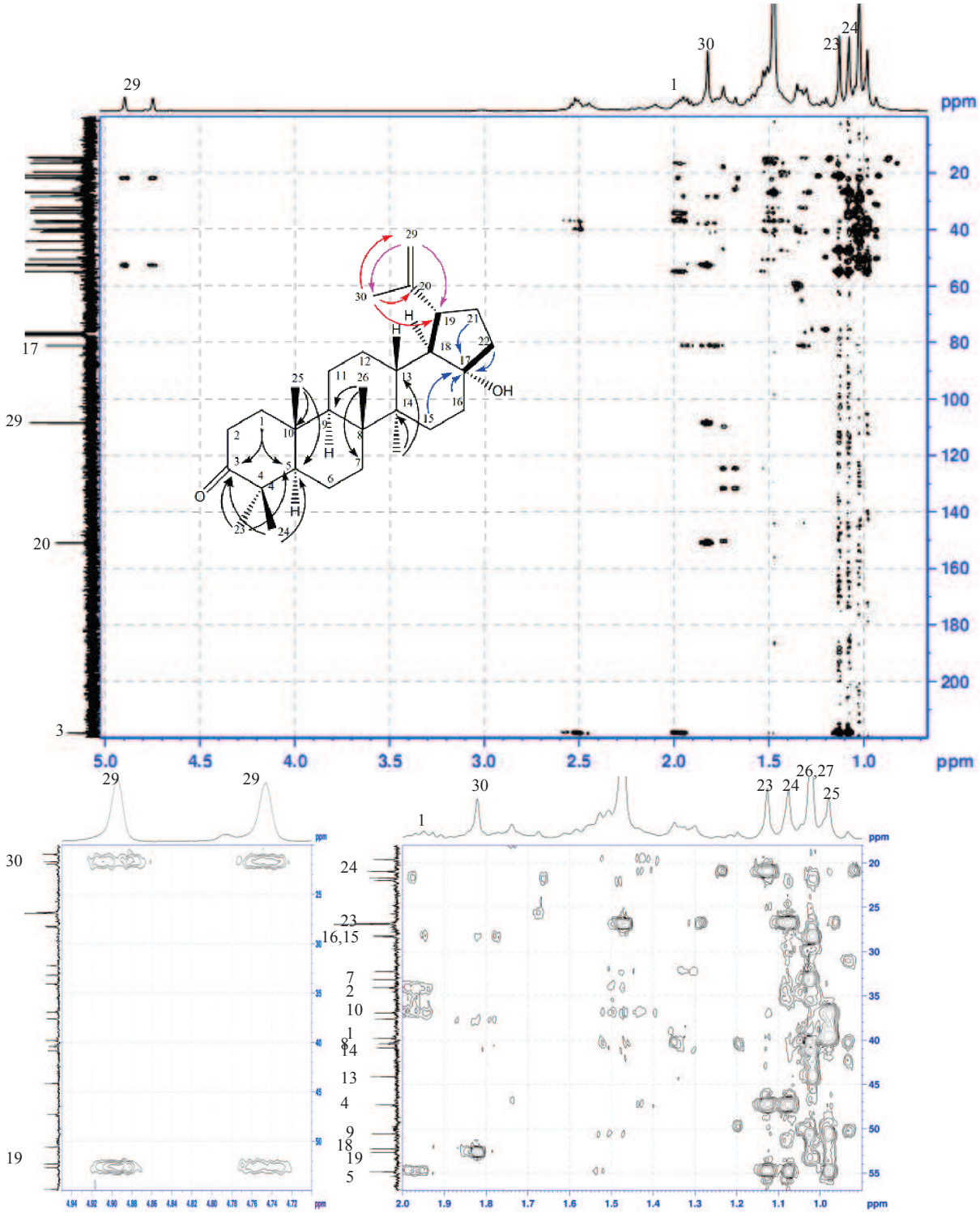

Figure 83. The HMBC correlation of **25** (in $CDCl_3$) and expanded spectrum in the range of δ_H 4.7-4.9 ppm, δ_C 20-55 ppm and δ_H 0.9-2.0 ppm, δ_C 18-57 ppm.

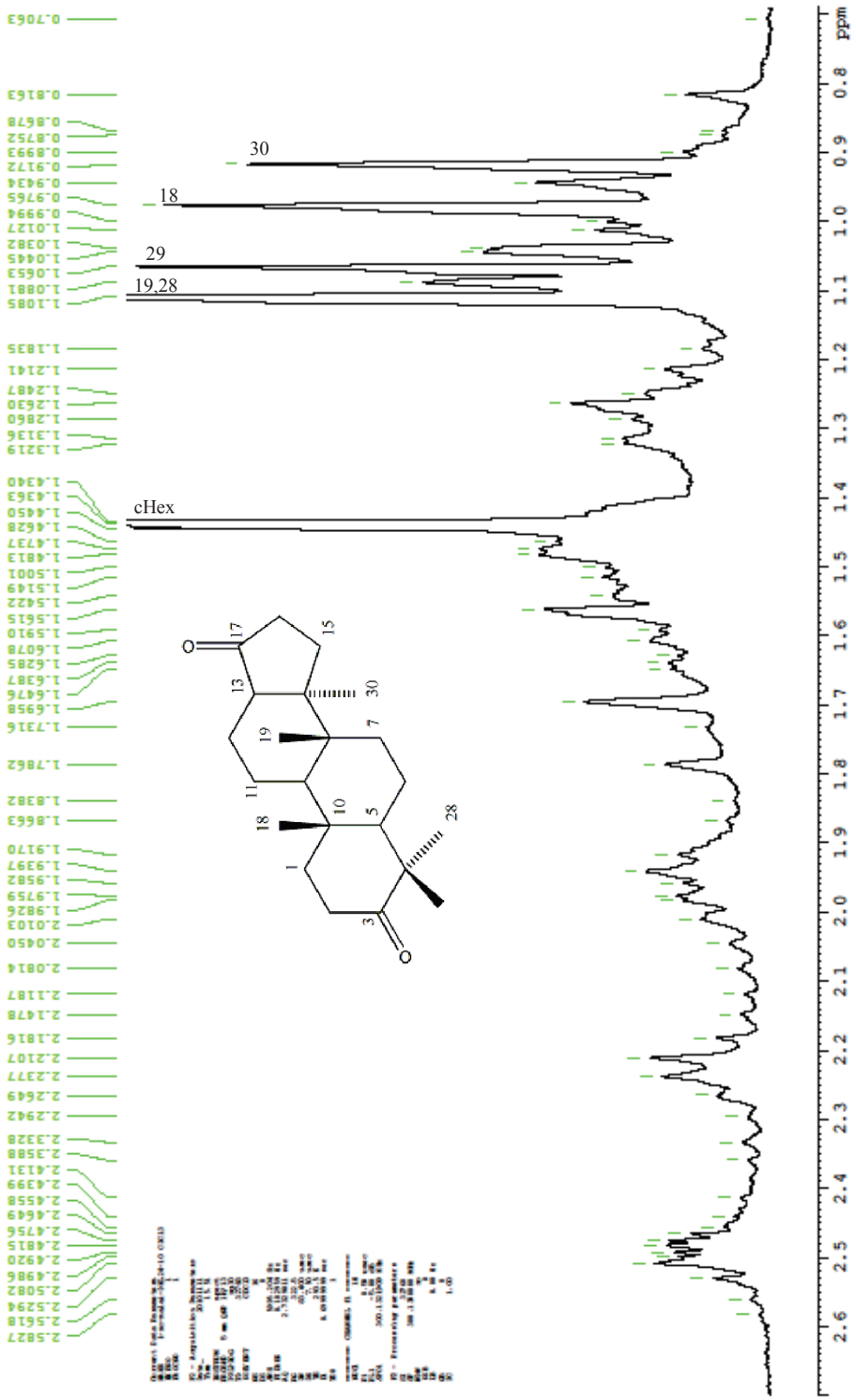

Figure 84. The expand ^{1}H NMR spectrum (300 MHz) of **<u>26</u>** (in $CDCl_3$).

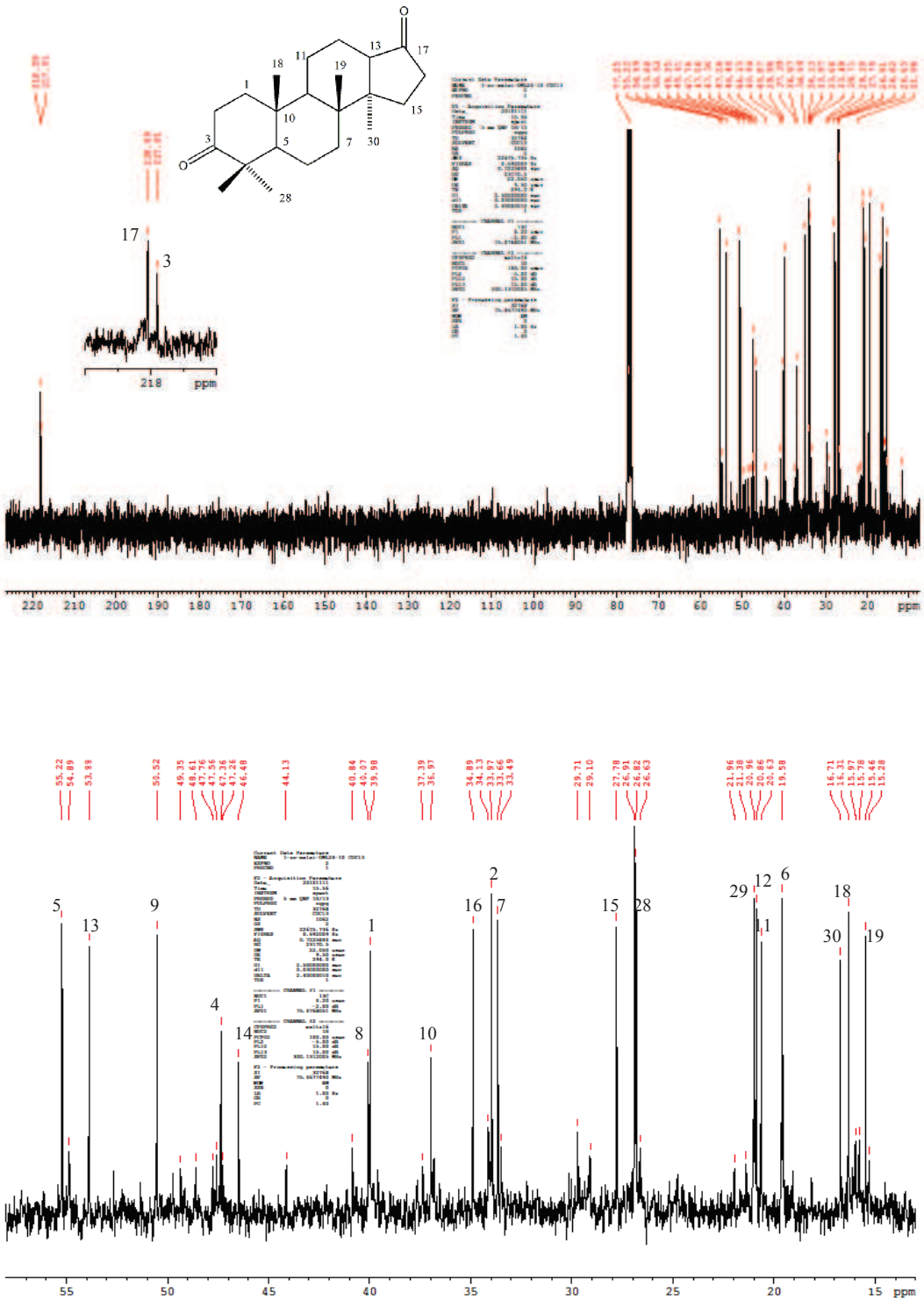

Figure 85. The ^{13}C NMR spectrum (75 MHz) of **26** (in $CDCl_3$) and expanded spectrum in the range of 13-58 ppm.

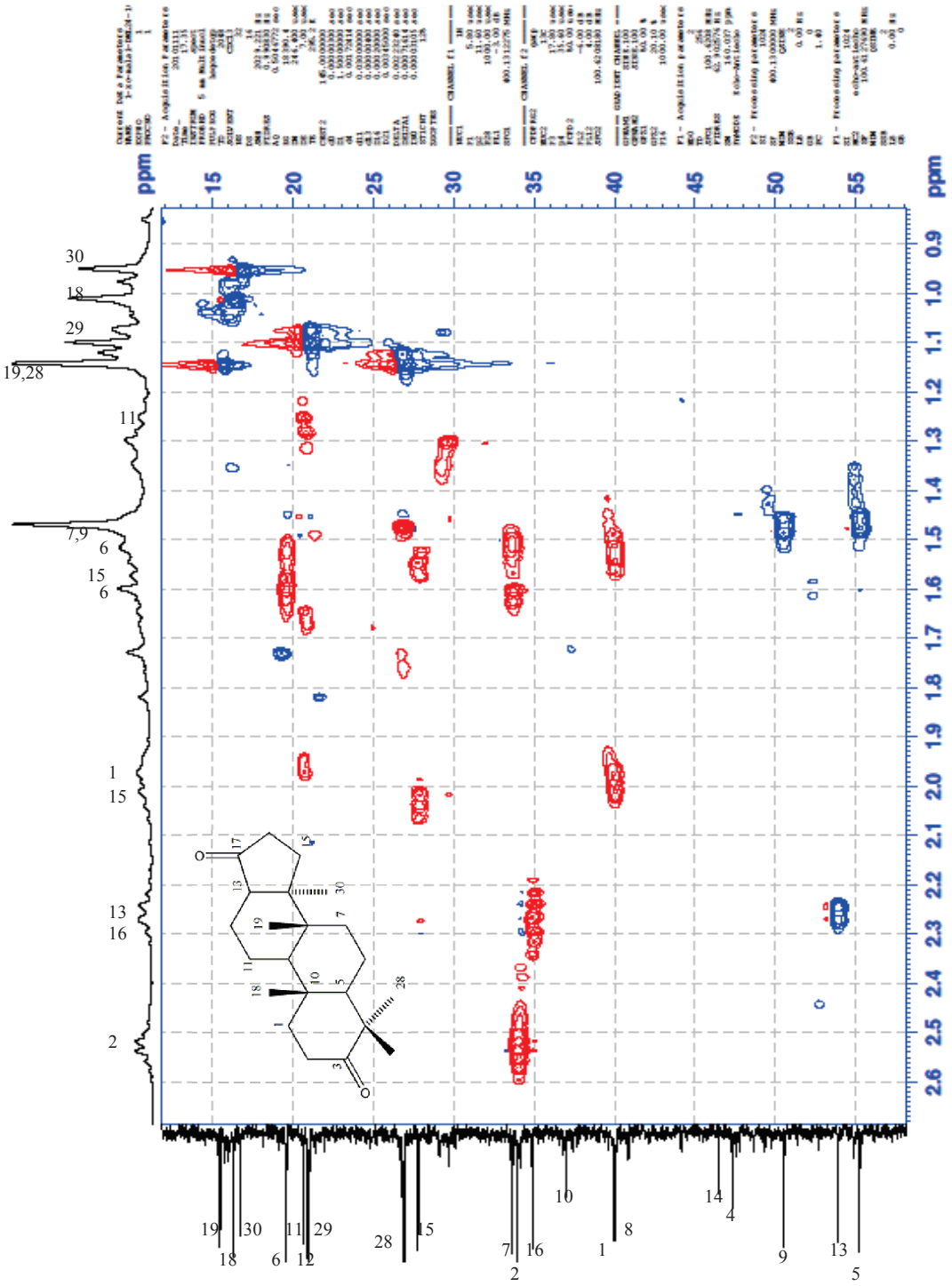

Figure 86. The expanded HSQCedited correlation of **26** (in $CDCl_3$) in the range of δ_H 0.8-2.7 ppm and δ_C 13-58 ppm.

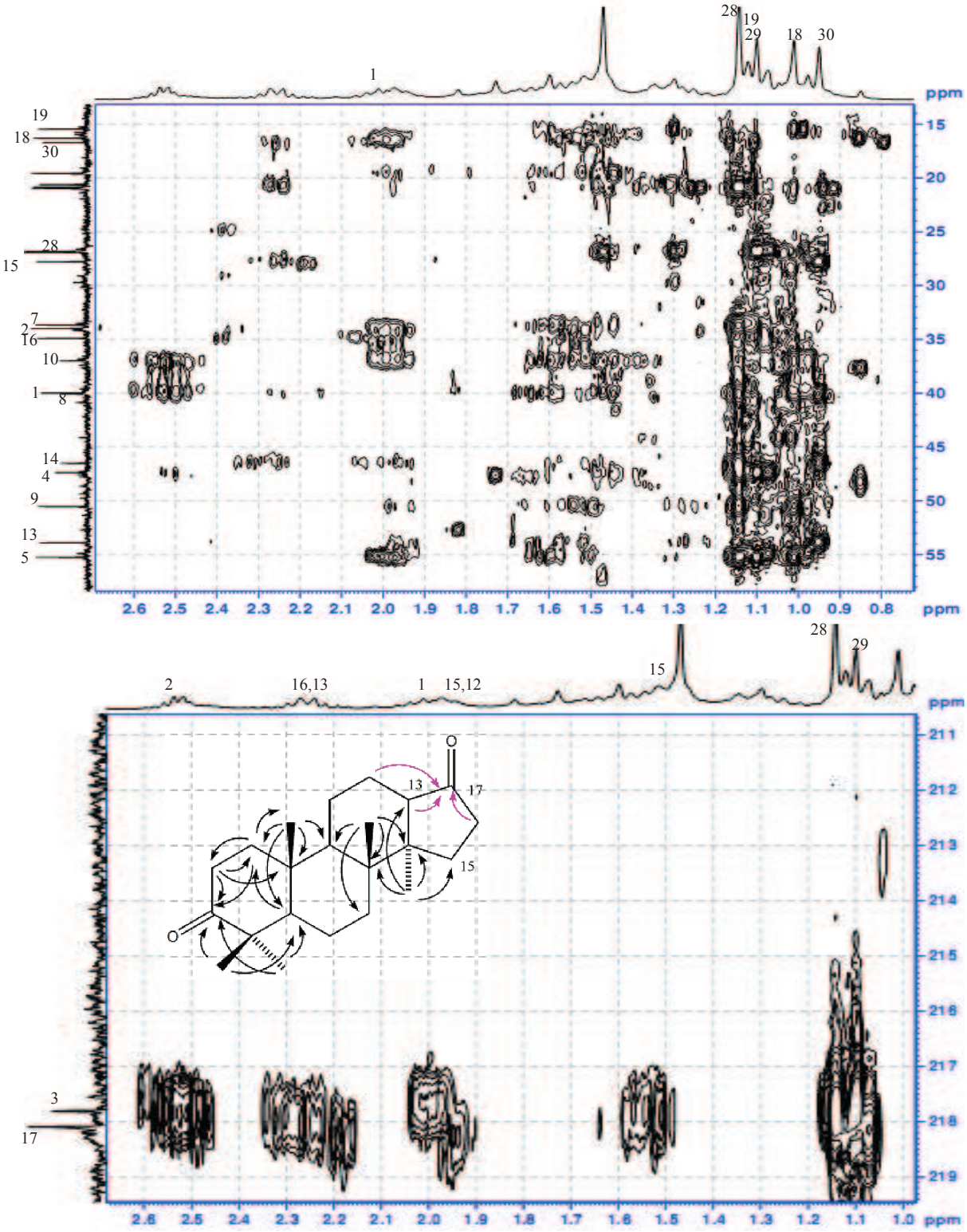

Figure 87. The expanded HMBC correlation of **<u>26</u>** (in $CDCl_3$) in the range of δ_H 0.7-2.7 ppm, δ_C 13-59 ppm and δ_H 1.0-2.7 ppm, δ_C 211-219 ppm.

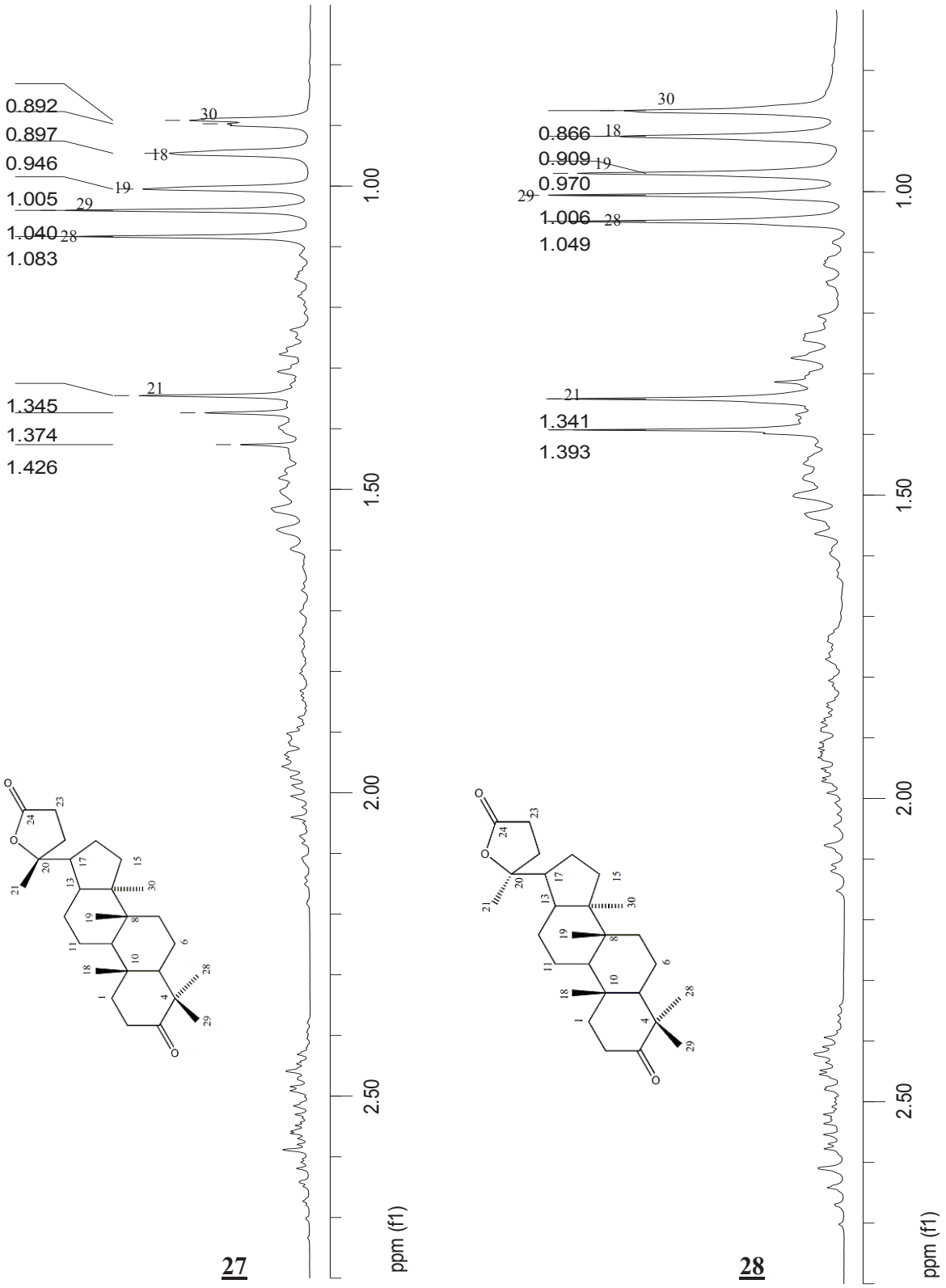

Figure 88. The expand ^{1}H NMR spectrum (300 MHz) of **27** and **28** (in $CDCl_3$) δ_H 0.7-2.7 ppm.

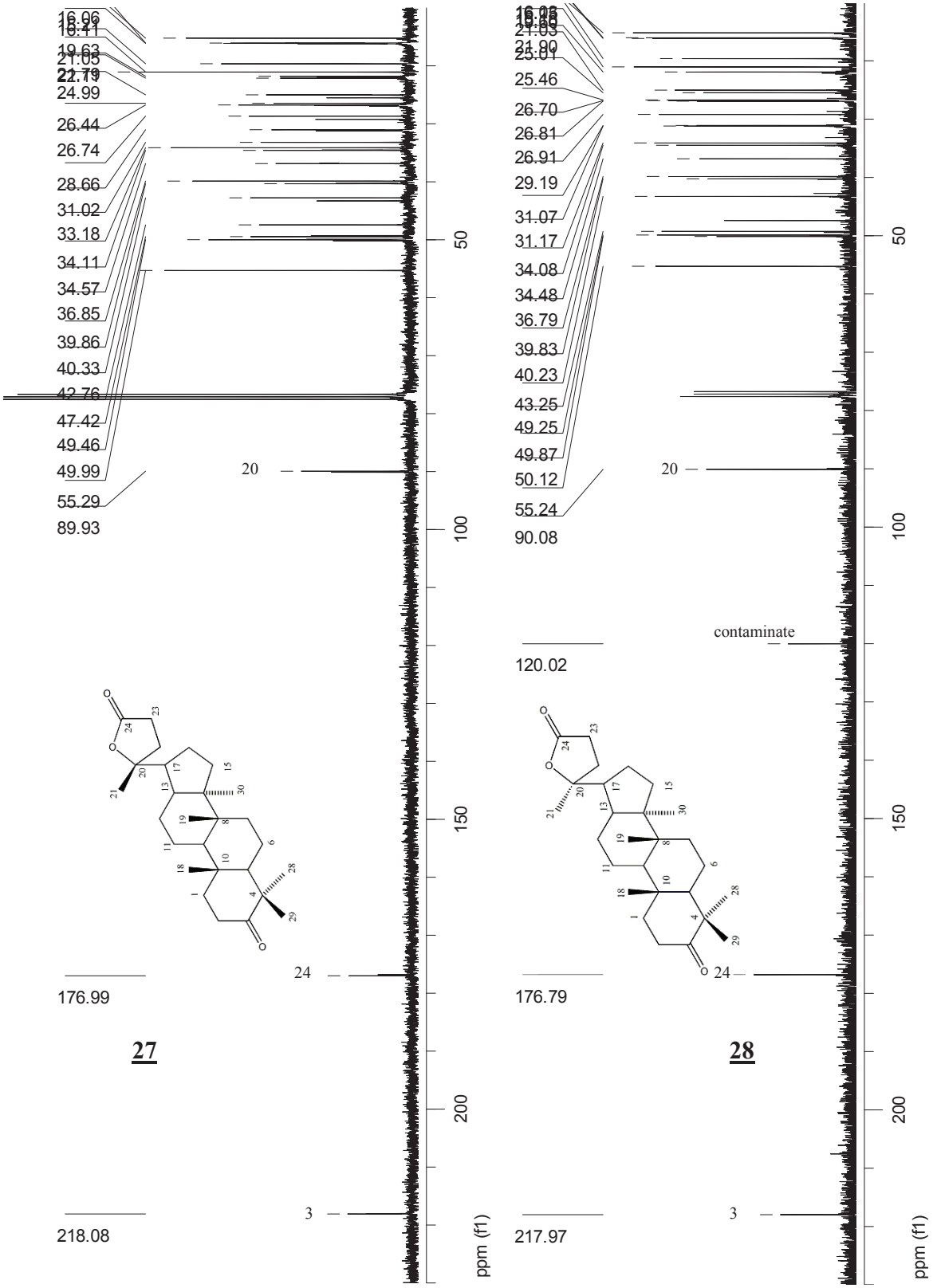

Figure 89. The ^{13}C NMR spectrum (75 MHz) of **27** and **28** (in $CDCl_3$).

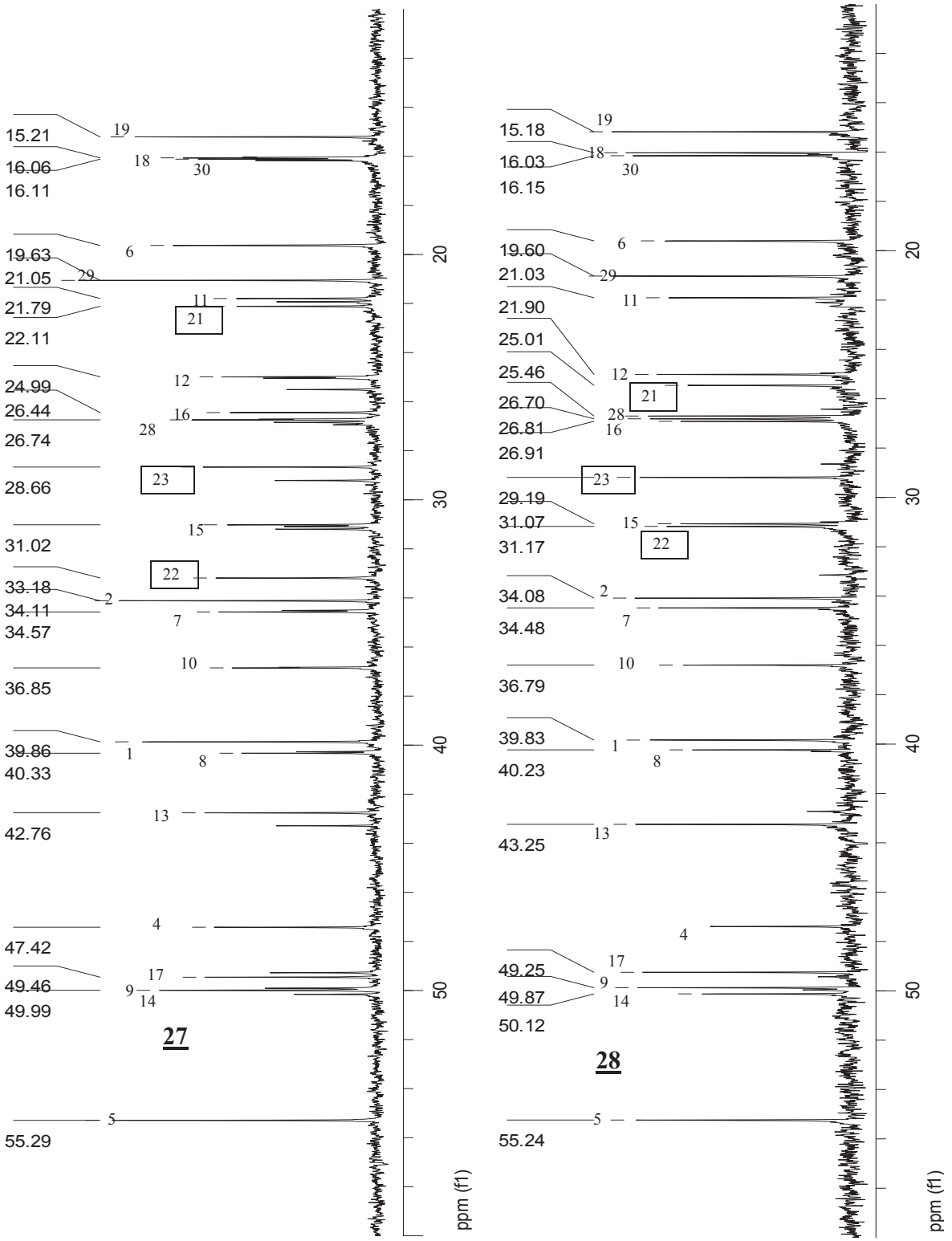

Figure 90. The expanded ^{13}C NMR spectrum (75 MHz) of **27** and **28** (in $CDCl_3$) in the range of δ_H 10-60 ppm.

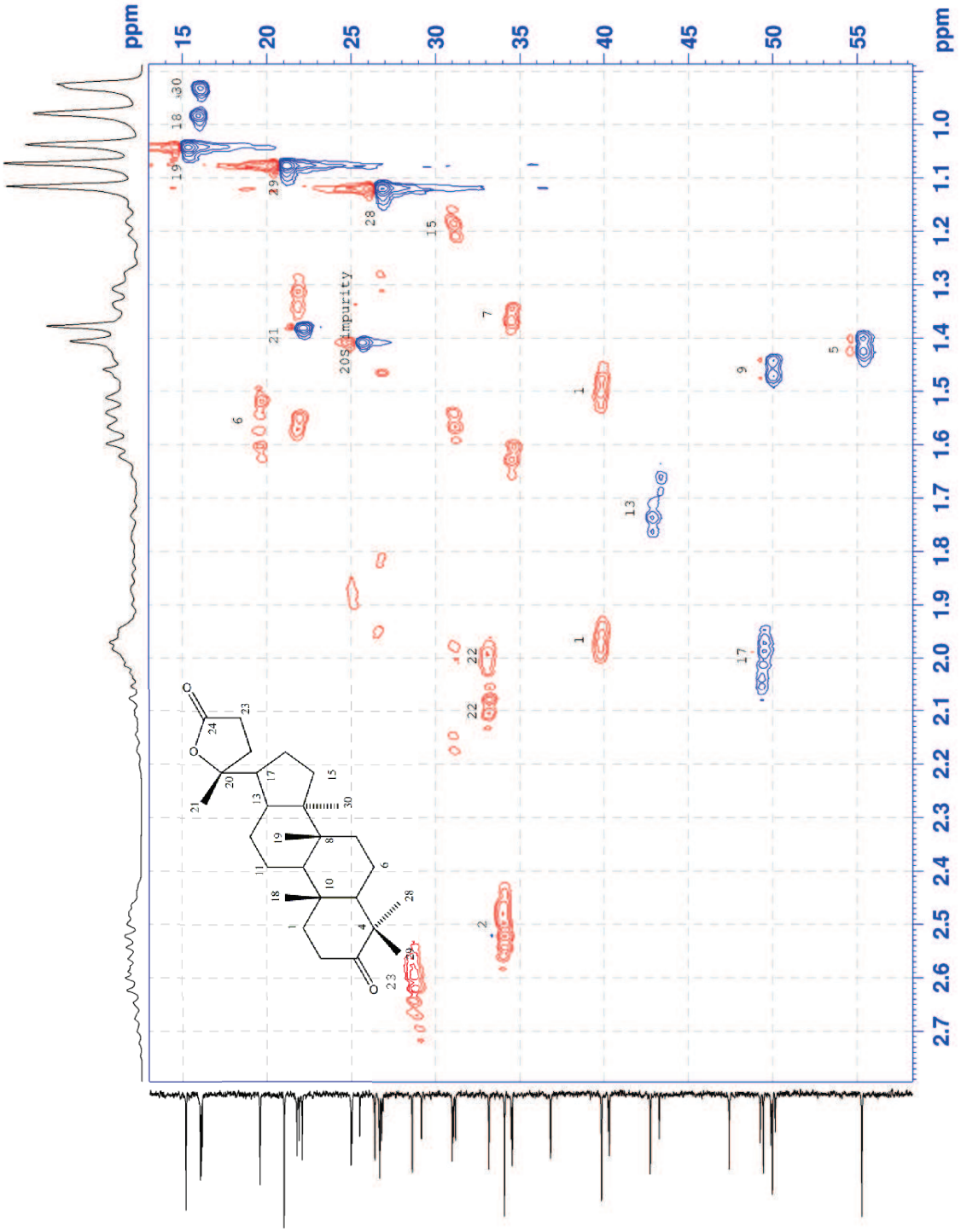

Figure 91. The expanded HSQCedited correlation of **27** (in $CDCl_3$) in the range of δ_H 0.8-2.8 ppm and δ_C 13-58 ppm.

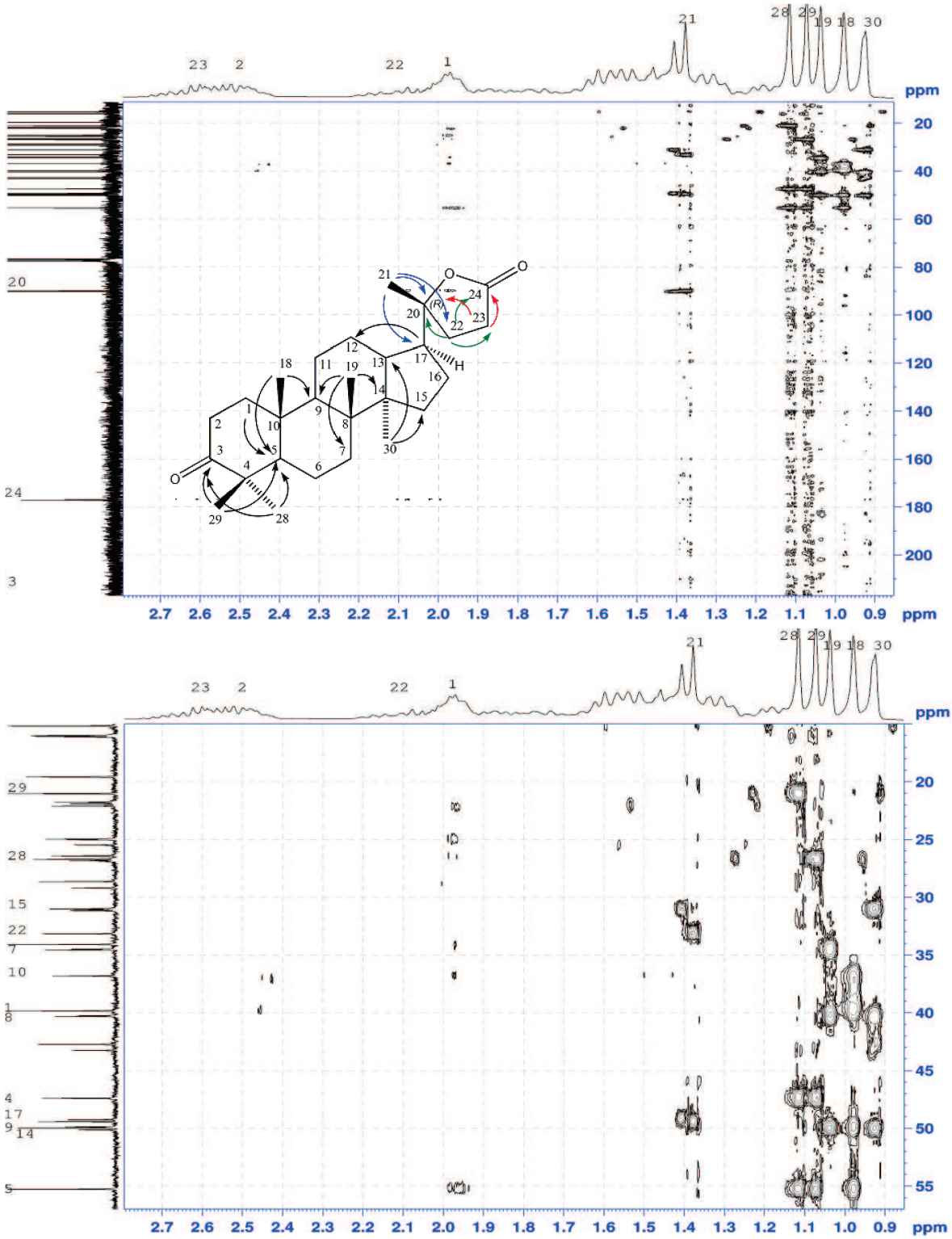

Figure 92. The HMBC correlation of **27** (in $CDCl_3$) and expanded spectrum in the range of δ_H 0.9-2.8 ppm, δ_C 15-57 ppm.

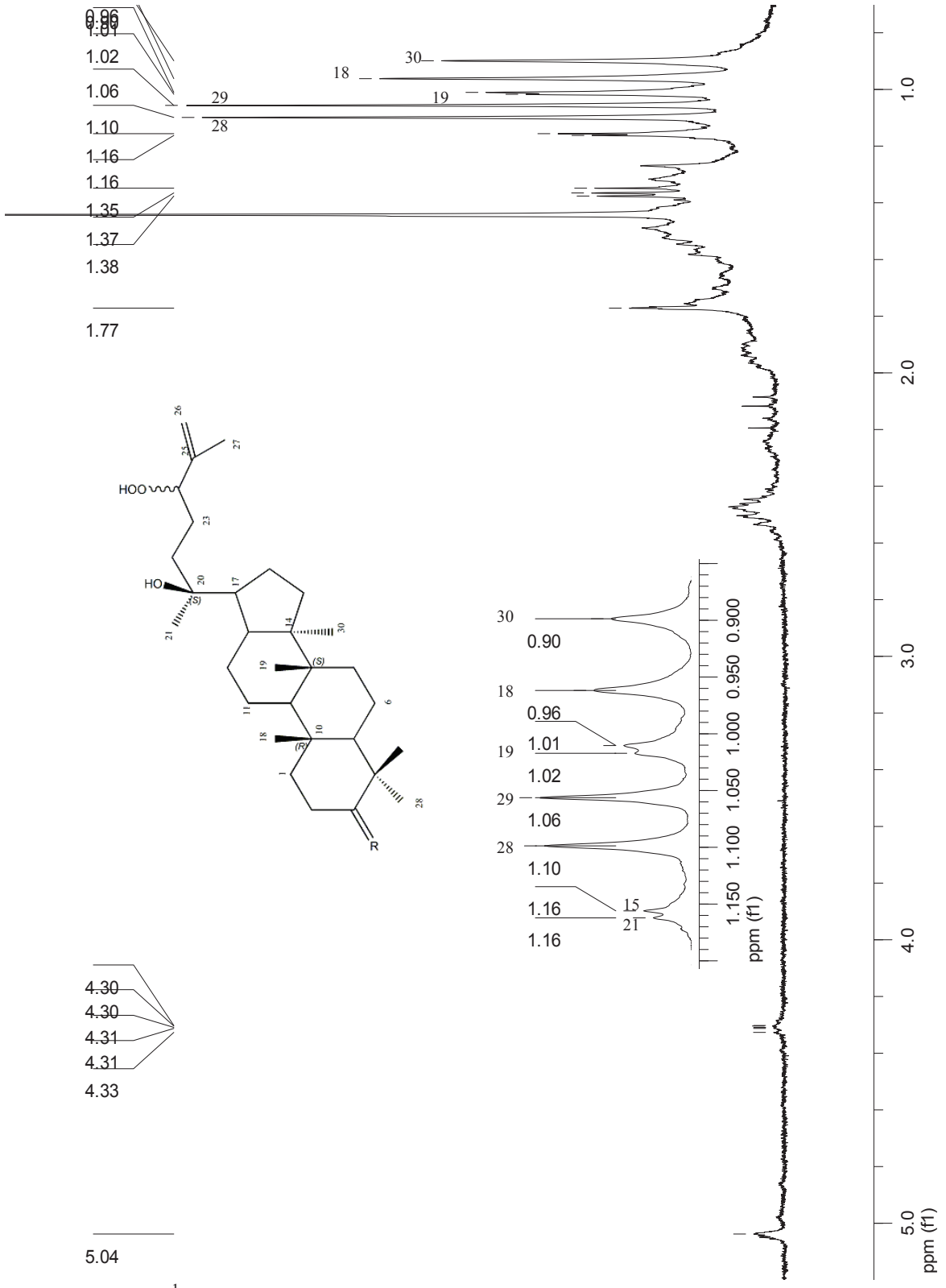

Figure 93. The ^{1}H NMR spectrum (300 MHz) of **29** (in $CDCl_3$) and expanded spectrum in the range of 0.85-1.20 ppm.

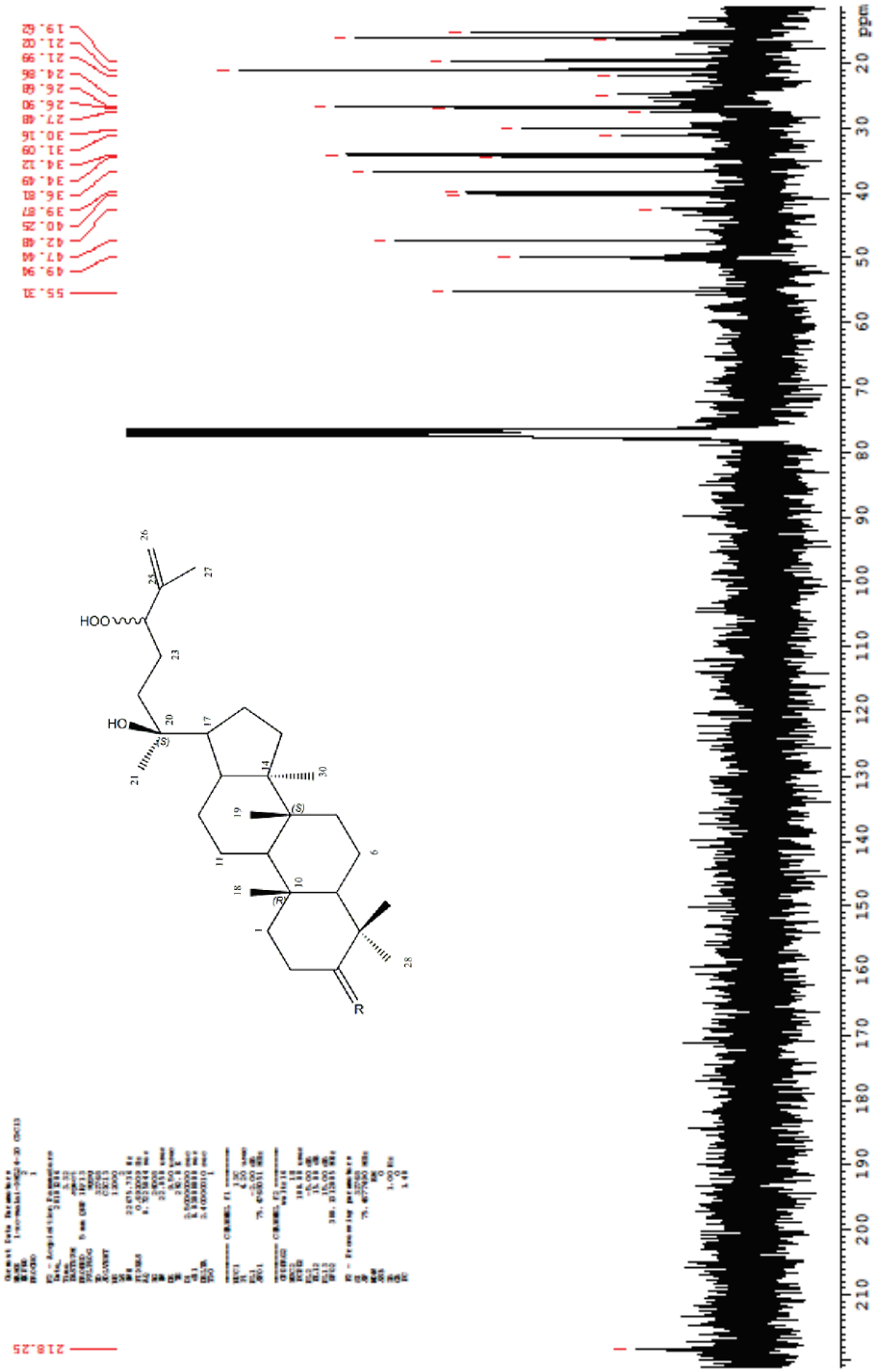

Figure 94. The ^{13}C NMR spectrum (75 MHz) of **29** (in $CDCl_3$).

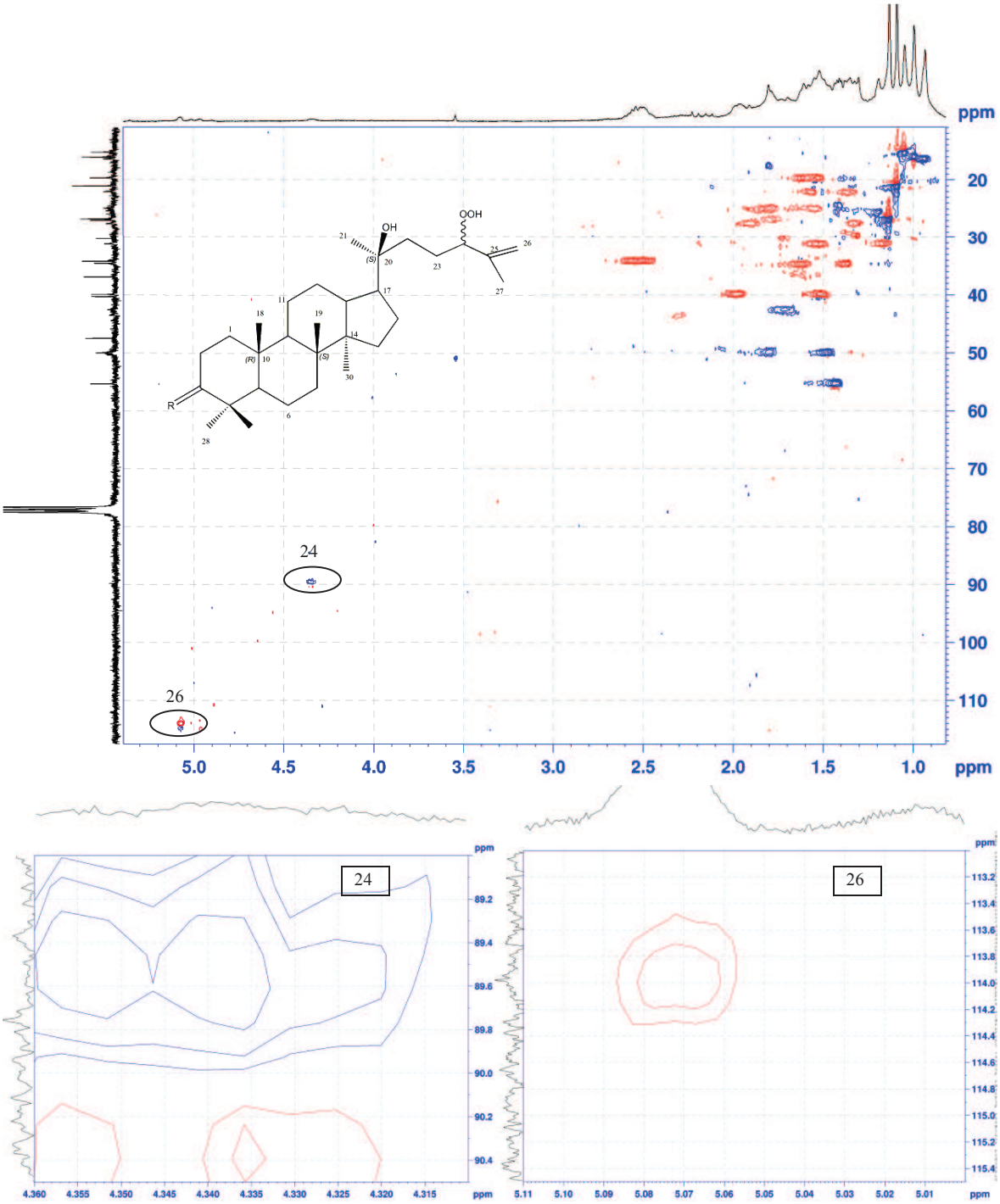

Figure 95. The HSQCedited correlation of **29** (in $CDCl_3$) and expanded spectrum in the range of δ_H 4.31-4.36 ppm, δ_C 89.00-90.50 ppm and δ_H 5.00-5.11 ppm, δ_C 113.00-115.50 ppm.

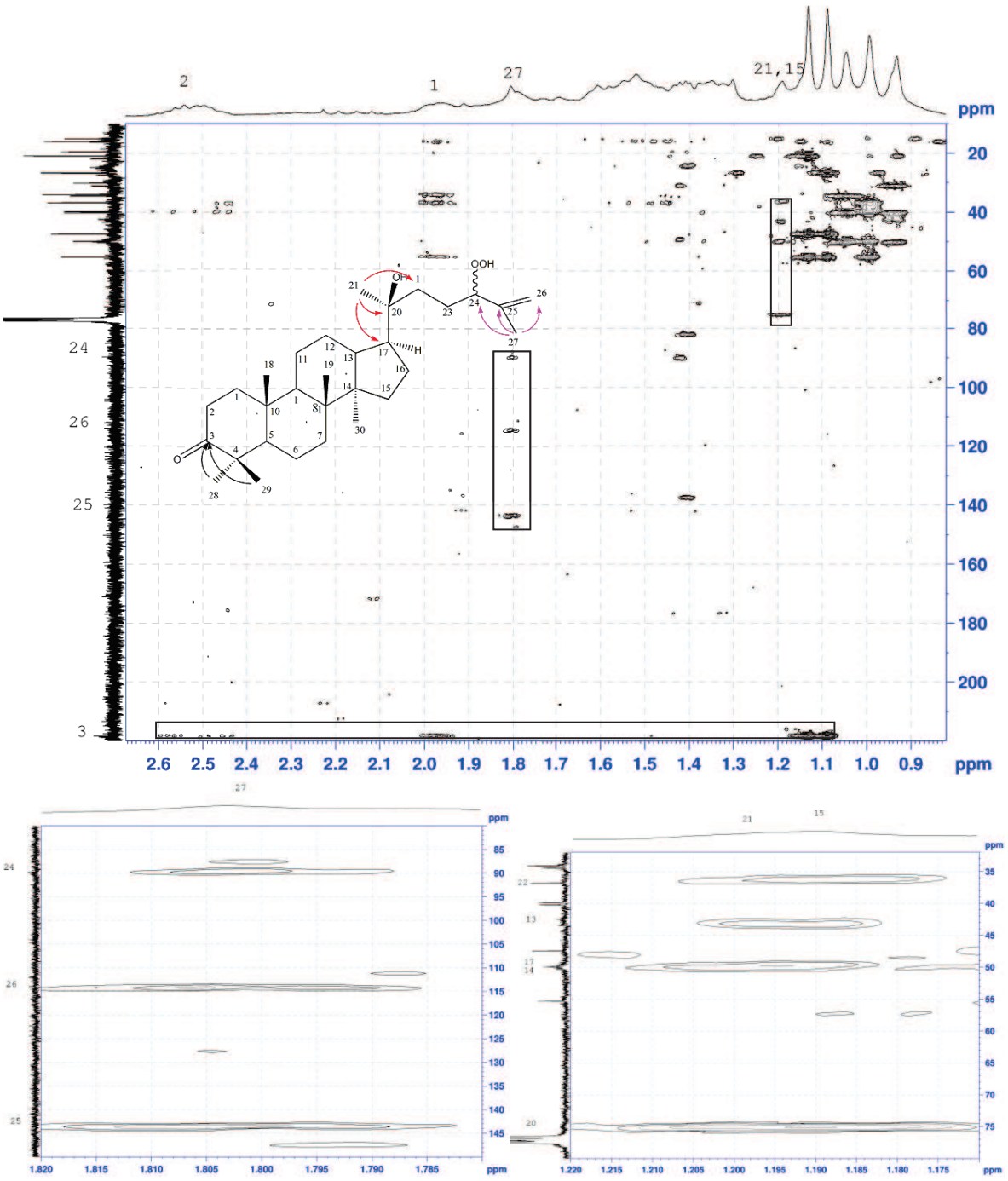

Figure 96. The HMBC correlation of **29** (in $CDCl_3$) and expanded spectrum in the range of δ_H 1.78-1.82 ppm, δ_C 86.00-150.00 ppm and δ_H 1.17-1.22 ppm, δ_C 32.00-80.00 ppm.

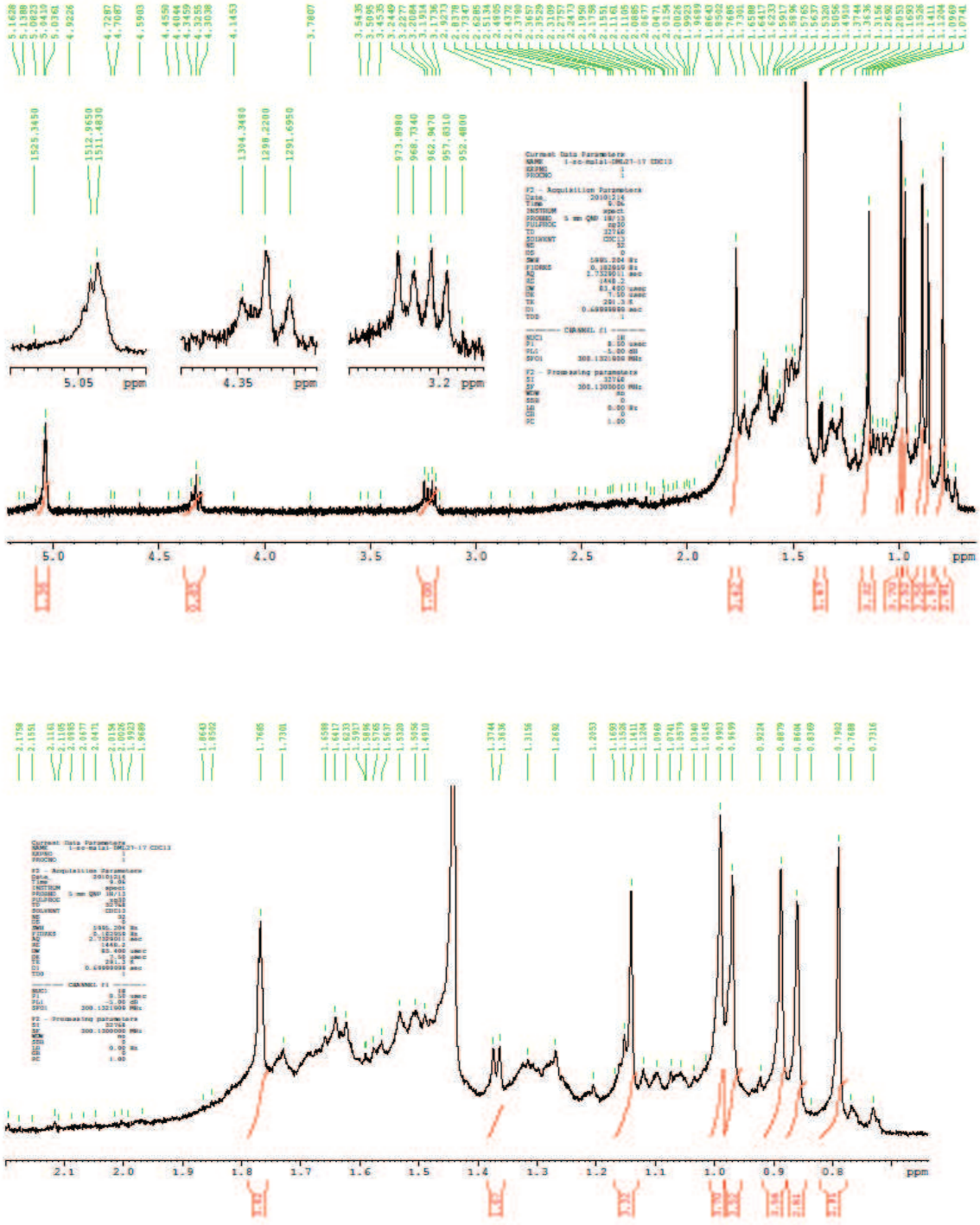

Figure 97. The ^{1}H NMR spectrum (300 MHz) of **32** (in $CDCl_3$) and expanded spectrum in the range of 0.7-2.2 ppm.

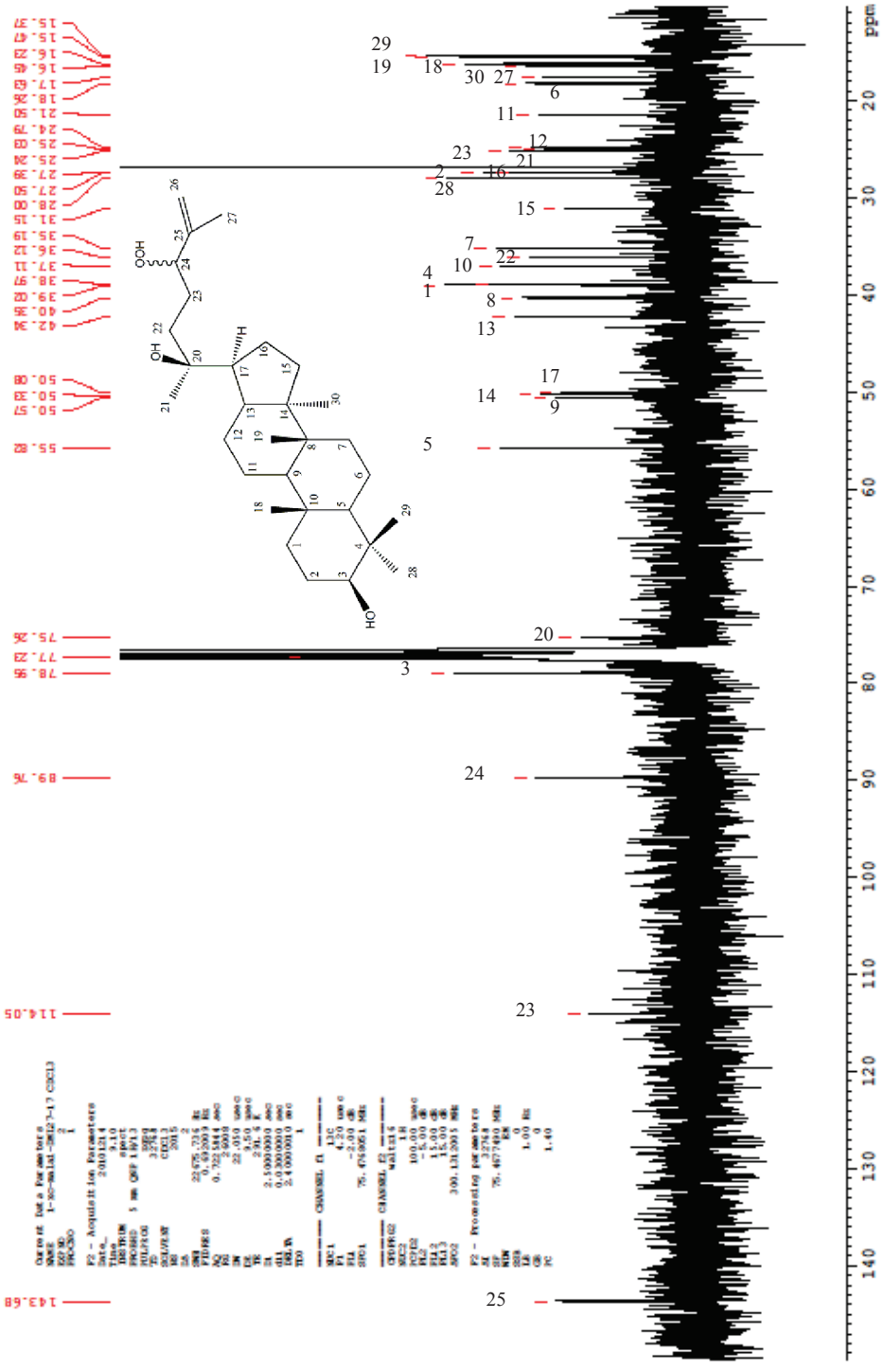

Figure 98. The ^{13}C NMR spectrum (75 MHz) of **32** (in $CDCl_3$).

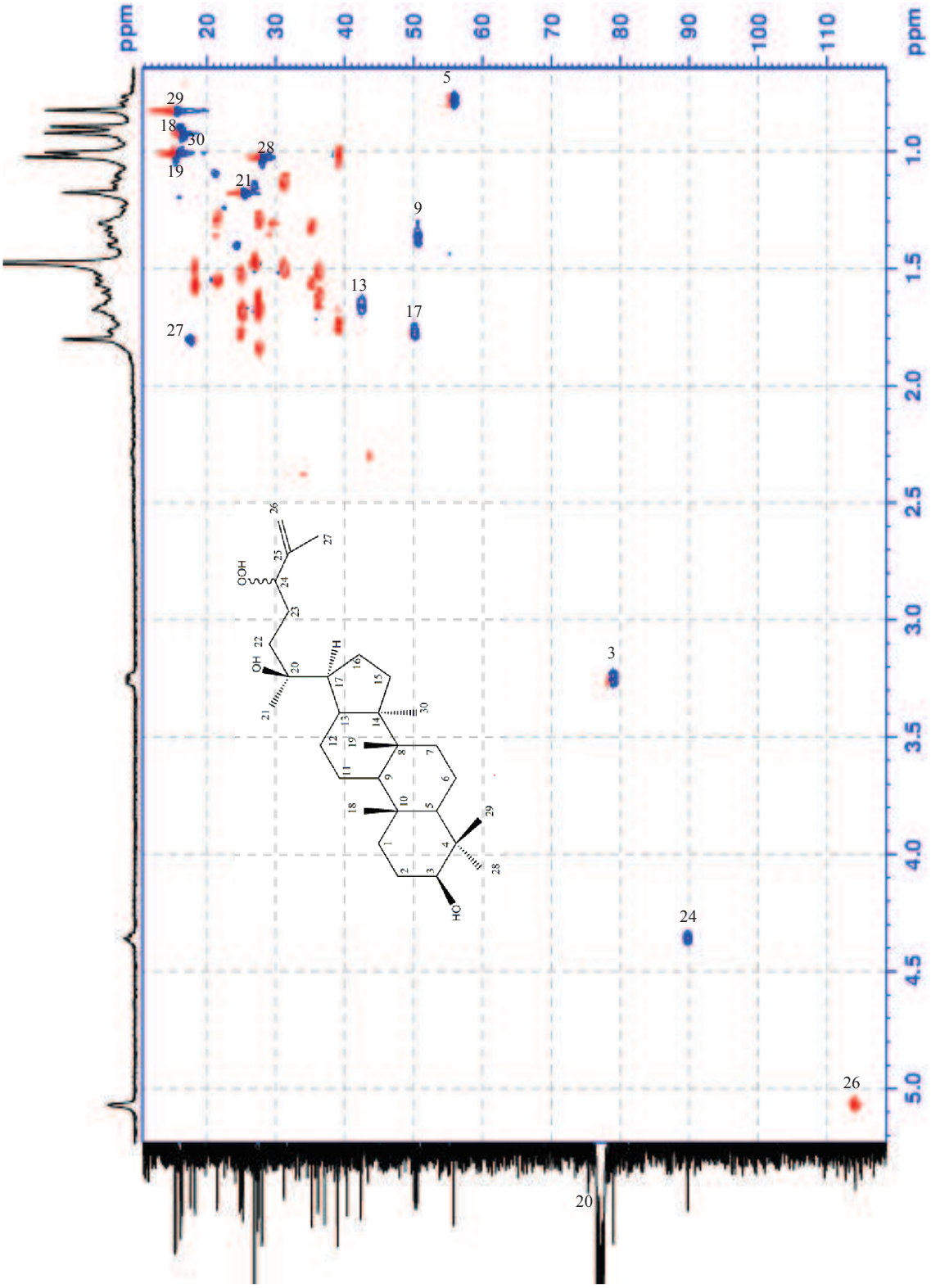

Figure 99. The HSQCedited correlation of **32** (in $CDCl_3$).

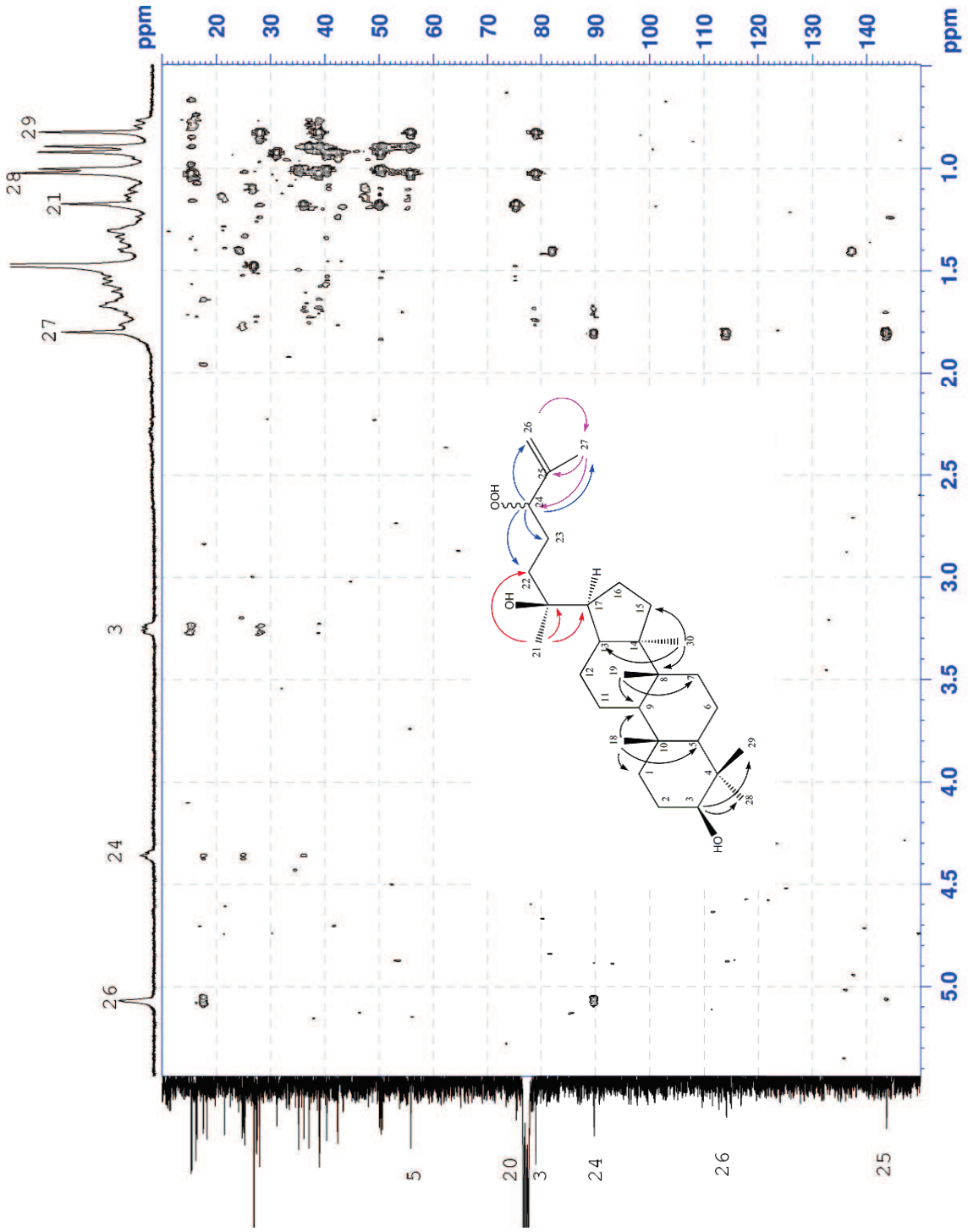

Figure 100. The HMBC correlation of **32** (in $CDCl_3$).

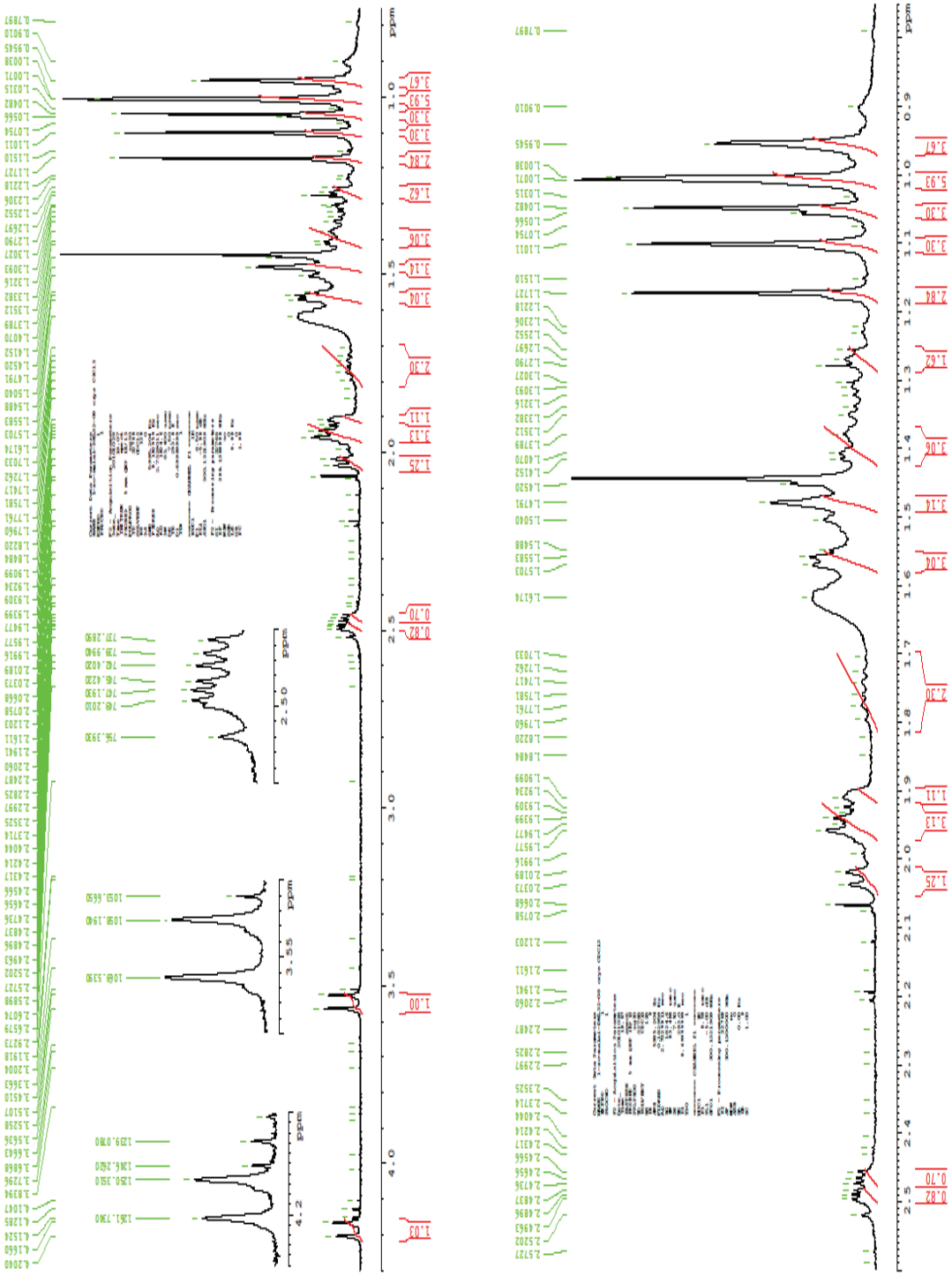

Figure 101. The ^{1}H NMR spectrum (300 MHz) of **36** (in $CDCl_3$) and expanded spectrum in the range of 0.8-2.6 ppm.

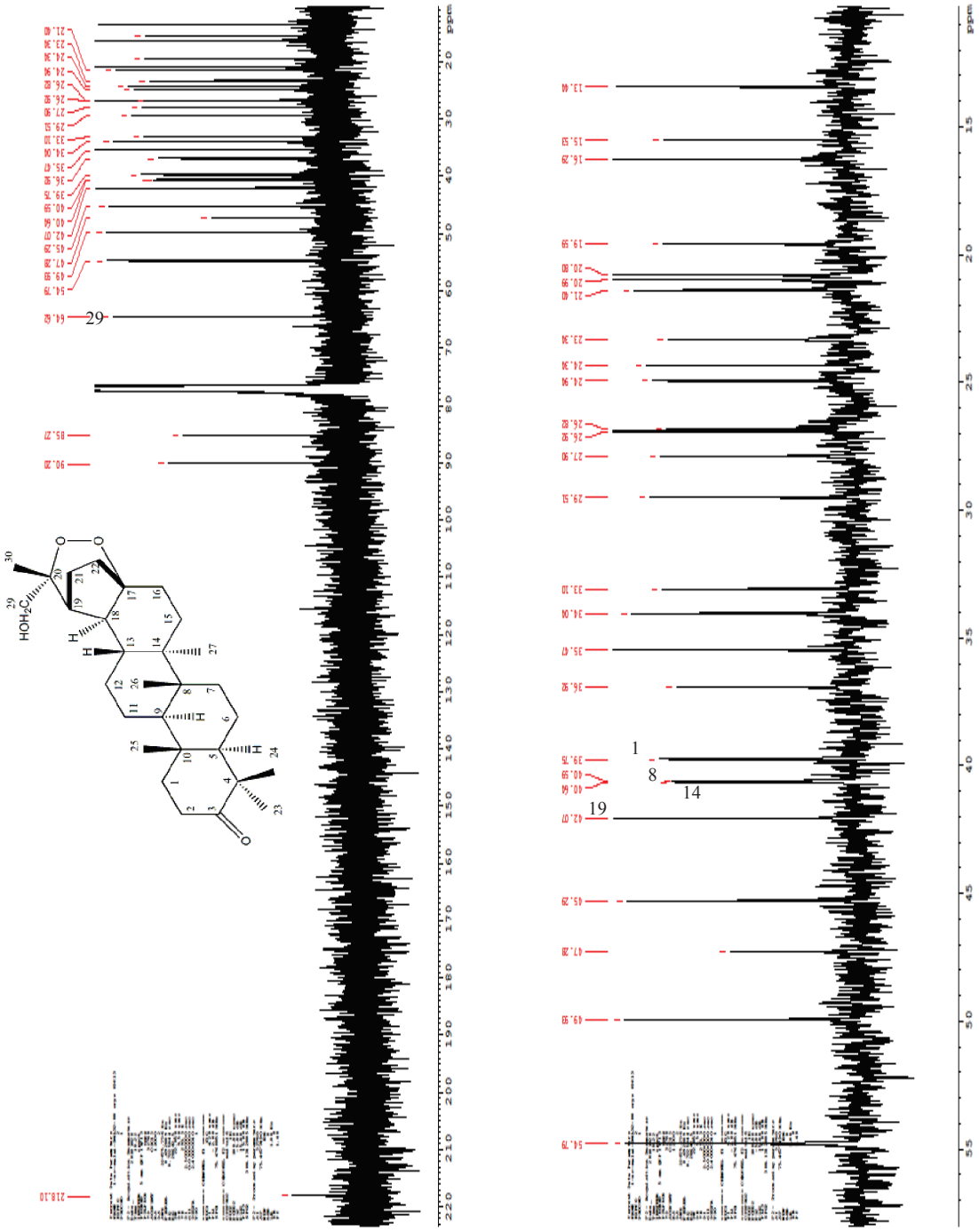

Figure 102. The ^{13}C NMR spectrum (75 MHz) of **36** (in $CDCl_3$) and expanded spectrum in the range of 11-58 ppm.

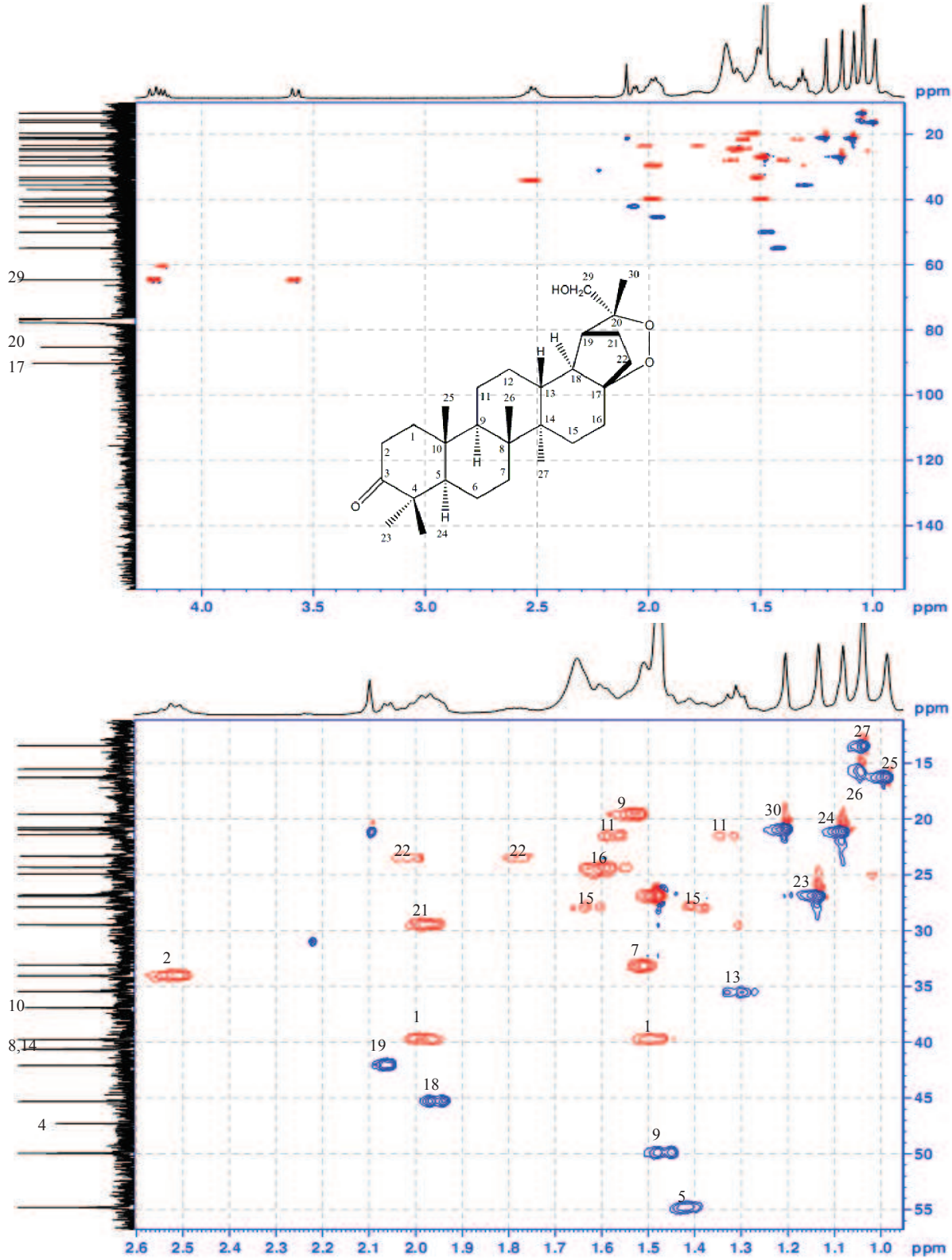

Figure 103. The HSQCedited correlation of **36** (in $CDCl_3$) and expanded spectrum in the range of δ_H 0.9-2.6 ppm and δ_C 10-56 ppm.

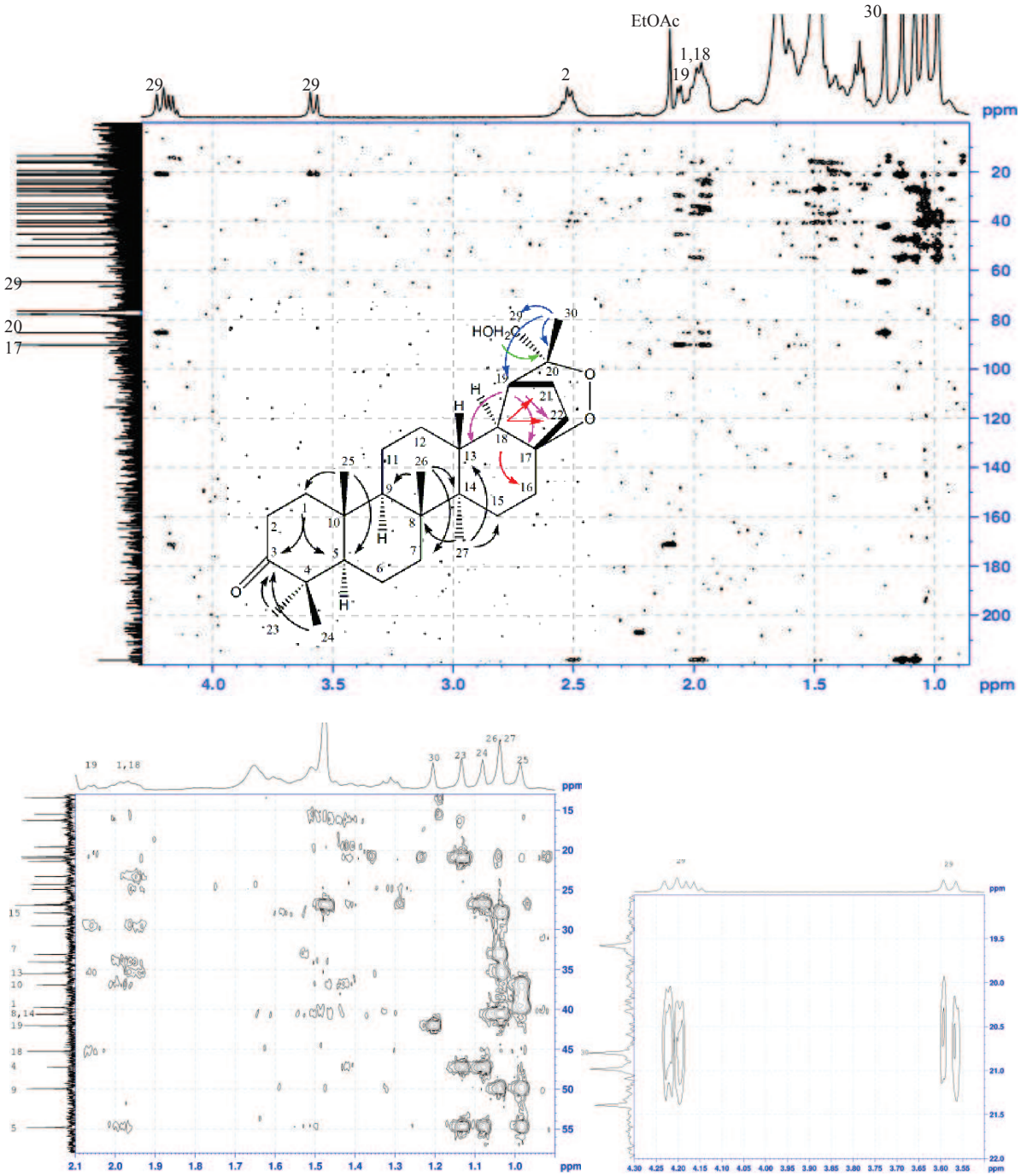

Figure 104. The HMBC correlation of **36** (in $CDCl_3$) and expanded spectrum in the range of δ_H 0.9-2.1 ppm, δ_C 13-58 ppm and δ_H 3.5-4.3 ppm, δ_C 19.5-22.0 ppm.

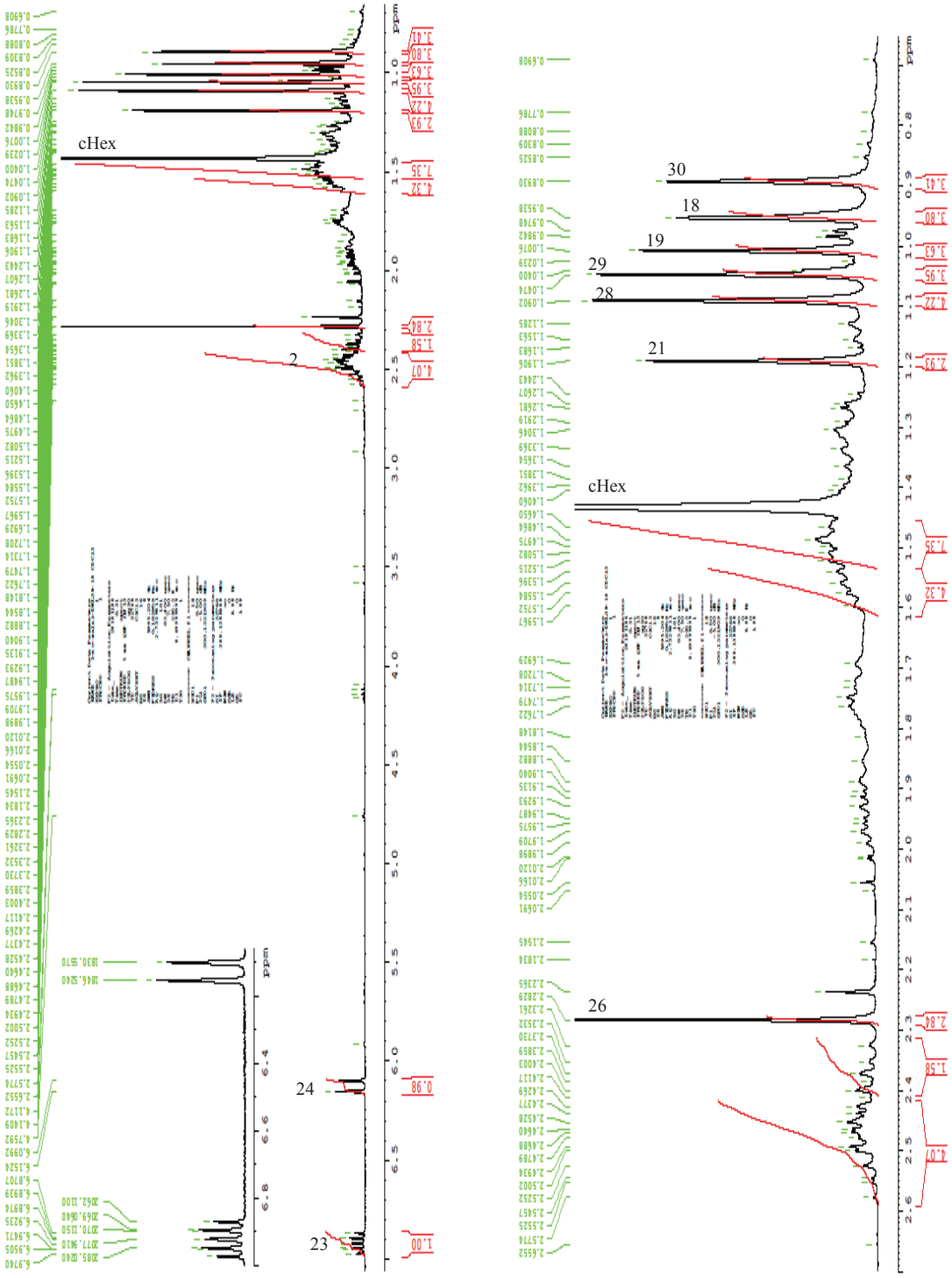

Figure 105. The ^{1}H NMR spectrum (300 MHz) of **39** (in $CDCl_3$) and expanded spectrum in the range of 0.7-2.7 ppm.

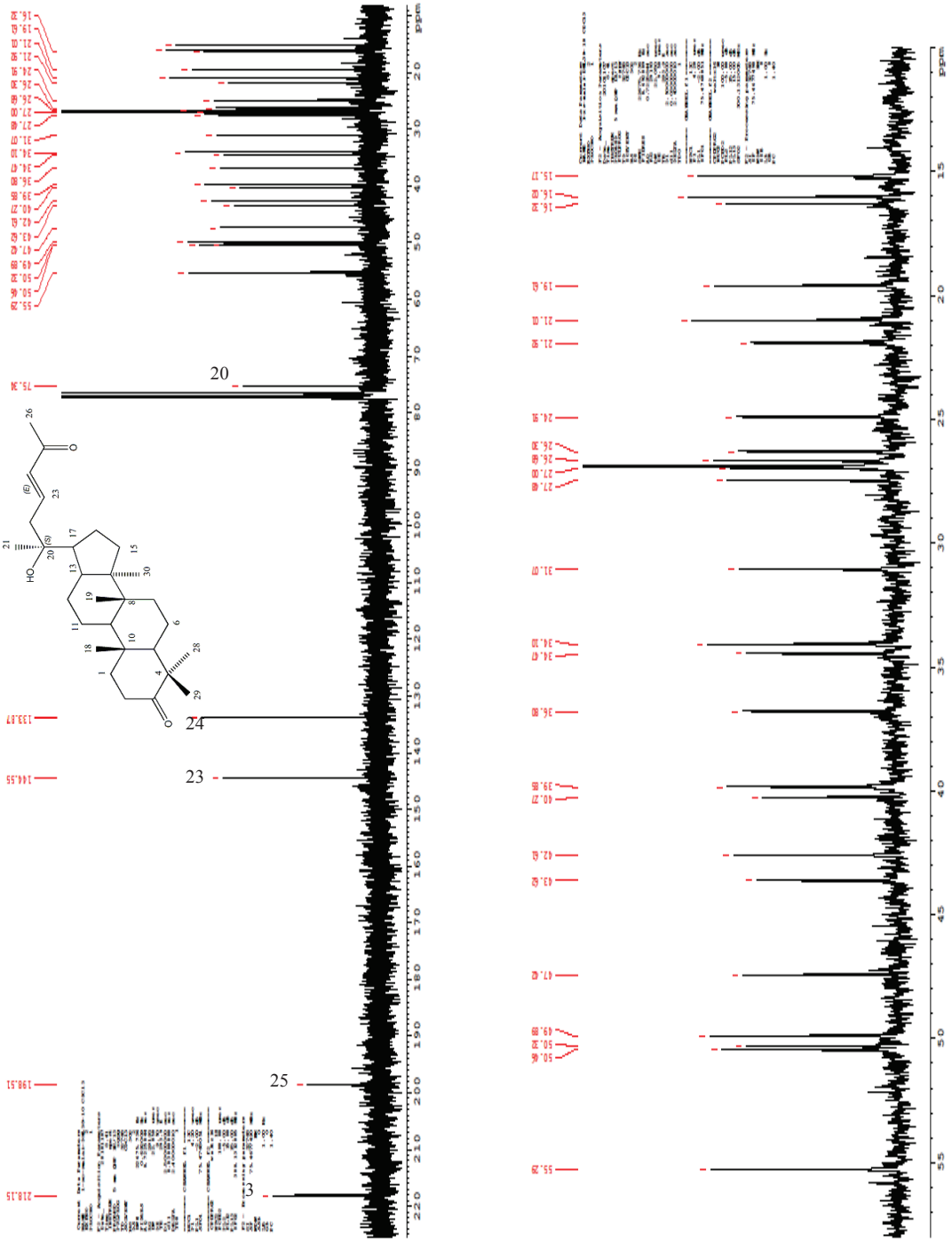

Figure 106. The ^{13}C NMR spectrum (75 MHz) of **39** (in $CDCl_3$) and expanded spectrum in the range of 10-58 ppm.

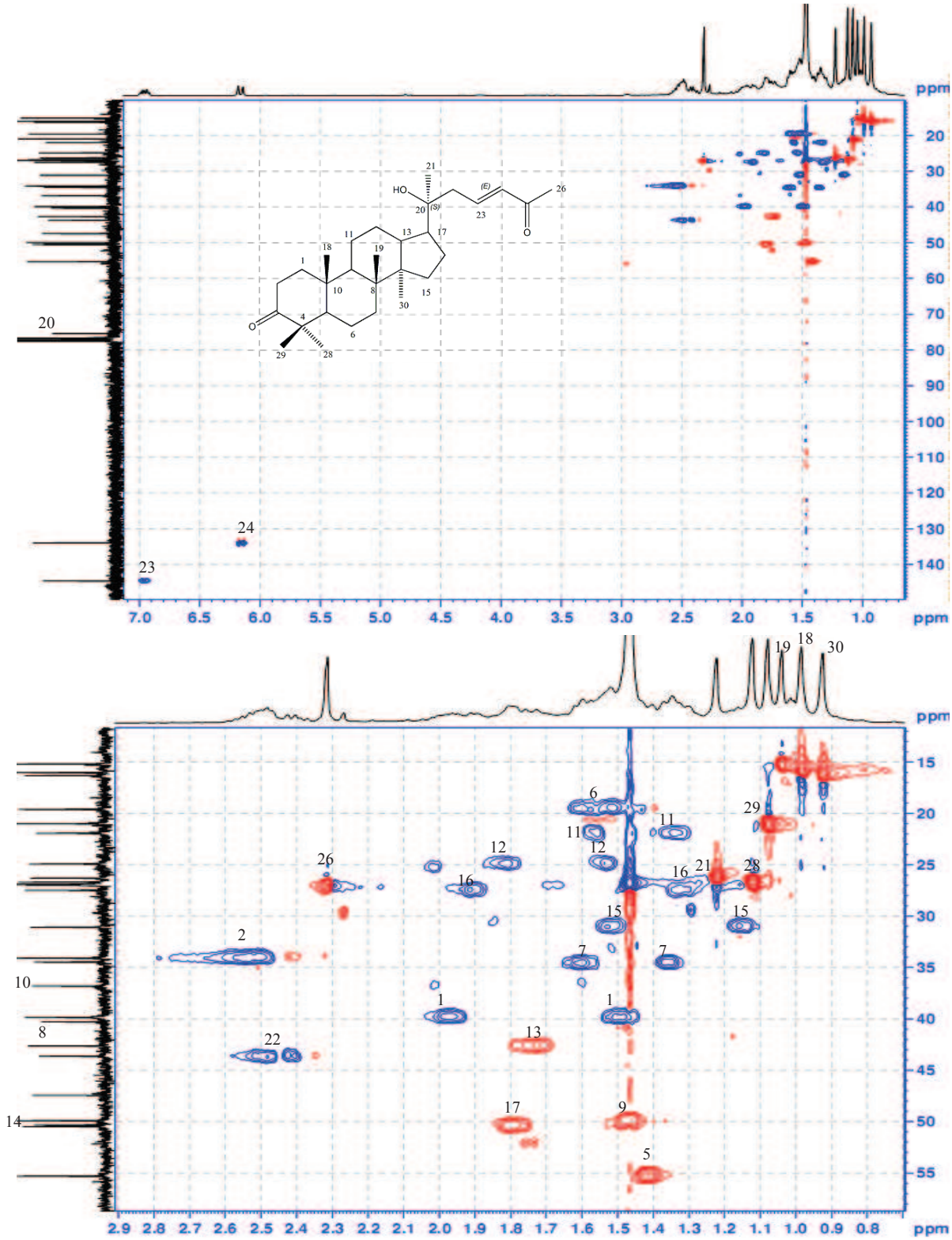

Figure 107. The HSQCedited correlation of **39** (in $CDCl_3$) and expanded spectrum in the range of δ_H 0.9-2.9 ppm and δ_C 12-58 ppm.

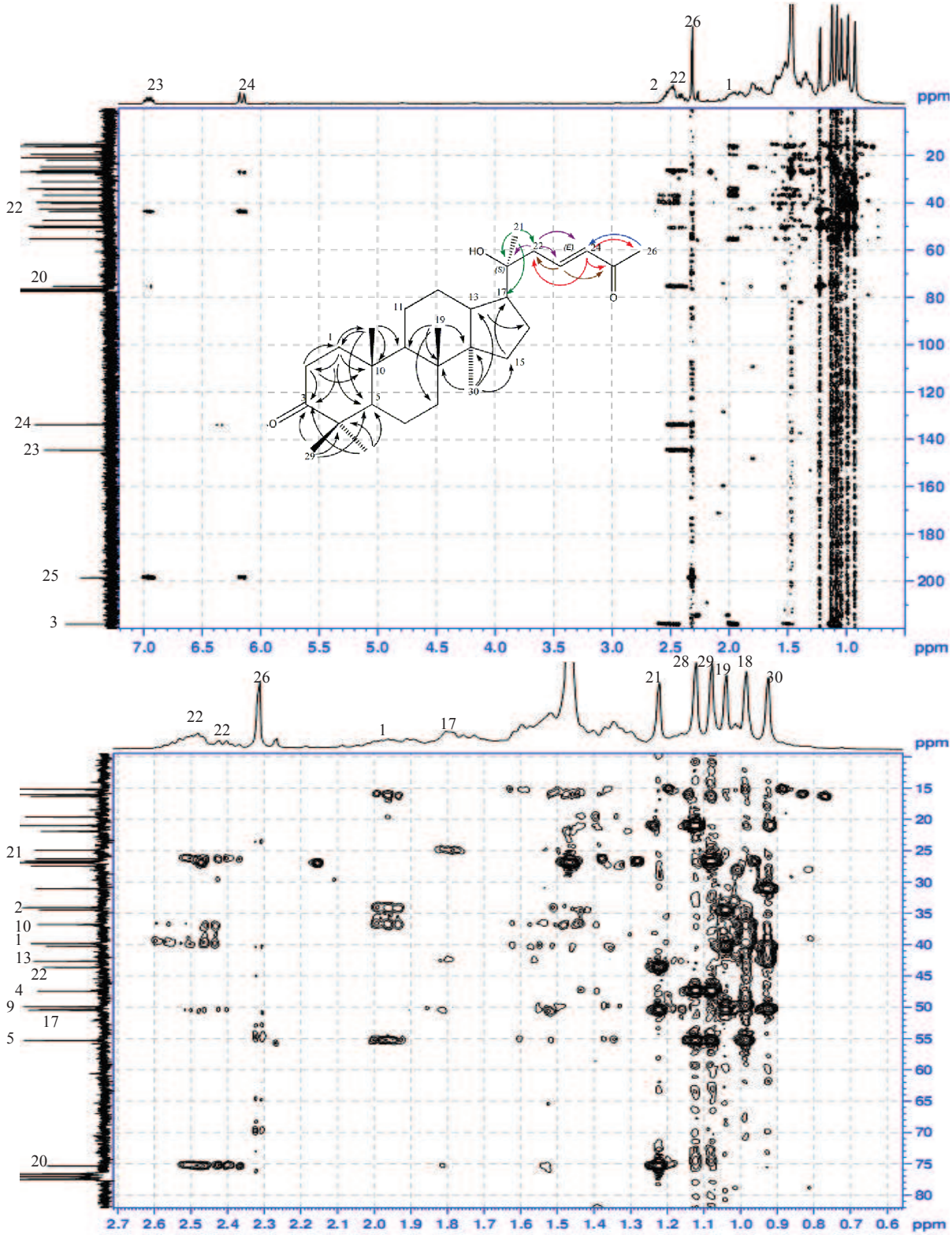

Figure 108. The HMBC correlation of **39** (in $CDCl_3$) and expanded spectrum in the range of δ_H 0.6-2.7 ppm and δ_C 10-80 ppm.

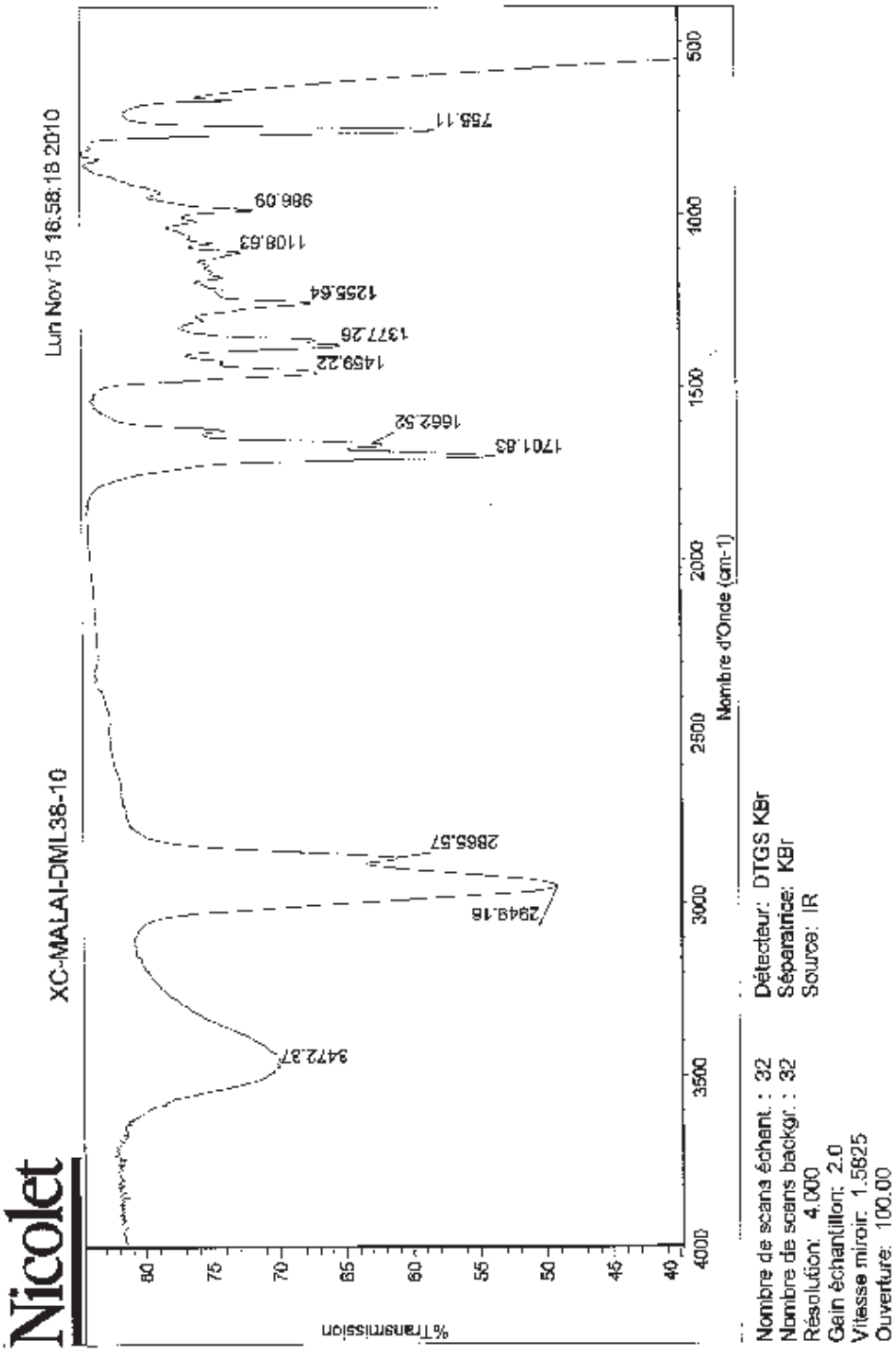

Figure 109. IR spectrum of **39**. (dry film).

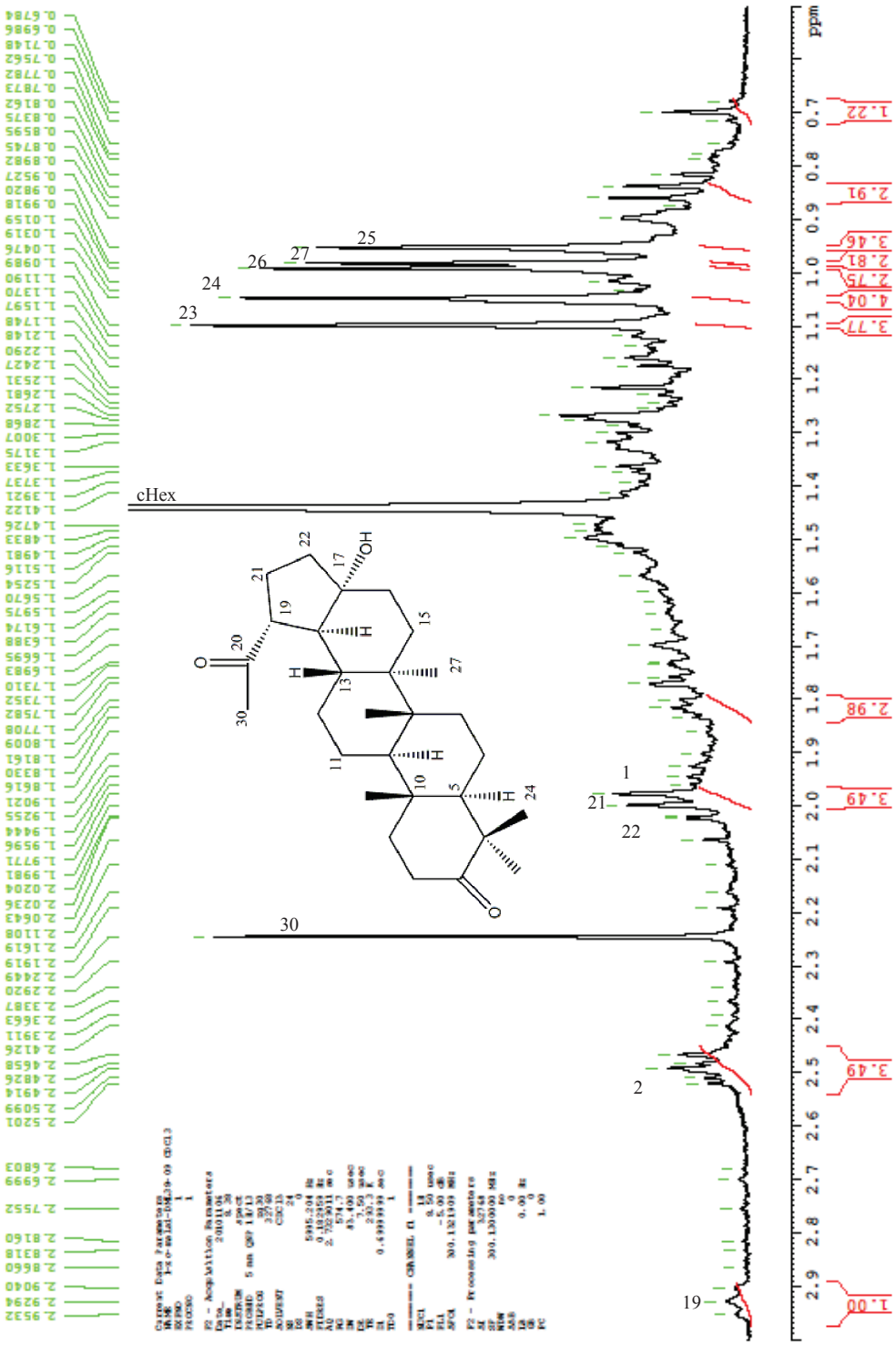

Figure 110. The ^{1}H NMR spectrum (300 MHz) of **41** (in $CDCl_3$).

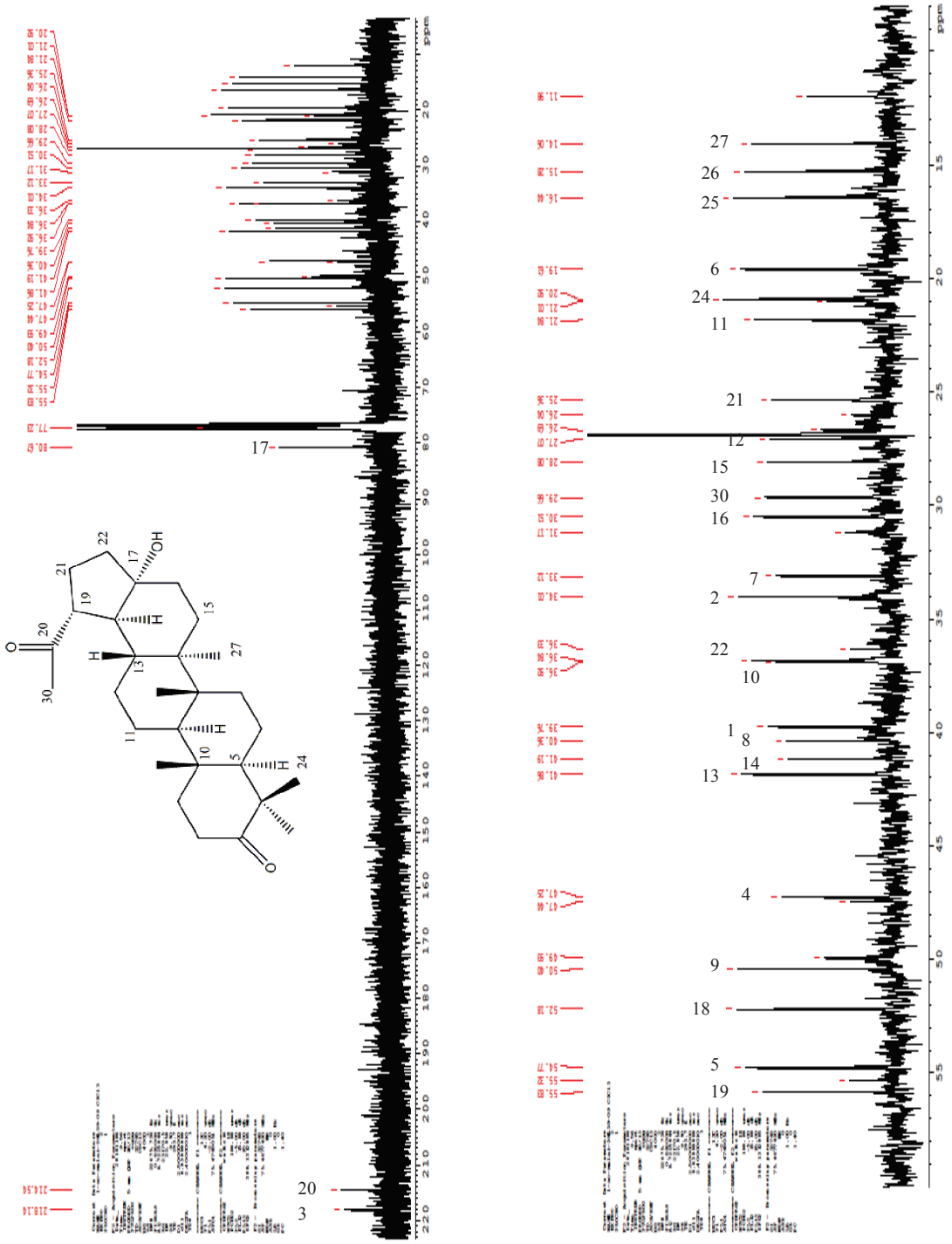

Figure 111. The ^{13}C NMR spectrum (75 MHz) of **41** (in $CDCl_3$) and expanded spectrum in the range of 10-59 ppm.

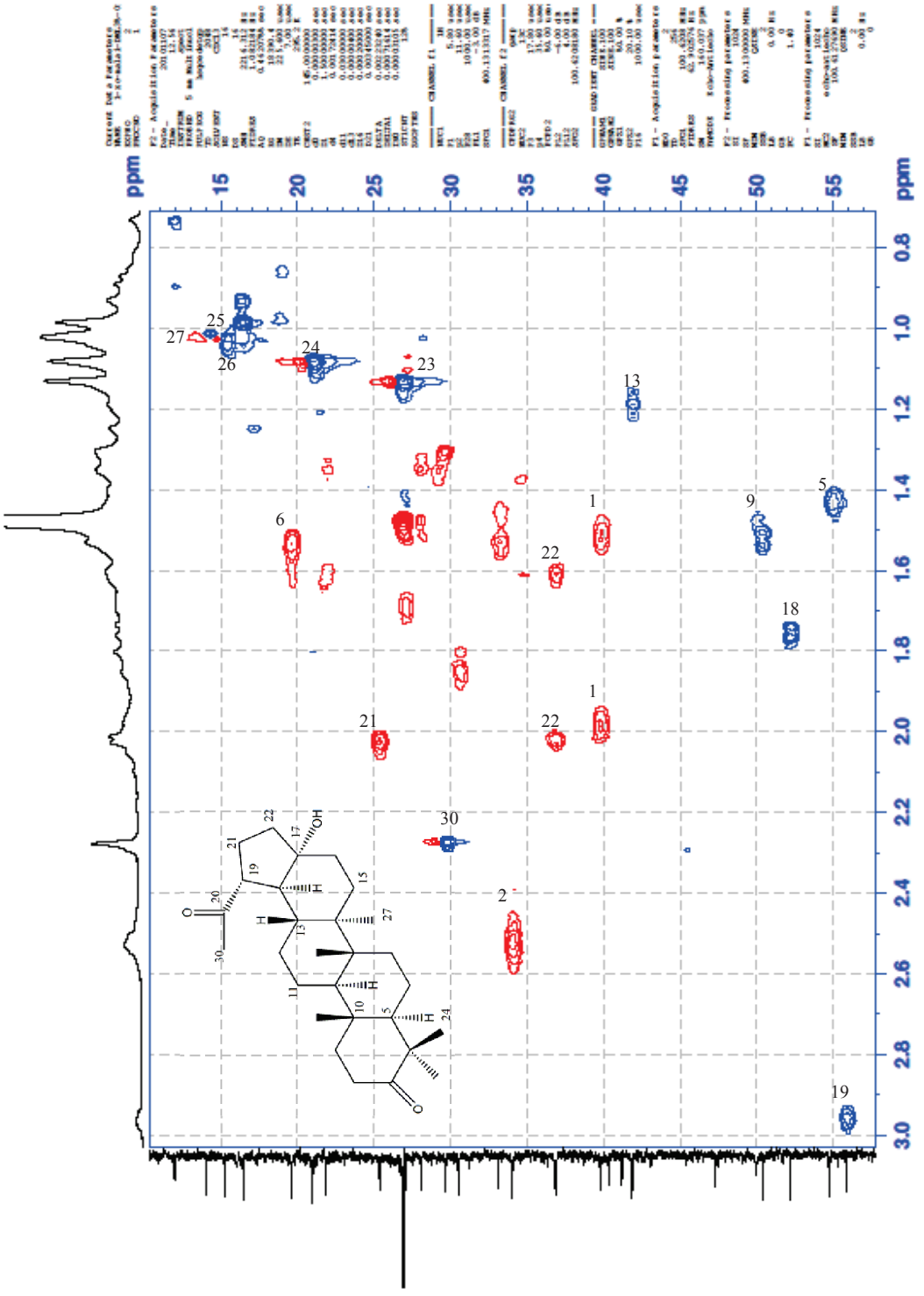

Figure 112. The expanded HSQCedited correlation of **41** (in $CDCl_3$) in the range of δ_H 0.8-3.0 ppm and δ_C 11-57 ppm.

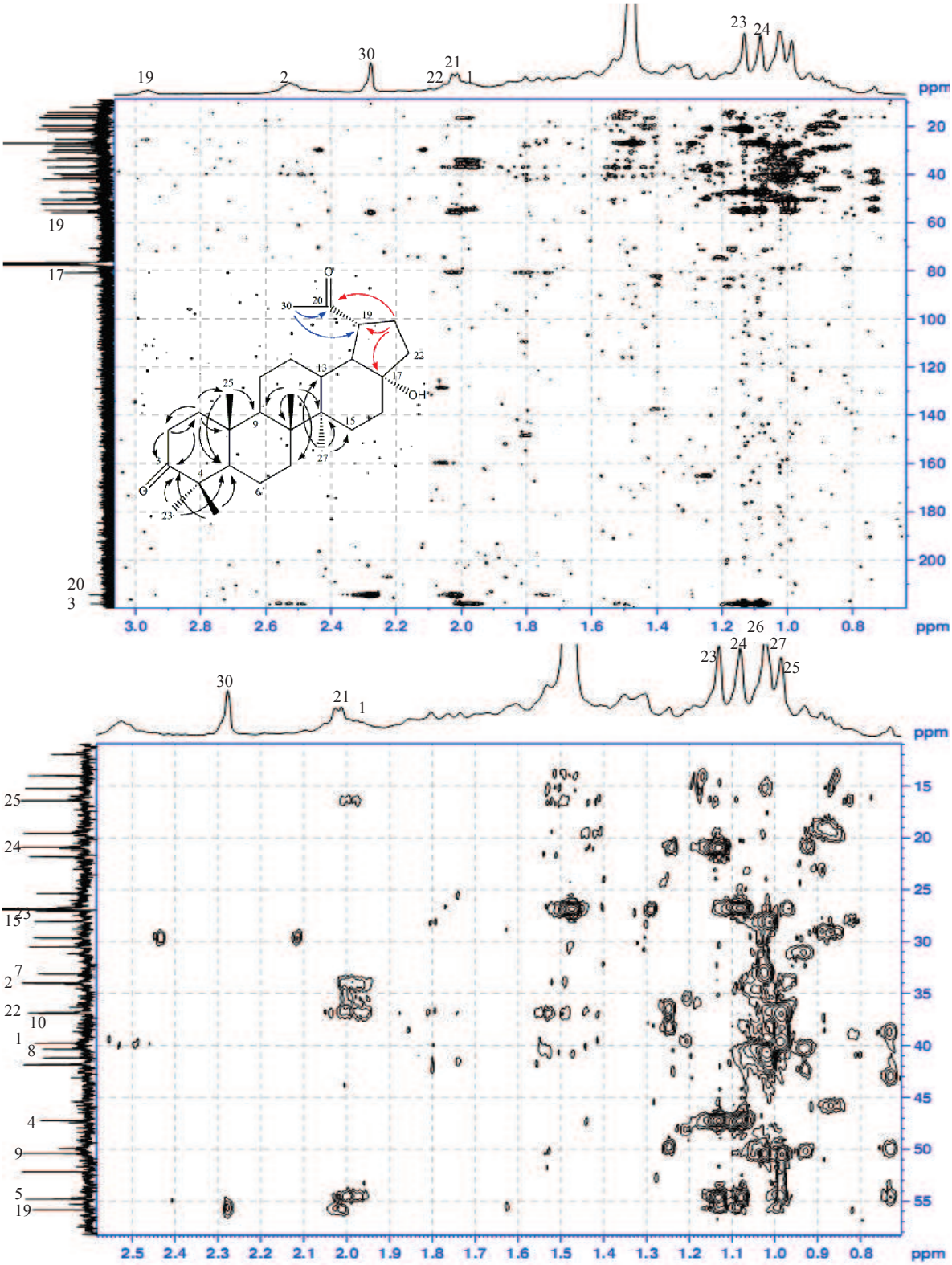

Figure 113. The HMBC correlation of **41** (in $CDCl_3$) and expanded spectrum in the range of δ_H 0.7-2.6 ppm and δ_C 10-59 ppm.

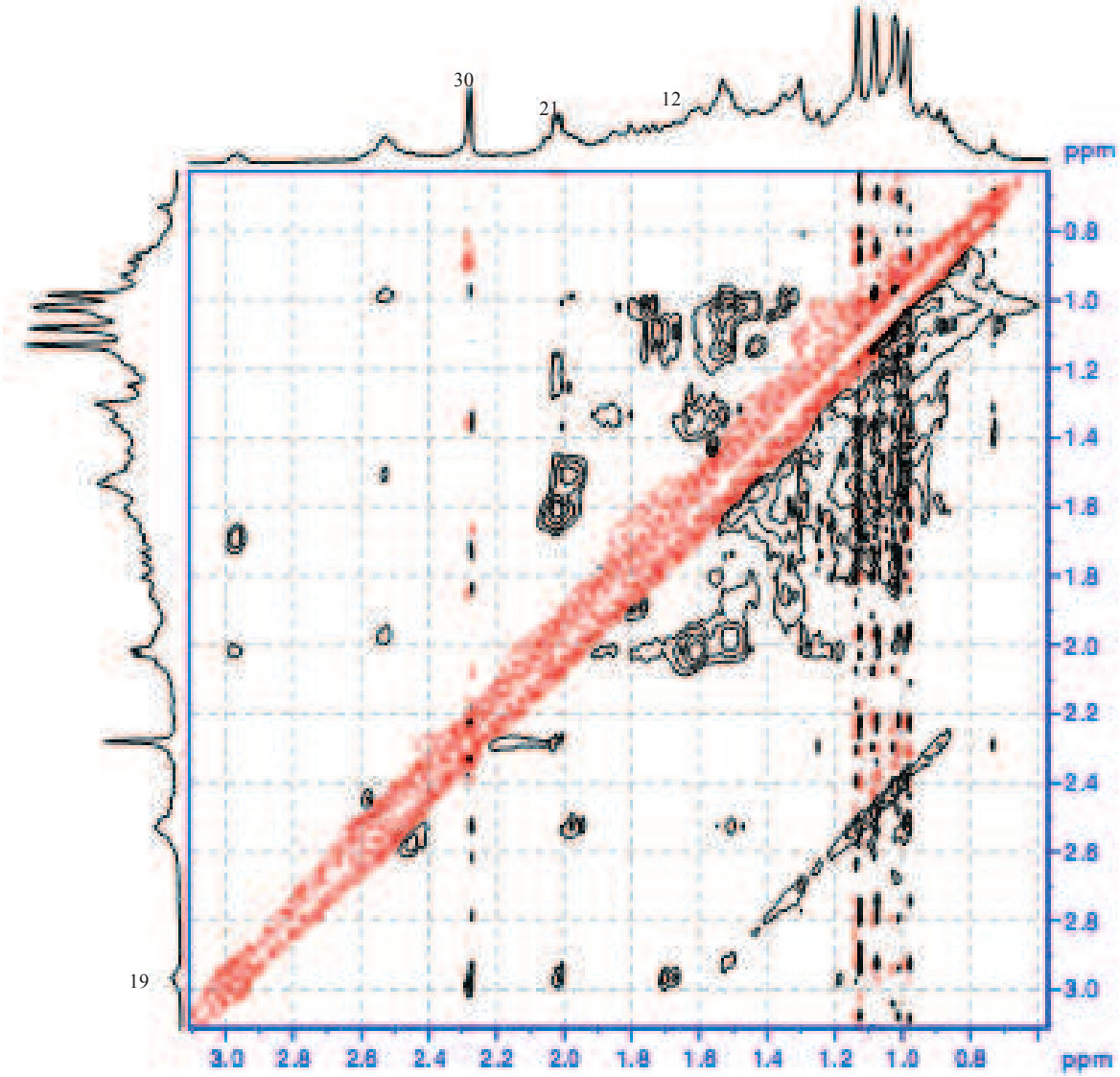

Figure 114. The NOE correlation of **41** (in $CDCl_3$).

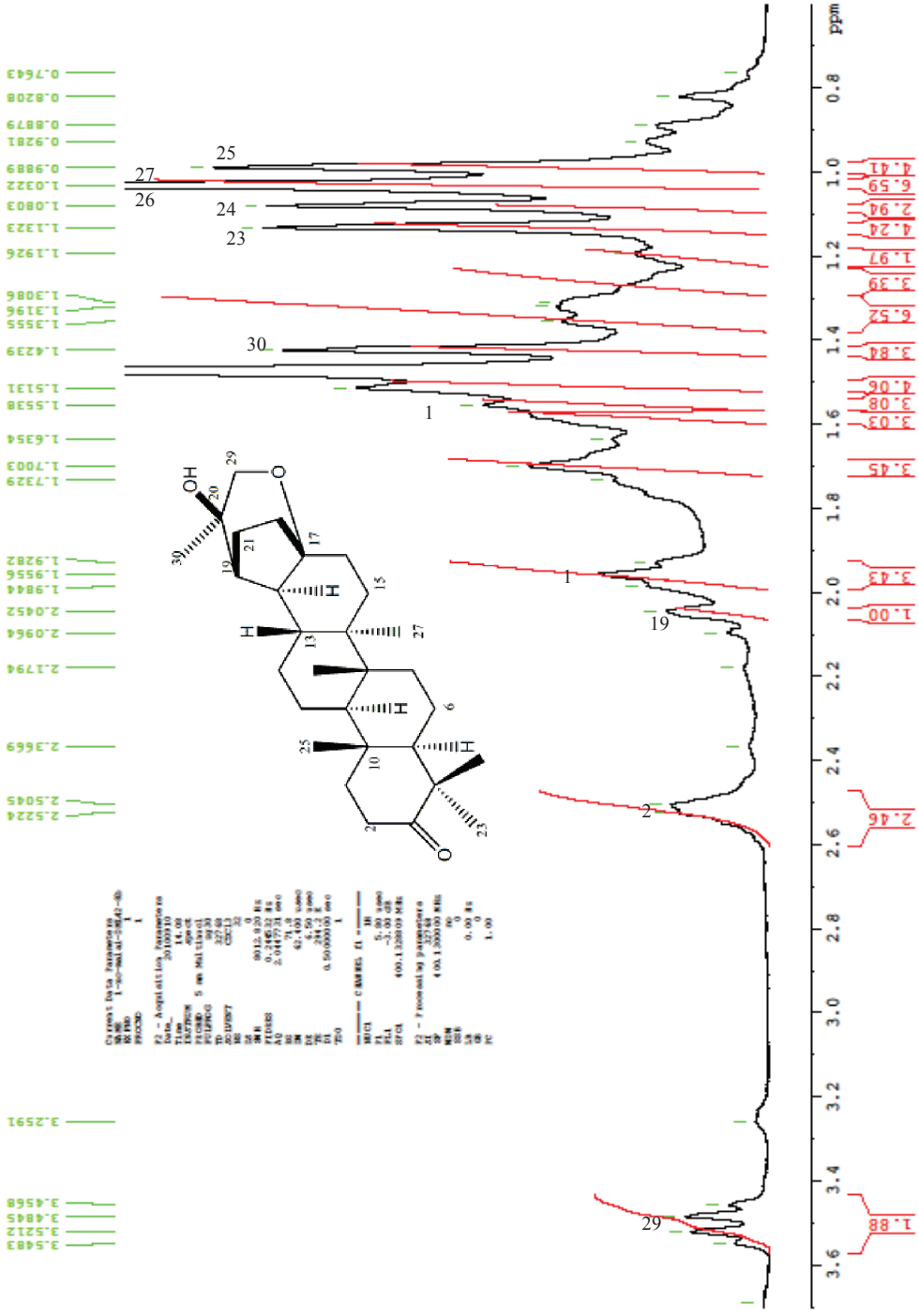

Figure 115. The ^{1}H NMR spectrum (300 MHz) of **42** (in $CDCl_3$) and expanded spectrum in the range of 0.8-2.6 ppm.

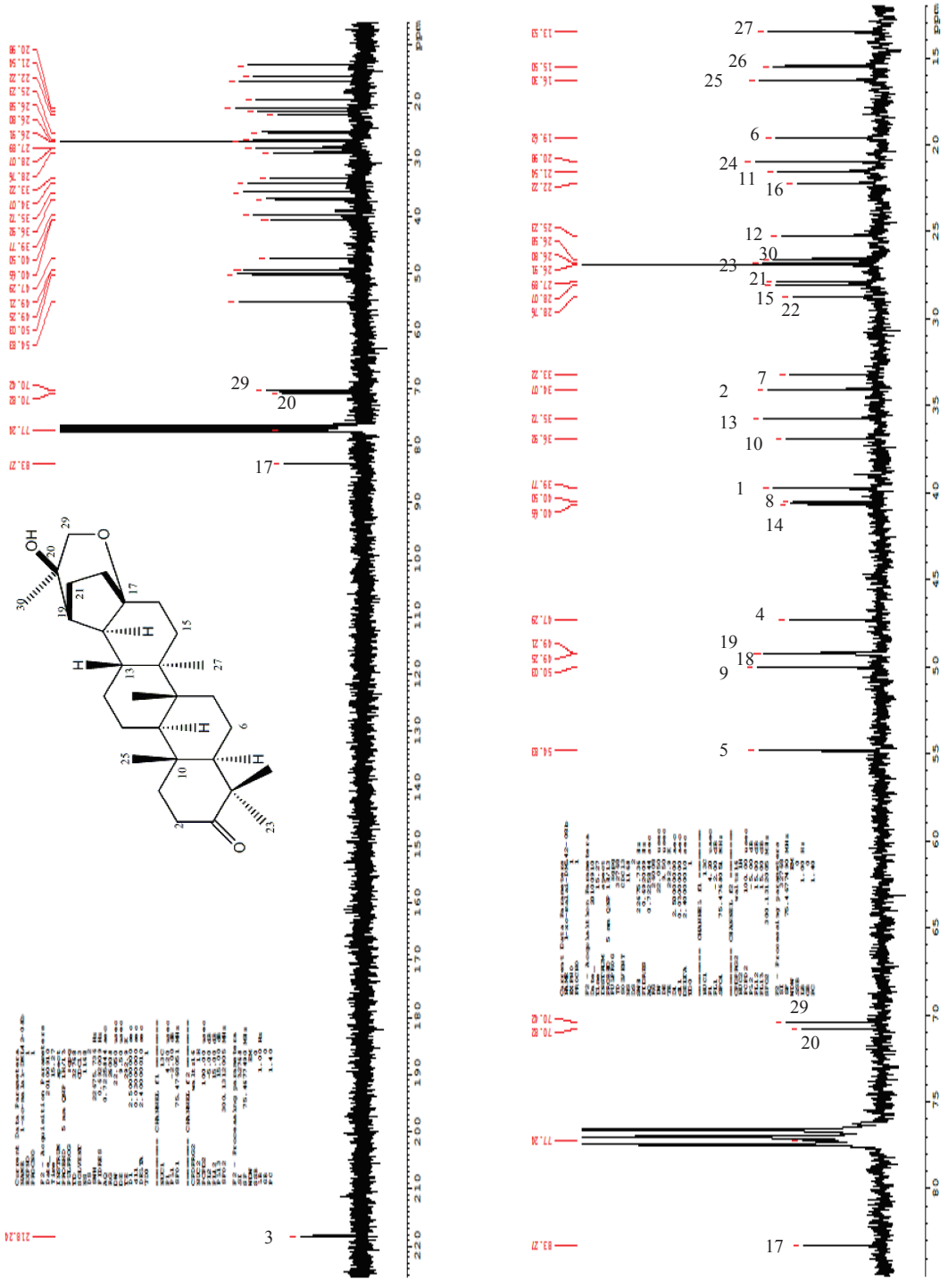

Figure 116. The ^{13}C NMR spectrum (75 MHz) of **42** (in $CDCl_3$) and expanded spectrum in the range of 12-84 ppm.

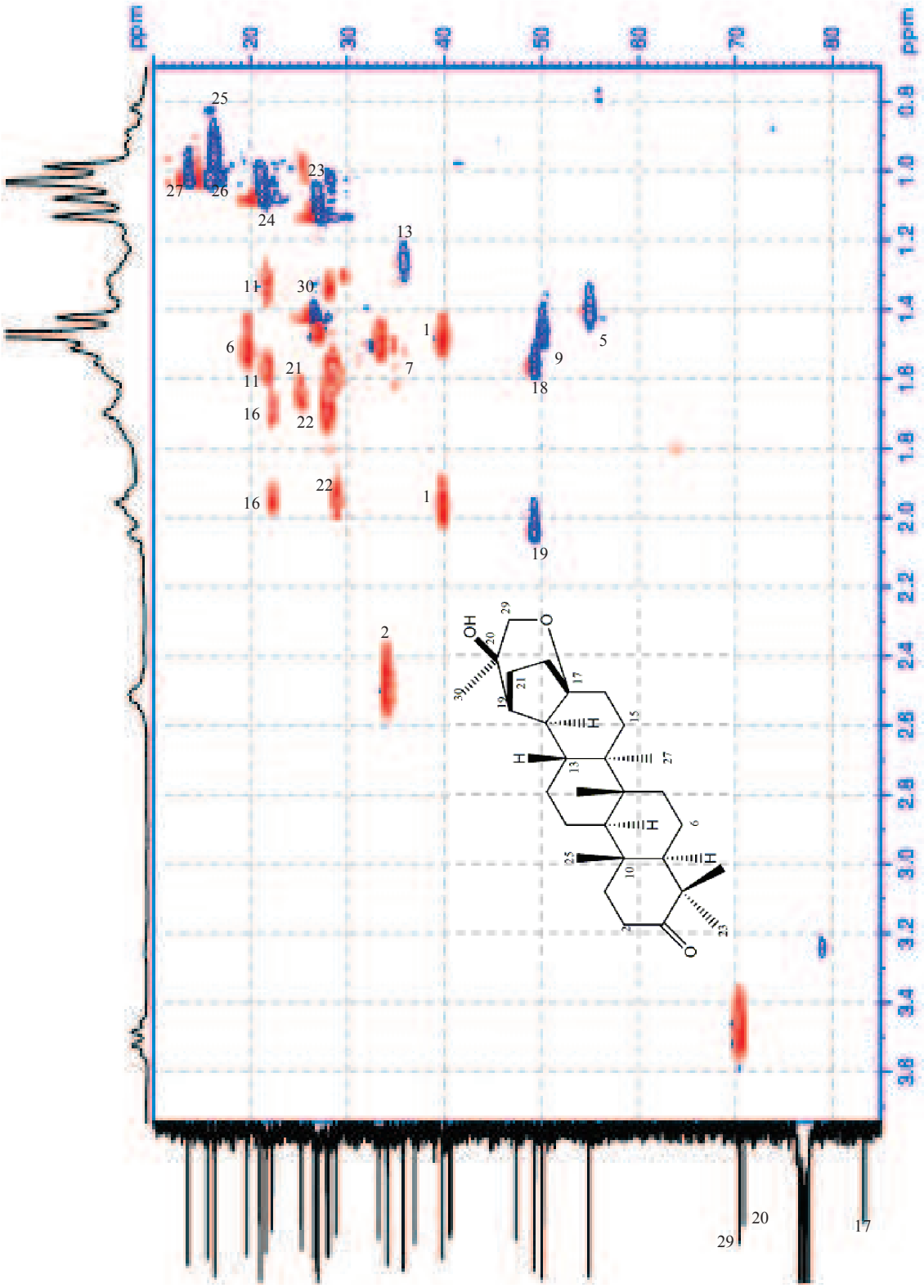

Figure 117. The expanded HSQCedited correlation of **42** (in $CDCl_3$) in the range of δ_H 0.8-3.6 ppm and δ_C 11-80 ppm.

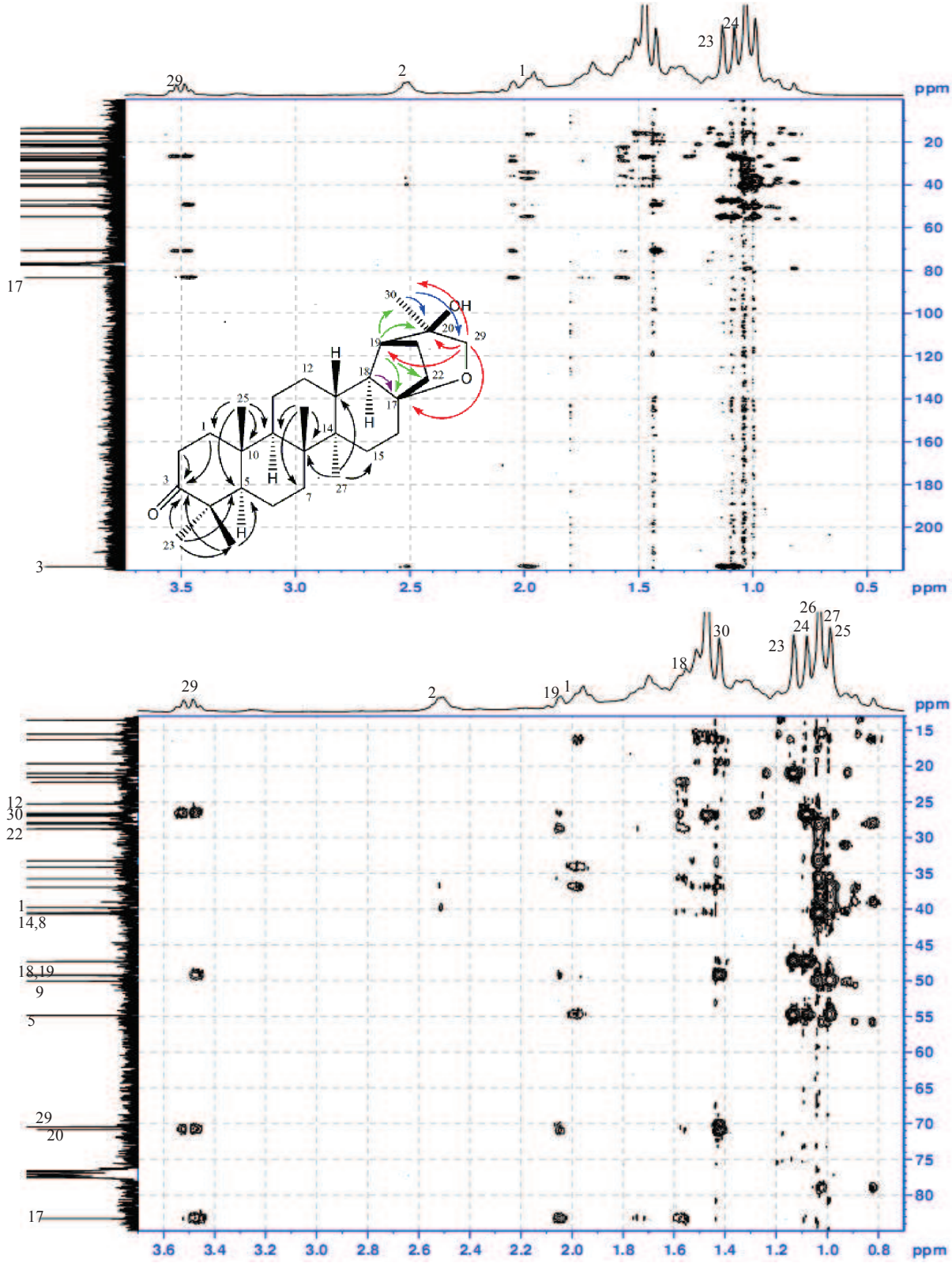

Figure 118. The HMBC correlation of **42** (in $CDCl_3$) and expanded spectrum in the range of δ_H 0.7-3.7 ppm and δ_C 13-90 ppm.

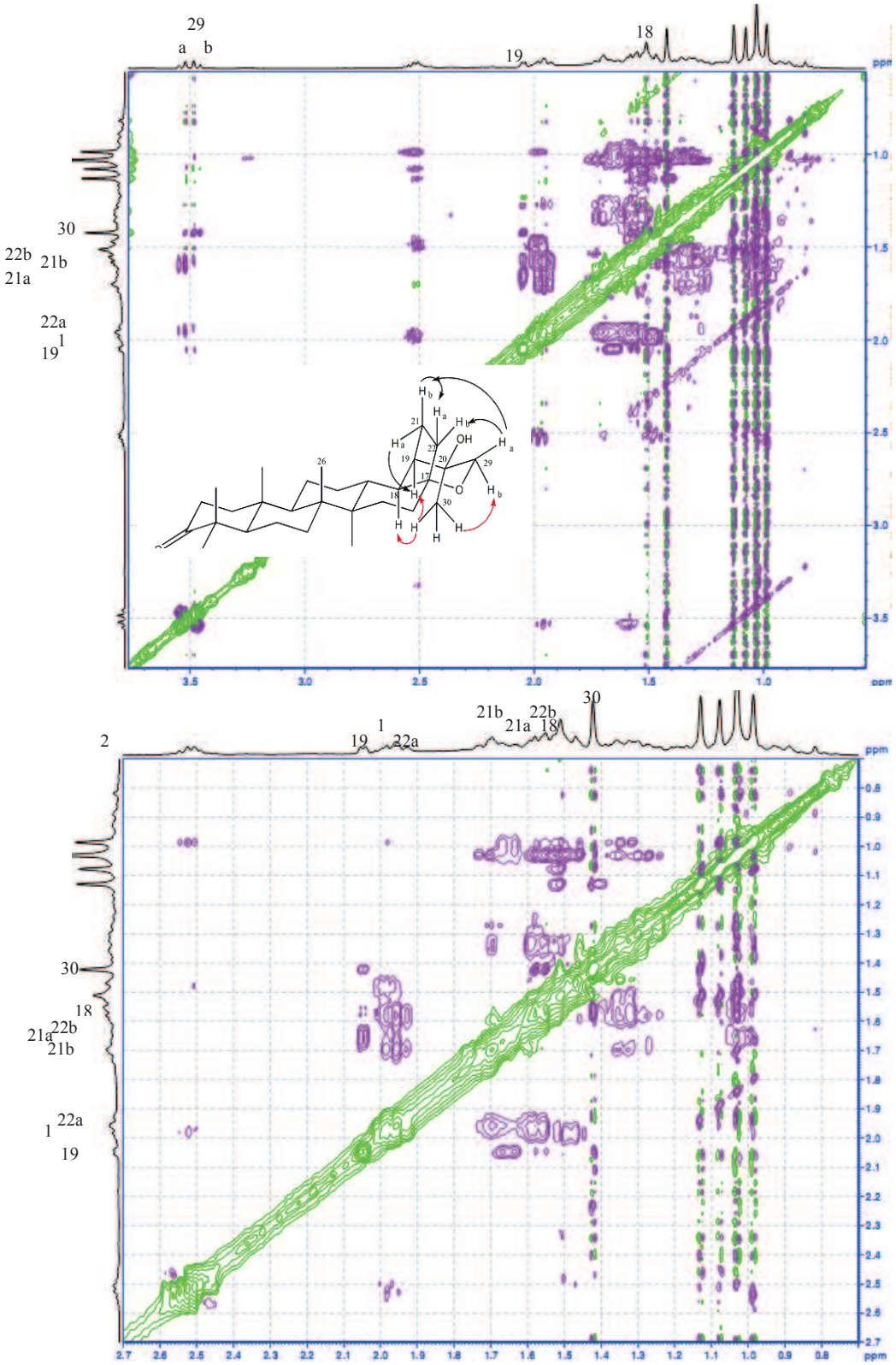

Figure 119. The NOE correlation of **42** (in $CDCl_3$) and expanded spectrum in the range of δ_H 0.7-2.7 ppm.

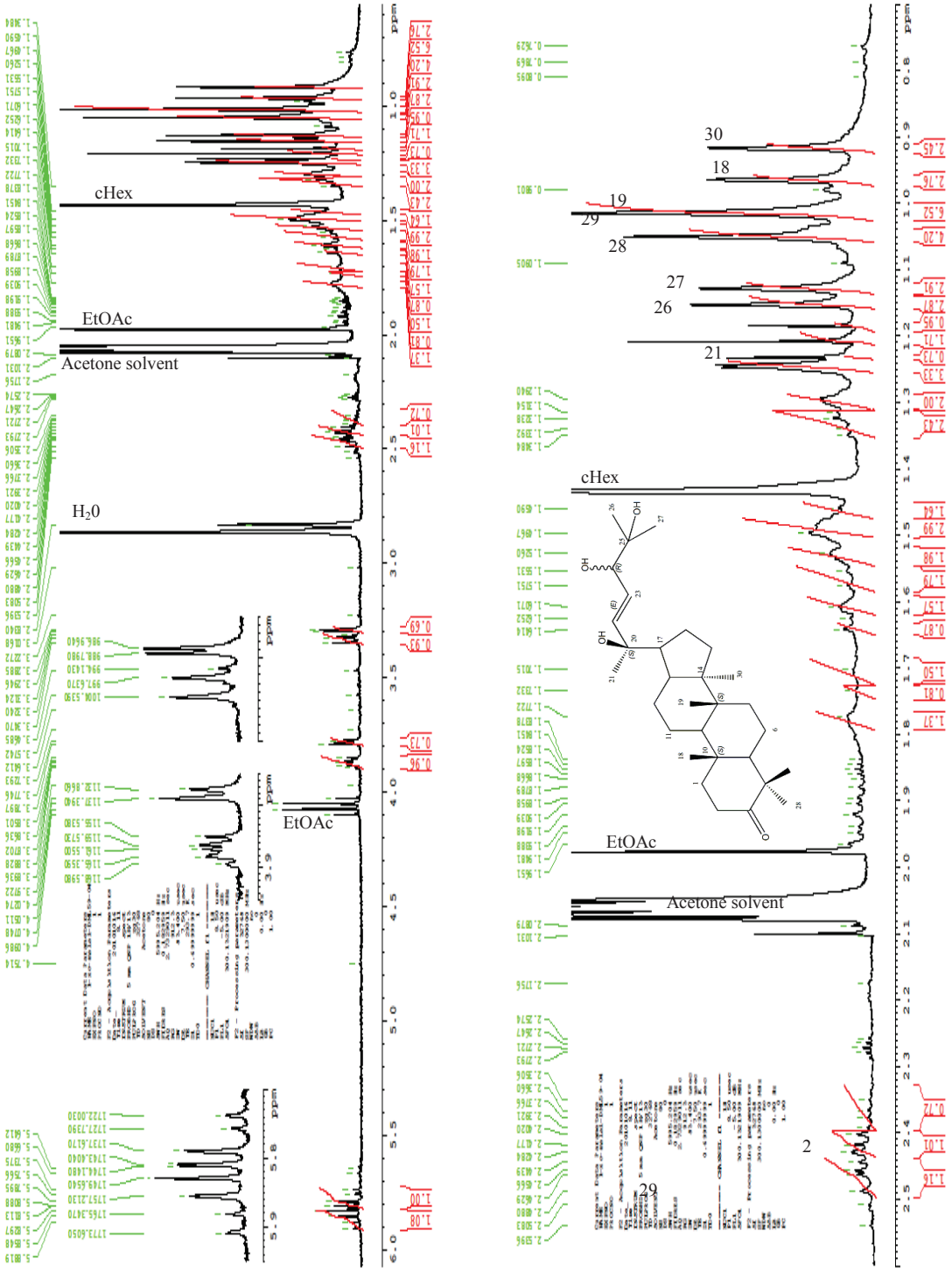

Figure 120. The ^{1}H NMR spectrum (300 MHz) of **45** (in acetone) and expanded spectrum in the range of 0.8-2.6 ppm.

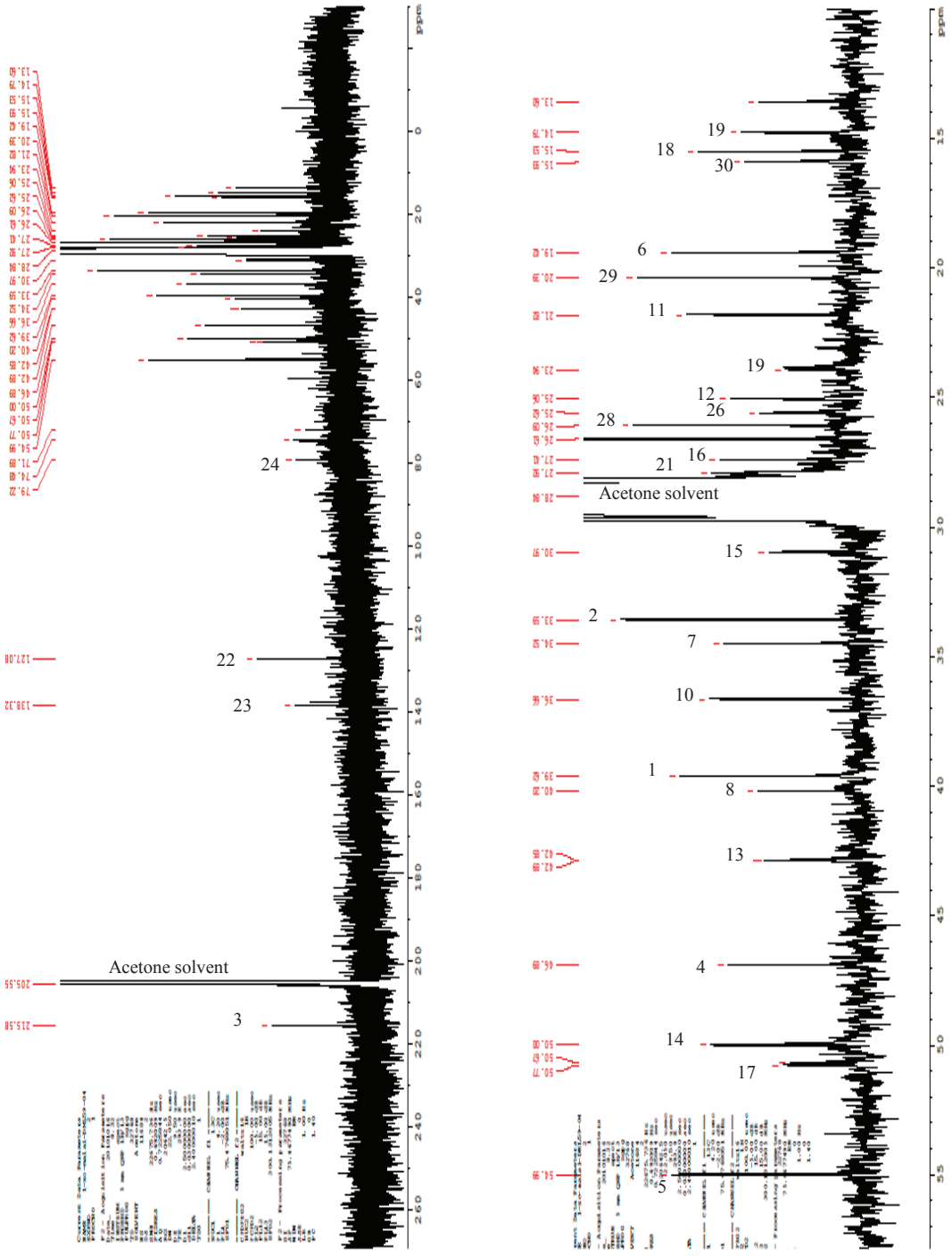

Figure 121. The ^{13}C NMR spectrum (75 MHz) of **45** (in acetone) and expanded spectrum in the range of 10-58 ppm.

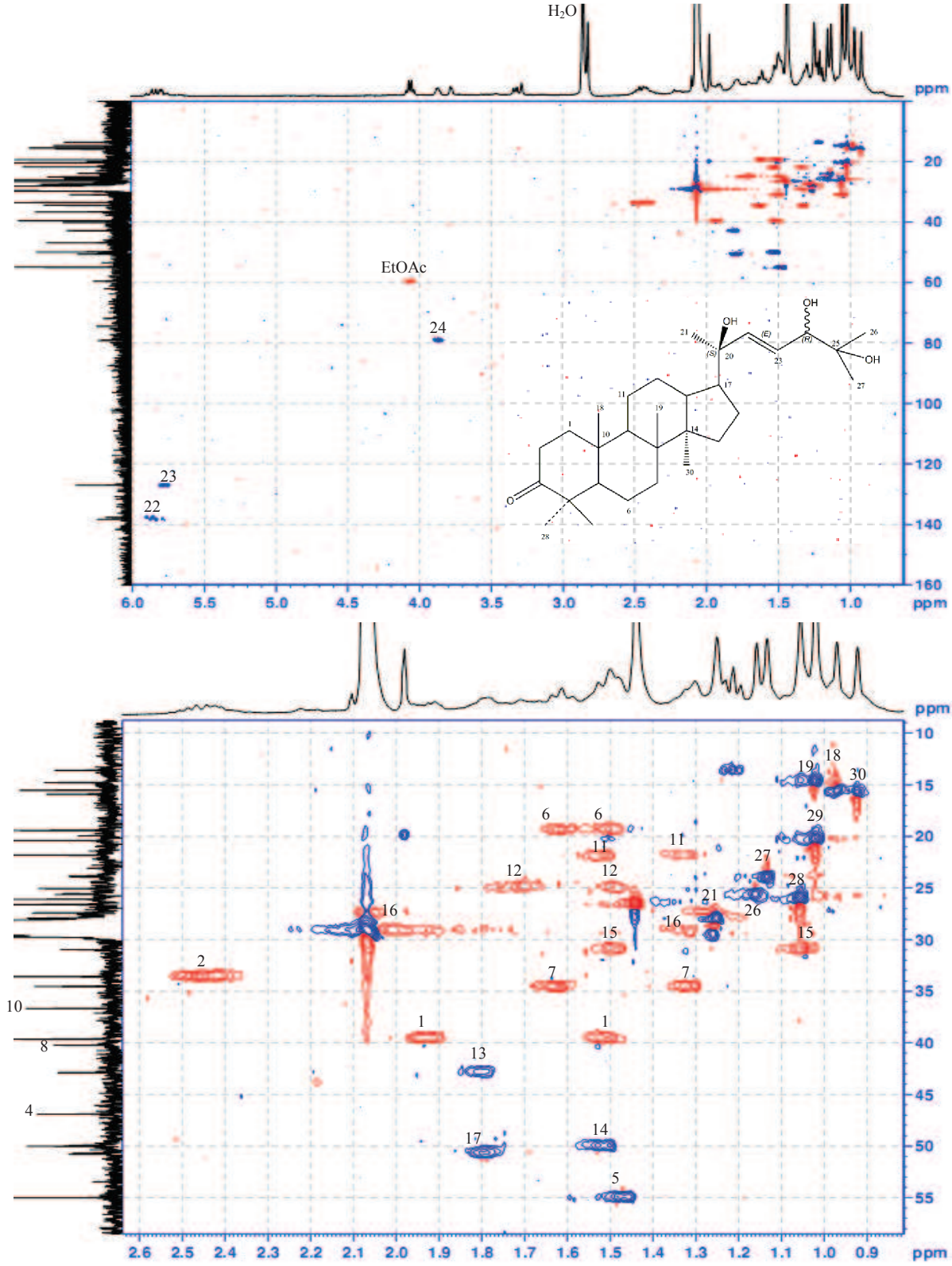

Figure 122. The HSQCedited correlation of **45** (in acetone) and expanded spectrum in the range of δ_H 0.8-2.6 ppm and δ_C 10-58 ppm.

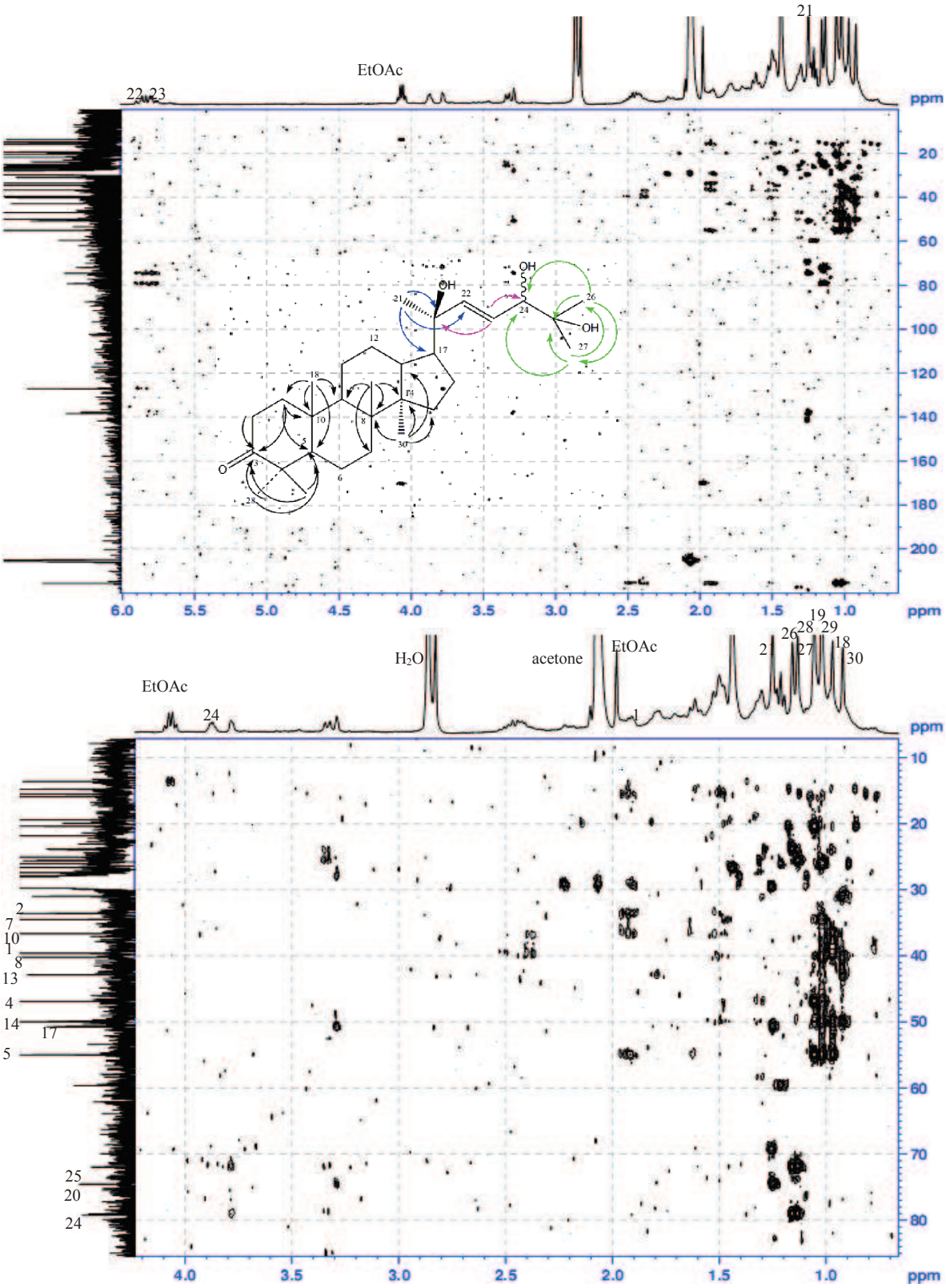

Figure 123. The HMBC correlation of **45** (in acetone) and expanded spectrum in the range of δ_H 0.6-4.2 ppm and δ_C 10-85 ppm.

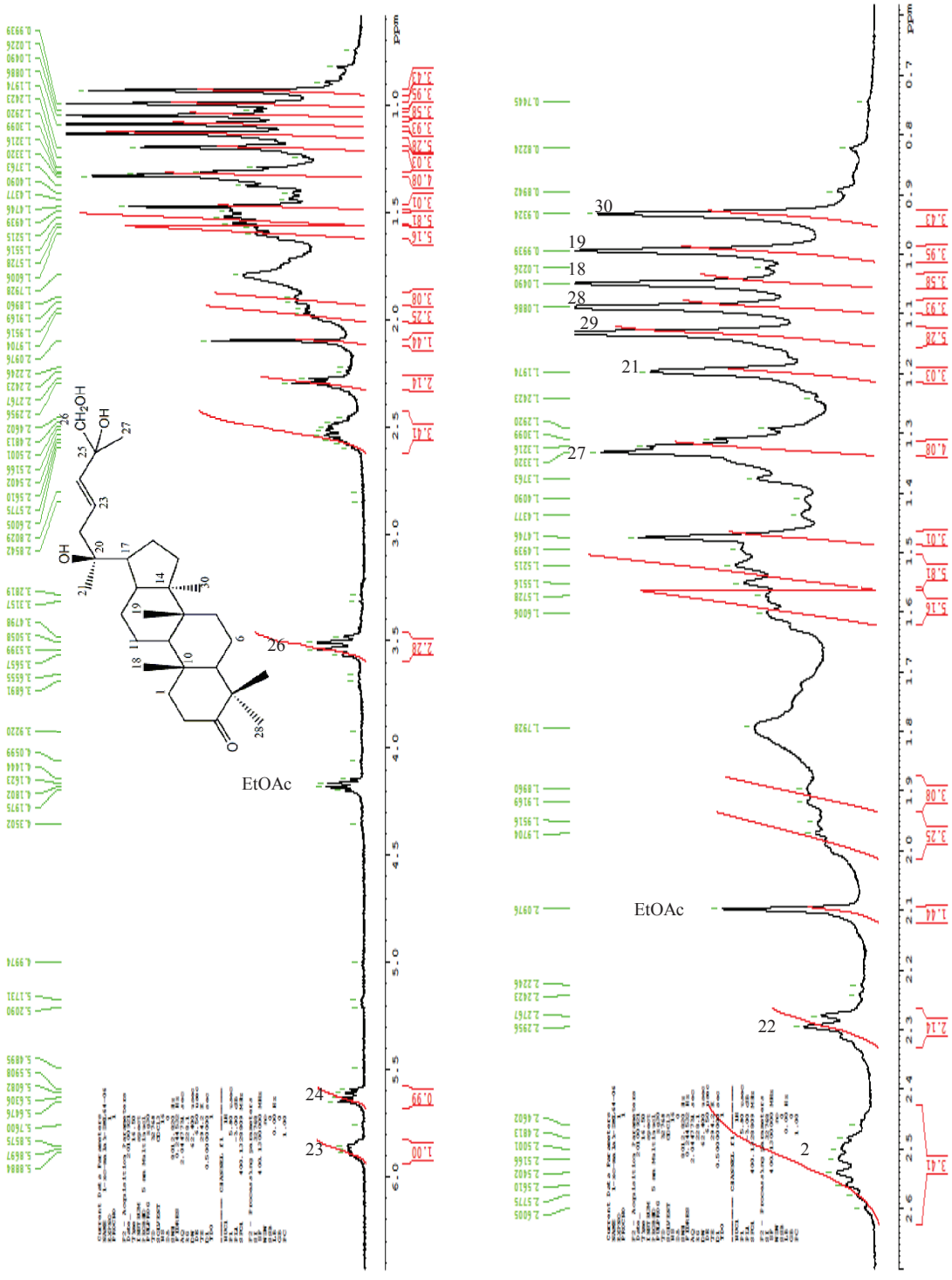

Figure 124. The ^{1}H NMR spectrum (300 MHz) of **46** (in $CDCl_3$) and expanded spectrum in the range of 0.7-2.7 ppm.

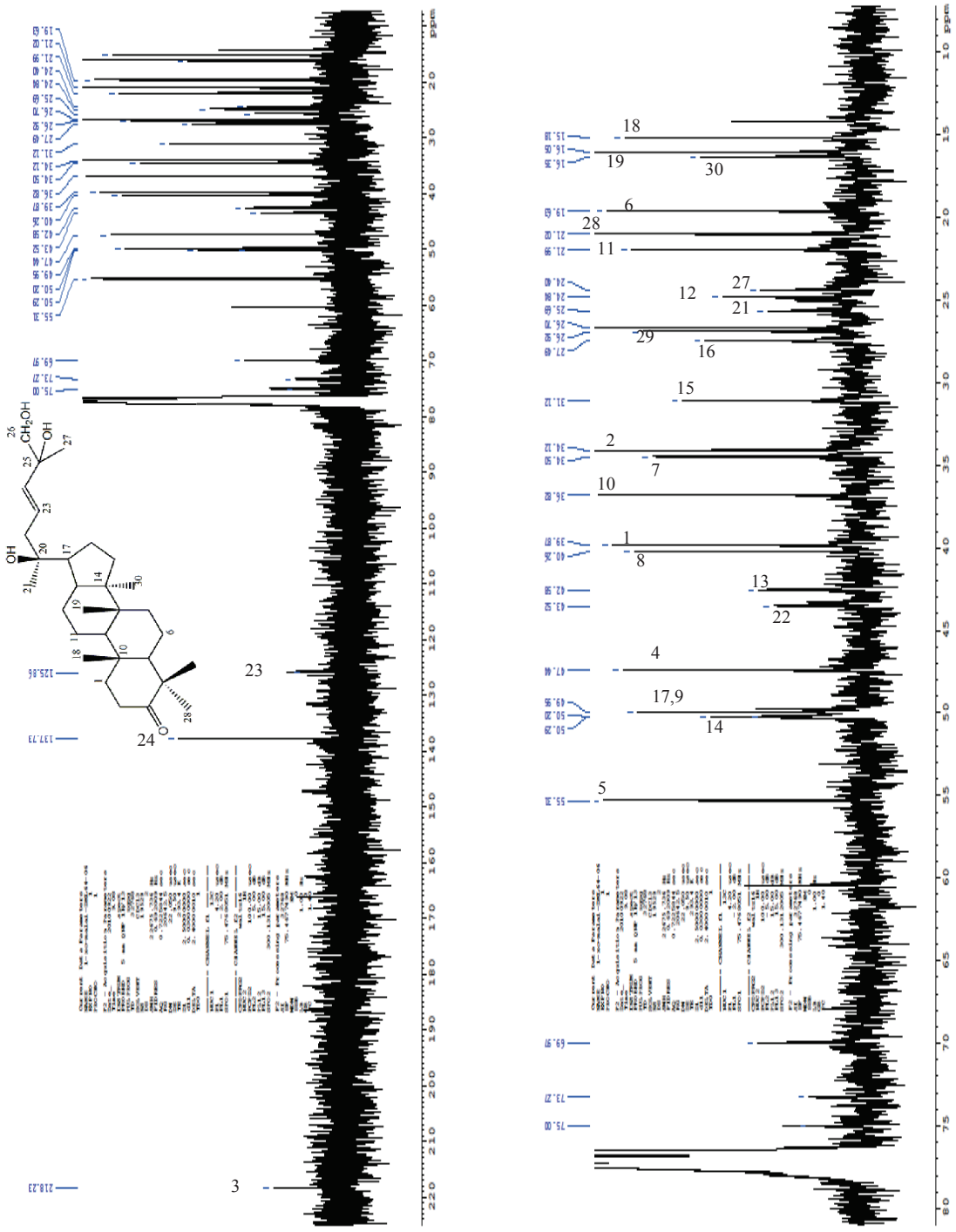

Figure 125. The ^{13}C NMR spectrum (75 MHz) of **46** (in $CDCl_3$) and expanded spectrum in the range of 10-58 ppm.

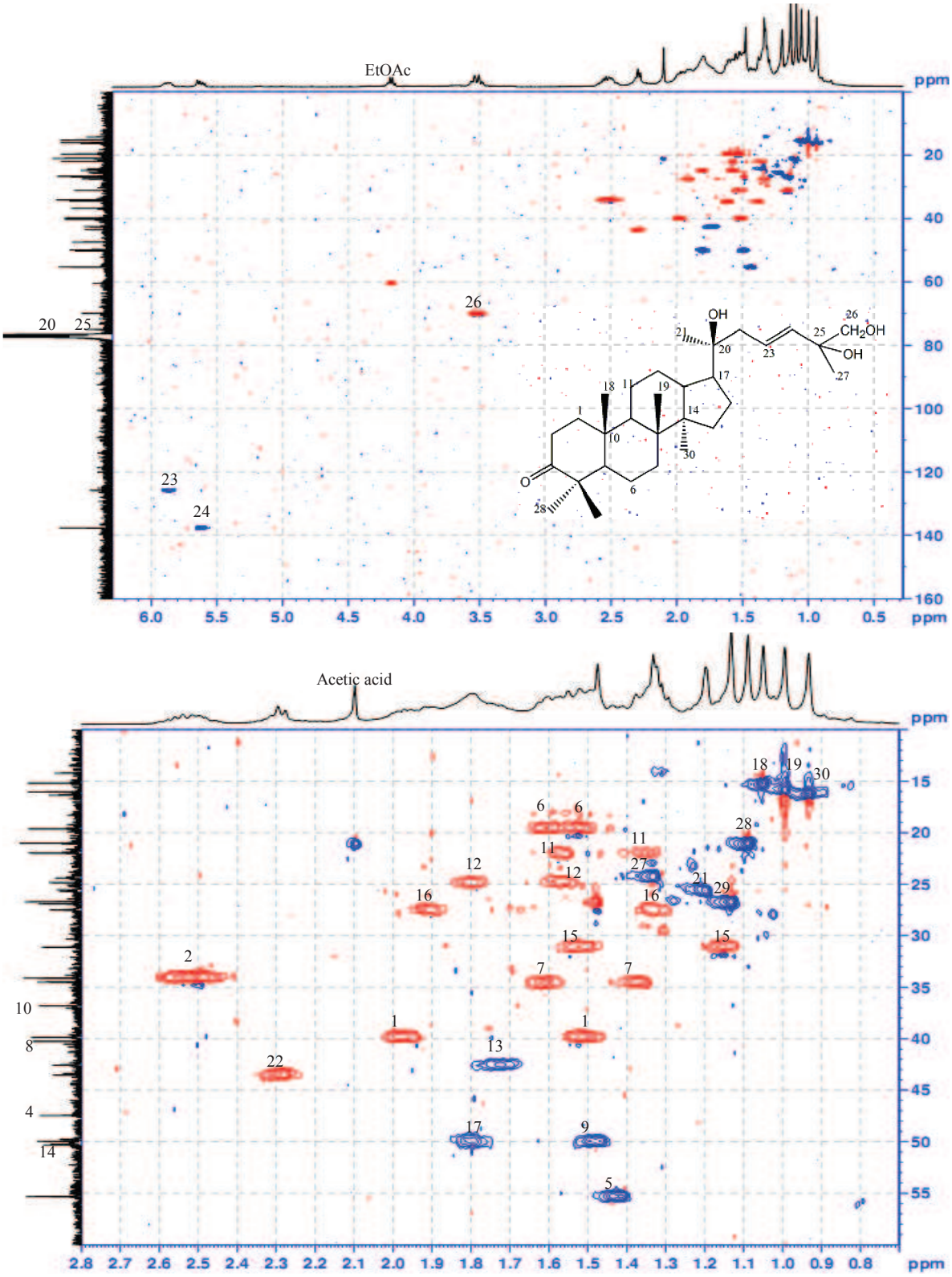

Figure 126. The HSQCedited correlation of **46** (in $CDCl_3$) and expanded spectrum in the range of δ_H 0.8-2.6 ppm and δ_C 10-58 ppm.

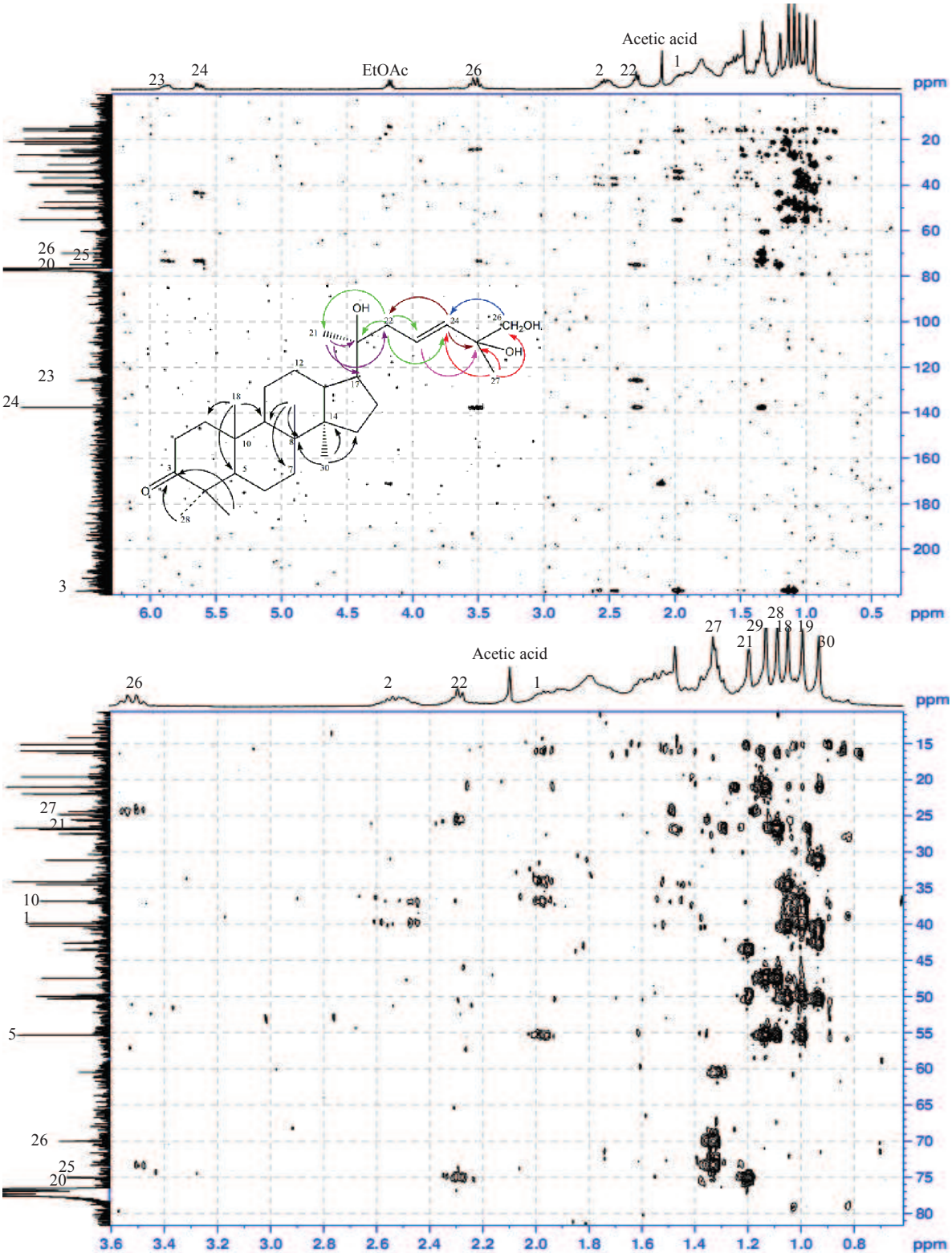

Figure 127. The HMBC correlation of **46** (in $CDCl_3$) and expanded spectrum in the range of δ_H 0.6-4.2 ppm and δ_C 10-85 ppm.

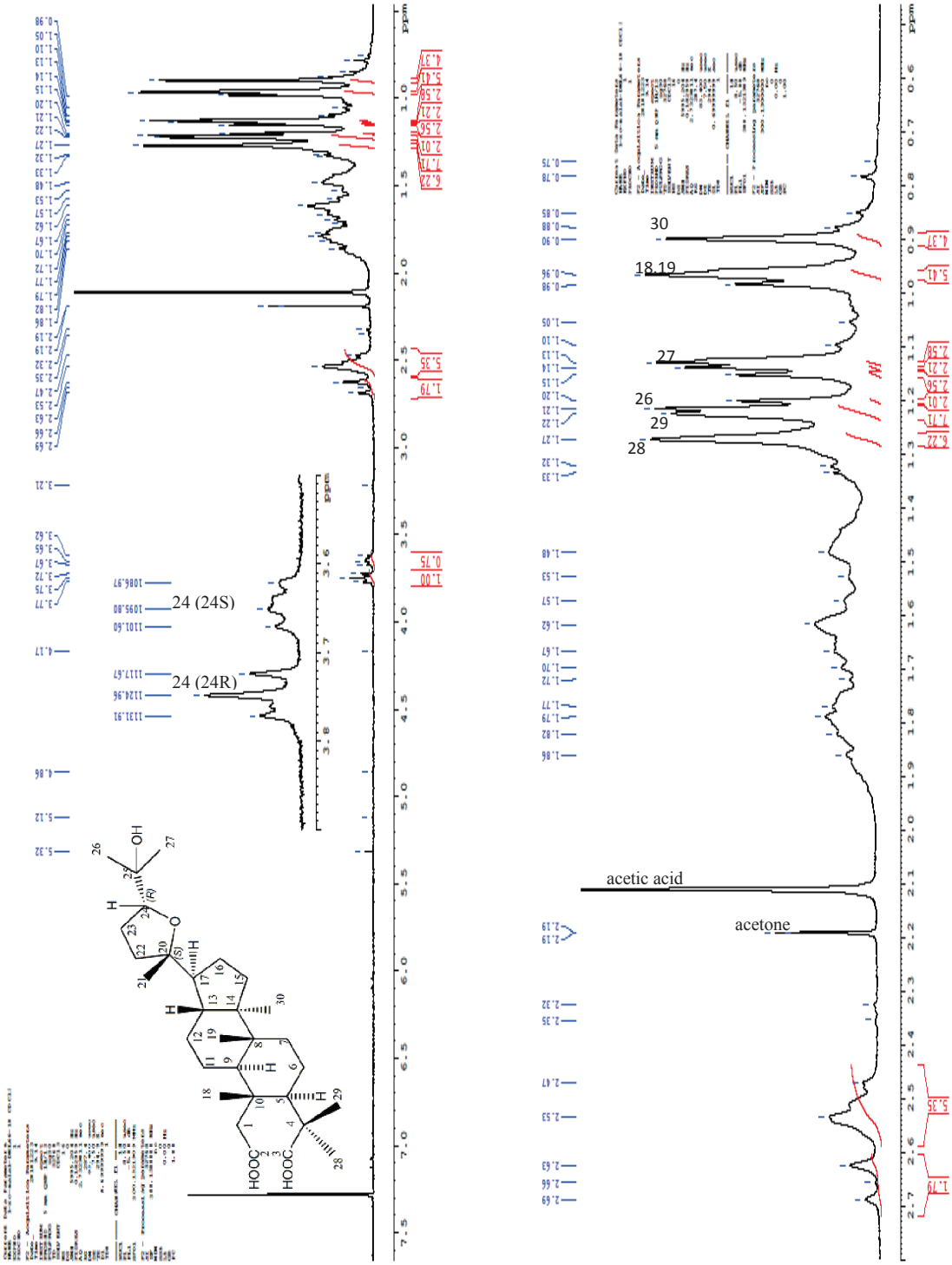

The stereochemistry of 20S,24S contaminated in the compound of 20S,24R (**47**).

Figure 128. The ^{1}H NMR spectrum (300 MHz) of **47** (in $CDCl_3$) and expanded spectrum in the range of 0.6-2.8 ppm.

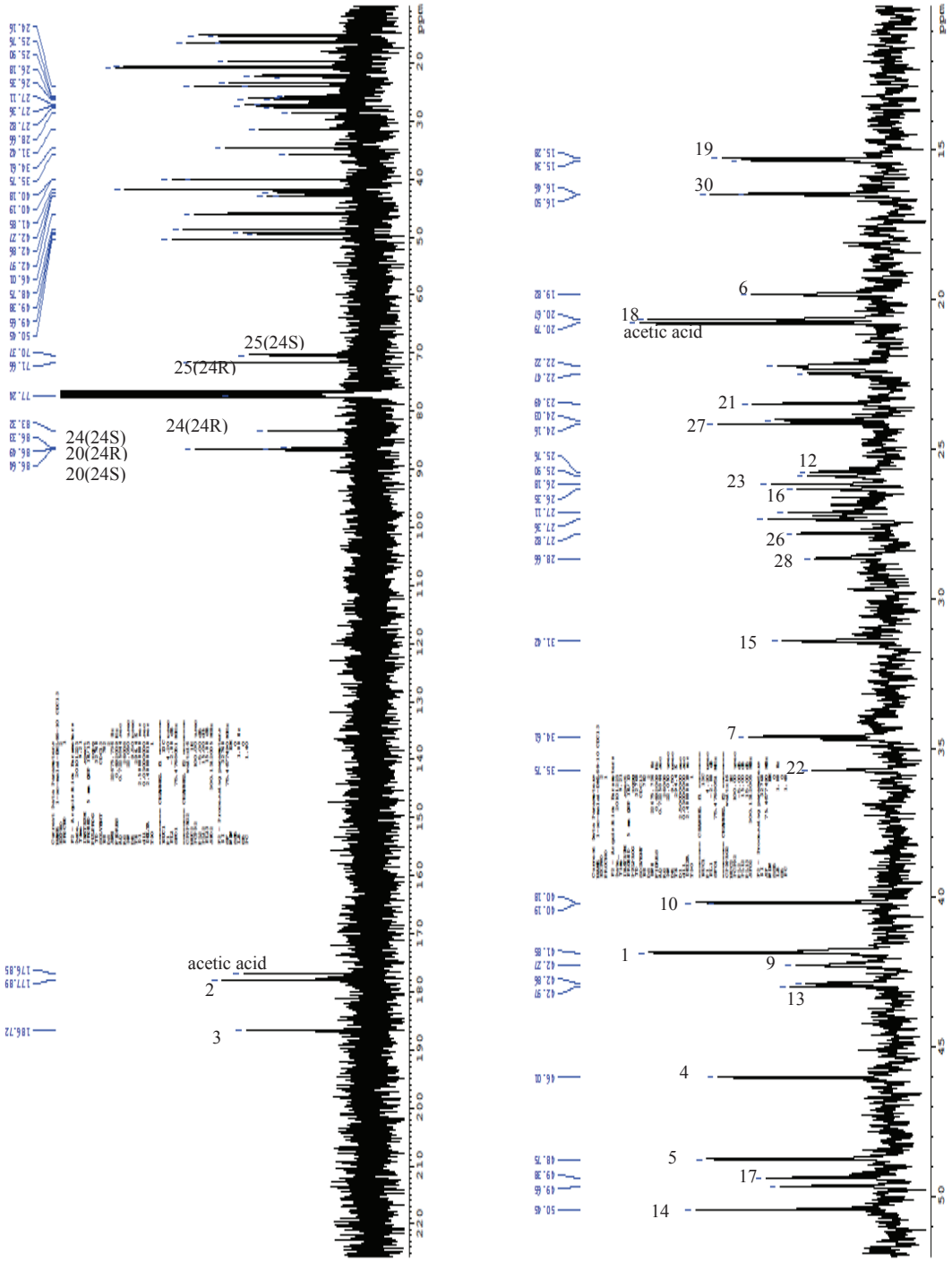

The stereochemistry of 20S,24S contaminated in the compound of 20S,24R (**47**).

Figure 129. The ^{13}C NMR spectrum (75 MHz) of **47** (in $CDCl_3$) and expanded spectrum in the range of 10-52 ppm.

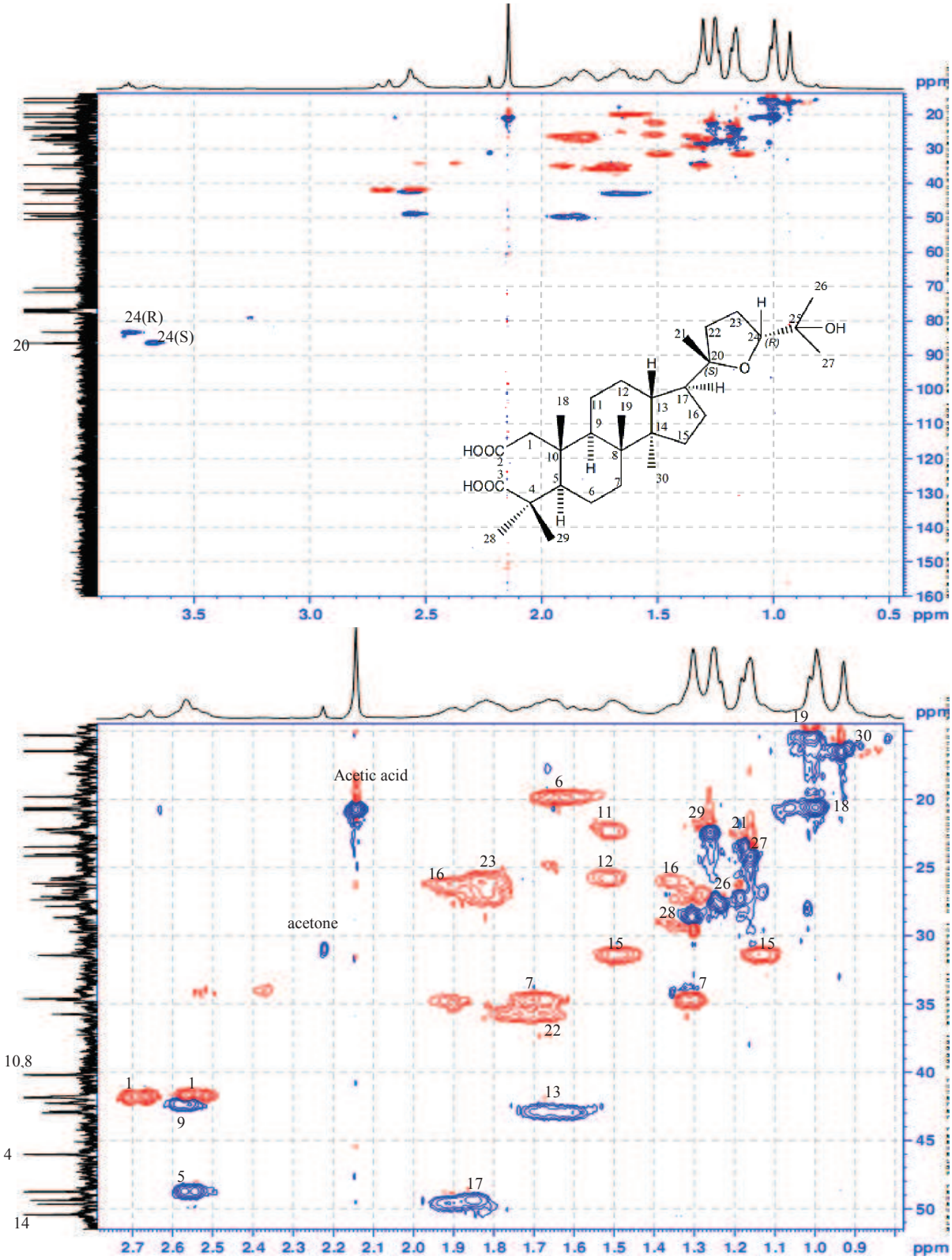

Figure 130. The HSQCedited correlation of **47** (in $CDCl_3$) and expanded spectrum in the range of δ_H 0.8-2.6 ppm and δ_C 10-58 ppm.

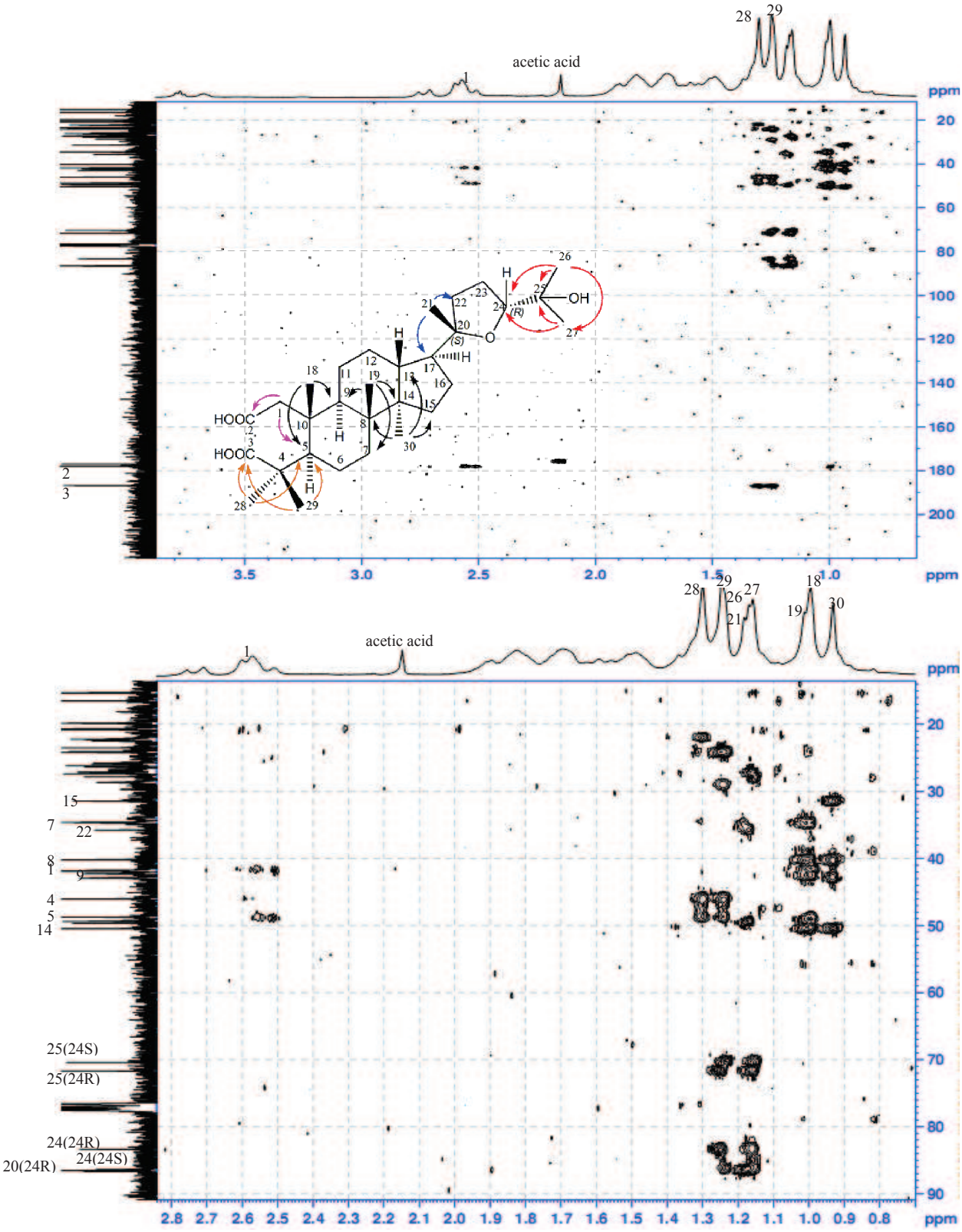

Figure 131. The HMBC correlation of **47** (in $CDCl_3$) and expanded spectrum in the range of δ_H 0.7-2.8 ppm and δ_C 10-90 ppm.

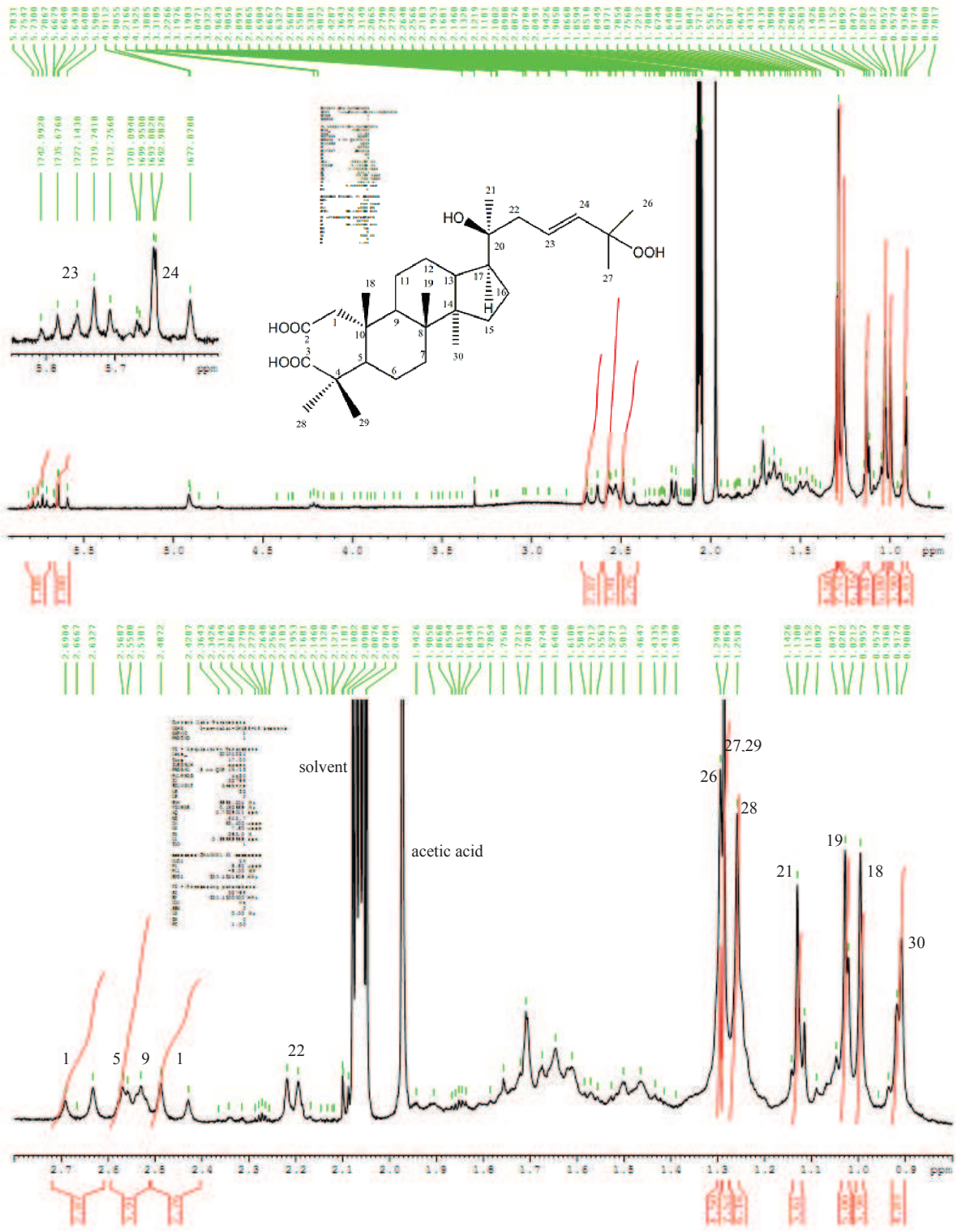

Figure 132. The ^{1}H NMR spectrum (300 MHz) of **48** (in acetone) and expanded spectrum in the range of 0.8-2.8 ppm.

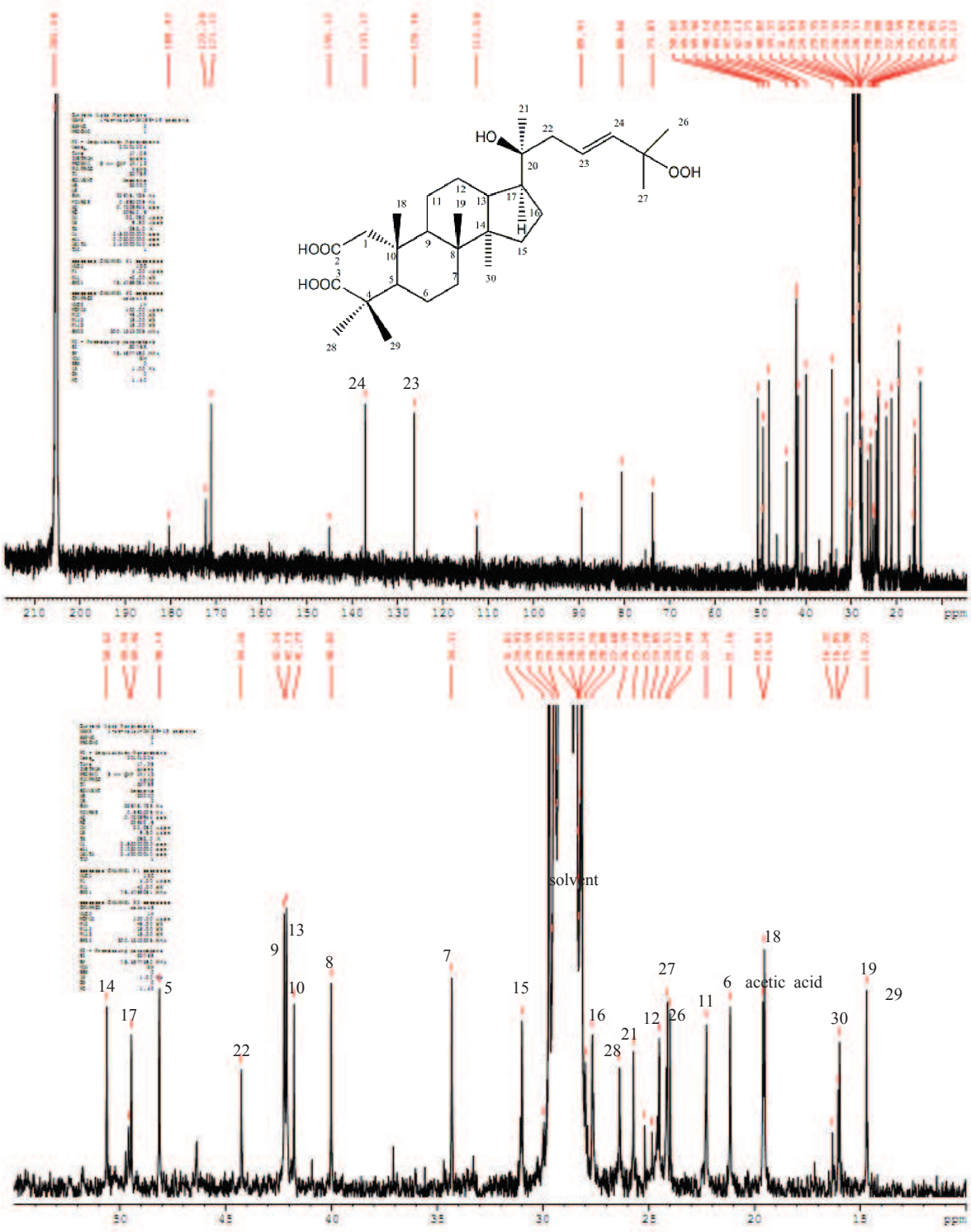

Figure 133. The ^{13}C NMR spectrum (75 MHz) of **48** (in acetone) and expanded spectrum in the range of 10-55 ppm.

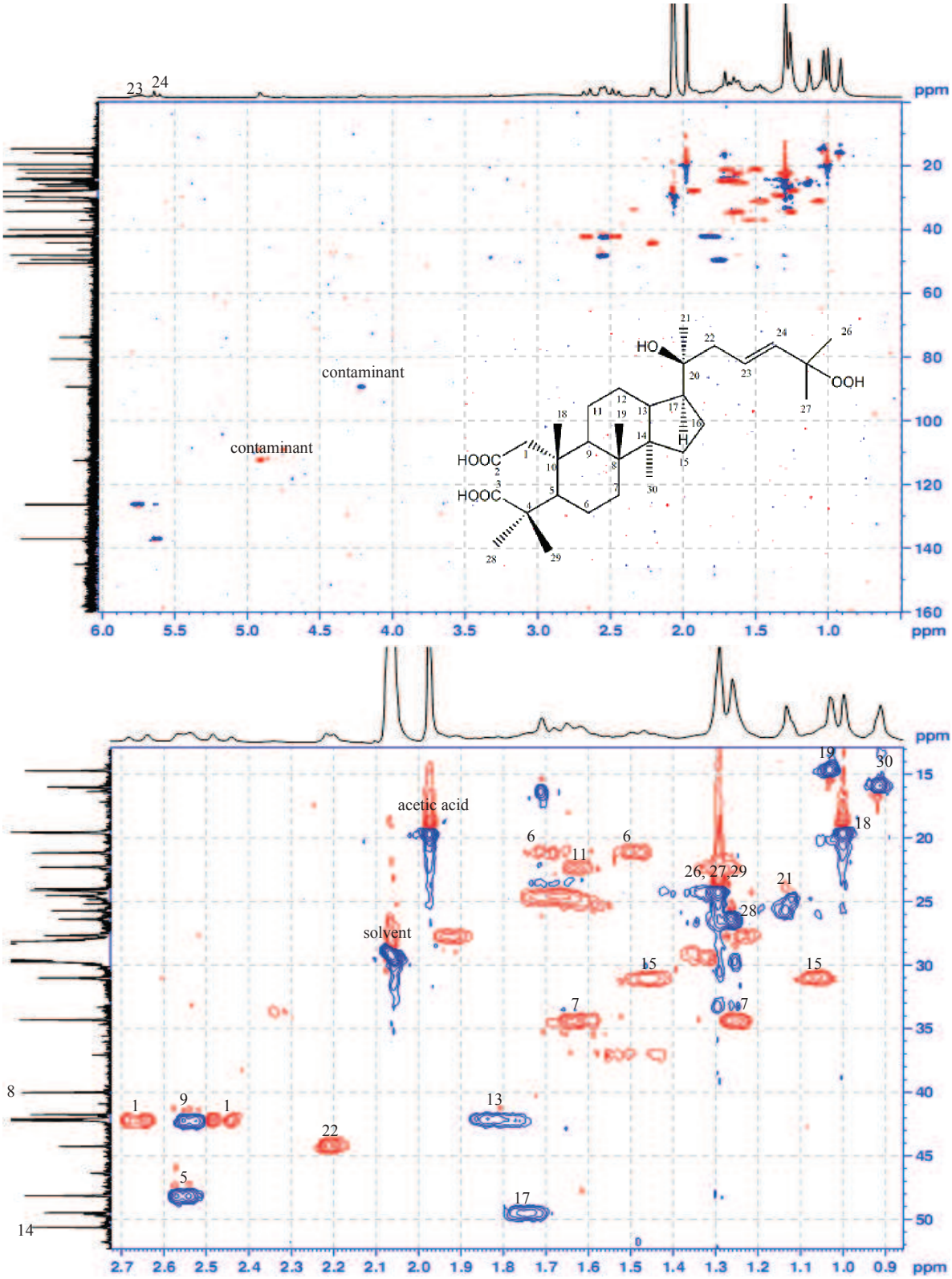

Figure 134. The HSQCedited correlation of **48** (in acetone) and expanded spectrum in the range of δ_H 0.9-2.7 ppm and δ_C 13-52 ppm.

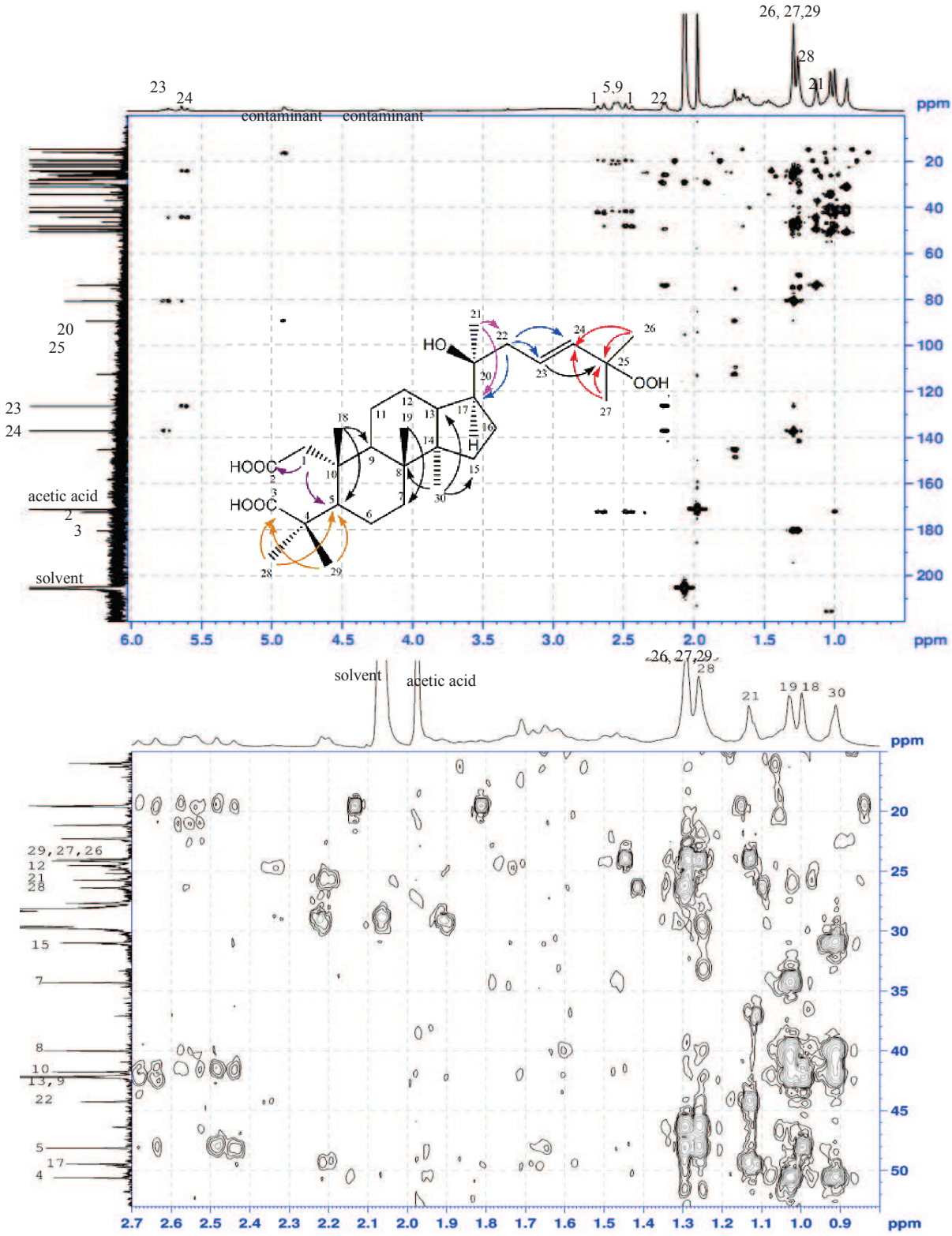

Figure 135. The HMBC correlation of **48** (in acetone) and expanded spectrum in the range of δ_H 0.8-2.7ppm and δ_C 15-53 ppm.

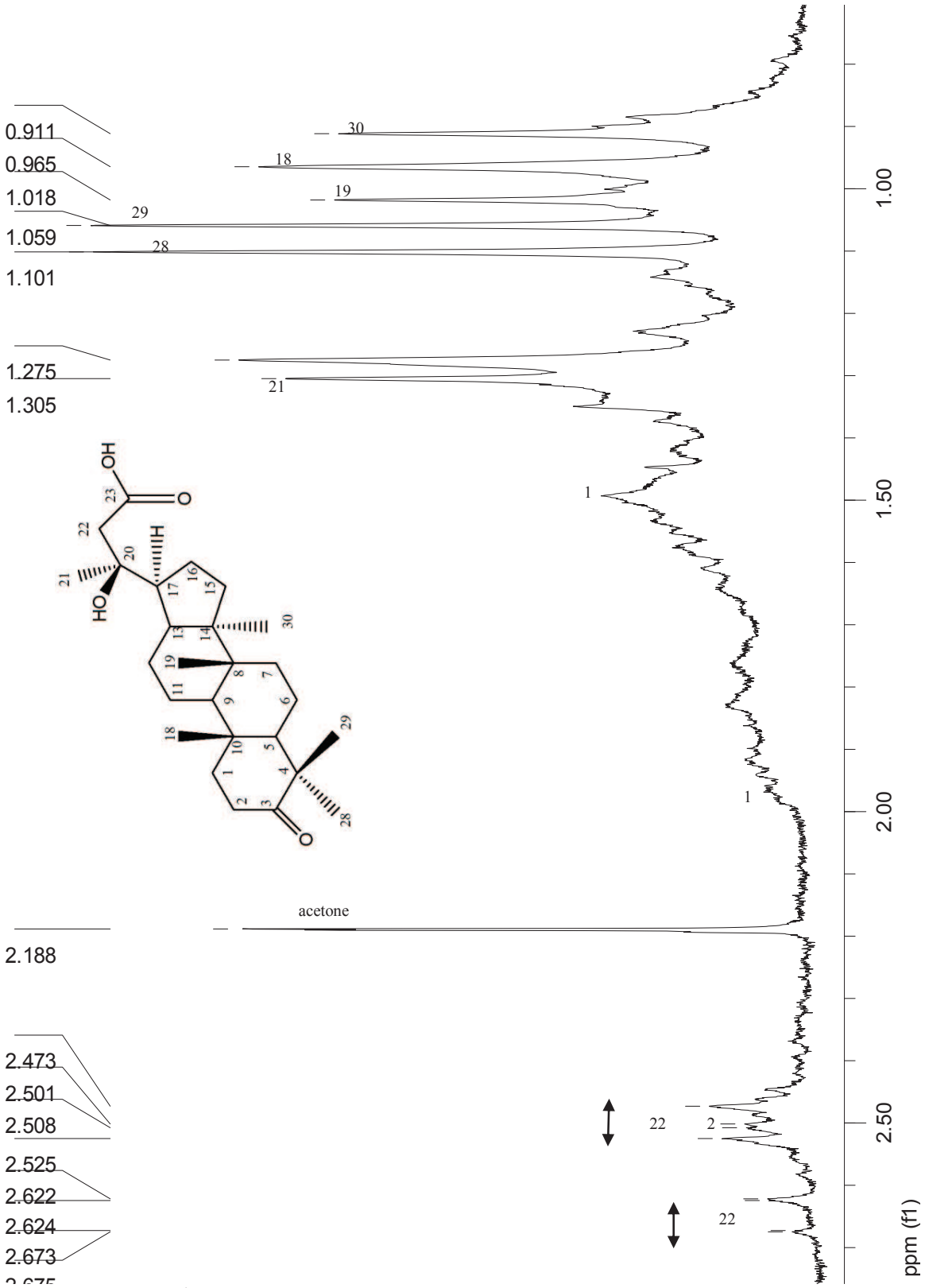

Figure 136. The ^{1}H NMR spectrum (300 MHz) of **49** (in $CDCl_3$).

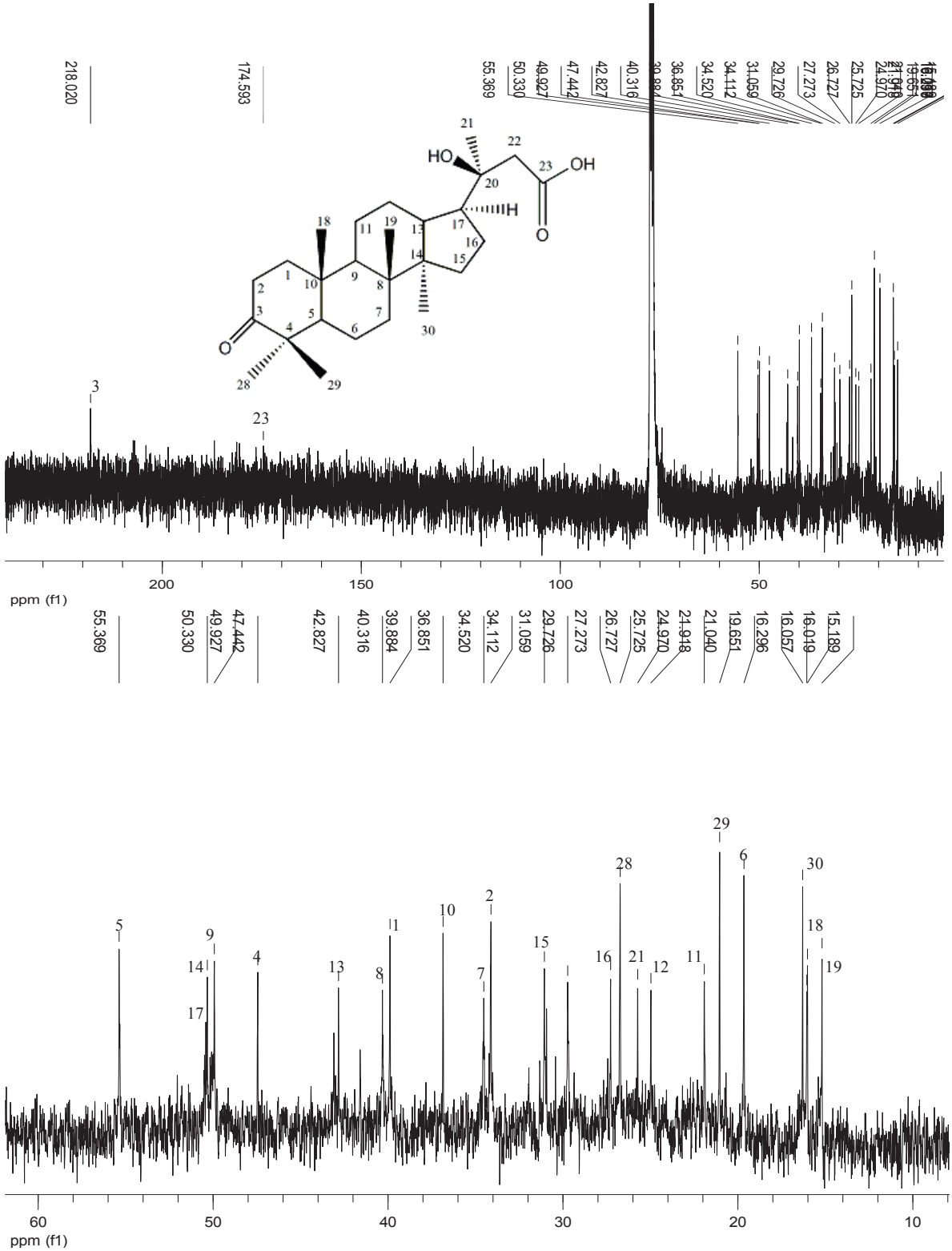

Figure 137. The ^{13}C NMR spectrum (75 MHz) of **49** (in $CDCl_3$) and expanded spectrum in the range of 10-60 ppm.

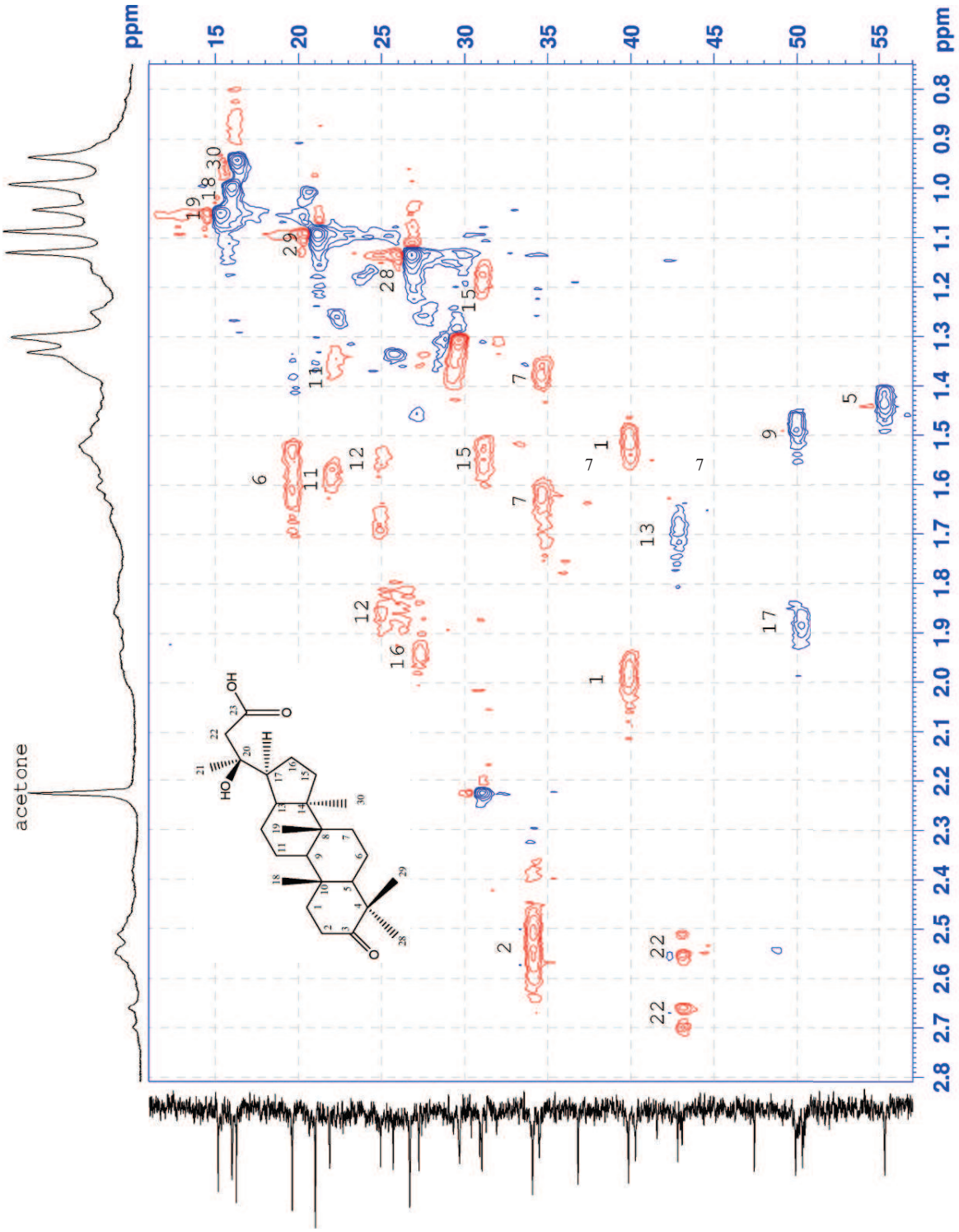

Figure 138. The expanded HSQCedited correlation of **49** (in $CDCl_3$) in the range of δ_H 0.9-2.8 ppm and δ_C 12-58 ppm.

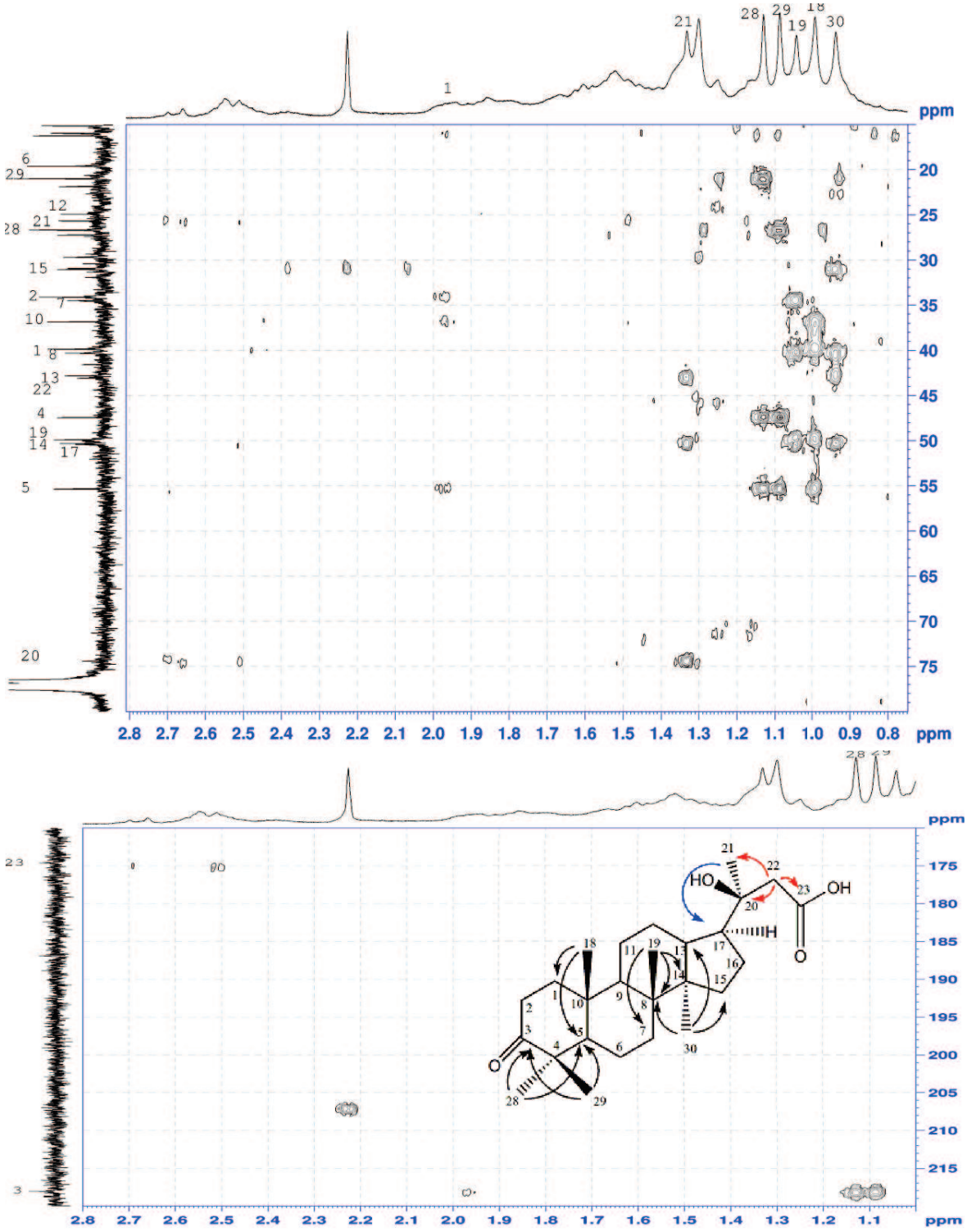

Figure 139. The expanded HMBC correlation of **49** (in $CDCl_3$) in the range of δ_H 0.9-2.7ppm, δ_C 15-53 ppm and δ_H 1.1-2.8ppm, δ_C 170-220 ppm.

Titre de la thèse : Etude phytochimique de deux Dipterocarpaceae de la forêt tropicale thaïlandaise : *Hopea odorata* Roxb. et *Dipterocarpus costatus* Gaertn.f.

Résumé :

Les extraits *n*-hexaniques respectivement des feuilles d'*Hopea odorata* Roxb. et du bois de *Dipterocarpus costatus* Gaertn.f. ont été sélectionnés sur la base d'un criblage biologique préliminaire. Ces extraits présentent des activités cytotoxiques significatives sur les lignées MCF-7 (cancer du sein) et NCI-H187 (cancer du poumon non à petite cellule). De plus, l'extrait du bois de *D. costatus* inhibe la croissance de la souche K1 de *Plasmodium falciparum*.

L'étude phytochimique de l'extrait *n*-hexanique des feuilles d'*Hopea odorata* a permis d'isoler 19 composés terpéniques dont 16 triterpènes des séries lupane (n=8), 3,4-*seco*-cycloartane (n=4), friedélane (n=2) et oléanane (n=2). Parmi les lupanes, l'acide 3,30-dioxolup-20(29)-èn-28-oïque a été isolé pour la première fois d'une source naturelle. L'évaluation de l'effet de ces lupanes sur la croissance de quatre lignées cancéreuses humaines (PC3, MDA-MB-231, HT-29 and HCT116) a permis d'identifier des composés actifs et d'apporter des éléments de relations structure-activité tels que l'influence du degré d'oxydation des positions C-3, C-28 et C-30 sur la cytotoxicité. Parmi les cycloartanes, deux nouveaux 3,4-*seco*-cycloartanes ont été identifiés. Il s'agit de deux esters d'acide gras saturés et de l'acide (24*S*, 25*S*, 26)-trihydroxy-3,4-*seco*cycloart-4(29)-èn-3-oïque. Par ailleurs, l'étude phytochimique de l'extrait *n*-hexanique du bois de *Dipterocarpus costatus* a permis d'isoler 30 terpènes dont 12 nouveaux triterpènes, parmi lesquels 5 norlupanes, 3 dammaranes, 2 nordammaranes et 2 *seco*dammaranes. Les activités biologiques de l'ensemble des composés isolés, ont été évaluées sur la croissance des lignées cancéreuses humaines précédemment citées et de muscle squelettique de rat L-6, ainsi que sur la croissance de la souche FcB1 du *Plasmodium falciparum*. En particulier, le norlupane **36** possédant une fonction endoperoxyde, montre une forte activité antiplasmodiale associée à une faible cytotoxicité.

Discipline :

Pharmacognosie

Mots-Clefs :

Dipterocarpaceae, *Hopea odorata*, *Dipterocarpus costatus*, triterpènes, cytotoxicité, 3,4-*seco*-cycloartane, lupane, norlupane, dammarane, nordammarane, 2,3-*seco*-dammarane

---

Adresse de l'auteur :

Faculty of Pharmacy, Silpakorn University, Sanamchandra Campus, Nakhon-Pathom 73000, Thailand.